P.O.Box 2345 Beijing 100023, China
Fax. 0086·10·65891893 Tel. 0086·10·65897901
E-mail.wcjd@public.bta.net.cn www.wd.org.cn

World J Gastroentero, 2001 April; 7(1):1 - 8
World Journal of Gastroenterology
Copyright©2001 by the WJG Press ISSN 1007 - 9327

Review

Advances in gene therapy of liver cirrhosis: a review

Wen Jie Dai and Hong Chi Jiang

Subject headings liver cirrhosis/therapy; gene therapy; transforming growth factor beta; interleukin 10; hepatocyte growth factor; telomerase; gene expression

Dai WJ, Jiang HC. Advances in gene therapy of liver cirrhosis: a review. ***World J Gastroenterol***, 2001;7(1):1-8

INTRODUCTION

Liver fibrosis or cirrhosis is a common progressively pathological lesion of chronic liver diseases in response to various liver-damaging factors. The main mechanisms of fibrotic or cirrhotic initiation and progression at the level of cellular and molecular events have been elucidated in the past two decades[1,2]. Various causes, including hepatitis virus infections, toxification, ischemia, congestion, parasites infection, abnormal cooper or iron load, etc, result in chronic inflammation and/or wound healing responses, of which the main characteristics manifest in the absolute increase of the excessive extracellular martrix (ECM) synthesis and the relative decrease of them, leading to ECM deposit. With the stimulation of inflammation or toxins, activated hepatic stellate cells(Ito cells), injuried or regenerated hepatocytes, Kupffer cells, sinusoidal cells and natural killer (NK) cells produce certain cytokines or immunoreactive factors, which exert various biological effects on their respective target cells or organs in an autocrine or paracrine manner. These consist of the cellular basis of hepatic fibrosis advances[3,4]. It is the vital molecular event in fibrosis progression that activated hepatic stellate cell exocrine ECM components and fibrosis-implementing factors, for example, the transforming growth factor β (TGF-β), which is considered the key cytokine to accelerate cirrhotic procession[5,6]. Various factors participate in fibrosis or cirrhosis formation. They could be simply divided into the fibrosis-implementing factors, such as TGF-β, platelet-derived growth factor (PDGF), epithelial growth factor (EGF), and antifibrotic factors, such as interferon γ and interleukin-10. These cytokines play important and unique roles in the interactive complicated network. Excessive ECM deposit, disappearance of sinusoidal endothelial fenestra and subsequent capillary vascularization cause the dysfunction of hepatocytes. The unblocked progressively pathological lesions with inevitably result in, lobular reconstruction, pseudolobule formation and nodular regeneration. With the elucidation of vital cellular and molecular events, gene delivery strategies for treatment of liver fibrosis or cirrhosis emerge on the basis of gene manipulations. Our interest focuses on the recent advances of gene therapy for liver fibrosis or cirrhosis.

Effective antifibrotic treatments, including medicinal or gene therapy, should satisfy several essential criteria. First, any therapy should have a sound biological basis. Additionally, the pharmacologically active drugs or compounds should reach or reside in the liver at a high concentration and have little side effect outside the liver. Specific targeting to hepatic stellate cells were preferentially chosen. Finally, in the ideal case, a therapeutic agent should keep the regional target environment for a relatively long period[7].

BLOCKADE OF TGF-β SIGNALING

It has been demonstrated that TGF-β is of great importance in fibrogenesis, and serves as a pivot in regulation of fibrogenic and antifibrogenic mediators. TGF-β exhibits stimulatory or inhibitory properties on cellular proliferation and differentiation, and is considered to represent a fundamental regulatory molecule acting through autocrine and/or paracrine mechanism[8].

TGF-β is clearly associated with hepatic fibrogenesis and cirrhosis in experimental animal models and in human liver diseases[9,10]. It regulates the gene expression of Ito cells, which in the course of liver fibrogenesis, proliferate and transform into the myofibroblast-like cells, synthesizing large amounts of connective tissue components, and also being involved in the ECM degradation by production of matrix metalloproteinases (MMP) inhibitors of MMP (TIMP), etc[11-13]. Because of the key role of TGF-β and Ito cells in the procession of liver fibrogenesis, lots of studies focus on their

Second Department of General Surgery, the First Clinical School, Harbin Medical University, Harbin 150001, Heilongjiang Province, China
Dr. Wen Jie Dai, graduated from seven-year system of Harbin Medical University in 1998, and now is a resident surgeon and doctoral student in the Second Department of General Surgery, the First Clinical School, Harbin Medical University, Harbin, China. Hismain research field is hepatobiliary and splenic surgery.
Correspondence to: Dr. Wen Jie Dai, Second Department of General Surgery, the First Clinical School, Harbin Medical University, Harbin 150001, Heilongjiang Province, China
Tel. 0086-451-3602829, Fax. 0086-451-3670428
Email. wenjiedai@etang.com
Received 2000-09-21 **Accepted** 2000-10-29

interactions. In *in vitro* studies, Ito cell cultures were found to be activated by TGF-β to increase the production of collagen type I, II, III, fibronectin, undulin and proteoglycans[14-16]. TGF-β enhanced the Ito cell transformation from resting to activated cells and inhibited Ito cell proliferation[17]. TGF-β signaling was mediated by specific receptors located on the target cell membrane. In non-activated Ito cells, type II and III were present, while in activated Ito cells, there were TGF-β/ activin receptor type I, II and III[18,20].

All the above showed clearly that anti-TGF-β intervention which could block the TGF-β signaling pathway may prevent liver fibrosis. Such interventions have come into being up to date. Qi *et al* have developed adenovirus-mediated gene transfer to rat liver for expressing a truncated type II TGF-β receptor[21]. It inhibits TGF-β activity by competing with binding of the cytokine to endogenous TGF-β receptors. The expression vector, AdCAT β-TR, was administrated via the portal vein for ensured infection and high-level expression in regional liver tissue.

Apparently, there needed a large excess of truncated receptor over the wild type full-length receptor for effective inhibition of TGF-β signaling[22,23]. Three days after AdCAT β-TR administration, two mRNAs corresponding to the truncated human receptor and the rat full-length receptor (5.5kb and 0.9kb) were detected respectively, and the former mRNA was about 20-fold that of the latter. Pathological examination showed that the extent of liver fibrosis, collagen type I, fibronectin, alpha smooth muscle actin (α-SMA), TGF-β 1 and monocytes/macrophages (ED-1) decreased significantly in AdCAT β-TR administration group. This inhibitory effect was observed in all areas of the liver. The content of liver hydroxyproline had no significant difference between AdCAT β-TR group and the intact group, while in the control group of dimethylnitrosamine (DMN)-treated persistent fibrotic rats, the amount of hydroxyproline was 3.4 times higher than that of the above two. It was evident that the activation of Ito cells and Kupffer cells was inhibited, suggesting that truncated type II TGF-β receptor gene transfer could prevent or abolish liver fibrogenesis effectively. More important, liver function of rats with AdCAT β-TR injection recovered with a marked decrease of serum hepatocyte enzyme AST and ALT[21].

Reports from Ueno *et al*[24] supported Qi *et al*'s results as well. They conducted an recombinant adenovirus expressing the entire extracellular domain of the human type ¢ò TGF-â receptor fused to the Fc portion of human immunoglobulin G (AdTβ-ExR) to produce a circulating soluble form of TGF-β receptor with remote vital organ targeting after intramuscular injection of AdT β-ExR. Soluble TGF-β receptor was detectable in circulation and its level peaked at 5-7 days after the injection. AdT β-ExR-infected COS cells secreted fused type II TGF-β receptors, which binded to TGF-β and consequently blocked the TGF-β signaling as the full-length TGF-β receptor did[24]. Injection of AdT β-ExR into the femoral muscle of DMN-induced fibrotic rats prevented hepatic fibrosis, while no side effects or complications were found either macroscopically or microscopically in the main organs including brain, heart, lung, liver and kidney. Histological examination in DMN-treated rats with i.m. injection of AdT β-ExR was essentially as the same as that in Qi *et al*'s report, which locally expressed truncated type II TGF-β receptor in the liver via the administration of AdCAT β-TR into the portal vein[21,24]. This research also disclosed that adenovirus-mediated expression of soluble TGF-β receptors exerted the binding effect to TGF-β in a TGF-β specific manner, that is, others, e.g., PDGF α-receptor and fibroblast growth factor (FGF), could not interfere with TGF-β. Although a large excess of soluble TGF-β receptor seems essential for blocking of TGF-β signaling, there was still apparent difference between specific soluble TGF-β receptor and non-receptor-specific binding proteins, e.g., decorin (would prevent TGF-β induced renal fibrosis), for blockade of TGF-β signaling[25]. Because the latter was lack of receptor specificity and selectivity when it binded to TGF-β, it may bind to other biological molecules, probably resulting in unexpected problems. More exact mechanism was also explored[26-29]. There was evidence that truncated type II TGF-β receptor may form a complex with other type TGF-β receptor and inhibit both the anti-proliferative effect of TGF-β and/or the transcriptional activation by TGF-β[30-31]. Each type of three TGF-β receptor isoforms may have its own distinct signaling pathway, each mediating a separate action setting of TGF-β[31]. Complete inhibition of TGF-β signaling was achieved via local expression of a kind of soluble TGF-β receptor in a remote area from the target organ. The fact suggested that such strategy should be applicable theoretically and therapeutically for other factors belonging to growth factor superfamily.

As a matter of fact, signaling pathways introduced by PDGF, FGF, epidermal growth factor (EGF), vascular endothelial growth factor (VEGF), insulin, etc, could be abolished specifically by their corresponding kinase-defective mutated form of receptors[23,32-36]. This kinase-defective or kinase-truncated receptors for signal transduction blockade of their growth factor may be a useful strategy for analysis of the *in vivo* role of these growth factors, because signaling pathway was blocked at the receptor level, not at the cytokine or gene level, without affecting the normal physiological status of these growth factors or signal transfer of other receptors[21,22,37]. Although no side effects were found during the study period, special attention should be paid to the surveillance

of the possible hazards, since Shull *et al* had demonstrated that there would be multifocal inflammation and tissue necrosis in TGF-β gene disrupted mice[38]. Adenovirus displayed the high degree of hepatotrophic activity. It could also mediate the targeted expression even if it was administrated in a remote site[21,24]. Immune responses would be elicited after repeated injection of adenovirus particles, therefore may lower the effectiveness of target gene expression.

STIMULATION OF HEPATOCYTE REGENERATION

In the course of liver fibrosis, the absolute and relative volume of hepatocytes was both reduced under the direct or indirect effect of liver-damaging factors. Stimulation of hepatocyte regeneration is the essential strategy in choice of treatment. Hepatocyte growth activators include an expanding list of complete mitogen and comitogen. Complete mitogen are defined as those that are capable of stimulating DNA synthesis and mitosis of cultured hepatocytes in serum-free media. Hepatocyte growth factor (HGF), EGF, TGF-α, and keratinocyte growth factor are in this category. Comitogens enhance the stimulatory action of complete mitogens and decrease the inhibitory effect of other inhibitors, while they have no direct proliferation-enhancing effect on cultured hepatocytes, including glucagon, insulin, insulin-like growth factors, adrenal cortical hormones, vasopressin, angiotensin, thyroid and parathyroid hormones, norepinephrine, as well as calcium and vitamin D[39]. HGF was regarded as the strongest hepatocyteproliferative agent up to date. It was a pleiotropic factor with potent morphogenic, mitogenic and motogenic effects and has anti-apoptotic action on hepatocytes and other several cells in culture, exhibiting a plethora of effects in many systems and organs[40-49]. The antifibrotic effect of HGF on hepatic fibrosis was first characterized by Yasuda *et al*[50]. In their experiment, the deletion variant of hepatocyte growth factor (dHGF) which was more mitogenic than full-length HGF, was used to examine its role in preventing fibrosis induced with dimethylnitrosamine in rats. Northern hybridization and immunohistochemical staining elucidated clearly the antifibrotic effect of dHGF on DMN-treated rats. The main mechanism appeared to be suppression of Ito cell activation, as demonstrated by the reduction of mRNA of procollagen α2(I), α1(III), α1(IV), TGF-β, desmin and α-SMA. Collagen content, as measured by hydroxyproline, was also decreased. Futhermore, dHGF exerted the mitogenic and antifibrotic activities even after the hepatic fibrosis had been established with DMN[50]. Their study showed that the antifibrotic effect of dHGF is not derived from the possible effect of dHGF on cytochrome P450-dependent metabolic degradation of DMN, but from the ability of dHGF to reduce or inhibit the TGF-β mRNA level[50,51], proliferation and activation of lipocytes and to stimulate liver regeneration[50]. Burr *et al* also demonstrated the vital role of HGF in liver regeneration[52]. After treatment with anti-HGF monoclonal antibody, the serum level of immunodetectable HGF was inhibited, as well as the parenchymal proliferative response to acute CCl_4-induced liver injury. Ueki *et al* developed a novel new gene therapy approach for rat liver cirrhosis by muscle-mediated gene transfer of HGF cDNA[53]. Plasmid containing HGF cDNA was embedded in the liposome, fused to the envelope protein of hemagglutinating virus of Japan (HVJ). This HVJ-liposome complex was intramuscularly injected repeatedly to achieve therapeutically detectable expression level of HGF. Repetitive administration resulted in a sound level of human HGF and increased level of endogenous rat HGF. The number of proliferative cellular nuclear antigen (PCNA) positive cells in HVJ-liposome-HGF injection group was markedly higher than that of control group. Apoptotic hepatocytes decreased significantly as well. The c-met, HGF-specific receptor located on the surface of hepatocytes, increased considerably in HVJ-liposome-HGF treated rats and stayed at this high level even after the repeated DMN administration, meanwhile strong tyrosine phosphorylation of c-met was observed. Immunohistochemistry revealed that with the administration of HVJ-HGF-liposome, staining of TGF-β1, expressed notably in persistent cirrhotic liver, decreased, as well as desmin and α-SMA, which were indicators of activated Ito cells. It suggested that expressed HGF could inhibit activation of Ito cells, decrease the synthesis of collagen type I and TGF-β, and prevent apoptosis of hepatocytes induced by DMN administration. After several injections of HVJ-HGF-liposome, complete remission was achieved, demonstrated by histology[53]. It can be inferred that HGF not only stimulated hepatocyte regeneration, but also remodeled the disorganized cirrhotic tissue. That is the pivotal potential for HGF gene therapy of liver cirrhosis[54]. It is of particular interest that HVJ-liposome was the ideal vehicle for gene transfer, because of the high efficiency, simplicity and lack of toxicity[55]. Another aspect of HGF on promoting neovascularization in certain ischemic diseases was also focused for possible application in the treatment of liver cirrhosis. Aoki *et al* delivered HGF cDNA into the myocardial infarction region in rats[56]. It promoted the neovascularization strongly in infarcted myocardium, including capillary, small- to medium-sized vessels. As an endothelium-specific growth factor with potent motogenic activity to endothelial cells, HGF's angiogenestic activity was also confirmed by the activation and upregulation of a transcription factor-ets, which is essential for angiogenesis[56]. Immunohistochemical staining revealed positive expression of ets 1 in endothelial cells and vascular smooth muscle cells (VSMC)

around the neovascularized vessels. The ets family participated in angiogenesis regulation by activating the transcription of several genes, including collagenase I, stromelysine 1 and urokinase plasminogen activator, which are proteases involved in ECM degradation, as well as migration of endothelial cells[57]. Overexpression of exogenous HGF activated ets family, initiated auto-loop up regulation mechanism of HGF resulting in up-regulation of endogenous HGF expression[53,56], since HGF gene promoter region comprised several putative regulatory elements, such as B cell- and macrophage-specific transcription factor binding sites (PU1/ETS), besides an interleukin-6 response element (IL-6RE), a TGF-β inhibitory element (TIE), and a cAMP response element (CRE)[56,58].

Another candidate for stimulation of hepatocyte proliferation is hepatic stimulatory substance (HSS), which was first described by LaBrecque *et al* in 1975. As a heat-stable stimulator for regenerating liver with partial hepatectomy, it is considered to be the unique liver-specific stimulatory factor and is universally located in mammal embryonic liver, weanling liver and regenerating liver[59]. In 1994, Hagiya *et al* obtained a gene product in rats, called augmenter of liver regeneration (ALR) with a full-length of 1.2kb and open reading frame of 378bp[60]. The molecular weight of ALR was approximately 30kDa, as a homodimeric complex[60,61]. The recombinant ALR expressed from ALR cDNA-transduced COS cells exerted potent and dose-dependent proliferative activity tested in canine Eck fistula (portal caval shunt) model[60]. Subsequent published reports have gradually come to a common view that ALR is actually the HSS. Yang *et al* cloned the human ALR gene in 1996[62,63]. Other groups also successfully cloned the rat and human ALR cDNA subsequently[64,65]. In comparison of the ALR encoding sequences of human and rat, homology of nucleotide sequence is about 87%, and that of protein sequence was 84.8%. Rat, mouse and human ALR genes and protein products were highly conserved and preferentially expressed in the testis and the liver, probably being involved in the synthesis and stability of the nuclear and mitochondrial transcripts, especially in spermatogenesis in actively regenerative tissues. Wang *et al* demonstrated that ALR or hepatopoietin (HPO) exerted the biological activity via the high affinity receptors for HPO on the surface of rat hepatocytes and human hepatoma cells. Each of the above cells has a mean of approximate 10 000 and 55 000 receptor sites respectively, as was identified with the binding of radioisotype ^{125}I-labelled HPO to a 90kDa polypeptide[66]. Updated research by Gandhi *et al* showed a certain new aspect of ALR funtion[67]. Hepatic levels of ALR decreased for 12 hours after 70% hepatectomy in adult rats and rose with no corresponding increase in ALR mRNA transcripts, while serum ALR level increased up to 12 hours. This implied that ALR was constitutively expressed in hepatocytes in an inactive form, and appeared to be an active form after being released outside the hepatocytes in response to partial hepatectomy or other regeneration-promoting circumstances[67]. Liver-derived NK cells are important regulators for liver regeneration[68]. Francavilla *et al*[69] connected the regulation activity of ALR in liver regeneration with the novel role of NK cells. Francavilla *et al* administrated three hepatotrophic factors (ALR, insulin-like growth factor II [IGF-II] and HGF) with the surely inducing sound hepatotrophic activities to assess the *in vivo* effects on NK cells in normal rats. Results showed that NK cell cytotoxic activities were inhibited in the population of mononuclear leukocytes (MNL) in the liver (liver-resident NK cells), but not in the MNL from the spleen or peripleral blood. Results obtained *in vitro* displayed that ALR, IGF-II and HGF had no effect on NK cell function in cultured MNL from the liver, spleen or blood[69]. Results from Polimeno *et al*also verified that ALR plays a pivotal role as growth factor and as immunoregulator by controlling the mitochondrial transcription factor A expression and lytic activity of liver-resident NK cells through IFN-γ levels[70] and regulates hepatocyte proliferation through enhancing cytochrome content and oxidative phosphorylation capacity of liver-derived mitochondia[71]. Liver injuries could also be prevented with recombinant ALR injected intraperitoneally[72-74]. Gene transfer of human ALR gene into cirrhotic rat may be an meaningful tool for reversing liver cirrhosis. Interestingly, no close or stringent homology was found between ALR and other polypeptide growth factor, while ALR has both structural and functional homology compared with yeast scERV1 gene which is involved in biogenesis of mitochondria and regulation of cell cycle, which may imply ALR's evolutional conservation and essentialness to growth and development[60,66].

INHIBITION OF INTERSTITIAL INFLAMMATION

Interstitial inflammation was characterized as the main pathological changes in fibrogenesis. Those inhibiting inflammatory responses would also be the target for gene transfer to block the fibrogenic inflammation. Interleukin-10 (IL-10) is suitable for this strategy. IL-10, originally identified as a cytokine synthesis inhibitory factor, inhibits production of a variety of cytokines in various cell types. It is produced under different conditions of immune activation by the T-H 2 and TH0 subsets of helper T cells, as well as by monocytes, macrophages, B cells, keratinocytes and stromal cells[75]. Sequences of open reading frame, not 5'- or 3'- flanking regions of mouse and human IL-10 cDNA showed high homology to two viruses,

Epstein-Barr virus and equine herpes virus[76]. Acquiring a mammalian IL-10 homology and subsequent inhibitory properties of IL-10 toward macrophages may help the virus escape from the antiviral immune attacks. IL-10 exerted multiple biological activities, including inhibition of T-H1 cells and antigen-presenting cells, stimulation of mast cell proliferation, protease expression, stimulation of B cell proliferation, antibody secretion and major histocompatibility complex II (MHC II) expression[75]. IL-10 takes part in the sophisticated regulation of fibrogenesis. In IL-10 gene knockout (KO) mice treated with tetrachloride (CCl_4), there existed no difference in hepatic toxicity of CCl_4 between KO mice and wild type (WT) mice.

In CCl_4-induced acute liver injury mice, serum TNF-α and TGF-β levels were markedly high in KO mice than that in WT mice. Administration of recombinant IL-10 inhibited cultured Kupffer cells producing superoxide radicals and TNF-α *in vitro*. In CCl_4-induced chronic liver injury model, the degree of hepatic fibrosis was severer and the level of tissue TNF-α was higher than that of WT mice. IL-10 knockout also seemed to enhance monocyte infiltration [77,78]. Up-regulation of IL-10 mRNA was found in both freshly isolated quiescent and activated Ito cells. Co-transfection of Ito cells with an IL-10 expression vector and collagen reporter genes showed a 40% inhibition of α1 (I) collagen promoter activity, suggesting the *in vivo* role of IL-10 in matrix remodeling and the possibility that failure for Ito cell to sustain IL-10 expression underlied pathologic progression to liver cirrhosis[79,80]. Kupffer cell also played a pivotal role in production of IL-10. Reports from Rai *et al*[81] revealed the subtle role of IL-10 in regulating production of TNF-α, a hepatocyte proliferative factor initiated after 70% partial hepatectomy. Kupffer cell depletion induced by gadolinium chloride (GdCl) abolished induction of IL-10, then elongated half-life of TNF-α mRNA. Overexpression of TNF-α promoted liver regeneration potently after partial hepatectomy. Meijer *et al* strengthened the common point of view that Kupffer cell depletion, physically induced with dichloromethylene-diphosphonate, resulted in an imbalanced hepatic cytokine expression, thereby suppressing important growth-stimulating factors, including HGF and TNF-α[82]. Similar results were found in alcoholic cirrhosis[83]. Contraversy existed with respect to effects of IL-10 on extracellular matrix regulation, for IL-10 was likely to have different effects relying upon the differently detailed experimental materials and conditions. In general, IL-10 inhibited α1 (I) collagen gene expression [79,84] stimulated collagenase (MMP-1), stromelysin (MMP-3)[84], gelatinase (MMP-9)[85] expression and elastin promoter activity.

Antifibrotic effect of IL-10 on hepatic fibrosis was also correlated with its inhibition of TGF-β expression in fibrotic tissue, which was verified as the key fibrotic regulator as stated above. This mechanism was also verified in other experiments[82,86]. As an inhibitory regulator with pleiotropic nature, IL-10 may be used as a target gene for gene transfer in the treatment of liver cirrhosis, based on the potent capacity of suppressing production of proinflammatory cytokines[75,77,78,82,83,87-92]. Nelson *et al* showed an exciting report that IL-10 could reduce liver fibrosis and normalize serum ALT levels in IFN-γ unresponsive hepatitis C patients[93].

TELOMERE AND TELOMERASE WITH CIRRHOSIS

Telomere is a special cap-like structure at the end of eukaryotic chromosomes, composed of a tandemly (TTAGGG)-rich repeat DNA sequences and relative catalyzing proteins. Length of telomere within a certain range is essential and vital for normal mitosis, for it enhances the stability of end chromosome, prevents abnormal chromosomal rearrangement and end-end fusion, and protects against the degradation or destruction by nuclease and/or ligase. When telomere was shortened to a checkpoint range of 2-4kb, the stabilization of chromosomes would collapse. Maintenance of telomere length depends on the telomerase, which consists of RNA and two protein subsets and serves as RNA-dependent DNA polymerase to achieve complete and entire replication of chromosome. There are large amounts of evidence to demonstrate that telomerase takes part in complex regulation and plays a crucial role in cell proliferation, aging, immortalization and tumorigenesis[94]. Except for the lymphocytes of peripheral bood, hematopoietic stem cells, germ cells, embryonic somatic cells and those resident in actively proliferating tissues, for example, hair, skin and endometrium, also have telomerase activities[95]. Other tissues exert no telomerase activity.

In cirrhotic liver, evidence verified no or a variety of low activity of telomerase, while telomere length decreased commonly[96-100]. Hytiroglou *et al* found a clear cut difference in telomerase activity levels between hepatocellular carcinoma (HCC) (positive or strongly positive) and cirrhotic liver tissues (weakly positive or negative). They considered that activation of telomerase was an early event in larger nodular cirrhosis formation, and consequently exerted facilitating effect on other factors in the progression of carcinogenesis[101]. A proportion of 86% of large noncancerous nodules exhibited similar telomerase activity to HCCs, and part of it was derived from large regenerative nodules, but not dysplastic nodules[101].

The importance of maintenance of telomere length has been verified in cultured telomerase-negative human retinal pigment epithelial cells and foreskin fibroblasts, transfected with vectors

encoding the human telomerase catalytic subunit[102]. A comparison between human telomerase reverse transcriptase subunit (hTRT) gene transfer group and control group showed that with hTRT gene transfer, the telomerase-negative cells displayed normal phenotype and karyotype, as well as exceeded their normal life-span by at least 20 doublings. The fact was also demonstrated by Kiyono *et al*[103]. Results obtained from telomerase-deficient mice verified the crucial role of telomerase and maintained telomere in development, which owned the nature of progressive telomere shortening from one generation to the next, for lack of active telomerase[104,105].

Based on the elucidation of telomerase's role in senescence and tumorigenesis, Rudolph *et al* brought new insight into the mechanism of telomerase gene transfer (mTR gene) in the treatment of liver injury and cirrhosis. They adopted three systems to gauge how telomere shortening influenced hepatocyte proliferation, survival and ultimately predisposition to cirrhosis[106]. The first was the albumin-directed urokinase plasminogen activator (Alb-uPA) transgenic mouse, in which Alb-uPA expression would cause widespread hepatocytes death and fatal liver failure in newborn mice. Results showed a progressive decline in telomere length of peripheral blood lymphocytes from the first generation (G1) to the third generation (G3), with a 3.6-fold increase in apoptotic hepatocytes and a decrease in proliferative hepatocytes. The second and third system was partial hepatectomy and CCl_4 mediated liver injury, respectively. Flow cytometry verified that telomerase dysfunction inhibited mitosis of mice hepatocytes. Pathology showed abnormal mitosis and formation of anaphase bridges in G6 $mTR^{-/-}$ mice. Induced apoptosis of hepatocytes delayed the volume recovery of hepatectomized liver. Repeated administration of CCl_4, caused liver cirrhosis first in G6 $mTR^{-/-}$ mice, followed by G3 $mTR^{-/-}$ mice and finally by $mTR^{+/+}$. It suggested that with the shortening of telomere, damage-resistant capacity of parenchymal cells decreased and cirrhosis was prone to be induced.

As gene transfer vector, adenovirus revealed good hepatotrophic property (an infection rate of 85%-100%). Telomere was shortened by about 70% in G6 $mTR^{-/-}$ mice, however, after mTR gene transfer, ascites reduced with gain of body weight, and serum levels of ALT and AST improved with active proliferation of hepatocytes. Compared with $mTR^{-/-}$ mice, mTR-transferred G6 $mTR^{-/-}$ mice survived during the experimental stage with 66% decrease of mitosis index and 58% reduction of anaphase chromatin bridges. No TGF-β was detected in mTR-transferred G6 $mTR^{-/-}$ mice, implying that mTR transfer may block TGF-β signaling and/or inhibit activation of Ito cell and TGF-β secretion. Target transfer of telomerase gene into affected organ created a new strategy and also a novel pathway for the treatment of aging and certain telomerase-related chronic disease.

Before actual application, over-high activity of telomerase may induce instablility of genomic structure and tumor formation. From a clinical point of view, telomerase gene therapy may be an ideal choice of treatment for patients awaiting liver transplantation, for it could actually improve liver function and extend survival, and the eventual surgical removal of diseased organ should at most minimize the potential cancer risk [105]. Telomerase gene therapy may be regarded as an effective short-term supporting procedure for patients with end-stage liver disease before carrying out of liver transplantation[107].

REFERENCES

1 Friedman SL. The cellular basis of hepatic fibrosis: mechanisms andtreatment strategies. *N Engl J Med,* 1993;328:1828-1835

2 Friedman SL. Molecular regulation of hepatic fibrosis, an integrated cellular response to tissue injury. *J Biol Chem,* 2000;275: 2247-2250

3 Bissell DM. Hepatic fibrosis as wound repair: a progress report. *J Gastroenterol,* 1998;33:295-302

4 Liu SR, Gu HD, Li DG, Lu HM. A comparative study of fat storing cells and hepatocytes in collagen synthesis and collagen gene expression. *Xin Xiaohuabingxue Zazhi,* 1997;5:761-762

5 Border WA, Noble NA. Transforming growth factor B in tissue fibrosis. *N Engl J Med,* 1994;331:1286-1291

6 Shetty K, Wu GY, Wu CH. Gene therapy of hepatic diseases: prospects for the new millennium. *Gut,* 2000;46:136-139

7 Rockey DC. Gene therapy for hepatic fibrosisa2bringing treatment into the new millennium. *Hepatology,* 1999;30:816-818

8 De Bleser PJ, Niki T, Rogiers V, Geerts A. Transforming growth factor-B gene expression in normal and fibrotic rat liver. *J Hepatol,* 1997;26:886-893

9 Liu F, Liu JX. Role of transforming growth factor betal in hepatic fibrosis. *Shijie Huaren Xiaohua Zazhi,* 2000;8:86-88

10 Wrana JL. Transforming growth factora-β signaling and cirrhosis. *Hepatology,* 1999;29:1909-1910

11 Casini A, Ceni E, Salzano R, Milani S, Schuppan D, Surrenti C. Acetaldehyde regulates the gene expression of matrixa2metalloproteinasea21 anda22 in human fata2storing cells. *Life Sci,* 1994;55:1311-1316

12 Milani S, Herbst H, Schuppan D, Grappone C, Pellegrini G, Pinzani M, Casini A, Calabró A, Ciancio G, Stefanini F, Burroughs AK, Surrenti C. Differential expression of matrix-metalloproteinase-1 and -2 genes in normal and fibrotic human liver. *Am J Pathol,* 1994;144:528-537

13 Gao Y, Wang Y, Yang JZ, Huang YQ. Dynamic changes of gelatinase A gene expression in the course of experimental hepatic fibrosis. *Shijie Huaren Xiaohua Zazhi,* 1999;7:1003-1004

14 Armendariza2Borunda J, Katayama K, Seyer JM. Transcriptional mechanisms of type collagen gene expression are differentially regulated by interleukin-1 β, tumor necrosis factor α, and transforming growth factor β in Ito cells. *J Biol Chem,* 1992;267: 14316-14321

15 Casini A, Pinzani M, Milani S, Grappone C, Galli G, Jezequel AM, Schuppan D, Rotella CM, Surrenti C. Regulation of extracellular matrix synthesis by transforming growth factor β_1 in human fat-storing cells. *Gastroenterology,* 1993;105:245-253

16 Ramadori G, Knittel T, Odenthal M, Schwöigler S, Neubauer K, Meyer zum Büschenfelde KH. Synthesis of cellular fibronectin by rat liver fat-storing (Ito) cells: regulation by cytokines. *Gastroenterology,* 1992;103:1313-1321

17 Xiang DD, Wei YL, Li QF. Molecular mechanism of transforming growth factor β_1 on Ito cell. *Shijie Huaren Xiaohua Zazhi,* 1999;7:980-981

18 Friedman SL, Yamasaki G, Wong L. Modulation of transforming growth factor β receptors of rat lipocytes during the hepatic wound healing response. Enhanced binding and reduced gene expression accompany cellular activation in culture and *in vivo. J Biol Chem,* 1994;269:10551-10558

19 Ebner R, Chen RH, Shum L, Lawler S, Zioncheck TF, Lee A, Lopez AR, Derynck R. Cloning of a type I TGF-β receptor and its effect on TGF-β binding to the type II receptor. *Science,* 1993; 260:1344-1349

20 Le Magueresse-Battistoni B, Morera AM, Goddard I, Benahmed M.

Expression of mRNAs for transforming growth factor-β receptors in the rat testis. *Endocrinology*, 1995;136:2788-2791
21 Qi Z, Atsuchi N, Ooshima A, Takeshita A, Ueno H. Blockade of type beta transforming growth factor signaling prevents liver fibrosis and dysfunction in the rat. *Proc Natl Acad Sci USA*, 1999; 96:2345-2349
22 Yamamoto H, Ueno H, Ooshima A, Takeshita A. Adenovirus-mediated transfer of a truncated transforming growth factor-β (TGF-β) type IIreceptor completely and specifically abolishes diverse signaling by TGF-β in vascular wall cells in primary culture. *J Biol Chem*, 1996;271:16253-16259
23 Ueno H, Colbert H, Escobedo JA, Williams LT. Inhibition of PDGFB receptor signal transduction by coexpression of a truncated receptor. *Science*, 1991;252:844-848
24 Ueno H, Sakamoto T, Nakamura T, Qi Z, Astuchi N, Takeshita A, Shimizu K, Ohashi H. A soluble transforming growth factor β receptor expressed in muscle prevents liver fibrogenesis and dysfunction in rats. *Hum Gene Ther*, 2000;11:33-42
25 Wang GQ, Kong XT. Action of cell factor and Decorin in tissue fibrosis. *Shijie Huaren Xiaohua Zazhi*, 2000;8:458-460
26 Bassing CH, Yingling JM, Howe DJ, Wang T, He WW, Gustafson ML, Shah P, Donahoe PK, Wang XF. A transforming growth factor β type I receptor that signals to activate gene expression. *Science*, 1994;263:87-89
27 Wrana JL, Attisano L, Wieser R, Ventura F, Massague J. Mechanism of activation of the TGF-β receptor. *Nature*, 1994;370: 341-347
28 Okadome T, Yamashita H, Franzen P, Moren A, Heldin CH, Miyazono K. Distinct roles of the intracellular domains of transforming growth factor-β type I and type II receptors in signal transduction. *J Biol Chem*, 1994;269:30753-30756
29 Vivien D, Attisano L, Wrana JL, Massague J. Signaling activity of homologous and heterologous transforming growth factor-β receptor kinase complexes. *J Biol Chem*, 1995;270:7134-7141
30 Brand T, MacLellan WR, Schneider MD. A dominanta2negative receptor for type β transforming growth factors created by deletion of the kinase domain. *J Biol Chem*, 1993;268:11500-11503
31 Chen RH, Ebner R, Derynck R. Inactivation of the type II receptor reveals two receptor pathways for the diverse TGF-β activities. *Science*, 1993;260:1335-1338
32 Ueno H, Escobedo JA, Williams LT. Dominant-negative mutations of platelet-derived growth factor (PDGF) receptors. Inhibition of receptor function by ligand-dependent formation of heterodimers between PDGFα-and β– receptors. *J Biol Chem*, 1993;268:22814-22819
33 Mima T, Ueno H, Fischman DA, Williams LT, Mikawa T. Fibroblast growth factor receptor is required for *in vivo* cardiac myocyte proliferation at early embryonic stages of heart development. *Proc Natl Acad Sci USA*, 1995;92:467-471
34 Millauer B, Shawver LK, Plate KH, Risau W, Ullrich A. Glioblastoma growth inhibited *in vivo* by a dominant-negative Flk-1 mutant. *Nature*, 1994;367:576-579
35 Kendall RL, Thomas KA. Inhibition of vascular endothelial cell growth factor activity by an endogenously encoded soluble receptor. *Proc Natl Acad Sci USA*, 1993;90:10705-10709
36 Kendall RL, Wang G, Thomas KA. Identification of a natural soluble form of the vascular endothelial growth factor receptor, FLT-1, and its heterod imerization with KDR. *Biochem Biophys Res Commun*, 1996;226:324-328
37 Ueno H, Gunn M, Dell K, Tseng A, Williams L. A truncated form of fibroblast growth factor receptor 1 inhibits signal transduction by multiple types of fibroblast growth factor receptor. *J Biol Chem*, 1992;267:1470-1476
38 Shull MM, Ormsby I, Kier AB, Pawlowski S, Diebold RJ, Yin M, Allen R, Sidman C, Proetzel G, Calvin D, Annunziata N, Doetschman T. Targeted disruption of the mouse transforming growth factor-β_1 gene results in multifocal inflammatory disease. *Nature*, 1992;359:693-699
39 Steer CJ. Liver regeneration. *FASEB J*, 1995;9:1396-1400
40 Michalopoulos GK, DeFrances MC. Liver regeneration. *Science*, 1997;276:60-66
41 Zarnegar R, Michalopoulos GK. The many faces of hepatocyte growth factor: from hepatopoiesis to hematopoiesis. *J Cell Biol*, 1995;129:1177-1180
42 Kopp JB. Hepatocyte growth factor : mesenchymal signal for epithelial homeostasis. *Kidney Int*, 1998;54:1392-1393
43 Nakamura Y, Morishita R, Higaki J, Kida I, Aoki M, Moriguchi A, Yamada K, Hayashi S, Yo Y, Matsumoto K, Nakamura T, Ogihara T. Expression of local hepatocyte growth factor system in vascular tissues. *Biochem Biophys Res Commun*, 1995;215:483-488
44 Böirset M, Hjorth-Hansen H, Seidel C, Sundan A, Waage A. Hepatocyte growth factor and its receptor c-met in multiple myeloma. *Blood*, 1996;88:3998-4004
45 Yamaguchi K, Nalesnik MA, Michalopoulos GK. Hepatocyte growth factor mRNA in human liver cirrhosis as evidenced by in situ hybridization. *Scand J Gastroenterol*, 1996;31:921-927
46 Itakura A, Kurauchi O, Morikawa S, Okamura M, Furugori K, Mizutani S. Involvement of hepatocyte growth factor in formation of bronchoalveolar structures in embryonic rat lung in primary culture. *Biochem Biophys Res Commun*, 1997;241:98-103
47 Luo YQ, Wu MC. Hepatocyte growth fuctor. *Xin Xiaohuabingxue Zazhi*, 1997;5:198-199
48 Shiota G, Wang TC, Nakamura T, Schmidt EV. Hepatocyte growth factor intransgenic mice: effects on hepatocyte growth, liver regeneration and gene expression. *Hepatology*, 1994;19:962-972
49 Phaneuf D, Chen SJ, Wilson JM. Intravenous injection of an adenovirus encoding hepatocyte growth factor results in liver growth and has a protective effect against apoptosis. *Mol Med*, 2000;6:96-103
50 Yasuda H, Imai E, Shiota A, Fujise N, Morinaga T, Higashio K. Antifibrogenic effect of a deletion variant of hepatocyte growth factor on liver fibrosis in rats. *Hepatology*, 1996;24:636-642
51 Ignotz RA, Endo T, Massague J. Regulation of fibronectin and type I collagen mRNA levels by transforming growth factor-β. *J Biol Chem*, 1987;262:6443-6446
52 Burr AW, Toole K, Chapman C, Hines JE, Burt AD. Anti-hepatocyte growth factor antibody inhibits hepatocyte proliferation during liver regeneration. *J Pathol*, 1998;185:298-302
53 Ueki T, Kaneda Y, Tsutsui H, Nakanishi K, Sawa Y, Morishita R, Matsumoto K, Nakamura T, Takahashi H, Okamoto E, Fujimoto J. Hepatocyte growth factor gene therapy of liver cirrhosis in rats. *Nature Med*, 1999;5:226-230
54 Wang FS, Wu ZZ. Current situation in studies of gene therapy for liver cirrhosis and liver fibrosis. *Shijie Huaren Xiaohua Zazhi*, 2000;8:371-373
55 Fujimoto J. Reversing liver cirrhosis: impact of gene therapy for liver cirrhosis. *Gene Ther*, 1999;6:305-306
56 Aoki M, Morishita R, Taniyama Y, Kida I, Moriguchi A, Matsumoto K, Nakamura T, Kaneda Y, Higaki J, Ogihara T. Angiogenesis induced by hepatocyte growth factor in non-infarcted myocardium and infarcted myocardium: up-regulation of essential transcription factor for angiogenesis, ets. *Gene Ther*, 2000;7:417-427
57 Gum R, Lengyel E, Juarez J, Chen JH, Sato H, Seiki M, Boyd D. Stimulation of 92-kDa gelatinase B promoter activity by *ras* is mitogen-activated protein kinase kinase 1-independent and requires multiple transcription factor binding sites including closely spaced PEA3/*ets* and AP-1 sequences. *J Biol Chem*, 1996;271: 10672-10680
58 Liu Y, Michalopoulos GK, Zarnegar R. Structural and functional characterization of the mouse hepatocyte growth factor gene promoter. *J Biol Chem*, 1994;269:4152-4160
59 He FC, Wu C, Tu Q, Xing G. Human hepatic stimulator substance: a product of gene expression of human fetal liver tissue. *Hepatology*, 1993;17:225-229
60 Hagiya M, Francavilla A, Polimeno L, Ihara I, Sakai H, Seki T, Shimonishi M, Porter KA, Starzl TE. Cloning and sequence analysis of the rat augmenter of liver regeneration (ALR) gene: expression of biologically active recombinant ALR and demonstration of tissue distribution. *Proc Natl Acad SciUSA*, 1994;91:8142-8146
61 Wang QM, Chen JZ, Tan YC, Fan GC, Jiang HL, Chen HP, He FC. Studies on chemicophysical properties of recombinant human hepatopoietin. *Junshi Yixue Kexueyuan Yuankan*, 2000;24:19-22
62 Yang XM, Xie L, Qiu ZH, Hu ZY, Wu ZZ, He FC. Isolation and sequence analysis of the human augmenter of liver regeneration. *Junshi Yixue Kexueyuan Yuankan*, 1996;20:241-244
63 Yang XM, He FC, Xie L, Hu ZY, Wang QM, Qiu ZH, Wu ZZ. Molecular cloning of new type augmenter of liver regeneration and research on its function. *Xin Xiaohuabingxue Zazhi*, 1997;5:335
64 Yi XR, Kong XP, Tong MH, Yang LP, Li RB, Zhang YJ. Cloning and sequencing of rat and human augmenter of liver regeneration gene. *Huaren Xiaohua Zazhi*, 1998;6:392-393
65 Liu Q, Wang ZY, Luo Y, Huang AL, Zhang DF. The cDNA clone and sequence analysis of the coding region of human augmenter of liver regeneration (hALR) gene. *Zhonghua Ganzhangbing Zazhi*, 1999;7:156-158
66 Wang G, Yang XM, Zhang Y, Wang QM, Chen HP, Wei HD, Xing GC, Xie L, Hu ZY, Zhang CG, Fang DC, Wu CT, He FC. Identification and characterization of receptor for mammalian hepatopoietin that is homologous to yeast ERV1. *J Biol Chem*, 1999;274:11469-11472
67 Gandhi CR, Kuddus R, Subbotin VM, Prelich J, Murase N, Rao AS, Nalesnik MA, Watkins SC, DeLeo A, Trucco M, Starzl TE. A fresh look at augmenter of liver regeneration in rats. *Hepatology*, 1999;29:

1435-1445
68 Luo DZ, Vermijlen D, Ahishali B, Triantis V, Plakoutsi G, Braet F, Vanderkerken K, Wisse E. On the cell biology of pit cells, the liver-specific NK cells. *World J Gastroenterol*, 2000;6:1-11
69 Francavilla A, Vujanovic NL, Polimeno L, Azzarone A, Iacobellis A, Deleo A, Hagiya M, Whiteside TL, Starzl TE. The *in vivo* effect of hepatotrophic factors augmenter of liver regeneration, hepatocyte growth factor, and insulin-like growth factor-II on liver natural killer cell functions. *Hepatology*, 1997;25:411-415
70 Polimeno L, Margiotta M, Marangi L, Lisowsky T, Azzarone A, Ierardi E, Frassanito MA, Francavilla R, Francavilla A. Molecular mechanisms of augmenter of liver regeneration as immunoregulator: its effect on interferon-γ expression in rat liver. *Digest Liver Dis*, 2000;32:217-225
71 Pomimeno L, Capuano F, Marangi LC, Margiotta M, Lisowsky T, Ierardi E, Francavilla R, Francavilla A. The augmenter of liver regeneration induces mitochondrial gene expression in rat liver and enhances oxidative phosphorylation capacity of liver mitochondria. *Digest Liver Dis*, 2000;32:510-517
72 Yang XM, Xie L, Qiu ZH, Gong F, Wu ZZ, He FC. Cloning and expression of rat augmenter of liver regeneration. *Shengwu Huaxue Zazhi*, 1997;13:130-135
73 Wang AM, Yang XM, Guo RF, Yang YW, Li PJ, Wang QM, He FC. Protection of recombinant human augmenter of liver regeneration to experimental hepaticfibrosis in rats. *Zhonghua Yixue Zazhi*, 1998;78:707-708
74 Yang XM, Wang AM, Zhou P, Wang QM, Wu ZZ, He FC. Effects of augmenter of liver regeneration on liver proliferation and anti-injury. *Kexue Tongbao*, 1998;43:616-620
75 Howard M, O Garra A. Biological properties of interleukin 10. *Immunol Today*, 1992;13:198-200
76 Moore KW, Vieira P, Fiorentino DF, Trounstine ML, Khan TA, Mosmann TR. Homology of cytokine synthesis inhibitory factor (IL-10) to the Epstein-Barr virus gene BCRF1. *Science*, 1990; 248:1230-1234
77 Thompson K, Maltby J, Fallowfield J, McAulay M, Millward-Sadler H, Sheron N. Interleukin-10 expression and function in experimental murine liver inflammation and fibrosis. *Hepatology*, 1998;28:1597-1606
78 Louis H, Van Laethem JL, Wu W, Quertinmont E, Degraef C, Van den Berg K, Demols A, Goldman M, Le Moine O, Geerts A, Devière J. Interleukin-10 controls neutrophilic infiltration, hepatocyte proliferation, and liver fibrosis induced by carbon tetrachloride in mice. *Hepatology*, 1998;28:1607-1615
79 Wang SC, Ohata M, Schrum L, Rippe RA, Tsukamoto H. Expression of interleukin-10 by *in vitro* and *in vivo* activated hepatic stellate cells. *J Biol Chem*, 1998;273:302-308
80 Thompson KC, Trowern A, Fowell A, Marathe M, Haycock C, Arthur MJP, Sheron N. Primary rat and mouse hepatic stellate cells express the macrophage inhibitor cytokine interleukin-10 during the course of activation *in vitro*. *Hepatology*, 1998;28: 1518-1524
81 Rai RM, Loffreda S, Karp CL, Yang SQ, Lin HZ, Diehl AM. Kupffer cell depletion abolishes induction of interleukin-10 and permits sustained overexpression of tumor necrosis factor alpha messenger RNA in the regenerating rat liver. *Hepatology*, 1997;25:889-895
82 Meijer C, Wiezer MJ, Diehl AM, Yang SQ, Schouten HJ, Meijer S, van Rooijen N, van Lambalgen AA, Dijkstra CD, van Leeuwen PAM. Kupffer cell depletion by CI_2MDP-liposomes alters hepatic cytokine expression and delays liver regeneration after partial hepatectomy. *Liver*, 2000;20:66-77
83 Le Moine O, Marchant A, De Groote D, Azar C, Goldman M, Deviere J. Role of defective monocyte interleukin-10 release in tumor necrosis factor-alpha overproduction in alcoholic cirrhosis. *Hepatology*, 1995;22:1436-1439
84 Reitamo S, Remitz A, Tamai K, Uitto J. Interleukin-10 modulates type I collagen and matrix metalloprotease gene expression in cultured human skin fibroblasts. *J Clin Invest*, 1994;94:2489-2492
85 Lacraz S, Nicod LP, Chicheportiche R, Welgus HG, Dayer JM. IL-10 inhibits metalloproteinase and stimulates TIMP-1 production in human mononuclear phagocytes. *J Clin Invest*, 1995;96:2304-2310
86 Van Vlasselaer P, Borremans B, Van Gorp U, Dasch JR, De Waal-Malefyt R. Interleukin 10 inhibits transforming growth factor-β (TGF-β) synthesis required for osteogenic commitment of mouse bone marrow cells. *J CellBiol*, 1994;124:569-577
87 Ertel W, Keel M, Steckholzer U, Ungethüm U, Trentz O. Interleukin-10attenuates the release of proinflammatory cytokines but depresses splenocyte functions in murine endotoxemia. *Arch Surg*, 1996;131:51-56
88 Zou XM, Yagihashi A, Hirata K, Tsuruma T, Matsuno T, Tarumi K, Asanuma K, Watanabe N. Downregulation of cytokine-induced neutrophil chemoattractant and prolongation of rat liver allograft survival by interleukin-10. *Surg Today*, 1998;28:184-191
89 Louis H, Le Moine O, Peny MO, Quertinmont E, Fokan D, Goldman M, Deviere J. Production and role of interleukin-10 in concanavalin A-induced hepatitis in mice. *Hepatology*, 1997;25:1382-1389
90 Louis H, Le Moine A, Quertinmont E, Peny MO, Geerts A, Goldman M, Le Moine O, Deviere J. Repeated concanavalin A challenge in mice induces an interleukin 10-producing phenotype and liver fibrosis. *Hepatology*, 2000;31:381-390
91 Sherry B, Espinoza M, Manogue KR, Cerami A. Induction of the chemokine B peptides, MIP-1 and MIP-1α, by lipopolysaccharide is differentially regulated by immunomodulatory cytokines γ-IFN, IL-10, IL-4 and TGF-β. *Mol Med*, 1998;4:648-657
92 Tsukamoto H. Is interleukin-10 antifibrogenic in chronic liver injury. *Hepatology*, 1998;28:1707-1709
93 Nelson DR, Lauwers GY, Lau JYN, Davis GL. Interleukin 10 treatment reduces fibrosis in patients with chronic hepatitis C: a pilot trial of interferon nonresponders. *Gastroenterology*, 2000;118: 655-660
94 Yakoob J, Hu GL, Fan XG, Zhang Z. Telomere, telomerase and digestive cancer. *World J Gastroenterol*, 1999;5:334-337
95 Counter CM, Gupta J, Harley CB, Leber B, Bacchetti S. Telomerase activity in normal leukocytes and in hematologic malignancies. *Blood*, 1995;85:2315-2320
96 Urabe Y, Nouso K, Higashi T, Nakatsukasa H, Hino N, Ashida K, Kinugasa N, Yoshida K, Uematsu S, Tsuji T. Telomere length in human liver diseases. *Liver*, 1996;16:293-297
97 Miura N, Horikawa I, Nishimoto A, Ohmura H, Ito H, Hirohashi S, Shay JW, Oshimura M. Progressive telomere shortening and telomerase reactivation during hepatocellular carcinogenesis. *Cancer Genet Cytogenet*, 1997;93:56-62
98 Komine F, Shimojima M, Moriyama M, Amaki S, Uchida T, Arakawa Y. Telomerase activity of needle-biopsied liver samples: its usefulness for diagnosis and judgment of efficacy of treatment of small hepatocellular carcinoma. *J Hepatol*, 2000;32:235-241
99 Ogami M, Ikura Y, Nishiguchi S, Kuroki T, Ueda M, Sakurai M. Quantitative analysis and in situ localization of human telomerase RNA in chronic liver disease and hepatocellular carcinoma. *Lab Invest*, 1999;79:15-26
100 Kojima H, Yokosuka O, Kato N, Shiina S, Imazeki F, Saisho H, Shiratori Y, Omata M. Quantitative evaluation of telomerase activity in small liver tumors: analysis of ultrasonography-guided liver biopsy specimens. *J Hepatol*, 1999;31:514-520
101 Hytiroglou P, Kotoula V, Thung SN, Tsokos M, Fiel MI, Papadimitriou CS. Telomerase activity in precancerous hepatic nodules. *Cancer*, 1998;82:1831-1838
102 Bodnar AG, Ouellette M, Frolkis M, Holt SE, Chiu CP, Morin GB, Harley CB, Shay JW, Lichtsteiner S, Wright WE. Extension of life-span by introduction of telomerase into normal human cells. *Science*, 1998;279:349-352
103 Kiyono T, Foster SA, Koop JI, McDougall JK, Galloway DA, Klingelhutz AJ. Both Rb/$p16^{INK4a}$ inactivation and telomerase activity are required to immortalize human epithelial cells. *Nature*, 1998;396:84-88
104 Lee HW, Blasco MA, Gottlieb GJ, Horner JW, Greider CW, DePinho RA. Essential role of mouse telomerase in highly proliferative organs. *Nature*, 1998;392:569-574
105 Blasco MA, Lee HW, Hande MD, Samper E, Lansdorp PM, DePinho RA, Greider CW. Telomere shortening and tumor formation by mouse cells lacking telomerase RNA. *Cell*, 1997;91: 25-34
106 Rudolph KL, Chang S, Millard M, Schreiber-Agus N, DePinho RA. Inhibition of experimental liver cirrhosis in mice by telomerase gene delivery. *Science*, 2000;287:1253-1258
107 Hagmann M. New genetic tricks to rejuvenate ailing livers. *Science*, 2000;287:1185-1187

Edited by Ma JY

P.O.Box 2345 Beijing 100023, China
Fax. 0086·10·65891893 Tel. 0086·10·65897901
E-mail.wcjd@public.bta.net.cn www.wd.org.cn

World J Gastroentero, 2001 April; 7(1):9 - 15
World Journal of Gastroenterology
Copyright©2001 by the WJG Press ISSN 1007 - 9327

Original Articles

Inhibitory effect and mechanism of acarbose combined with gymnemic acid on maltose absorption in rat intestine

Hong Luo[1], Le Feng Wang[2], Toshiaki Imoto[1] and Yasutake Hiji[1]

Subject headings diabetes mellitus; maltose; gymnemic acid; alpha-glucosidases; intestinal mucosa; rats; nutrition

Luo H, Wang LF, Imoto T, Hiji Y. Inhibitory effect and mechanism of acarbose combined with gymnemic acid on maltose absorption in rat intestine. ***World J Gastroenterol***, 2001;7(1):9-15

Abstract

AIM To compare the combinative and individual effect of acarbose and gymnemic acid (GA) on maltose absorption and hydrolysis in small intestine to determine whether nutrient control in diabetic care can be improved by combination of them.

METHODS The absorption and hydrolysis of maltose were studied by cyclic perfusion of intestinal loops in situ and motility of the intestine was recorded with the intestinal ring *in vitro* using Wistar rats.

RESULTS The total inhibitory rate of maltose absorption was improved by the combination of GA (0.1g/L - 1.0g/L) and acarbose (0.1mmol/L - 2.0mmol/L) throughout their effective duration (P <0.05, U test of Mann-Whitney), although the improvement only could be seen at a low dosage during the first hour. With the combination, inhibitory duration of acarbose on maltose absorption was prolonged to 3 h and the inhibitory effect onset of GA was fastened to 15 min. GA suppressed the intestinal mobility with a good correlation (r = 0.98) to the inhibitory effect of GA on maltose absorption and the inhibitory effect of 2 mmol/L (high dose) acarbose on maltose hydrolysis was dual modulated by 1 g/L GA in vivo indicating that the combined effects involved the functional alteration of intestinal barriers.

CONCLUSION There are augmented effects of acarbose and GA,which involve pre-cellular and paracellular barriers. Diabetic care can be improved by employing the combination.

[1]Departments of Physiology, and [2]Internal Medicine, Faculty of Medicine, Tottori University, Yonago 683-0826, Japan
Supported by Grant for Promotion of Science from Tottori Bioscience Foundation (1997-1998), Japan and Japanese Government (Ministry of Education, Science and Culture of Japan, MONBUSHO) scholarship No. 933241 (1994-1999), Japan in part. Dr. Luo was supported by the scholarships.
Correspondence to: Dr. Hong Luo, Department of Physiology, the Institute of Basic Medicine, Chinese Academy of Medical Sciences and Peking Union Medical College, 5 Dongdansantiao Beijing 100005, China
Tel. 0086-10-65296463, Fax. 0086-10-67611572
Received 2000-05-12 **Accepted** 2000-06-23

INTRODUCTION

Hyperglycemia and hyperinsulinaemia are characters of non-insulin-dependent diabetes mellitus (NIDDM). Their interaction further impairs the action and secretion of insulin in NIDDM[1]. With the aim of reducing the possibility of developing long-term various complications such as microvascular disorder or neuropathy[2], a good diet regimen and control of nutrient entry are broadly accepted as basic treatment for diabetes mellitus.

Acarbose, an alpha-D-glycosidase inhibitor, was first extracted from the culture broths of actinomycetes by Puls and his colleagues in the 1970s, and was applied in clinical studies for more than 10 years[3-5]. It reversibly inhibits alpha-glycosidases that exist in the brush-border of the small intestinal mucosa[6]. Its efficacy has been reported as a potent inhibitory effect on sucrose hydrolysis, but a weak effect on the maltose. For instance, in humans, even if high doses of 300 mg of acarbose are orally used, there is little effect on the absorption of maltose[7] and no obvious effects on body weight have been observed in most studies possibly due to its short effective duration. During daytime, blood glucose levels were hardly decreased although the postprandial blood glucose amplitudes were reduced, that also due to its short effective duration[8]. In addition, there is no interaction with the intestinal Na^+/glucose- cotransporter[9], although an inhibitory effect on glucose absorption and an osmotic stimulus-mediating glucagon-like peptide-1 secretion has been reported[10,11].

Gymnemic acid (GA)[12], a mixture of triterpene glucuronides, which was found in the leaves of the Indian plant Gymnema sylvestre, not only inhibits glucose absorption in the small intestine[13], but also suppresses hyperglycemia and hyperinsulinaemia in an oral glucose tolerance test[14]. It is especially noteworthy that the body weight gain in fat rats is suppressed by GA treatment [15]. In an ordinary human diet, carbohydrates normally represent the quantitatively greatest part and are the primary source of energy. The typical diet contains far more starch than all other carbohydrates combined. More than 80% final products of intestinal carbohydrate digestion are glucose.

Maltose is a rather important product during starch hydrolysis. In this report, the combined effect of acarbose with GA on maltose absorption in

the rat small intestines is reported. The mechanism and application in perspective are discussed.

METHODS

Animals

Male 8 - 9 weeks old Wistar rats (body weight 300 g ± 25g) obtained from Shimizu (Kyoto), were housed in an air-conditioned room at 22℃ ± 2℃ with a natural lighting schedule for 1 to 3 weeks until the experiment began. They were fed with a standard pellet diet (Oriental Yeast CO., Tokyo) and tap water. Care and treatment of the experimental animals conformed to Tottori University guidelines for the ethical treatment of laboratory animals.

Perfusion of small intestine in vivo

A modified technique as elaborated by Yoshioka[13] was used in the small intestine perfusion experiment. Animals that had fasted overnight with free access to water were anesthetized by an intraperitoneal injection of 50 mg/kg body weight sodium pentobarbital (Dainabot, Osaka). After a catheter was inserted in the trachea, the abdominal cavity was opened. The small intestine of 30 cm length from the 2 cm caudal ward of Treitz's ligament was selected. Two L-shaped cannulae were inserted into each end of the intestine and connected with a peristaltic pump (SJ-1211H, Atto, Tokyo). After the abdominal cavity was closed, the intestinal loop was rinsed with Ringer's solution (145.4 mmol/L NaCl,5.4 mmol/L KCl, 1.8mmol/L $CaCl_2$ and 2.4 mmol/L $NaHCO_3$) for 60 min. Each chemical that was dissolved in Ringer's solution was continuously perfused through the intestine at a constant flow rate of 3 mL/min. The perfusing solution was adjusted to pH 7.5- pH 7.8 with NaOH and used at 37℃.

The animals were randomly grouped and exposed to 20 mL 10 mmol/L maltose (Sigma, ST. Louis) with or without GA (extracted by ourselves from Gymnema sylvestre) and acarbose (Bayer, Osaka) by cyclic perfusion through the loops for 1h (first perfusion), then 10 mmol/L maltose only was perfused for one hour again following an intestinal rinse with Ringer's solution for 30 min (second perfusion). To compare the combined and individual effective duration, 5 groups were chosen, in which the rinse time between the two perfusions was prolonged from 30 min to 60 min, 120 min and 180 min respectively. The perfusates at the first perfusion in the 5 groups were as follows: ① control group,10 mmol/L maltose; ② acarbose group, 2 mmol/L acarbose + 10 mmol/L maltose; ③ GAa2 group, 1 g/L GA + 2 mmol/L acarbose + 10 mmol/L maltose; ④ GAa 0.2 group, 1 g/L GAa + 0.2 mmol/L acarbose +10 mmol/L maltose; and ⑤ GA group, 1 g/L GA +10 mmol/L maltose.

Measurement of maltose absorption and hydrolysis

The samples (20 μL) from perfusion fluid were taken every 15 min during 1 h perfusion period, which were kept at 0℃ until next step to prevent the possibility of further hydrolysis. The maltose hydrolyzed by over dosage of alpha-glucosidase (Funacoshi, Tokyo) and glucose in sample was measured with the glucose-B-test-kit (Wako, Osaka)[16], and by the percentages of absorption and hydrolysis of maltose in perfusate were calculated.

Recording of isometric contraction of the intestinal rings

To explain the combined effect of acarbose and GA, the effect of GA on contraction of the intestinal smooth muscle was investigated *in vitro*. Fasted animals were sacrificed by stunning and exsanguinations. The intestines at the same position as the perfusion experiments were removed, cleaned of adhering fat and connective tissues in the serous membrane, and cut into transverse rings of 1cm wide. The rings were mounted on stainless steel hooks under 5 grams of resting tension and bathed in 25 mL organ bath at 37℃ in Locke's solution containing (mmol/L) NaCl: 154, KCl: 5.6, $CaCl_2$: 2.1, $NaHCO_3$: 2.4 and Glucose: 5.6, which was saturated with 95% O_2 and 5% CO_2. Tension was recorded isometrically using a force transducer (NEC Sanei, Tokyo) through its amplifier on an ink recorder (FBR-252A, TOA, Tokyo). Tissues were allowed to equilibrate at least 90min before the experiments begun. The rings were treated with GA and the alterations of auto-rhythmic contraction were recorded.

GA extraction

Dry Gymnema sylvestre leaves were obtained from Okinawa (Japan), from which GA was extracted with water, ethanol and diethyl carbonate by a slightly modified version of Imoto's method and freeze-dried into GA powder which was confirmed at 230 nm UV with a high-performance liquid chromatography (HPLC, Shimadzu SPD-6AV, Kyoto)[12].

Statistical and pharmacological analyses

Statistical analyses were performed with the *U* test of Mann-Whitney or ANOVA, which was indicated in the result when ANOVA was used, by StatView for a Macintosh computer. $P < 0.05$ was considered to be a significant difference.

The dose-response curves were analyzed by the least-squares fitting method using Cricket Graph for a Macintosh computer. The *r* (correlation coefficient) was tested with the limit table of *r*. If the value of *r* was under $P < 0.05$, the curve and function were accepted, from which the IC_{50} s (50% inhibitory concentrations) were calculated.

RESULTS

Dose-effect relationship and effective onset

The inhibitory effects of GA and acarbose, or both

of them, on 10 mmol/L maltose absorption obtained from the intestinal loop experiments *in situ* are illustrated in Figure 1 as a function of uptake time and compared at different doses of acarbose 0.2 mmol/L (Figure 1A) and 2 mmol/L (Figure 1B), respectively. Both agents inhibited maltose absorption significantly. The first point difference between the treated and control groups in maltose absorption was considered as the onset point of the inhibitory effect on maltose absorption. The duration from GA and/or acarbose perfused to that point was regarded as the onset time. The onset time was 30 min in the GA group and 15 min in both the acarbose and combining groups, in other words the longer onset time of GA was overcome by the combined. The inhibitory rates at 60 min were 50.7% ± 3.68% (1g/L GA), 51.72% ± 2.21% (0.2 mmol/L acarbose) and 68. 97% ± 2.71% (both of them), while at the high dose of acarbose they were increased to 80.68% ± 1.81% (2 mmol/L acarbose) and 72.27% ± 2.57% (both of them) indicating that the inhibitory effects were improved by the combination only in the lower doses during the first perfusion.

Time course of the inhibition

Time-effect curves of the GA and acarbose on absorption of maltose are shown in Figure 2. Even though the intestine was rinsed for 120 min, the altered maltose absorption remained at the inhibitory level in GA, GAa2 and GAa 0.2 groups. In the case of acarbose only application, the absorption returned to almost normal after 30 min rinsing ($P > 0.05$ *vs* control). The present results suggest that the short effective duration of acarbose be overcome by the combination. The peak effect appeared during the first perfusion in GAa2 and acarbose (2 mmol/L) groups and the second perfusion following rinse for 30 min in GAa0.2 and GA groups. The altered absorption of maltose was recovered in each group to the control level after 180 min rinse with Ringer's solution.

The IC_{50}

The acarbose dose dependently inhibited the absorption of maltose with IC_{50s} of 0.65 mmol/L, 0.27 mmol/L, 0. 22 mmol/L and 0.28 mmol/L ($r >$ or $= 0.99$) during 15 min, 30 min, 45 min and 60 min perfusion, respectively. The inhibitory effects were improved when combined with GA ($P < 0.001$ ANOVA). The IC_{50} s in an hour duration decreased to about 73% and 40% of acarbose with 0.1 g/L and 0.25 g/L GA, respectively. The inhibitory effects of GA ($IC_{50} = 0.85$g/L, $r = 0.99$) were also improved by lower doses of acarbose ($P < 0.001$ ANOVA) with IC_{50} s of 0.35 g/L (0.1 mmol/ L acarbose) and 0.04g/L (0.2 mmol/L acarbose) respectively.

Augment of GA and acarbose

The amount of total maltose absorbed during the two perfusions is compared in Figure 3. The first perfusion was performed for 1 h by 10mmol/L maltose containing GA and/or acarbose and the second was performed again for 1 h by 10 mmol/L maltose only, after rinsing for 30 min. The absorption of maltose during 1 h in control group was 42.2 mg and 43.0 mg in the first and second perfusions respectively, which had no significant difference. If the total absorbed maltose in control is taken as 100%, the relative maltose absorption was 64.2% ± 5.0% and 54.0% ± 7.3% in the 0.2 and 2 mmol/L acarbose groups respectively, which was further decreased to only 26.9% ± 2.9% and 31.0% ± 2.7% respectively by the combined 1 g/L GA. In GA (1g/L) group the relative maltose absorption was 38.1% ± 4.3% but still higher than that in combined groups ($P < 0.05$). These values implied that augmented inhibitory effects are highly revealed throughout effective duration in either combined group of GA and acarbose.

Modulation of the acarbose activity by GA

The percentages of maltose hydrolysis during perfusion maltose and acarbose with or without GA are shown in Figure 4A. It is noted that the inhibitory effect of 2 mmol/L acarbose on maltose hydrolysis was time-dependently decreased by combination with 1 g/L GA in the first perfusion. The hydrolysis of maltose in GAa2 group, which was similar to that in 0.2 mmol/L acarbose, was higher than that in 2 mmol/L acarbose group at 30 min ($P < 0.05$), 45 min and 60 min ($P < 0.$ 01) except that at 15 min. On the contrary, the hydrolysis of maltose in the GAa2 group was lower than that in 2 mmol/L acarbose group ($P < 0.05$) in the second perfusion after the intestine was washed out for 120 min (Figure 4B). The hydrolyses at 15 min, 30 min, 45 min and 60 min were 15.77% ± 0.89%, 29. 44% ± 0.18%, 45.18% ± 3.20% and 59.67% ± 5.86% in the former while 21.94% ± 1.36%, 45.38% ± 2.87%, 57.52% ± 1.69% and 73.14% ± 3.92% in the latter. No significant difference was observed in lower dosages of acarbose (0.2 mmol/L) with the presence or absence of GA.

Correlation of GA's inhibitory effects on absorption and mobility of the intestine

To explain mechanism of the combination, the effect of GA on auto-rhythmic contraction of the intestinal ring was recorded isometrically using a force transducer. Although the frequency of auto-rhythmic contraction was 17.2 ± 0.77 times per minute in the intestinal rings, and the tension induced by auto-rhythmic contraction was 1406.67 mg ± 565.33 mg under normal conditions, they were dose-dependently decreased when treated with GA (Figure 5A,B). The inhibitory effects of GA on the absorption of maltose and auto-rhythmic contractions of the ring in the small intestine had a good linear correlation ($r = 0.98$, Figure 5C).

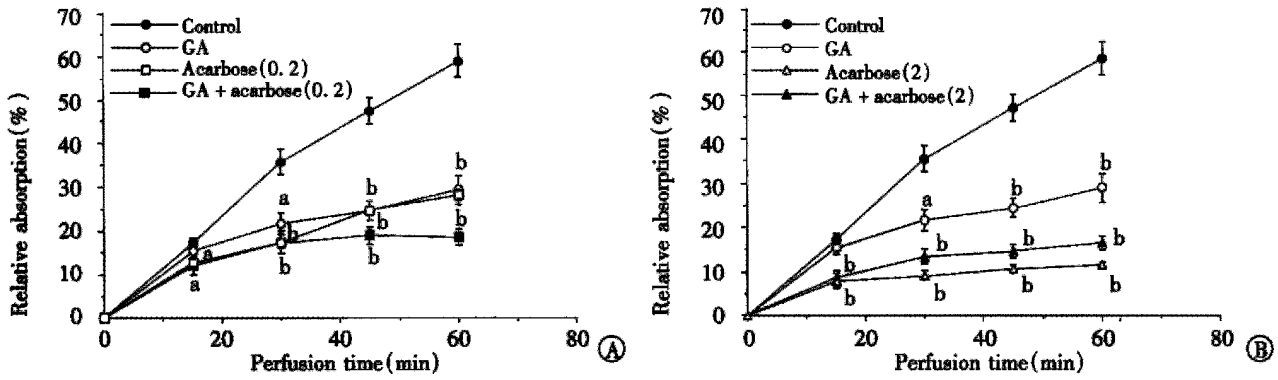

Figure 1 Inhibitory effect of GA and acarbose on maltose absorption. The intestinal loops *in situ* were perfused with 10 mmol/L maltose in the presence or absence of GA (1 g/L) and acarbose (mmol/L). The absorption of maltose is shown as percentage of maltose contained in the beginning of perfusion. Each point is expressed as mean ± SD of 5-10 determinations. ($^aP < 0.05$, $^bP < 0.01$)

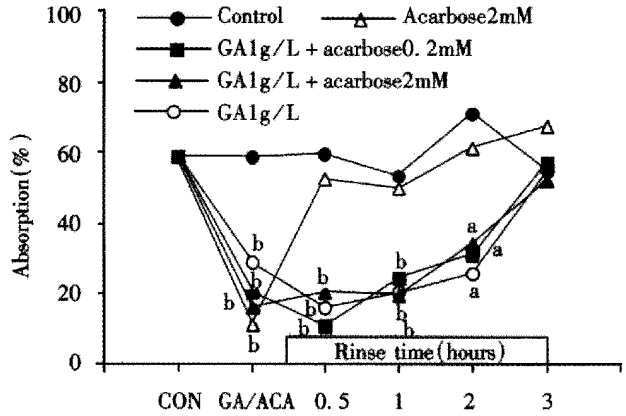

Figure 2 Alteration of maltose (10 mmol/L) absorption following application with GA and/or acarbose. Each point shows the maltose absorption during 60 min perfusion of 10 mmol/L maltose following rise with Ringer's solution after treatment of GA and/or acarbose (the second perfusion) except the points of "CON" or "GA/ACA" which shows the absorption during the first 1 hour perfusion with or without GA and acarbose (the first perfusion). The absorption of maltose is shown as percentage of maltose contained in the beginning of perfustion ($^aP < 0.05$, $^bP < 0.01$).

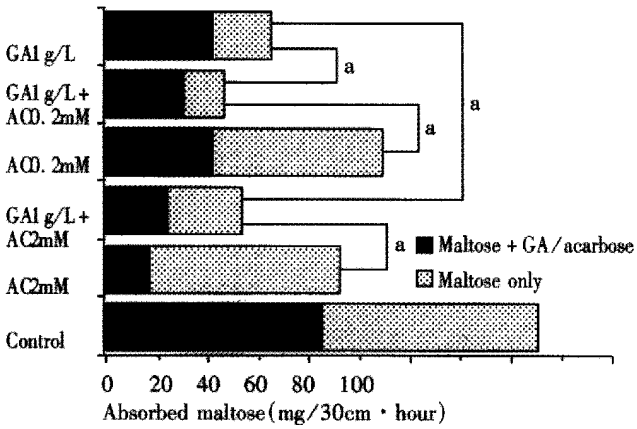

Figure 3 Maltose absorption during the two perfusions in the first 2.5 hours. Maltose+GA/acarbose: first perfusion, 10 mmol/L maltose containing GA and/or acarbose was perfused for 1 hour. Maltose only: after first perfusion the intestinal loops were rinsed for 30 min, then 10 mmol/L maltose only was perfused for 1 hour again. The absorbed maltose is shown as the absorption in each perfusion. There was significant difference between each treated group versus control. ($^aP < 0.05$, n = 5-10).

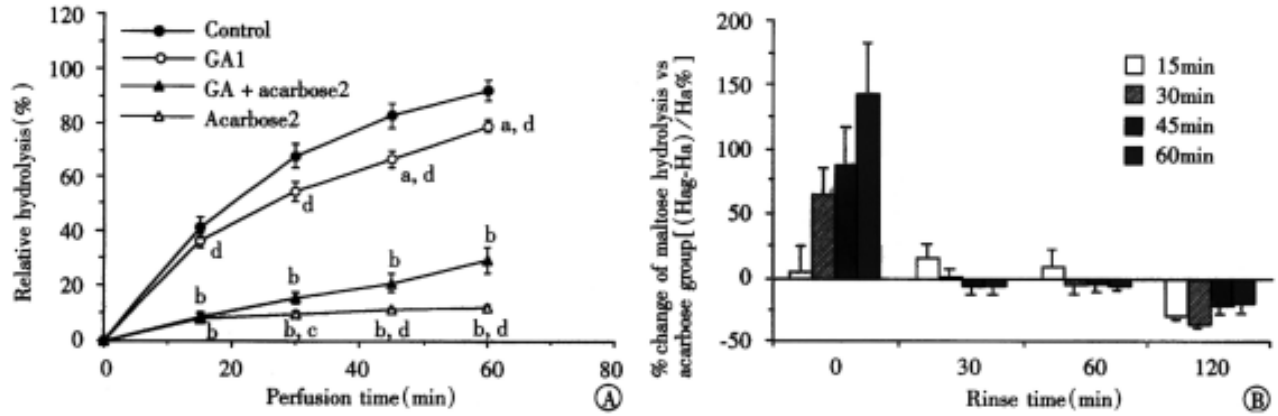

Figure 4 The dual effects of GA (1mg/mL) on the activity of acarbose during the first perfusion (A), maltose with GA and/or acarbose was presented in the perfusates. Maltose contained in the fluid at perfusion starting point was taken as 100%. $^aP < 0.05$ and $^bP < 0.01$ *vs* control; $^cP < 0.05$ and $^dP < 0.01$ *vs* GAa2. (n = 6-10) and second perfusion (B), the intestinal loops were rinsed for 30 min to 120 min, then 10 mmol/L maltose only was perfused for 1 h again. Each bar shows the percentage change of maltose hydrolysis (Hc%) in GAa2 group versus 2 mmol/L acarbose group in different perfusing times, which was calculated by the following equation: Hc% = (Hag-Ha)/Ha × 100%, where Hag and Ha represent, respectively, the hydrolyzed maltose in GAa2 group and in 2 mmol/L acarbose group. Hydrolysis of maltose in the acarbose group is believed as 100% (n = 3-10). A diminished effect in the beginning and improved effect in the end were observed.

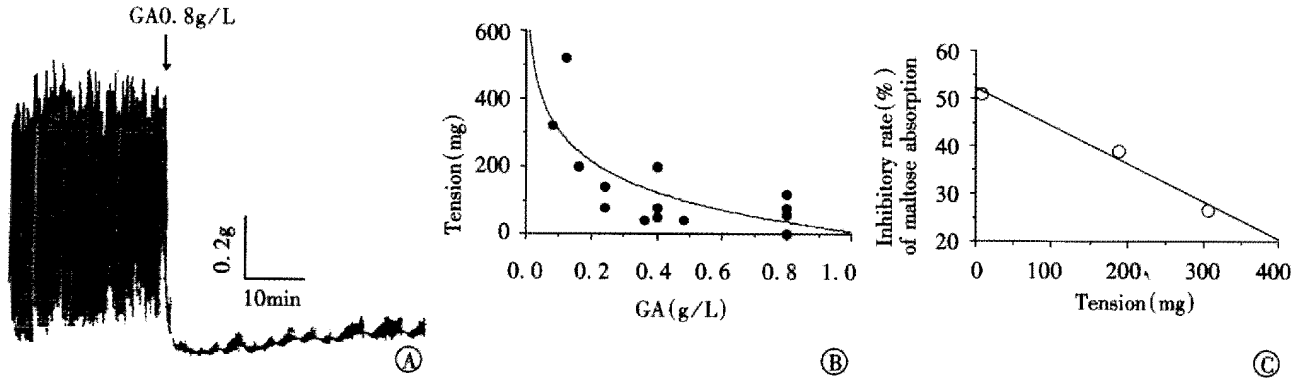

Figure 5 The relationship of GA's inhibitory effects on absorption of the maltose and on mobility of the intestinal ring. A, an example of the inhibitory effect of GA (0.8 g / L) on the intestinal auto-rhythmic contraction. B, dose-dependently inhibitory effect of GA on amplitude of the small intestinal rings which is expressed as the tension induced by the auto-rhythmic contraction in the present different doses of GA. C, correlation of GA's inhibitory effects on absorption of maltose and on tension of the intestinal ring. Each point comes from one dose of GA. The tension is calculated from the function of curve in the Figure B.

DISCUSSION

The combined effects of acarbose and GA are first reported in this paper. With the combination, inhibitory duration of acarbose was prolonged and onset time of GA was shortened, while the total inhibitory rate of maltose absorption was improved each other throughout their effective duration. Subsequently, a more effective reduction of postprandial hyperglycemia and hyperinsulinaemia could be expected by employing the combination in humans.

Acarbose is a pseudo-tetrasaccharide that is structurally similar to the typical oligosaccharides derived from starch digestion and can attach to the carbohydrate binding site of alpha-glycosidases in a competitive manner with a rank order of inhibitory potency of glucoamylase > sucrase > maltase > isomaltase. To alpha-amylase, acarbose has only a weak noncompetitive inhibitory effect[17]. In our experiment, the IC_{50} of acarbose for the 10 mmol/L (3.42 g/L) maltose absorption was 0.65 mmol/L during 15 min perfusion compared with a previous study of Krause *et al*, in which acarbose inhibits the absorption of maltose (1 g/L and 2 g/L) with IC_{50s} of 36 mg/L (0. 06 mmol/L) and 57 mg/L (0.09 mmol/L) respectively during 15 min in perfused loops[18]. The IC_{50s} and concentrations of maltose in the 3 points had a good semilog linear correlation (r = 0.94).

The inhibitory effects of GA on intestinal glucose absorption and oral glucose tolerance were first noticed in the 1980s[13,14], although there has been more than a century's history of treating diabetes mellitus with the leaves of Gymnema sylvestre in India [19-24]. Recently, various effects of GA including decreased body weight[15], improved hyperinsulinaemia[14] and inhibited glucose-stimulated gastric inhibitory peptide secretion[25] have been published. In a previous study in our laboratory[13], GA inhibited intestinal glucose absorption consistent with the present results, but with a difference in time (5 mmol/L glucose). Rinsed with Ringer's solution, the loops tended to recover their absorption of glucose. Those contrary results could be coming from the different effects of the unstirred layer and the tight junction on the absorption of maltose and lower concentration of glucose. In a recent study that we performed[26], GA inhibited the absorption of oleic acid and glucose (5 mmol/L) simultaneously with a time course same as the experiment of only 5 mmol/L glucose[13], which implies that the inhibitory effect of GA on the absorption of oleic acid has some relationship with the inhibitory effect of GA on glucose absorption.

Mechanism of the combination

The mechanisms for GA's actions have been considered as participating in the glucose receptor[25], Na^+/glucose cotransporter[13], ATPase[27] and insulin release[28]. In the present experiment, a new mechanism of GA's action was suggested concerned with an influence of the precellular and paracellular barriers of absorption in the intestinal brush borders.

Intestinal absorption of solute requires that the compound cross two barriers, the unstirred layer as an aqueous diffusion barrier, and epithelium which consist of enterocytes and paracellular factors[29-34]. Disaccharides are absorbed at a faster rate than monosaccharides *in vivo*, but inversely *in vitro* for the absorption of disaccharides coupled with the membrane digestion. Oligomers invariably appear in monomeric form at the serosal side of the epithelial cell or in the blood stream[35]. The concentration of glucose hydrolyzed from maltose (10 mmol/L) in the microenvironment of enterocytes and the tight junction is nearly 200 mmol/L-300 mmol/L with membrane

digestion[36], which is 10-15 times of that contained in the perfusate and is a power to drive absorption through paracellular pathway. If the tight junctions were narrowed or the membrane digestion was limited, the effect on the absorption of maltose would be more than that on the absorption of glucose.

"Membrane digestion" was defined by Ugolev and De-Laey[37] as that action of the cellular membranes on enzyme activities combined with the transport of their products of hydrolysis across membrane forms. The structural foundation of the model is presented as enterocytes projecting microvilli and the unstirred layer that is mainly formed by a glycocalyx entrapping water mixture with mucin from nearby goblet cells. Most of the disaccharidases produced by the enterocytes are binding with the membrane (under the unstirred layer) and a small amount of saliva and pancreatic amylase is in the glycocalyx. The maltose is hydrolyzed during it passes through the glycocalyx and enterocytes[38].

On the other hand, thickness of the unstirred layer (glycocalyx) largely depends on motility of the intestine, which becomes relatively thin when the intestine exhibits motility[29,37]. Suppressed by GA, the tension and intestinal auto-rhythmic contraction had un-negligible effects on unstirred layer not only, but also on the tight junction around the enterocytes. When the intestine relaxes, the paracellular pathways become narrow[36,39]. Consequently both hydrolysis and absorption could be inhibited by GA through pre-epithelium and epithelium barriers, in the latter containing transcellular (same as glucose) and paracellular factors (only for maltose or high concentration of glucose), that could be a main reason for the different time courses of GA on maltose and glucose.

It is another evidence altering the function of unstirred layer, that the activity of acarbose in the higher concentration (2 mmol/L) was decreased at the beginning and increased after rinsing by the combination with GA (Figure 4). The unstirred layer limits the diffusion of acarbose entering (at the beginning) and leaving (during rinse) the microenvironment nearest the membrane maltase resulting in the dual effects of GA on the activity of acarbose. It should be due to lower affinity[40] of acarbose with alpha-amylases, that the dual effects only appeared with higher concentration of acarbose. When the activity of alpha-amylases in the unstirred layer (glycocalyx) was inhibited, the glycocalyx digestion itself was decreased. With a combination of high concentration of acarbose and GA, the unstirred layer became thick enough to suppress the diffusion of acarbose. The glycocalyx is estimated to impede solute diffusion to the surface in a manner that is directly proportional to its solubility and inversely proportional to the square root of its molecular weight. The molecular weight of acarbose is nearly 2 times that of maltose, therefor in same condition the barrier of unstirred layer on acarbose is more effective than that on maltose. On the other hand, the solubility of GA (molecular weight about 800) was lower (about 10 g/L) than that of acarbose and maltose, which also is one of the reasons for GA's longer onset time (30 min).

The merits of combination

Tolerability should be considered when a drug is administered to a patient. Acarbose has contained in the drug list of diabetic management either type 1 or type 2 [5,40-46]. The most common adverse effect of acarbose is a gastrointestinal disturbance, which is induced by producing gas with fermentation of the unabsorbed carbohydrates in the bowel[17,43,47-50]. Acarbose has rarely been associated with systemic adverse effects, but in some case acute severe hepatotoxicity has been reported[3,51,52]. These adverse effects tend to increase with higher doses. GA not only improves the effect with a decrease in the IC_{50} of acarbose, but also inhibits the growth of anaerobia[53]. Bacterial overgrowth plays a role in the development of gastrointestinal symptoms[54], therefore the adverse effects of acarbose induced by fermentation are expected to be diminished by the combination of GA.

CONCLUSION

Acarbose inhibits maltose absorption through the inhibition of maltase under the unstirred layer and alpha-amylase in the unstirred layer. The latter is only involved at a higher dose (2 mmol/L) of acarbose. GA inhibits maltose absorption possibly by making the unstirred layer thicker and shutting the paracellular pathway, besides other reported mechanisms that are the same as glucose[13-15,25,27,28]. The effects of GA on maltose absorption and the combined effects of acarbose and GA are first reported in this paper. With the combination, the effective duration of acarbose is prolonged and the effective onset of GA is faster. Improvements in postprandial hyperglycemia, hyperinsulinaemia and insulin resistance, treatments of an overweight condition and diminishing of the adverse effects of acarbose in diabetic control by this combination are also in perspective.

REFERENCES

1 Higgins JA, Brand-Miller JC, Denyer GS. Development of insulin resistance in the rat is dependent on the rate of glucose absorption from the diet. *J Nutr*, 1996;126:596-602
2 Jennings PE. Oral antihyperglycaemics. Considerations in older patients with non-insulin-dependent diabetes mellitus. *Drugs Aging*, 1997;10:323-331
3 Coniff R, Krol A. Acarbose: a review of US clinical experience. *Clin Ther*, 1997;19:16-26
4 Scheen AJ. Clinical efficacy of acarbose in diabetes mellitus: a critical review of controlled trials. *Diabetes Metab*, 1998;24:311-320
5 Junger C, Rathmann W, Giani G. Prescribing behavior of primary care physicians in diabetes therapy: effect of drug budgeting. *Dtsch Med Wochenschr*, 2000;125:103-109
6 Clissold SP, Edwards C. Acarbose. A preliminary review of its pharmacodynamic

and pharmacokinetic properties, and therapeutic potential. *Drugs*, 1988;35:214-243
7 Hayakawa T, Kondo T, Okumura N, Nagai K, Shibata T, Kitagawa M. Enteroglucagon release in disaccharide malabsorption induced by intestinal alpha-glucosidase inhibition. *Am J Gastroenterol*, 1989;84:523-526
8 Herrmann BL, Schatz H, Pfeiffer A. Continuous blood glucose monitoring: the acute effect of acarbose on blood glucose variations. *Med Klin*, 1998;93:651-655
9 Bischoff H. Pharmacology of alpha-glucosidase inhibition. *Eur J Clin Invest*, 1994;24:3-10
10 Hirsh AJ, Yao SY, Young JD, Cheeseman CI. Inhibition of glucose absorption in the rat jejunum: a novel action of alpha-D-glucosidase inhibitors. *Gastroenterology*, 1997;113:205-211
11 Ranganath L, Morgan L. An osmotic stimulus-mediating glucagon-like peptide-1 (7-36 amide) (GLP-1) secretion in acarbose-induced sucrose malabsorption? *Nutrition*, 2000;16:64-65
12 Imoto T, Yamamoto FM, Miyasaka A, Hatano H. High-performance liquid chromatography-atmospheric pressure ionization mass spectrometry of gymnemic acids. *J Chromatogr*, 1991;557: 383-389
13 Yoshioka S. Inhibitory effects of gymnemic acid and an extract from the leaves of Zizyphus jujuba on glucose absorption in the rat small intestine. *J Yonago Med Assoc*, 1986;37:142-145
14 Hirata S, Abe T, Imoto T. Effects of crude gymnemic acid on the oral glucose tolerance test in the human being. *J Yonago Med Assoc*, 1992;43:392-396
15 Terasawa T, Miyoshi M, Imoto T. Effects of long-term administration of Gymnema sylvestre watery-extract on variations of body weight, plasma glucose, serum triglyceride, total cholesterol and insulin in Wistar fatty rats. *J Yonago Med Assoc*, 1994;34: 117-127
16 Barham D, Trinder P. An improved colour reagent for the determination of blood glucose by the oxidase system. *Analyst*, 1972; 97:142-145
17 Salvatore T, Giugliano D. Pharmacokinetic-pharmacodynamic relationships of Acarbose. *Clin Pharmacokinet*, 1996;30:94-106
18 Krause HP, Keup U, Puls W. Inhibition of disaccharide digestion in rat intestine by the alpha-glucosidase inhibitor acarbose (BAY g 5421). *Digestion*, 1982;23:232-238
19 Arai K, Ishima R, Morikawa S, Miyasawa A, Imoto T. Three-dimensional structure of gurmarin, a sweet taste-suppressing polypeptide. *J Biomol NMR*, 1995;5:297-305
20 Baskaran K, Kizar Ahamath B, Radha Shanmugasundaram K, Shanmugasundaram ER. Antidiabetic effect of a leaf extract from Gymnema sylvestre in non-insulin-dependent diabetes mellitus patients. *J Ethnopharmacol*, 1990;30:295-300
21 Shanmugasundaram ER, Rajeswari G, Baskaran K, Rajesh Kumar BR, Radha Shanmugasundaram K, Kizar Ahmath B. Use of Gymnema sylvestre leaf extract in the control of blood glucose in insulin-dependent diabetes mellitus. *J Ethnopharmacol*, 1990;30: 281-294
22 Shanmugasundaram ER, Gopinath KL, Radha Shanmugasundaram K, Rajendran VM. Possible regeneration of the islets of Langerhans in streptozotocin-diabetic rats given Gymnema sylvestre leaf extracts. *J Ethnopharmacol*, 1990;30:265-279
23 Okabayashi Y, Tani S, Fujisawa T, Koide M, Hasegawa H, Nakamura T, Fujii M, Otsuki M. Effect of Gymnema sylvestre, R.Br. on glucose homeostasis in rats. *Diabetes Res Clin Pract*, 1990;9:143-148
24 Dogar IA, Ali M, Yaqub M. Related Articles. Effect of Grewia asiatica, Gossypium herbacium and Gymnema sylvestre on blood glucose, cholesterol and triglycerides levels in normoglycaemic and alloxan diabetic rabbits. *J Pak Med Assoc*, 1988;38:289-295
25 Fushiki T, Kojima A, Imoto T, Inoue K, Sugimoto E. An extract of Gymnema sylvestre leaves and purified gymnemic acid inhibits glucose-stimulated gastric inhibitory peptide secretion in rats. *J Nutr*, 1992;122:2367-2373
26 Wang LF, Luo H, Miyoshi M, Imoto T, Hiji Y, Sasaki T. Inhibitory effect of gymnemic acid on intestinal absorption of oleic acid in rate. *Can J Physiol Pharmacol*, 1998;76: 1017-1023
27 Koch RB, Desaiah D, Cutkomp LK. Inhibition of ATPases by gymnemic acid. *Chem Biol Interact*, 1973;7:121-125
28 Persaud SJ, Al-Majed H, Raman A, Jones PM. Gymnema sylvestre stimulates insulin release *in vitro* by increased membrane permeability. *J Endocrinol*, 1999;163:207-212
29 Levitt MD, Fine C, Furne JK, Levitt DC. Use of maltose hydrolysis measurements to characterize the interaction between the aqueous diffusion barrier and the epithelium in the rat jejunum. *J Clin Invest*, 1996;97:2308-2315
30 Levitt MD, Strocchi A, Levitt DG. Human jejunal unstirred layer: evidence for extremely efficient luminal stirring. *Am J Physiol*, 1992;262:G593-G596
31 Thomson AB, Wild G. Adaptation of intestinal nutrient transport in health and disease. Part II. *Dig Dis Sci*, 1997;42:470-488
32 Thomson AB, Wild G. Adaptation of intestinal nutrient transport in health and disease. Part I. *Dig Dis Sci*, 1997;42:453-469
33 Teichberg S, Lifshitz F, Bayne MA, Fagundes-Neto U, Wapnir RA, McGarvey E. Disaccharide feedings enhance rat jejunal macromolecular absorption. *Pediatr Res*, 1983;17:381-389
34 Oliver RE, Jones AF, Rowland M. What surface of the intestinal epithelium is effectively available to permeating drugs. *J Pharm Sci*, 1998;87:634-639
35 Heitlinger LA, Sloan HR, DeVore DR, Lee PC, Lebenthal E, Duffey ME. Transport of glucose polymer-derived glucose by rabbit jejunum. *Gastroenterology*, 1992;102:443-447
36 Pappenheimer JR. On the coupling of membrane digestion with intestinalabsorption of sugars and amino acids. *Am J Physiol*, 1993;265:G409-G417
37 Ugolev AM, De Laey P. Membrane digestion. A concept of enzyme hydrolysis on cell membranes. *Biochim Biophys Acta*, 1973; 300:105-128
38 Moran ET. Digestion and absorption of carbohydrates in fowl and events through perinatal development. *J Nutr*, 1985;115:665-674
39 Luo H, Groot JA, van Leeuwen PA, Houdijk AP. Reduction of phorbol ester induced hyperpermeability by glutamine in HT-29CL. 19A intestine cells: the role of glutamate. *Gastroenterology*, 2000; 118(Suppl):A72
40 Hiele M. Georges Brohee Prize 1988-1989. Assimilation of nutritional carbohydrates: influence of hydrolysis. *Acta Gastroenterol Belg*, 1991;54:3-11
41 Riddle MC. Oral pharmacologic management of type 2 diabetes. *Am Fam Physician*, 1999;60:2613-2620
42 Mozersky RP. Pharmacologic management of diabetes mellitus. *J Am Osteopath Assoc*, 1999;99:S15-S19
43 Riccardi G, Giacco R, Parillo M, Turco S, Rivellese AA, Ventura MR, Contadini S, Marra G, Monteduro M, Santeusanio F, Brunetti P, Librenti MC, Pontiroli AE, Vedani P, Pozza G, Bergamini L, Bianchi C. Efficacy and safety of acarbose in the treatment of Type 1 diabetes mellitus: a placebo-controlled, double-blind, multicentre study. *Diabet Med*, 1999;16:228-232
44 Ozgen AG, Hamulu F, Bayraktar F, Cetinkalp S, Yilmaz C, Tuzun M, Kabalak T. Long-term treatment with acarbose for the treatment of reactive hypoglycemia. *Eat Weight Disord*, 1998;3:136-140
45 Juntti-Berggren L, Pigon J, Hellstrom P, Holst JJ, Efendic S. Influence of acarbose on post-prandial insulin requirements in patients with Type 1 diabetes. *Diabetes Nutr Metab*, 2000;13:7-12
46 Koch HH, Wudy A, Eberlein G, Quast C. Use of acarbose for eliminating the interval between meal consumption and insulin injection in patients with Type 1 diabetes. *Diabetes Nutr Metab*, 1999;12:195-201
47 Zarate A, Ochoa R, Hernandez M, Basurto L. Effectiveness of acarbose in the control of glucose tolerance worsening in pregnancy. *Ginecol Obstet Mex*, 2000;68:42-45
48 Balfour JA, McTavish D. Acarbose. An update of its pharmacology and therapeutic use in diabetes mellitus. *Drugs*, 1993;46:1025-1054
49 Kelley DE, Bidot P, Freedman Z, Haag B, Podlecki D, Rendell M, Schimel D, Weiss S, Taylor T, Krol A, Magner J. Efficacy and safety of acarbose in insulin-treated patients with type 2 diabetes. *Diabetes Care*, 1998;21:2056-2061
50 Kentrup H, Bongers H, Spengler M, Kusenbach G, Skopnik H. Efficacy and safety of acarbose in patients with cystic fibrosis and impaired glucose tolerance. *Eur J Pediatr*, 1999;158:455-459
51 Carrascosa M, Pascual F, Aresti S. Acarbose-induced acute severe hepatotoxicity. *Lancet*, 1997;349:698-699
52 Mennecier D, Zafrani ES, Dhumeaux D, Mallat A. Acarbose-induced acute hepatitis. *Gastroenterol Clin Biol*, 1999;23:1398-1399
53 Miyoshi M, Imoto T, Kasagi T. Antieurodontric effect of various fractions extracted from the leaves of gymnema sylvestre. *J YonagoMed Assoc*, 1987;38:127-137
54 Zheng JJ, Zhu XS, Wang YM. Breath hydrogen determination in patients following partial gastrectomy. *World J Gastroenterol*, 1998;4(Suppl 2):49-52

Edited by You DY and Ma JY

P.O.Box 2345 Beijing 100023, China
Fax. 0086·10·65891893 Tel. 0086·10·65897901
E-mail.wcjd@public.bta.net.cn www.wd.org.cn

World J Gastroentero 2001 April; 7(1):16 - 21
World Journal of Gastroenterology
Copyright©2001 by the WJG Press ISSN 1007 - 9327

The development of colon innervation in trisomy 16 mice and Hirschsprungs disease

Ji Cheng Li[1], Kai Hong Mi[1], Ji Lin Zhou[1], LC Busch[2] and W Kuhnel[2]

Subject headings Hirschsprungs disease;colon; down syndrome; immunohistochemistry; nervous system; trisomy 16 mouse

Li JC, Mi KH, Zhou JL, Busch LC, Kuhnel W. The development of colon innervation in trisomy 16 mice and Hirschsprung s disease. ***World J Gastroenterol***, 2001;7(1):16-21

Abstract

AIM To study the colon innervation of trisomy 16 mouse, an animal model for Down's syndrome, and the expression of protein gene product 9.5 (PGP 9.5) in the stenosed segment of colon in Hirschsprungs disease (HD).

METHODS Trisomy 16 mouse breeding; cytogenetic analysis of trisomy 16 mice;and PG P9.5 immunohistochemistry of colons of trisomy 16 mice and HD were carried out.

RESULTS Compared with their normal littermates, the nervous system of colon in trisomy 16 mice was abnormally developed. There existed developmental delay of muscular plexuses of colon, no submucosal plexus was found in the colon, and there was 5 mm aganglionic bowel aparting from the anus in trisomy 16 mice. The mesentery nerve fibers were as well developed as shown in their normal littermates. Abundant proliferation of PGP 9.5 positive nerve fibers was evealed in the stenosed segment of HD colon.

CONCLUSION Trisomy 16 mice could serve as an animal model for Hirschsprung's disease for aganglionic bowel in the distal part of colon. Abundant proliferation of PGP 9.5 positive fibers resulted from extrinsic nerve compensation, since no ganglionic cells were observed in the stenosed segment of the colon in HD. HD has a genetic tendency.

[1]Department of Lymphology, Department of Histology and Embryology, Zhejiang University Medical School, Hangzhou 310031, China
[2]Institute of Antomy, Medical University of Lubeck, Germany
Dr. Ji Cheng Li, graduated from Zhejiang Medical University in 1983, now professor of histology and embryology, engaged in the research of Hirschsprung's disease, having 50 papers published.
Project supported by the Grants of Analysis and Measurement of Zhejiang Province and Education Committee of Zhejiang Province.
Correspondence to: Dr. Ji Cheng Li, Department of Lymphology, Department of Histology and Embryology, Zhejiang University Medical School, Hangzhou 310031, Zhejiang Province, China
Tel. 0086-571-7217139, Fax. 0086-571-8855930
Email. lijc@mail.hz.zj.cn
Received 2000-09-02 **Accepted** 2000-10-22

INTRODUCTION

The most significant pathophysiological change of Hirschsprung's disease is its characteristic abnormal enteric nervous development of colon which resulted in the regional enterospasm and narrowed lumen, loss of intestinal peristalsis and relaxing reflex of the internal enteric sphincter[1]. The physiological peristalsis of the proximal gut pushes the intestinal contents forward, leading to the second megacolon in the proximal part of the narrowed gut. Since the cause of HD is still unknown and the experiment on humans is impossible, we used protein gene product 9.5 to study the enteric nerve development of colon in trisomy 16 mice, an animal model for Down's syndrome[2,3], and the innervation of stenosed segment of the colon in HD so as to reveal the possibility of developing the congenital megacolon in trisomy 16 mice and the genetic tendency of HD in human[4-7].

MATERIALS AND METHODS

Animal stocks and breeding[8-10]

Trisomy 16 mouse embryos examined in this study were produced by crossing NMRI-female mice provided by the Experimental Center of Medical University of Lubeck, with male mice carrying the two Robertsonian (Rb) translocation chromosomes Rb (16,17) 8Lubt^{wLub3} perpendicularly and Rb (11,16)2H. The day on which a vaginal plug was observed was considered to be the first embryonic day (ED).

Cytogenetic analysis

The pregnant female mice were sacrificed one hour after intraperitoneal injection of colchicine (0.02 mg/25-35 mg body weight) by dislocation of the neck. The embryos were collected by laparatomy. Small samples of liver were taken from each embryo for direct preparation of karyotypes, by using the standard technique of hypotonic treatment with 0.563% KCl and methanol : acetic acid fixation (3 : 1). Air-dried slides were observed under light microscope. Accurate ascertainment of trisomy 16 was provided by the demonstration of two Rb metecentric chromosomes and a count of 41 chromosome arms. After the defrimy of the chromosomal status, the trisomic and the normal euploid embryos of each litter could be separated (Figure 1).

Immunohistochemical methods[11]

The guts were taken from trisomy 16 embryos and

normal littermates, and fixed in a solution containing 4% paraformaldehyde and 2% picric acid in phosphate-buffered saline (PBS) for approximately 2 hours at room temperature. Fifteen pieces of narrowed HD guts were obtained from the patients aged between 18 months and 9 years. Six segments of normal colons served as controls. The diagnosis of HD was based on the case history, clinical manifestations, examination of barium enema and pressure measurement of rectum and anal. All the cases were confirmed postoperatively by pathological examinations.

Whole mount preparations of the gut were dissected out under stereomicroscopic control[12-14], and freezing sections were made at a thickness of 12 μm, then washed in 0.01 M PBS and 50% ethanol for 2 hours at room temperature. For immunohistochemistry, peroxidase-anti-peroxidase (PAP) was used in the present experiment.

The specimens were treated with 10% normal goat serum (Dakopatts × 907) for 30 min, then incubated in a primary antiserum protein gene product 9.5 (PGP 9.5) (Ultraclone RA 95101, UK) overnight at room temperature, diluted to 1 : 400 in a solution containing 10% normal goat serum, 0.01% sodium azide and 0.05% thimerosal in PBS. After three washes in PBS for 30 min, the specimens were incubated in goat anti-rabbit IgG (Dakopatts Z421) overnight at room temperature as the secondary antiserum, and diluted to 1 : 100 in the above solution. The specimens were then exposed in rabbit PAP (rabbit antibody to horseradish peroxidase and horseradish peroxidase) overnight at room temperature and diluted to 1 : 100 in a solution containing 0.1% bovine serum albumin and 0.05% thimerosal in PBS pH 7.4. 4 Cl1-naphtol or DAB was used as the chromogen for the peroxidase reaction. Control included the omission of the primary antiserum. PGP 9.5 is a cytoplastic protein composed of 212 amino acids with molecular weight of 2.45 kb. This protein only exists in the neurons and neuroendocrine cells. PGP 9.5 is a specific protein with an excellent localizing function for the neurons[15-19].

RESULTS

Development of trisomy 16 mice and their normal littermates

Owing to the abnormality of their chromosomes, the trisomy 16 mice were characterized by their small size, generalized edema and a failure of closed eyelids after embryonic day 16 (ED 16). Both the small size and lid-gap defect were attributed to the generalized growth retardation and developmental delay, leading death at the time of birth in most mice. The trisomy 16 mice in the present study were chosen from the gestational age between ED13 and ED 18. The survival rate of the trisomy 16 mice was lower with the gestational age. The lowest survival rate of trisomy 16 mice was observed at the time of their birth (Figure 2).

Development of colon innervation in trisomy 16 mice and their normal littermates

The nerve development of colon in normal littermates is a continuous process. Based on the morphology and staining degree of the PGP 9.5 positive reactions, the nerve development of colon could be divided into three stages: primary stage (ED14), juvenile stage (ED15 and ED16) and mature stage (ED17 and ED18). At ED14, scantly-distributed PGP 9.5 positive neurons were observed with light staining and round nucleus in the center of the neurons. At ED15, the distribution density of neurons increased greatly with some nervous processes, through which the neurons were connected with each other (Figure 3A). At ED16, muscular plexuses appeared with gathered neurons to form the light-stained ganglion. But the number of neurons in the ganglion was less and sparely arranged. At ED17 and ED18, the precursor cells of muscular plexuses migrated into the submucosal layer to form submucosal plexuses. The arrangement of nervous fibers in submucosal plexus was irregular, accompanied by some small-sized and sparely-distributed ganglions, while muscular plexuses were composed of primary, secondary and tertiary strands displaying a nerve meshwork with regular wide meshes and numerous large ganglia. The muscular and submucosal plexuses were further developed with much stronger PGP 9.5 staining at ED18 (Figure 4A). The increasing number of large-sized ganglions was observed with stronger immunostaining and arranged along the primary nerve strands. Numerous fine nerve strands in the gut villi were observed at ED18 (Figure 5).

When compared with the normal littermates, the developmental delay of the colon- innervation was observed in trisomy 16 mice. Some neurons appeared with a scattered distribution and light staining at ED15 (Figure 3B) and the neurons were found with some nerve processes by which irregular nervous meshwork formed at ED16. In the colon of trisomy 16 mice at ED17 and ED 18, only one plexus was visible, i.e., the myenteric plexus with a few small-sized ganglions (Figure 4B). From ED14 to ED18 there was no submucosal layer in colon, and 5mm aganglionic bowel was found at the distal end of the colon in trisomy 16 mice (Figure 6), which was revealed as a characteristic morphological evidence of the development of congenital megacolon in trisomy 16 mice. This important finding was constantly verified in all the experimental trisomy 16 mice.

The exogenous innervation of colon in trisomy 16 mice and their littermates

As early as ED14, PGP 9.5 positive nerve fibers occurred in the mesentery of both trisomy 16 mice and their normal littermates, which gradually

increased with the embryonic development. At ED17 and ED18, rich mesenteric nerve fibers were detected. In all whole mounts of PGP 9.5 nerve fibers in mesentery, they were observed regularly running in parallel and close to the blood vessels and innervated the colon in both trisomy 16 mice and their normal littermates (Figure 7). Thus, the arcades of the mesenteric vessels were clearly delineated by their immunostained perivascular plexuses.

The distribution of PGP 9.5 positive nerve fibers in the stenosed segment of HD and normal colons

The ganglions of the muscular plexus and submucosal plexus from the normal colon all revealed highly positive reaction to PGP 9.5 (Figure 8). The number of ganglion in muscular plexus was greater than that in the submucosal ones. The neurons presented a dark brown color and gathered as a mass. The adjacent neurons extended processes, by which they were connected with each other. PGP 9.5 positive nerve fibers were distributed in all intestinal layers. The richest part was in the circular muscular layer and parallel to the muscular fibers. In the proper mucous membrane, nerve network was formed around the intestinal glands. In the submucosal layer, the nerve fibers were arranged around the vessels. But in the stenosed segment of HD colon, no ganglionic cell was observed in the muscular and submucosal plexuses. At the distal end of the stenosed segment of the colon, no nerve plexus was found. Occasionally, a few neurons existed, but with abnormal morphology, while PGP9.5 positive nerve fibers were great in number in all intestinal layers. Big, strong, disordered and even twisted nerve tracts could be observed (Figure 9). Such disorderly arranged nerve fibers could also be found in the submucosal layer and proper mucous membrane layer of the colon. Some of the proliferated fibers were twisted along the vessels.

Table 1 The development of the colon and mensenteric innervation of trisomy 16 mice and their normal littermates in chronological sequence

	ED13		ED14		ED15		ED16		ED17		ED18	
	N	T	N	T	N	T	N	T	N	T	N	T
PM	-	-	+	-	++	+	++	+	+++	++	+++	++
PS	-	-	-	-	-	-	+	-	++	-	+++	-
MF	-	-	+	+	++	++	+++	+++	+++	+++	+++	+++

N: normal littermates; T: trisomy 16 mice.
PM: myenteric plexus; PS: submucosal plexus; MF: mesentery nervour fiber
-: no neurons and immunoreactive nerve fibers detected;
+: a few scattering neurons and no enteric plexus or sparse immunoreactive fibers detected;
+: lowly developed enteric plexus or moderate immunoreactive fibers detected;
+++: moderately developed enteric plexus or abundant immunoreactive fibers detected;
++++: fully developed enteric plexus or very abundant immunoreactive fibers detected.

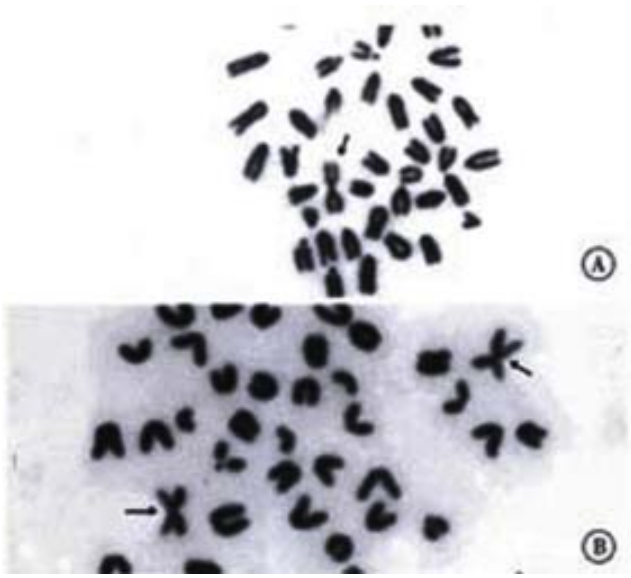

Figure 1 a. The chromosome of normal mice. b. The chromosome of trisomy 16 mice: two Rb metecentric chromosomes (↑) and 41 chromosome arms. × 1000

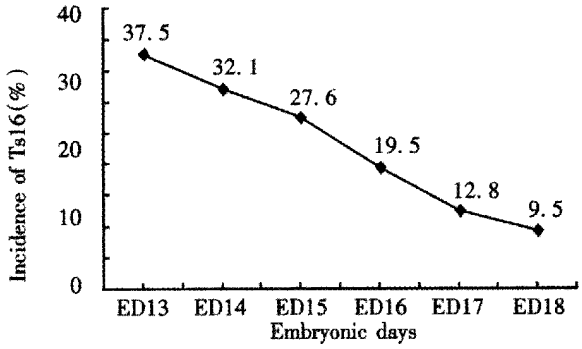

Figure 2 The survival rate of trisomy 16 mice with different embryonic days (ED).

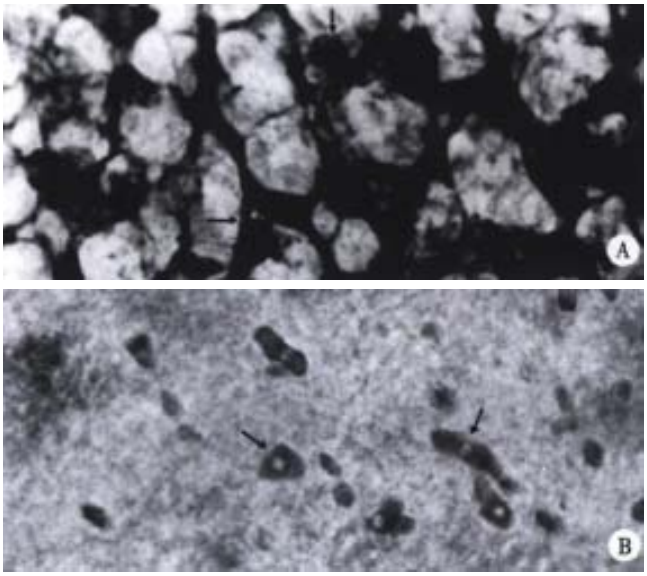

Figure 3 a. Myenteric plexus of normal littermates at ED 15. The nerve meshworks had regular meshes with many neurons (↑). × 400 b. The colon of trisomy 16 mice contained some neurons (arrow) with different staining and size at ED15. × 400

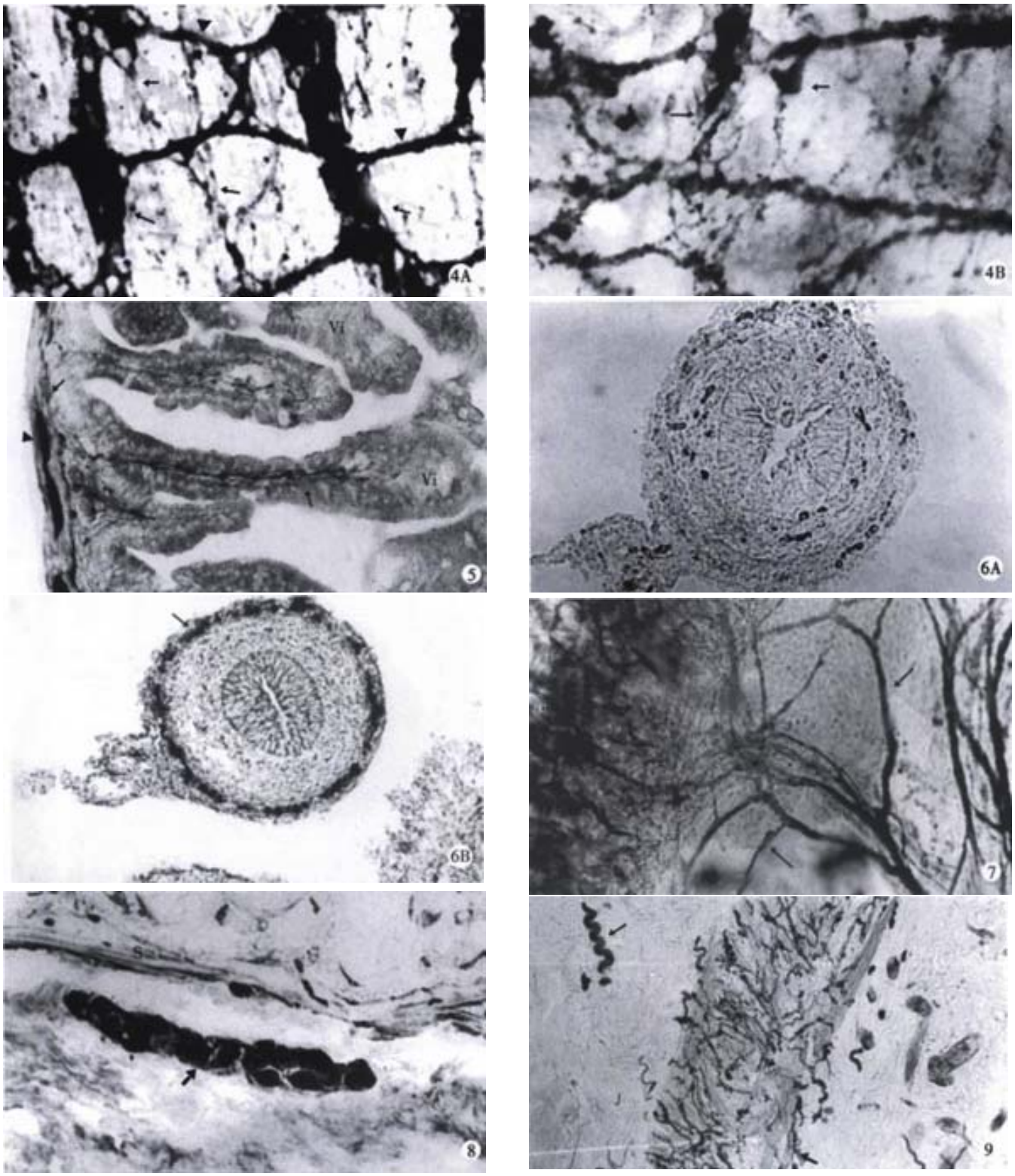

Figure 4 At ED 18, the myenteric plexuses of trisomy 16 mice and their normal littermates in whole mount preparation. × 250
A. The developed myenteric plexus with primary (long arrow), secondary (arrow) and tertiary (arrowhead) strands were displayed in the colon of normal littermates. The primary strands were composed of broad fiber bundles and numerous ganglia with longitudinally arranged meshes. B. The myenteric plexus of trisomy 16mice was poor with less ganglia containing some neurons (arrow) at different staining.

Figure 5 At ED 18, the nerve fibers (long arrow) stretching from the enteric plexuses reached the gut villi (Vi). The myenteric (arrowhead) and submucosal (arrow) plexuses were clear. × 160

Figure 6 Aganglionic segment of trisomy 16 mouse colon. × 160 B. The colon of normal littermate with ganglia (arrow). × 100

Figure 7 The myenteric nervous fibers (arrow) were detected in the colon (C) mesentery of trisomy 16 mice. × 160

Figure 8 The submucosal ganglia (arrow) of normal colon of human. S: submucosal muscular layer. × 100

Figure 9 The aganglionic colon of Hirschprung's disease. Abundant proliferation of nerve fibers (large arrow) was found in the stenosed segment of colon. A wave-like nerve fiber (arrow). × 100

DISCUSSION

The incidence of HD is 1/5000 due to the developmental defect of enteric nervous system[20-23]. Recently, HD incidence is increasing, especially the genetic HD and Down's syndrome with congenital megacolon[24-29], which greatly aroused researchers' interest in investigating the causes. The present study was based on PGP 9.5 as primary antibody to reveal the innervation of the narrowed gut in HD and the nerve development of the colon in trisomy 16 mice.

Enough evidences have been obtained from this study that trisomy 16 mice had a significant anomaly and developmental delay in colon innervation as well as 5 mm aganglionic colon at the distal end, which was the result of the chromosome abnormality. Our present experiment, found that there was a chronological sequence in the nerve development and a clear link between the gestational age and the morphological development in colon innervation of trisomy 16 mice and their normal littermates (Table 1). At ED 14, the precursor cells of ectoderm migrated into the gut along the course of the vagus nerves; at ED 15, nerve processes were observed in the neuron migrated gut; at ED 16, the muscular plexuses and ganglions appeared in the gut; at ED17, the precursor cells in muscular layer migrated into the submucosal layer and developed into submucosal nervous plexuses; at ED 18, the relatively matured muscular and submucosal plexuses occurred, the former controls the intestinal peristalsis, and the latter manages the intestinal secretions and absorption[30, 31]. The lack of submucosal nerve plexuses of trisomy 16 mice accounted for the lower material absorption and poor intestinal secretions while the distal aganglionic colon could result in the neurotrophic and innervating disorders. It is now recognized that the intestinal nerve development begins from the cephalic part to the caudal end[32-41]. But HD was due to the stagnated development of the precursor cells. The earlier the stagnation of the precursor cells, the longer the aganglionic bowel. Since colon is the last segment of gut for the precursor cells to migrate into, colon is most likely to develop HD. The aganglionic colon in trisomy 16 mice strongly confirmed the above findings. The euchromosome 16 of trisomy 16 mice has the same sequence as the 21q22 genes of human euchromosome 21[8]. It is often used as an animal model for Down's syndrome. Besides, trisomy 16 mice have constant genetic tendency and aganglionic colon, being easy to develop congenital megacolon. Epstein and associates believed that the intestinal innervation was composed of intrinsic and extrinsic ones[42]. The well-developed mesenteric nervous system of trisomy 16 mice could be regarded as a compensation for the intrinsic nerves. When there were no ganglionic cells in the intestine, the extrinsic nerve fibers would proliferate greatly. In our experiment, considerable PGP9.5 positive nerve fibers were verified in the stenosed HD colon, which was obviously the compensative nerve proliferation to the innervation of aganglionic HD colon. Since trisomy 16 mice had severe cardiovascular abnormalities, multi-organ deformities[43-45] and could hardly survive after delivery, so in the present study, the distal colon end of trisomy 16 mice showed no such extrinsic compensating nerve proliferations.

Among all clinically verified HD cases, 20% were caused by the lack of genetic factors[46]. Trisomy 16 mice, with its constant chromosome abnormality, is a reliable animal model for studying the genetic tendency of HD. The regional microcircumstance was closely related to the changes of the genetic inheritance. Tennyson and associates have found two striking abnormalities, i.e., an overgrowth of the muscularis mucosa, particularly in the outer longitudinal layer and an extensive thickening of the basal lamina around smooth muscle cell.

These excessive accumulation of basal lamina material and muscularis mucosa interfered with normal migration of precursor cells[47-51]. Payette and associates [52] thought that the excessive accumulation of components of basal lamina material in the aganglionic region of the lethal spotted mutant mouse stopped precursor cells from migrating into the terminal bowel of lethal spotted mutant mice. Our study revealed that 5mm aganglionic bowel in length aparting from anus in trisomy 16 mice, might be caused by the change of regional micro-circumstance due to the abnormal chromosome, finally resulting in the nerve defect.

REFERENCES

1 Li JC, Mi KH, Busch LC, Liu WG, Kühnel W. The expression of protein gene product 9.5 in trisomy 16 mouse colon and Hirschsprung's disease. *Zhongguo Bingli Shengli Zazhi*, 1999;15: 1030-1033

2 Miyabara S. Animal model for congenital anomalies induced by chromosome aberrations. *Cong Anom*, 1990;30:49-68

3 Epstein CJ, Cox DR, Epstein LB. Mouse trisomy 16: an animal model of humantrisomy 21 (Down syndrome). *Ann New York Acad Sci*, 1985;450:157-168

4 Romeo G, Ronchetto P, Luo Y, Barone V, Seri M, Ceccherini I, Pasini B, Bocciardi R, Lerone M, Kääriäinen H, Martucciello G. Point mutations affecting the tyrosine kinase domain of the RET proto-oncogene in Hirschsprung's disease. *Nature*, 1994;367:377-378

5 Pelet A, Attie T, Goulet O, Eng C, Ponder BAJ, Munnich A, Lyonnet S. De-novo mutations of the RET proto-oncogene in Hirschsprung's disease. *Lancet*, 1994;344:1769-1770

6 Martucciello G, Favre A, Takahashi M, Jasonni V. Immunohistochemical localization of RET protein in Hirschsprung's disease. *J Pediatr Surg*,1995;30:433-436

7 Edery P, Lyonnet S, Mulligan LM, Pelet A, Dow E, Abel L, Holder S, Nihoul-Fekete C, Ponder BA, Munnich A. Mutations of the RET proto-oncogene in Hirschsprung's disease. *Nature*, 1994; 367:378-380

8 Cox DR, Epstein CJ. Comparative gene mapping of human chromosome 21 and mouse chromosome 16. *Ann New York Acad Sci*, 1985;450:169-177

9 Holtzman DM, Kayney RM, Li YW, Khosrovi H, Berger CN, Epstein CJ, Mobley WC. Dysregulation of gene expression in mouse trisomy 16, an animal model of Down syndrom. *EMBO J*, 1992;11:619-627

10 Miyabara S, Gropp A, Winking H. Trisomy 16 in the mouse fetus associated with generalized edema and cardiovascular and urinary tract anomalies. *Teratology*, 1982;25:369-380

11 Krammer HJ, Karahan ST, Sigge W, K1hnel W.

Immunohistochemistry of markers of the enteric nervous system in whole-mount preparations of the human colon. *Eur J Pediatr Surg*, 1994;4:274-278
12 Wedel T, Roblick U, Gleiss J, Schiedeck T, Bruch HP, Kuhnel W, Krammer HJ. Organization of the enteric nervous system in the human colon demonstrated by wholemount immunohistochemistry with special reference to the submucous plexus. *Anat Anz*, 1999;181:327-337
13 Wedel T, Krammer HJ, Kuhnel W, Sigge W. Alterations of the enteric nervous system in neonatal necrotizing enterocolitis revealed by whole-mount immunohistochemistry. *Pediatr Pathol Lab Med*, 1998;18:57-70
14 Watanabe Y, Ito F, Ando H, Seo T, Kaneko K, Harada T, Iino S. Morphological investigation of the enteric nervous system in Hirschsprung's disease and hypoganglionosis using whole-mount colon preparation. *J Pediatr Surg*, 1999;34:445-449
15 Krammer HJ, Meier-Ruge W, Sigge W, Eggers R, Kühnel W. Histopathological features of neuronal intestinal dysplasia of the plexus submucosus in whole mounts revealed by immunohistochemistry for PGP 9.5. *Eur J Pediatr Surg*, 1994;4:358-361
16 Jackson P, Thomson VM, Thompson RJ. A comparison of the evolutionary distribution of the two neuroendocrine markers, neurone-specific enolase and protein gene product 9.5. *J Neurochem*, 1985;45:185-190
17 Thompson RJ, Doran JF, Jackson P, Dhillon AP, Rode J. PGP 9.5-a new marker for vertebrate neurons and neuroendocrine cells. *BrainRes*, 1983;278:224-228
18 Wilson PO, Barber PC, Hamid QA, Power BF, Dhillon AP, Rode J, Day IN, Thompson RJ, Polak JM. The immunolocalization of protein gene product 9.5 using rabbit polyclonal and mouse monoclonal antibodies. *Br J Exp Pathol*, 1988;69:91-104
19 Doran JF, Jackson P, Kynoch PA, Thompson RJ. Isolation of PGP 9.5, a new human neurone-specific protein detected by high resolution two-dimensional electrophoresis. *J Neurochem*, 1983; 40:1542-1547
20 Kato H, Yamamoto T, Yamamoto H, Ohi R, So N, Iwasaki Y. Immunocytochemical characterization of supporting cells in the enteric nervous system in Hirschsprung's disease. *J Pediatr Surg*, 1990;25:514-519
21 OKelly TJ, Davies JR, Tam PKH, Brading AF, Mortensen NJMC. Abnormalities of nitric-oxide-producing neurons in Hirschsprung's disease: morphology and implications. *J Pediatr Surg*, 1994;29: 294-300
22 Kuroda T, Ueda M, Nakano M, Saeki M. Altered production of nerve growth factor in aganglionic intestines. *J Pediatr Surg*, 1994;29:288-293
23 Neunlist M, Schemann M. Projections and neurochemical coding of myenteric neurons innervating the mucosa of the guinea pig proximal colon. *Cell Tissue Res*, 1997;287:119-125
24 Hassold T, Merrill M, Adkins K, Freeman S, Sherman S. Recombination and maternal age-dependent nondisjunction: Molecular studies of trisomy 16. *Am J Hum Genet*, 1995;57:867-874
25 Sherman SL, Petersen MB, Freeman SB, Hersey J, Pettay D, Taft L, Frantzen M, Mikkelsen M, Hassold TJ. Non-disjunction of chromosome 21 in maternal meiosis I: evidence for a maternal age-dependent mechanism involving reduced recombination. *Hum Mol Genet*, 1994;3:1529-1535
26 Zaragoza MV, Jacobs PA, James RS, Rogan P, Sherman S, Hassold T. Nond isjunction of human acrocentric chromosomes: studies of 432 trisomic fetuses and liveborns. *Hum Genet*, 1994;94: 411-417
27 Zheng CJ, Byers B. Oocyte selection: a new model for the maternal-age dependence of Down syndrome. *Hum Genet*, 1992; 90:1-6
28 Meijers JHC, van der Sanden MP, Tibboel D, van der Kamp AWM, Luider TM, Molenaar JC. Colonization characteristics of enteric neural crest cells: embryological aspects of Hirschsprung's disease. *J Pediatr Surg*, 1992;27:811-814
29 Barone V, Weber D, Luo Y, Brancolini V, Devoto M, Romeo G. Exclusion of linkage between RET and neuronal intestinal dysplasia type B. *Am J Med Genet*, 1996;62:195-198
30 OKelly TJ. Nerves that say NO: a new perspective on the human rectoanal inhibitory reflex. *Ann R Coll Surg Engl*, 1996;78: 31-38
31 Joq F. A new generation of model system to study the blood brain barrier: the in vitro approach. *Acta Physio Hung*, 1993;81:207-218
32 Tennyson VM, Pham TD, Rothman TP, Gershon MD. Abnormalities of smooth muscle, basal laminae, and nerves in the aganglionic segments of the bowel of lethal spotted mutant mice. *Anat Rec*, 1986;215:267-281
33 Newgreen DF, Hartley L. Extracellular matrix and adhesive molecules in the early development of the gut and its innervation in normal and spotting lethal rat embryos. *Acta Anat*, 1995;154:243-260
34 Gershon MD, Chalazonitis A, Rothman TP. From neural crest to bowel: development of the enteric nervous system. *J Neurobiol*, 1993;24:199-214
35 Levy J. The gastrointestinal tract in Down syndrome. *Prog Clin BiolRes*, 1991;373:245-256
36 Kapur RP, Yost C, Palmiter RD. A transgenic model for studying development of the enteric nervous system in normal and aganglionic mice. *Development*, 1992;116:167-175
37 Branchek TA, Gershon MD. Time course of expression of neuropeptide Y, calcitonin gene-related peptide, and NADPH diaphorase activity in neurons of the developing murine bowel and the appearance of 5-Hydroxytryptamine in mucosal enterochromaffin cells. *J Comp Neurol*, 1989;285:262-273
38 Epstein ML, Poulsen KT, Thiboldeaux R. Formation of ganglia in the gut of the chick embryo. *J Comp Neurol*, 1991;307:189-199
39 Kablar B. Structural study on the appearance of innervation in the stomach of mouse and rat embryos. *Tissue Cell*, 1995;27:309-315
40 Pham TD, Gershon MD, Rothman TP. Time of origin of neurons in the murine enteric nervous system: sequence in relation to phenotype. *J Comp Neurol*, 1991;314:789-798
41 Hoehner JC, Wester T, Påhlman S, Olsen L. Localization of neurotrophins and their high-affinity receptors during human enteric nervous system development. *Gastroenterology*, 1996;110: 756-767
42 Epstein ML, Poulsen KT, Thiboldeaux R. Formation of ganglia in the gutof the chick embryo. *J Comp Neurol*, 1991;307:189-199
43 Miyabara S, Gropp A, Winking H. Trisomy 16 in the mouse fetus associated with generalized edema and cardiovascular and urinary tract anomalies. *Teratology*, 1982;25:369-380
44 Webb S, Brown NA, Anderson RH. Cardiac morphology at late fetal stages in the mouse with trisomy 16: consequences for different formation of the atrioventricular junction when compared to humans with trisomy 21. *Cardiovasc Res*, 1997;34:515-524
45 Ludwig M, Busch LC, Winking H. The embryonic development of sensory organs and the skull in the trisomy 16 mouse, an animal model for Down's syndrome. *Anat Anz*, 1997;179:525-538
46 Robertson K, Mason I, Hall S. Hirschsprung s disease: genetic mutations in mice and men. *Gut*, 1997;41:436-441
47 Buselmaier W, Bacchus C, Sterz H. Genesis and systematization of cardi ovascular anomalies in murine trisomy 16. *Prog Clin Biol Res*, 1991;373:203-214
48 Leffler A, Ludwig M, Schmitt O, Busch LC. Germ cell migration and early development of the gonads in the trisomy 16 mouse-an animal model for Down's syndrome. *Anat Anz*, 1999;181: 247-252
49 Pomeranz HD, Gershon MD. Colonization of the avian hindgut by cells derived from the sacral neural crest. *Dev Biol*, 1990;137: 378-394
50 Payette RF, Tennyson VM, Pham TD, Mawe GM, Pomeranz HD, Rothman TP, Gershon MD. Origin and morphology of nerve fibers in the aganglionic colon of the lethal spotted (ls/ls) mutant mouse. *J Comp Neurol*, 1987;257:237-252
51 Fekete E, Resch BA, Benedeczky I. Histochemical and ultrastructural features of the developing enteric nervous system of the human foetal small intestine. *Histol Histopathol*, 1995;10: 127-134
52 Payette RF, Bennett GS, Gershon MD. Neurofilament expression in vagal neural crest-derived precursors of enteric neurons. *Dev Biol*, 1984;105:273-287

Edited by Ma JY

P.O.Box 2345 Beijing 100023, China
Fax. 0086·10·65891893 Tel. 0086·10·65897901
E-mail.wcjd@public.bta.net.cn www.wd.org.cn

World J Gastroentero, 2001 April; 7(1):22 - 27
World Journal of Gastroenterology
Copyright©2001 by the WJG Press ISSN 1007 - 9327

Reduction of tumorigenicity of SMMCa27721 hepatoma cells by vascular endothelial growth factor antisense gene therapy

Yu Cheng Tang, Yu Li and Guan Xiang Qian

Subject headings liver neoplasms; endothelial growth factors; gene therapy; endothelium vascular; enzymea2linked immunosorbent assay; carcinoma, hepatocellular; RNA, antisense

Tang YC, Li Y, Qian GX. Reduction of tumorigenicity of SMMCa27721 hepatoma cells by vascular endothelial growth factor antisense gene therapy. ***World J Gastroentero***, 2001;7(1):22-27

Abstract

AIM **To test the hypothesis to block VEGF expression of SMMC-7721 hepatomacells may inhibit tumor growth using the rat hepatoma model.**

METHODS **Amplifiy the 200 VEGF cDNA fragment and insert it into human U6 gene cassette in the reverse orientation transcribing small antisense RNA which could specifically interact with VEGF165, and VEGF121 mRNA. Construct the retroviral vector containing this antisense VEGF U6 cassette and package the replication-deficient recombinant retrovirus. SMMC-7721 cells were transduced with these virus and positive clones were selected with G418. PCR and Southern blot analysis were performed to determine if U6 cassette integrated into the genomic DNA of positive clone. Transfected tumor cells were evaluated for RNA expression by ribonuclease protection assays. The VEGF protein in the supernatant of parental tumor cells and genetically modified tumor cells was determined with ELISA. In vitro and in vivo growth properties of antisense VEGF cell clone in nude mice were analyzed.**

RESULTS **Restriction enzyme digestion and PCR sequencing verified that the antisense VEGF RNA retroviral vector was successfully constructed. After G418 selection, resistant SMMC-7721 cell clone was picked up. PCR and Southern blot analysis suggested that U6 cassette was integrated into the cell genomic DNA. Stable SMMC-7721 cell clone transduced with U6 antisense RNA cassette could express 200 bp small antisense VEGF RNA and secrete reduced levels of VEGF in culture condition. Production of VEGF by antisense transgenea2expressing cells was 65 ± 10 ng/L per 10^6 cells, 420 ± 45 ng/L per 10^6 cells in sense group and 485 ± 30 ng/L per 10^6 cells in the negative control group, (P<05). The antisense-VEGF cell clone appeared phenotypically indistinguishable from SMMC-7721 cells and SMMC-7721 cells transfected sense VEGF. The growth rate of the antisense-VEGF cell clone was the same as the control cells. When S.C. was implanted into nude mice, growth of antisense-VEGF cell lines was greatly inhibited compared with control cells.**

CONCLUSION **Expression of antisense VEGF RNA in SMMC-7721 cells could decrease the tumorigenicity, and antisense-VEGF gene therapy may be an adjuvant treatment for hepatoma.**

Department of Biochemistry, Shanghai Second Medical University, Shanghai 200025, China
Dr. Yu Cheng Tang, graduated in 2000 from Shanghai Second Medical University, specialized in tumor biology.
Project supported by National Natural Science Foundation of China, No.863-Z20-01-04
Correspondence to: Yu Cheng Tang, Department of Biochemistry, Shanghai Second Medical University, Shanghai 200025, China
Tel. 0086-21-63846590 Ext. 504, Fax. 0086-21-63842916
Email. tangyc@shsmu.edu.cn
Received 2000-09-21 **Accepted** 2000-10-29

INTRODUCTION

Neovascularization is critical for supporting the rapid growth of solid tumors[1]. Tumor angiogenesis appears to be achieved by the expression of angiogenic agents within solid tumors that stimulate host vascular endothelial cell mitogenesis and possibly chemotaxis. One such protein, vascular endothelial growth factor (VEGF) or vascular permeability factor[2-5], is a selective endothelial cell mitogen and angiogenic agent .Many tumor cell lines secrete VEGF *in vitro*, suggesting that this diffusible molecule is a mediator of tumor angiogenesis. The clinical results showed high levels of VEGF expression in primary hepatoma, elevated levels of flt-1, the receptors of VEGF in hepatoma blood vessels, and the relationship between VEGF levels and hepatoma invasion and transfer[6]. These data indicated that VEGF and its receptors play important roles in the development of hepatoma vasculature and progressive growth of hepatoma.

In this study, we used the SMMC-7721 hepatoma cell line which has a high expression of

VEGF, as established model for human hepatoma. The strategy of exogenous expression of antisense VEGF transcribed by POL III promoter in the SMMC-7721 cell line was applied to assess the feasibility of disrupting the VEGF/VEGF receptor pathway of angiogenesis and decreasing their tumorigenicity *in vivo*.

MATERIALS AND METHODS

Materials

Bam HI, T4 DNA ligase was purchased from Promega Company. RNase A and RNase T1 were the products of MBI Fermentas, G418 was purchased from Sigma Company and SMMC-7721 cell line from Chinese Academy of Cell Biology.

Methods

Construction of vectors VEGF antisense vector to generate the VEGF anti-sense vector, a DNA fragment containing 250 bp of human VEGF cDNA, was ligated in reverse orientation in the *sal* I, *xho* I sites of the U6 cassette, and subcloned into the *Bam* H I site of pLXSN vector. Expression of the antisense molecule in pLXSN was driven by POLIII promoter of U6 cassette. The pLXSN vector also contained the G418 resistance gene driven by the simian virus (SV40) promoter. To generate infectious virions, PA317 packaging cells were transfected with pLXSN-U6-as-VEGF and selected in the culture medium containing 500 mg/L G418. Virus-containing supernatants were harvested and used to infect SMMC-7721 cells.

Genetic modification of SMMC-7721 cells The SMMC-7721 cells were incubated with the viral stock containing 8 mg/L polybrene. On the following day, the cells were split and selected in 500 mg/L G418. Cultures were added every 3-4 days with the fresh G418 supplemented media for 14 days. Resistant colonies were expanded, and subcloned and the clone which produced the reduced levels of VEGF was selected for further research.

Ribonuclease protection assay A 200bp VEGF PCR product was cloned into T7,T3 vector pBlueScript-SK, the plasmid was linearized by *Eco* R V, treated with proteinase K and purified. The α-^{32}P UTP sense VEGF RNA was generated by addition of T7 polymerase. Ribonuclease protection assays were made as follows, 20 μg of total cellular RNA was hybridized with RNA probes overnight at 45℃. The remaining single-stranded probe RNA and unhybridized RNA were digested with a mixture of RNase A and RNase T1, added yeast RNA, extracted by phenol, precipitated by ethanol, seperated on 7M urea/polyacrylamide gels, and then exposed to X-ray film.

PCR, southern blot analysis PCR was performed on genomic DNA isolated from human SMMC-7721 cells and individual clones of transfected cells using a sense primer corresponding to the U6 promoter (5'-TATACTAAGTCGACTCCTATGTGCTGG-3') and an antisense primer corresponding to the VEGF cDNA (5'-TAGAGAGGGCAGAATCATCACG-AAGTGG-3'). Using the NeoR primer, the sense primer is 5'-CAAGATGGAATTGCACGCAGG-3', the reversal primer is 5'-CCCGCTCAGAAAGAACTCGTC-3'. The PCR was performed using the following protocol: 95℃ 1min, 60℃ 1min, 72℃ 1min 30s; in the last cycle, extend 10 min at 72℃. Southern blot, 20 μg genomic DNA was digested overnight, electrophoresed on 1% agarose gels, transferred onto Hybond N nylon membrane, and hybridized with the DIG labeled NeoR probe at 68℃ for 6 h, the membrane was washed in 2 × SSC for 5 min × 2, and 0.1 × SSC for 15 min. The fragments were visualized by chemiluminescent, and exposed to X-ray film.

Quantitation of VEGF The supernatant of parental or transfected SMMC-7721 cells were measured by ELISA. To generate the conditional medium, the cells were seeded onto 3.0×10^5/well plates. The media was changed next day to MEM /0.5% bovine serum albumin/ 1% dialyzed fetal calf serum for another 24 h. The media was then replaced by the fresh MEM and cells were allowed to grow for another 48 h. The CM was generated by centrifugation at 14 000rpm at 4℃ for 15 min, then for ELISA analysis according to the manufacturer's instructions.

***In vitro* growth rate** SMMC-7721 hepatoma cells and cells transfected with antisense, and sense-VEGF were cultured at 1×10^4 and grown under standard culture conditions. Cell count was made every 24 h for a total of 144 h. The total number of cells from duplicate experiments was determined as a function of time.

Determination of *in vivo* tumor growth Subcutaneous inoculation and tumor growth measurements were carried out, 1×10^6 cells of the parental SMMC-7721 cells or antisense, sense expressing clones were injected into the flank of normal BALB/C nude mice. Tumors were measured in two dimensions every 5 days for 25 days. Tumor volume was calculated using the formula $v = l \times w^2/2$, where v = volume (mm^3), l = long diameter, and w = short diameter.

RESULTS

Construction of the antisense-VEGF RNA expression vector based on U6 POLIII promoter

All of the major transcriptional promoter elements for U6 RNA polymerase III are upstream of the transcription start, which has a potential advantage of the less exogenous RNA coding sequence. Another advantage of the U6 promoter is that U6

gene is heavily expressed in human cells. The U6 cassette contained the first 5' initial 27 nucleotides and 3' stem 19 nucleotides for transcript terminator and the U6+27 transcript was predicted to be most stable because of the γ-phosphomethyl-GTP cap. The fragment of VEGF was cloned into U6 cassette through sense or antisense direction, and verified by DNA sequence. U6 cassette containing sense or antisense VEGF was cleaved by *Hind* III, *Pst* I digestion and cloned into pBlue-SK vector, and subcloned into *Bam* HI restriction site of retroviral expression vector. The positive plasmid was verified by *Bam* HI digestion (Figure 1).

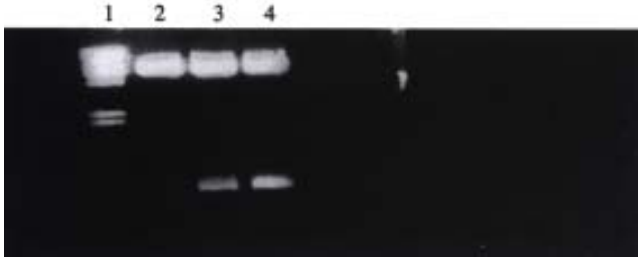

Figure 1 Electrophoresis pattern of pLXSN-U6 sense, antisense VEGF plasmid digested by *Bam* HI.
Lane 1: λ DNA *Hind* III Marker; Lane 2: pLXSN digested by *Bam* HI; Lane 3: pLXSN-U6 sense VEGF digested by *Bam* HI; Lane 4: pLXSN-U6 antisense VEGF digested by *Bam* HI.

SMMC-7721 cells expressing antisense-VEGF

Following transfection by recombinant antisense VEGF or sense VEGF retrovirus, the SMMC-7721 cells were selected by antibiotic G418, the individual clones were isolated and expanded. And the selected clone expressed low VEGF for further analysis and was referred to as anti-1. This clone was evaluated for gene expression in ribonuclease protection assays. In this assay, hybridization of RNA with the complementary RNA probe protects the probe from the subsequent digestion with RNase A and RNase T1. From Figure 2, it can be seen that 200 bp antisense VEGF RNA was only expressed in SMMC-7721 transfected by pLXSN U6 antisense VEGF.

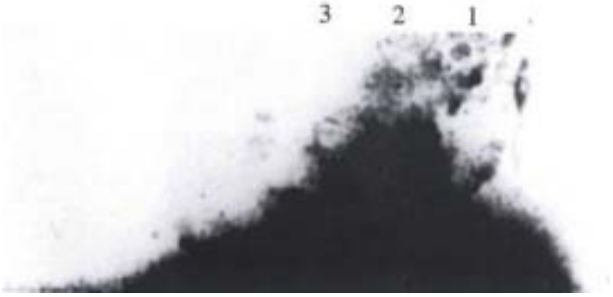

Figure 2 Detection of antisense VEGF RNA expression by RNase protection assay.
Lane 1: Hybridization with total RNA from SMMC-7721 antisense clone showed 200 bp antisenseVEGF RNA; Lane 2: Hybridization with total RNA from SMMC-7721 sense clone showed no positive band; Lane 3: Hybridization with total RNA from SMMC-7721 cells showed no positive band.

PCR analysis of DNA isolated from the antisense-VEGF, sense VEGF clones showed foreign gene integration into the genomic DNA, and the results of PCR using the specific primer, showed that the antisense VEGF U6 gene cassette had inserted the genomic DNA of SMMC-7721 cells. Southern blot analysis was performed on genomic DNA of these antisense VEGF, senseVEGF clones to verify again that there was foreign integrated cDNA (Figures 3, 4).

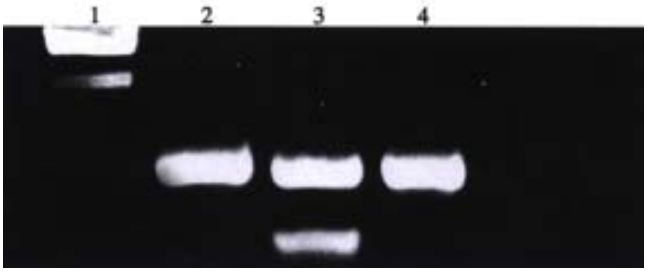

Figure 3 PCR amplification of genomic DNA from SMMC-7721 antisense, sense VEGF clone.
Lane 1: Marker; Lane 2: SMMC-7721 / sense VEGF clone showed of neo gene 790 bp; Lane 3: SMMC-7721 / antisense VEGF clone showed neo gene 790 bp, U6 cassette 260 bp; Lane 4: SMMC-7721 / pLXSN clone showed neo gene 790 bp

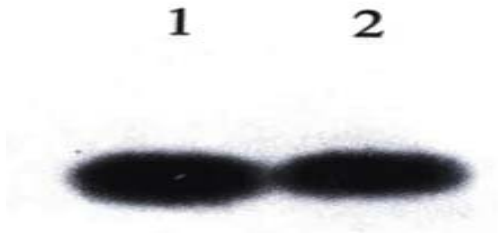

Figure 4 Genomic analysis of SMMC-7721 / U6 antisense VEGF, SMMC-7721 / U6 sense VEGF clones.Lane 1: SMMC-7721 / U6 sense VEGF clone; Lane 2: SMMC-7721 / U6 antisense VEGF clone.

Diminished production of VEGF by SMMC-7721 cells transduced with antisense VEGF cDNA

In order to determine if the expression of the antisense VEGF transgene reduced production of secreted protein, supernatant from control-transduced (SMMC-7721 sense VEGF) and antisense VEGF transduced cells were assayed for VEGF by ELISA. Production of VEGF by antisense transgene-expressing cells was 65 + 10ng/L per 10^6 cells, as compared with 420 + 45 ng/L per 10^6 cells in sense group and 485 + 30 ng/L per 10^6 cells in negative control group, $P < 0.05$.

In vitro growth rate of antisense-VEGF cell lines

The antisense-VEGF cell lines appeared phenotypically indistinguishable from normal SMC-7721 cells and SMMC-7721 transfected sense VEGF cells. And growth rates of antisense-VEGF cell lines were the same as the control cells (Figure 5).

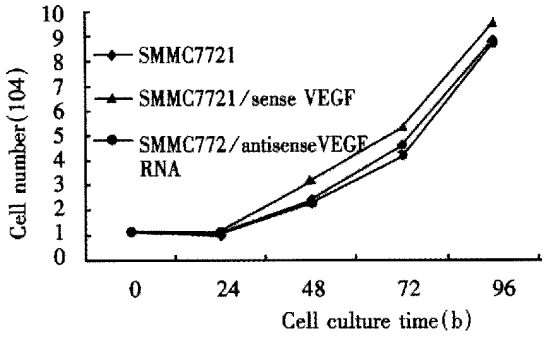

Figure 5 Proliferation curves of parental SMMC-7721 cells and antisense-VEGF, sense-VEGF cell lines.

In vivo growth of the antisense-VEGF cell lines

Control SMMC-7721 cells and antisense-VEGF SMMC-7721 cells were s.c. injected into nude mice, tumor volumes were measured every 5 days. Tumor growth was detectable and measurable for control SMMC-7721 cells 5 days post-implantation, while the antisense VEGF cell lines gave rise to tumors. Examination of mice at 25 days post-implantation revealed that the negative control SMMC-7721 group produced tumors of 630.92 ± 85 mm^3, sense-VEGF SMMC-7721 group produced tumors of 601.07 ± 52 mm^3, while the antisense VEGF SMMC-7721 group produced tumors of 76.33 ± 20 mm^3. This experiment demonstrates that the reduced tumorigenicity of antisense-VEGF SMMC-7721 cells in nude mice may be attributed to the reduced expression of VEGF (Figure 6).

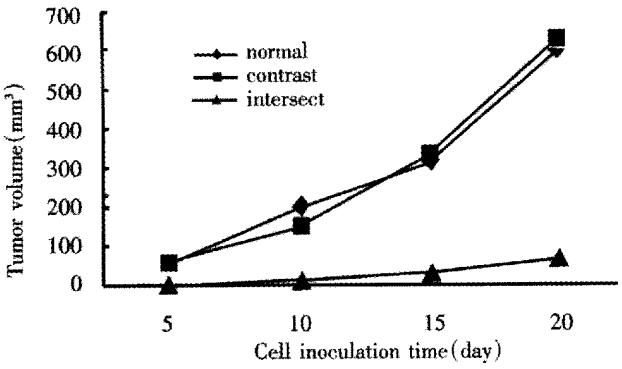

Figure 6 Tumorgenicity of antisense VEGF SMMC-7721 in nude mice.

DISCUSSION

Angiogenesis, the formation of new blood vessels , is essential for both tumor growth and metastasis [7-10]. Tumor angiogensis is a process controlled by certain chemicals produced in cancer cells. These chemicals stimulate endothelail cells to form new blood vessels. Candidates as major physiological stimulators include VEGF[11], bFGF. VEGF, and its receptors play critical roles in tumor-associated angiogenesis and represent good targets for therapeutic intervention[12-15]. VEGF was initially termed vascular permeability factor, its first function was discovered by Dvorak and colleagues[16]. There are several VEGF isoforms, in which VEGF121 and VEGF165 are readily secreted. Unlike bFGF, VEGF is a very specific mitogen for vascular endothelial cells. It also functions as a potent pro-survival factor for endothelial cells in nearby formed vessels and this may be one of its most important functions[17,18].

It is reported that VEGF is an angiogenic factor most closely associated with the neovascularization in solid tumors. VEGF is expressed by vast majority of cancers at elevated levels and blocks its activity by specific neutralizing antibodies to VEGF[19,20]. VEGF-toxin conjugates[21], aptamers[21] and small molecule VEGF receptor antagonists[22] could inhibit the growth of cancer in animal models. In human hepatocellular carcinoma, abundant tumor vascularity was observed. And vascular endothelial growth factor gene and protein expression was analyzed by means of Northern hybridization and immunohistochemistry, increased expression of VEGF has been reported in hepatocellular carcinoma cells (HCC)[23-26]. So VEGF gene expression is significantly associated with angiogenesis of HCC. Tang Zhao You *et al* studied the angiogenesis induced by liver cancer with different metastatic potentials using corneal micropocket model in nude mice. It was suggested that highly metastatic liver cancer was more angiogenic than low metastatic cancer and liver tissue[26]. In HCC with metastasis, mRNA of VEGF is closely related to the growth of HCC as well as its metastasis[27].

In China, the hepatocarcinogenesis is closely related with the hepatitis virus[28], the results of the researches showed that, after viral infection,there is abnormal expression of oncogene such as ras, bcl-2, especially P53[29-33], and there is also a possible link between oncogenes and tumor angiogenesis. Expression of mutant ras can lead to a marked induction of a potent paracrine stimulator of angiogenesis. In addition, hypoxia stimulates expression of VEGF and tumor angiogenesis[34-40]. The results of therapeutic experiments showed that the chimeric protein consisting of DT390-VEGF165 or DT390-VEGF exon7 can efficiently kill the HepG2 and gastric carcinoma cells and may kill vascular endothelial cells in the cancer[41, 42] and antiangiogenesis inhibitor TNP-470 plus lipiodol greatly decreased the hepatoma growth in animal models which depend on the reduction of microvessel density[43].

Blocking the interaction between the VEGF and its receptor can inhibit the growth of tumor through the antiangiogenesis effect[44-47]. From our

previous experiment, we found VEGF expression in hepatoma cell line SMMC-7721 cells. We there fore sought to determine if inhibition of secretion of VEGF in SMMC-7721 tumor cells would inhibit the growth of this tumor in animal model.

In order to improve the expression of the antisense VEGF RNA in the target cell, we constructed the retrovirus vector containing the human U6 promoter cassette that had the POL III promoter to transcribe the small therapeutic RNA in the nuclei of cells. Compared with other transcriptional promoters such as POL II, tRNA, there are two advantages of U6 promoter: ① high expression in human cells, and ② the therapeutic RNA contains less unnecessary RNA encoding the intragenic ptomoter. In the same time, we amplified a common VEGF cDNA and inserted reversely into U6 cassette[48-52]. U6 promoter transcribed a small antisense VEGF RNA fragment that could specifically interacted with VEGF165 and VEGF121 mRNA. Our previous results, verified that U6 cassette could effectively express antisense VEGF RNA molecules and decreased the expression of mRNA VEGF165, and VEGF121. Then U6 cassette that expressed antisense VEGF RNA was inserted into the retroviral construct. After packaging the recombinant retrovirus, this cassette was introduced into the SMMC-7721 cells. Ribonuclease protection analysis using the RNA probe specific for antisense VEGF demonstrated that there was antisense VEGF RNA expression in the SMMC-7721 cells genetically modified by antisense U6 cassette. The antisense clone selected for further study showed radical decrease in VEGF protein in supernatant compared with the sense and negative SMMC-7721 cell group. Inhibition of VEGF expression in SMMC-7721 cells resulted in severely impaired growth of this tumor *in vivo*. This may be related with the reduced levels of VEGF produced by the antisense-VEGF-transfected SMMC-7721 cell clone, and this resulted in a decrease of number of tumor blood vessels. Our findings demonstrate that the inhibition of VEGF is sufficient to control the tumor growth *in vivo*. The antisense VEGF srategy offers a way for gene therapy as an adjuvant treatment for hepatoma.

REFERENCES

1 Shweiki D, Itin A, Soffer D, Keshet E. Vascular endothelial growth factor induced by hypoxia may mediate hypoxia-initiated angiogenesis. *Nature*, 1992;359:843-845

2 Carmeliet P, Jain RK. Angiogenesis in cancer and other diseases. *Nature*, 2000;407:249-257

3 Lewin M, Bredow S, Sergeyev N, Marecos E, Bogdanov A, Weissleder R. *In vivo* assessment of vascular endothelial growth factor-induced angiogenesis. *Int J Cancer*, 1999;83:798-802

4 Millauer B, Longhi MP, Plate KH, Shawver LK, Risau W, Ullrich A, Strawn LM. Dominant-negative inhibition of Flk-1 suppresses the growth of many tumor types *in vivo*. *Cancer Res*, 1996;56:1615-1620

5 Asano M, Yukita A, Matsumoto T, Kondo S, Suzuki H. Inhibition of tumor growth and metastasis by an immunoneutralizing monoclonal antibody to human vascular endothelial growth factor/vascular permeability factor$_{121}$. *Cancer Res*, 1995;55:5296-5301

6 Li J, Wang WL, Liu B. Angiogenesis and apoptosis in human hepatocellular carcinoma. *Huaren Xiaohua Zazhi*, 1998;6:1057-1060

7 Jia L, Chen TX, Sun JW, Na ZM, Zhang HH. Relationship between microvessel density and proliferating cell nuclear antigen and prognosis in colorectal cancer. *Shijie Huaren Xiaohua Zazhi*, 2000;8:74-76

8 Gao GL, Yang Y, Yang S, Ren CW. Relationship between proliferation of vascular andothelial cells and gastric cancer. *Shijie Huaren Xiaohua Zazhi*, 2000;8:282-284

9 Yoshiji H, Kuriyama S, Ways DK, Yoshii J, Miyamoto Y, Kawata M, Ikenaka Y, Tsujinoue H, Nakatani T, Shibuya M, Fukui H. Protein kinase C lies on the signaling pathway for vascular endothelial growth factor-mediated tumor development and angiogenesis. *Cancer Res*, 1999;59:4413-4418

10 Weidner N. Intratumor microvessel density as a prognostic factor in cancer. *Am J Pathol*, 1995;147:9-19

11 Danielsen T, Rofstad EK. The constitutive level of vascular endothelial growth factor (VEGF) is more important than hypoxia-induced VEGF up-regulation in the angiogenesis of human melanoma xenografts. *Br J Cancer*, 2000;82:1528-1534

12 Benjamin LE, Golijanin D, Itin A, Pode D, Keshet E. Selective ablation of immature blood vessels in established human tumors follows vascular endothelial growth factor withdrawal. *J Clin Invest*, 1999;103:159-165

13 Cheng SY, Huang HJS, Nagane M, Ji XD, Wang D, Shi CCY, Arap W, Huang CM, Cavenee WK. Suppression of glioblastoma angiogenicity and tumorigenicity by inhibition of endogenous expression of vascular endothelial growth factor. *Proc Natl Acad Sci USA*, 1996;93:8502-8507

14 Kim KJ, Li B, Winer J, Armanini M, Gillett N, Phillips HS, Ferrara N.Inhibition of vascular endothelial growth factor-induced angiogenesis suppresses tumour growth *in vivo*. *Nature*, 1993;362:841-844

15 Petit AMV, Rak J, Hung MC, Rockwell P, Goldstein N, Fendly B, Kerbel RS. Neutralizing antibodies against epidermal growth factor and ErbB-2/neu receptor tyrosine kinases down-regulate vascular endothelial growth factor production by tumor cells *in vitro* and *in vivo*: angiogenic implications for signal transduction therapy of solid tumors. *Am J Pathol*, 1997;151:1523-1530

16 Dvorak HF, Brown LF, Detmar M, Dvorak AM. Vascular permeability factor/vascular endothelial growth factor, microvascular hyperpermeability and angiogenesis. *Am J Pathol*, 1995;146:1029-1039

17 Wong EYM, Morgan L, Smales C, Lang P, Gubby SE, Staddon JM. Vascular endothelial growth factor stimulates dephosphorylation of the catenins p120 and p100 in endothelial cells. *Biochem J*, 2000;346:209-216

18 Neufeld G, Cohen T, Gengrinovitch S, Poltorak Z. Vascular endothelial growth factor (VEGF) and its receptors. *FASEB J*, 1999;13:9-22

19 Presta LG, Chen H, OConnor SJ, Chisholm V, Meng YG, Krummen L, Winkler M, Ferrara N. Humanization of an anti-vascular endothelial growth factor monoclonal antibody for the therapy of solid tumors and other disorders. *Cancer Res*, 1997;57:4593-4599

20 Zhu Z, Rockwell P, Lu D, Kotanides H, Pytowski B, Hicklin DJ, Bohlen P, Witte L. Inhibition of vascular endothelial growth factor-induced receptor activation with anti-kinase insert domain-containing receptor single-chain antibodies from a phage display library. *Cancer Res*, 1998;58:3209-3214

21 Ramakrishnan S, Olson TA, Bautch VL, Mohanraj D. Vascular endothelial growth factor-toxin conjugate specifically inhibits KDR/flk-1-positive endothelial cell proliferation *in vitro* and angiogenesis *in vivo*. *Cancer Res*, 1996;56:1324-1330

22 Seo MS, Kwak N, Ozaki H, Yamada H, Okamoto N, Yamada E, Fabbro D, Hofmann F, Wood JM, Campochiaro PA. Dramatic inhibition of retinal and choroidal neovascularization by oral administration of a kinase inhibitor. *Am J Pathol*, 1999;154:1743-1753

23 Suzuki H, Seto K, Shinoda Y, Mori M, Ishimura Y, Suematsu M, Ishii H. Paracrine upregulation of VEGF receptor mRNA in endothelial cells by hypoxia-exposed Hep G2 cells. *Am J Physiol*, 1999;276:G92-97

24 El-Assal ON, Yamanoi A, Soda Y, Yamaguchi M, Igarashi M, Yamamoto A, Nabika T, Nagasue N. Clinical significance of microvessel density and vascular endothelial growth factor expression in hepatocellular carcinoma and surrounding liver: possible involvement of vascular endothelial growth factor in the angiogenesis of cirrhotic liver. *Hepatology*, 1998;27:1554-1562

25 Jin-no K, Tanimizu M, Hyodo I, Nishikawa Y, Hosokawa Y, Doi T, Endo H, Yamashita T, Okada Y. Circulating vascular endothelial growth factor (VEGF) is a possible tumor marker for metastasis in

human hepatocellular carcinoma. *J Gastroenterol*, 1998;33:376-382
26 Sun HC, Li XM, Xue Q, Chen J, Gao DM, Tang ZY. Study of angiogenesis induced by metastatic and non-metastatic liver cancer by corneal micropocket model in nude mice. *World J Gastroenterol*, 1999;5:116-118
27 Yamaguchi R, Yano H, Iemura A, Ogasawara S, Haramaki M, Kojiro M. Expression of vascular endothelial growth factor in human hepatocellular carcinoma. *Hepatology*, 1998;28:68-77
28 Gu GW, Zhou HG. New concept in etiology of liver cancer. *Huaren Xiaohua Zazhi*, 1998;6:185-187
29 Feng DY, Chen RX, Peng Y, Zheng H, Yan YH. Effect of HCV NS_3 protein on P53 protein expression in hepatocarcinogenesis. *World J Gastroenterol*, 1999;5:45-46
30 Peng XM, Peng WW, Chen Q, Yao JL. Apoptosis, Bcl-2 and P53 protein expressions in tissues from hepatocellular carcinoma. *Huaren Xiaohua Zazhi*, 1998;6:834-836
31 Zheng SX, Liu LJ, Shao YS, Zheng QP, Ruan YB, Wu ZB. Relationship between ras p53 gene RNA and protein expression and HCC metastasis. *Huaren Xiaohua Zazhi*, 1998;6:104-105
32 Yuan FP, Huang PS, Wang Y, Gong HS. Relationship between EBV infection in Fujian HCC and HBV and P53 protein expression. *Shijie Huaren Xiaohua Zazhi*, 1999;7:491-493
33 Dameron KM, Volpert OV, Tainsky MA, Bouck N. Control of angiogenesis in fibroblasts by p53 regulation of thrombospondina 21. *Science*, 1994;265:1582-1584
34 Yamagishi S, Yonekura H, Yamamoto Y, Fujimori H, Sakurai S, Tanaka N, Yamamoto H. Vascular endothelial growth factor acts as a pericyte mitogen under hypoxic conditions. *Lab Invest*, 1999; 79:501-509
35 Carmeliet P, Dor Y, Herbert JM, Fukumura D, Brusselmans K, Dewerchin M, Neeman M, Bono F, Abramovitch R, Maxwell P, Koch CJ, Ratcliffe P, Moons L, Jain RK, Collen D, Keshet E. Role of HIF-1α in hypoxia-mediated apoptosis, cell proliferation and tumour angiogenesis. *Nature*, 1998;394:485-490
36 Mazure NM, Chen EY, Laderoute KR, Giaccia AJ. Induction of vascular endothelial growth factor by hypoxia is modulated by a phosphatidylinositol 3-kinase/Akt signaling pathway in Ha-ras-transformed cells through a hypoxia inducible factor-1 transcriptional element. *Blood*, 1997;90:3322-3331
37 Maxwell PH, Dachs GU, Gleadle JM, Nicholls LG, Harris AL, Stratford IJ, Hankinson O, Pugh CW, Ratcliffe PJ. Hypoxia-inducible factor-1 modulates gene expression in solid tumors and influences both angiogenesis and tumor growth. *Proc Natl Acad Sci USA*, 1997;94:8104-8109
38 Raleigh JA, Calkins-Adams DP, Rinker LH, Ballenger CA, Weissler MC,Fowler WC, Novotny DB, Varia MA. Hypoxia and vascular endothelial growth factor expression in human squamous cell carcinomas using pimonidazole as a hypoxia marker. *Cancer Res*, 1998;58:3765-3768
39 Kim KW, Bae SK, Lee OH, Bae MH, Lee MJ, Park BC. Insulin-like growth factor II induced by hypoxia may contribute to angiogenesis of human hepatocel lular carcinoma. *Cancer Res*, 1998;58:348-351
40 Biroccio A, Candiloro A, Mottolese M, Sapora O, Albini A, Zupi G, Del Bufalo D. Bcl-2 overexpression and hypoxia synergistically act to modulate vascular endothelial growth factor expression and *in vivo* angiogenesis in a breast carcinoma line. *FASEB J*, 2000;14:652-660
41 Pan X, Ke CW, Pan W, He X, Cao GW, Qi ZT. Killing effect of DT/VEGF system on gastric carcinoma cell. *Shijie Huaren Xiaohua Zazhi*, 2000;8:393-396
42 Pan X, Pan W, Ni CR, Ke CW, Cao GW, Qi ZT. Killing effect of tetracy cline-controlled expression of DT/VEGF system on liver cell cancer. *Shijie Huaren Xiaohua Zazhi*, 2000;8:867-873
43 Cao W, Wang ZM, Liang ZH, Zhang HX, Wang YQ, Huan Y, Li WX, Pan BR. Effects of angiogenesis inhibitor TNP-470 with lipiodol in arterial embolization of liver cancer in rabbit model. *Shijie Huaren Xiaohua Zazhi*, 2000;8:629-632
44 Brekken RA, Overholser JP, Stastny VA, Waltenberger J, Minna JD, Thorpe PE. Selective inhibition of vascular endothelial growth factor (VEGF) receptor 2 (KDR/Flk-1) activity by a monoclonal anti-VEGF antibody blocks tumor growthin mice. *Cancer Res*, 2000;60:5117-5124
45 Drevs J, Hofmann I, Hugenschmidt H, Wittig C, Madjar H, Müller M, Wood J, Martiny-Baron G, Unger C, Marme D. Effects of PTK787/ZK 222584, a specific inhibitor of vascular endothelial growth factor receptor tyrosine kinases, on primary tumor, metastasis, vessel density, and blood flow in a murine renal cell carcinoma model. *Cancer Res*, 2000;60:4819-4824
46 Takayama K, Ueno H, Nakanishi Y, Sakamoto T, Inoue K, Shimizu K, Oohashi H, Hara N. Suppression of tumor angiogenesis and growth by gene transfer of a soluble form of vascular endothelial growth factor receptor into a remote organ. *Cancer Res*, 2000;60:2169-2177
47 Klement G, Baruchel S, Rak J, Man S, Clark K, Hicklin DJ, Bohlen P, Kerbel RS. Continuous low-dose therapy with vinblastine and VEGF receptor-2 antibody induces sustained tumor regression without overt toxicity. *J Clin Invest*, 2000;105:R15-24
48 Ohkawa J, Taira K. Control of the functional activity of an antisense RNA by a tetracycline-responsive derivative of the human U6 snRNA promoter. *Hum Gene Ther*, 2000;11:577-585
49 Lobo SM, Ifill S, Hernandez N. Cis-acting elements required for RNA polymerase and (r) transcription in the human U2 and U6 snRNA promoters. *Nucleic Acids Res*, 1990;18:2891-2899
50 Chalker DL, Sandmeyer SB. Sites of RNA polymerase III transcription initiation and Ty3 integration at the U6 gene are positioned by the TATA box. *Proc Natl Acad Sci USA*, 1993;90:4927-4931
51 Goomer RS, Kunkel GR. The transcriptional start site for a human U6 small nuclear RNA gene is dictated by a compound promoter element consisting of the PSE and the TATA box. *Nucleic Acids Res*, 1992;20:4903-4912
52 Good PD, Krikos AJ, Li SXL, Bertrand E, Lee NS, Giver L, Ellington A, Zaia JA, Rossi JJ, Engelke DR. Expression of small, therapeutic RNAs in human cell nuclei. *Gene Ther*, 1997;4:45-54

Edited by Ma JY

P.O.Box 2345 Beijing 100023, China
Fax. 0086·10·65891893 Tel. 0086·10·65897901
E-mail.wcjd@public.bta.net.cn www.wd.org.cn

World J Gastroentero, 2001 April; 7(1):28 - 32
World Journal of Gastroenterology
Copyright©2001 by the WJG Press ISSN 1007 - 9327

Multimodality treatment in hepatocellular carcinoma patients with tumor thrombi in portal vein

Jia Fan, Zhi Quan Wu, Zhao You Tang, Jian Zhou, Shuang Jian Qiu, Zeng Chen Ma, Xin Da Zhou and Sheng Long Ye

Subject headings carcinoma, hepatocellular/therapy; neoplasm circulating cells; portal vein; antineoplastic agents; combined modality therapy; chemoembolization, therapeutic

Fan J, Wu ZQ, Tang ZY, Zhou J, Qiu SJ, Ma ZC, Zhou XD, Ye SL. Multimodality treatment in hepatocellular carcinoma patients with tumor thrombi in portal vein. ***World J Gastroenterol***, 2001;7(1):28-32

Abstract

AIM **To compare the therapeutic effect and significances of multimodality treatment for hepatocellular carcinoma (HCC) with tumor thrombi in portal vein (PVTT).**

METHODS **HCC patients (*n* = 147) with tumor trombi in the main portal vein or the first branch of portal vein were divided into four groups by the several therapeutic methods. There were conservative treatment group in 18 out of patients (group A); and hepatic artery ligation (HAL) and/or hepatic artery infusion (HAI) group in 18 patients (group B), in whom postoberative chemoembolization was done periodically; group of removal of HCC with PVTT in 79 (group C) and group of transcatheter hepatic arterial chemoembolization (TACE) or HAI and/or portal vein infusion (PVI) after operation in 32 (group D).**

RESULTS **The median survival period was 12 months in our series and the 1-, 3-, and 5-year survival rates were 44.3%, 24.5% and 15.2%, respectively. The median survival times were 2, 5, 12 and 16 months in group A, B, C and D, respectively. The 1-, 3- and 5-year survival rates were 5.6%, 0% and 0% in group A; 22.2%, 5. 6% and 0% in group B; 53.9%, 26.9% and 16.6% in group C; 79.3%, 38.9% and 26.8% in group D, respectively. Significant difference appeared in the survival rates among the groups (*P*<05).**

CONCLUSION **Hepatic resection with removal of tumor thrombi and HCC should increase the curative effects and be encouraged for the prolongation of life span and quality of life for HCC patients with PVTT, whereas the best therapeutic method for HCC with PVTT is with regional hepatic chemotherapy or chemoemblization after hepatic resection with removal of tumor thrombi.**

Liver Cancer Institute, Zhongshan Hospital, Fudan University Medical Center (Former Shanghai University), 136 Yixueyuan Road, Shanghai 200032, China
Dr. Jia Fan, doctor degree from Shanghai Medical University in 1995, professor of surgery, major in surgical oncology of liver, having more than 60 papers published.
Surported by the Funds of Hundred Outsdanding Persons project of Shanghai (97BR029) and Science and Technology Commission of Shanghai (984419067)
Correspondence to: Jia Fan, M.D., Ph.D. Liver Cancer Institute, Zhongshan Hospital, Fudan University Medical Center (Former Shanghai University), 136 Yixueyuan Road, Shanghai 200032, China
Tel/Fax. +86-21-64037181
Email. jiafan 99 @ yahoo.com
Received 2000-08-08 **Accepted** 2000-09-29

INTRODUCTION

Hepatocellular carcinoma (HCC) with tumor thrombi in the main trunk or the first branch of the portal vein would be considered to be advanced stage of liver cancer[1], which often results in intrahepatic metastasis and can only be treated with conservative or non-operative methods such as per oral chemotherapy, biotherapy, traditional Chinese medicine, etc. In China, some patients even give up all the therapeutic methods for HCC. The majority of those patients usually die of liver failure or bleeding of the upper digestive tract within several months[2,3]. In recent decade, the active therapeutic measure for HCC with tumor thrombi in portal vein (PVTT) was performed at the Liver Cancer Institute of Shanghai Medical University, i. e., hepatic resection with removal of PVTT. After the operation, some patients obtained satisfactory curative effects through transcatheter chemotherapy or transcatheter hepatic arterial chemoembolization (TACE), or hepatic artery infusion (HAI) and/or portal vein infusion of chemotherapeutic agents (PVI).

MATERIALS AND METHODS

Patients

By December 1996, 147 patients with pathologically proven HCC with tumor thrombi in the main trunk or the first branch of the portal vein had been treated at the Liver Cancer Institute of Shanghai Medical University. Among them, 144 were males and 3 females, the median age was 48. 2 years (ranged from 20 to 70 years). Serum hepatitis B surface antigen was found positive in 123 cases (83.7%). Coexisting cirrhosis was found in 138

cases (93.9%): macronodular cirrhosis (cirrhotic nodule >3 mm) in 81 patients and micronodular cirrhosis (cirrhotic nodule ≤3 mm) in 57 patients. Alpha-fetoprotein (AFP) levels were elevated (21-16 000 μg·L^{-1}) in 120 cases (81.6%). The tumors were situated in the left lobe in 53 cases, the right lobe in 61 and both lobes in 33.

Groups of patients

One hundred and forty-seven patients were divided into 4 groups. Group A: conservative treatment group, receiving only oral medications of chemotherapy or Chinese herbal decoction and supporting treatment, 18 cases; Group B: hepatic artery ligation (HAL) and/or HAI or PVI (postoperative chemotherapy through hepatic artery or portal vein, and periodical chemoembolization through hepatic artery), 18 cases; Group C: removal of HCC with PVTT in 79 cases; among them, 5 patients were lost to follow-up. The tumors and tumor thrombi were resected simultaneously or tumor thrombi were extracted from the portal vein after removal of the tumors for the HCC patients with PVTT; Group D: Intrahepatic arterial chemoembolization or chemotherapy and/or intraportal chemotherapy by catheterization or TACE were periodically performed after resection of HCC with PVTT in 32 cases; among them, 3 cases were lost to follow-up.

Location of tumor thrombi

Fifty-one cases had tumor thrombi in left branch of portal vein, 47 in right branch, 10 in both branches, 14 in left branch extending to the main portal vein, 9 in right branch extending to the main trunk of portal vein, and 16 in both branches and the main portal vein.

Comparison of clinical data in different groups in HCC patients with PVTT

These data are shown in Table 1, indicating that there were no statistical differences between groups.

Table 1 Comparison of several treatments groups for HCC with PVTT

	Group A (n = 18)	Group B (n = 18)	Group C (n = 74)	Group D (n = 29)	P
Tumor diameter					
<10 cm	2	5	39	14	NS
≥10 cm	16	13	35	15	
Tumor number					
Single	7	13	46	18	NS
≥2	11	5	28	11	
Encapsulation					
Well	1	3	16	5	NS
Poor	17	15	58	24	
PVTT in main trunk					
-	6	12	58	24	NS
+	12	6	16	5	

NS: no significance statistically.

Resection of HCC and catheterization after resection

Resection of left lateral lobe was performed in 18 cases, resection of left lateral lobe and partial right hepatic resection in 3, left hemihepatectomy in 40, left trilobectomy in 9, resection of hepatic medial lobe in 3, right hemihepatectomy in 4 and right partial hepatectomy in 34. PVI was followed by resection in 5 cases, HAI in 7 and HAI + PVI in 9. The catheters were cannulated into the hepatic artery and portal vein, and the ports were completely implanted beneath the abdominal wall.

Treatment methods for PVTT

For the tumor thrombi in left branch of portal vein, the right branch of portal vein was detached at first and then ligated by using a cotton ribbon or a fine rubber tube. The purpose was to prevent spreading of cancer cells of tumor thrombi from the left branch of portal vein to the right lobe during the resection or PVTT removal. After resection of left lateral lobe or left hemihepatectomy, the tumor thrombi were taken out from the stump of left branch of portal vein and irrigation was done with physiological saline, then the stump of portal vein was sutured and the ligature of the right branch of portal vein was released.

For tumor thrombi in the right branch of portal vein, the treatment for HCC with PVTT was similar to that in the left branch.

For the tumor thrombi in both branches of portal vein, the stump of one branch of portal vein was exposed after resection of liver cancer in left or right lobe, the hepatoduodenal ligament was ligated to block the blood flow entering the liver, and then the tumor thrombi were sucked or taken out through the stump.

For the tumor thrombi in the left or right branch of portal vein extending to the main trunk, the liver cancer in left or right lobe was removed first after detaching and ligating the right or left branch of portal vein, the stump of portal vein was clipped, then the main portal vein over the duodenum was gently held by the thumb and index finger. While the stump was being loosened, the tumor thrombi would flow out with the on-going portal blood flow.

For the tumor thrombi in both branches and the main trunk of portal vein, the tumor thrombi were sucked through the stump of one branch of portal vein, while pressing the opposite branch with an index finger for preventing dissemination of tumor cells. If the tumor thrombi were difficult to be sucked or taken out, the main portal vein should be detached. A longitudinal incision of 1.5 to 2.0 cm was made on anterior or right vascular wall of the main trunk of portal vein, and then the tumor thrombi were taken out directly. After the operation, B-mode ultrasonography was performed to make out whether the tumor thrombi had been

removed completely from the portal vein.

Chemotherapy after operation

Group D: After operation, 11 patients received 1 to 3 times of TAI or TACE (median 1.5 times) and other 21 patients received 2 to 4 times (median 2.5 times) of HAI and/or PVI or hepatic arterial chemoembolization (HAE). Group B: All patients were treated by HAI or HAE and/ or PVI 1 to 4 times (median 2 times). The dosages of chemotherapy in HAI or TAI and/or PVI were 5-fluorouracil (5-Fu) 1 000 mg, mitomycin (MMC) 12 to 20 mg and cisplatin or carborlatinum 80 mg, and lipoidal 5 mL in group D to 20 mL in group B of lipiodol was used in the TACE or HAE.

Statistical method

All the data were calculated with the digital Cox model and the limit of significant difference was $P<0.05$.

RESULTS

Curative effects of several therapeutic methods for HCC patients with PVTT

Among the series, the follow-up survey was lost in 8 cases. The median survival period of the 139 patients was 12 months, and the 1-, 3 and 5- year survival rates were 44.3%, 24.5% and 15.3% respectively. The median survival period and the 1, 3 and 5- year survival rates in different groups are shown in Table 2.

Table 2 Survival time and rates of patients with PVTT

	Group A (n = 18)	Group B (n = 18)	Group C (n = 74)	Group D (n = 29)
Median survival periods (months)	2.0	5.0	12.0	16.0
Survival rates				
1-year(%)	5.6	22.2	53.9[a2]	79.3[a1]
3-year (%)	0	5.6	26.9[a2]	38.9[a1]
5-year(%)	0	0	16.6[a2]	26.8[a1]

[a1]$P<0.05$, *vs* Group C, B and A; [a2]$P<0.05$, *vs* Group B and C.

Table 3 Survival time and rates of patients with the tumor thrombi in the main trunk and the first branch of portal vein

	Tumor thrombi in the main trunk				Tumor thrombi in the first branch			
	Gr.A (n = 12)	Gr.B (n = 6)	Gr.C (n = 16)	Gr.D (n = 5)	Gr.A (n = 6)	Gr.B (n = 12)	Gr.C (n = 58)	Gr.D (n = 24)
MST* (months)	2.0	5.5	8.0	16.0	2.0	5.0	13.0	16.5
Survival rate								
1-year(%)	8.3	33.3	29.4	80.0	0	16.7	59.7	79.2
3-year (%)	0	0	14.3	20.0	0	8.3	27.4	54.6
5-year(%)	0	0	11.1	0	0	0	8.8	42.0

* MST: median survival time.

Curative effects between PVTT in the main trunk and the first branch

Table 3 shows the results of multimodality treatment in patients with tumor thrombi in the main trunk and the first branch of portal vein. It indicates that the results of treatment in patients with PVTT in the first branch were better than that in patients with PVTT in the main trunk in groups C and D.

Curative effects and factors influencing the prognosis of the patients

after resection of HCC with PVTT (Table 4) The results of resection followed by chemotherapy or chemoembolization in patients with a diameter of tumor mass less than 10 cm, without tumor thrombi in the main portal vein were better than those in patients with diameter of more than 10 cm, with tumor thombi in the main portal vein and without chemotherapy or chemoembolization after resection.

Table 4 Curative effects and factors influencing the prognosis of patients after removal of HCC with PVTT

	Patients	1-year(%)	3-year(%)	5-year(%)	P
Removal of PVTT	103	61.7	32.3	22.4	
Tumor diameter					
<10 cm	53	64.2	41.5	27.0	0.014[a1]
⩾10 cm	50	59.7	25.2	19.3	
PVTT in main trunk					
-	82	66.3	36.9	26.1	0.027[a2]
+	21	42.9	14.3	8.6	
Encapsulation					
Well	21	75.6	30.9	8.6	0.928
Poor	82	58.4	32.9	26.7	
Chemotherapy or chemoembolization after operation					
No	74	53.9	26.9	16.6	0.012[a3]
Yes	29	79.3	38.9	26.8	
Tumor number					
Single	64	59.4	27.7	18.7	0.561
⩾2	39	65.4	38.7	27.7	

[a1]$P<0.05$ *vs* ⩾10 cm group; [a2]$P<0.05$ *vs* PVTT in main trunk (+) group; [a3]$P<0.05$ *vs* chemotherapy or chemoembolization after operation (yes) group.

DISCUSSION

HCC with tumor thrombi in the main trunk or the first branch of the portal vein is considered to be a late stage of liver cancer, lacking in ideal therapeutic measures. The treatment was often given up in former times. As the majority of the patients with HCC have been in advanced stage when first seen, a large probortion of the patients are associated with tumor thrombi in the main trunk or the first branch of the portal vein. Therefore, it is very important to explore effective therapeutic methods for HCC with PVTT and to raise the survival rates of these patients.

Until now, the treatments for HCC with PVTT are limited. In the medical literaures about the treatments of HCC with PVTT, there were the following methods: TACE, PVI, percutaneous ethanol injection in tumor thrombi, TACE + radiotherapy and surgical removal of tumor thrombi etc. Chung *et al*[4] reported that the 1 and 2-year survival rates were 30% and 18% respectively in 110 HCC patients with PVTT by TACE. Katsumori *et*

al[5] reported that the 3-year survival rate was 44% in 9 cases of tumor thrombi in the main portal vein by hepatic arterial chemotherapy through the implanted ports beneath the abdominal wall. It was also reported that the percutaneous ethanol injection in PVTT and TACE + radiotherapy gave satisfactory curative effects for PVTT[6-8]. There were only a few papers about the resection of HCC with removal of tumor thrombi in the main trunk or the first branch of the portal vein[9,10]. Yamaoka *et al*[9] adopted 5 resection modes for PVTT. The operative mortality of 29 patients with PVTT was 11%, and the 1, 2 and 3-year survival rates after operation were 52.2%, 23. 2%, and 11.6%, respectively. Four different procedures were used for the patients with PVTT in our series, and the results revealed poor efficacy in the conservative treatment group. The median survival time was only 2 months (group A). The best curative effect was in group of removal of HCC with PVTT + HAI and/or PVI or TACE (group D). The median survival time was 16 months and the 5-year survival rate was 26.8%. For this reason, if the tumors with PVTT are limited in the left or right lobe of liver and liver function as evaluated is able to tolerate the operation, we should adopt active therapeutic procedure. The best try should be made for removal of HCC with PVTT and hepatic regional chemotherapy or chemoembolization are periodically performed after operation. This procedure can further raise the treatment efficacy and prolong the survival for the HCC patients with PVTT.

The conservative treatment (only per oral chemotherapy or Chinese herbal decoctions) can not inhibit or kill cancer cells in the HCC patients with PVTT. Rapid progression of liver cancer will result in death in a short time due to liver failure or portal hypertension, with vigorous variceal bleeding. Among 18 patients undergoing conservative treatment, 12 cases died of vigorous bleeding of upper digestive tract within 3 months and only one case had the longest survival of 13 months. Although the survival time of 18 patients treated with HAL and/or HAI were shorter, the curative efficacy was better than that of conservative treatment group. The 1-year survival rate was 22.2%. Perhaps the periodical hepatic artery chemotherapy or chemoembolization can inhibit the tumor growth in various degrees and result in partial necrosis of tumor thrombi. The results of Katsumori[5] and Ando[11] also support this viewpoint. The result in the group of removal of HCC and PVTT (Group C) was evidently better than those of Groups A and B, the median survival time being 12 months and the 1, 3 and 5-year survival rates being 53.9%, 26.9%, 16.6% respectively. If HCC is limited to one lobe and the residual liver is estimated to be functionally efficient, we should first choose surgical resections for the patients with PVTT. The residual cancer and residual tumor thrombi are primary factors influencing the survival of the HCC patients with PVTT. According to patient's conditions, periodical HAI/PVI or TACE are effective methods to improve the survival rate after operation. In the group of HAI/PVI or TACE after resection of HCC with PVTT (group D), the median survival time was 16 months and the 1, 3, and 5-year survival rates were 79.3%, 38.9%, 26.8% respectively. The result was better than the other three groups. These results indicate that the best therapeutic method is sequential regional hepatic chemotherapy or TACE after surgical removal of HCC and PVTT. Table 3 shows curative effects in HCC patients with tumor thrombi in the main trunk of portal vein were inferior to those in patients with tumor thrombi in the first branch. The tumor thrombi in the main trunk represent the disease in advanced stage, which is often accompanied with tumor thrombi in both branches and disseminated foci in the opposite side of liver. Moreover, the resection of thrombi in the main trunk of portal vein may lead to cancer cell dissemination or incomplete extermination and rapid formation of thrombi in the main trunk after operation. The above factors cause the poor efficacy for HCC patients with tumor thrombi in the main trunk of portal vein, and poor quality of life than those with tumor thrombi in the first branch.

It has been convinced that the factors influencing curative effects for HCC with PVTT such as location of tumor thrombi (in the main trunk or the first branch of portal vein), tumor size and regional hepatic chemotherapy, etc. To our experience, the treatment methods for removal of tumor thrombi are closely related to the efficacy. Before operation, we must find out the scope of tumorthrombi with ultrasonography, CT or magnetic resonance angiography (MRA). During resection, we should block the blood flow of portal vein into liver or blood flow of the opposite branch, suck the tumor thrombi completely as far as possible and not break it. Then, we scrape off with curet the residual tumor thrombi attached on the vascular wall, and perform repeated irrigation and exsuction with physiological saline. Furthermore, anticoagulant injections through the portal vein during several postoperative days may also be an effective procedure to prevent and reduce the rapid recurrence of thrombi in the portal vein[12,13].

The therapeutic methods for HCC with PVTT are still at the investigative stage. Such patients occupy a considerable proportion in the liver cancer clinic. As PVTT is an important factor resulting in intrahepatic metastasis and recurrence after operation, it will be very valuable to study the mechanism of the PVTT formation in HCC patients and to explore more effective treatment measures for prolonging survival and improving their quality of life.

REFERENCES

1 Mitsunobu M, Toyosaka A, Oriyama T, Okamoto E, Nakao N. Intrahepatic metastases in hepatocellular carcinoma: the role of the portal vein as an efferent vessel. *Clin Exp Metastasis*, 1996; 14:520-529

2 Yu YQ, Xu DB, Zheng YX, Zhang BH. Resection of hepatocellular carcinoma with tumor thrombi for the patients with hepatocellular carcinoma-report of 25 cases. *Zhongguo Shiyong Waike Zazhi*, 1994;14:18-19

3 Pirisi M, Avellini C, Fabris C, Scott C, Bardus P, Soardo G, Beltrami CA, Bartoli E. Portal vein thrombosis in hepatocellular carcinoma: age and sex distribution in an autopsy study. *J Cancer Res Clin Oncol*, 1998;124:397-400

4 Chung JW, Park JH, Han JK, Choi BI, Han MC. Hepatocellular carcinoma and portal vein invasion: results of treatment with transcatheter oily chemoembolization. *Am J Roentgenol*, 1995;165:315-321

5 Katsumori T, Fujita M, Takahashi T, Satoh O, Ichijima S, Nakamura T, Morishita H, Ohno K, Nakano Y, Maeda T. Effective segmental chemoembolization of advanced hepatocellular carcinoma with tumor thrombus in the portal vein. *Cardiovasc Intervent Radiol*, 1995;18:217-221

6 Livraghi T, Grigioni W, Mazziotti A, Sangalli G, Vettori C. Percutaneous alcohol injection of portal thrombosis in hepatocellular carcinoma: a new possible treatment. *Tumori*, 1990;76:394-397

7 Chen SC, Lian SL, Chang WY. The effect of external radiotherapy in treatment of portal vein invasion in hepatocellular carcinoma. *Cancer Chemother Pharmacol*, 1994;33:S124-127

8 Raoul JL, Guyader D, Bretagne JF, Heautot JF, Duvauferrier R, Bourguet P, Bekhechi D, Deugnier YM, Gosselin M. Prospective randomized trial of chemoembolization versus intra-arterial injection of ^{131}I-labeled-iodized oil in the treatment of hepatocellular carcinoma. *Hepatology*, 1997;26:1156-1161

9 Yamaoka Y, Kumada K, Ino K, Takayasu T, Shimahara Y, Mori K, Tanaka A, Morimo to T, Taki Y, Washida M, Manaka D, Hayashi M, Fujita T, Ozawa K. Liver resection for hepatocellular carcinoma (HCC) with direct removal of tumor thrombi in the main portal vein. *World J Surg*, 1992;16:1172-1177

10 Tanaka A, Morimoto T, Yamaoka Y. Implications of surgical trea tment for advanced hepatocellular carcinoma with tumor thrombi in the portal vein. *Hepatogastroenterology*, 1996;43: 637-643

11 Ando E, Yamashita F, Tanaka M, Tanikawa K. A novel chemotherapy for advanced hepatocellular carcinoma with tumor thrombosis of the main trunk of the portal vein. *Cancer*, 1997;79: 1890-1896

12 Gurgey A, Buyukpamukcu M, Baskut C, Yalcin B, Gogus S.Portal vein thrombosis in association with factor V Leiden mutation in a patient with hepatocellular carcinoma. *Med Pediatr Oncol*, 1997; 29:224-225

13 Engelberg H. Actions of heparin that may affect the malignant process. *Cancer*, 1999;85:257-272

Edited by Pan BR
proofread by Ma JY

P.O.Box 2345 Beijing 100023, China
Fax. 0086·10·65891893 Tel. 0086·10·65897901
E-mail.wcjd@public.bta.net.cn www.wd.org.cn

World J Gastroentero, 2001 April; 7(1):33 - 36
World Journal of Gastroenterology
Copyright©2001 by the WJG Press ISSN 1007 - 9327

Effect of phosphorylation of MAPK and Stat3 and expression of c-fos and c-jun proteins on hepatocarcinogenesis and their clinical significance

De Yun Feng, Hui Zheng, Yi Tan and Rui Xue Cheng

Subject headings liver neoplasms; mitogen-activated protein kinases; signal transduction; trans-activators; oncogenes; immunohistochemistry; precancerous conditions

Feng DY, Zheng H, Tan Y, Cheng RX. Effect of phosphorylation of MAPK and Stat3 and expression of c-fos and c-jun proteins on hepatocarcinogenesis and their clinical significance. ***World J Gastroenterol***, 2001;7(1):33-36

Abstract

AIM To study the effect of phosphorylation of MAPK and Stat3 and the expression of c-fos and c-jun proteins on hepatocellular carcinogenesis and their clinical significance.

METHODS SP immunohistochemistry was used to detect the expression of p42/44^{MAPK}, p-Stat3, ca2fos and c-jun proteins in 55 hepatocellular carcinomas (HCC) and their surrounding liver tissues.

RESULTS The positive rates and expression levels of p42/44^{MAPK}, p-Stat3, c-fos and c-jun proteins in HCCs were significantly higher than those in pericarcinomatous liver tissues (PCLT). A positive correlation was observed between the expression of p42/44^{MAPK} and c-fos proteins, and between pa2Stat3 and c-jun, but there was no significant correlation between p42/44^{MAPK} and p-Stat3 in HCCs and their surrounding liver tissues.

CONCLUSION The abnormalities of Ras/Raf/MAPK and JAKs/Stat3 cascade reaction may contribute to malignant transformation of hepatocytes.Hepatocytes which are positive for p42/44^{MAPK}, c-fos or c-jun proteins may be potential malignant pre-cancerous cells. Activation of MAPK and Stat3 proteins may be an early event in hepatocellular carcinogenesis.

Department of Pathology, Hunan Medical University, Changsha 410078, Hunan Province, China
New England Biolab, MA, USA
Dr. De Yun Feng, graduated from Hunan Medical University as postgraduate in 1991, now associate professor of pathology, specialized in hepatic pathology, having 21 papers published.
Supported by New England Biolab, MA, USA.
Correspondence to: Dr. De Yun Feng, Department of Pathology, Hunan Medical University, Changsha 410078, Hunan Province, China
Tel. 0086-731-4805407
Email. cslj4841401@public.cs.hn.cn
Received 2000-09-21 **Accepted** 2000-10-29

INTRODUCTION

The regulation of cellular mitogenesis and proliferation under normal circumstances are dependent on a number of separate, yet integrated, signaling pathways responsible for the transduction of extracellular signals to the cell nucleus[1-3]. Similar to other tumorigenic cells, hepatocellular carcinoma (HCC) is characterized by the imbalance of the normal growth-promoting and growth-arresting signal transduction cascade reaction, the net result of which leads to uncontrolled hepatocyte growth [1,2]. Mitogen-activated protein kinase (MAPK) and signal transducer and activator of transcription 3 (Stat3) are important molecules in signal transduction cascades, which take part in cellular physiological growth, development, mitogenesis and differentiation, and play key roles in cellular malignant transformation[4,5]. In order to study the function of signal transduction cascade in hepatocarcinogenesis, the phosphorylation of MAPK (p42/44 MAPK, Erk1/Erk2) and Stat3 (p-Stat3), and the expression of c-fos and c-jun proteins were investigated by immunohistochemical method in HCCs and their surrounding liver tissues.

MATERIALS AND METHODS

Tissue samples

Fifty-five HCCs with pericarcinomatous tissue (PCLT) and 5 normal liver tissues were obtained by surgical resection in Xiang Ya Hospital and the Affiliated Second Hospital of Hunan Medical University, Changsha, People's Republic of China. Of 55 HCC patients, 43 were men and 12 women. The age ranged from 36 to 69 years (mean, 51.8 years). The tumor sizes were less than 3cm in diameters in 3 cases, 2.1 cm-5 cm in 32 cases, 5.1 cm-10 cm in 18, and larger than 10 cm in 2 cases. All patients were HBsAg negative. Remote metastasis was not found, and preoperative radiological or chemical therapy was nor performed in all patients. All HCCs and PCLTs were fixed in 10% formalin and embedded in paraffin. Five μm serial sections were cut. According to Edmondson's criteria[6], 10 HCCs were grade I, 21 grade II, 17 grade III, and 7 grade IV. Thirty-eight atypical hyperplasia cases were observed in 55 PCLTs.

Reagents

p42/44 MAPK(Erk1/Erk2, Thr202/Tyr204) and p-Stat3(Ser727) MAbs, were used to detect the

phosphorylation of MAPK and Stat3, and S-P detection kit were kindly donated by New England Biolab, USA. Anti-c-fos and anti-c-jun protein MAbs were purchased from GIB Com (Beijing, China).

Methods

Immunohistochemical staining Five μm tissue sections were deparaffinized, washed in 0.05 M PBS, and treated with 2% H_2O_2 for 20 min. According to the SP method, the tissues were detected with immunohistochemical technique. PBS was used as substitutes of MAbs for negative control groups[7].

Histological assessment Semi-quantity analysis was made as Formowitz described[8].

Statistical analysis

The difference between each group was analyzed by Chi-Square test and correlativity.

RESULTS

Expression of p42/44^{MAPK} and p-Stat3 proteins in HCCs, PCLTs and normal liver tissues

p42/44^{MAPK} was negative in normal liver tissues. The positive rate of p42/44^{MAPK} in HCCs (87.3%, 48/55) was significantly higher than that in PCLTs (32.7%, 18/55, $P<0.01$) (Figure 1). Positive signals were mainly located in the nucleus. The distribution of positive cells for p42/44^{MAPK} was clustered and/or diffused in HCCs (Figure 2), and scattered in PCLTs, but also clustered in atypical hyperplasia regions of some PCLTs near cancer tissues. The expression level of p42/44^{MAPK} in HCCs was higher than that in PCLTs ($P<0.01$), but it was not correlated with the differentiation degree of cancer cells (Table 1). Positive signals of p-Stat3 were of nuclear-type. Of 9 normal liver tissues, 1 case was p-Stat3 positive. The positive rate of p-Stat3 in HCC (74.5%, 41/55) was significantly higher than that in PCLTs (23.6%, 13/55) ($P<0.01$). The p-Stat3 positive cells were clustered in HCC (Figure 3), and scattered in PCLTs. The expression intensity of p-Stat3 in HCCs was also higher than that in PCLTs ($P<0.01$), but it was not correlated with differentiation degree of cancer cells ($P>0.05$) (Table 1).

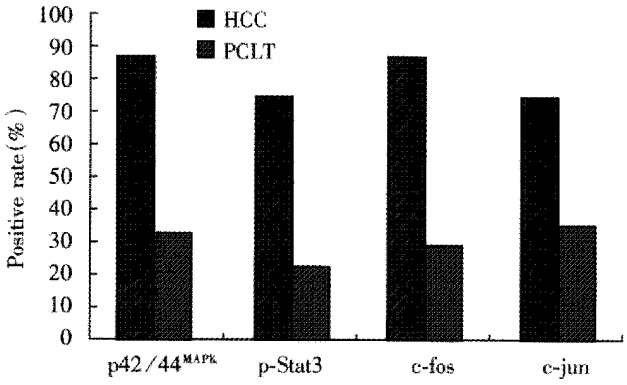

Figure 1 The positive rates of p42/44^{MAPK}, p-Stat3, c-fos and c-jun proteins in HCCs and PCLTs.

Table 1 Expressions of p42/44^{MAPK}, p-Stat3, c-fos and c-jun proteins in HCCs, PCLTs and normal liver tissues

Groups	No	p42/44^{MAPK}				p-Stat3				c-fos				c-jun			
		-	+	++	+++	-	+	++	+++	-	+	++	+++	-	+	++	+++
Normal	9	9	0	0	0	8	1	0	0	9	0	0	0	9	0	0	0
PCLT	55	37	9	7	2	42	4	7	2	36	12	7	0	39	13	3	0
HCC																	
Grade I	10	1	4	4	1	5	1	2	2	8	1	1	0	4	4	1	1
Grade II	21	3	6	12	0	2	12	5	2	3	12	4	2	1	15	4	1
Grade III	17	1	9	2	5	4	3	6	4	2	4	8	3	2	8	5	2
Grade IV	7	2	1	3	1	3	1	3	0	0	1	2	4	0	0	2	5

Expression of c-fos and c-jun proteins in HCCs, PCLTs and normal liver tissues

The expression of c-fos and c-jun proteins was not found in normal liver tissues. The rates of c-fos and c-jun protein expression in HCCs (76.4%, 87.3%) were significantly higher than those in PCLTs (34.5%, 29.1%) ($P<0.01$). Their positive signals were mainly of nuclear type in HCCs (Figures 4, 5) and nuclear-plasmic type in PCLTs. The positive intensity in HCCs was distinctly higher than that in PCLTs, and related to the differentiation degree of HCC cells. The poorer the differentiation of HCC cells, the stronger the expression of c-fos and c-jun proteins. The distribution of positive cells for c-fos or c-jun protein in HCCs was diffuse, and scattered in PCLTs.

Relativity of expression intensities of p42/44^{MAPK} and p-Stat3 in HCCs and PCLTs

No relationship was found between p42/44^{MAPK} and p-Stat3 signal intensities in HCCs and PCLTs (r = -0.167 and 0.0844, $P>0.05$).

Relationship between expression strength of p42/44^{MAPK} and c-fos proteins, between p42/44^{MAPK} and c-jun in HCCs and PCLTs (Table 2)

In HCCs, the expression of p42/44^{MAPK} was positively related to the expression intensities of c-fos and c-jun proteins. The stronger the expression of p42/44^{MAPK}, the higher the signal intensities of c-fos and c-jun proteins. In PCLTs, there was a positive relationship between the expression of p42/

44^{MAPK} and c-fos proteins, and no relationship between the expression of p42/44^{MAPK} and c-jun proteins.

Table 2 Relationship in expressive strengthes of p42/44^{MAPK}, c-fos and c-jun proteins between HCCs and PCLTs

Groups	*r*	*P*
HCC		
p42/44^{MAPK}/c-fos	0.44835	<0.01
p42/44^{MAPK}/c-jun	0.3054	<0.01
PCLT		
p-MAPK/c-fos	0.9433	<0.01
p-MAPK/c-jun	0.1472	>0.05

Relationship between expression strength of p-Stat3 and c-fos proteins, between p-Stat3 and c-jun in HCCs and PCLTs (Table 3)

In HCCs, the expression of p42/44^{MAPK} was significantly positively related to expression intensities of c-fos and c-jun proteins. In PCLTs, there was a positive relationship between the expression of p-Stat3 and c-jun proteins, whereas no relationship between the expression of p-Stat3 and c-fos proteins was observed.

Table 3 Relationship in expression strength of p-Stat3, c-fos and c-jun proteins between HCCs and PCLTs

Groups	*r*	*P*
HCC		
p-Stat3/c-fos	0.3967	<0.01
p-Stat3/c-jun	0.5444	<0.01
PCLT		
p-Stat3/c-fos	0.0499	>0.05
p-MAPK/c-jun	0.3596	<0.01

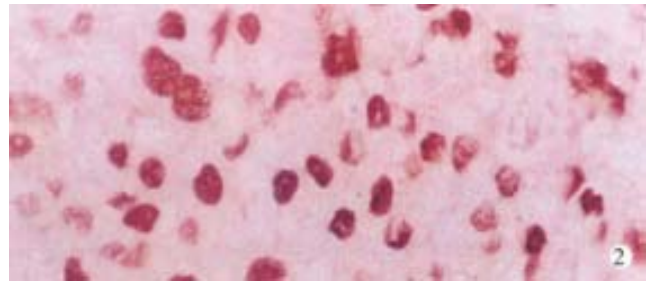

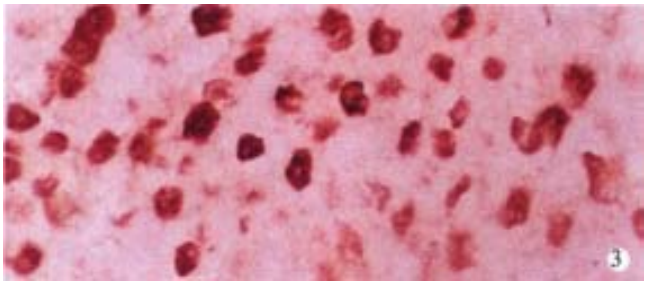

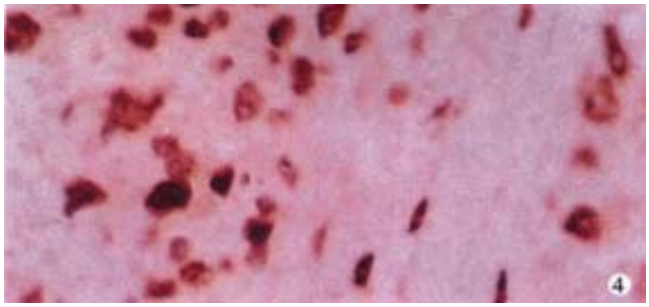

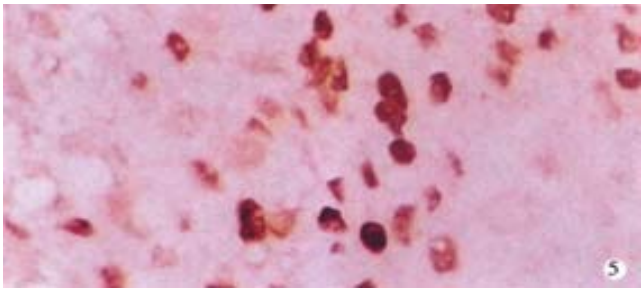

Figure 2 Localization of positive signal and distribution of positive cells for p42/44^{MAPK} protein in HCC. SP×400
Figure 3 Localization of positive signal and distribution of positive cells for Stat3 protein in HCC. SP×400
Figure 4 Positive expression of c-fos protein in HCC. SP×400
Figure 5 Positive expression of c-jun protein in HCC. SP×400

DISCUSSION

Ras/Raf/MAPK and Janus protein tyrosine kinases (JAKs)/Stat3 cascades are two major signaling pathways of growth factors and cytokines[1,2,4,5,9,10]. The former involves transient formation of ras-GTP and activation of raf kinase at the cell membrane to activate MAPK kinase which in turn activates MAPK through dual phosphorylation on threonine and tyrosine residues[11-14]. Activated MAPK then transduces into the nucleus and phosphorylates the ternary complex factor TCF which activates the expression of immediate-early genes, such as c-fos and egr-1[14,15]. There have been a few reports concerning MAPK activation in human cancers[1,2,16-21]. It was reported that MAPK activity level in HCC was significantly higher than that in the adjacent non-cancerous lesions[1,2,18]. Our results showed that the positive signal of p42/44^{MAPK} was almost located in the nucleus, indicating that the detected MAPK is activated MAPK. The positive rate and intensity of p42/44^{MAPK} in HCCs were all distinctly higher than those in PCLTs, which is consistent with the results reported in literature. Statistical analysis found that the expression intensity of p42/44^{MAPK} in HCCs was significantly positively correlated with the expression strength of immediate-early genes (c-fos and c-jun), and the expressive intensity of p42/44^{MAPK} in PCLTs was also significantly positively correlated with the expression strength of c-fos. These findings further suggest that the imbalance of Ras/Raf/MAPK cascade components may play a key role in hepatocarcinogenesis.

JAKs associate with cytokine receptors which lack intrinsic tyrosine kinase activity and become activated upon cytokine stimulation. Activated JAKs activate Stat3 through phosphorylation of Tyr-705[22]. Phosphorylated Stat3 (p-Stat3) then

translocates into the nucleus and binds to DNA response elements and transactivates gene expression [14,23,24]. The data presented here showed that the positive signals of p-Stat3 were mainly of nuclear type, and the positive rate and strength of p-Stat3 in HCCs were significantly higher than those in PCLTs, and the signal intensity of p-Stat3 was positively correlated with the expression level of the c-jun protein in HCCs and PCLTs. These results suggest that JAKs signaling cascade may also contribute to malignant transformation of hepatocytes besides Ras/Raf/MAPK signaling pathway in hepatocellular carcinogenesis.

Results in literature were inconsistent on the correlation between Ras/Raf/MAPK and JAKs/Stat3 pathways in tumor genesis and development[14,25,26]. Chung *et al*[25] reported that MAPK activated Stat3 through phosphorylation of Ser-727. Leaman *et al*[26] found that JAKs may not be required for the activation of Stat3 by some growth factors such as EGF and PDGF. As the MAPK and Stat3 become activated upon many growth factors and cytokines, it was considered that MAPK may promote activation of Stat3, but in Jain's results MAPK may inhibit transcription activity of Stat3[14]. Our data indicated that there was no correlation between expression intensities of $p42/44^{MAPK}$ and p-Stat3 in HCCs and PCLTs. The Stat3 phosphorylation is a complex event. Because the Stat3 can be phosphorylated through different protein kinases and pathways, detecting Stat3 at different phases of signaling cascades may produce entirely contradictory results about Stat3 activity. We think that both Ras/Raf/MAPK and JAKs/Stat3 pathways may play important roles in hepatocellular carcinogenesis, but their detailed mechanisms need to be further studied.

Up to now, the characteristics of pericar-cinomatous hepatocytes has not been clear[27]. The results showed that pericarcinomatous hepatocytes, especially proliferative or atypical hyperplasia hepatocytes, strongly express $p42/44^{MAPK}$, p-Stat3, c-fos and c-jun proteins, which suggest that activation of MAPK and Stat3 may be an early event in hepatocellular carcinogenesis. It also implys that the hepatocytes which express $p42/44^{MAPK}$ and/or p-Stat3 may be potentially malignant precancerous cells. Therefore, in order to avoid local recurrence, the operative range should be as extended as possible in the resection of HCCs.

REFERENCES

1 Ito Y, Sasaki Y, Horimoto M, Wada S, Tanaka Y, Kasahara A, Ueki T, Hirano T, Yamamoto H, Fujimoto J, Okamoto E, Hayashi N, Hori M. Activation of mitogen-activated protein kinases/extracellular signal-regulated kinases in human hepatocellular carcinoma. *Hepatology*, 1998;27:951-958

2 Schmidt CM, McKillop IH, Cahill PA, Sitzmann JV. Increased MAPK expression and activity in primary human hepatocellular carcinoma. *Biochem Biophy Res Com*, 1997;236:54-58

3 Gu SQ, Liang YY, Fan LR, Li BY, Wang DS. Co-regulative effects of the cAMP/PKA and DAG/PKC signal pathways on human gastric cancer cells during differentiation induced by traditional Chinese medicines. *China Natl J New Gastroen terol*, 1997;3:50-53

4 Hill CS, Treisman R. Transcriptional regulation by extracellular signals: mechanisms and specificity. *Cell*, 1995;80:199-211

5 Kim H, Baumann H. Dual signaling role of the protein tyrosine phosphatase SHP-2 in regulating expression of acute-phase plasma proteins by interleukin- 6-cytokine receptors in hepatic cells. *Mol Cell Biol*, 1999;19:5326-5338

6 Edmondson HA, Sterner PE. Primary carcinoma of liver study of 100 cases among 48900 necropsies. *Cancer*, 1954;7:462-503

7 Feng DY, Cheng RX, Peng Y, Zheng H, Yan YH. Effect of HCV NSa-3 protein on P53 protein expression in hepatocarcinogenesis. *World J Gastroenterol*, 1999;5:45-46

8 Fromowitz FB, Viola MV, Chao S, Oravez S, Mishriki Y, Finkel G, Grimson R, Lundy J. ras p21 expression in the progression of breast cancer. *Hum Pathol*, 1987;18:1268-1275

9 Yu CL, Jove R, Burakoff SJ. Constitutive activation of the Janus kinase-STAT pathway in T lymphoma overexpressing the Lck protein tyrosine kinase. *J Immunol*, 1997;159:5206-5210

10 Yu CL, Burakoff SJ. Involvement of proteasomes in regulating Jak-STAT pathways upon interleukin-2 stimulation. *J Biol Chem*, 1997;272:14017-14020

11 Leevers SJ, Paterson HF, Marshall CJ. Requirement for Ras in Raf activation is overcome by targeting Raf to the plasma membrane. *Nature*, 1994;369:411-414

12 Marshall CJ. MAP kinase kinase kinase, MAP kinase kinase and MAP kinase. *Curr Opin Genet Dev*, 1994;4:82-89

13 Stokoe D, Macdonald SG, Cadwallader K, Symons M, Hancock JF. Activation of Raf as a result of recruitment to the plasma membrane [see comments]. *Science*, 1994;264:1463-1467

14 Jain N, Zhang T, Fong SL, Lim CP, Cao X. Repression of Stat3 activity by activation of mitogen-activated protein kinase (MAPK). *Oncogene*, 1998;17:3157-3167

15 Treisman R. Journey to the surface of the cell: Fos regulation and theSRE. *EMBO J*, 1995;14:4905-4913

16 Hoshino R, Chatani Y, Yamori T, Tsuruo T, Oka H, Yoshida O, Shimada Y,Arii S, Wada H, Fujimoto J, Kohno M. Constitutive activation of the 41-/43-kDa mitogen-activated protein kinase signaling pathway in human tumors. *Oncogene*, 1999;18:813-822

17 Sivaraman VS, Wang H, Nuovo GJ, Malbon CC. Hyperexpression of mitogen-act ivated protein kinase in human breast cancer. *J Clin Invest*, 1997;99:1478-1483

18 Toyoda M, Hashimoto N, Tokita K, Goldstein BJ, Yokosuka O, Kanatsuka A, Suzuki Y, Saito Y. Increased activity and expression of MAP kinase in HCC model rats induced by 3 2methyl-4-dimethylamino-azobenzene. *J Hepatol*, 1999;31:725-733

19 McKillop IH, Schmidt CM, Cahill PA, Sitzmann JV. Altered expression of mitogen-activated protein kinases in a rat model of experimental hepatocellular carcinoma. *Hepatology*, 1997;26: 1484-1491

20 Arbuthnot P, Capovilla A, Kew M. Putative role of hepatitis B virus X protein in hepatocarcinogenesis: effects on apoptosis, DNA repair, mitogen-activated protein kinase and JAK/STAT pathways [see comments]. *J Gastroenterol Hepatol*, 2000;15:357-368

21 Ostrowski J, Woszczynski M, Kowalczyk P, Wocial T, Hennig E, Trzeciak L, Janik P, Bomsztyk K. Increased activity of MAP, p70S6 and p90rs kinases is associated with AP-1 activation in spontaneous liver tumours, but not in adjacent tissue in mice. *Br J Cancer*, 2000;82:1041-1050

22 Kaptein A, Paillard V, Saunders M. Dominant negative stat3 mutant inhibits interleukin-6-induced Jak-STAT signal transduction. *J Biol Chem*, 1996;271:5961-5964

23 Darnell JE Jr, Kerr IM, Stark GR. Jak-STAT pathways and transcriptional activation in response to IFNs and other extracellular signaling proteins. *Science*, 1994;264:1415-1421

24 Ihle JN. STATs: signal transducers and activators of transcription. *Cell*, 1996;84:331-334

25 Chung J, Uchida E, Grammer TC, Blenis J. STAT3 serine phosphorylation by ERK-dependent and -independent pathways negatively modulates its tyrosine phosphorylation. *Mol Cell Biol*, 1997;17: 6508-6516

26 Leaman DW, Pisharody S, Flickinger TW, Commane MA, Schlessinger J, Kerr IM, Levy DE, Stark GR. Roles of JAKs in activation of STATs and stimulation of c-fos gene expression by epidermal growth factor. *Mol Cell Biol*, 1996;16:369-375

27 Feng DY, Cheng RX, Yan YH. Comparative study of expression of p21 and c-myc protein in hepatocellular carcinoma with pericarcinomatous liver tissue. *Hunan Yike Daxue Xuebao*, 1997;22: 310-312

Edited by Ma JY

P.O.Box 2345 Beijing 100023, China
Fax. 0086·10·65891893 Tel. 0086·10·65897901
E-mail.wcjd@public.bta.net.cn www.wd.org.cn

World J Gastroentero, 2001 April; 7(1):37 - 41
World Journal of Gastroenterology
Copyright©2001 by the WJG Press ISSN 1007 - 9327

Expression changes of activin A in the development of hepatic fibrosis

Xin Huang[1], Ding Guo Li[1], Zhi Rong Wang[1], Hong Shan Wei[1], Ji Lin Cheng[1], Yu Tao Zhan[1], Xin Zhou[1], Qin Fang Xu[1], Xin Li[2] and Han Ming Lu[1]

Subject headings liver cirrhosis; transforming growth factor beta; carbon tetrachloride; polymerase chain reaction; immunohistochemistry; RNA, messenger

Huang X, Li DG, Wang ZR, Wei HS, Cheng JL, Zhan YT, Zhou X, Xu QF, Li X, Lu HM. Expression changes of activin A in the development of hepatic fibrosis. ***World J Gastroentero***, 2001;7(1):37-41

Abstract

AIM To examine the expression of activin A, a member of the transforming growth factor (TGF-β) superfamily, recently has been reported to beoverexpressed in liver cirrhosis, in the course of carbon tetrachloride-induced rat hepatic fibrosis.

METHODS Hepatic fibrosis was induced in rats by subcutaneous injections of 40% carbon tetrachloride oily solution for a period of 1 to 7 weeks. At the end of 1, 2, 3, 4, 5, 6 and 7 weeks after carbon tetrachloride injections, the rats were killed in group (6-10 rats each time) for study. The activin A messenger RNA expression and its protein localization were assessed by semi-quantitative reverse transcription polymerase chain reaction (RT-PCR) and immunohistochemistry.

RESULTS The normal rat liver expressed activin A mRNA and protein, and its expression was transiently decreased and became undetectable after carbon tetrachloride injections for 2 or 3 weeks and then increased gradually. After injection of carbon tetrachloride for 6 and 7 weeks, activin A mRNA and protein expressions were significantly enchanced in rat liver. Compared with that of the normal rat liver. Activin A mRNA expression levels in rats receiving carbon tetrachloride injections for 6 and 7 weeks were 1.6 and 2.2 times that of those in normal rat liver respectively (0.456 ± 0.094 *vs* 0.286 ± 0.0670, *P*<0.01; 0.620 ± 0.134 *vs* 0.286 ± 0.0670, *P*<0.01). Immunohistochemistry showed that activin A expressed in hepatocytes of normal liver, and its expression was decreased in rats receiving carbon tetrachloride for 2 or 3 weeks. Compared with normal liver, activin A expression distribution mode changed in fibrotic liver, being increased significantly in hepatocytes around fibrotic areas.

CONCLUSION Activin A expression was increased in late stage of hepatic fibrosis, and this may be involved in hepatic fibrosis formation in this period.

[1]Xinhua Hospital, Shanghai Second Medical University, Shanghai 200092, China
[2]Ninth Hospital, Shanghai Second Medical University, Shanghai 200011, China
Dr. Xin Huang, is studying in Shanghai Second Medical University Affiliated Xinhua Hospital for doctor degree, specialized in hepatic pathophysiology, having 3 papers published.
Correspondence to: Dr. Xin Huang, Gastroenterology Department, Xinhua Hospital, Shanghai Second Medical University, Shanghai 200092, China
Tel. 0086-21-65790000 Ext. 5319, Fax. 0086-21-55571294
Received 2000-07-19 **Accepted** 2000-10-19

INTRODUCTION

Many researchers have tried to elucidate the pathogenesis of hepatic fibrosis[1-11]. Multiple studies have proved that cytokines play a vital role in this process, especially transforming growth factor β (TGF-β) superfamily[12-21]. Activins are newly found multifunctional proteins that belong to the TGF-β superfamily[22]. There are three kinds of activins, A(βAβA), B(βBβB) and AB(βAβB), which are hetero/homodimers closely related β-subunits of inhibin (βA and βB)[23]. Discovered by virtue of their capacity to stimulate production of follicle-stimulated hormone (FSH) from pituitary gland, activins have widespread anatomical distribution and are implicated in the regulation of many biological processes, including proliferation and differentiation of various types of cells[24]. In liver, ACT A inhibits growth of heptocytes and induces apoptosis, but promotes mesenchymal proliferation and extracellular matrix (ECM) production, and these effects are similar to those of TGF-β[25-27]. Activins and TGF-β may implicate in development of hepatic fibrosis jointly. Sugiyama *et al*[27] have demonstrated that activin A expression was significantly enhanced in cirrhotic and fibrotic rat livers induced by dimethylnitrosamine (DMN) and porcine serum. However, there has been no consensus of opinion about activin expression changing mode and its cell origins in fibrotic rats liver yet, for some researchers have got different results from those of Sugiyama. By means of RT-PCR and immunohistochemstry, we have examined the activin A expression mode in carbon tetrachloride (CCl_4) induced fibrotic rat liver.

MATERIALS AND METHODS

Animals

Adult male Sprague Dawley rats, weighing 180 g-210 g, were obtained from Shanghai Experimental Animal Institute of the Chinese Academy of Sciences. Hepatic fibrosis rat model was created by subcutaneous injections of CCl_4[28-36]. Altogether 72 rats were used. They were randomly divided into the normal control group (6 rats) and model group (64 rats). For the model group rats, CCl_4 olive solution (40% CCl_4) was injected subcutaneously at a dose of 0.4 mL/100 g twice a week. A double dose was used for the first injection. A same volume of saline was injected in normal control group animals. For study by lots every week (from the 1st to 7 th week), 72 hours after last injection of CCl_4, 6-10 model group rats were sacrificed. One portion of each liver was immediately frozen in liquid nitrogen for RNA extraction, and the remainder was fixed with 10%(vol/vol) formalin for van Gieson (VG) staining or immunostaining.

Immunohistochemistry

Deparaffinized 5 μm thick liver sections were washed three times with phosphate-buffered saline (PBS; pH 7.4), incubated in endogenous peroxidase blocking solution (Immunostain EliVision Kit, Maxim Biotech, Inc), and then treated with 0.01 M citrate buffer pH 6.0 for 10 minutes in a microwave oven at 650W. Non-specific-antibody binding was blocked by pretreatment with PBS containing 0.5% bovine serum albumin (fraction V powder, Sigma). Sections were then rinsed in PBS and incubated overnight at 4℃ with diluted monoclonal antibody against activin βA subunit (Serotic, UK) at 1: 100 in PBS followed by three washes in PBS containing 0.05% Tween-20. The steps were performed using Immunostain EliVision kit according to the manufacturer's instructions. Sections were stained with 3,3'-diaminobenzidine tetrahydrochloride (DAB) as a chromogen. The slide was rinsed with distilled water, counterstained with hematoxylin, dehydrated, air dried, and mounted. The negative control slides were treated with nonspecific mouse IgG. The sections were examined under light microscopy.

Preparation of RNA

Total RNA was extracted from liver tissues according to the guanidinium isothiocyanate single-step methods (Kit from Watson Biological Inc, Shanghai).The RNA concentration of each sample was estimated by measuring the absorbance at 260 nm.

Reverse transcription and polymerase chain reaction (PCR)

Reverse transcription (RT) was performed using RT kit from Bioneer. The 20 μL reaction contains total RNA 2 μg, and oligo$(dT)_6$ 12.5pmol (Sangon, Shanghai). The first-strand cDNA sample (2 μL) was added to 25 μL of a PCR reaction mixture containing 0.5 μM gene-specific primers, 2 mM $MgCl_2$, 0.2 mM dNTP, and 1.5 units Taq polymerase, 2.5 μL 10 × buffer. Activin βA[37] sense primer: 5'-cagtcgtggacggtgcagaagt-3'; antisense primer: 5'-gcctgcggtgaggatggtctt-3'; the predicted size of the amplification products was 474 bp. The glyceraldehyde-3-phosphate dehydrogenase (GAPDH) gene (house-keeper gene) sense primer [38]: 5'-catggtctacacgttccagt-3'; antisense primer: 5'-ggctaagcagttggtggtgc-3'; the 329 bp fragment amplification product was used as a positive control of the reverse-transcriptase receation and tissue mRNA integrity. Amplification conditions included initial denaturation for 5 minutes at 94℃, 30 cycles of amplification for activinβA and 28 cycles for GAPDH, with denaturation at 94℃ for 45 seconds, annealing at 60℃ for 45 seconds, and extension at 72℃ for 1 minute. PCR products were analyzed by electrophoresis through agarose gel(2% wt/vol) and visualized by ethidium bromide staining and ultraviolet illumination. The length of PCR products was measured by comparison with standard molecular-weight marker. The signal intensity of each band was normalized by comparing it with the intensity of GAPDH.

Statistical analysis

Results were expressed as mean ± SE. To compare the mean values, ANOVA analysis was applied. Differences were considered significant if $P<0.05$.

RESULTS

Van Gieson staining

Hepatic fibrosis gradually developed with increasing CCl_4 injections. After 6-7 weeks, VG staining showed that liver from most of model group animals were forming fake liver lobuli with reticulin fibers spreading radially between the portal tracts and central veins (Figure 1).

Immunohistochemistry

Activin βA subunit was detected in normal liver. Figure 2 shows that activinβA immunoreactivity was distributed within the lobuli and localized in parenchymal cells. More staining was found in hepatocytes around central veins. No staining was found in hepatocytes around portal tracts. After CCl_4 injection for 2-3 weeks, activin βA immunostaining was decreased but still detectable, and its distribution was changed, localizing mainly in hepatocytes around fibrotic areas (Figure 3). After CCl_4 injection for6-7 weeks, activinβA immunostaining was enhanced. Many hepatocytes around fibrotic areas (around portal tracts, fibrotic septa and central veins areas) were stained positive (Figures 4,5).

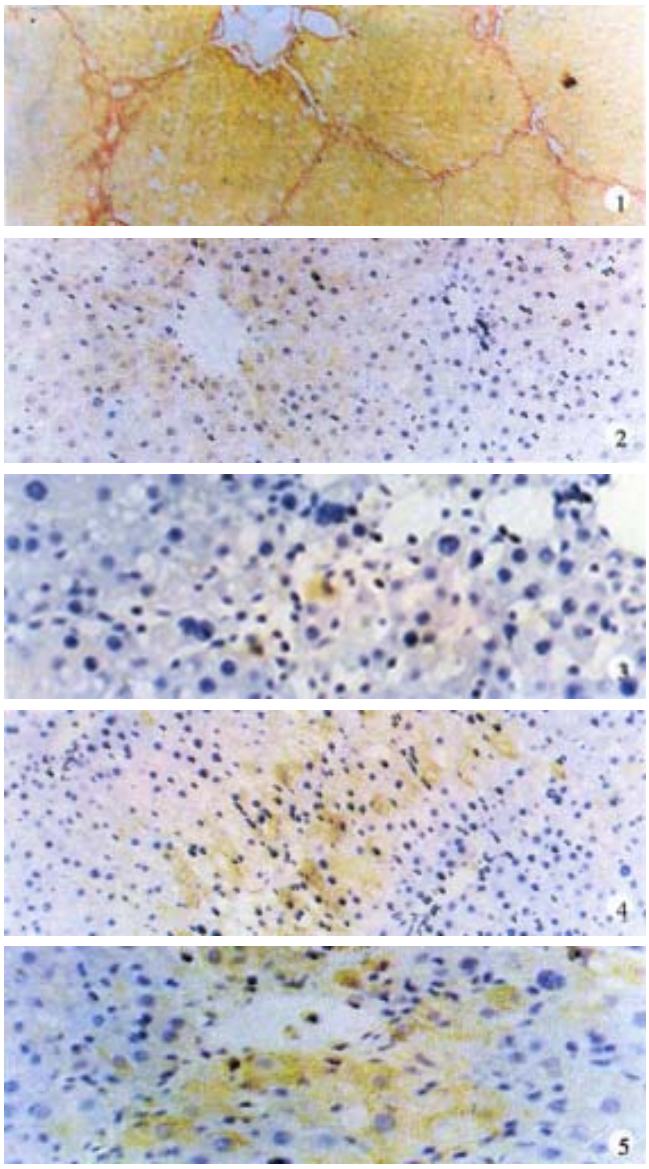

Figure 1 Fake lobuli formed after CCl_4 was injected for 7 weeks. VG staining, ×100

Figure 2 Normal rat liver activin βA immunostaining, immunoreactivity was detected in hepatocytes. DAB, ×100

Figure 3 Activin βA immunostaining after 3-week CCl_4 injections. DAB, ×400

Figure 4 Hepatocytes around connective septa were detected by immunostaining after 7 weeks' CCl_4 treatment. DAB, ×200

Figure 5 Hepatocytes around central veins by activin β immunostaining after 7-weeks CCl_4 treatment. DAB, ×400

PCR

ActivinβA mRNA subunit was detected in normal rat liver, but it became undetectable after CCl_4 was injected for 2-3 weeks. Four weeks after CCl_4 injections, activin βA mRNA levels increased gradually, and were significantly enhanced after 6 or 7 weeks when compared with normal rat liver ($P<0.01$) (Figures 6,7). Activin βA mRNA levels in rats treated with CCl_4 for 6 and 7 weeks were 1.6 and 2.1 times of those in normal rat liver respectively.

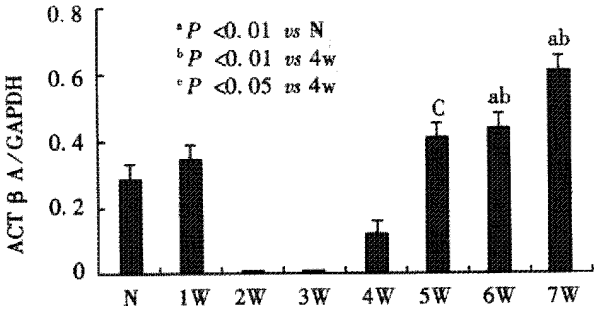

Figure 6 The mRNA expression of activin A at the different stages of CCl_4 induced hepatic fibrosis. N: normal, W: week, M: marker

Figure 7 A relative amount of activin βA mRNA were quantified using an image analyzer.
ᵃ$P<0.01$ *vs* N; ᵇ$P<0.01$ *vs* 4w; ᶜ$P<0.05$ *vs* 4w.
N: normal group, W: week

DISCUSSION

Liver cirrhosis is a final stage of various chronic liver diseases and is characterized by a marked deposition of extracellular matrix, combined with impared hepatic regeneration. Several cytokines are involved in the pathogenesis of this disease[39]. In particular, TGF-β1 is overexpressed in nonparenchymal cells of fibrotic liver of human or animals, and plays a pivotal role in the development of cirrhosis by stimulating fibroblast proliferation and ECM secretion[40-44]. Recent studies showed that activin may also be involved in the development of cirrhosis.

Activin A has mutiple effects including proliferation and differentiation of various types of cells[24]. In terms of its effects on hepatocytes, activin A inhibits DNA synthesis and induces apoptosis of hepatocytes[25,26,45]. In fibrotic or cirrhotic rat liver induced by CCl_4, De Bleser found that activin A disappeared in parenchymal cells, and it was expressed when the liver was normal. The normal hepatic stellate cells showed no activin A expression, but its expression was significantly enhanced when hepatic fibrosis had formed[17,46]. Subsequently, Sugiyama[27] found activin A expression was greatly increased in fibrotic rat liver induced by DMN and porcine serum, but it was in hepatocytes but not hepatic stellate cell that activin

A expression was significantly increased. Obviously, results from De Bleser and Sugiyama were not completely consistent with each other. Our research showed that activin A expression was increased in CCl_4-induced fibrotic rat liver, being localized in hepatocytes. These results were consistent with those of Sugiyama.

We had used the same hepatic fibrosis model as De Bleser's, but the results were different. This may be due to a difference in the period of model-making. We found that normal liver expressed activin A, but after injection of CCl_4 for 2-3 weeks, activin A mRNA became undetectable, although its protein could still be found. Four weeks later, activin A mRNA increased gradually. But it was not significantly increased until CCl_4 was injected for 6 or 7 weeks when hepatic fibrosis had formed completely. This means that most of livers have formed pseudo lobuli. Sugiyama also found that in the early period of hepatic fibrosis induced by DMN, the expression of activin β A mRNA was discreased transiently, and then increased gradually with lapse of time. However, the expression was enhanced continuously in porcine serum-induced cirrhosis. This difference may be due to serious hepatocytic damage caused by CCl_4, which is also found in the early stage of the development of DMN induced liver cirrhosis but not in porcine serum induced cirrhosis[47-50]. As activin A acts as an autocrine growth inhibitor of hepatocytes, this transient decrease in expression may promote hepatocytic regeneration. De Bleser reported that activin βA expression disappeared in parenchymal cells of CCl_4 induced cirrhosis, but we think that it might be a transient disappearance, for liver cirrhosis was not formed completely. In addition, De Bleser found that activin A expressed in activated hepatic stellate cells (HSC) of fibrotic liver, but according to our result, activin A immunostaining was mainly distributed in hepatocytes around fibrotic areas (Figures 4,5), a result also consistent with Sugiyama's reports. So it is worthy of further study to confirm whether HSC expresses activin A or not.

The expression of activin A protein was not complete in conformity with its mRNA. Its mRNA became undetectable after CCl_4 injections for 2 to 3 weeks, but activin A protein could be detected by immunohistochemistry. Sugiyama described similar phenomenon in DMN-induced cirrhosis. This may be because of the fact that the mRNA level was too low to be detected by our method. Of course, other reasons may exist and worth further studying.

In summary, our study shows that in CCl_4-induced rat cirrhosis, the expression of activin A is decreased transiently at first, and then increased gradually. Activin A may be involved in the late stage of the development of liver cirrhosis. Distribution of activin A also changes with the development of fibrosis, that is from hepatocytes around central veins to hepatocytes around fibrotic areas including central vein, connective septa and portal tracts.

REFERENCES

1 Yan JC, Liu JH, Ma Y. Vascular obstruction in pathogenesis of hepatitis B fibrosis. *Xin Xiaohuabingxue Zazhi*, 1997;5:647-649

2 Jia JB, Han DW, Xu RL, Gao F, Zhao LF, Zhao YC, Yan JP, Ma XH. Effect of endotoxin on fibronectin synthesis of rat primary cultured hepatocytes. *World J Gastroentero*, 1998;4:329-331

3 Liu CH, Hu YY, Wang XL, Liu P, Xu LM. Effects of salvianolic acid-A on NIH/3T3 fibroblast proliferation, collagen synthesis and gene expression. *World J Gastroenterol*, 2000;6:361-364

4 Chang XM, Xue H, Duan ZB, Feng XL, Jia AL. Diagnostic value of simutaneous determination of serum protocollagen III and hyaluronic acid in patients with chronic liver diseases. *Xin Xiaohuabingxue Zazhi*, 1994;2:223-224

5 Liu SR, Gu HD, Li DG, Lu HM. A comparative study of fat storing cells and hepatocytes in collagen synthesis and collagen gene expression. *Xin Xiaohuabingxue Zazhi*, 1997;5:761-762

6 Pan XF, Zhang CF, Qiu WW, Lu GQ, Zhou MW, Chang J, Ni Y, Li SQ, Han TQ. Alterations of serum laminin and hyaluronic acid in patients with chronic liver diseases. *Xin Xiaohuabingxue Zazhi*, 1996;4:373-374

7 Gao CF, Kong XT, Fan LY. Isolation, culture and identification of lipocytes and Kupffer cells in rats. *Xin Xiaohuabingxue Zazhi*, 1995;3:8-10

8 Yang SM, Fang DC, Feng HF, Chen GM, Gao LQ. Diagnostic value of serum prolidase, procollagen type III and hyaluronic acid levels for liver fibrosis. *Xin Xiaohuabingxue Zazhi*, 1995;3:27-28

9 Gu SW, Luo KX, Zhang L, Wu AH, He HT, Weng JY. Relationship between ductule proliferation and liver fibrosis of chronic liver disease. *Shijie Huaren Xiaohua Zazhi*, 1999;7:845-847

10 Yan JC, Chen WB, Liu JH, Ma Y, Xu CJ. Immunohistochemical studies on intrahepatic vascular proliferation in hepatitis B. *Huaren Xiaohua Zazhi*, 1998;6:780-782

11 Yan JC, Ma Y, Chen WB, Shun XH. Dynamic observation on liver fibrosis and cirrhosis of hepatitis B. *Huaren Xiaohua Zazhi*, 1998; 6:699-702

12 Ueki T, Kaneda Y, Tsutsui H, Nakanishi K, Sawa Y, Morishita R, Matsumoto K, Nakamura T, Takahashi H, Okamoto E, Fujimoto J. Hepatocyte growth factor gene therapy of liver cirrhosis in rats. *J Hepatol*, 1999;30:461-471

13 Kogure K, Zhang YQ, Shibata H, Kojima I. Immediate onset of DNA synthesis in remnant rat liver after 90% hepatectomy by an administration of follistatin. *J Hepatol*, 1998;29:977-984

14 Li XQ, Zeng MX, Ling QH. Effects of interferon-B on DNA synthesis and collagen production of cultured rat hepatocytes. *Huaren Xiaohua Zazhi*, 1998;6:488-490

15 Huang X, Li DG, Wang ZR, Wei HS, Cheng JL, Zhan YT, Xu QF, Lu HM. Follistatin on hepatic fibrotic rat liver PCNA, BrDU and activin A expression. *Shijie Huaren Xiaohua Zazhi*, 2000;8: 993-997

16 Wang X, Chen YX, Xu CF, Zhao GN, Huang YX, Wang QL. Relationship between tumor necrosis factor-α and liver fibrosis. *World J Gastroenterol*, 1998;4:18

17 De Bleser PJ, Niki T, Xu G, Rogiers V, Geerts A. Localization and cellular sources of activins in normal and fibrotic rat liver. *Hepatology*, 1997;26:905-912

18 Zhang YQ, Mashima H, Kanzaki M, Shibata H, Kojima I. Assessment of the role of activin A and transforming growth factor beta in the regulation of AML12 cell growth. *Hepatology*, 1997;25: 1370-1375

19 Qi Z, Atsuchi N, Ooshima A, Takeshita A, Ueno H .Blockade of type beta transforming growth factor signaling prevents liver fibrosis and dysfunction in the rat. *Proc Natl Acad Sci USA*, 1999; 96:2345-2349

20 Liu F, Liu JX, Cao ZC, Li BS, Zhao CY, Kong L, Zhen Z. Relationship between TGF-β1, serum indexes of liver fibrosis and hepatic tissue pathology in patients with chronic liver diseases. *Shijie Huaren Xiaohua Zazhi*, 1999;7:519-521

21 Kogure K, Zhang YQ, Maeshima A, Suzuki K, Kuwano H, Kojima I. The role of activin and transforming growth factor-beta in the regulation of organ mass in the rat liver. *Hepatology*, 2000;31: 916-921

22 Eto Y, Tsuji T, Takezawa M, Takano S, Yokogawa Y, Shibai H. Purification and characterization of erythroid differentiation factor (EDF) isolated from human leukemia cell line THP-1. *Biochem Biophys Res Commun*, 1987;142:1095-1103

23 Hubner G, Alzheimer C, Werner S. Activin: a novel player in tissue repair processes. *Histol Histopathol*, 1999;14:295-304
24 Woodruff TK. Regulation of cellular and system function by activin. *Biochem Pharmacol*, 1998;55:953-963
25 Hully JR, Chang L, Schwall RH, Widmer HR, Terrell TG, Gillett NA. Induction of apoptosis in the murine liver with recombinant human activin A. *Hepatology*, 1994;20:854-861
26 Zhang YQ, Kanzaki M, Mashima H, Mine T, Kojima I. Norepinephrine reverses the effects of activin A on DNA Synthesis and apoptosis in cultured rat hepatocytes. *Hepatology*, 1996;23:288-293
27 Sugiyama M, Ichida T, Sato T, Ishikawa T, Matsuda Y, Asakura H. Expression of activin A is increased in cirrhotic and fibrotic rat livers. *Gastroenterology*, 1998;114:550-558
28 Sun ZQ, Wang YJ, Quan QZ, Han GY, Jin XH. Change of serum phosphonate esterase in hepatic fibrosis in rats. *Xin Xiaohuabingxue Zazhi*, 1994;2:206-207
29 Han GY, Jin XH, Wu CQ, Wang HF, Liu WJ. Alteration of serum phosphonate esterase in liver fibrosis in rats. *Xin Xiaohuabingxue Zazhi*, 1996;4:369-370
30 Li BS, Wang J, Zhen YJ, Liu JX, Wei MX, Sun SQ, Wang SQ. Experimental study on serum fibrosis markers and liver tissue pathology and hepatic fibrosis in immuno-damaged rats. *Shijie Huaren Xiaohua Zazhi*, 1999;7:1031-1034
31 Wang Y, Gao Y, Huang YQ, Yu JL, Fang SG. Gelatinase A proenzyme expression in the process of experimental liver fibrosis. *Shijie Huaren Xiaohua Zazhi*, 2000;8:165-167
32 Yan JC, Ma Y, Chen WB, Xu CJ. Dynamic observation on vascular diseases of liver tissues of rats induced by CCla-4. *Shijie Huaren Xiaohua Zazhi*, 2000;8:42-45
33 Sun DL, Sun SQ, Li TZ, Lu XL. Serologic study on extracellular matrix metabolism in patients with viral liver cirrhosis. *Shijie Huaren Xiaohua Zazhi*, 1999;7:55-56
34 Hu YY, Liu C, Liu P, Gu HT, Ji G, Wang XL. Anti-fibrosis and anti-peroxidation of lipid effects of Fuzhenghuayu decoction on rat liver induced by CCla-4. *Xin Xiaohuabingxue Zazhi*, 1997;5:485-486
35 Huang ZG, Zhai WR, Zhang YE, Zhang XR. Study of heteroserum-induced rat liver fibrosis model and its mechanism. *World J Gastroenterol*, 1998;4:206-209
36 Du WD, Zhang YE, Zhai WR, Zhou XM. Dynamic changes of type I, III and IV collagen synthesis and distribution of collagen-producing cells in carbon tetrachloride-induced rat liver fibrosis. *World J Gastroenterol*, 1999;5:397-403
37 Woodruff TK, Meunier H, Jones PBC, Hsueh AJW, Mayo KE. Rat inhibin: Molecular cloning of alpha- and β-subunit complementary deoxyribonucleic acids and expression in the ovary. *Mol Endocrinol*, 1987;1:561-568
38 Sonoyama K, Rutatip S, Kasai T. Gene expression of activin, activin receptors, and follistatin in intestinal epithelial cells. *Am J Physiol Gastrointest Liver Physiol*, 2000;278:G89-G97
39 Kovalszky I, Nagy P, Szende B, Lapis K, Szalay F, Jeney A, Schaff Z. Experimental and human liver fibrogenesis. *Scand J Gastroenterol*, 1998;228(Suppl):51-55
40 Date M, Matsuzaki K, Matsushita M, Tahashi Y, Sakitani K, Inoue K. Differential regulation of activin A for hepatocyte growth and fibronectin synthesis in rat liver injury. *J Hepatol*, 2000;32:251-260
41 Yasuda H, Mine T, Shibata H, Eto Y, Hasegawa Y, Takeuchi T, Asano S, Kojima I. Activin A: an autocrine inhibitor of initiation of DNA synthesis in rat hepatocytes. *J Clin Invest*, 1993;92:1491-1496
42 Ohga E, Matuse T, Teramoto S, Katayama H, Nagase T, Fukuchi Y, Ouchi Y. Effects of activin A on proliferation and differentiation of human lung fibroblasts. *Biochem Biophys Res Commun*, 1996;228:391-396
43 Schwall RH,Robbins K, Jardieu P, Chang L, Lai C, Terrell TG. Activin induces cell death in hepatocytes *in vivo* and *in vitro*. *Hepatology*, 1993;18:347-356
44 Dooley S, Delvoux B, Lahme B, Mangasser-stephan, Gressner AM. Modulation of transforming growth factor β response and signaling during transdifferentiation of rat hepatic stellate cells to myofibroblasts. *Hepatology*, 2000;31:1094-2000
45 Zhang YQ, Kanzaki M, Shibata H, Kojima I. Regulation of the expressionof follistatin in rat hepatocytes. *Biochem Biophys Acta*, 1993;1354:204-210
46 Qiu DK, Li H, Zeng MD, Li JQ. Effect of cordyceps polysaccharidesliposome on the expression of interstitial mRNA in rats with hepatic fibrosis. *Xin Xiaohuabingxue Zazhi*, 1997;5:417-418
47 Sun ZQ, Wang YJ, Quan QZ, Liu XF, Pan X, Jiang XL. Prevention and treatment action of tetrandrine on experimental liver fibrosis in rats. *Xin Xiaohuabingxue Zazhi*, 1994;2:19-20
48 Wang YJ, Sun ZQ, Quan QZ, Zhang ZJ, Liu XF, Jiang XL, Pan X. Study on type I collagen and fat-storing cells in fibrotic rat liver treated by tetrandrine. *Xin Xiaohuabingxue Zazhi*, 1994;2:78-79
49 Gong AY, Ma XH, Xu RL, Yin L, Chen XM, Zhao YC, Han DW. Changes of laminin in the liver of rats with experimental cirrhosis. *Xin Xiaohuabingxue Zazhi*, 1997;5:3-5
50 Li BS, Wang J, Zhen YJ, Wang XG, Sun YH, Wang SQ, Wu ZQ. Blocking effect of Chinese herbs Yiganxian and PHGF on immuno-damaged hepatic fibrosis in rats. *Huaren Xiaohua Zazhi*, 1998;6:786-788

Edited by Ma JY

P.O.Box 2345 Beijing 100023, China
Fax. 0086·10·65891893 Tel. 0086·10·65897901
E-mail.wcjd@public.bta.net.cn www.wd.org.cn

World J Gastroentero, 2001 April; 7(1):42 - 48
World Journal of Gastroenterology
Copyright©2001 by the WJG Press ISSN 1007 - 9327

Animal experiment and clinical study of effect of gamma-interferon on hepatic fibrosis

Hong Lei Weng, Wei Min Cai and Rong Hua Liu

Subject headings recombinant human gamma-interferon; liver fibrosis; carbon tetrachloride; dimethylnitrosamine; medium chronic hepatitis B virus

Weng HL, Cai WM, Liu RH. Animal experiment and clinical study of effect of gamma-interferon on hepatic fibrosis. ***World J Gastroenterol***, 2001;7(1):42-48

Abstract

AIM **To evaluate the antifibrotic effect of different doses of recombinant human Gamma-Interferon (IFN-γ) in two rat models of hepatic fibrosis, and to observe its effect on moderate chronic hepatitis B virus fibrosis.**

METHODS **Hepatic fibrosis was successfully induced in 150 and 196 rats by subcutaneous injection of carbon tetrachloride ($CCla_4$) and intraperitoneal injection of dimethylnitrosamine (DMN), respectively. Each of the two model groups was divided into: ① fibrotic model group; ② colchicine treatment group (0.1 mg/kg/day, gastrogavage for 8 weeks); ③ high-dose IFN-γ group (15 MU/kg per day, i.m. for 8 weeks); ④ medium-dose IFN-γ group (5MU/kg daily, i.m. for 8 weeks); and ⑤ low-dose IFN-γ group (1. 67 MU/kg daily, i.m. for 8 weeks). Another group of 10 rats without any treatment was used as normal controls. At the end of the experiment, semi-quantitative histopathological scores of inflammation and fibrosis, liver α smooth muscle actin (α-SMA) expression level, liver hydroxyl proline content and serum hyaluronic acid levels were compared. And 47 medium chronic hepatitis B viral fibrosis patients were studied. They were given IFN-γ treatment, 100 MU/day i.m. for the first three months and 100 MU qod i.m. for the next six months. Semi-quantitative pathological scores of inflammation and fibrosis and serum hepatic fibrosis indices were compared within the 9 months.**

RESULTS **In animal experiment, the pathological fibrosis scores and liver hydroxyl proline content were found to be significantly lower in rats treated with different doses of IFN-γ as compared with rats in fibrotic model group induced by either $CCla_4$ or DMN, in a dose-dependent manner. For $CCla_4$-induced model, pathological fibrosis scores in high, medium and low doses IFN-γ groups were 5.10 ± 2.88, 7.70 ± 3.53 and 8.00 ± 3.30, respectively, but the score was 14.60 ± 7.82 in fibrotic model group. Hydroxyl proline contents were 2.83 ± 1.18, 3. 59 ± 1.22 and 4.80 ± 1.62, in the three IFN-γ groups, and 10.01 ± 3.23 in fibrotic model group. The difference was statistically significant (P<0.01). Similar results were found in DMN-induced model. Pathological fibrosis scores were 6.30 ± 0.48, 8.10 ± 2.72 and 8.30 ± 2.58, in high, medium and low doses IFN-γ groups, and 12. 60 ± 3.57 in fibrotic model group. Hydroxyl proline contents were 2.72 ± 0.58, 3.14 ± 0.71 and 3.62 ± 1.02, in the three IFN-γ groups, and 12.79 ± 1.54 in fibrotic model group. The difference was statistically significant (P<0.01). Serum hepatic fibrosis indices decreased significantly in the 47 patients after IFN-γ treatment (HA: 433.38 ± 373.00 *vs* 281.57 ± 220.48; LN: 161.22 ± 41.02 *vs* 146.35 ± 44.67; PC(r): 192.59 ± 89.95 *vs* 156.98 ± 49.22; C-I: 156.30 ± 44.01 *vs* 139.14 ± 34.47) and the differences between the four indices were significant (P<0.05). Thirty-three patients received two liver biopsies, one before and one after IFN-γ treatment. In thirty of 33 patients IFN-γ had better effects according to semi-quantitative pathological scores (8.40 ± 5.83 *vs* 5.30 ± 4.05, P<0.05).**

CONCLUSION **All the three doses of IFN-γ are effective in treating rat liver fibrosis induced by either $CCla_4$ or DMN, the higher the dose, the better the effect. And IFN-γ is effective for patients with moderate chronic hepatitis B viral fibrosis.**

Institute of Infectious Diseases, First Affiliated Hospital, Medical School, Zhejiang University, Hangzhou 310003, Zhejiang Province, China
Dr. Hong Lei Weng, graduted from Medical School of Zhejiang University as a postgraduate in 1999, now associate professor of Institute of Infectious Diseases, First Affiliated Hospital, Medical School, Zhejiang University.
Correspondence to: Wei Min Cai, Institute of Infectious Diseases, First Affiliated Hospital, Medical School, Zhejiang University, 261 Qingchun Lu, Hangzhou 310003, Zhejiang Province, China
Tel. 0086-571-7236580, Fax. 0086-571-7086731
Email. syliao@netease. com
Received 2000-09-18 **Accepted** 2000-10-20

INTRODUCTON

Hepatic fibrosis can cause liver cirrhosis in chronic liver diseases (viral, schistosomal, alcoholic). Regardless of causes, hepatic fibrosis is characterized by a large deposition of extracellular matrix, collagen being a major component. Studies on interferon-gamma (IFN-γ) *in vitro* or *in vivo* are increasing[1-7]. Although the interferons were initially described for their antiviral properties, IFN-γ has also been found to have significant effects against hepatic fibrosis and to inhibit the synthesis

of extracellular matrix[8-14]. However, there have been few studies on the relationship between different doses and effects of IFN-γ for hepatic fibrosis. Our previous study showed that IFN-γ could lower serum hyaluronic acid levels in chronic hepatitis patients with hepatic fibrosis[15]. But no reports concerning histological changes after IFN-γ treatment have ever been found. We were prompted to systematically observe the effect of IFN-γ and investigate its effective doses on rat hepatic fibrosis induced by intraperitoneal injection of two different toxins, carbon tetrachloride (CCl_4) and dimethylnitrosamine (DMN). Once hepatic fibrosis emerged in two rat models, different doses of IFN-γ were injected intramuscularly to observe the following changes after IFN-γ treatment: pathological fibrosis scores, liver hydroxylproline content and serum hyaluronic acid levels. In the meantime, we observated 47 chronic hepatitis B patients with hepatic fibrosis who received IFN-γ treatment for 9 months. Liver biopsy and other laboratory tests were performed within the 9 months, the effect of IFN-γ was assessed.

MATERIALS AND METHODS

Animal experimental design

Sprague-Dawley rats (n = 483) weighing 200 gm-250 gm were used. They were fed with Good Laboratory Practice diet in pellets (provided by Zhejiang University Animal Study Center). Rats were maintained under 12 h light/dark cycles and allowed free access to food and water. Experiments were performed in accordance with the institutional ethical guidelines.

Hepatic fibrosis was induced by intraperitoneal injections of CCl_4 or DMN. Recombinant human IFN-γ was kindly provided by Shanghai Clonbiotech Co., Ltd (Shanghai, China, Batch Number 970521).

Rats (n = 205) were subcutaneously administered dissolved CCl_4 in olive oil (a proportion of 4:6) at 0.3 mL/kg of body weight, i.p., for 2 consecutive days a week for 16 weeks. Five rats were killed at the end of each week to examine their pathological changes.

For DMN-induced fibrosis, 278 rats were injected i.p. repeatedly, for 3 consecutive days at the first week and 2 consecutive days for the next 5 weeks. Five rats were killed at the end of each week to examine their pathological changes.

According to histological sections, hepatic fibrosis appeared at the end of the fourth week from the start of the study. One hundred and fifty rats in CCl_4 induced model and 196 rats in DMN-induced model could be used for the next study. Rats in the two models were divided into five groups: ① fibrotic model group; ② colchicine treatment group (0.1mg·kg^{-1}·day^{-1}, gastrogavage); ③ high-dose IFN-γ group (15 MU·kg^{1}·day^{-1}, i.m.); ④ medium-dose IFN-γ group (5 MU·kg^{1}·day^{1}, i.m.); and ⑤ low-dose IFN-γ group (1.67 MU·kg^{-1}·day^{1}, i.m.). In addition, 10 rats were chosen as the normal control group. Rats in the normal control and fibrotic model groups were given 0.9% sodium chloride by intramuscular injection instead of IFN-γ.

Rats of CCl_4 induced model received 8-week treatment. At the end of the eighth week, 10 rats of each group were killed, and histological sections of their livers were evaluated by hematoxylin and eosin and Sirius red stains. α-smooth muscle actin (α-SMA) was examined with immunohistochemical technique. Liver hydroxylproline content and serum hyaluronic acid level were also detected. In the next 4 weeks, all treatments stopped. The rest of the rats were killed at the end of the sixteenth week from the start of the experiment.

Rats of DMN-induced model received 4-week treatment. At the end of the fourth week, 10 rats of each group were killed. All items performed in CCl_4-induced model were detected, too. The other rats were killed at the end of the 12 th week from the start of the study.

Histological study

Excised liver tissues from rats were fixed in 10% neutralized formaldehyde, embedded in paraffin, and then stained with hematoxylin and eosin. Alternatively, the Sirius red stain method was used to specifically stain fibrous tissue components. These sections were observed under polarization microscopy (Leica DMLB, Leica Wetalar, Germany.) to distinguish type I and III collagen[16]. Specimens were reviewed under code by a single pathologist who graded and scored the specimens according to the criteria of Scheuer and Chevallier *et al*[17,18]. In Scheuer criteria, the transformation of grade and stage was as follows: stage 0, = 2°; grade or stage 1, = 2^1; grade or stage 2, = 2^2; grade or stage 3, = 2^3; grade or stage 4, = 2^4.

Identification of activated hepatic stellate

α-SMA, a marker of activated hepatic stellate (HSC) [19,20], was detected in formaldehyde-fixed paraffin-embedded section. Briefly, liver tissue was incubated with a monoclonal IgG_2a recognizing α-SMA (Dako M851) and reactive sites were detected using the labeled streptavidin-biotin technique (Dako M680), resulting in a brown staining after incubation with Tris-buffered saline containing diammobenzidine and H_2O_2. In control slides, the primary antibody was substituted by the Tris-buffers.

Biochemical measurements

The liver was homogenated into powder and hydrolyzed with 6 mol/L HCl. The hydroxyl proline content was measured by the means of Kivirikko *et al*[21]. The routine serum biochemical tests, including serum aspartate transaminase and alanine transaminase, were performed.

Examination of serum hyaluronic acid level

Serum hyaluronic acid level was detected by radioimmunoassay technique. The kit was provided by the Shanghai Navy Medical Institute. The operations were performed according to the manufacturer's instructions.

Patients

Fourty-seven hepatic fibrosis patients with chronic hepatitis B, 37 males and 10 females, were chosen for the study. They were confirmed to have moderate hepatic fibrosis pathologically according to Scheuer and Chevallier scoring system[17,18] and had chronic hepatitis B for 6 months to 30 years. Additional criteria included: age between 18 and 65 years; presence of HBsAg in serum for at least 6 months; positive serum tests for anti-HBe documented on four occasions, at least 1 month apart, during the 6 months before entry into the study. Among four serum hepatic fibrosis indices, including hyaluronic acid (HA, upper nomal limit <110 μg/L), laminin (LN, upper normal limit <150 μg/L), type III procollagen (PCIII, upper normal limit <120 μg/L) and type IV collagen (C-IV, upper normal limit <80 μg/L), two indices were higher than upper normal limit. Patients were excluded when the haemoglobin ≤10 g/dL, platelet count ≤50 000/mL, and white cell count ≤4 000/mL. Other exclusion criteria were patients with decompensated liver disease (serum albumin <3.5 g/dL; serum total bilirubin ≥85.5 μmol/L; prothrombin time prolongation >3sec), histories of hepatic encephalopathy or ascites, esophageal or gastric varices at risk of bleeding, hepatitis delta virus, hepatitis C virus infections, causes of liver disease other than HBV, intravenous drug abuse, pregnancy, malignancy, chronic heart and/or renal failure, anti-virus therapy (such as IFN-α, lamivudine, Famciclovir and Penciolovir therapy) and immune modulation therapy (such as Thymosin α_1) within a period of 3 months, and anti-hepatic fibrosis drugs (such as colchicines, herbal recipe 861 and Extractum Semen Percise).

Study protocol

In this open label study, all the patients were given routine therapy and received rhIFN-γ (kindly provided by Shanghai Clonbiotech Co., Ltd, Shanghai, China, Batch Number 981210) at a dose of 1 MU intramuscularly daily for the first three months and every other day for the following six months. They were asked to take rhIFN-γ in local hospitals near their homes. They were visited every three months during the treatment and thereafter followed up for 3 months after the treatment stopped. At each visit, clinical and laboratory assessments were made, including serum biochemical tests, such as serum hepatic fibrosis indices, routine serum biochemical tests, such as ALT, AST and γ-glutamyl transpeptidase, alkaline phosphatase, albumin, total bilirubin and alfha fetoprotein (AFP), routine blood tests, and HBV serology. Ethical Committee of the Centers involved approved the study. All the patients were volunteers.

Histology

Liver biopsies were performed twice within the 9 months, one before the treatment and one after it. All liver biopsy specimens were stained with hematoxylin-eosin and Sirius red. A single pathologist who was blinded with respect to treatment regimen evaluated specimens according to the criteria of Scheuer and Chevallier *et al*[9,10].

Statistical analysis

Results were expressed as mean ± standard deviation and compared when appropriate, by Student's two-tailed paired and unpaired *t* test and Kruskall Wallis nonparametric one-way ANOVA.

RESULTS

Animal experiment

In normal control group, Sirius red staining showed a normal distribution of collagen in a small amount in the portal tracts and around the terminal hepatic veins.

CCl_4- induced model showed different pathological changes from DMN-induced model. In the former, besides hepatocyte necrosis, fatty degeneration was the major feature[22] while in the latter, lymphomonocyte infiltration and local hepatocyte necrosis were the main characteristics[23]. However, after 12 weeks of CCl_4 and 8 weeks of DMN treatment, all the rats in fibrotic model groups showed complete fibrotic septum, forming a pattern of micronodular cirrhosis to the parenchyma (Figure 1).

In animal treated with high-dose of IFN-γ, Sirius red staining showed a small collagen deposition in the portal tracts and lobules. Only collagen fibers around the terminal hepatic veins were observed (Figure 2). Collagen depositions in liver sections taken from animals treated with medium or low dose of IFN-γ were particularly evident but only thin bands of collagen which formed short, incomplete septum could be seen (Figures 3, 4). In colchcine treated animals, complete fibrotic septum departing from the central vein were present, and no cirrhosis could be observed (Figure 5). Tables 1 and 2 show the histological stage and grade of different groups.

Table 1 Histological grading and staging in CCl_4-induced specimens after 8 week treatment

Groups	2^{g*}	2^{s*}	SSS△
Normal control group	1.00 ± 0.00	1.00 ± 0.00	0
Fibrotic model group	9.20 ± 5.01	10.40 ± 5.06	14.60 ± 7.82
Colchicine treatment group	10.40 ± 5.06	7.40 ± 4.99[a]	10.60 ± 3.34[a]
High-dose IFN-γ group	9.60 ± 3.37	3.00 ± 1.05[bc]	5.10 ± 2.88[bc]
Medium-dose IFN-γ group	6.00 ± 4.22	5.60 ± 4.20[bc]	7.70 ± 3.53[bc]
Low-dose IFN-γ group	7.60 ± 4.79	5.40 ± 2.32[bc]	8.00 ± 3.30[bc]

* Scheuer's criteria; △ Chevallier's criteria

[a]$P<0.05$ *vs* fibrotic model group; [b]$P<0.01$ *vs* fibrotic model group; [c]$P<0.05$ *vs* colchicines treatment group.

Table 2 Histological grading and staging in DMN-induced specimens after 4 week treatment

Groups	2^{g*}	2^{s*}	SSS△
Normal control group	1.00 ± 0.00	1.00 ± 0.00	0
Fibrotic model group	7.00 ± 2.16	9.60 ± 4.70	12.60 ± 3.57
Colchicine treatment group	6.80 ± 4.13	7.00 ± 3.92[a]	11.3 0 ± 2.37[a]
High-dose IFN-γ group	6.40 ± 2.07	2.60 ± 0.97[bc]	6.3 0 ± 0.48[bc]
Medium-dose IFN-γ group	4.80 ± 2.35	4.00 ± 2.32[bc]	8. 10 ± 2.72[bc]
Low-dose IFN-γ group	5.00 ± 2.71	4.40 ± 2.07[bc]	8.30 ± 2.58[bc]

*Scheuer's criteria; △ Chevallier's criteria
[a]P<0.05 *vs* fibrotic model group; [b]P<0.01 *vs* fibrotic model group; [c]P<0.05 *vs* colchicines treatment group.

In the normal control group, α-SMA positive cells were detected mainly in the portal space as elements of vascular walls or as fibroblastlike cells scattering in the connective tissue or near bile ductules. In lobule, α-SMA positive cells were present on the walls of large and medium sized terminal hepatic veins. The pattern of distribution of α-SMA positive cells was modified in CCl_4 or DMN treated animals as compared with the normal control rats. In fibrotic model groups, α-SMA positive cells were detected in portal space, sinusoid, lobule and areas where fibrotic septum appeared. Different doses of IFN-γ appeared to strikingly decrease the activation of HSC. After 8 weeks of IFN-γ treatment in CCl_4 model or 4 weeks in DMN model, only thin and incomplete parenchymal α-SMA positive septum joining thickened centrilobular veins were observed. α-SMA positive cells were mainly found in portal space and areas around fibrotic septum. Few α-SMA positive cells were present in sinusoid and lobule.

Analysis of total collagen content in liver substantiated the histological impression. Hydroxylproline evaluation in fibrotic model groups showed that the amount of Hydroxyl proline content increased approximately 5-fold (in CCl_4 model) or 6-fold (in DMN model) as compared with the normal control group, whereas, figures of different doses of IFN-γ groups were lower (<2-fold). The results in Tables 3 and 4 indicate the serum hyaluronic acid level of different groups. Except for low-dose IFN-γ group in CCl_4-induced model, other IFN-γ treatment groups had obvious decrease of serum hyaluronic acid level in both models.

Table 3 Serum hyaluronic acid level and liver hydroxylproline content in CCl_4-induced specimens after 8 weeks treatment

Groups	HA (μg/L)	Hyp (mg/g liver dry weight)
Normal control group	147.64 ± 19.28	2.43 ± 0.33
Fibrotic model group	900.04 ± 508.84	10.01 ± 3.23
Colchicine treatment group	745.57 ± 170.44[a]	6.90 ± 1.70
High-dose IFN-γ group	482.05 ± 210.57	2.83 ± 1.18
Medium-dose IFN-γ group	765.51 ± 586.65[a]	3.59 ± 1.22[bd]
Low-dose IFN-γ group	981.52 ± 509.95	4.80 ± 1.62

[a]P<0.05 *vs* fibrotic model group; [b]P<0.01 *vs* fibrotic model group; [c]P<0.05 *vs* colchicines treatment group; [d]P<0.01 *vs* colchicines treatment group.

Table 4 Serum hyaluronic acid level and liver hydroxylproline content in DMN-induced specimens after 4-weeks treatment

Groups	HA (μg/L)	Hyp (mg/g liver dry weight)
Normal control group	147.64 ± 19.28	2.43 ± 0.33
Fibrotic model group	969.52 ± 257.80	12.79 ± 1.54
Colchicine treatment group	323.72 ± 388.45[a]	6.40 ± 1.84[a]
High-dose IFN-γ group	144.25 ± 105.66	2.72 ± 0.58
Medium-dose IFN-γ group	334.10 ± 420.06	3.14 ± 0.71
Low-dose IFN-γ group	407.95 ± 386.61[a]	3.62 ± 1.02[bd]

[a]P<0.05 *vs* fibrotic model group; [b]P<0.01 *vs* fibrotic model group; [c]P<0.05 *vs* colchicines treatment group; [d]P<0.01 *vs* colchicines treatment group.

Clinical study

All the 47 patients completed the 9-month treatment. Table 5 shows the changes of symptoms after the 9-month IFN-γ treatment. Except for these changes, 12 patients (12/47, 25.5%) had a better appetite than before the treatment.

Thirty-three patients were given a second biopsy after the 9-month treatment (33/47, 70.2%). According to Chevallier's criteria, semi-quantitative system score (SSS) was calculated. After the 9-month IFN-γ treatment, the SSS decreased significantly in 14 patients (14/33, 42.4%) and the SSS dropped over 2 points, increased in 3 patients (3/33, 9.1%), and remained unchanged or dropped 1 point in the remaining 16 patients (16/33, 48.5%). Table 6 shows the mean SSS change during the treatment. A significant decrease of hepatic fibrosis score in accordance with the SSS was seen at the end of the IFN-γ treatment (8.40 ± 5.83 *vs* 5.30 ± 4. 05, P<0.05). In the meantime, a decrease of inflammation score in accorda nce with the SSS was also found although the difference was not statistically significant (P>0.05). Figures 6-9 display the collagen deposition changes within the IFN-γ treatment.

Table 7 shows the mean serum hepatic fibrosis indices, including HA, LN, PCIII and C-IV, and changes during the entire study. Decreases were present in the four indices (HA: 433.38 ± 373.00 *vs* 281.57 ± 220.48; LN: 161.22 ± 41.02 *vs* 146.35 ± 44.67; PCIII: 192.59 ± 89.95 *vs*. 156.98 ± 49.22; C-IV: 156.30 ± 44.01 *vs*. 139. 14 ± 34.47) and the differences between the four indices were significant (P<0.05).

As described by Cannon *et al*[24], the main side-effects in our study during the IFN-γ treatment were: fever (25) , joint pain (13), nausea (1), myagias (18), headache (10), leukopenia (5) and platelet decreases (7). Fever presenting in some patients was temporary and only 1 person had persistent fever (about 38℃), which disappeared when the treatmentended.

We also performed other routine serum biochemical tests, including ALT, AST and γ-GT, AFP. The results showed that the mean serum ALT, AST, γ-GT levels lowered in those patients as compared with those of IFN-γ treatment. No obvious change in serum AFP level was present within the 9 months (data not shown).

Table 5 Symptom change after IFN-γ treatment

	Fatigue	Abdominal distention	Nausea	Liver area pain
Before treatment	33	31	12	22
After treatment	4	4	0	4

Table 6 Histological grading and staging of liver biopsy specimens before and after 9-month treatment

	Grade*	Score of grade△	Stage*	Score of stage△
Before treatment	2.30 ± 0.98	7.30 ± 5.39	2.60 ± 0.88	8.40 ± 5.83
After 9-month treatment	1.95 ± 0.69	4.90 ± 2.27	2.05 ± 0.76	5.30 ± 4.05
t		2.719		2.719
P		0.051		0.014[a]

* Scheuer's criteria; △ Chevallier's criteria; [a]$P<0.05$ *vs* before treatment

Table 7 Serum hepatic fibrosis indices before and after 9-month treatment

Hepatic fibrosis indices	HA (μg/L)	LN (μg/L)	PCIII (μg/L)	C-IV (μg/L)
Before treatment	435.38 ± 373.00	161.22 ± 41.02	192.59 ± 89.95	156.30 ± 44.01
After 9-month treatment	281.57 ± 220.48	146.35 ± 44.67	156.98 ± 49.22	139.14 ± 34.47
t	2.341	2.434	2.381	2.104
P	0.017[a]	0.021[a]	0.020[a]	0.038[a]

[a]$P<0.05$ *vs* before treatment.

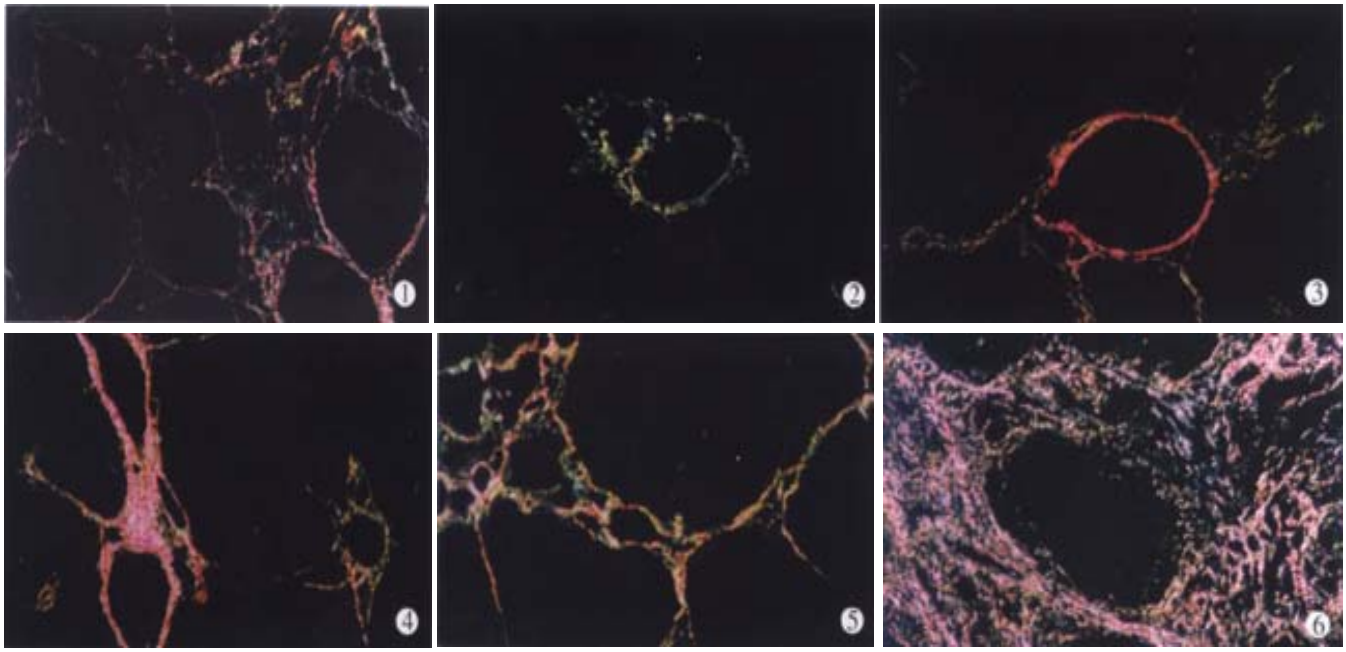

Figure 1 Histological section of rat liver after 12- weeks of CCl_4 treatment under polarizes after staining with Sirius Red. Red and yellow represented collagen type I and green collagen type III (the same below). The pattern of micronodular cirrhosis is evident. ×100

Figure 2 Histological section of rat liver after 8- weeks of treatment with high-dose IFN-γ and 12 weeks of CCl_4 under polarizes after staining with Sirius Red. ×100

Figure 3 Histological section of rat liver after 8-weeks of treatment with medium-dose IFN-γ and 12 weeks of CCl_4 under polarizes after staining with Sirius Red. ×100

Figure 4 Histological section of rat liver after 8- weeks of treatment with low-dose IFN-γ and 12 weeks of CCl_4 under polarizes after staining with Sirius Red. ×100

Figure 5 Histological section of rat liver after 8- weeks of treatment with colchicine and 12 weeks of CCl_4 under polarizes after staining with Sirius Red. ×100

Figure 6 and 7 Histological section of liver biopsy of a patient with chronic hepatitis B before IFN-γ treatment under polarizes after staining with Sirius Red. Figures 6 and 7 show two different fields. ×100

Figure 8 and 9 Histological section of liver biopsy of a patient with chronic hepatitis B after 9-month treatment with IFN-γ under polarizes after staining with Sirius Red. Figures 8 and 9 show two different fields. ×100

DISCUSSION

CCl_4 is one of the most widely used hepatic toxins for experimental induction of liver fibrosis cirrhosis in laboratory[22,25,26]. The model was used even in 1936. But, disadvantages of the model were apparent, such as higher mort ality rate. For this reason, 205 rats were used to produce CCl_4-iduced hepatic fibrosis model in our study. By killing some animals at the end of each week, we successfully got the hepatic fibrosis model at the fourth week. A total of 150 rats were used for the following study. We used DMN-induced hepatic fibrosis model. The characteristics of this model had been described by Madden *et al* [23]. Low mortality rate, shortproduction period and easy reproduction were the main advantages. We could investigate the effect of IFN-γ on hepatic fibrosis caused by different toxins because the two models had different mechanisms of inducing hepatic fibrosis.

Earlier report on the effect of IFN-γ anti-fibrosis could be found in 1984[8]. Studies *in vitro* or *in vivo* later proved that IFN-γ had a better effect on hepatic fibrosis[9-14]. However, IFN-γ and toxins were used at the same time in these studies. In the strict sense, their results only demonstrated that IFN-γ could prevent hepatic fibrosis, but failed to prove the effect of IFN-γ. In this study, IFN-γ was used on the first day of the fifth week when hepatic fibrosis had appeared so as to observe its effect on hepatic fibrosis.

In our study, we substantiated the impression that pathological changes taking place in CCl_4-induced model were different from those in DMN-induced model[22,26]. But, all the animals in fibrotic model groups showed complete fibrotic septum, forming a pattern of micronodular cirrhosis. Treatments with different doses of IFN-γ indicated significant decreases in the SSS, liver hydroxylproline content and serum hyarunic acid level. Among the three IFN-γ treatment groups, the best effect was present in the high-dose IFN-γ group.

To our knowledge, this is the first study on the effect of IFN-γ using different doses in animals. Our results showed that the effect of IFN-γ was associated significantly with doses. The higher the dose, the better the effect (Tables 1-4). The dose of IFN-γ used for virus is as high as 600MU/day. However, in our study, the medium dose of IFN-γ (5 MU/kg/day) used in rats is equal to 100 MU/day used in human. Whether the dose of IFN-γ could be increased clinically needs further studies.

Colchicine was used as the control drug in the experiment. Its effect on hepatic fibrosis in rats was not as good as that of IFN-γ according to the pathological and biochemical examinations (Tables 1-4).

In order to complete the animal experiment, we substantiated the effect of IFN-γ on chronic hepatitis B patients with hepatic fibrosis. Fourty-seven patients conforming to the study criteria were chosen in our study. After a 9-month IFN-γ treatment, 33 patients underwent a second liver biopsy. The results showed that the SSS decreased or unchanged in 30 patients (Table 5). The mean fibrosis score in accordance with SSS decreas ed from 8.40 ± 5.83 to 5.30 ± 4.05 (Table 6). And serum indices (including HA, C-IV, PCIII and LN) strengthened the pathological impression. All the four indices decreased significantly after the IFN-γ treatment (Table 7).

It was concerned that IFN-γ would increase inflammation[27]. However, our study showed a decrease of inflammation as compared with the previous IFN-γ treatments although the difference was not statistically significant (Table 6). We chose chronic hepatitis patients for the experiment so as not to cause patients any worries at the stage of acute inflammation. The results showed that IFN-γ treatment was safe for chronic hepatic patients. In the study, we also performed routine serum biochemical tests, including ALT, AST, and γ-GT, AFP. The mean serum ALT, AST, and γ-GT level lowered in those patients as compared with those of IFN-γ treatment. No obvious change in serum AFP level was found within the 9 months.

It is well known that collagen type I is the predominant extracellular matrix protein in fibrosis and cirrhosis but few techniques could discriminate different collagens in the same section[28,29]. We used Sirius red stain to resolve the problem as described by Zhang *et al*[16]. Under Polarization microscopy, sections stained with Sirius red showed different colors, red and yellow representing collagen type I and green collagen type III.

In our previous report, decrease of serum hepatic fibrosis indices was observed[15] after 3 months of IFN-γ treatment. So, at the earlier stage of the experiment, we adopted a 6-month treatment. There were 2 patients who received a second liver biopsy. No obvious changes were found in liver sections. We considered that a 9-month IFN-γ treatment was appropriate.

In this study, we paid more attention to side-effects. Symptoms including fever, joint pain, myagias, headache, nausea, leukopenia and platelet decrease were found in the experiment. IFN-γ was first used to treatrheumatoid [30,31], for as long as 24- months[24]. No serious side-effects were reported. However, whether IFN-γ may cause any side effects when it is used to treat hepatic fibrosis needs further observations.

ACKNOWLEDGEMENT We are indebted to Prof. Pei Hui Chen from the Department of Pathology, Second Affiliated Hospital, Medical College, Zhe jiang University for his help with the pathological technique.

REFERENCES

1 Pan X, Ke CW, Pan W, Wu WB, Zhang B, He X, Cao GW, Qi ZT. Construction of eukaryotic expression vector carrying IFN-β gene under control of human HBV promoter. *Shijie Huaren Xiaohua Zazhi*, 2000;8:520-523

2 Chen SB, Miao XH, Du P, Wu QX. Assessment of natural and interleukin-2-induced production of interferon-gamma in patients with liver diseases. *China Natl J New Gastroenterol*, 1996; 2:173-175

3 Fan K. Regulatory effects of lipopolysaccharide in murine macrophage proliferation. *World J Gastroenterol*, 1998;4:137-139

4 Wang JY, Wang XL, Liu P. Detection of serum TNF-α, IFN-γ, IL-6 and IL-8 in patients with hepatitis B. *World J Gastroentero*, 1999;5:38-40

5 Liu ZG, Yang JH, Aa HZ, Wang HY, He FT, Han ZY, Han Y, Wu HP, Xiao B, Fan DM. Cloning and identification of an angiostatic molecule IP-10/crg-2. *World J Gastroenterol*, 1999;5:241-244

6 Yin T, Tong SQ, Xie YC, Lu DY. Cyclosporin A protects Balb/c mice from liver damage induced by superantigen SEB and D-GalN. *World J Gastroenterol*, 1999;5:209-212

7 Zhong QP. Pathogenic effects of O-polysaccharide from Shigella flexneri strain. *World J Gastroenterol*, 1999;5:245-248

8 Granstein RD, Murphy GF, Margolis RJ, Byme MH, Amento EP. Gamma-interferon inhibits collagen synthesis *in vivo* in the mouse. *J Clin Invest*, 1987;79:1254-1258

9 Czaja MJ, Weiner FR, Takahashi S, Giambrone MA, van der Meide PH, Schellekens H, Biempica L, Zern MA. B-interferon treatment inhibits collagen deposition in murine schistosomiasis. *Hepatology*, 1989;10:795-800

10 Baroni GS, Ambrosio LD, Curto P, Casini A, Mancini R, Jezeqeel AM, Benedetti A. Interferon gamma decreases hepatic stellate cell activation and extracellular matrix deposition in rat liver fibrosis. *Hepatology*, 1996;23:1189-1199

11 Rockey DC, Maher JJ, Jarnagin WR, Gabbiani G, Friedman SL. Inhibition of rat hepatic lipocyte activation in culture by interferon-γ. *Hepatology*, 92;16:776-784

12 Weng HL, Cai WM, Wang GY, Chen F, Liu RH. Experiment study of recombinant human gamma-interferon on anti-hepatic fibrosis. *Zhonghua Ganzangbing Zazhi*, 1999;7(Suppl):33-35

13 Yang YH, Cai WM, Jin GL, Zhu SJ, Chen F, Weng HL, Liu RH. Dynamic changes in hepatic myofibroblast of rabbits with schistosoma japonicum. *Zhonghua Yixue Zazhi*, 1999;79:870-873

14 Li XQ, Zeng MX, Ling QH. Effects of interferon-γ on DNA synthesis and collagen production of cultured rat hepatocytes. *Huaren Xiaohua Zazhi*, 1998;6:488-490

15 Cai WM, Chen Z, Chen F, Weng HL, Liu RH. The primary observation on the effect of γ-interferon for antifibrosis. *Linchuang Gandanbing Zazhi*, 1998;14:21-23

16 Zhang J, He JW, Wang TL, Zhao JB. Discriminate collagen type I and collagen type III by Sirius red stain and polarization microscopy. *Zhonghua Binglixue Zazhi*, 1996;25:180-181

17 Desmet VJ, Gerber M, Hoofnagle JH, Manns M, Scheuer PJ. Classification of chronic hepatitis: diagnosis, grading and staging. *Hepatology*, 1994;19:1513-1520

18 Chevallier M, Guerret S, Chossegros P, Gerard F, Grlmaud JA. A histological semiquantitative scoring system for evaluation of hepatic fibrosis in needle liver biopsy specimens: comparison with morphometric studies. *Hepatology*, 1994;20:349-355

19 Lortat-Jacob H, Baltzer F, Desmoulière A, Peyrol S, Grimaud JA. Lobular-but not periovular-inhibition of collagen deposition in the liver of S. Mansoni infected mice using interferon-γ. *J Hepatol*, 1997;26:894-903

20 Rockey DC, Housset CN, Friedman SL. Activation-dependent contractility of rat hepatic lipocytes in culture and *in vivo*. *J Clin Invest*, 1993;92:1795-1804

21 Kivirikko KL, Laitinen O, Prockop DJ. Modifications of a specific assay for hydroxyproline in urine. *Anal Biochem*, 1967;19: 249-255

22 Jiang Z, You DY, Chen XC, Wu J. Monitoring of serum markers for fibrosis during CCla-4-induced liver damage. Effects of antifibrotic agents. *J Hepatol*, 1992;16:282-289

23 Madden JW, Gertman PM, Peacock EE. Dimethylnitrosamine-induced hepatic cirrhosis:a new canine model of an ancient human disease. *Surgery*, 1970;68:260-268

24 Cannon GW, Emkey RD, Denes A, Cohen SA, Saway PA, Wolfe F, Jaffer AM,Weaver AL, Cogen L, Gulinello J, Kennedy SM, Schindler JD. Prospective two-year followup of recombinant interferon-γ in rheumatoid arthritis. *J Rheumatol*, 1990;17:304-310

25 Wang YJ, Wang SS, Bickel M, Guenzler V, Gerl M, Bissell DM. Two novel antifibrotics, HOE O77 and Safironil, modulate stellate cell activation in rat liver injury. *Am J Pathol*, 1998;152: 279-287

26 Fort J, Pilette C, Veal N, Oberti F, Gallois Y, Douay O, Rosenbaum J, Cals P. Effects of long-term administration of interferon in two models of liver fibrosis in rats. *J Hepatol*, 1998;29:263-270

27 Napoli J, Bishop GA, McGuinness PH, Painter DM, McCaughan GW. Progressive liver injury in chronic hepatitis C infection correlates with increased intrahepatic expression of Th1-associated cytokines. *Hepatology*, 1996;24:759-765

28 Alpini G, Elias I, Glaser SS, Rodgers RED, Phinizy JL, Robertson WE, Francis H, Lasater J, Richards M, LeSage GD. Gamma-interferon inhibits secretin-induced choleresis and cholangiocyte proliferation in a murine model of cirrhosis. *J Hepatol*, 1997;27:371-380

29 Brenner DA, Westwick J, Breindl M. Type I collagen gene regulation and the molecular pathogenesis of cirrhosis. *Am J Physiol*, 1993;264:G589-G595

30 Firestein GS, Weisman MH, Zvaifler NJ. Parenteral IFN-γ in rheumatoid arthritis: Effect on disease activity and peripheral blood monocytes (abstr). *Arthritis Rheum*, 1987;30:S115

31 Machold KP, Smolen JS. Recombinant human gamma interferon (gifn) in the treatment of rheumatoid arthritis (RA): Double-blind placebo-controlled crossover study (abstr). *Arthritis Rheum*, 1989; 32:S131

Edited by Ma JY

P.O.Box 2345 Beijing 100023, China
Fax. 0086·10·65891893 Tel. 0086·10·65897901
E-mail.wcjd@public.bta.net.cn www.wd.org.cn

World J Gastroentero, 2001 April; 7(1):49 - 52
World Journal of Gastroenterology
Copyright©2001 by the WJG Press ISSN 1007 - 9327

Inhibition of hepatitis B virus by oxymatrine *in vivo*

Xiao Song Chen, Guo Jun Wang, Xiong Cai, Hong Yu Yu and Yi Ping Hu

Subject headings hepatitis B virus; antiviral agents; oxymatrine; hepatitis B surface antigens; hepatitis B core antigens; immunohistochemistry

Chen XS, Wang GJ, Cai X, Yu HY, Hu YP.Inhibition of hepatitis B virus by oxymatrine *in vivo*. ***World J Gastroenterol***, 2001;7(1):49-52

Abstract

AIM To investigate the anti-HBV effect of oxymatrine (oxy) *in vivo*.

METHODS HBV transgenic mice were produced by micro-injection of a 4.2 kb fragment containing the complete HBV genomes. Expression level of HBsAg and HBcAg in the transgenic mice liver was determined by immunohistochemical assay.

RESULTS Four groups (6 mice in each group) were injected intraperitoneally with oxy at the dosage of 100, 200, and 300 mg/kg or with saline once a day for 30 days. Both HBsAg and HBcAg were positive in livers of all the six mice in the control group (injected with saline), and were positive in livers of two mice in 100 mg/kg group and 300 mg/kg group. In 200 mg/kg group, HBsAg and HBcAg were negative in livers of all the six mice. Based on the results, 200 mg/kg is the ideal dosage to explore the effect of oxy at different time points. According to the oxy treatment time, mice were divided into four groups: 10 d, 20 d, 30d and 60 d (4 mice in each group). Each mouse underwent liver biopsy two weeks before the treatment of oxy. Down-regulation of HBsAg and HBcAg appeared after treatment of oxymatrine for 10 d and 20 d, Dane-like particles disappeared after the treatment of oxy for 20 d under electron microscopy, however, the expression level of HBsAg and HBcAg returned to normal 60 d later after oxy treatment.

CONCLUSION oxymatrine can reduce the contents of HBsAg and HBcAg in transgenic mice liver,longer treatment time and larger dosage do not yield better effects.

[1]Department of Infectious Diseases, Changzheng Hospital, the Second Military Medical University, Shanghai 200003, China
[2]Department of Pathology, [3]Department of Cell Biology, Department of Basic Medicine, the Second Military Medical University, Shanghai 200433, China
Xiao Song Chen, graduated from Second Military Medical University as a postgraduate in 1999, specialized in viral hepatitis B.
Supported by Projects of the Science Development Foundation of Shanghai, No.994919033 and Tackling Key Problems in Science and Technology from the State Science and Technology Ministry, TJ99-LA01.
Correspondence to: Yi Ping Hu, Department of Cell Biology, Department of Basic Medicine, the Second Military Medical University, Shanghai 200433, China
Tel. 0086-21-25070240
Email. Yphu@smmu.edu.cn
Received 2000-08-08 **Accepted** 2000-09-29

INTRODUCTION

There are about 30 million patients suffering from chronic hepatitis B in China. Patients with active liver disease carry a high risk of developing cirrhosis and hepatocellular carcinoma. At present, the most effective medicine is IFN-α, but it is too expensive for most patients. Even in the patients treated by IFN-α, the sera negative-convertion rate of HBeAg and HBVDNA is about 40%[1-3]. Previous works in our department by Cai X *et al* showed that the sera negative-convertion rates of HBeAg in patients with chronic active hepatitis B treated with oxymatrine was 61%[4]. To investigate the inhibiting mechanism of oxymatrine (oxy) on HBV replication, transgenic mice were employed as animal model to observe the changes of HBsAg and HBcAg expression in liver tissues.

MATERIALS AND METHODS

Materials

Matrine injection is the product of Ningxia Pharmaceutical Company Ltd., containing 98% oxymatrine. The restriction enzymes were purchased from PROMEGA. Taq enzyme purchased from SANGON. Immunohistochemical kits were purchased from DAKO. Primers of PCR were designed by ourselves and synthesized by GIBCO. ^{32}P labeled kit was the product of PROMEGA. Other reagents were purchased from WASON, HUAMEI and so on.

Methods

Preparation of animals HBV transgenic mice (official designation: ICR-TgN HBV adr1.2 SMMU) were produced by micro-injection of a 4.2 kb fragment containing the complete HBV genome (adr subtype)[5]. Structural analysis of the transgene revealed that at least one complete uninterrupted HBV genome was present. HBsAg and HBeAg were not detectable in the sera of the mice, but can be detected in livers by immunohistochemical assay (ABC), which was used to determine the expression level of HBV.

PCR and Southern-blot analysis Total tail genome DNA was analyzed by PCR using HBV-specific primers 5'CCCAATGGAACACTCACC[sense], 5' AGGAACCACTGAACAAATGGC [antisense]), generating a 380 bp fragment. Twenty mililiter of PCR products were analyzed by electrophoresis on a 1% agarose gel in the presence of 0.5 mg of ethidium bromide per mililiter. DNA bands were visualized by UV fluorescence. Southern-blot analysis was performed on total genomic DNA by agarose gel electrophoresis of 30 mg restricted

genomic DNA. Samples added on nylon filters were hybridized with HBV specific ^{32}P labeled DNA probes.

Histological analysis and electron microscopy were carried out as routine methods. The expression of HBsAg and HBcAg in liver tissues were assessed by immunohistochemical analysis according to Guidotti *et al*[6].

RESULTS

Effect of oxy at different doses on the expression of HBsAg and HBcAg Twenty-four age and sex-matched mice were divided into four groups. Each group was injected intraperitoneally with oxy at the dosage of 100, 200 and 300 mg/kg or with saline separately once a day for 30 days. Livers were harvested 2 hours after the last injection for immunohistochemical assay. Both HBsAg and HBcAg were positive in livers of all the six mice in the control group (injected with saline). In 100 mg/kg group, HBsAg and HBcAg were positive in two mice, while HBsAg and HBcAg were negative in the other four mice. In the 200 mg/kg group, both HBsAg and HBcAg were negative in all the six mice, none of the six mice had detectable HBV antigen in the livers. In the 300 mg/kg group, HBsAg and HBcAg were positive in two mice, and negative in the other four mice. No pathological changes were found in the transgenic mice. Based on the results, we considered that 200 mg/kg is the ideal dosage of oxy for further study.

The effect of oxy at different time on the expression of HBsAg and HBcAg

Mice were divided into four groups according to the oxy treatment time, 10d (group 1), 20 d (group 2), 30 d and 60 d (group 3 and 4). In each group, 4 mice were randomly entered. Each mouse underwent liver biopsy two weeks before the treatment of oxy (200 mg/kg). The liver samples before and after oxy treatment were collected, and immunohistochemical analysis was performed to determine the expression level of HBsAg and HBcAg. All the samples contained HBsAg and HBcAg positive cells, and the positive and negative cells were counted in 5 randomly selected high field vision, and χ^2 test was made to compare the HBV expression level before and after oxy treatment. In group 1, the number of HBsAg and HBcAg positive cells was significantly lower than before treatment of oxy in all the four mice livers. In group 2, the similar results were observed (Figures 1 and 2), and Dane-like particles could be found in the livers before oxy treatment under electron microscope and such particles could not be found after the treatment of oxy for 20 d (Figure 3). In group 3, the expression of HBV was decreased only in two of four mice. No difference was observed on the expression of HBsAg and HBcAg between the two liver samples harvested before and after the treatment of oxy in group 4.

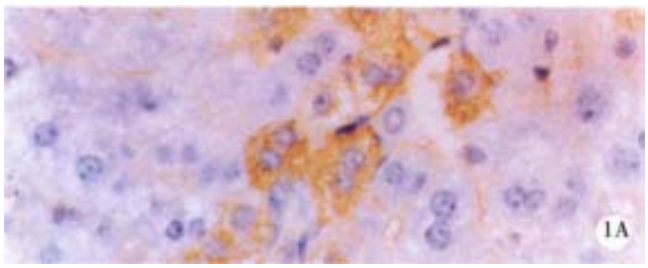

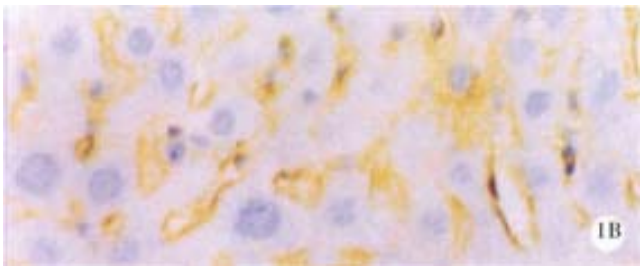

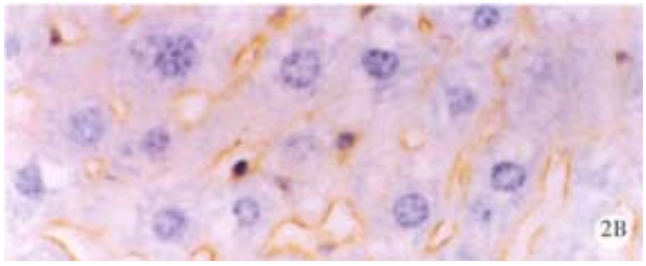

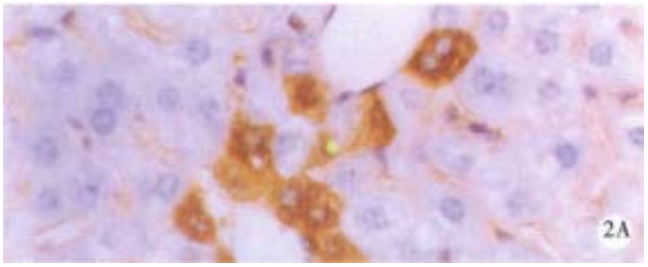

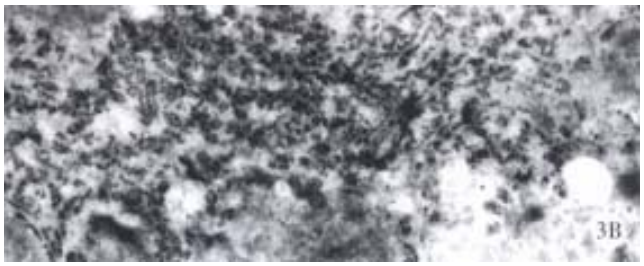

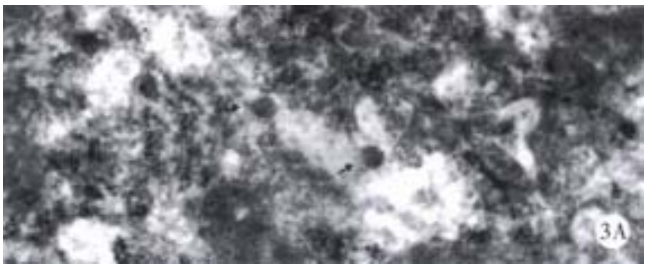

Figure 1 HBsAg in liver of the mice before (A) and after (B) treatment with 200 mg/kg oxy for 20 d.
Figure 2 HBcAg in liver of the mice before (A) and after (B) treatment with 200 mg/kg oxy for 20 d.
Figure 3 Dane's like particles can be seen in the liver of untreated mice (A) and disappeared after treatment with 200 mg/kg oxy for 20 d (B).

DISCUSSION

As a traditional Chinese medicine, *Sophra Flavescens Ait* has been used for the treatment of many diseases for thousands of years. Its extract, oxy, has long been extensively used in China. It is reported that oxy has a lot of pharmacological functions which can be divided into four classes: ① Anti-bacterial and anti-parasitic actions. It has been reported that oxy can cure acute dysentery, *Trichomonas vaginalis* and Giardia lamblia infection [7-9], but the mechanism is still unclear. ② Regulating immune reaction. Oxy can stimulate immune response at a low concentration while inhibiting immune response at a high concentration[10]. Recently, more researchers have paid attentions to the immune inhibitory effect of oxy. It has been reported that oxy has many functions such as anti-inflammation, anti-hypersensitive reactions, inhibiting histamine releasing[11-14]. The mechanism may be related to the changes of cAMP in the cell[15] and inhibiting production of cytokine[16]. ③ Inducing production of cytochrome P450. Oxy can increase the content of P450 in the rat liver significantly after treatment of oxy at the dosage of 200 mg/kg for 4d [17]. ④ Anti-virus actions. Liu JX reported that oxy could inhibit coxsackie virus B3 *in vivo* and *in vitro* [18,19]. Cai X found that the sera negative convertion rates of HBVDNA and HBeAg were 61.9% and 61.0% in chronic active hepatitis treated by oxy, while such rates in the therapy of IFN-α were 57.9% and 55.3%[4]. In our study, the content of HBV antigen in livers of transgenic mice decreased significantly after treatment of oxy for 10 and 20 d. Dane-like particles disappeared in the liver of transgenic mice after oxy treatment for 20 d. However, HBV expression level returned to normal after treatment by oxy for 60 d. We concluded that oxy can be used as an effective drug in managing HBV infection. There are two features of oxy on HBV: ① HBsAg and HBcAg was down regulated at the same time, ② longer time and larger dose did not yield better effect.

Our results strongly suggested that oxy can significantly inhibit the expression of HBV antigen in transgenic mice and the replication of HBV as well[20]. But how oxy give play to its effect can not be concluded from our experiments. However, based on the previous researches, it seems that oxy may act by two ways: ① oxy acts as an immune reaction regulator: Since HBV transgenic mice were first found by Chisari in 1985[21], *in vivo* study of HBV has become convenient and objective. Different lineage of HBV transgenic mice has also been found in our country[5,22]. A serial studies by Chisari *et al* have shown that certain soluble products of the immune response, especially IFN-γ, TNF-α, IFN-α, IL-2 and IL-12[23-28] could suppress the steady-state content of HBV messenger RNA in the hepatocytes of transgenic mice. Furthermore, these effects were found to be mediated by a post-transcriptional mechanism that selectively accelerates the degradation of cytoplasmic HBV mRNA[27]. The same events were set in motion when HBsAg-specific CTL secreted IFN-γ and induced TNF-α after antigen recognition[23,29]. The interhepatic nucleocapsid particles and replicative intermediates were also eliminated during unrelated virus infection[30,31] or during hepatocellular regeneration after partial hepatectomy[32]. Oxy is a strong immune regulator, Wang HX has reported that oxy can inhibit the competence of LAK cell killing P815 cell by about 70%-80%[33], and Shang HS reported that oxy has the same effect of marcophage on P815 cell[34], which proved that oxy may be an agonist of IL-2. Thus, IL-2 could not be the mediator of oxy inhibiting HBV. Whether other cytokines may be the mediator remains unclear. ② Oxy acts as an inducer of cytochrome P450. HBV antigen is exogenous proteins in mice hepatocytes. mRNA of HBV in hepatocytes may be degraded by cytochrome P450. Therefore, oxy can induce the production and enhance the activity of cytochrome P450[17], hence accelerating the degradation of HBV mRNA and inhibiting HBV replication. Further study is needed.

Oxy is a broad-spectrum anti virus drug, at least to HBV and coxsackie B virus 3 so far. This may give us new hope for the treatment of chronic hepatitis HBV infection including other viral infection such as HCV and HIV infection.

Cirrhosis is a servere consequence of chronic HBV infection and preventing the development of cirrhosis is very difficult[35]. Gan LW *et al* reported that oxy can inhibit the liver fibrosis induced by CCl_4 in rats[36]. Oxy can not only down-regulate HBV expression but also inhibit the liver fibrosis. Based on the two points, we concluded that oxy can be used as an effective drug in managing HBV infection. However, the exact mechanism of oxy inhibiting expression of HBV and liver fibrosis has not yet been fully understood. Further studies both basicaly and clinically are needed.

REFERENCES

1 Hoofnagle JH, Peters M, Mullen KD, Jones DB, Rustgi V, Bisceglie AD, Hallahan C, Park Y, Meschievitz C, Jones EA. Randomized, controlled trial of recombinant human α-interferon in patients with chronic hepatitis B. *Gastroenterology*, 1988;95:1318-1325

2 Zhu Y, Wang YL, Shi L. Clinical analysis of the efficacy of interferon alpha treatment of hepatitis. *World J Gastroenterol*, 1998; 4(Suppl 2):85-86

3 Shi JJ, Miao F, Liu FL. Therapeutic effect of medicinal herbs and western drugs on hepatitis B virus. *World J Gastroenterol*, 1998;4 (Suppl 2):61-62

4 Cai X,Wang GJ, Qu Y, Fan CH, Zhang RQ, Xu WS. Clinical efficacy of kurorinone in the treatment of chronic hepatitis B. *Dier Junyi Daxue Xuebao*, 1997;18:47-49

5 Hu WJ, Dai DS, Li JX, Wang XM, Sun W, Hao GR, Hu YP. The generation of hepatitis B virus transgenic mice homozygote. *Dier Junyi Daxue Xuebao*, 1999;20:598-600

6 Guidotti LG, Matzke B, Schaller H, Chisari FV. High-level hepatitis B virus replication in transgenic mice. *J Virol*, 1995;69:6158-6169

7 Tang ZW. Report of 60 case acute dysentery treated by matrine. *Zhonghua Neike Zazhi*, 1960;8:357-358
8 Sun DX. Chinese medicine matrine can cure Trichomonas vaginalis. *Zhonghua Fuchanke Zazhi*, 1958;6:544
9 Chen JL, Yu SZ, Wang HJ, Yang GJ, Wang PH, Shi Y. Report of 100 case Giardia lamblia infection treated by matrine. *Zhonghua Neike Zazhi*, 1965;13:614
10 Qian YK, Cheung HT, Richardson A. Chinese herbs (SFA, LLA)act as immunoregulator to immune cells and cytokine (IL-2,IL-3) *in vitro*. *Zhonghua Weishengwuxue He Mianyixue Zazhi*, 1988;8:312-315
11 Han CL, Chen XR, Ma JJ, Lin ZB. Study of oxymatrine s pharmacodynamic effect on allergic contact dermatitis. *Beijing Yike Daxue Xuebao*, 1996;28:59-61
12 Liao J, Zhang BH. Anti-inflammatory effects of oxymatrine. *Beijing Yike Daxue Xuebao*, 1988;20:313-315
13 Ma JJ, Si LP, Ding Y, Lin ZB, Chen XR, Han CL, Peng QS, Fang Y. Inhibition of type I-I allergic reactions by oxymatrine. *Beijing Yike Daxue Xuebao*. 1991;23:445-447
14 Zhang Q, Zhao FS, Hao ZM, Yin JZ, Qian YK. Study of effects and its mechanisms of oxymatrine on histamine release from peritoneal mast cells. *Zhonghua Weishengwuxue He Mianyixue Zazhi*, 1992;12:41-44
15 Wang HX, Yu XZ, Qian YK. The effects of oxymatrine on lymphocytes' second messengers. *Zhongguo Mianyixue Zazhi*, 1993; 9:315-317
16 Ding GF, Shang HS, Xu H, Deng YL, Long ZZ, Han GQ. The study of monokines-the measurement of IL-1 from the macrophages activated by different agents. *Zhongguo Mianyixue Zazhi*, 1986; 2:336-339
17 Yuan C, Lu SQ, Yao X. Effect of oxymatrine on the antitumor activity and toxicity of cyclophosphamide in mice. *Yaoxue Xuebao*, 1987;22:245-249
18 Liu JX, Lu DY, Yang ZM, Chen SX, Qian FR. Preliminary studies on the role of anti coxsackie group B virus of Chinese medicine sophora flavescens. *Shanghai Dier Yike Daxue Xuebao*, 1991;11: 140-142
19 Chen FX, Liu JX, Lu DY. The effects of sophora flavescens alkaloids of coxsackie virus B3 in vitro and a preliminary study of its mechanism. *Zhonghua Shiyan He Linchuang Bingduxue Zazhi*, 1995;9:115-117
20 Tang RX, Gao FG, Zeng LY, Wang YW, Wang YL. Detection of HBV DNA and its existence status in liver tissues and peripheral blood lymphocytes from chronic hepatitis B patients. *World J Gastroenterol*, 1999;5:359-361
21 Chisari FV, Pinkert CA, Milich DR, Filippi P, Mclachlan A, Palmiter RD, Brinster RL. A transgenic mouse model of the chronic hepatitis B surface antigen carrier state. *Science*, 1985;230:1157-1160
22 Hu YP, Yao YC, Li JX, Wang XM, Li H, Wang ZH, Lei ZH. The cloning of 3'-truncated preS/S gene from HBV genomic DNA and its expression in transgenic mice. *World J Gastroenterol*, 2000;6: 734-737
23 Guidotti LG, Ando K, Hobbs MV, Ishikawa T, Runkel L, Schreiber RD,Chisari FV. Cytotoxic T lymphocytes inhibit hepatitis B virus gene expression by a noncytoly tic mechanism in transgenic mice. *Proc Natl Acad Sci USA*, 1994;91:3764-3768
24 Gilles PN, Fey G, Chisari FV. Tumor necrosis factor alpha negatively regulates hepatitis B virus gene expression in transgenic mice. *J Virol*, 1992;66:3955-3960
25 Wang JY, Wang XL, Liu P. Detection of serum TNF-α, IFN-γ, IL-6 and IL-8 in patients with hepatitis B. *World J Gastroentero*, 1999;5:38-40
26 Guidotti LG, Guilhot S, Chisari FV. Interleukin-2 and Alpha/Beta interferon down-regulate hepatitis B virus gene expression *in vivo* by tumor necrosis factor-dependent and independent pathways. *J Virol*, 1994;68:1265-1270
27 Guilhot S, Guidotti LG, Chisari FV. Interleukin-2 downregulates hepatitis B virus gene expression in transgenic mice by a posttranscriptional mechanism. *J Virol*, 1993;67:7444-7449
28 Cavanaugh VJ, Guidotti LG, Chisari FV. Interleukin-12 inhibits hepatitis B virus replication in transgenic mice. *J Virol*, 1997;71: 3236-3243
29 Guidotti LG, Ishikawa T, Hobbs MV, Matzke B, Schreiber R, Chisari FV. Intracellular inactivation of the hepatitis B virus by cytotoxic T lymphocytes. *Immunity*, 1996;4:25-36
30 Cavanaugh VJ, Guidotti LG, Chisari FV. Inhibition of hepatitis B virus replication during adenovirus and cytomegalovirus infections in transgenic mice. *J Virol*, 1998;72:2630-2637
31 Guidotti LG, Borrow P, Hobbs MV, Matzke B, Gresser I, Oldstone MBA,Chisari FV.Viral cross talk:intracellular inactivation of the hepatitis B virus duringan unrelated viral infection of the liver. *ProcNatl Acad Sci USA*, 1996;93:4589-4594
32 Guidotti LG, Matzke B, Chisari FV. Hepatitis B virus replication is cell cycle independent during liver regeneration in transgenic mice. *J Virol*, 1997;71:4804-4808
33 Wang HX, Zhang LH, Huang Y, Qian YK. Effect of oxymatrine on LAK cell activity. *Mianyixue Zazhi*, 1994;10:17-19
34 Shang HS, Zhao J, Chen WF. The effect of matrine on macrophage inhibiting P815 cell proliferation. *Beijing Yike Daxue Xuebao*, 1986;18:127-130
35 Cheng ML, Wu YY, Huang KF, Luo TY, Ding YS, Lu YY, Liu RC, Wu J. Clinical study on the treatment of liver fibrosis due to hepatitis B by IFN-α_1 and traditional medicine preparation. *World J Gastroenterol*, 1999;5:267-269
36 Gan LW, Wang GJ, Li YL. Effects of oxymatrine on liver fibrosis in rats. *Dier Junyi Daxue Xuebao*, 1999;20:445-448

Edited by Ma JY

P.O.Box 2345 Beijing 100023, China
Fax. 0086·10·65891893 Tel. 0086·10·65897901
E-mail.wcjd@public.bta.net.cn www.wd.org.cn

World J Gastroentero, 2001 April; 7(1):53 - 59
World Journal of Gastroenterology
Copyright©2001 by the WJG Press ISSN 1007 - 9327

Relationship between phenotypes of cella2function differentiation and pathobiological behavior of gastric carcinomas

Yan Xin, Xiao Ling Li, Yan Ping Wang, Su Min Zhang, Hua Chuan Zheng, Dong Ying Wu and Yin Chang Zhang

Subject headings stomach neoplasms; cell differentiation; lymphatic metastasis; prognosis; cell-function classification; immunohistochemistry; absorptive function differentiation type

Xin Y, Li XL, Wang YP, Zhang SM, Zheng HC, Wu DY, Zhang YC. Relationship between phenotypes of cell-function differentiation and pathobiological behavior of gastric carcinomas. ***World J Gastroenterol***, 2001;7(1):53-59

Abstract

AIM **To reveal the correlation between the functional differentiation phenotypes of gastric carcinoma cells and the invasion and metastasis by a new way of cell-function classification.**

METHODS **Surgically resected specimens of 361 gastric carcinomas(GC) were investigated with enzyme-, mucin-, and tumor-related marker immunohistochemistry. According to the direction of cell-function differentiation, stomach carcinomas were divided into five functionally differentiated types.**

RESULTS **① Absorptive function differentiation type (AFDT): there were 82 (22.7%) patients including 76 (92.7%) aged 45 years. Sixty-nine (84.1%) cases belonged to the intestinal type. Thirty-eight (46.3%) expressed CD44v6 and 9 (13.6%) of 66 male patients developed liver metastasis. The 5-year survival rate of patients in this group (58.5%) was higher than those with the other types (*P*<0.01). ② Mucin secreting function differentiation type (MSFDT): 54 (15%) cases. Fifty-three (98.1%) tumors had penetrated the serosa, 12 (22.2%) expressed ER and 22 (40.7%) expressed CD44v6. The postoperative 5-year survival rate was 28.6%. ③ Absorptive and mucin-producing function differentiation type (AMPFDT): there were 180 (49.9%) cases, including 31 (17.2%) aged yanger than 45 years. The tumor was more common in women (62, 34.4%,) and expressed more frequently estrogen receptors (ER)(129, 81.7%) than other types (*P*<0.01). Ovary metastasis was found in 12 (19.4%) out of 62 female subjects. The patients with this type GC had the lowest 5-year survival rate (24.7%) among all types. ④ Specific function differentiation type (SFDT): 13 (3.6%) cases. Nine (69.2%) tumors of this type derived from APUD system, the other 4 (30.7%) were of different histologicaldifferentiation. Sixty per cent of the patients survived at least five years. ⑤ Non-function differentiation type (NFDT): 32 (8.9%) cases. Nineteen (59.%) cases had lymph node metastases but no one with liver or ovary metastasis. The 5-year survival rate was 28.1%.**

CONCLUSION **This new cell-function classification of GC is helpful in indicating the characteristics of invasion and metastasis of GC with different cell-function differentiation phenotypes. Further study is needed to disclose the correlation between the cell-functional differentiation phenotypes and the relevant genotypes and the biological behavior of gastric carcinoma.**

The Fourth Laboratory of Cancer Institute, China Medical University, Shenyang 110001 ,Liaoning Province, China
Yan Xin, graduated from China Medical University in 1993 with M.D, Ph.D, now Professor, Director of the Fourth Laboratory of Cancer Institute of China Medical University, specialized in tumor pathology, focusing on the pathobiological behavior of gastrointestinal carcinoma and the mechanism of metastasis, having more than 60 papers published.
Project supported by the National Natural Science Foundation of China, No.39270300, No.39370772 and Training Program for Trans-Century Talents by the State Education Commission of China.
Correspondence to: Prof. Yan Xin, The Fourth Laboratory of Cancer Institute, China Medical University, Shenyang 110001, Liaoning Province, China
Tel. 0086-24-23256666 Ext.6351, Fax. 0086-24-23252377
Received 2000-05-18 **Accepted** 2000-06-23

INTRODUCTION

Gastric carcinoma is one of the most common malignancies and has the highest mortality in China [1,2]. The most important reason causing patients' death is the metastasis to distant important organs. It was reported that 64.2% of gastric carcinomas developed distant organ metastases, among which the rate of liver metastasis was 31.8% of all patients, and ovary metastasis rate was 43.6% of the female patients[3]. As liver is the biggest parenchymatous organ in the body, the micrometastasis of it is very difficult to be diagnosed early. The same is true in ovary metastasis because ovaries lie in the bottom of abdominal cavity. There has been no good indicator so far to objectively predict the risk of liver and ovary metastases, making the diagnosis for micrometastases of these two organs very difficult. The present study put

forward a new classification of gastric carcinoma based on the cell-function differentiation features, in an attempt to reveal the relationship between the characteristics of cell-function differentiation and the local invasion and distant organ metastases of gastric carcinomas, and to clarify the causes and molecular mechanism of metastasis to the liver or ovary.

MATERIALS AND METHODS

Subjects

Three hundred and sixty-one cases of surgically resected gastric carcinomas (from Cancer Institute, China Medical University) were involved in the study, consisting of 258 men and 103 women, including 11 without metastasis, 224 with lymph node metastases, 12 with liver metastases, and 14 with ovary metastases. At least 2 blocks were cut from each primary tumor and 1 block from each metastatic tumor of any organ involved respectively.

Principle and standards of cell-functional differentiation classification

Glandular epithelial cells of gastrointestinal tract can be divided into three main groups: ① absorptive cells of the small intestine, ② mucinous cells including goblet and columnar mucous cells; and ③ cells with specific secretary function, such as parietal, chief, paneath, and APUD system cells. According to the principle that cancer cells maintain more or less the functional differentiation potential of their ancestors, a group of comprehensive indicators that could objectively reflect absorptive, mucin-secreting, and specific function differentiation were selected: indicators of absorptive function differentiation were brush border enzymes, such as alkaline phosphatase (AKP) and L-aminopeptidase (LAP); indicators of mucin secreting function differentiation were sulfomucin (HID+), sialomucin (ABpH2.5+) and neutral mucin (PAS+), and indicators of specific function differentiation were antibodies to hormones produced by APUD cells, cellular keratin and others. According to the expressions of these indicators, the gastric carcinomas were divided into five cell-function differentiation types: ① gastric carcinomas, in which more than two thirds of cancer cells expressed AKP and LAP but did not secrete mucin or hormone, were defined as absorptive function differentiation type (AFDT); ② those in which more than two thirds of the cancer cells secreted only mucin but not AKP or LAP, were defined as mucin secreting function differentiation type (MSFDT); ③ those in which more than two thirds of the cancer cells not only expressed AKP and LAP but also produced mucin, were defined as absorptive and mucin-producing function differentiation type (AMPFDT); ④ those which neither expressed AKP and LAP nor produced mucin, were defined as non-function differentiation type (NFDT); and ⑤ specific function differentiation type (SFDT) was defined as that more than two thirds of cancer cells possessed some special functions, such as the tumors from APUD system and squamous cell cancer (Table 1 and Figures 1-6).

Table 1 Standards of cell-function classification of gastric carcinoma

Type	Brush border enzyme		Mucin			Immunohistochemistry	
	AKP	LAP	HID	ABpH2.5	PAS	Ch-A	Keratin
AFDT	+	+	-	-	-	-	-
MSFDT	-	-	+	+	+	-	-
ANOFDT	+	+	+	+	+	-	-
SFDT	-	-	-	-	-	+	+*
NFDT	-	-	-	-	-	-	-

*Chosen according to practice.

Detection of cell-functional differentiations

Enzyme histochemistry[4]: alkaline phosphatase (AKP) was detected by Gomori's method, and L-aminopeptidase (LAP) by Nachal's method. Mucin histochemistry was done by the HID/ABpH2.5 / PAS method[5]; endocrine histochemistry was performed by ABC immunostaining with antibodies to hormones produced by APUD cells. The results were evaluated using the standards given in references[6,7].

Detection of tumor associated markers[8-13]

The sections from all cases were stained by ABC histochemistry using antibodies to ER and CD44v6 respectively. The ploidy of DNA patterns of the cases with liver or ovary metastasis was examined by flow cytometry (FCM). p53 and laminin expressions in the gastric carcinomas with liver or ovary metastasis were also detected immunohistochemically.

Statistics

χ^2 test was employed in this study to analyze the results of histochemistry and survival data.

RESULTS

The carcinomas were divided into five types: 82 cases classified as AFDT (22.7%); 54 MSFDT (15%); 180 AMPFDT (49.9%); 32 NFDT (8.9%) and 13 SFDT (3.6%). Tables 2 and 3 illustrate the relationship between the cell function classification and the patients' age and sex. The relationship between the cell-function classification and histological types, growth patterns, clinicopathological stages, ER expression, CD44v6 expression, ability forming laminin-positive basement membraneous structure, lymph node metastasis, liver and ovary metastases, and postoperative 5-year survival rates are shown in Tables 4-13 and Figures 1-12.

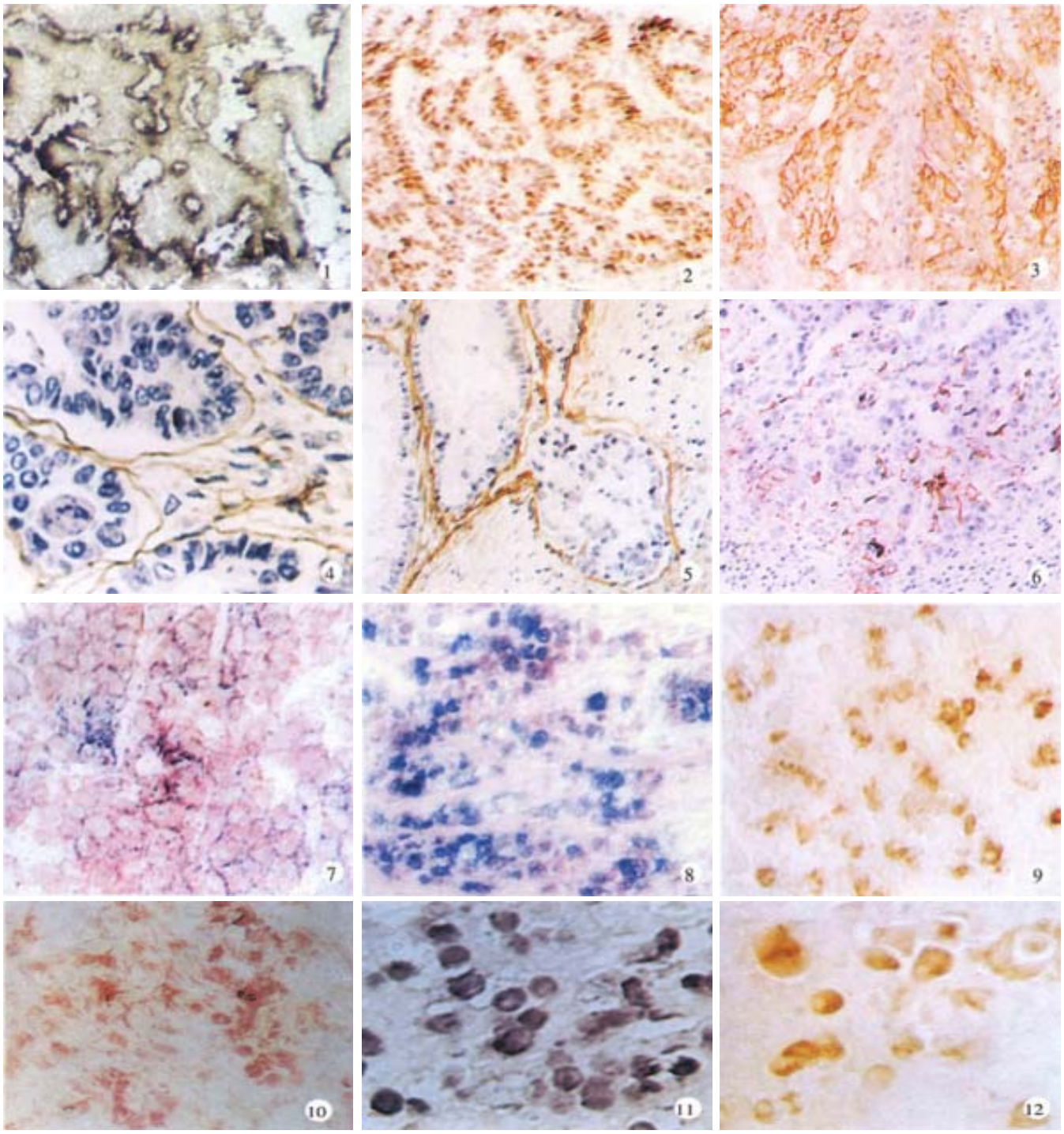

Figure 1 Primary stomach cancer of AFDT with liver metastasis. AKP was moderately positive and distributed along the free edge of cancerous papillary structure. Frozen section. ×20

Figure 2 The same case in Figure 1, Tp53 protein was expressed in most of primary cancer cells. Immunostain, ×16

Figure 3 The same case of Figure 1. CD44v6 was expressed in most of primary cancer cells. Immunostain, ×20

Figure 4 The same case of Figure 1. There was obvious basement membrane like structure with Laminin positive in the primary tumor. Immunostain, ×40

Figure 5 The same case of Figure 1. There was also obvious basement membrane like structure with laminin positive in the liver metastatic tumor. Immunostain, ×20

Figure 6 The same case of Figure 1. CD44v6 was also expressed in the liver metastatic cancer cells. Immunostain, ×20

Figure 7 Primary gastric carcinoma of AMPFDT with ovary metastasis. LAP was moderately positive and distributed in the membrane and cytoplasm of cancer cells. Frozen section, ×40

Figure 8 The same case of Figure 7. Sialomucin and neutral mucin were positive in the primary cancer cells. Mucin histochemistry, ×20

Figure 9 The same case of Figure 7. Most of primary cancer cells expressed ER, which was distributed in the nuclei and cytoplasm. Immunostain, ×20

Figure 10 The same case of Figure 7. LAP was moderately positive in the ovary metastatic cancer cells. Frozen section, ×20

Figure 11 The same case of Figure 7. Sulfomucin was positive in the ovary metastatic cancer cells. Mucin histochemistry, ×40

Figure 12 The same case of Figure 7. Most of the ovary metastatic cancer cells expressed ER. Immunostain, ×40

Table 2 Relationship between cell function classification and age of patients with gastric carcinoma

Type	*n*	Age		
		<45 yrs(%)	45-65 yrs(%)	>65 yrs(%)
AFDT	82	6 (7.3)	59 (72.0)	17 (20.7)
MSFDT	54	2 (3.7)	43 (79.6)	9 (14.7)
AMPFDT	180	31 (17.2)[a]	118 (65.5)	31 (17.2)
SFDT	13	1 (7.7)	9 (69.2)	3 (23.1)
NFDT	32	6 (18.8)	17 (53.1)	9 (28.1)
Total	361	46 (12.7)	246 (68.1)	69 (19.1)

[a]$P<0.05$ ($\chi^2 = 4.5575$), *vs* AFDT of the patients below 45 years old.

Table 3 Relationship between cell-function classification and sex of patients with gastric carcinoma

Type	*n*	Female (%)		Male (%)	
		n	%	*n*	%
AFDT	82	16	(19.5)	66	(80.5)
MSFDT	54	15	(27.8)	39	(72.2)
AMPFDT	180	62	(34.4)[a]	118	(65.6)
SFDT	13	3	(23.1)	10	(76.9)
NFDT	32	7	(21.9)	25	(78.1)
Total	361	103	(28.5)	258	(71.5)

[a]$P<0.05$ ($\chi^2 = 6.0079$), *vs* AFDT of female patients.

Table 4 Relationship between cell-function and WHO's histological classifications of gastric carcinoma

Types	*n*	AFDT(%)	MSFDT(%)	AMPFDT(%)	SFDT(%)	NFDT(%)
Papillary adenocarcinoma	37	29 (78.4)[a]	2 (5.4)	6 (16.2)	0	0
Tubular adenocarcinoma						
Well-diff. ade.	20	17 (85.0)	0	2 (10.0)	0	1 (5.0)
Mode. diff. ade.	59	20 (33.9)	5 (8.5)	27 (45.8)	1 (1.7)	6 (10.2)
Poor. diff. ade.	126	15 (11.9)	14 (11.1)	79 (62.7)	2 (1.6)	16 (12.7)
Undiff. car.	30	1 (3.3)	7 (23.3)	13 (43.3)	0	9 (30.0)
SRC	41	0	5 (12.2)	6 (87.8)[b]	0	0
Mucous ade.	38	0	21 (55.3)	17 (44.7)	0	0
Carcinoid	9	0	0	0	9 (100.0)	0
Squamous car.	1	0	0	0	1 (100.0)	0
Total	361	82 (22.7)	54 (15.0)	180 (49.9)	13 (3.6)	32 (8.9)

[a]$P<0.01$ ($\chi^2 = 28.6784$), *vs* others of the papillary adenocarcinomas; [b]$P<0.01$ ($\chi^2 = 46.8780$), *vs* others of signetring cell carcinomas. ade: adenocarcinoma; diff.: differentiated; mode.: moderately; undiff.: undifferentiated; SRC: signet ring cell carcinoma

Table 5 Relationship between cell-function and Lauren£§s classifications of gastric carcinoma

Types	*n* (%)	AFDT(%)	MSFDT(%)	AMPFDT(%)	SFDT(%)	NFDT(%)
Intestinal	124(36.4)	69(84.1)[a]	11(20.4)	33(18.3)	11(84.6)[b]	0
Diffuse	237(63.6)	13(15.9)	43(79.6)	147(81.7)	2(15.4)	32(100.0)
Total	361	82	54	180	13	32

[a]$P<0.01$ ($\chi^2 = 102.6339$), *vs* AMPFDT; [b]$P<0.01$ ($\chi^2 = 15.11320$),*vs* AMPFDT.

Table 6 Relationship between cell-function classification and histological growth patterns of gastric carcinomas

Patterns	*n*(%)	AFDT(%)	MSFDT(%)	AMPFDT(%)	SFDT(%)	NFDT(%)
Mass	19(6.1)	12(19.4)	0	0	7(53.8)	0
Nest	84(27.0)	37(59.7)	12(22.2)	23(14.8)	6(46.2)	6(22.2)
Diffuse	208(66.9)	13(21.0)[a]	42(77.8)	132(85.2)	0	21(77.8)
Total	311	62(19.9)	54(17.4)	155(49.8)	13(4.2)	27(8.7)

[a]$P<0.01$(Exact test: $\chi^2 = 12.2793$), *vs* MSFDT, AMPFDT and NFDT.

Table 7 Relationship between cell-function classification and clinicopathological stages of gastric carcinomas

Stages	*n*(%)	AFDT(%)	MSFDT(%)	AMPFDT(%)	SFDT(%)	NFDT(%)
EGC	50(13.9)	20(24.4)	0	25(13.9)	0	5(15.6)
AGC						
Subserosa	42(11.6)	8(9.8)	1(1.9)	28(25.6)	1(7.7)	4(12.5)
Through serosa	269(74.5)	54(65.9)	53(98.1)[a]	127(70.6)	12(92.3)	23(71.9)
Total	361	82	54	180	13	32

[a]$P<0.01$($\chi^2 = 10.1203$, 8.9078 and 6.7487 respectively), *vs* AFDT, AMPFDT and NFDT.

Table 8 Relationship between cell-function classification and ER expression of gastric carcinomas

ER expression	AFDT	MSFDT	AMPFDT	SFDT	NFDT	Total
Positive / examined	7 / 82	12 / 54	129 / 180	0 / 13	7 / 32	155 / 361
Positive rate(%)	8.5	22.2	71.7[a]	21.9	42.9	

[a]$P<0.01$($\chi^2 = 45.6418$), *vs* others.

Table 9 Relationship between cell-function classification and CD44v6 expression in gastric carcinoma tissues

CD44v6	*n*	AFDT(%)	MSFDT(%)	AMPFDT(%)	SFDT(%)	NFDT(%)
-	241	44	32	132	9	24
+ (%)	120(33.2)	38(46.3)[a]	22(40.7)[b]	48(26.7)	4(30.8)	8(25.0)
Total	361	82	54	180	13	32

[a]$P<0.01$ ($\chi^2 = 9.8900$), *vs* AMPFDT; [b]$P<0.05$ ($\chi^2 = 3.9245$), *vs* AMPFDT.

Table 10 Relationship between cell-function classification and metastases of gastric carcinomas

Types	*n*(%)	AFDT(%)	MSFDT(%)	AMPFDT(%)	SFDT(%)	NFDT(%)
No mets	111(30.7)	28(34.1)	13(24.1)	51(28.3)	6(46.2)	13(40.6)
LN mets	224(62.0)	45(54.9)	38(70.4)	116(64.4)	6(46.2)	19(59.4)
Liver mets	12(3.3)	9(11.0)[a]	1(1.9)	1(0.6)	1(7.7)	0
Ovary mets	14(3.9)	0	2(3.7)	12(6.7)	0	0
Total 361	82(22.7)	54(15.0)	180(49.9)	13(3.6)	32(8.9)	

[a]$P<0.05$ (Exact test: $\chi^2 = 5.4385$), *vs* AMPFDT.Mets: metastasis; LN: lymph node.

Table 11 Relationship among cell-function classification, metastasis and sex of patients with gastric carcinoma

Types	Liver metastasis		Ovary metastasis
	Male (%)	Female (%)	
AFDT	9/ 66 (13.6)[a]	0/ 16	0/ 16
MSFDT	0/ 39	1/ 15 (6.7)	2/ 15 (13.3)
AMPFDT	1/ 118 (0.8)	0/ 62	12/ 62 (19.4)[b]
SFDT	1/ 10 (10.0)	0/ 3	0/ 3
NFDT	0/ 25	0/ 7	0/ 7
Total	11/258 (4.3)	1/103 (1.0)	14/103 (13.6)

[a]$P<0.01$ (Exact test $\chi^2 = 8.9527$), *vs* AMPFDT of the male with liver metastasis;[b]$P<0.05$ (Exact test $\chi^2 = 4.2992$), *vs* AFDT, SFDT and NFDT of the female with ovary metastasis.

Table 13 Relationship between postoperative survival rates and cell function classification of gastric carcinomas

Types	*n*	Cases survived over 5 years (%)	
AFDT	82	48	(58.5)[a]
MSFDT	49	14	(28.6)
AMPFDT	174	43	(24.7)
SFDT	5	3	(60.0)
NFDT	32	9	(28.1)
Total	342	117 (34.2)	

[a]$P<0.01$($\chi^2 = 11.0478$, 28.7138 and 10.3250), *vs* MSFDT, AMPFDT and NFDT, respectively.

Table 12 Comparison of cell-function differentiation classification and molecular biological features of gastric carcinoma with liver or ovary metastases

Comparison	GC with liver mets.	GC with ovary mets.
	Positive / 12 cases(%)	Positive / 14 cases(%)
Cell-function differentiation types		
AFDT	9 (75.0)[a]	0
MSFDT	1 (8.3)	2 (14.3)
AMPFDT	1 (8.3)	12(85.7)[b]
SFDT	1 (8.3)	0
NFDT	0	0
Comparison of molecular biological features		
Estrogen-dependent ER(+)	0	12(85.7)[c]
LN (+) BM structure (+)	12 (100.0)	0
Mutant p53 protein (+)	10 (83.3)[d]	3 (21.4)
DNA ploidy:Diploid	3 (25.0)	10 (71.4)
Tetraploid	0	2 (14.3)
Aneuploid	9 (75.0)[e]	2 (14.3)
CD44v6 expression (+)	10 (83.3)[f]	0

LN: laminin; BM: basement membrane; Mets: metastasis
[a]$P<0.01$ (Exact test $\chi^2 = 12.9160$), *vs* AFDT with ovary mets;
[b]$P<0.01$ (Exact test $\chi^2 = 12.5357$), *vs* AMPFDT with liver mets;
[c]$P<0.01$ (Exact test $\chi^2 = 15.8087$), *vs*GC with liver mets;
[d]$P<0.01$ (Exact test $\chi^2 = 7.5833$), *vs* GC with ovary mets;
[e]$P<0.01$ (Exact test $\chi^2 = 6.0420$), *vs* GC with ovary mets;
[f]$P<0.05$ (Exact test $\chi^2 = 15.6010$), *vs* GC with ovary mets.

DISCUSSION

In the light of differentiation degree, malignant tumors from epithelial cells of gastrointestinal tract may retain more or less the functional differentiation potential of their ancestors, which has effects on their biological behavior. Previous studies revealed the relationship between the morphological differentiation and the pathobiological behavior of gastric cancer[14-22], but so far there have been very few studies on the phenotypes of functional differentiation of gastric cancer cells[23-25]. We have studied simple morphological and the functional differentiation indicators of gastric carcinoma to infer its biological behavior during last fifteen years, and found that there was a correlation between the functional differentiation of gastric carcinoma cells and their biological behavior[26-32]. In this study, we investigated more cases and compared the degree of functional differentiation and morphological differentiation features of gastric carcinomas, and found no definite correlation between them. Although most well-differentiated papillary and tubular adenocarcinomas possessed absorptive functions, all signet ring cell cancers were classified as AMPFDT and carcinoid tumors as SFDT, the direction of functional differentiation of most moderately and poorly differentiated adenocarcinomas were undetermined. Most so-called undifferentiated cancers determined histologically displayed some functional differentiation, and were mostly MSFDT or AMPFDT gastric carcinomas; truly undifferentiated cancers made up only 8.3% in our study. Interestingly, 55.3% of mucinous adenocarcinomas classified by histology had mucin-secreting function (MSFDT) but the other 44.7% had absorptive and mucin-producing function (AMPFDT). Furthermore, Tumors of MSFDT were significantly different from those of AMPFDT in patient age, the serosa involvement, estrogen dependence and the CD44v6 expression. The results indicated that the cancer cells of mucinous adenocarcinoma possessed obvious heterogenicity in cell function differentiation and biological behavior, which should be paid special attention to predict the invasive and metastatic features.

The results also indicated that stomach cancers with different functional characteristics often possessed different pathobiological behavior. For example, the MSFDT tumors, constantly growing invasively, were mostly accompanied by the

serosa involvement, and were not obviously dependent on estrogen. NFDT independent of estrogen invades weakly, of which about 60% metastasized to lymph node. Among different functionally differentiated gastric carcinomas, AFDT and AMPFDT had specific clinicopathologically biological features as follows. Gastric carcinomas of ATDT were most common in the middle aged and senile (92.7%), only 7.3% were found in the young; with men (80.5%) surpassing women (19.5%), and intestinal type gastric carcinoma (84.1%) exceeding diffuse ones; and exhibited mainly "mass" or "nest" styles of growth. The invasion of this type of tumor was often beneath the serosa, which resisted local infiltration as a barrier. AFDT, whose growth was not very much dependent on estrogen, expressed metastasis-associated cell adhesion molecule CD44v6 at a higher rate than AMPFDT, and its postoperative 5-year survival rate was 58.5% revealed its best prognosis. Liver metastasis was frequently observed in patients with AFDT tumor whose biological behavior was as follows: ① mutant p53 protein positively expressed at a rate of 83.3%; ② among 75.0% of cases, DNA showed aneuploid; ③ 83.3% of this type presented positive expression of CD44v6; and ④ the thread-like basement membraneous structure containing LN was often formed. Special attention should be paid clinically to the characteristics of AFDT stomach cancer mentioned above. AMPFDT gastric carcinoma often occurried in the young aged below 45 years (17.2%) with more female patients (34.3%) than in other types, and histologically, 81.7% were diffusing invasive type and 71.7% were estrogen-dependent type, and there were more ovary metastases (19.4%) than in the other types. The 5-year survival rate of 24.7% embodied the worst prognosis. AMPFDT gastric carcinoma that grew in women with ovary metastasis had the following biological behavior: 85.7% of cases had high ER expression; mutant P53 protein displayed low expression at a rate of 21.4%; no expression of metastasis-associated adhesion molecule CD44v6; and diploid DNA occurred in 71.4% of tumors. Although the molecular mechanism of liver and ovary metastases was not clear, we should pay much more attention to the cell-function differentiation and biological behavior of gastric carcinomas mentioned above in order to help with the early diagnosis and treatment of the micrometastasis in the liver and ovary.

Much attention has been paid to the mechanism of cancer invasion and metastasis[33-42], especially to the mechanism of the liver and ovary metastases from gastric carcinomas. Several hypotheses have been proposed but cannot explain the specific organic affinity satisfactorily[43-50]. Our study found that the gastric carcinomas with liver metastasis possessed different cellular biological behaviors from those with ovary metastasis (Tables 10-12). It is thus possible to consider a new explanation of the mechanisms of the organic affinity of liver and ovary metastases: the fact that the gastric carcinoma with liver metastasis displayed absorptive function differentiation and expressed LN positive basement membrane-like structure suggested that these cancer cells may have increased the number of exposed laminin receptors. When the cells with exposed laminin receptors (LR) encounter the basement membrane of capillaries, the cancer cells can combine with the basement membrane by the specific affinity between LN and LR, making it possible for the cancer cells to invade the blood vessels. Therefore, we can hypothesize that the presence of exposed LR on the surface of cancer cells is an important precondition for the metastasis through the blood vessels. Most gastric cancers with ovary metastasis displayed disordered functional differentiation in the directions of absorption and mucin-production, and all these cancers expressed estrogen receptors (ER). This finding suggests that the specific organic affinity between the ovary and the specific type of gastric carcinomas may be related to an estrogen-estrogen receptor (E-ER) link.

In addition, our study found that gastric carcinomas exhibiting "mass" or "nest" growth pattern, all expressed thread-like structure containing LN. The reason for this phenomenon is probably that LR is polarized on the basal side of the cancer cells which grow in masses or nests, so these cancer cells can arrange in a row along basement membranes containing LN. On the contrary, the laminin receptors were absent or disordered on those cancer cells which grow diffusely, so that they cannot form a regular structure[51-53].

In summary, the findings of the study indicate that there was some correlation between the cell-function differentiation and invasion and metastasis of gastric carcinomas. A further study is necessary to make clear the genotypes of different functional phenotypes of gastric carcinomas and find out new molecular biological markers for the early diagnosis and treatment of the metastasis. Additionally, the remarkable difference between liver and ovary metastasis of gastric carcinoma in cell-function differentiation, P53 gene mutation, ploidy of DNA, CD44v6 expression and laminin expression indicates their different pathways of gene regulation.

REFERENCES

1 Li LD, Lu FZ, Zhang SW, Mu R, Shun XD, Huangpu XM. Analyses variation trend and short term detection of Chinese malignant tumor mortality during twenty years. *Zhonghua Zhongliu Zazhi*, 1997;19:3-9

2 Li LD, Zhang SW, Lu FZ, Mu R, Shun XD, Huangpu XM. Research characteristics of mortality spectrum and type composition of malignant tumors in China. *Zhonghua Zhongliu Zazhi*, 1997;19: 323-328

3 National Pathological Association of Stomach Cancer Research.

Pathological study on the postmortems of 360 gastric carcinomas. *Zhonghua Binglixue Zazhi*, 1983;12:124-128
4 Takeuchi T editor. New Enzyme Histochemistry. Tokyo: Asakura Publishing House, 1980:228
5 Jass JR. Sulphomucin, precancerous lesion of the human stomach. *Histopathology*, 1980;4:291-296
6 Xin Y, Zhang YC, Zhang PF, Wang MX. Comparative study of cyclic nucleotide phosphodiesterases and marker enzymes of small intestinal absorptive cell in gastric cancer tissue. *Zhongguo Yike Daxue Xuebao*, 1991;20:333-337
7 Xin Y, Wu DY, Zhang SM, Wang YP, Xu L, Zhao FK, Zhang YC. Relationship between the expression of glucagon and liver metastasis of gastric carcinoma. *Zhongguo Yike Daxue Xuebao*, 1998; 27(Suppl):1-5
8 Xin Y, Zhao FK, Li HZ, Zhang YC. Relationship between the expression of ER and pathobiological behavior of gastric carcinomas. *Zhongguo Yike Daxue Xuebao*, 1991;20:231-233
9 Xin Y, Leader M, Henry K. DNA ploidy, expression of p53 and metastatic behavior of gastric carcinoma. *Chin Med Sci J*, 1996; 11:147-151
10 Xin Y, Grace A, Leader M, Kay E. CD44 splice variant 6(CD44v6) in gastric carcinomas. *Lab Invest*, 1999;79:495
11 Xin Y, Zhao FK, Zhang SM, Wu DY, Wang YP, Xu L. Relationship between CD44v6 expression and prognosis in gastric carcinoma patients. *Shijie Huaren Xiaohua Zazhi*, 1999;7:210-214
12 Xin Y, Zhao FK, Wu DY, Zhang PF, Zhang YC, Wang YH. Immunohistochemical study on the content and distribution of laminin in stomach cancer tissues. *Zhongguo Yike Daxue Xuebao*, 1993;22:179-181
13 Xin Y, Zhao FK, Wu DY, Wang YP, Xu L, Zhang YC. Relationship between the mutation of p53 gene and infiltration,metastasis and prognosis of gastric carcinoma. *Chin J Cancer Res*, 1996;8: 263-266
14 Zhang YC, Zhang PF, Zhang WF. Study of the morphological and biological features of 60 cases of stomach cancers. *Zhonghua Binglixue Zazhi*, 1964;8:234-237
15 Lauren P. The two histological main types of gastric carcinoma: diffuse and socalled intestinal-type carcinoma. *Acta Path*, 1965;64:31-37
16 Ming SJ. Gastric carcinoma. *Cancer*, 1977;33:2475-2481
17 Japanese Research Society for gastric Cancer. The general rules for the gastric cancer study in surgery and pathology. Part II. Histological classification of gastric cancer. *Jpn J Surg*, 1981;48: 2084-2087
18 Watanabe H, Jass JR, Sobin LH. In collaboration with pathologists in 8 countries. Histological typing of esophageal and gastric tumors, 2nd edition. *WHO International Histological Classification of Tumours*. Berlin: Springer-Verlag, 1994:40-52
19 UICC, TNM classification of malignant tumors. 4th edition. Hermaneck P, Sobin IH, eds. Berlin; Springer-Verlag, 1987
20 Martin IG, Dixon MF, Sue-Ling H, Axon ATR, Johnston D. Goseki histological grading of gastric cancer is an important predictor of outcome. *Gut*, 94;35:758-763
21 Carneiro F. Classification of gastric carcinomas. *Curr Diag Pathol*, 1997;4:51-59
22 Zhang YC. Metastatic carcinoma of the cervix uteri from the gastrointe stinal tract. *Gynecol Oncol*, 1983;15:287-290
23 Zhang QX, Dou YL, Shi XY, Ding Y. Expression of somatostatin mRNA in various differentiated types of gastric carcinoma. *World J Gastroenterol*, 1998;4:48-51
24 Yu JY, Wang LP, Meng YH, Hu M, Wang JL, Bordi C. Classification of gastric neuroendocrine tumors and its clinicopathologic significance. *World J Gastroentero*, 1998;4:158-161
25 Yi YF, Cheng BK. Expression of sialylated mucin-associated carbohydrate structures in human gastric carcinoma. *World J Gastroenterol*, 1998;4:233
26 Xin Y,Zhao FK,Wu DY,Wang YP.Comparative study of functional and histological differentiation of 104 gastric carcinomas. *Zhongguo Yike Daxue Xuebao*, 1993;22:259-261
27 Xin Y, Zhao FK, Gong W, Wang YP, Zhang YC, Yan RF. A new classification of stomach cancer and its pathobiological and clinical significance. *Chin Med Sci J*, 1994;9:119-124
28 Xin Y, Zhao FK, Wu DY, Wang YP, Zhang YC. Recommendation of a new functional classification of gastric cancer. *Zhonghua Binglixue Zazhi*, 1995;24:320-321
29 Xin Y, Zhao FK, Wang YP, Zhang YC. Comparative study of the biological behavior of signet ring cell carcinoma and mucinous adenocarcinoma of the stomach. *Zhongguo Yike Daxue Xuebao*, 1996;25:441-445
30 Zhao FK, Xin Y, Zhang SM. Relationship between Collagen I and Laminin and the pathobiological behavior of gastric carcinomas. *Zhongguo Yike Daxue Xuebao*, 1998;27(Suppl):6-8
31 Xin Y, Zhao FK, Wang YP, Wu DY. Study of the biological characteristics of the metastatic tumor cells in the liver from the cancers of gastrointestinal tract. *Zhongguo Yike Daxue Xuebao*, 1994;23:443-445
32 Xin Y, Zhao FK, Wang YP, Wu DY. Study of biological characteristics of the metastatic tumour cells in the ovary and uterus cervix from the cancers of gastrointestinal tract. *Zhongguo Yike Daxue Xuebao*, 1995;24:1-4
33 Albelda SM. Role of intergrins and other cell adhesion molecules in tumour progression and metastasis. *Lab Invest*, 1993;68:4-17
34 Matsui S, Shiozaki H, Inoue M. Immunohistochemical evaluation of alpha-catenin expression in human gastric cancer. *Virchows Arch*, 1994;424:375-381
35 Su LK, Vogelstein B, Kinzler KW. Association of the APC tumour suppresor protein with catenins. *Science*, 1993;262:1734-1737
36 Rubinfeld R, Robbins P, E1-Gamil M, Albert I, Porfiri E, Polakis P. Stabilization of β-catenin bu genetic defects in melanoma cell lines. *Science*, 1997;275:1790-1792
37 Morin PJ, Sparks AB, Korinek V. Activation of B-catenin-Tcf signaling in colon cancer by mutations in B-catenin or PAC. *Science*, 1997;275:1787-1790
38 Joseph-Silverstein J, Silverstein RL. Cell adhesion molecules: an overview. *Cancer Invest*, 1998;13:1225-1231
39 Postel EH. NM23-NPD kinase. *Int J Biochem Cell Biol*, 1998;30: 1291-1295
40 Ma D, Luyten GP, Luider TM, Jager MJ, Niederkorn JY. Association between NM23-H1 gene expression and metastasis of human Uveal melanoma in an animal model. *Invest Opththalm Visual Sci*, 1996;37:2293-2301
41 Sass PM. The involvement of selectins in cell adhesion, tumour progression and metastasis. *Cancer Invest*, 1998;51:191-196
42 Liotta LA, William G, Stevenson WG. Tumour invasion and metastasis: an imbalance of positive and negative regulation. *Cancer Res*, 1991;51(Suppl):5054s
43 Liotta LA, Steeg PS, Stetler-Stevenson WG. Cancer metastasis and angiogenesis:an imbalance of positive and negative regulation. *Cell*, 1991;64:327-336
44 Stetler-Stevenson WG. Type I collagenases in tumour invasion and metastasis. *Cancer Metastasis Rev*, 1990;9:289-303
45 Hruban RH, Offerhaus GJ. Molecular diagnosis of cancer and micrometast ases. *Adv Anat Pathol*, 1998;5:175-181
46 Morris VL, Schmidt EE, MacDonald IC. Sequential steps in hematogenous metastasis of cancer cells studied by *in vivo* videomicroscopy. *Invasion Metastasis*, 1999;17:281-287
47 Nicolson GL. Gene expression, cellular diversification and tumour progression to the metastatic phenotype. *Bioessays*, 1991;13: 337-342
48 Liotta LA, Kleinerman J, Saidel G. Quantitative relationships of intravascular tumour implantation. *Cancer Res*, 1996;56:4063-4670
49 Meyer T, Hart IR. Mechanism of tumour metastasis. *Eur J Cancer*, 1998;34:214-221
50 Woodhouse EC, Chuaqui RF, Liotta LA. General mechanisms of metastasis. *Cancer*, 1997;80:1529-1537
51 Liotta LA, Horan HP, Rao CN. Monoclonal antibodies to the human laminin receptor recognized structurally distinct sites. *Exp Cell Res*, 1985;156:117-121
52 De-Manzoni G,Gnugliemi A,Verlato G. Prognostic significance of 67kD laminin receptor expression in advanced gastric cancer. *Oncology*, 1998;55:456-460
53 Li XL, Wang YP, Wu DY, Zhang SM, Xin Y. Expression of 67Kda laminin receptor in human gastric cancer and its significance. *Zhongguo Aizheng Yanjiu Jinzhan*, 2000;5:130-134

Edited by Ma JY

P.O.Box 2345 Beijing 100023, China

Inh a-tocopheryl succinate on)-induced forestomach car nice

World J Gastroentero, 2001 April; 7(1):60 - 65

Kun Wu[1], Yu Juan Shan[1], Yan Zhao[1], Jian Wu Yu[2] and Bai He Liu[1]

Fax: 0086-10-65891893 Tel. 0086-10-65897901
E-mail:wcjd@public.bta.net.cn www.wjd.org.cn
World Journal of Gastroenterology
Copyright©2001 by the WJG Press. ISSN 1007 - 9327

Subject headings stomach neoplasms; antineoplastic agents; vitamin E; transforming growth factors; apoptosis; benzo(a)pyrene

Wu K, Shan YJ, Zhao Y, Yu JW, Liu BH. Inhibitory effects of RRR-a-tocoph eryl succinate on benzo(a)pyrene (B(a)P)-induced forestomach carcinogenesis in female mice. ***World J Gastroenterol***, 2001;7(1):60-65

Abstract

AIM **To study the inhibitory effects of VES (RRR-α-tocopheryl Succinate, VES), a derivative of natural Vitamin E, on benzo(a)pyrene(B(a)P)-induced forestomach tumor in female mice.**

METHODS **The model of B(a)P-induced forestomach tumor was established according to the methods of Wattenberg with slight modifications. One hundred and eighty female mice (6 weeks old) were divided into six groups equally; negative control (Succinic acid), vehicle control (Succinate+B(a)P),positive control(B(a)P), high VES(2.5 g/kg.b.w+B(a)P), low VES(1.25 g/kg.b.w+B(a)P) ig as well as VES by ip (20 mg/kg.b.w + B(a)P). Except the negative control group, the mice were administrated with B(a)P ig. and corresponding treatments for 4 weeks to study the anti-carcinogenetic effect of VES during the initiation period. The experiment lasted 29 weeks, in which the inhibitory effects of VES both on tumor incidence and tumor size were tested.**

RESULTS **The models of B(a)P-induced forestomach tumor in female mice were established successfully. Some were cauliflower-like, others looked like papilla, even a few were formed into the ulcer cavities. VES at 1.25 g/kg.b.w, 2.5 g/kg.b.w. by ig and 20 mg/kg.b.w. via ip could decrease the number of tumors per mouse (1.7.±0.41, 1.6.0±0.34 and 1.1.±0.43), being lower than that of B(a)P group (5.4.±0.32, *P*<0.05). The tumor incidence was inhibited by 18.2%, 23.1% and 50.0%. VES at 1.25 g/kg.b.w., 2.5 g/kg.b.w. by ig and 20 mg/kg.b.w. via ip reduced the total volume of tumors per mouse (54.8 ± 8.84, 28.4 ± 8.32 and 23.9 ± 16.05), being significantly lower than that of B(a)P group (150.2 ± 20.93, *P*<0.01). The inhibitory rates were 63.5%, 81.1% and 84.1%, respectively.**

CONCLUSION **VES has inhibitory effects on B(a)P-induced forestomach carcinogenesis in female mice, especially by ip and it may be a potential anti-cancer agent *in vivo*.**

[1]Department of Nutrition and Food Hygiene, School of Public Health, Harbin Medical University, Harbin 150001, Heilongjiang Province, China
[2]The Second Affiliated Hospital, Harbin Medical University, Harbin 150001, Heilongjiang Province, China
Kun Wu, Professor, engaged in the study on anti-carcinogenetic nutrients in food, having more than 40 papers published.
Project Supported by National Natural Science Foundation of China, No.39870662
Correspondence to: Prof. Kun Wu, Department of Nutrition and Food Hygiene, School of Public Health, Harbin Medical University, Harbin 150001, Heilongjiang Province, China
Tel. 0086-451-3648665, Fax. 0086-451-3648665
Email. wukun@public.hr.hl.cn
Received 2000-07-17 **Accepted** 2000-10-28

INTRODUCTION

RRR-α-Tocopheryl Succinate (referred to Vitamin E Succinate, VES) is a derivative of natural vitamin E (RRR-α-tocopheryl)[1]. The interest in this derivative of vitamin E is the fact that it can inhibit the proliferation of a variety of tumor cells *in vitro*[2]. Tumor cells responsive to VES antiproliferative effects include human monoblastic leukemia cells[3], murine B-16 melanoma cells[4], human prostatic adenocarcinoma cells[5], avian lymphoid cells[6,7], human promyelocytic cells[8], human breast cancer cells[9,10]and murine EL4 T lymphoma cells[11,12].

Although the mechanisms whereby VES inhibits the proliferation of rapidly dividing cells are not well understood, induction of cell cycle blockage[13], increasing secretion and activation of potent negative growth factors, i.e., transforming growth factor-βs and their type II- cell surface receptors [2,7,11,14], and induction of apoptosis[15-17] have been observed in VES-treated cells. Earlier studies in our laboratory using the SGC-7901 cell lines (human gastric cancer cells) as model indicated that VES has antagonistic effects on cell growth and DNA synthesis[18], and can obviously induce apoptosis of SGC-7901 cells[19,20].

To date, VES has not been extensively studied on its antitumor properties as well as its mechanism of action *in vivo*. Schwartz J and co-workers[21] found that injection of VES directly into the tumor-bearing buccal pouch of hamsters (twice a week for

four weeks at a dose of 250 μg/injection) caused chemically induced oral epidermoid carcinomas to regress. As VES is found to be a potential chemopreventive and chemotherapeutic agent, it is of interest to ascertain the manner in which tumor growth is inhibited in VES-treated mice and to better understand the relationship between the structure and the function involved. This study characterizes the ability of VES to inhibit B(a)P-induced forestomach carcinogenesis in mice, addresses the involvement of different administration ways in this experiment, and shows that VES is capable of lowering both the tumor incidence and the total tumor size. The inhibitory effects of VES may be attributed to its intact compound.

MATERIALS AND METHODS

Materials

Reagents VES (purity>98%) was obtained from Sigma Co. Ltd, 10% buffered formalin phosphate (10% formalin in neutral phosphate buffer) was purchased from Shanghai Chemical Co. (China), and B(a) P (purity>98%) from Fluka Chemical Co. Ltd (Switzerland).

Animals Female Kunming mice (4-5 weeks old) were purchased from the Animal Center of the Cancer Institute in Heilongjiang Province, China. Fifteen mice were placed in a plastic cage and the animals were maintained under the following standard conditions: 22℃ ± 2℃, 45% ± 10% relative humidity, and 12 h light/12 h dark cycles each day. All animals were fed with basic diet (purchased from the Center of Animal Experiment, Heilongjiang, China) and water.

Methods

B(a)P-induced forestomach tumorgenesis Female Kunming mice (6 weeks old) were divided into six groups, each group was composed of 30 mice. Succinic acid, B(a)P and VES were dissolved in corn oil. In group 1 (negative control) and group 2 (vehicle control), the mice were intubated with 1 g/(kg b.w.) succinic acid 4 times per week for 4 weeks. In all groups except group 1, the mice were intubated with 1mg per mouse B(a)P twice a week for 4 weeks. The mice in group 3 (positive control) were given nothing except B(a)P. Groups 4 and 5 were given 2. 5 g/(kg b.w.) or 1.25g/(kg b.w.) VES by the same way 4 times/week for 4 weeks. Group 6 was given 20 mg/(kg b.w.) VES via ip twice a week for 4 weeks. The mice were then sacrificed at week 11, 16 and 29 after the first administration of B(a) P. Buffered formalin-phosphate (10%) was immediately injected into the stomach by intubation into the mouth so that the stomach was distended and fixed. Each stomach was removed and placed on a plastic sheet and the number of tumors in each forestomach was counted. The samples were stored in 10% buffered formalin-phosphate for histological examination.

Tumor volume All tumors were examined with the aid of a magnifying lens, and tumor size was measured. As described previously[22], tumor volume was determined by measuring the three dimension size of all tumors using the average of the three measurements to calculate radium. Tumor volume was calculated with the formula: volume = $4/3\pi R^3$

Histological examination of tumors Tumors found by visual examinations were further confirmed histologically. The stomach samples were excised, fixed in 10% buffered formalin-phosphate, embedded in paraffin and processed for histologic slides with hematoxylin and eosin (HE) staining. Slides were read blindly by a pathologist and the tumors were classified according to the pathological principle.

Statistical analysis

The significance of data was determined by *t* test.

RESULTS

Establishment of B(a) P-induced forestomach tumor model On the basis of previous method with some slight modifications, the model of B(a) P-induced forestomach tumor was successfully established. Treatment of Kunming mice with 1 mg/mouse of B(a) P by ig twice a week for 4 weeks mainly resulted in four forms of tumors (Figure 1). Some bigger ones appeared cauliflower-like, the moderate tumors looked like papilloma, and the smaller ones were usually grain-like. A few tumors had broken into ulcer-like cavities.

The dynamic processes of tumorigenesis in pathology at the week 11, 16 and finally 29 were observed. Before the treatment with B(a) P, the thickness of normal gastric mucosa was uniform with all characterizstics of gastric mucosa in previous studies[23-25]. The pathological changes at week 11 after the first administration of B(a)P were mainly the hyperplasia of the gastric mucosa, just as what we said "precancerous lesions"[26], and only a few papillomas could be seen. Under this condition, the thickness of epidermins was not uniform, some positions were very thin, while others were very thick. The nuclei of hyperplastic neoplastic cells were enlarged, round or ovoid with prominent necleoli. At week 16, the dominant features were papillomas, being more serious than those at week 11, and the proportion of squamous cell carcinomas in the positive group (B (a)P) was 20%, which was more malignant than before. Tumor cells proliferated lumpy into the connective tissues and were polyhedral, with abundant cytoplasms and large nuclei, in which nucleolus was prominent and some were polynucleolar. The desmosomes were clear, the mitotic figures and a few keratinized cells could be seen. The typical pathological alterations

of B(a)P-induced forestomach tumor at the week 29 were that the number of papilloma and squamous cell carcinoma were both increased. The pathological changes of B(a)P-induced forestomach tumor are illustrated in Figure 2 and the dynamic processes of tumorigenesis in each period are shown in Table 1.

Inhibitory effects of VES on B(a)P-induced forestomach tumorigenesis The treatment with 1mg/mouse- B(a)P twice a week for 4 weeks by ig in group 3 resulted in 100% incidence of forestomach tumors. There was an average of 5.4 tumors/mouse at week 29 of the experiment (Table 2, group 3). Similar results were obtained from group 2. The results in both groups showed that the succinic acid alone had no anticarcinogenic effect. Administration of 1.25 g/(kg b.w.) and 2.5 g/(kg b.w.) VES by ig 4 times/week for 4 weeks inhibited the number of B(a) P-induced forestomach tumors per mouse by 68.5% and 70.4%, respectively (Table 2, groups 4 and 5). When 20 mg/(kg b.w.) VES was injected intraperitoneally into the mice twice a week for 4 weeks, the number of B(a)P-induced forestomach tumors was inhibited by 79.6% (Table 2, group 6). These results suggested that VES could significantly decrease the number of B(a)P-induced tumors per mouse with a dose-dependent manner.

Inhibitory effects of VES on the size of B(a)P-induced forestomach tumor Administration of 1.25g/(kg b.w.) and 2.5 g/(kg b.w.) VES by ig significantly decreased the total tumor volume per mouse by 63.5% and 81.1%, respectively. Notably, the treatment with VES via ip at a much lower dose of 20 mg/(kg b.w.) and shorter time of twice a week for 4 weeks showed even higher rate of decreasing the total tumor volume per mouse (84.1%) (Table 3).

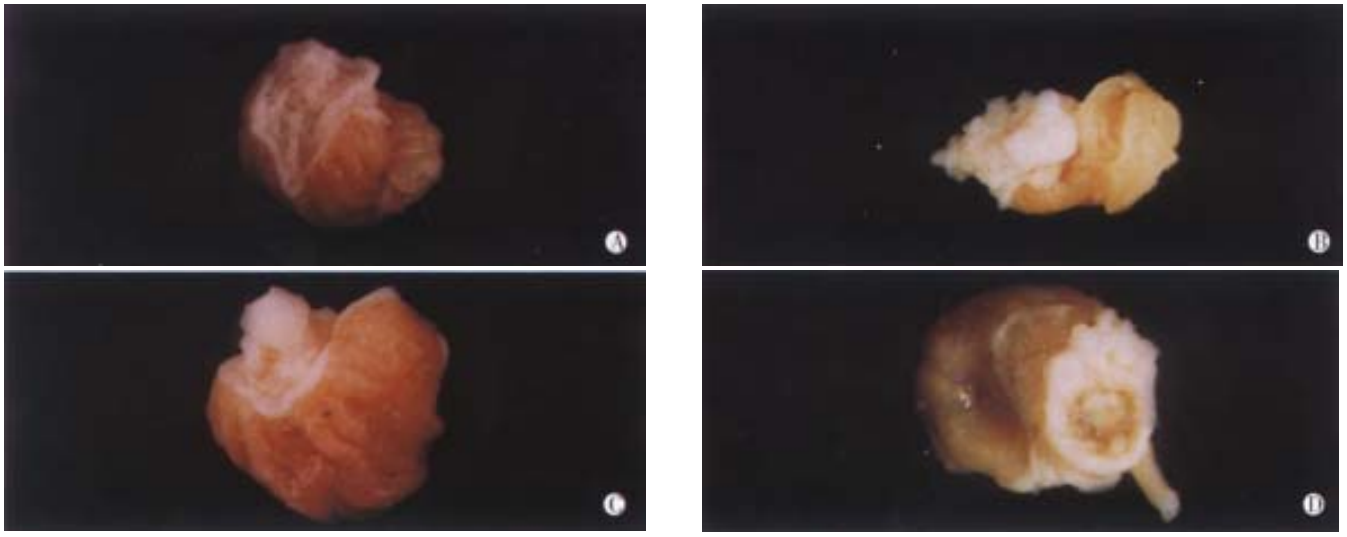

Figure 1 The model of B(a)P-induced forestomach tumor.
A. Normal mucosa of forestomach; B. Cauliflower-like tumor; C. Papilla-like tumor; D. Ulcer cavities-like tumor.

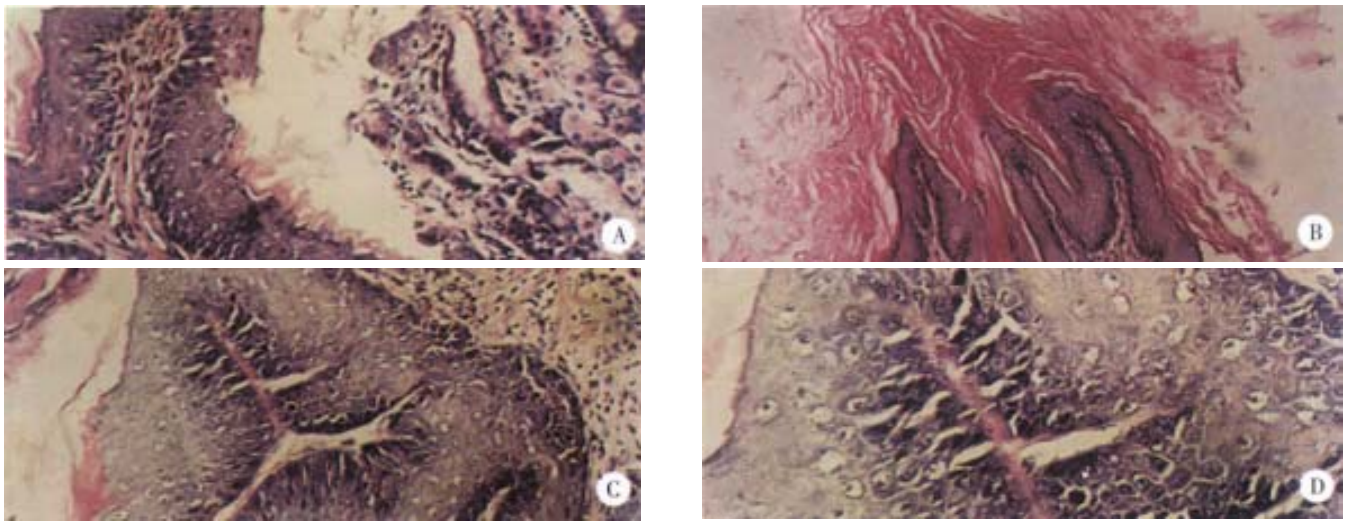

Figure 2 Pathological observation of B(a)P-induced forestomach tumor (HE staining) in mice.
A. The normal gastric mucosa ×200; B. The epithelium of gastric mucosa formed papillary projection ×100; C. Squamous tumor cells proliferated into connective tissues and they were polyhedral ×100; D. The mitotic figures (white arrow) in the squamous cell carcinoma ×400

Table 1 Pathological alterations in each group at different periods of the experiment

Groups	Week 11			Week 16			Week 29		
	H(%)	P(%)	S(%)	H(%)	P(%)	S(%)	H(%)	P(%)	S(%)
1. Succinic acid	0	0	0	0	0	0	0	0	0
2. Succinic acid+B(a)P	100	17.9	0	100	100	18.3	100	100	76.8
3. B(a)P	100	9.6	0	100	100	19.9	100	100	70.4
4. 1.25g / kgVES+B(a)P	80.3	0	0	100	80.1	0	100	91.8	56.9
5. 2.5g / kgVES+B(a)P	79.7	0	0	100	60.4	0	100	90.3	49.8
6. 20mg / kgVES(ip)+B(a)P	69.7	0	0	100	49.7	0	100	80.7	18.4

H: Hyperplasia, P: Papillomas, S:Squamous cell carcinoma

Table 2 Inhibitory effects of VES on B(a)P induced forestomach tumorgenesis ($\bar{x} \pm s_{\bar{x}}$)

Groups	No.of mice	Body weight (g)	Total tumors	
			Tumors / mouse	% of mice with tumors
1. Succinic acid	12	39.5±1.58	0	0
2. Succinic acid+B(a)P	9	40.2±1.12	5.3±0.48	100
3. B(a)P	10	40.6±1.14	5.4±0.32	100
4. 1.25g / kgVES+B(a)P	11	40.1±1.22	1.7±0.41[a](68.5)	81.8 (18.2)
5. 2.5g / kgVES+B(a)P	13	39.9±1.66	1.6±0.34[a]	76.9 (23.1)
6. 20mg / kgVES(ip)+B(a)P	10	38.7±1.06	1.1±0.43[a] (79.6)	50.0 (50.0)

[a]Compared with B(a)P group (group 3), $P<0.05$ (using Student *t* test)
Numbers in parentheses are % of inhibition compared to group 3.

Table 3 Inhibitory effects of VES on the size of B(a)P-induced forestomach tumors ($\bar{x} \pm s_{\bar{x}}$)

Groups	No.of mice	Vol / tumor(mm^3)	Total tumor Vol / mouse(mm^3)
1. Succinic acid	12	0	0
2. Succinic acid+B(a)P	9	31.5±4.51	169.5±33.42
3. B(a)P	10	27.8±8.52	150.2±20.93
4. 1.25g / kgVES+B(a)P	11	31.7±8.62 (0)	54.8±8.84[b] (63.5)
5. 2.5g / kgVES+B(a)P	13	17.6±5.54 (36.7)	28.4±8.32[b]
6. 20mg / kgVES(ip)+B(a)P	10	21.7±2.13 (21.9)	23.9±16.05[b] (84.1)

[b]Compared with the B(a)P group (group 3), $P<0.01$ (using Student's *t* test)[a]¤Numbers in parentheses are % of inhibition of tumors compared to group 3.

DISCUSSION

The results of our study demonstrated that administration of VES to mice, by both ig. and ip., inhibited B(a)P-induced forestomach tumorigenesis during the initiation period. VES may be useful in the future as a chemopreventive agent of carcinogenesis. A study *in vitro* indicated that VES is able to inhibit the proliferation of tumor cells without adverse effects on non-tumor cells[27]. Kline *et al*[2] showed that VES did not inhibit the proliferation of normal murine bone marrow cells and the non-mitogen-stimulated normal avian B and T cells. They also reported that VES can retard the growth of MCF-7, a kind of human breast cancer cell, while it has no inhibitory effects on MCF-10A, a non-tumorigenic mammary cell. Since 1997, we have studied the antagonistic effects of VES on gastric cancer, and found the inhibitory effects of VES on the growth of human gastric cancer cell (SGC-7901), DNA synthesis arrest and induction of apoptosis[18,19].These findings also supported the possibilities of VES as prospective chemopreventive and chemotherapeutic agent of tumors in the future. VES given intraperitoneally was more effective than given by ig. in lowering both the number and size of B(a)P-induced forestomach tumors even at a much lower dose. Therefore, it seems that VES administrated by ig. may be decomposed by some non-specific esterases which may normally exist in stomach, thus losing its original intact structure. VES contains a succinic acid moiety attached to the chroman head structure of RRR-α-tocopherol via an ester linkage. Esterification eliminates the hydroxy moiety that mediates RRR-α-tocopherol's classical antioxidant properties that prevents VES from acting as an antioxidant, unless the esterified succinic acid moiety is removed by cellular esterases, thereby generating free RRR-α-tocopherol. After VES was proteolyzed into succinic acid and Vitamin E, succinic acid had no inhibitory effects on B(a)P-induced forestomach tumors, as shown in group 2. Previous studies have proved that the inhibitory effect of Vitamin E on

tumors was performed through its antioxidant functions, and the inhibitory effects of natural vitamin E on human promyelocytic leukemia (HL-60) cell proliferation were much weaker than that of VES *in vitro*. All these data suggest that the inhibitory effects of VES may be attributed to its intact structure, as suggested by Fariss and co-workers[27].

The mechanisms by which VES has the inhibitory effects on chemically induced forestomach tumorigenesis in mice are still unknown. VES may influence the metabolic activation and detoxification of carcinogens as well as the postinitiation phase of carcinogenesis[28-30]. B(a)P is a suspected human carcinogen and is known to cause tumors in the forestomach of mice. Singh and Hu *et al*[31-33] reported that GST plays a major role in the detoxification of the ultimate carcinogen of B(a)P (+) anti-BPDE. In our lab, VES has been found to increase the activity of glutathione S transferase (GST) which is phase II metabolic enzyme and inhibits the activity of ethoxyresorufin O-deethylase (EROD) of liver S-9 fraction in mice, a phaseIxenobiotic-metabolizing enzyme. This was the same as the results of Wu[34,35] and Seng[36]. During the developing process of cancer, the immune functions will be decreased[37-39]. Of course, this is a very complex process and it may be involved in many factors[40-42], such as IL-2, IL-4[43,44], TNF[45,46], TGF-β[47-52] and so on. In 1993, Kline *et al*[52] found that RRR-α-tocopheryl succinate could induce IL-2 production by avian splenic T lymphocytes and murine EL-4 thymic lymphoma cells. And they suggested that VES-induced IL-2 production may involve a mechanism other than antioxidant effects of Vitamin E. In addition, administration of VES to mice increased the serum levels of IL-2 and IL-4 (unpublished data). The information indicates that the mechanisms of VES *in vivo* may be related to the activation pathway of B(a) P metabolism in liver and regulation of the immune system.

Our findings that VES can inhibit chemically induced carcinogenesis in the forestomach of mice suggest a need for further studies on pharmacology and toxicology to determine whether VES may be a useful chemopreventive agent against human gastric carcinogenesis.

ACKNOWLEDGEMENTS We would like to thank Dr. Wei Ping Yu for his technical assistance, and Dr. Dong Lai Wu for reading the pathological slides and taking the pathological photos. We are also grateful to Dr. Love for his critical review of this manuscript.

REFERENCES

1 Bendich A, Machlin LJ. Safety of oral intake of vitamin E. *Am J Clin Nutr*, 1988;48:612-619
2 Kline K, Yu WP, Zhao BH, Israel K, Charpentier A, Simmons-Menchaca M,Sanders BG. Vitamin E Succinate: Mechanisms of action as tumor cell growth inhibitor. In: Prasad KN. Santamaria L and Willams RM, eds. Nutrients in cancer prevention and treatment. Totowa NY: Humana, 1995:39-56
3 Kim SJ, Bang OS, Lee YS, Kang SS. Production of inducible nitric oxide is required for monocytic differentiation of U937 cells induced by vitamin E-succinate. *J Cell Sci*, 1998;111:435-441
4 Ottino P, Duncan JR. Effect of α-tocopherol succinate on free radical and lipid peroxidation levels in BL6 melanoma cells. *Free Radical Biol & Med*, 1997;22:1145-1151
5 Israel K, Sanders BG, Kline K. RRR-α-Tocopheryl Succinate inhibits the proliferation of human prostatic tumor cells with defective cell cycle/differentiation pathways. *Nutr Cancer*, 1995;24: 161-169
6 Kline K, Yu WP, Sanders BG. Vitamin E: Mechanisms of action as tumor cell growth inhibitors. In: Prasad KN, Cole WC, eds. Cancer and nutrition. *IOS Press*, 1998:37-53
7 Simmons-Menchaca M, Qian M, Yu WP, Sanders BG, Kline K. RRR-α-Tocopheryl succinate inhibits DNA synthesis and enhances the production and secretion of biologically active transforming growth factor-B by avian retrovirus-transformed lymphoid cells. *Nutr Cancer*, 1995;24:171-185
8 Turley JM, Sanders BG, Kline K. RRR-α-Tocopheryl Succinate modulation of human promyelocytic leukemia (HL-60) cell proliferation and differentiation. *Nutr Cancer*, 1992;18:201-213
9 Turley JM, Ruscetti FW, Kim SJ, Fu T, Gou FV, Birchenall-Roberts MC. Vitamin E succinate inhibits proliferation of BT-20 human breast cancer cells: increased binding of cyclin A negatively regulates E2F transactivation activity. *Cancer Res*, 1997;57:2668-2675
10 Yu WP, Simmons-Menchaca M, You HH, Brown P, Birrer MJ, Sanders BG,Kline K. RRR-α-Tocopheryl Succinate induction of prolonged activation of c-jun amino-terminal kinase and c-jun during induction of apoptosis in human MDA-MB-435 breast cancer cells. *Mol Carcinogenesis*, 1998;22:247-257
11 Yu WP, Sanders BG, Kline K. Modulation of murine EL-4 thymic lymphoma cell proliferation and cytokine production by Vitamin E succinate. *Nutr Cancer*, 1996;25:137-149
12 Yu WP, Sanders BG, Kline K. RRR—tocopheryl succinate inhibits EL4 thymic lymphoma cell growth by inducing apoptosis and DNA synthesis arrest. *Nutr Cancer*, 1997;27:92-101
13 Boscoboinik D, Szewczyk A, Azzi A. α-Tocopherol (vitamin E) regulates vascular smooth muscle cell proliferation and protein kinase C activity. *Arch Biochem Biophys*, 1991;286:264-269
14 Ariazi EA, Satomi Y, Ellis MJ, Haag JD, Shi W, Sattler CA, Gould MN. Activation of the transforming growth factor B signaling pathway and induction of cytostasis and apoptosis in mammary carcinomas treated with the anticancer agent perillyl alcohol. *Cancer Res*, 1999;59:1917-1928
15 Turley JM, Fu T, Ruscetti FW, Mikovits JA, Bertolette III DC, Birchenall-Roberts MC. Vitamin E succinate induces Fas-mediated apoptosis in estrogen receptor-negative human breast cancer cells. *Cancer Res*, 1997;57:881-890
16 Yu WP, Israel K, Liao QY, Aldaz CM, Sanders BG, Kline K. Vitamin E succinate (VES) induces Fas sensitivity in human breast cancer cells: role for Ma-r 43000 Fas in VES-triggered apoptosis. *Cancer Res*, 1999;59:953-961
17 Malafa MP, Neitzel, LT. Vitamin E succinate promotes breast cancer tumor dormancy. *J Surg Res*, 2000;93:163-170
18 Wu K, Ren Y, Guo J. The effects of Vitamin E Succinate on the cyclic regulation protein of human gastric cancer cells. *Weisheng Dulixue Zazhi*, 1998;12:203-207
19 Liu BH, Wu K. Study on the growth inhibition of Vitamin E Succinate in human gastric cancer cell. *Aibian Jibian Tubian*, 2000;12:79-81
20 Wu K, Guo J, Shan YJ, Liu BH. Effects of Vitamin E succinate on inducing apoptosis of human gastric carcinoma cells. *Weisheng Dulixue Zazhi*, 1999;13:84-87
21 Schwartz J, Shklar G. The selective cytotoxic effect of carotenoids and -tocopherol on human cancer cell lines *in vitro*. *J Oral Maxillofac Surg*, 1992;50:367-373
22 Huang MT, Lou YR, Ma W, Newmark HL, Reuhl KR, Conney AH. Inhibitory effects of dietary curcumin on forestomach, duodenal and colon carcinogenesis in mice. *Cancer Res*, 1994;54:5841-5847
23 Ji XL, Cheng YQ, Wang SQ. Gastroendoscopic biopsy diagnosis of mucosa-associated lymphoid tissue lyphoma. *China Natl J New Gastroenterol*, 1995;1:30-32
24 Yin GY, He XF, Yin YF. Clinical and experimental study on gastric mucosal pathology, DNA, cAMP, and trace elements of pixu patients. *China Natl J New Gastroenterol*, 1996;2:44-50
25 Yu JY, D' Adda T. Quantitative ultrastructure analysis of neuroendocrine cells of gastric mucosa in normal and pathological conditions. *China Natl J New Gastroenterol*, 1996;2:155-157
26 Zhang XC, Zhao FZ, Shan PY, Dai X, Tian DL. Ultrastructural

effect of xiaopiling chongji on gastric precancerous lesions in rats. *Xin XiaohuabingxueZazhi*, 1996;4:669-671
27 Fariss MW, Fortuna MB, Everett CK, Smith JD, Trent DF, Djuric Z.The selective antiproliferative effects of tocopheryl hemisuccinate and cholesteryl hemisuccinate on murine leukemia cells result from the action of the intact compounds. *Cancer Res*, 1994;54:3346-3351
28 Gudi VA, Singh SV. Effect of diallyl sulfide, a naturally occurring anticarcinogen, on glutathione-dependent detoxification enzymes of female CD-1 mouse tissues. *Biochem Pharmacol*, 1991;42:1261-1265
29 Yoshida S, Matsui M, Shirouzu Y, Fujita H, Yamana H, Shirouzu K. Effects of glutamine supplements and radiochemotherapy on systemic immune and gut barrier function in patients with advanced esophageal cancer. *Ann Surg*,1998;227:485-491
30 Srivastava SK, Hu X, Xia H, Awasthi S, Amin S, Singh SV. Metabolic fate of glutathione conjugate of benzo(a)pyrene-(7R,8S)-diol(9S,10R)-epoxide in human liver. *Arch Biochem Biophys*, 1999;371:340-344
31 Hu X, Singh SV. Glutathione S-transferases of female A/J mouse lung and their induction by anticarcinogenic organosulfides from garlic. *Arch Biochem Biophys*, 1997;340:279-286
32 Xia H, Pan SS, Hu X, Srivastava SK, Pal A, Singh SV. Cloning, expression, and biochemical characterization of a functionally novel alpha class glutathione S-transferase with exceptional activity in the glutathione conjugation of (+)-anti-7,8-dihydroxy-9,10-oxy-7,8,9,10-tetrahydrobenzo(a)pyrene. *Arch Biochem Biophys*, 1998;353:337-348
33 Srivastava SK, Singhal SS, Hu X, Awasthi YC, Zimniak P, Singh SV. Differential catalytic efficiency of allelic variants of human glutathione S-transferase Pi in catalyzing the glutathione conjugation of thiotepa. *Arch Biochem Biophys*, 1999;366:89-94
34 Wu K, Leslie CL, Stacey NH. Effects of mutagenic and nonmutagenic aniline derivatives on rat liver drug-metabolizing enzymes. *Xenobiotica*, 89;19:1275-1283
35 Wu K, Bonin AM, Leslie CL, Baker RSU, Stacey NH. Genotoxicity and effects on rat liver drug-metabolizing enzymes by possible substitutes for 4,4 -methylene bis (2-chloroaniline). *Carcinogenesis*, 1989;10:2119-2122
36 Seng JE, Gandy J, Turturro A, Lipman R, Bronson RT, Parkinson A, Johnson W, Hart RW, Leakey JEA. Effects of caloric restriction on expression of testicular cytochrome P450 enzymes associated with the metabolic activation of carcinogens. *Arch Biochem Biophys*, 1996;335:42-52
37 Araghi-Niknam M, Zhang Z, Jiang S, Call O, Eskelson CD, Watson RR. Cytokine dysregulation and increased oxidation is prevented by dehydroepiandrosterone in mice infected with murine leukemia retrovirus. *Proc Soc Exp Biol Med*, 1997;216:386-391
38 Gammon MD, John EM, Britton JA. Recreational and occupational physical activities and risk of breast cancer. *J Natl Cancer Inst*, 1998;90:100-117
39 Mullins DW, Burger CJ, Elgert KD. Paclitaxel enhances macrophage IL-12 production in tumor-bearing hosts through nitric oxide. *J Immunol*, 1999;162:6811-6818
40 Liu Y, Lu MZ, Pan BR. Cells proliferation and regulation in digestive tumors. *Xin Xiaohuabingxue Zazhi*, 1997;5:532-533
41 Yuan Y, Dong M, Lu P, Wang XJ, Jin CL, He AG. Restriction fragment length polymorphism of pepsinogen C gene in patients with stomach carcinoma and in its high risk population. China *Natl J New Gastroenterol*, 1996;2:223-225
42 Yuan Y, Lin HZ, Zhang YC, Wang XJ, Wu YQ, Gao H, Wang L, Liu YH, Lu F, Lou SQ. Study on the pathogenetic effect of salted pork from a high risk area of stomach cancer in China. *China Natl J New Gastroenterol*, 1997;3:93-94
43 Belli F, Mascheroni L, Gallino G, Lenisa L, Arienti F, Melani C, Colombo MP, Parmiani G, Cascinelli N. Active immunization of metastatic melanoma patients with IL-2 or IL-4 gene transfected, allogeneic melanoma cells. *Gene Ther Cancer*, 1998:543-545
44 Saijo Y, Hong X, Tanaka M, Tazawa R, Liu SQ, Saijo K, Ohno T, Koike K, Ohkuda K, Nukiwa T. Autologous high-killing cytotoxic T lymphocytes against human lung cancer are induced using interleukin (IL)-1β,IL-2,IL-4 and IL-6: possible involvement of dendritic cells. *Clinical Cancer Res*, 1999;5:1203-1209
45 Gogos CA, Ginopoulos P, Salsa B, Apostolidou E, Zoumbos NC, Kalfarentzos F. Dietary omega-3 polyunsaturated fatty acids plus vitamin E restore immunodeficiency and prolong survival for severely ill patients with generalized malignancy: a randomized control trial. *Cancer*, 1998;82:395-402
46 Arbabi S, Garcia I, Bauer GJ, Maier RV. Alcohol (ethanol) inhibits IL-8 and TNF: role of the p38 pathway. *J Immunol*, 1999;162: 7441-7445
47 Moses HL, Yang EY, Pietenpol JA. TGF-β stimulation and inhibition of cell proliferation: New Mechanistic Insights. *Cell*, 1990; 63:245-247
48 Aaronson SA. Growth factors and cancer. *Science*, 1991;254: 1146-1153
49 Gleizes PE, Munger JS, Nunes I, Harpel JG, Mazzieri R, Noguera I, Rifkin DB. TGF-β latency: biological significance and mechanisms of activation. *Stem Cells*, 1997;15:190-197
50 Zhuang ZH, Chen YL, Wang CD, Chen YG. Expressions of TGF-β1 and TGF-β receptor I in gastric carcinoma and precancerous lesions. *Shijie Huaren Xiaohua Zazhi*, 1999;7:507-509
51 Deng DH, Luo JY, Zhu HH, Li DL, Wang KM.The expression of TGF-β1 in squamous oesophagus cancer and heteroproliferation. *Xin Xiaohuabingxue Zazhi*, 1997;5:465
52 Kline K, Sanders BG. RRR-α-tocopheryl succinate inhibition of lectin-induced T cell proliferation. *Nutr Cancer*, 1993;19:241-252

Edited by Ma JY

P.O.Box 2345 Beijing 100023, China
Fax. 0086·10·65891893 Tel. 0086·10·65897901
E-mail.wcjd@public.bta.net.cn www.wd.org.cn

World J Gastroentero, 2001 April; 7(1):66 - 73
World Journal of Gastroenterology
Copyright©2001 by the WJG Press ISSN 1007 - 9327

Effect of bowel rehabilitative therapy on structural adaptation of remnant small intestine: animal experiment

Xin Zhou, Yuan Xin Li, Ning Li and Jie Shou Li

Subject headings short bowel syndrome; intestinal mucosa; somatotropin; glutamine; dietary fiber; parenteral nutrition, total; rats

Zhou X, Li YX, Li N, Li JS. Effect of bowel rehabilitative therapy on structural adaptation of remnant small intestine: animal experiment. ***World J Gastroentero***, 2001;7(1):66-73

Abstract

AIM **To investigate the individual and the combined effects of glutamine, dietary fiber, and growth hormone on the structural adaptation of the remnant small bowel.**

METHODS **Forty-two adult male Sprague-Dawley rats underwent 85% mid-small bowel resection and received total parenteral nutrition (TPN) support during the first three postoperational days. From the 4 th postoperational day, animals were randomly assigned to receive 7 different treatments for 8 days: TPNcon group, receiving TPN and enteral 20 g·L^{-1} glycine perfusion; TPN+Gln group, receiving TPN and enteral 20 g·L^{-1} glutamine perfusion; ENcon group, receiving enteral nutrition (EN) fortified with 20 g·L^{-1} glycine; EN+Gln group, enteral nutrition fortified with 20 g·L^{-1} glutamine; EN+Fib group, enteral nutrition and 2 g·L^{-1} oral soybean fiber; EN+GH group, enteral nutrition and subcutaneous growth hormone (GH) (0.3IU) injection twice daily; and ENint group, glutamine-enriched EN, oral soybean fiber, and subcutaneous GH injection.**

RESULTS **Enteral glutamine perfusion during TPN increased the small intestinal villus height (jejunal villus height 250 μm ± 29 μm in TPNcon *vs* 330 μm ± 54 μm in TPN+Gln, ileal villus height 260 μm ± 28 μm in TPNcon *vs* 330 μm ± 22 μm in TPN+Gln, *P*<0.05) and mucosa thickness (jejunal mucosa thickness 360 μm ± 32 μm in TPNcon *vs* 460 μm ± 65 μm in TPN+Gln, ileal mucosa thickness 400μm ± 25 μm in TPNcon *vs* 490 μm ± 11 μm in TPN+Gln, *P*<0.05) in comparison with the TPNcon group. Either fiber supplementation or GH administration improved body mass gain (end body weight 270 g ± 3.6 g in EN+Fib, 265.7 g ± 3.3 g in EN+GH, *vs* 257 g ± 3.3 g in ENcon, *P*<0.05), elevated plasma insulin-like growth factor (IGF-I) level (880 μg·L^{-1} ± 52 μg·L^{-1} in EN+Fib, 1 200 μg·L^{-1} ± 96 μg·L^{-1} in EN ± GH, *vs* 620 μg·L^{-1} ± 43 μg·L^{-1} in ENcon, *P*<0.05), and increased the villus height (jejunum 560 μm ± 44 μm in EN ± Fib, 530 μm ± 30 μm in EN ± GH, *vs* 450 μm ± 44 μm in ENcon, ileum 400 μm ± 30 μm in EN+Fib, 380 μm ± 49 μm in EN ± GH, *vs* 320 μm ± 16 μm in ENcon, *P*<0.05) and the mucosa thickness (jejunum 740 μm ± 66 μm in EN ± Fib, 705 μm ± 27 μm in ENGH, *vs* 608 μm ± 58 μm in ENcon, ileum 570 μm ± 27 μm in EN ± Fib, 560 μm ± 56 μm in EN ± GH, *vs* 480 μm ± 40 μm in ENcon, *P*<0.05) in remnant jejunum and ileum. Glutamine-enriched EN produced little effect in body mass, plasma IGF-I level, and remnant small bowel mucosal structure. The ENint group had greater body mass (280 g ± 2. 2 g), plasma IGF-I level (1450 μg·L^{-1} ± 137 μg·L^{-1}), and villus height (jejunum 620 μm ± 56 μm, ileum 450 μm ± 31 μm) and mucosal thickness (jejunum 800 μm ± 52 μm, ileum 633 μm ± 33 μm) than those in ENcon,EN+Gln (jejunum villus height and mucosa thickness 450 μm ± 47 μm and 610 μm ± 63 μm, ileum villus height and mucosa thickness 330 μm ± 39 μm and 500 μm ± 52 μm), EN+GH groups (*P*<0.05), and than those in EN+Fib group although no statistical significance was attained.**

CONCLUSION **Both dietary fiber and GH when used separately can enhance the postresectional small bowel structural adaptation. Simultaneous use of these two gut-trophic factors can produce synergistic effects on small bowel structural adaptation. Enteral glutamine perfusion is beneficial in preserving small bowel mucosal structure during TPN, but has little beneficial effect during EN.**

[1]Department of General Surgery, Medical School, Nanjing University, Nanjing 210093, Jiangsu Province, China
[2]Research Institute of General Hospital, Chinese PLA General Hospital of Nanjing Military Area, Nanjing 210002, Jiangsu Province, China
Xin Zhou, graduated from Medical School of Nanjing University in 1998, now a doctoral candidate of Nanjing University, majoring general surgery.
Supported partially by the Medical and Health Research Foundation of PLA, No. 98Q015
Correspondence to: Xin Zhou, Research Institute of General Surgery, Chinese PLA General Hospital of Nanjing Military Area, 305 East Zhongshan Road, Nanjing 210002, Jiangsu Province, China
Tel. 0086-25-3387871 Ext.58088, Fax. 0086-25-4803956
Received 2000-09-21 **Accepted** 2000-11-20

INTRODUCTION

Various clinical conditions necessitate therapeutic massive small bowel resection, which is often followed by serious malabsorption, characterized by intractable diarrhea, steatorrhea, and weight loss. This malabsorptive state is defined as short bowel syndrome. Traditionally, parental nutrition (PN) is prescribed for these patients to assure adequate nutritional status and obtain enough time to wait for the remnant small bowel to undergo adaptation, with the hope of eventual transition from parental nutrition support to volitional enteral nutrition. Under this supportive therapeutic strategy, however, some patients may never achieve complete adaptation, i.e., sustaining completely on enteral nutrition, and life-long total parental nutrition (TPN) become lifesaving unless successful small bowel transplantation is conducted[1-3]. Unfortunately, long-term TPN is associated with great expense, vitamin or trace element malnutrition, recurrent catheter sepsis, and progressive cholestatic liver disease[4], whereas small bowel transplantation is still used currently as a salvage therapy for patients with severe metabolic complications, hepatic failure, or lack of venous access due to imperfect management of post-transplantational rejection[5]. Therefore, any therapy aimed at actively accelerating or enhancing the adaptive process in the residual bowel is likely to impact greatly on the patients' life style and the costs of medical care. Since 1995 Byrne *et al* have published a series of studies, which demonstrated that a combination of growth hormone, glutamine, and modified fiber-enriched diet can improve nutrient absorption, decrease stool output, and reducte TPN requirement[6-8]. These reports are the first to introduce the concept that further bowel adaptation can occur with the use of specialized nutrients and growth factors, and ushered in a new era in the treatment of short bowel syndrome. However, many questions about this therapy are to be answered, e.g., whether this therapy has enhanced the structural adaptation in the remnant small bowel and how each component of the remedy contributes to bowel adaptation.

Due to the heterogeneity in patient age, underlying diseases, and anatomy of the remnant bowel as well as ethic concerns, it is rather difficult to answer these questions directly from the patients. Consequently, we conducted this animal experiment in an attempt to assess the individual and combined effect of glutamine, dietary fiber and growth factor on the structural small bowel adaptation immediately after massive small bowel resection.

MATERIALS AND METHODS

Animals and surgical procedures

The animal protocols and procedures were approved by the Laboratory Animal Medicine Ethics Committee of Nanjing Military Area General Hospital of Chinese PLA. Male Sprague Dawley rats weighing between 220 g and 250 g (Shanghai Laboratory Animals Center, Chinese Academy of Sciences) were allowed 1 week to get acclimatized to our laboratory conditions before surgery. They were kept in individual stainless steel cages and fed a standard rat chow with free access to tap water in a room maintained at 22℃ on a 12 h day/night cycle (06:00/18:00).

The animals weighed about 260 g to 290 g at the end of acclimation period, and were fasted for 12 hours before surgery. Surgical procedures were performed using aseptic technique under anesthesia by intramuscular ketamine cocktail (ketamine, 100 $mg \cdot kg^{-1}$; and xylazine 8 $mg \cdot kg^{-1}$). Three surgeries were performed on each animal in the following sequence: placement of TPN catheter in the superior vena cava via the external jugular vein, installation of gastrotomy tube for liquid diet delivery, and 85% mid-small bowel resection. Both tubes were tunneled subcutaneously, and the dorsal cervical region exited through a spring-swivel apparatus. Normal saline was administered at 1 $mL \cdot h^{-1}$ through the TPN catheter with a minipump. Small bowel resection left the first 6 cm jejunum from the Treitz ligament and the terminal 6 cm ileum. The day when operations were performed was dated as day 0. The postoperative days were dated as day *n*.

Experimental design

After the operation, animals were placed back to stainless steel cages and supported with total parenteral nutrition (TPN), the composition of which is indicated in Table 1. TPN was administered at a half-rate of 1.25 $mL \cdot h^{-1}$ on day 1, and full-rate of 2.5 $mL \cdot h^{-1}$ on day 2 and 3. From day 4, animals were randomly allocated to seven experimental groups: ENcon group, receiving control liquid enteral nutrition (EN); EN+Gln group, receiving EN enriched with 20 $g \cdot L^{-1}$ glutamine; EN+Fib group, receiving control EN and fed with 2 g/d soybean fiber, containing 70% total dietary fiber (provided by Nanjing Military Area General Hospital of Chinese PLA, Nanjing, China), and was mixed with water to the consistency of porridge; EN+GH group, injected with control EN and 0.3IU recombinant human growth hormone (rhGH) (Saizen, provided by Laboratories Serona S.A., 1170 Aubonne, Switzerland) subcutaneously twice a day; ENint group, receiving subcutaneous injection of EN enriched with 20 $g \cdot L^{-1}$glutamine, 2 $g \cdot d^{-1}$ soy bean fiber, and 0.3IU rhGH twice a day; TPNcon group, receiving TPN, and 20 $g \cdot L^{-1}$glycine perfusion *via* gastrotomy tube; and TPN+Gln group, receiving TPN, and 20 $g \cdot L^{-1}$ glutamine perfusion *via* gastrotomy tube. Each experimental group contained 6 animals. The liquid EN was fiber-free with the compositions as indicated in Table 2, and was reconstituted with sterile water before

perfusion and used within 12 hours to avoid bacteria growth. Gastrotomy tube feeding of EN or amino acid solution was introduced gradually by the following schedule: half-strength solution at 1.25 mL·h^{-1} on day 4, full-strength solution at 1.25 mL·h^{-1} on day 5, and full-strength solution at 2.5 mL·h^{-1} from day 6-until day 12. PN was continued until full-strength EN was administered at full-rate, thus combined EN and PN to supply 251kJ calorie to the animals. Our formulas for TPN and EN supplied isocaloric and isonitrogenous nutrition to all animals, i.e., 251Kj nonprotein calories, 0. 414 g nitrogen from PN or Pepti-2000 variant, and 0. 272 g nitrogen from glutamine enrichment or glycine for control per day for each animal. Glutamine enrichment constituted 39.5% of the total nitrogen. Water was provided *ad lib* throughout the study.

Table 1 Total parenteral nutrition composition (400 mL)

Ingredients	mL
500 g·L^{-1} glucose	100.0
Fat (300 g·L^{-1} intralipid *)	67.5
Amino acid (114g·L^{-1} Novamin *)	150.0
100 g·L^{-1} NaCl	10.0
100 g·L^{-1} KCl	10.0
100 g·L^{-1} calcium gluconate	5.0
Multi-electrolytes (Addemel *)	2.5
Water-soluble vitamins (Soluvit *)	2.5
Lipid-soluble vitamins (Vitalipid *)	2.5
Nonprotein energy (kJ·mL^{-1})	4.2
Total nitrogen (g)	2.7
NPC / N (kJ·g^{-1})	620

*Provided by Sino-Swed Pharmaceutical Corp. Ltd., Wuxi, China. NPC / C: nonprotein energy per gram of nitrogen.

Table 2 Enteral nutrition composition (420 mL)

Ingredients	Control EN	Glutamine enriched EN
Pepti-2000 variant * (g)	126.0	126.0
Protein hydrolysate (g)	19.9	19.9
Nitrogen (g)	2.9	2.9
Fat (g)	4.9	4.9
Vegetable (g)	2.45	2.45
MCT (g)	2.45	2.45
Linoleic acid	1.12	1.12
Carbohydrates (g)	93.1	93.1
Malto^{a2}dextrin (g)	91.7	91.7
Lactose (g)	<1.12	<1.12
Organic acid (g)	0.01	0.01
Minerals (g)	2.6	2.6
Vitamins (g)	0.4	0.4
Glycine (g)	10.0	0
Glutamine (g)	0	10.0
Nonprotein energy (kJ·mL^{-1})	4.2	4.2
NPC / N	610	610

*A commercial, nutritional complete, short-chain peptide based elemental diet (Nutricia, the Netherland). NPC / N: nonprotein energy per gram of nitrogen from Pepti-2000 variant.

Plasma and tissue isolation

Body mass was monitored every three days after surgery as an index of nutritional status. At about 12:00 am on the 12 th postoperative day, laparotomy was performed on all animals under anesthesia with ketamine hydrochloride (100 mg·kg^{-1}). Blood was obtained from the inferior vena cava and placed on ice in a heparin-pretreated tube. Plasma was then isolated by centrifugation at 4℃ and stored at -20℃ for later analysis.

The residual small intestine was rapidly resected from peritoneal and vascular connections, and the luminal content was removed. After the intestine was flushed with ice-cold normal saline, 2 cm segments from both jejunum and ileum located between 2 and 4 cm from the anastomosis were removed and fixed in phosphate-buffered neutral formalin. The animals were then killed by exsanguination.

Plasma insulin-like growth factor (IGF-I) assay and histological image analysis

Total plasma IGF-I concentrations were measured after acid-ethanol extraction with the rat IGF-I RIA DSL-2900 kit (Diagnostic Systems Laboratories, Inc., Webster, USA) in duplication, following the instruction of the manufacturer. This measurement was taken both as indicator of nutritional status and evidence of rhGH treatment.

Villus height (from villus base to villus tip), crypt depth (from crypt base to villus base), and mucosal thickness (from crypt base to villus tip) were taken as indicators of structural adaptation. Routine hematoxylin and eosin stained sections were prepared, and HPIAS-1000 True Color Image Analysis System (Tongji Qianping Image Engineering Corp., Wuhan, China) was employed to analyze the image. Fifteen intact axially oriented villi and crypts selected from each specimen were measured.

Statistical analysis

Data were expressed as $\bar{x} \pm s$. Multiple comparison tests were performed after analysis of variance with the Student-Newman-Keuls test. Differences with P value less than 0.05 were considered to be statistically significant.

RESULTS

Body mass

As shown in Table 3 and Figure 1, the initial body mass on day 0 was similar among the 7 experimental groups. The body mass on day 3 was not significantly different among the 7 groups, which reflected similar operative stress and postoperative nutritional support remedy. The overall body mass loss during the first three postoperative days averaged 26.3 g. Marked body mass difference was evident from day 6. The two TPN-supported groups had gained remarkable body mass by day 6 which was kept steady during the remainder of the experimental period, suggesting the ebbing of stress and fixed nutrition supply. No significant body mass difference was observed between the two TPN groups throughout the experiment. In ENcon, EN+Gln, and EN+GH groups, the introduction of EN resulted in further body mass loss, which was accompanied by a moderate to a large amount of liquid stool production, indicating insufficient

nutrition assimilation from the remnant small bowel. From day 6, diarrhea in these groups became increasingly milder and almost disappeared after day 9, which was associated with gradual body mass gain. Each animal in two fiber-supplied groups ate up daily fiber supply, and fiber-containing solid stool instead of large liquid stool was observed after EN introduction. Continuous body mass gain began from day 3 in ENint group, and after day 6 in EN+Fib group. From day 3, the mean body mass of ENint group maintained higher than those of the other groups, which bore statistical significance on day 6 when compared with ENcon, EN+Fib, and EN+GH groups, and on day 9 and day 12 when compared with TPNcon, ENcon, EN+Fib, and EN+GH groups. Throughout the study, ENcon and EN+Gln groups had similar body mass, which remained significantly lower than that of TPNcon on day 6 and day 9 and rose to the similar level as TPNcon on day 12. From day 6, mean body mass of EN+Fib groups began to distinguish itself significantly from ENcon, and became markedly higher than both ENcon and TPNcon on day 12. On day 9, the mean body mass of EN+GH groups was significantly higher than that in ENcon group, and on day 12 significantly higher than both ENcon and TPNcon groups.

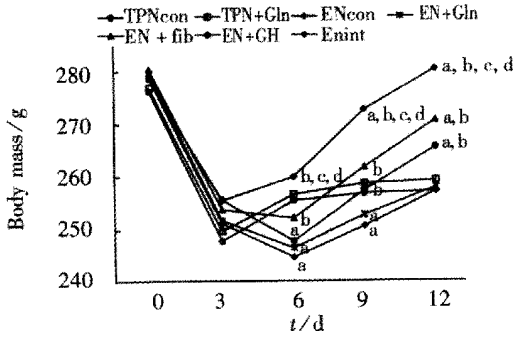

Figure 1 Body mass before and after surgery.
[a]*P*<0.05, *vs* TPNcon; [b]*P*<0.05, *vs* ENcon; [c]*P*<0.05, *vs* EN+GH; [d]*P* <0.05, *vs* EN+Fib. Day 0, refers to the day operation was performed, from which the time was dated.

Plasma IGF -I concentrations

Plasma IGF-I concentrations were similar among TPNcon, TPN+Gln, ENcon, and EN+Gln groups. Plasma IGF-I level in EN+fib group was significantly higher than that in ENcon group. GH treatment resulted in significant increase in plasma IGF-I concentration as compared with ENcon group. ENint group had the highest level of plasma IGF-I (Figure 2).

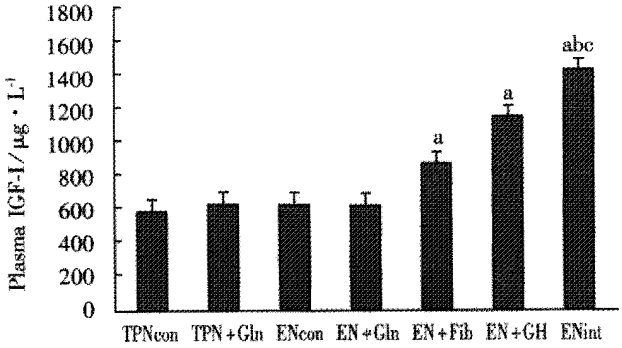

Figure 2 Plasma insulin-like growth factor level on day 12.
[a]*P*<0.05, *vs* Encon; [b]*P*<0.05, *vs* EN+Fib; [c]*P*<0.05, *vs* EN+GH.

Remnant intestinal mucosal structure

Compared with ENcon group, TPNcon group had significantly lower mean villus height and mucosal thickness in both remnant jejunum and ileum, and significantly shallower jejunal crypt (Figures 3 and 4). Luminal glutamine perfusion completely restored the villus height and mucosal thickness in ileum and partially restored the villus height, crypt depth, and mucosal thickness in jejunum. However, glutamine-enriched EN had a little impact on mucosal structural parameters whether in remnant jejunum or ileum when compared with ENcon group. The villus height and mucosal thickness in both remnant jejunum and ileum were more significantly increased by fiber supplementation than in ENcon group. GH treatment produced significant increase in villus height in both remnant jejunum and ileum, and mucosal thickness in remnant ileum when compared with ENcon group. Combined treatment with glutamine, fiber, and GH significantly deepened the crypt in remnant ileum as against TPNcon group, and further increased villus height and mucosal thickness in both remnant jejunum and ileum, which, when compared with EN+GH group, achieved statistical significance in villus height of both jejunum and ileum, and in mucosal thickness of ileum.

Table 3 Comparison of body mass before and after operation between each experiment groups (n = 6, $\bar{x} \pm s$, g)

Groups	Day 0	Day 3	Day 6	Day 9	Day 12
TPNcon	276.3 ± 9.0	247.8 ± 7.4	255.5 ± 3.6	256.8 ± 3.4	257.3 ± 2.9
TPN+Gln	277.0 ± 6.1	249.7 ± 6.5	256.7 ± 4.0	258.7 ± 3.7	259.3 ± 2.9
Encon	278.8 ± 7.8	251.2 ± 8.0	244.7 ± 3.2[a]	250.7 ± 3.5[a]	257.3 ± 3.3
EN+Gln	279.8 ± 8.9	251.8 ± 7.1	246.5 ± 3.4[a]	252.8 ± 2.7	258.0 ± 2.5
EN+fib	280.5 ± 8.0	253.8 ± 6.6	252.2 ± 2.0[b]	261.8 ± 3.4[b]	270.7 ± 3.6[a,b]
EN+GH	278.7 ± 12.9	255.7 ± 6.2	247.8 ± 2.3[a]	257.5 ± 3.3[b]	265.7 ± 3.3[a,b]
ENint	278.8 ± 8.1	255.5 ± 6.2	260.5 ± 2.4[b,c,d]	272.7 ± 2.3[a,b,c,d]	280.5 ± 2.2[a,b,c,d]

[a]*P*<0.05, *vs* TPNcon; [b]*P*<0.05, *vs* ENcon; [c]*P*<0.05, *vs* EN+Fib; [d]*P*<0.05, *vs* EN+GH.
Day 0, refers to the day operation was performed, from which the time was dated.

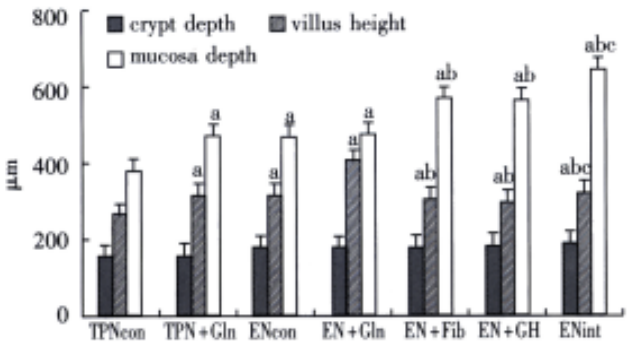

Figure 3 Crypt depth, villus height and mucosal thickness of the remnant ileum.
[a]*P*<0.05, *vs* TPNcon; [b]*P*<0.05, *vs* ENcon; [c]*P*<0.05, *vs* EN+GH.

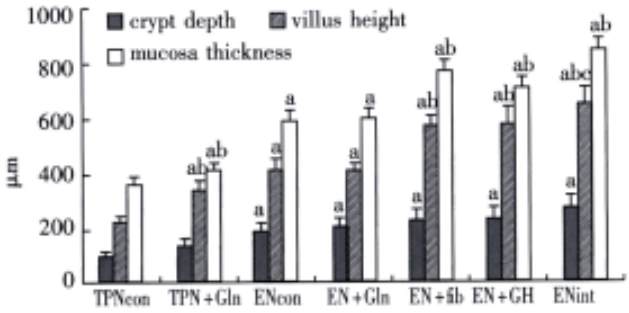

Figure 4 Crypt depth, villus height and mucosal thickness of the remnant jejunum.
[a]*P*<0.05, *vs* TPNcon; [b]*P*<0.05, *vs* ENcon; [c]*P*<0.05, *vs* EN+GH.

DISCUSSION

After massive small bowel resection, the structural adaptation of the remnant small bowel was characterized by mucosal hyperplasia. The villus height and crypt depth are both increased, while cell hypertrophy is considered unimportant[9]. This process is influenced by many factors, among which, both the quantity and route of nutrient intake are important regulators. Luminal nutrient supply, which is essential for structural adaptation, serves as not only energy source, but also signal for endogenous secretions and the release of various gut-trophic hormones and growth factors. On the other hand, normal nutritional status, which usually needs the facilitation of TPN to maintain, favors bowel adaptation[1]. In this study, great efforts were made to ensure strict control on the quantity and route of nutritent supply, and TPN was used immediately after bowel resection and during the period of reintroduction of enteral nutrition to improve the nutritional status. The compositions and delivery schedules for TPN and EN were set to provide isocaloric and isonitrogenus nutrition and to produce comparable overall nutritional status in animals of each experimental group. And the goal of producing comparable nutritional status was attained, which was attested by similar body mass and plasma total IGF-I concentration among TPNcon, TPN+Gln, ENcon, and EN+Gln groups. The utilization of plasma IGF-I as index of nutritional status is justified by sensitive IGF-I response to dietary intake, close correlation with body composition, short half-life, and its nycthermeral stability[10]. Thus the risk of confounding effects of variation in nutritional supplementation had been minimized.

Substantial researches have been done to modify the formulation of enteral nutrition to optimize the postresectional small bowel adaptation. Pepti-2000 variant has often been recommended as fiber-free EN to patients with short bowel syndrome in Nanjing Military Area General Hospital of Chinese PLA and has been chosen in this experiment as the EN formulation. This is justified by its compositional feature as peptide-based, polymeric nutrient-complete diet, which provide equal energy from medium-chain triglycerides and long-chain triglycerides. Polymeric diets are more trophic for intestinal adaptive hyperplasia compared with monomeric diets. Partial hydrolysation or protein facilitates amino acid absorption from peptide transporters while preserves gut trophic effect. Medium-chain triglycerides are water-soluble and are better absorbed in the presence of bile acid or pancreatic insufficiency, while long-chain triglycerides are more effective in inducing adaptation[11].

Glutamine is an essential nutrient for intestinal mucosa. Besides serving as the structural unit of protein synthesis, a precursor for synthesis of nucleotides and other micromolecules, it is the major respiratory fuel for intestinal mucosa[12]. *in vitro* studies have indicated that intracellular mitogenic signal transduction can be modified by glutamine supply and metabolism[13]. Animal studies have consistently shown that total parenteral nutrition (TPN)-induced intestinal hypoplasia can be attenuated by parenteral glutamine supplementation[14-16]. Glutamine-fortified-parent-eral or enteral nutrition has also been demonstrated to accelerate small intestinal healing and improves survival outcome after chemotherapy and radiation[17,18].

Following massive bowel resection, malabsorption occurs and patients may be intolerable to enteral nutrition and have to sustain on TPN for a certain period. Efforts made to preserve intestinal mucosal mass and absorption area during TPN will assist early reintroduction of enteral nutrition, which is essential for the initiation of intestinal adaptation. Parenteral glutamine supplementation has been shown to prevent TPN induced mucosal atrophy in the remnant small intestine after 85% resection[19]. Since enteral glutamine can be readily absorbed by small intestinal epithelium, and glutamine oxidation

stimulates enterocyte Na^+/H^+ exchange, leading to a high rate of electroneutral NaCl absorption in healthy and diseased jejunum[20], we studied the effect of enteral glutamine perfusion on the remnant intestinal mucosal structure during TPN. Because previous studies have not confirmed the beneficial effect of enteral glutmine supplementation during EN[21-25], we also studied the effect of adding extra glutamine to nutrition-complete enteral diet. Our results confirmed the existence of TPN induced intestinal hypoplasia, which was indicated by significantly lower villi in both jejunum and ileum and markedly shallower crypts in jejunum in TPNcon group compared with ENcon group. Luminal glutamine perfusion was effective to reverse TPN-induced hypoplasia in ileum and partially reverse TPN-induced hypoplasia in jejunum. In contrast, glutamine-supplemented enteral nutrition has little impact on small intestinal structural parameters. This finding is surprising, yet is similar to the results of several other studies[19-23]. The dosage ranged approximately from 2 $g \cdot kg^{-1} \cdot day^{-1}$ to 5.6 $g \cdot kg^{-1} \cdot day^{-1}$. And a dosage of more than 4 $g \cdot kg^{-1} \cdot day^{-1}$ was found effective in preventing TPN-induced intestinal hypoplasia in rats[12]. In all these studies, glutamine-fortified enteral nutrition was compared with standard rat chow or non-glutamine-containing elementary diet, or EN with insufficient glutamine due to partial hydrolysation of protein. Therefore, the lack of effect cannot be interpreted as insufficient glutamine delivered to intestine, or overload of glutamine. Different routes of administration were tried. Extra glutamine was mixed with enteral diet to form *ad lib* diet, or was administrated separately in bolus form, or administered as 24 h continuous enteral perfusion. The remnant intestines were analyzed 2, 7, 14 or 21 days after small bowel resection. The time points represent the beginning, active, and maximal remnant intestinal hyperplasia. In most of those studies, the animals gained body mass. In our study, the animals maintained the body mass lower than that of preoperation, reflecting our restrict nutrition supply. Nevertheless, despite different experimental protocols, similar results were obtained that during enteral nutrition, enteral glutamine supplementation produced little effect on remnant small intestinal morphological parameters. Therefore, the current available data raise the hypothesis that for otherwise healthy small intestine, with adequate enteral nutrition stimulation, glutamine delivered by arterial blood is sufficient for optimal intestinal growth. In consistent with this hypothesis, *in vitro* studies have shown that in a number of cell lines, maximal proliferation occurs when glutamine concentrations are maintained at 0.5 $mmol \cdot L^{-1}$ or above, a concentration approximates normal plasma concentration[26]. With the maximal mitogenic stimulation of epidermal growth factor, the optimal proliferation of IEC-6, a rat jejunum cell line, occurred at a glutamine concentration of 1.0 $mmol \cdot L^{-1}$ in the cultural medium, a concentration within the physiologic ranges of glutamine found in rat plasma[27]. Under normal nutritional status, plasma glutamine homeostasis can be maintained without nutritional glutamine supply[28]. However, in the absence of luminal nutrition stimulation during TPN, glutamine delivered by blood flow may be insufficient for optimal intestinal growth, as is attested by the fact that parenteral or enteral glutamine supplementation is effective in reducing TPN-induced intestinal hypoplasia. This insufficiency may be caused by decreased blood flow induced by TPN, or enteral nutrition can stimulate the uptake of glutamine through the basolateral membrane by modifying the activity of the transporters. However, our data do not exclude the possibility that when inadequate enteral nutrition is received, enteral glutamine may exert a trophic effect on small intestine, since minimum luminal nutrition has been found indifferent in stimulating small intestinal mucosal growth as compared with TPN[29].

Dietary fiber includes a wide variety of carbohydrates that, as a group, are resistant to enzymatic hydrolysis within the human gastrointestinal tract. The principal physiologic function of dietary fiber are regulating gastric emptying and intestinal transit time, based on the bulking action of the fiber. Insoluble fibers are minimally fermented and function almost solely as bulking agents that decrease colonic transit time and increase fecal mass. Soluble fibers are largely fermented by anaerobic gut flora, resulting in increase of the bacterial quantity, and fecal mass, and production of short-chain fatty acids (SCFAs), which are quickly absorbed by the colonic mucosa. The importance of dietary fiber in maintenance of normal colonic morphology and function has been widely acknowledged. However, its role in short-bowel syndrome has not been investigated thoroughly. Previous studies on the effect of dietary fiber on colon were mostly carried out in normal animals with intact small and large intestine. In contrast, after massive small bowel resection, the colon in continuity with the remnant small bowel will receive substantial unabsorbed carbohy drates and protein, which will undergo fermentation in colon by various anaerobic bacteria and produce SCFAs. This represents an important mechanism whereby the colon compensates some energy absorption function of the lost small intestine[30,31]. How colon with this altered environment responses to additional dietary fiber loading is not clear. Although there is the speculation that in carbohydrates malabsorption, dietary fiber supplementation seemed to be redundant in

enhancing the SCFAs production[11], available data from massive small bowel resection models showed the beneficial effect of dietary fiber supplementation on residual small bowel as well as colon adaptation[32-34]. In contrast, dietary fiber had little effect on intact intestinal function[35]. Therefore, it seems that the effect of dietary fiber is modified by the absorptive function of intestine.

We fed the animals with fiber-free enteral nutrition of 2 g soy bean fiber daily, containing about 70% total dietary fiber consisting predominantly of insoluble fiber, and found that soy bean fiber supply led to large solid fiber-containing stool, instead of large liquid stool as seen in non-fiber supplied EN groups. This indicates that fiber supply may alter the colon absorptive and moving function. Significantly improved body mass recovery was associated with this improved stool consistency. In addition, the plasma IGF-I concentration was simultaneously elevated, which implied that the improved body mass was not solely caused by colonic fiber retention. Both the residual jejunum and ileum displayed significantly greater mean villus height and mucosal thickness. The exact mechanism that soybean fiber enhanced the postresectional adaptation was not investigated in this study. Since the soy bean fiber consisted predominantly of insoluble fiber which mainly influences the intestinal transit, it is most likely that the presence of fiber in combination with unabsorbed carbohydrates and proteins in the colon had delayed the intestinal transit through direct bulk effect, hence promoting the colonic fermentation of unabsorbed carbohydrate and protein. Consequently, the secretion of colon-derived enteric hormones, such as enteroglucagon and peptide YY, might be augmented, which in turn exerted their small bowel trophic effect and stimulated further structural adaptation in small bowel.

Besides gut-special nutrients such as glutamine and dietary fiber, the possible role of many growth factors has met with intense research interest. Strong evidence has demonstrated that growth hormone (GH) is an important growth factor for intestine. Complete GH depletion due to hypophysectomy caused pronounced hypoplasia of small intestinal mucosa with decreased villus height and reduced crypt cell proliferation[36]. Simple replacement of GH can restore mucosal proliferative activity[37]. The study of the transgenic mice overexpressing the bovine growth hormone demonstrated that chronic excessive GH can produce hyperplasia in small intestinal mucosa whether food intake was *ad lib* or restricted[38]. Hypophysectomy could impair the adaptive hyperplasia in response to small bowel resection[39]. In an unpaired-fed study, exogenous GH was found to enhance mucosal hyperplasia after extensive small bowel resection[40]. Our pair-fed study revealed that exogenous GH administration significantly elevated the plasma IGF-I level, increased villus height in both remnant jejunum and ileum, and significantly increased ileum mucosal thickness. Postresectional body mass recovery was also accelerated by GH administration, suggesting the enhanced nutrient absorption. Our data further confirmed the gut-trophic property of GH. The more important findings of our study are that concomitant fiber supplementation further enlarged the villus height and mucosal thickness in both remnant ileum and jejunum, enhanced body mass gain, and increased the plasma IGF-I concentration in ENint group. These results suggest that gut-trophic growth factor, GH, can be used in combination with gut-special nutrient, dietary fiber, to bring about synergistic effect on postresectional remnant small bowel structural adaptation.

In summary, our study demonstrated that both dietary fiber and growth hormone can enhance the postresectional small bowel structural adaptation, promote bodymass-gain, and increase plasma IGF-I level when used separately. Simultaneous use of these two gut-trophic factors produced synergistic effect on structural adaptation parameters, body mass, and plasma IGF-I concentration. In contrast, the gut essential nutrient, glutamine when enterally administered with enteral nutrition, showed little beneficial effect on remnant small bowel structural adaptation, and the body mass did not alter in comparison with the control enteral nutrition. However, enteral glutamine is effective in preserving intestinal mucosal structure during TPN. These findings raise the doubt about the necessity of enteral glutamine supplementation during enteral nutrition. On the other hand, they provide the evidence favoring the combined utilization of GH and dietary fiber with enteral nutrition in patients with short bowel syndrome.

REFERENCES

1 Li N, Li JS, Liao CX, Li YS. Antirejection therapy with Tripterygium woifordii and low-dose cyclosporine in small bowel transplantation in pigs. *China Natl J New Gastroenterol*, 1996;2:36-40

2 Li YS, Li JS, Li N, Jiang ZW, Li YX, Li XH. Endoscopic monitoring in small bowel transplantation. *China Natl J New Gastroenterol*, 1997;3:137-138

3 Li YS, Li JS, Li N, Jiang ZW, Zhao YZ, Li NY, Liu FN. Evaluation of various solutions for small bowel graft preservation. *World J Gastroenterol*, 1998;4:140-143

4 Liang LJ, Yin XY, Luo SM, Zheng JF, Lu MD, Huang JF. A study of the ameliorating effects of carnitine on hepatic steatosis induced by total parenteral nutrition in rats. *World J Gastroenterol*, 1999;5:312-315

5 Wilmore DW, Byrne TA, Persinger RL. Short bowel syndrome: New therapeutic approaches. *Curr Probl Surg*, 1997;34:389-444

6 Byrne TA, Morrissey TB, Nattakom TV, Ziegler TR, Wilmore DW. Growth hormone, glutamine, and a modified diet enhance nutrient absorption in patients with severe short bowel syndrome. *JPEN*, 1995;19:296-302

7 Byrne TA, Persinger RL, Young LS, Ziegier TR, Wilmore DW. A new treatment for patients with short-bowel syndrome. *Ann Surg*, 1995;222:243-255

8 Wilmore DW, Lacey JM, Soultanakis RP, Bosch RL, Byrne TA. Factors predicting a successful outcome after pharmacologic bowel compensation. *Ann Surg*, 1997;226:288-293

9 Williamson RCN, Chir M. Intestinal adaptation. Structural, functional

and cytokinetic changes. *N Eng J Med*, 1978;298:1393-1402
10 Thissen JP, Ketelslegers JM, Underwood LE. Nutritional regulation of the insulin-like growth factors. *Endocr Rev*, 1994;15:80-101
11 Vanderhoof JA, Langnas AN. Short-bowel syndrome in children and adults. *Gastroenterology*, 1997;113:1767-1778
12 Souba WW, Smith RJ, Wilmore DW. Glutamine metabolism by the IntestinalTract. *JPEN*, 1985;9:608-617
13 Rhoads JM, Argenzio RA, Chen W, Rippe RA, Westwick JK, Cox AD, Berschneider HM, Brenner DA. L-Glutamine stimulates intestinal cell proliferation and activates mitogen-activated protein kinases. *Am J Physiol*, 1997;272:G943-G953
14 O Dwyer ST, Smith RJ, Hwang TL, Wilmore DW. Maintenance of small bowel mucosa with glutamine-enriched parenteral nutrition. *JPEN*, 1989;13:579-585
15 Li J, Langkamp-Henken B, Suzuki K, Stahlgren LH. Glutamine prevents parenteral nutrition-induced increases in intestinal permeability. *JPEN*, 1994;18:303-307
16 Platell C, McCauley R, McCulloch R, Hall J. The influence of parenteral glutamine and branched-chain amino acids on total parenteral nutrition-induced atrophy of the gut. *JPEN*, 1993;17: 348-354
17 Klimberg *VS*, Souba WW, Dolson DJ, Salloum RM, Hautamaki RD, Plumley DA, Mendenhall WM, Bova FJ, Khan SR, Hackett RL, Bland KI, Copeland III EM. Prophylactic glutamine protects the intestinal mucosa from radiation injury. *Cancer*, 1990; 66:62-68
18 Fox AD, Kripke SA, De Paula J, Berman JM, Settle RG, Rombeau JL. Effect of a glutamine-supplemented enteral diet on methotrexate-induced enterocolitis. *JPEN*, 1988;12:325-331
19 Tamada H, Nezu R, Matsuo Y, Imamura I, Takagi Y, Okada A. Alanyl glutamine-enriched total parenteral nutrition restores intestinal adaptation after either proximal or distal massive resection in rats. *JPEN*, 1993;17:236-242
20 Desjeux JF, Nath SK, Taminian J. Organic substrate and electrolyte solutions for oral rehydration in diarrhea. *Annu Rev Nutr*, 1994;14:321-342
21 Vanderhoof JA, Blackwood DJ, Mohammadpour H, Park JHY. Effects of oral supplementation of glutamine on small intestinal mucosal mass following resection. *J Am Coll Nutr*, 1992; 11:223-227
22 Michail S, Mohammadpour H, Park JHY, Vanderhoof JA. Effect of glutamine-supplemented elemental diet on mucosal adaptation following bowel resection in rats. *J Pediatr Gastroenterol Nutr*, 1995;21:394-398
23 Wiren ME, Permert J, Skullman SP, Wang F, Larsson J. No differences in mucosal adaptive growth one week after intestinal resection in rats given enteral glutamine supplementation or deprived of glutamine. *Eur J Surg*, 1996;162:489-498
24 Alavi K, Kato Y, Yu D, Schwartz MZ. Enteral glutamine does not enhance the effects of hepatocyte growth factor in short bowel syndrome. *J Pediatr Surg*, 1998;33:1666-1669
25 Yang H, Larsson J, Permert J, Braaf Y, Wiren M. No effect of bolus glutamine supplementation on the postresectional adaptation of small bowel mucosa in rats receiving chow ad libitum. *Dig Surg*, 2000;17:256-260
26 Smith RJ. Glutamine metabolism and its physiologic importance. *JPEN*, 1990;14:40S-44S
27 Ko TC, Beauchamp RD, Townsend CM, Thompson JC. Glutamine is essential for epidermal growth factor-stimulated intestinal cell proliferation. *Surgery*, 1993;114:147-154
28 Van Der Hulst RRWJ, Von Meyenfeldt MF, Deutz NEP, Stockbrugger RW, Soeters PB. The effect of glutamine administration on intestinal glutamine content. *J Surg Res*, 1995;61:30-34
29 Heel KA, Kong SE, McCauley RD, Erber WN, Hall JC. The effect of minimum luminal nutrition on mucosal cellularity and immunity of the gut. *J Gastroenterol Hepatol*, 1998;13:1015-1019
30 Bond JH, Currier BE, Buchwald H, Levitt MD. Colonic conservation of malabsorbed carbohydrate. *Gastroenterology*, 1980;78: 444-447
31 Nordgaard I, Hansen BS, Mortensen PB. Colon as a digestive organ in patients with short bowel syndrome. *Lancet*, 1994;343: 373-376
32 Koruda MJ, Rolandelli RH, Settle RG, Saul SH, Rombeau JL. The effect of a pectin-supplemented elemental diet on intestinal adaptation to massive small bowel resection. *JPEN*, 1986;10:343-350
33 Roth JA, Frankel WL, Zhang W, Klurfeld DM, Rombeau JL. Pectin improves colonic function in rat short bowel syndrome. *J Surg Res*, 1995;58:240-246
34 Michail S, Mohammadpour M, Park JH, Vanderhoof JA. Soy-polysaccharide-supplemented soy formula enhances mucosal disaccharidase levels following massive small intestinal resection in rats. *J Pediatr Gastroenterol Nutr*, 1997;24:140-145
35 Kapadia SA, Raimundo AH, Grimble GK, Aimer P, Silk DBA. Influence of three different fiber-supplemented enteral diets on bowel function and short-chain fatty acid production. *JPEN*, 1995; 19:63-68
36 Bastie MJ, Balas D, Laval J, Senegas-Balas F, Bertrand C, Frexinos J,Ribet A. Histological variations of jejunal and ileal mucosa on days 8 and 15 after hypophysectomy in rat: morphometrical analysis in light and electron microscopy. *Acta Anat (Basel)*, 1982; 112:321-337
37 Scow RO, Hagan SN. Effect of testosterone propionate and growth hormone on growth and chemical composition of muscle and other tissues in hypophysectomized male rats. *Endocrinology*, 1965;77:852-858
38 Ulshen MH, Dowling RH, Fuller CR, Zimmermann EM, Lund PK. Enhanced growth of small bowel in transgenic mice overexpressing bovine growth hormone. *Gastroenterology*, 1993;104:973-980
39 Taylor B, Murphy GM, Dowling RH. Effect of food intake and the pituitary on intestinal structure and function after small bowel resection in the rat. *Gut*, 1975;16:397-398
40 Shulman DI, Hu CS, Duckett G, Lavallee-Grey M. Effects of short-term growth hormone therapy in rats undergoing 75% small intestinal resection. *J Pediatr Gastroenterol Nutr*, 1992;14:3-11

Edited by Ma JY

P.O.Box 2345 Beijing 100023, China
Fax. 0086·10·65891893 Tel. 0086·10·65897901
E-mail.wcjd@public.bta.net.cn www.wd.org.cn

World J Gastroentero, 2001; 7(1):74 - 79
World Journal of Gastroenterology
Copyright©2001 by the WJG Press ISSN 1007 - 9327

Comparison of a new stent and Wallstent for transjugular intrahepatic portosystemic shunt in a porcine model

Gao Jun Teng[1], Michael A. Bettmann[2], P. Jack Hoopes[2] and Li Yang[3]

Subject headings hypertention/portal; portosystemic shunt/surgical; stents; radiology/interventional; balloon dilatation; swine

Teng GJ, Bettmann MA, Hoopes PJ, Yang L. Comparison of a new stent and Wallstent for transjugular intrahepatic portosystemic shunt in a porcine model. ***World J Gastroenterol***, 2001;7(1):74-79

Abstract

AIM To evaluate a new balloon-expandable stainless steel stent (Cordis stent) in a transjugular intrahepatic portosystemic shunt (TIPS) porcine model and compared with Wallstent.

METHODS TIPS was performed in 26 normal domestic pigs weighing 20 kg-30 kg using a Cordis stent or Wallstent (13 pigs in each stent). All pigs were sacrificed at the 14 th day after TIPS. The stent deployment delivery system, stent patency, and stent recoil after placement were evaluated.Proliferative response in representative histological sections from the center,hepatic and portal regions of the two stent designs were quantified.

RESULTS The shunt was widely patent in 4 pigs in the Cordis stent group (4/12, premature dead in 1 pig), and in 5 pigs in the Wallstent group (5/13). All remaining stents of both designs were occluded or stenotic. The mean quantified proliferation including thickness of the proliferation and the ratio of proliferation: total area in three assayed regions in Cordis stent and Wallstent was 2.18 mm² 2:00 mm, and 59.18 mm². 51.66 mm², respectively (*P*<0. 05). The delivery system and mechanical properties of the Cordis stent fuctioned well.

CONCLUSION The new Cordis stent is appropriate for TIPS procedure.

[1]Department of Radiology, Zhong-Da Hospital, Southeast University, Nanjing 210009, China
[2]Department of Radiology, Dartmouth-Hitchcock Medical Center, USA
[3]Department of Radiology, PLA General Hospital, Beijing
Corresponding to: Gao Jun Teng, M.D., Department of Radiology, Zhong-Da Hospital, Southeast University, 87 Dingjiaqiao Road, Nanjing 210009, China
Tel/Fax. 0086-25-3311083
Email. gjteng@public1.ptt.js.cn
Received 2000-04-03 **Accepted** 2000-07-30

INTRODUCTION

The high incidence of stenosis following transjugular intrahepatic portosystemic shunt (TIPS) remains the major barrier in this relatively new technique which is effective in controlling variceal hemorrhage secondary to portal hypertension and utilized in refractory ascites[1, 2]. The exact mechanism for TIPS restenosis is not well understood and seems multifactorial. One relevant factor may be stent design. Wallstent is the most common stent currently used for TIPS procedures, but various stent designs may be effective. To evaluate a new balloon-expandable stent (Cordis stent) in TIPS, a comparative study of the Cordis stent and Wallstent was performed in a TIPS porcine model.

MATERIALS AND METHODS

TIPS was performed in 26 domestic swine weighing 20 kg-30 kg, with two stent designs: balloon-expandable stainless steel stents (Cordis Co., Miami, FL) in 13 pigs and Wallstents (Schneider, Minneapolis, MN) in 13 pigs, respectively. The Cordis stent is made up of one stainless steel wire, which is formed into a sinusoidal wave pattern, wrapped in a tubular helical fashion and held in place by a series of welded joints (Figure 1). Either Cordis stent or Wallstent with an diameter of 8 mm and 4 cm in length was used in each pig.

TIPS was performed with a 22 G, 80 cm long puncture needle with a 5-F,70 cm long coaxial Teflon catheter (AngioDynamic, Queenshury, NY), a 9 F sheath set and a 14 G metal cannula with a curved tip (Cook, Bloomington, IN).

The animals in this study had normal livers and did not have portal hypertension. All protocols were approved by the Dartmouth Animal Care and Use Committee. Animals were sedated with intramuscular Ketamine (20 mg/kg) injection, intubated and maintained with 1%-3% halothane and oxygen.

The sheath was assembled with a 9-F Teflon catheter with a tapered tip and was introduced into the IVC by a standard percutaneous Seldinger method from the right jugular vein. A 7-F NIH catheter was advanced into the right lateral hepatic vein. The sheath was then placed into the hepatic vein and followed by the metal cannula containing the coaxial puncture needle. Through the metal cannula, the puncture needle together with the coaxial catheter was advanced into the hepatic parenchyma in an anterior direction targeted toward

the right branch of portal vein. Following confirmation of suitable portal vein puncture by contrast injection, a 0.035 inch steerable guidewire (Cordis Co., Miami, FL) was advanced into the portal vein and followed by the 5-F catheter. Following portography, the floppy-tip guide wire was exchanged for an Amplatz super stiff guide wire, and a hepatic parenchymal tract was dilated using an 8 mm balloon catheter. The Cordis balloon catheter-stent delivery system was introduced into the sheath by advancing the insertion tool over the wire through the hemostasis valve, until a hand stop was reached. A stent mounted balloon was introduced through the insertion tool and advanced over the guidewire until the stent was in the desired location for deployment. The stent was deployed by inflating the balloon with a 50% saline and 50% Renografin76 solution using a standard manual technique (Le Veen balloon inflator). A 10 mm diameter balloon catheter was used with 6 atm pressure for 2 minutes with 3 repetitions. The Wallstent was deployed in a standard fashion and inflated using equivalent inflation pressures and technique for Cordis stent deployment.

Since the coagulation process is much faster in pigs than in humans based on our previous experience, 500U/kg heparin was routinely administered in each procedure. No anticoagulants or other medicines were used after the procedure.

A numerical rating system was developed in the evaluation of the following deployment factors at implantation: stent insertion through the sheath, insertion tool function, stent tracking, balloon inflation and deflation, stent expansion, ease of positioning, balloon catheter removal, and stent architecture and visibility under fluoroscopy. The rating system was scored as follows: excellent = 1; satisfactory = 2; poor = 3; and not achieved = 4.

Portal venography was performed following TIPS placement and prior to sacrifice. Plain radiography was taken and the following factors were assessed: stent migration, distortion of stent architecture and changes of diameter and length of the stent.

Animals were euthanized 2 weeks after TIPS placement by intravenous injection of 15 mL saturated KCL. All of the shunts were examined by portography via transjugular i mmediately prior to euthanasia.

Necropsy was performed i mmediately following euthanasia. The TIPS shunt and involved adjacent tissues were evaluated by gross examination at necropsy and preserved for histologic assessment. Representative crossections from the central, hepatic and portal vein regions of the stent were cut after fixation in buffered 4% formalin for at least 24 hours. The metal of Wallstent was removed before embedding while the metal of Cordis stent had to be removed using a hand saw after embedding and then reembedded in JB-4. The tissues were then cut at 5 microns and stained with modified Giemsa and basic fuchsin.

At least 3 sections in each region of stent were prepared and reviewed. Histologic quantification including thickness, the area of the proliferative response and the ratio of the proliferative area/total area of the stent was achieved using standard planimetry techniques and Nikon microscopy and Camera Lucita with Micro-Plan II Image Analysis (Laboratory Computer Systems, INC).

All quantitated data were expressed as the mean value ± SD. Stent patency and quantified proliferative reaction within the stent were compared using Chi-Square test and Student's *t* test, respectively. Statistical significance was defined as $P<0.05$.

RESULTS

TIPS was successfully performed in all pigs with both stent designs (100%). No difficulties were encountered in delivering and deploying the Cordis stents. All pigs remained healthy until the scheduled date of euthanasia except one. This pig died 2 days following Cordis stent placement from introgenic hemorrhage secondary to inadvertent gastric puncture during the TIPS procedure. This early death was excluded from the numerical results.

Patency

Stent patency was determined by venography and pathohistological examinations, 33.3% (4/12) of the Cordis stent group and 38.5% (5/13) of the Wallstent group were patent at 2 weeks post-deployment (Figure 2). This difference did not reach a statistical significance ($P>0.05$, Chi-Square test). One pig had an occluded Cordis stent because its proximal end wedged into the liver parenchyma due to its stiff property (Figure 3). Likewise, one pig had an occluded Wallstent due to longitudinal recoiling of the stent causing the distal end to withdraw from the portal vein into the liver parenchyma.

Stent deployment factors

The mean score for stent deployment factors are listed in Table 1. Stent insertion through the sheath and stent expansion were scored excellent in all procedures performed with both Cordis stent and Wallstent. Cordis stent had a higher score than Wallstent in stent tracking, positioning, and visibility by fluoroscopy. The factors of tool function, balloon in/de-flation and catheter removal which are unique to Cordis stent, were scored excellent for all procedures.

Recoiling of stents

No stent migration or stent distortion was demonstrated in either Cordis stent or Wallstent groups. Stent diameter and length i mmediately after TIPS placement and 2 weeks after TIPS are shown in Tables 2 and 3. The interval change in the Wallstent group at 2 weeks after TIPS is larger than

in the Cordis stent group. The Wallstent demonstrated an average shortening of 5.18% as compared with 0. 69% with Cordis stent.

Histopathologic characteristics

Pseudointimal proliferation (PIH) formed within the shunt with both stent designs, and histology was similar in all three assayed areas. PIH was primarily composed of myofibroblasts (Figures 2,4), organized thrombus, and collagen. Infla mmatory cells were mainly lymphocytes and mononuclear cells co mmonly located around the stent wires. Organized thrombus was characterized by palisading and herringbone deposition of the fibrin and the invasion of blood vessels (neovascularization). A single-cell lining of endothelial-like cells covering the lumen was observed only in specimens with a patent shunt. The liver tissue adjacent to the stent showed minimal injury characterized by sinusoidal dilatation, hemorrhage, focal necrosis, mononuclear infla mmation and fibrosis. There was no major difference in histological characteristics between the two groups with the different stent designs.

In 10 specimens (5 in each stent group), bile leak was identified by bile staining of thrombus. Histologic sections demonstrated extensive neo-bile duct proliferation within the PIH or on the surface of the lumen in some specimens with bile leak (Figure 4). This partially contributed to occlusion of the stent.

Quantified histological results

PIH thickness and the ratio of proliferative area/total area within both stent designs are shown in Table 4. The portal vein aspect of the stents had the highest proliferative response, the hepatic region the second highest and the middle region of the stents the least proliferative. There was no statistically significant difference among the three assayed regions between Cordis stent and Wallstent specimens (P>0.05).

DISCUSSION

Various stent designs including Palmaz stent, Gianturco-Rosch Z stent, Strecker stent and Memotherm stent have been utilized in TIPS procedures[3-6]. Wallstent is the most co mmon stent used for TIPS currently within the United States due to its flexibility which allows easy negotiation of the angles bridging a hepatic vein and a portal vein[7]. Unfortunately, TIPS stent stenosis rates are high with all stent designs, although PTFE covered stent seems to decrease the stenosis of TIPS shunt in pigs[8,9]. The mechanism and process of restenosis in TIPS remains poorly understood. However, it is well accepted that stent design including mechanical properties are important factors influencing stent patency.

Table 1 Scores of deployment factors

Stent types	Insert thru sheath	Tool function	Stent tracking	Balloon in / de flation	Stent expansion	Position	Catheter removal	Architecture & visibility
Cordis	1 ± 0.0	1 ± 0.0	1.07 ± 0.27	1 ± 0.0	1.14 ± .53	1.29 ± .61	1 ± 0.0	1.86 ± .54
Wallstent	1 ± 0.0	*	2.17 ± .84	*	1.00 ± 0.00	*	1.75 ± .87	2.42 ± .52

*Not applicable to the device.

Table 2 Recoil data in Cordis stent

Interval	Diameter (mm)				Length (CM)
	Proximal	Middle	Distal	Overall	
I mm post-TIPS	7.46 ± .80	7.32 ± .70	7.43 ± .73	7.40 ± .73	4.35 ± .33
2 weeks	7.51 ± .79	7.25 ± .73	7.50 ± .74	7.42 ± .74	4.32 ± .32
Change (%)	+0.67	-0.96	+0.94	+0.27	-0.69

I mm: I mmediately

Table 3 Recoil data in Wallstent

Interval	Diameter (mm)				Length (CM)
	Proximal	Middle	Distal	Overall	
I mm post-TIPS	9.17 ± .94	7.42 ± .60	7.72 ± .71	7.98 ± 1.05	4.83 ± .42
2 weeks	9.28 ± .83	7.67 ± .53	7.94 ± .52	8.22 ± 0.90	4.58 ± .48
Change (%)	+1.2	+3.37	+2.77	+3.01	-5.18

I mm: I mmediately

Table 4 Quantified histological proliferation in specimens with Cordis stent *vs*. Wallstent

Region	Thickness (mm)			Proliferation area / total area (%)		
	Cordis stent	Wallstent	P value*	Cordis stent	Wallstent	P value*
Hepatic	2.04 ± 1.28	1.85 ± .96	0.66	57.49 ± 23.60	51.43 ± 24.61	0.74
Middle	1.42 ± 0.82	1.31 ± .87	0.63	49.89 ± 17.31	47.91 ± 20.12	0.60
Portal	2.46 ± 0.98	2.38 ± .23	0.61	71.88 ± 21.18	69.97 ± 29.45	0.57
Average	2.18 ± 1.07	2.00 ± .02	0.73	59.18 ± 23.06	51.66 ± 25.11	0.78

*Two-tail t test.

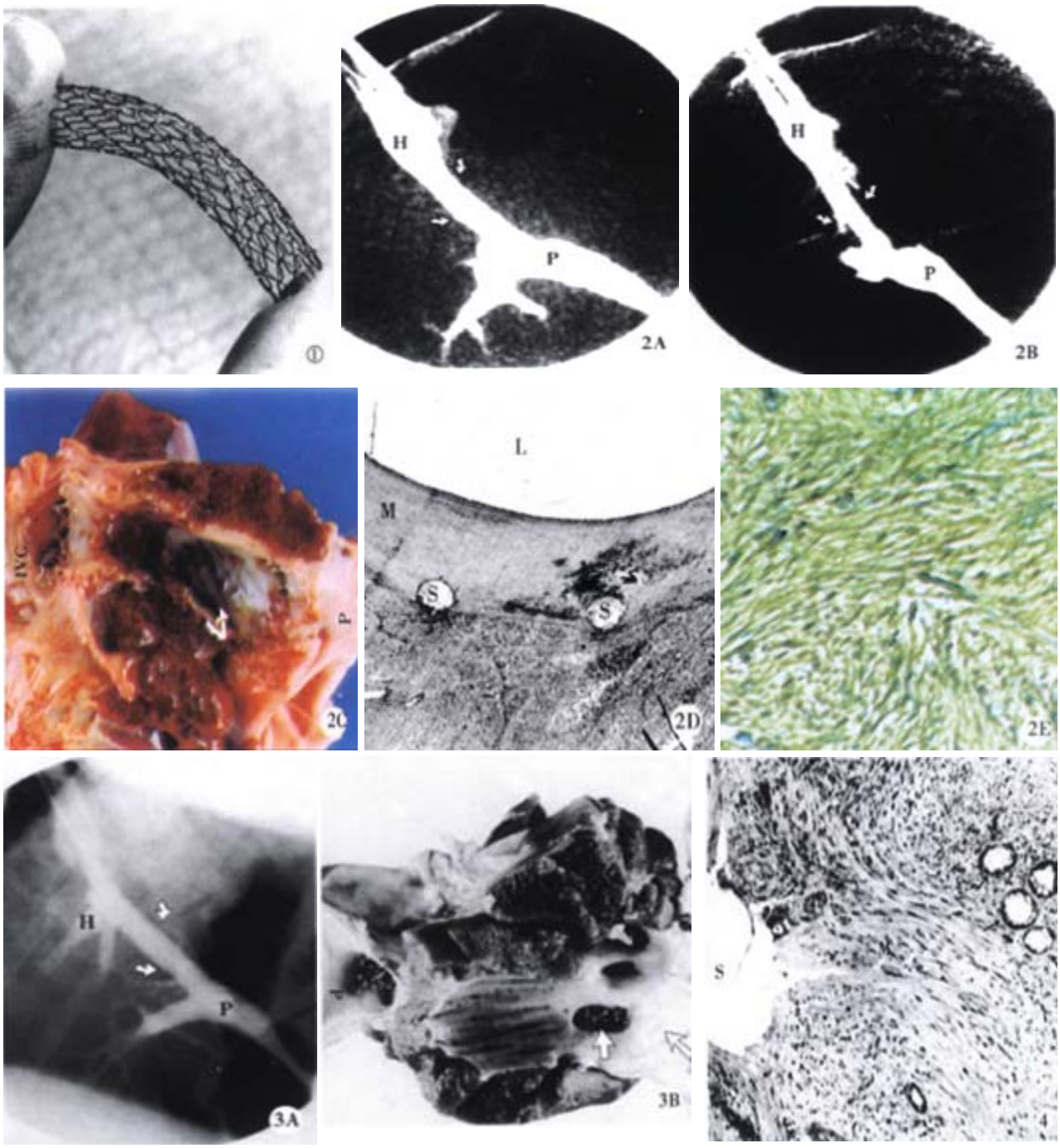

Figure 1 The Cordis balloon-expandable stent, which is constructed as a sinusoidal wave pattern by one stainless steel wire, with high rigidity.

Figure 2 a. The portal venography obtained i mmediately shows that the TIPS shunt (arrows) is well created between the hepatic vein (H) and the portal vein (P). **b.** The shunt remains patent in the portography taken i mmediately before the euthanasia at 2 weeks after stent placement. **c.** The gross examination of the specimen shows that the surface of the stent (straight arrows) is covered by a smooth and thin layer endothelia-like tissue (curved arrows) which does not extend to the ends of the stent at the IVC and the portal vein (P). **d.** Low magnification photomicrography of the TIPS reaction shows a mild myofibroblastic cell proliferation (M) under stent meshes (S) (Modified Giemsa and basic Fuchsin stain, ×3.12). **e.** The myofibroblastic cells are primarily composed of smooth muscle cells. (Anti-SMCα actin stain, ×125).

Figure 3 a. An occluded TIPS shunt from a pig using a Cordis stent. The i mmediate portal venography after TIPS shows a patent TIPS shunt (arrows). **b.** The occluded shunt was confirmed by the portography obtained i mmediately before the euthanasia in two weeks after the stent placement. The gross examination of the specimen demonstrates that the hepatic end of the stent wedges into the liver parenchyma and the proximal end of the shunt is totally occluded by the healed hepatic vein (arrows), while the portal end (P) of the stent keeps patent.

Figure 4 Photomicrography from an occluded TIPS shunt using a Wallstent shows that a massive pseudointimal proliferative tissue under the stent (S), which primarily composed of myofibroblastic cells (M). Neo-bile duct proliferation within the proliferation is also noted (arrows). Modified Giemsa and basic Fuchsin stain, ×125

Since multiple interdependent mechanical characteristics of stents may play a role in stent restenosis [10-19], the ideal stent appears to be non-existent. To produce a satisfactory stent, the following factors should be considered: stent wire material and diameter, longitudinal flexibility, hoop strength (circumferential strength), stent texture and stent surface area.

A layer of metal oxide provides the ultimate interface between stent and host following stent implantation. This is independent of metal content[10]. Similar thrombogenicity and patency rate have been observed in stented arteries using different stent metals[16,20]. Hehrlein *et al*[18] evaluated stent biocompatibility as related to surface texture and charge. Palmaz-Schatz stents were coated either by electrochemical metal deposition (platinum, gold, copper) or coated with a metallic film implanted onto the stent surface by argon ion bombardment. These stents were implanted and evaluated in a rabbit iliac arterial model. The results demonstrated that the most electropositive coating (platinum or gold) induced markedly less neointima formation than the least electropositive (copper). The authors therefore concluded that stent surface texture was the most important factor determining biocompatibility of the stent while the charge on stents appeared to be less important[18]. Strength, elasticity, and plasticity of various stents co mmonly used were recently investigated in an *in vitro* model[12,13]. The results suggested that the Palmaz stent is appropriate for insertion into highly resistant obstructions due to its superior resistance to deformation. Strecker stents and Wallstents required good wall contact to achieve adequate strength and Wallstent may not function well if implanted into eccentric stenoses of tough consistency due to its unique deformation. The Gianturco stent showed the lowest resistance and deformed more readily. We did not evaluate such criteria regarding the Cordis stent in this study. However, the higher longitudinal rigidity and hoop strength of this new stent may have merit for placement within tough and highly resistant cirrhotic liver tissue. Strong mechanical support by a stent is important to prevent proliferation as demonstrated by Ikari *et al*[17]. They demonstrated significantly higher proliferation at the articulation of Palmaz-Schats stents in stented conorary arteries and partially attributed this to lack of mechanical support in the articulation area of the stent. Surface area occupied by the metal stent mesh also influences restenosis.

A predominant difference between Cordis stent and Wallstent evaluated in this study is the rigid characteristic of Cordis stent and the flexible characteristic of Wallstent. The benefits of the Palmaz stent and Wallstent in TIPS were compared in a prospective randomized study[21]. The authors illustrated that early shunt thrombosis was more frequent with Wallstent (4/45 *vs* 0/45). Palmaz suggests that the relatively more rigid Palmaz stent could provide a stable, nonshifting surface for endothelial growth, whereas dimensional change in a prosthetic surface causes increased endothelial slough and platelet proliferation[10]. However, late observation in the same study[21] showed more frequent shunt insufficiency with Palmaz stent than Wallstent (6/45 *vs* 2/45). This indicates that the process of TIPS stenosis should be multifactorial.

Wallstent is frequently associated with unpredictable shortening in TIPS at follow-up due to the self-expanding force from elasticity[6,22]. Wallstent shortened 5.18% in our study at 2 weeks as compared with 0. 69% shortening of the Cordis stent. Stent flexibility is required to negotiate curves when delivering the stent by catheter through tortuous vessels leading to the target area. Is it possible to compromise flexibility and rigidity without the drawback of shortening like a Wallstent in TIPS Several other stent designs have been utilized in TIPS. Gianturco-Rosch stent was the first stent designed in experimental TIPS, but it seems to be unco mmonly used. Strecker stent is highly radiopaque, flexible and shortens minimally but tends to dislodge and is difficult to be recatheterized[23]. Preliminary experience in TIPS using the Memotherm stent (Angiomed, Germany) showed promising results, but the number of samples was small[6]. The new Cordis stent used in this study is relatively more flexible than the Palmaz stent, and has the added advantage of being highly radiopaque with minimal shortening. From a technical perspective, the Cordis stent deployment system consistently works well and is easy to use, compared with Wallstent. In our opinion, the Cordis stent is an appropriated compromise between the rigid Palmaz and the flexible but foreshortening Wallstent.

The similar histologic characteristics of proliferative response were observed in the two groups using different designs of stent, which is also very similar to the findings described previously by us and other authors[24-26].

To date, there are few experimental studies or clinical trials available to compare different stent designs in TIPS. It is difficult to directly compare different stent designs following deployment. For instance, although equal stent diameters and balloons with equal inflation pressures were used in our study, TIPS stent length was not equivalent following deployment. Stent diameter following TIPS completion in the Wallstent group was larger than the Cordis stent group (7.98 mm *vs* 7.40 mm). This unexpected size variation may contribute to the relative rigidity of Cordis stents compared with the relative flexibility of Wallstents and the stronger circumferential strength of Cordis stents compared with the relatively decreased hoop strength of Wallstents. Perhaps the difference in luminal diameter contributed to the increased PIH in the pigs with Cordis stents (not statistically

significant). Such an explanation is favored by our recent study (unpublished data, 1996) which demonstrated significantly thicker pseduointimal formation within the lumen (2.07 mm *vs* 1.25 mm, P = 0.006) when comparing a smaller diameter Wallstent (6.50 mm) to larger Wallstent (7.25 mm) in a TIPS porcine model. Nevertheless, the short-term patency rate using the Cordis balloon-expandable stainless steel stent in a TIPS porcine model in this study is comparable to that found using Wallstent.

There were interesting findings in two occluded stents in this study: one stent probably occluded because of Cordis stent rigidity, and the other probably occluded because of Wallstent longitudinal recoil. This probably reflects the inherent drawbacks of Cordis stent and Wallstent respectively. However, Cordis stent rigidity may be an advantage when deployed in stiff cirrhotic liver parenchyma in TIPS rather than in healthy, compliant normal pig livers, although Cordis stent should not be deployed where sharp curves are required to bridge the portal and hepatic veins. Use of a longer Wallstent than the exact length of the tract required in TIPS may overcome the shortening disavantage of Wallstent[22]. However, it is important to accurately place the stent in the hepatic vein to ensure patency and not to compromise future opportunity for liver transplantation[27]. The easy to use, reliable Cordis deployment system and increased radiopacity allow for accurate manipulation and precise positioning under fluoroscopy.

Therefore, our study suggests that the Cordis stent merits further investigation for potential use in TIPS patients.

REFERENCES

1 Cello JP, Ring EJ, Olcott EW, Koch J, Gordon R, Sandhu J, Morgan DR, Ostroff JW, Rochey DC, Bacchetti P, LaBerge JM, Lake JR, Somberg K, Doherty C, Davild M, McQuaid K, Wall SD. Endoscopic sclerotherapy compared with percutaneous transjugular intrahepatic portosystemic shunt after initial sclerotherapy in patients with acute variceal hemorrhage. A randomized, controlled trial. *Ann Intern*, 1997;126:907-910

2 Ochs A, Rossle M, Haag K, Hauenstein KH, Deibert P, Siegerstetter V, HusnkerM, Langer M, Blum HE. The transjugular intrahepatic portosystemic stent-shunt procedure for refractory ascites. *N Eng J Med*, 1995;332:1192-1197

3 Noeldge G, Richter GM, Roessle M, Haag K, Katzen BT, Becker GJ, Palmaz JC. Morphologic and clinical results of the transjugular intrahepatic portosystemic stent-shunt (TIPSS). *Cardiovasc Intervent Radiol*, 1992;15:342-348

4 Matsuzaka S, Kanazawa H, Kobyashi M, Kumazaki T. An experience of transjugular intrahepatic portosystemic shunt in the treatment of gastroesophageal varices. *Nippon Shokakibyo Gakkai Zasshi*, 1994;91:257-266

5 Echenagusia AJ, Gamunez F, Simo G, Deilo J, Garag MG, Rodriguez LJM, Banares R. Variceal hemorrhage: efficacy of transjugular intrahepatic portosystemic shunts created with Strecker stents. *Radiology*, 1994;192:235-240

6 Tesdal IK, Jaschke W, Buhler M, Adamus R, Filser J, Holm E, Georgi M. Transjugular intrahepatic portosytemic shunting (TIPS) with balloon-expandable and self-expanding stents: technical and clinical aspects after 3 1/2 years experience. *Cardiovasc Intervent Radiol*, 1997;20:29-37

7 Kerlan RK, LaBerge JM, Gordon RL, Ring EJ. Transjugular intrahepatic portosystemic shunts: Current Status. *AJR*, 1995;164: 1059-1066

8 Nishimine K, Saxon R, Kichkawa K, Mendel-Hartvig J, Ti mmermans HA, Shim HJ, Uchida BT, Barton RE, Keller FS, Rosch J. Improved transjugular intrahepatic portosystemic shunt patency with PTFE-covered stent-grafts: experimental results in swine. *Radiology*, 1995;196:341-347

9 Haskal ZJ. Improved patency of transjugular intrahepatic portosystemic shunts in humans: creation and revision with PTFE stent-grafts. *Radiology*, 1999;213:759-766

10 Palmaz JC. Intravascular stents: tissue-stent interactions and design considerations. *AJR*, 1993;160:613-618

11 Fontaine AB, Spigo DG, Eaton G, Das Passos S, Christofridis G, Khabiri H, Jung S. Stent-induced intimal hyperplasia: are there fundamental differences between flexible and rigid stent designs? *JVIR*, 1994;5:739-744

12 Lossef SV, Lutz RJ, Mundorf J, Barth KH. Comparison of mechanical deformation properties of metallic stents with use of stress-strain analysis. *JVIR*, 1994;5:341-349

13 Flueckiger F, Sternthal H, Klein GE, Aschauer M, Szolar D, Kleinhappl G. Strength, elasticity, and plasticity of expandable metal stents: *in vitro* studies with three types of stress. *JVIR*, 1994;5:745-750

14 Tominaga R, Kambic HE, Emoto H, Harasaki H, Hollmen J. Effects of design geometry of intravascular endoprostheses on stenosis rate in normal rabbits. *Am Heart J*, 1992;23:21-28

15 Tominaga R, Harasaki H, Sutton C, Emoto H, Kambic H, Hollmen J. Effects of stent design and serum cholesterol level on the restenosis rate in atherosclerotic rabbits. *Am Heart J*, 1993;126: 1049-1058

16 Hausegger KA, La mmer J, Fluckiger F, Lafer M, Klein GE, Pilger E. Iliac artery stenting-clinical experience with the Palmaz stent, Wallstent, and Strecker stent. *Act Radiol*, 1992;3:292-296

17 Ikari Y, Hara K, Tamura T, Saeki F, Yamaguchi T. Luminal loss and site of restenosis after Palmaz-Schatz coronary stent implantation. *Am J Cardiol*, 1995;76:117-120

18 Hehrlein C, Zi mmermann M, Metz J, Ensinger W, Kubler W. Influence of surface texture and charge on the biocompatibility of endovascular stents. *Coron Arter Dis*, 1995;6:581-586

19 Schurmann K, Vorwerk D, Kulisch A, Straehmer-Kulisch E, Biesterfelds, Stopinski T, Gunther RW. Experimental arterial stent placement comparison of anew nitinol stent and Wallstent. *Invest Radiol*, 1995;30:412-420

20 Scott NA, Robinson KA, Nunes GL, Thomas CN, Viel K, King SB 3rd, Harker LA, Rowland SM, Juman I, Cipolla GD. Comparison of the thrombogenicity of stainless steel and tantalum coronary stents. *Am Heart J*, 1995;129:866-872

21 Hauenstein KH, Vinee P, Haag K, Ochs A, Rossle M. Palmaz stent versus Wallstent for transjugular intrahepatic portosystemic shunts: Results of a prospective randomized study in 90 patients (abstr.). *Radiology*, 1994;193(p):166

22 Hausegger KA, Sternthal HM, Linbichler F, Ascharuer M, Karaic R, Stauber R. Progressive shortening of the Wallstent after TIPS: A co mmon cause for shunt occlusion (abstr.). *Eur Radiol*, 1995; 5(Suppl):219

23 Ugolotti U, Larini P, Marcato C, Saccani A, Puccianti F, Pedretti G.Is the tantalum Strecker stent suitable for TIPS creation? Short- and mid-term results in 20 consecutive patients. *Cardiovasc Intervent Radiol*, 1997;20:38-42

24 Rosch J, Uchida BT, Putnam JS, Buschman RW, Law RD, Hershey AI. Experimental intrahepatic portacaval anastomosis: use of expandable Gianturco stents. *Radiology*, 1987;162:481-485

25 Teng GJ, Bettmann, MA, Hoopes PJ, Ermerling BL, Yang L, Wagner RJ. Transjugular intrahepatic portosystemic shunt in a porcine model: histological characeristics. *Academic Radiol*, 1998; 5:547-555

26 Teng GJ, Bettmann, MA, Hoopes PJ, Wagner RJ, Park BH, Yang L, Baxter BR. Transjugular intrahepatic portosystemic shunt: effect of bile leak on smooth muscle cell proliferation. *Radiology*, 1998;208:799-805

27 Wilson MW, Gordon RL, LaBerge JM, Kerlan RK, Radosevich PM, Roberts JP, Ring EJ. Liver transplantation complicated by malpositioned transjugular intrahepatic portosystemic shunts. *JVIR*, 1995;6:695-699

Edited by Ma JY

P.O.Box 2345 Beijing 100023, China
Fax. 0086·10·65891893 Tel. 0086·10·65897901
E-mail.wcjd@public.bta.net.cn www.wd.org.cn

World J Gastroentero, 2001; 7(1):80 - 82
World Journal of Gastroenterology
Copyright © 2001 by the WJG Press ISSN 1007 - 9327

Brief Reports

Intensify standardized therapy for esophageal and stomach cancer in tumor hospitals

Shi Jie Wang, Deng Gui Wen, Jing Zhang, Xin Man and Hui Liu

Subject headings esophageal neoplasms/therapy; stomach neoplasms/therapy; endoscopy, digestive system; chemotherapy, adjuvant; radiotherapy; surgery, operative

Wang SJ, Wen DG, Zhang J, Man X, Liu H. Intensify standardized therapy for esophageal and stomach cancer in tumor hospitals. ***World J Gastroenterol***, 2001;7(1):80-82

INTRODUCTION

Cancer treatment situation in tumor hospitals in China has its own unique characteristics which are not found in other parts of the world. Because of the huge population and high incidence rates of esophageal and stomach cancer[1-5], the number of cancer patients waiting for admission is inconceivably large. It is estimated that there are about 1.6-2.0 million new cases per year in China. In 1999, the Hebei Tumor Hospital had 6884 carcinoma patients hospitalized, among them there were 1035 esophageal cancer and 1057 stomach cancer patients. Because of the financial problem and most peasants have not joined the medical care insurance plan. Therefore, they are not benefited by the ideal treatment regimen after being diagnosed with TNM staging.

Hebei Tumor Hospital was established in 1958 to provide medical care to cancer patients in the central and southern parts of Hebei Province. It has 621 beds. The southern part of Hebei Province around Chixian is adjacent to Linxian of Henan Province, both Chixian and Linxian counties have the highest incidence rates of esophageal cancer which are 135/100 000. Besides, stomach carcinoma is another major cancer in this region.

With a view to standardize the therapy of esophagus and stomach cancer, the authors reviewed the national and international standard treatment and recent progress in this field, and the therapeutic modalities given in this hospital from 1981 to 1997, and hope this analysis may benefit the development of standardized therapy for the above two malignances in clinical management.

Dr. Shi Jie Wang, graduated from Hebei Medical University in 1973, Professor of Cancer Surgery, President of Hebei Tumor Hospital (Fourth Affiliated Hospital of Hebei Medical University) and Hebei Cancer Institute, having 27 papers published.
Supported by the Hebei Provincial Scientific Commission, No. 97276162D
Correspondence to: Dr.Shi Jie Wang, Hebei Tumor Hospital, 5 Jiankanglu, Shijiazhuang 050011, Hebei Province, China
Received 2000-07-12 **Accepted** 2000-07-26

MATERIALS AND METHODS

A database was constructed for esophageal and stomach cancer patients who had been hospitalized in Hebei Tumor Hospital from 1981 to 1997 by the Foxprow database management techniques. Each hospitalized patient had his or her own record in the dataset. Percentages of therapeutic modalities as surgery, radiotherapy, chemotherapy, separate or in combination were calculated by the programs written in the Foxprow language. Finally, the results were analyzed according to *Diagnosis and Treatment Criteria for Common Malignances in China* by Ministry of Health of China and *Manual of Clinical Oncology* by UICC, and recent advances in these fields so as to find out the most rational suggestions for esophageal and gastric cancer.

RESULTS AND DISCUSSION

Esophageal carcinoma

As seen in Table 1, surgery and radiotherapy are two major options for esophageal cancer. Only 2.76% of the patients were treated by chemotherapy alone, and even fewer cases had been treated by multimodality treatment regimens such as surgery + radiotherapy, surgery + chemotherapy, chemoradiotherapy, and surgery + chemoradio-therapy. Radiotherapy as a preoperative option is eligible for esophageal cancer of various locations[6]. Preor postoperative radiotherapy in addition to surgery could reduce tumor recurrence and metastasis[7,8]. Either surgery or radiotherapy alone is not satisfactory because of the high rate of recurrence and metastasis[9,10]. The rationale for preoperative radiotherapy includes cytoreduction, improved resectability and reduced chance of marginal dissemination of tumor during the surgical procedure[11]. Therefore, preoperative radiotherapy is especially beneficial to patients with middle or late stage esophageal cancer[12].

Postoperative radiotherapy had been proved to be useful in reducing recurrence and metastasis[11]. Recent trials showed that although the 5-year survival rate of esophageal cancer was still poor, it had improved somewhat from 3% 30 years ago to 10%-15% today[13]. It was reported that multimodality approaches combining surgery, radiotherapy, and chemotherapy had resulted in 5-year survival rate of 40%-75% for advanced stage patients with a complete histological response to

preoperative chemotherapy[14]. These results suggest that further improvement in multimodality treatment regimens may allow a significant increase in survival period for esophageal carcinoma patients in the future [15].

Preoperative chemotherapy has been shown in nonrandomized trials to have similar side effects and mortality rate with surgery alone. Furthermore, phase two trials have suggested higher survival rates for combination of preoperative chemotherapy and surgery than that seen in surgery alone[16]. Another randomized study of 113 patients with esophageal carcinoma found that preoperative Cisplatin and 5-Fu given concurrently with 40 Gy of radiation significantly improved 3-year survival rate (32% vs 6%)[17]. Criticism of the study included poor preoperative staging and small sample size (113 patients). However, this trial offered hope that multimodality treatment regimens may ultimately prove beneficial in improving the overall survival period in esophageal cancer.

As seen in Table 1, although the cured and improved rate on discharge was highest in patients treated by surgery + radiotherapy, the percentage was only 3.58%, far less than those with surgery alone (48.93%) or radiotherapy alone (32.87%). The percentage of multimodality treatment regimens was only 4.32%, this was because in the past, we adopted the policy of elimination of symptoms rather than eradication of the disease. Therefore, in the future, we should focus our attention on the multimodality treatment regimens and to search for the most eligible combinations.

Table 1 Treatment modalities of esophageal and stomach cancer patients from 1981 to 1997 in Hebei Tumor Hospital

Treatment modality	Esopageal cancer			Stomach cancer		
	n	%	Cured & improved(%)	*n*	%	Cured & improved(%)
Surgery	4683	48.93	92.70	5328	67.48	59.51
Radiotherapy	3146	32.87	93.01	1758	22.26	56.66
Chemotherapy	264	2.76	91.67	117	1.48	84.67
Surgery+radiotherapy	343	3.58	95.04	260	3.29	93.83
Surgery+chemotherapy	41	0.43		114	1.44	88.60
Chemo-radiotherapy	24	0.25	87.50	8		87.50
Surgery+radio+chemotherapy	5			4		75.00
Other therapy	1064	11.12	53.20	307	3.89	83.71
Total	9570	100.00	88.46	7896	100.00	84.04

Gastric carcinoma

As seen in Table 1, surgery remains the first choice as curative treatment for patients with gastric cancer, especially at the early stages[18-20]. Early intraepithelial gastric cancer without nodal metastasis by surgery alone can yield a 5-year survival rate as high as 90%-95%. These early carcinomas may also be treated by endoscopic resection or endoscopic mucosectomy[21-24]. Gastric cancer survival is clearly stage dependent and is significantly affected by lymph node involvement[25]. The 5-year survival rate for patients with early gastric carcinoma after treatment approaches 90% but only less than 5% for cancer that involves the serosa[26]. The better survival statistics among Japanese are mainly due to greater frequency of early gastric cancer. Early detection of gastric carcinoma relies upon advanced development of X-ray and endoscopies[27,28], and also upon massive screening in high risk populations.

Although surgery has been proven to be the curative therapy for early gastric cancer, unfortunately, only 10% are early cancers[29]. In fact, locoregional recurrence is also common even after curative resection[30,31], therefore adjuvant chemo and radiotherapies are absolutely necessary[32-34].

Currently, preoperative chemotherapy and intraoperative radiotherapy are used as adjuvant therapies.

The operative morbidity of gastrectomy is high. It frequently precludes patients from entering into adjuvant therapy in a timely manner. Therefore, many studies are investigating the use of preoperative therapy. Wilke *et al*[35] described 34 patients who were demonstrated at laparotomy to have locally advanced unresectable cancer, these patients received two to five cycles of etoposide, doxorubicin, and cisplatin (EAP), 70% responders were offered a second laparotomy, and 15 were without clinical evidence of local extension. Kelsen *et al*[36] reported 56 patients who underwent preoperative therapy with FAMTX combined with postoperative intraperitoneal 5-FU and Cisplatin, among whom 34 patients received a potentially curative resection. For the entire group, the median survival period was 15 months; however, for those who underwent the above preoperation chemothe rapy and surgical resection, the median survival period was 31 months. Lowy *et al*[37] reported 24 patients who responded to similar- therapy, 84% had a 5-year disease-free survival, while 30% of those who did not respond had a 5-year disease-free survival. These studies suggest an appealing potential benefit of preoperative chemotherapy by inducing positive response in some patients[38].

The largest experience with intraoperative radiotherapy (IORT) came from Japan, where it had been studied for over 20 years. Abe *et al*[39] performed a prospective randomized trial of IORT in over 200 gastric cancer patients, and a more significant survival advantage was found for patients treated with IORT and surgery over those treated by surgery alone. This 5-year survival advantage was seen in patients with stage two (84% vs 62%) and stage three (62% vs 37%). Patients with stage one disease received no benefit from IORT. In addition, the only 5-year survivors in stage four were those who received IORT. This study suggests that IORT may be able to control locoregional recurrence after resection, which alone is often a major cause of treatment failure.

According to the criteria for gastric cancer

therapy modality planning of the Diagnosis and Treatment Criteria for Common Malignances in China for early gastric carcinomas with no nodal metastasis, no adjuvant therapy is necessary following curative resection depending on whether the disease is restricted to the mucosa or submucosa, but if there is nodal metastasis, adjuvant chemotherapy should be considered. For stage two and/or stage three progressive gastric cancer patients, preoperative radiotherapy is helpful to improve resectability. Postoperative chemotherapy should be considered for all progressive gastric cancer patients whether they have undergone curative or noncurative resection, and whether there is nodal metastasis or not. Intraoperative radiotherapy should be applied for stage two or stage three patients who are undergoing curative resection[40].

As seen in Table 1, the percent of surgery alone for treatment of gastric cancer is 67.48%, surgery plus chemotherapy and surgery plus radiotherapy account for only 1.44% and 3.29% respectively. Considering only 10% of gastric cancer patients diagnosed in hospitals are early cancer and may be treated by surgery alone, all other patients present with advanced disease should be treated by multimodality regimens such as preoperative chemotherapy, pre, intra or postoperative radiotherapy etc.

CONCLUSIONS

The advent of multimodality treatment is introduced in the last decade. Pre-operational chemotherapy can eliminate micro-metastasis and post-operational radiotherapy can kill the residual cancer cells, therefore in the future surgical resection with preoperational chemotherapy and postoperational radiotherapy should be considered to achieve better results and longer-survival periods.

REFERENCES

1 Zhou Q, Wang LD, Gao SS, Li YX, Zhao X, Wang LX. *p*53 immunostaining positive cells correlated positively with S phase cells as measured by BrdU in the esophageal precancerous lesions from the subjects at high incidence area for esophageal cancer in northern China. *World J Gastroenterol*, 1998; 4(Suppl 2):106-107

2 Zhang XY. Some recent works on diagnosis and treatment of gastric cancer. *World J Gastroentero*, 1999;5:1-3

3 Yuan Y, Gong W, Xu RT, Wang XJ, Gao H, Dong M, Wu HQ, Wang L, Wang MX, Song XJ, Wang FC, Jiang H, Song LY, Li X, Zhou BS, Zhang YC. A gastric cancer surveillance on 50 000 natural inhabitants of 16 villages and towns in Zhanghe China. *Huaren Xiaohua Zazhi*, 1998;6 (Suppl 7):478

4 Cai L, Yu SZ. A molecular epidemiologic study on gastric cancer in Changle, Fujian Province. *Shijie Huaren Xiaohua Zazhi*, 1999;7:652-655

5 Zhong YR, Ye TS. Incidence distribution of gastric,cardiac, and esophageal cancer of 1 436 cases. *Huaren Xiaohua Zazhi*, 1998;6(Suppl 7):445

6 Sherman Jr CD. Digestive carcinomas. In: Union Internationale Contre Le Cancer (UICC). Manual of clinical oncology 5. Beijing: The joint publishing house of Beijing Medical University and China. *Saint Medical University*, 1992:37-38

7 Chen KN, Xu GW. Diagnosis and treatment of esophageal cancer. *Shijie Huaren Xiaohua Zazhi*, 2000;8:196-202

8 Chen DF. Outside-radiotherapy in combination with intra-radiotherapy in the treatment of 121 cases of esophageal cancer. *Huaren Xiaohua Zazhi*, 1998;6:127

9 China Ministry Of Health. Esophageal cancer. In: China Ministry Of Health, ed. *Diagnosis and treatment criteria for common malignances in China* 2. Beijing: The joint publishing house of Beijing Medical University and China Saint Medical University, 1991:30-31

10 Zou HY, Huang GD, Liu JH, Wang M, Zheng GJ. Radiotherapy in the treatment of above-collarbone nodal metastasis in 111 cases of esophageal cancer. *Huaren Xiaohua Zazhi*, 1998;6(Suppl 7):408

11 Yin YB. Advances in radiotherapy for the treatment of esophageal cancer in China. *Huaren Xiaohua Zazhi*, 1998;6(Suppl 7):15-16

12 Wu SG, Li DB, Xin BQ, Chen JL, Wang GD. High-dose short time preoperative radiotherapy of esophageal cancer. *Huaren Xiaohua Zazhi*, 1998;6(Suppl7):421

13 Parker SL, Tong T, Bolden S, Wingo PA. Cancer statistics, 1996 (abstract). Ca Cancer J Clin, 1996;65:5-27

14 Swisher SG, Holmes EC, Hunt KK, Doty JE, Zinner MJ, McFadden DW. The role of neoadjuvant therapy in surgically resectable esophageal cancer. *Arch Surg*, 1996;131:819-825

15 Naunheim KS, Petruska PJ, Roy TS, Schlueter JM, Kim H, Baue AE. Multimodality therapy for adenocarcinoma of the esophagus. *Ann Thorac Surg*, 1995;59:1085-1091

16 Forastiere AA, Orringer MB, Perez-Tamayo C, Urba SG, Zahurak M. Preoperative chemoradiation followed by transhiatal esophagectomy for carcinoma of the esophagus: final report. *J Clin Oncol*, 1993;11:1118-1123

17 Walsh TN, Noonan N, Hollywood D. A comparision of multimodal therapy and surgery for esophageal adenocarcinoma. *N Engl J Med*, 1996;335:462-467

18 Lin CH. A new method of extensive resection for gastric carcinoma: selective type III operation. *World J Gastroenterol*, 1998;4:264-265

19 Wu XY, Zhang XF, Yin FS, Cai JC, Guan GX. Surgical treatment of residual stomach cancer with a new technique of alimentary tract reconstruction. *World J Gastroentero*, 1998;4(Suppl 2):69-70

20 Lin CH. Resection of gastric carcinoma with preservation of pancreas and clearance of lymph nodes along splenic artery: theory, technique and results. *World J Gastroentero*, 1999;5:81-83

21 Akahoshi K, Chijiiwa Y, Tanaka M, Harada N, Nawata H. Endosonography probe-guided endoscopic mucosal resection of gastric neoplasms. *Gastrointest Endosc*, 1995;42:248-252

22 Torii A, Sakai M, Kajiyama T, Kishimoto H, Kin G, Inoue K, Koizumi T, Ueda S, Okuma M. Endoscopic aspiration mucosectomy as curative endoscopic surgery: analysis of 24 cases of early gastric cancer. *Gastrointest Endosc*, 1995;42:475-479

23 Jia KL, Yang XL, Zhang JC, Ma LS, Guo TM. Advances in the study of gastric precancer diseases. *Xin Xiaohuabingxue Zazhi*, 1993;1(Suppl 1):17-19

24 Wang GT. Progress in the diagnosis and treatment of early gastric cancer. *Huaren Xiaohua Zazhi*, 1998;6(Suppl 7):62-65

25 Noguchi Y, Imada T, Matsumoto A, Coit DG, Brennan MF. Radical surgery for gastric cancer: a review of the Japanese experience. *Cancer*, 1989; 64:2053-2062

26 Roder JD, Böttcher K, Siewert JR, Busch R, Hermanek P, Meyer HJ, the German Gastric Carcinoma Study Group. Prognostic factors in gastric carcinoma: results of the german gastric carcinoma study 1992. *Cancer*, 1993;72:2089-2097

27 Zhou WQ. Endoscopic diagnosis of 506 cases of early gastric cancer. *Shijie Huaren Xiaohua Zazhi*, 1999;7:668

28 Zhuang XQ, Sun GH, Zhang YF. Value of foetal-tumorantigen, X-ray, and endoscopy in the diagnosis of early and middle gastric cancer. *Shijie Huaren Xiaohua Zazhi*, 1999;7:545-546

29 Antonioli DA. Precursors of gastric carcinoma: critical review with a brief description of early gastric cancer. *Hum Pathol*, 1994;25:994-1005

30 Gunderson LL, Sosin H. Adenocacinoma of the stomach: areas of failure in a re-operation series (second or symptomatic look): clinicopathologic correlation and implications for adjuvant therapy. *Int J Radiat Oncol Biol Phys*, 1982;8:1-11

31 Weng HR, Yang WP, Yang JS, Chen YQ, Chen YP, Yang XH. Analysis of 100 dead cases of cardiac carcinoma metastasis after operation. *Huaren Xiaohua Zazhi*, 1998;6:234-235

32 Lu DD. Survival analysis of late-staged gastric cancer patients after adjuvant chemotherapy. *Huaren Xiaohua Zazhi*, 1998;6:803

33 Yang QL, Li L, Li JQ, Guo WX. Clinical observation on the effects of reformed FAM programme in the treatment of late-staged gastric cancer. *HuarenXiaohua Zazhi*, 1998;6(Suppl 7):408

34 Lin YJ. Further improvement of therapy results for gastric cancer. *Huaren Xiaohua Zazhi*, 1998;6(Suppl 7):8-9

35 Wilker H, Preusser P, Fink U. Preoperative chemotherapy in locally advanced and nonresectable gastric cancer: a phase two study with etoposide, doxorubicin, and Cisplatin. *J Clin Oncol*, 1989;7:1318-1326

36 Kelsen D, Karpeh M, Schwartz G, Gerdes H, Lightdale C, Botet J, Lauers G, Klimstra D, Huang Y, Saltz L, Quan V, Brennan M. Neoadjuvant therapy of high-risk gastric cancer: a phase IItrial of preoperative FAMTX and postoperative intraperitoneal fluorouracil-cisplatin plus intravenous fluorouracil. *J Clin Oncol*, 1996;14: 1818-1828

37 Lowy A, Leach S, Mansfield P. Response to neoadjuvant chemotherapy best predicts survival after curative resection of gastric cancer. Presented at the society of surgical oncology 49th annual cancer symposium; Atlanta, Georgia, 1996

38 Zou SC, Qiu HS, Zhang CW, Tao HQ. A clinical and long-term follow-up study of peri-operative sequential triple therapy for gastric cancer. *World J Gastroenterol*, 2000;6:284-286

39 Abe M, Takahashi M. Intraoperative radiotherapy: the Japanese experiense. *Int J Radiat Oncol Biol Phys*, 1981;7:863-868

40 China Ministry Of Health. Gastric cancer. In: China Ministry Of Health,ed. *Diagnosis and treatment criteria for common malignances in China* 2. Beijing: The Joint Publishing House of Beijing Medical University and China Saint Medical University, 1991:52-53

Edited by Wu XN
proofread by Ma JY

P.O.Box 2345 Beijing 100023, China
Fax. 0086·10·65891893 Tel. 0086·10·65897901
E-mail.wcjd@public.bta.net.cn www.wd.org.cn

World J Gastroentero, 2001; 7(1):83 - 87
World Journal of Gastroenterology
Copyright © 2001 by the WJG Press ISSN 1007 - 9327

Effect of vitamin E succinate on expression of TGF-β_1, c-Jun and JNK1 in human gastric cancer SGC-7901 cells

Kun Wu, Bai He Liu, Dan Yang Zhao and Yan Zhao

Subject headings stomach neoplasms; apoptosis; signal transduction; vita min E; enzyme- linked immunosorbent assay; blotting, western; flow cytometry

Wu K, Liu BH, Zhao DY, Zhao Y. Effect of vita min E succinate on expression of TGF-β1, c-Jun and JNK1 in human gastric cancer SGC-7901 cells. ***World J Gastroenterol***, 2001;7(1):83-87

INTRODUCTION

Vita min E succinate (RRR-α-Tocopheryl Succinate, VES), a derivative of natural vita min E, is a compound esterified by succinic acid and 6-hydroxyl-α-tocopheryl. VES can increase the stability of á-tocopheryl and protect 6-hydroxyl from oxidation. Nowadays, this kind of vita min E has been on sale on the markets. Previous researches indicate that VES has an evident inhibitory effect on the growth of various tumor cells, but has no harm to the growth of normal cells[1-7]. The experiment *in vivo* has demonstrated that VES can cause the tumor to retrogress by regional injection[8,9]. Thus it is presumed that VES may be a potential tumor chemopreventive and chemotherapeutic agent.

Gastric cancer is one of the most common tumors in China. Up to now, most studies have focused on the preventive measures for tumors[10-13], but there has been few reports that VES inhibits the growth of gastric cancer. Our study showed that VES has an obviously inhibitory effect in the growth and DNA synthesis of human gastric cancer SGC-7901 cells[14]. The observation under electron microscope and the detection by flow cytometry and *in situ* end-labeling methods implicated that VES can induce gastric cancer cells to undergo apoptosis[15]. The exact mechanism of VES-induced growth inhibition in tumor- cells has still been unclear, but it has been reported that transforming growth factor beta (TGF-β) played a critical role in VES-induced apoptosis in tumor cells[16,17]. In addition, VES-triggered apoptosis was inhibited when c-Jun mutant was transfected into breast cancer cells[18]. The data above show that both TGF-β and c-Jun may be important factors for VES-induced apoptosis. In this study, the expression of TGF-β_1, c-Jun and c-Jun NH_2-ter minal kinase (JNK) was deter mined in SGC-7901 cells treated with VES so as to explore the mechanisms of VES-triggered apoptosis in gastric cancer cells.

MATERIALS AND METHODS

Materials

Human gastric cancer SGC-7901 cell line was obtained from the Beijing Cancer Institute and cultured in RPMI1640 medium plus 10% fetal bovine serum and routinely incubated with 5% carbon dioxide at 37℃. VES was purchased from the Sigma Corporation. Quantikine human TGF-β_1 ELISA kit was purchased from R&D Systems Company. Rabbit JNK1 polyclonal antibodies were kindly presented as a gift by Dr. Rui Hai Liu of Cornell University, USA. Rabbit c-Jun/AP_1 polyclonal antibodies were purchased from Beijing Zhongshan Biotechnical Company.

Drug treatment

VES was prepared at 5, 10 and 20mg/L by 100% ethanol. The concentration of ethanol in VES solution was adjusted to 0.1% (v/v) by 100% ethanol. Exponentially growing SGC-7901 cells were treated with VES. RPMI1640 complete condition media containing 1 μL/mL ethanol served as control.

Methods

ELISA When the cells were cultured for 12 h,18 h, 24 h and 48 h respectively, condition media was aspirated and centrifuged. The supernatant was prepared for the detection of activated TGF-β_1. Next, 500 μL culture supernatant was added into 0.1 mL 1N HCl and centrifuged for 10 min at room temperature. Then 0.1 mL 1.2N NaOH was used to neutralize the acidified samples for the detection of total TGF-β_1. Standard solution was prepared at different concentrations according to the instructions in the kit. Standard solution (200 μL per well) or activated samples were added into the 96-well plates bound with human recombinant TGF-

Department of Nutrition and Food Hygiene, School of Public Health, Harbin Medical University, Harbin 150001, Heilongjiang Province, China
Kun Wu, a professor, engaged in the study on anti-carcinogenetic nutrients in food, having more than 40 papers published.
Project supported by National Natural Science Foundation of China, No. 39870662
Correspondence to: Prof. Kun Wu, Department of Nutrition and Food Hygiene, School of Public Health, Harbin Medical University, Harbin 150001, Heilongjiang Province, China
Tel. 0086-451-3648665
Email. wukun@public.hr.hl.cn
Received 2000-07-17 **Accepted** 2000-12-17

βs RII. Then the steps proceeded as instructed. Finally, the value of optical density (OD) of each well was deter mined at 450 nm within 30 min, using a microplate reader set to 450 nm, and corrected at 540 nm.

Western blot SGC-7901 cells were harvested, decomposed on ice and centrifuged. Total protein contents in the supernatant were detected by nucleic acid and protein analyzer. Total protein (100 μg) was used for 12% SDS-PAGE electrophoresis and transferred onto nitrocellulose membrane, which was hybridized with rabbit c-Jun/AP-1 or JNK1 polyclonal antibodies (1:1000 dilution) and then with the secondary horseradish peroxidase-labeled antibody to detect the expression of c-Jun and JNK1.

RESULTS

Effects of VES on the expression of TGF-â₁ protein

Standard curve Standard curve was created by plotting the mean absorbance for each standard on the y-axis against the concentration of TGF-β_1 on the x-axis. The linear regression equation was as follows:

$$Y = -0.037+8.559\times10^{-4}\,x \qquad r = 0.9991$$

Detection of total TGF-β_1 When SGC-7901 cells were collected following VES treatment for varying time periods, the OD value of TGF-β_1 was measured by microplate reader and converted into the concentration of total TGF-β_1 according to the regression equation above. Compared with the control, the expression of total TGF-β_1 in VES-treated cells was enhanced with a dose-time effect. After 48h treatment of VES at 5, 10, and 20 mg/L, the level of total TGF-β_1 was increased by 44.8%, 92.4% and 182. 3%, respectively (Figure 1).

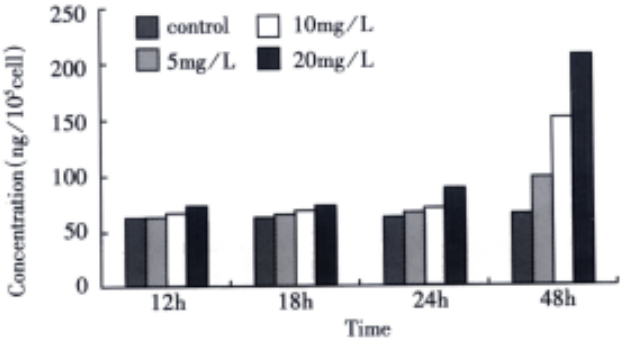

Figure 1 The effects of VES on total TGF-β_1 in SGC-7901 cells.

Detection of activated TGF-β_1 The OD value was directly measured in SGC-7901 cells harvested without acidification, and converted into the concentration of activated TGF-β_1 by means of the equation above. In comparison with the control, VES-treated cells exhibited increased level of activated TGF-β_1 in a dose-dependent manner. When the cells were treated with VES at 10 mg/L for 48 h and at 20 mg/L for 24 h and 48 h, the expression of activated TGF-β_1 was increased by 130.9%, 115.8% and 559.6%, respectively (Figure 2).

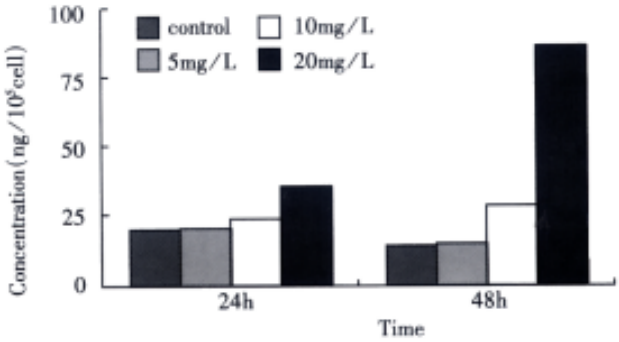

Figure 2 The effects of VES on the expression of active TGF-β_1 in SGC-7901 cells.

Effects of VES on c-Jun expression

The transferred filter membrane was hybridized with rabbit c-Jun/AP-1 polyclonal antibodies, then with the secondary antibody, colorated with DAB and imaged by digital imaging maker (Figures 3 and 4). From Figure 3, it can be seen that VES-treated SGC-7901 cells at 10 mg/L for 3 h exhibited evidently increased level of c-Jun protein. It was in a high state within 24 h and began to decrease after 24 h. Figure 4 indicates that the expression of c-Jun in VES-treated SGC-7901 cells at different concentrations at the same time was increased with a significant dose-effect relationship.

Effects of VES on JNK1 expression

The procedure was similar to that for c-Jun (Figures 5 and 6). Figure 5 shows that when SGC-7901 cells were treated with VES at 10 mg/L for 3 h, the expression of JNK1 was obviously promoted and further promotion occurred with the lapse of time within 24 h. Figure 6 implicates that the level of JNK1 expression was different in VES treated SGC-7901 cells at different concentrations at the same time. Compared with the control, the expression of JNK1 was evidently elevated in a dose-dependent manner.

Figure 3 The expression of c-Jun in VES treated SGC-7901 cells at 10 mg/L for different time.
A. Protein marker; B. VES treatment for 0 h; C. VES treatment for 3 h; D. VES treatment for 6 h; E. VES-treatment for 12 h; F. VES treatment for 24 h; G. VES- treatment for 48 h.

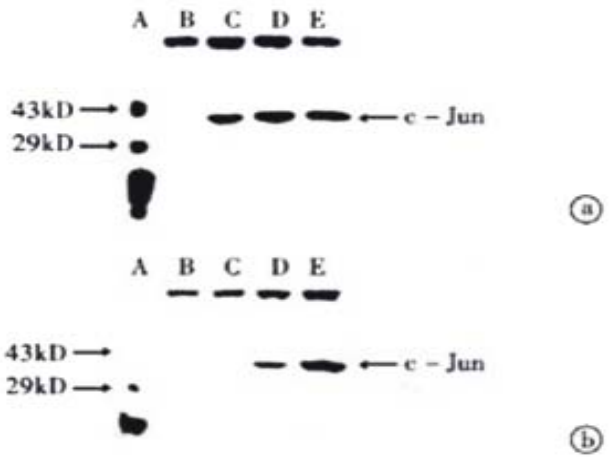

Figure 4 The expression of c-Jun in VES-treated SGC-7901 cells.
(**a**) VES-treated SGC-7901 cells for 24 h; (b) VES-treated SGC-7901 cells for 48 h.
A. Protein marker; B. Control; C. VES at 5 mg/L; D. VES at 10 mg/L; E. VES at 20 mg/L.

Figure 5 The expression of JNK1 in VES-treated SGC-7901 cells at 10 mg/L for different time points.
A. Protein marker; B. VES- treatment for 0 h; C. VES treatment for 3 h; D. VES treatment for 6 h; E. VES treatment for 12 h; F. VES treatment for 24 h; G. VES treatment for 48 h.

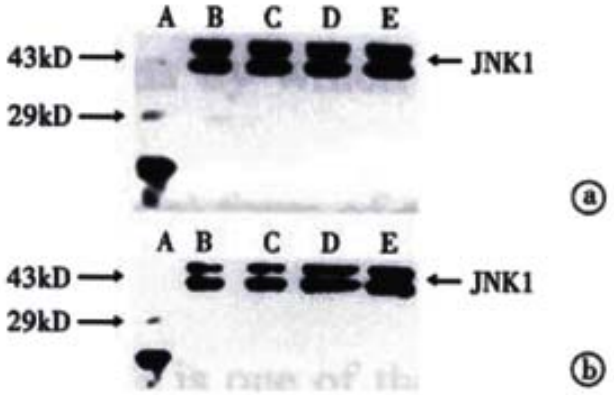

Figure 6 The expression of JNK1 in VES-treated SGC-7901 cells.
(**a**) VES-treated SGC-7901 cells for 24 h; (b) VES-treated SGC-7901 cells for 48 h.
A. Protein marker; B. Control; C. VES at 5 mg/L; D. VES at 10 mg/L; E. VES at 20 mg/L.

DISCUSSION

Previous researches showed that induction of apoptosis in tumor cells is one of the important mechanisms by which VES inhibits tumor cell growth[15,19]. Apoptosis is the most common physiological form of cell death and occurs-during embryonic development, tissue remodeling, immune regulation and tumor regression. Thus, initiation of apoptotic signal pathway and induction of apoptosis in tumor cells will be an effective approach for treating tumors[20-23]. Apoptosis is controlled by genes. Now hundreds of regulatory factors have been identified. These factors form many apoptotic signal transduction pathways which are complex[24-28]. In this study, several apoptosis-related proteins were deter mined to investigate the possible pathways involved in VES-induced apoptosis of human gastric cancer SGC-7901 cells.

Transfor ming growth factor (TGF) is a large family of multifunctional cytokines which can regulate cell proliferation, differentiation and death[29-31]. It has been proved that TGF-β, a latent inhibitor of epidermal proliferation, plays a role in the inhibition of more than three quarters of human primary tumors (such as breast cancer[32,33], prostatic carcinoma[34], lung cancer[35,36], colic carcinoma[37] and liver cancer[38,39]). Inhibition of the activation of latent TGF-β, down-regulation or loss of the expression of TGF-β receptors and deficiency of important elements responsible for cellular message transmitting pathway cause tumor cells to escape the growth inhibition of TGF-β, resulting in cancer [40-42]. Yu *et al*[43] found that VES can improve the secretion of activated TGF-β_1 and induce apoptosis in human breast cancer MDA-MB-435 cells. When TGF-β antibody neutralization assay was applied or antisense TGF-βRII oligonucleotide was transfected into breast cancer cells, the ability of VES-induced apoptosis was blocked by 50%, which implicated that the increase of TGF-β expression was related to induction of tumor cell-undergoing apoptosis. In our study, activated TGF-β_1 was directly measured with the kit in VES-treated SGC-7901 cells and its expression was distinctly increased; yet total TGF-β_1 was detected when the samples were acidified and its expression was also clearly promoted. These facts suggested that VES can induce not only the activation of active TGF-β_1 but also an increased secretion of latent TGF-β_1. Latent TGF-β_1 is released from cells into media and activated by some enzyme outside the cell membrane.

c-Jun is an early and transient gene[44] and its response to many kinds of stimuli is rapid and transient. The expression of c-Jun can be enhanced and prolonged by many stress stimuli such as ultraviolet, irradiation, hydrogen peroxide, tumor necrosis factor α and other apoptosis-triggering factors[45,46]. As mentioned above, VES-induced apoptosis rate was obviously decreased when human breast cancer cells were transfected with antisense c-Jun oligonucleotide or c-Jun mutant[18]. Our results showed that the expression of c-Jun was elevated and prolonged in VES-treated SGC-7901 cells (usually the expression of c-Jun only lasted 3 h-4 h or even shorter), indicating that c-Jun was also involved in apoptosis of VES-treated SGC-7901

cells.

It is reported that the mainly biological roles of c-Jun are the induction of cell cycle arrest and apoptosis [47-49]. JNK can directly bind with transcription factor c-Jun and activate c-Jun through phosphorylation of serine 63/73, suggesting that the activation of JNK is the upstream events involved in phosphorylation of c-Jun. It is also known that JNK belongs to mitogen-activated protein kinases (MAPK) family whose activation can be evidently affected by TGF-β, which shows that the activation of JNK can be possibly influenced by TGF-β[50-52]. These data suggest that JNK may be involved in VES-mediated apoptosis in tumor cells. In our study, the expression of JNK protein in VES-treated SGC-7901 cells was obviously increased with a dose-dependent relationship. Therefore, we suspect that JNK1 may be involved in apoptotic signal transduction similar to TGF-β_1 and c-Jun. When SGC-7901 cells were treated with VES, the secretion and activation of TGF-β were improved, TGF-β increased the activity of JNK, JNK caused the phosphorylation of c-Jun, and finally activated c-Jun triggered apoptosis in tumor cells.

Although we presumed a signal pathway responsible for VES-induced apoptosis in SGC-7901 cells, several interrelated pathways may trigger apoptosis simultaneously owing to the fact that the mechanisms of apoptosis are complicated and precisely regulated. So the observation that the expression of these three proteins is increased is only the preli minary survey on VES. With the development of molecular biological technology, if the strategies that a point in designed signal pathway is "knockout" by different means and then the blockage of downstream events is observed can be carried out, it will be critical for further studies on the mechanisms of VES-mediated growth inhibition in tumor cells.

ACKNOWLEDGEMENTS We would like to thank Dr. Wei Ping Yu, Genetics Institute, Texas University of USA, for the technical assistance.

REFERENCES

1 Turley JM, Sanders BG, Kline K. RRR-α-tocopheryl succinate modulation of human promyelocytic leukemia (HL-60) cell proliferation and differentiation. *Nutr Cancer*, 1992;18:201-203

2 Fariss MW, Fortuna MB, Everett CK, Smith JD, Trent DF, Djuric Z. The selective antiproliferative effects of α–tocopheryl hemisuccinate and cholesteryl hemisuccinate on murine leukemia cells result from the action of the intact compounds. *Cancer Res*, 1994;54:3346-3351

3 Yu WP, Israel K, Liao QY, Aldaz CM, Sanders BG, Kline K. Vita min E succinate (VES) induces Fas sensitivity in human breast cancer cells: role for Ma-r 43000 Fas in VES-triggered apoptosis. *Cancer Res*, 1999;59:953-961

4 Turley JM, Ruscetti FW, Kim SJ, Fu T, Gou FV, Birchenall-Roberts MC. Vita minE succinate inhibits proliferation of BT-20 human breast cancer cells: increased binding of cyclin A negatively regulates E2F transactivation activity. *Cancer Res*, 1997;57:2668-2675

5 Ottino P, Duncan JR. Effect of α-tocopheryl succinate on free radical and lipid peroxidation levels in BL6 melanoma cells. *Free Radical Biol Med*, 1997;22:1145-1151

6 Kim SJ, Bang OS, Lee YS, Kang SS. Production of inducible nitric oxide is required for monocytic differentiation of U937 cells induced by vita min E-succinate. *J Cell Sci*, 1998;111:435-441

7 Turley JM, Fu T, Ruscetti FW, Mikovits JA, Bertolette III DC, Birchenall-Roberts MC. Vita min E succinate induces Fas-mediated apoptosis in estrogen receptor-negative human breast cancer cells. *Cancer Res*, 1997;57:881-890

8 Schwartz J, Shklar G. The selective cytotoxic effect of carotenoids and -tocopherol on human cancer cell lines *in vitro*. *J Oral Maxillofac Surg*, 1992;50:367-373

9 Malafa MP, Neitzel LT. Vita min E succinate promotes breast cancer tumor dormancy. *J Surg Res*, 2000;93:163-170

10 Fang DC, Liu WW. Expression of Span-1 and Ypan-1 in gastric cancer and subtypes of intestinal metaplasia. *China Natl J New Gastroenterol*, 1995;1:9-12

11 Ma LS, Pan BR. Strengthen international academic exchange and promote development of gastroenterology. *World J Gastroenterol*, 1998;4:1

12 Li XG, Xie JY, Lu YY. Suppressive action of garlic oil on growth and differentiation of human gastric cancer cell line BGC-823. *Huaren Xiaohua Zazhi*, 1998;6:10-12

13 Zou SC, Qiu HS, Zhang CW, Tao HQ. A clinical and long-term follow-up study of peri-operative sequential triple therapy for gastric cancer. *World J Gastroentero*, 2000;6:284-286

14 Liu BH, Wu K. Study on the growth inhibition of vita min E succinate in human gastric cancer cell. *AibianQibianTubian*, 2000; 12:79-81

15 Wu K, Guo J, Shan YJ, Liu BH. The effects of vita min E succinate on apoptosis in human gastric cancer. *Weisheng Dulixue Zazhi*, 1999;13:84-90

16 Simmons-Menchaca M, Qian M, Yu WP, Sanders BG, Kline K. RRR-α-tocopheryl succinate inhibits DNA synthesis and enhances the production and secretion of biologically active transfor ming growth factor-β by avian retrovirus-transformed lymphoid cells. *Nutr Cancer*, 1995;24:171-185

17 Ariazi EA, Satomi Y, Ellis MJ, Haag JD, Shi WG, Sattler CA, Gould MN. Activation of the transfor ming growth factor β signaling pathway and induction of cytostasis and apoptosis in mammary carcinomas treated with the anticancer agent perillyl alcohol. *Cancer Res*, 1999;59:1917-1928

18 Yu WP, Simmons-Menchaca M, You HH, Brown P, Birrer MJ, Sanders BG, Kline K. RRR -α-tocopheryl succinate induction of prolonged activation of c-jun a mino-ter minal kinase and c-jun during lnduction of apoptosis in human MDA-MB-435 breast cancer cells. *Mol Carcinog*, 1998;22:247-257

19 Wu K,Ren Y,Guo J.The effects of vita min E succinate on the cyclin regulation protein of human gastric cancer cell. *Weisheng Dulixue Zazhi*, 1998;12:203-207

20 Green DR, Reed JC. Mitochondria and apoptosis. *Science*, 1998; 281:1309-1312

21 Liu HF, Liu WW, Fang DC, Men RP. Relationship between Fas antigen expression and apoptosis in human gastric carcinoma and adjacent noncancerous tissues. *Huaren Xiaohua Zazhi*, 1998;6: 321-322

22 Vaux DL, Korsmeyer SJ. *Cell death in development*. Cell, 1999; 96:245-254

23 Xu HY, Yang YL, Guan XL, Song G, Jiang AM, Shi LJ. Expression of regulating apoptosis gene and apoptosis index in primary liver cancer. *World J Gastroenterol*, 2000;6:721-724

24 Thompson CB. Apoptosis in the pathogenesis and treatment of disease. *Science*, 1995;267:1456-1462

25 Yang WC, Wang LD. The mechanisms of cell proliferation control by tumor inhibitory genes and oncogenes. *Xin Xiaohuabingxue Zazhi*, 1997;5:262-263

26 Kroemer G, Zamzami N, Susin SA. Mitochondrial control of apoptosis. *Immunol Today*, 1997;18:44-51

27 Aravind L, Dixit VM, Koonin EV. The domains of death: evolution of the apoptosis machinery. *TIBS*, 1999;24:47-53

28 Sun BH, Zhao XP, Wang BJ, Yang DL, Hao LJ. FADD and TRADD expression and apoptosis in primary human hepatocellular carcinoma. *World J Gastroenterol*, 2000;6:223-227

29 Koff A, Ohtsuki M, Polyak K, Roberts JM, Massague J. Negative regulation of G1 in mammalian cells inhibition of cyclin E-dependent kinase by TGF-β. *Science*, 1993;260:536-539

30 Hu PPC, Datto MB, Wang XF. Molecular mechanisms of transfor ming growthfactor-β signaling. *Endocrine Rev*, 1998;19:349-363

31 Yang YH, Fu XB, Sun TZ, Jiang LX, Gu XM. bFGF and TGFβ expression in rat kidneys after ischemic/reperfusional gut injury and its relationship with tissue repair. *World J Gastroenterol*, 2000;6:147-149

32 Butta A, MacLennan K, Flanders KC, Sacks NPM, Smith I, McKinna A, Dowsett M, Wakefield LM, Sporn MB, Baum M, Colletta AA. Induction of transfor ming growth factor β_1 in human breast cancer *in vivo* following tamoxifen treatment. *Cancer Res*, 1992;52:4261-4264

33 Erbas H, Lai LC. Effect of transfor ming growth factor β_2 on oestrogen metabolism in the MCF-7 breast cancer cell line. *J Clin Pathol*, 2000;53:322-324

34 Guo YP, Kyprianou N. Restoration of transfor ming growth factor β signaling pathway in human prostate cancer cells suppresses tumorigenicity via inducation of caspase-1-mediated apoptosis. *Cancer Res*, 1999;59:1366-1371

35 Yang YH, Fu XB, Sun TZ, Jiang LX. bFGF and TGFβ mRNA expression in liver and lungs following intestinal ischemia-reperfusion injury in rats. *Huaren Xiaohua Zazhi*, 1998;6:850-852

36 Fu XB, Yang YH, Sun TZ, Gu XM, Jiang LX, Sun XQ, Sheng ZY. Effect of intestinal ischemia-reperfusion on expressions of endogenous basic fibroblast growth factor and transfor ming growth factor β in lung and its relation with lung repair. *World J Gastroenterol*, 2000;6:353-355

37 Engle SJ, Hoying JB, Boivin GP, Ormsby I, Gartside PS, Doetschman T.Transfor ming growth factor β_1 suppresses nonmetastatic colon cancer at an early stage of tumorigenesis. *Cancer Res*, 1999;59:3379-3386

38 He FY, Zheng YL, Wang Y, Liu SX, Wang ZZ. Clinical significance of TGF-β_1 and PCNA expression in primary human hepatocarcinoma tissues. *Huaren Xiaohua Zazhi*, 1998;6(Suppl 7):165-166

39 Huang YX, Zhang GX, Lu MS, Fan GR, Chen NL, Wu GH. Increased expression of transfor ming growth factor-β_1 in hepatocellular carcinoma. *Shijie Huaren Xiaohua Zazhi*, 1999;7:150-152

40 Hayashi H, Abdollah S, Qiu YB, Cai JX, Xu YY, Grinnell BW, Richardson MA, Topper JN, Gimbrone MA Jr, Wrana JL, Falb D. The MDA-related protein smad7 associates with the TGF-β receptor and functions as an antagonist of TGFβ signaling. *Cell*, 1997;89:1165-1173

41 Deng DH, Luo JY, Zhu HH, Li DL, Wang KM. The expression of TGF-β_1 in squamous oesophagus cancer and heteroproliferation. *Xin Xiaohuabingxue Zazhi*, 1997;5:465

42 Zhuang ZH, Chen YL, Wang CD, Chen YG. Expressions of TGF-β1 and TGF-β receptor I in gastric carcinoma and precancerous lesions. *Shijie Huaren Xiaohua Zazhi*, 1999;7:507-509

43 Kline K, Yu WP, Sanders BG. Vita min E: mechanisms of action as tumor cell growth inhibitors. In: Prasad KN, Cole WC (eds), *Cancer and Nutrition*. Amsterdam: IOS press, 1998:37-53

44 Meyer-ter-Vehn T, Covacci A, Kist M, Pahl HL. Helicobacter pylori activates mitogen-activated protein kinase cascades and induces expression of the proto-oncogenes c-fos and c-jun. *J Biol Chem*, 2000;275:16064-16072

45 Tchou WW, Yie TA, Tan TH, Rom WN, Tchou-Wong KM. Role of c-Jun N-ter minal kinase 1 (JNK1) in cell cycle checkpoint activated by the protease inhibitor N-acetyl-leucinyl-leucinyl-norleucinal. *Oncogene*, 1999;18:6974-6980

46 Amato SF, Swart JM, Berg M, Wanebo HJ, Mehta SR, Chiles TC. Transient stimulation of the c-Jun-NH_2-Ter minal kinase/activator protein 1 pathway and inhibition of extracellular signal-regulated kinase are early effects in paclitaxel-mediated apoptosis in human B lymphoblasts. *Cancer Res*, 1998;58:241-247

47 Kyrlakls JM, Banerjee P, Nikolakakl E, Dal T, Ruble EA, Ahmad MF,Avruch J, Woodgett JR. The stress-activated protein kinase subfamily of c-Jun kinases. *Nature*, 1994;369:156-160

48 Leppa S, Böhmann D. Diverse functions of JNK signaling and c-Jun in stress response and apoptosis. *Oncogene*, 1999;18:6158-6162

49 Jiang LX, Fu XB, Sun TZ, Yang YH, Gu XM. Relationship between oncogene c-jun activation and fibroblast growth factor receptor expression of ischemia-reperfusion intestine in rats. *Shijie Huaren Xiaohua Zazhi*, 1999;7:498-500

50 Yamaguchi K, Shirakabe K, Shibuya H, Irie K, Oishi I, Ueno N, Taniguchi T, Nishida E, Matsumoto K. Identification of a member of the MAPKKK family as a potential mediator of TGF-β signal transduction. *Science*, 1995;270:2008-2011

51 Shibuya H, Yamaguchi K, Shirakabe K, Tonegawa A, Gotoh Y, Ueno N, Irie K, Nishida E, Matsumoto K. TAB1: an activator of the TAK1 MAPKKK in TGF-β signal transduction. *Science*, 1996; 272:1179-1182

52 Ricos MG, Harden N, Sem KP, Lim L, Chia W. Dcdc42 acts in TGF-β signaling during Drosophila morphogenesis: distinct roles for the Drac1/JNK and Dcdc42/TGF-β cascades in cytoskeletal regulation. *J Cell Sci*, 1999;112:1225-1235

Edited by Ma JY

P.O.Box 2345 Beijing 100023, China
Fax. 0086·10·65891893 Tel. 0086·10·65897901
E-mail.wcjd@public.bta.net.cn www.wd.org.cn

World J Gastroentero, 2001; 7(1):88 - 92
World Journal of Gastroenterology
Copyright © 2001 by the WJG Press ISSN 1007 - 9327

Relationship between Fas/FasL expression and apoptosis of colon adenocarcinoma cell lines

Zhi Hai Peng, Tong Hai Xing, Guo Qiang Qiu and Hua Mei Tang

Subject headings colonic neoplasms/drug therapy; apoptosis; cisplatin/therapeutic use; mitomycins/therapeutic use; fluorouracil/therapeutic use; epirubicin/therapeutic use; flow cytometry

Peng ZH, Xing TH, Qiu GQ, Tang HM. Relationship between Fas/FasL expression and apoptosis of colon adenocarcinoma cell lines. ***World J Gastroentero***, 2001;7(1):88-92

INTRODUCTION

Fas/FasL system has been identified as a key mediator of apoptosis in tumor cells[1-4]. The occurrence and development of neoplasm are closely related to apoptosis [5-7]. Most chemotherapeutic drugs kill cancer cells mainly by inducing apoptosis[8-14]. We determined the Fas/FasL expression and apoptosis of colon adenocarcinoma cell lines induced by chemotherapeutic drugs with flow cytometry (FACScan), and studied the relation ship between Fas/FasL expression and apoptosis of colon adenocarcinoma cell lines for selection of sensitive chemotherapeutic drugs and appropriate dosage.

MATERIAL AND METHODS

Cell lines and cell culture

Colon adenocarcinoma cell lines (LS174-T cells and LoVo cells, provided by the Cell Bank of Chinese Academy of Sciences) were cultured in RPMI 1640 medium at 37℃ in a humidified 5% CO_2 atmosphere. Cells were seeded at a concentration of 1×10^6/well in 6-well plates and incubated at 37℃ in a humidified 5% CO_2 atmosphere overnight to ensure that the cells adhere to the walls, then chemotherapeutic drug of various concentrations was added and incubated again for 24 h or 48h.

Treatment with chemotherapeutic drugs

Different cell lines were treated with Cisplatin (CDDP), Mitomycin (MMC), 5-fluorouracil (5-FU) and epirubicin Hydrochloride (EPH) at concentrations of plasma peak concentration (PPC), 1/10 PPC, 1/5 PPC, 5 PPC and 10 PPC for 24 h and 48 h. The PPC of CDDP, MMC, 5-FU, EPH was 3 mg/L, 3 mg/L, 10 mg/L and 0.6 mg/L[5].

Apparatus and reagent

EPHCS-XL FACScan was purchased from Coulter Co. of America. Annexin-V-Fluos labeling reagent for identifying apoptosis was purchased from Boehringer Mannheim Co., and reagent for identifying Fas/FasL expression was purchased from Pharmingen Co..

Determination of apoptosis and Fas/FasL expression

Early apoptotic changes were identified using Annexin-V-Fluos, which binds to phosphati dylserine on the outer leaflet of apoptotic cell membranes. Propidium iodide was used for the discrimination of necrotic cells from the annexin V positively stained cell cluster. Cells were trypsinized, washed with PBS twice, centrifuged at 200×g for 5 min, and resuspended in 100mL Annexin-V-Fluos labeling solution containing Annexin-V-Fluos reagent and propidium iodide. Cells were incubated for 10-15 min and analyzed on FACScan. Percentage of apoptosis = 100% [experimental apoptosis (%)-spontaneous apoptosis in medium (%)]/[100%-spontaneous apoptosis in medium (%)][16]. For determination of Fas expression, cells were stained with anti-Fas IgG1 monoclonal antibody (mAb 1 g/mL) for 45 min at 4℃ followed by rat anti-mouse IgG1-FITC for 30min at 4℃. FII23 IgG3 antibody was used as isotype-matched antibody to control non-specific binding. For determination of FasL expression, cells were stained with FITC-conjugated rat anti-FasL mAb for 45 min at 4℃ followed by goat anti-mouse Igs-biotinylated. Rat IgG2a antibody was used as isotype-matched control antibody. Fas/FasL expression was assessed by FACScan. Fas expression = (%Fas + treated cells - %IgG1 - FITC + treated cells) - (%Fas + control cells - %IgG1 - FITC + control cells)[16]. FasL expression was calculated according to the formula as that of Fas expression. Cells were analyzed by FACScan using Cell Quest software.

DNA extration and gel electrophoresis

LS174T cells and LoVo cells of colon adenocarcinoma cell lines were added to 6-well culture plates at a concentration of 1×10^6/mL.

Supported by the Health Committee of Shanghai
Correspondence to: Dr. Zhi Hai Peng, Shanghai No.1 People's Hospital, 85 Wujin Road, Shanghai 200080, China
Tel. 0086-21-63240090 Ext.3102, Fax. 0086-21-63240825
Email. pengpzhb@online.sh.cn
Received 2000-09-18 **Accepted** 2000-09-29

Cell cultures without treatment, or with treatment at different PPC of above chemotherapeutic drugs were harvested from the culture plates after 24 h or 48 h, washed twice with PBS (pH 7.4), and moved to the micro-centrifuging tube. Cells were pelleted at 300×*g* and the medium was removed by aspiration. Cell pellets were resuspended in 100 mL lysis buffer and incubated at 50℃ for 1 h, then mixed with 10 μL RNase and incubated at 50℃ for another 1 h. The DNA was resuspended in sample buffer and quantified by absorbance at 260 nm. Ten micrograms of DNA was applied to a 1.5% agarose gel in TBE buffer and resolved at 75 mA constant current for 2 h. The DNA was then visualized by ethidium bromide staining for 5 min and washed twice with distilled water. The result was observed under ultraviolet radiation (Figures 5 and 6).

Statistical analysis

Fas expression FasL expression and apoptosis percentage of each treated group were compared and checked with *F* test, and their relationship was analyzed.

RESULTS

The drug concentrations of CDDP, MMC, 5-Fu and EPH ranged between 1/10 PPC and 10 PPC[15], among which we set 1/5 PPC, PPC, and 5 PPC[17]. We treated LS174T cells and LoVo cells with chemotherapeutic drugs fo 24 h and 48 h respectively, and detected apoptosis and Fas/FasL expression with FACScan.

In untreated control group of LS174T cells, Fas expression, FasL expression and apoptosis percentage was 0.5%, 1.5% and 2.8% separately. The percentage in those treated with chemotherapeutic drug for 24 h was similar in that treated for 48 h, but figures were lower. LS174T cells treated with chemotherapeutic drugs for 48 h showed that Fas expression was upregulated when drug concentration was below 1/5 PPC or at PPC, and downregulated when drug concentration was above 1/5 PPC or at PPC (Figure 1). FasL expression was upregulated obviously when drug concentration was above PPC (Figure 2). When drug concentration of CDDP, MMC and EPH was below 1/5 PPC or PPC, apoptosis was upregulated, and downregulated at a concentration above 1/5 PPC or PPC. Apoptosis of 5-Fu group cells was upregulated with increase of drug concentration. Apoptosis in various drug concentrations in each group is shown in Figure 3.

We did not detect Fas expression of LoVo cells treated with chemotherapeutic drugs for 24 h. FasL expression was lower than that of LS174T cells. Apoptosis of 5-Fu group was upregulated with ascending drug concentration which was 54.8% when drug concentration was 10PPC. The effect of apoptosis induced by 5-Fu was the best while that induced by EPH was the worst. The results were just opposite to the results in LS174T cells. Apoptosis of CDDP group and MMC group were downregulated with ascending drug concentration (Figure 4). We could not detect Fas expression or FasL expression of LoVo cells treated with chemotherapeutic drugs for 48 h. Necrosis was found mainly in LoVo cells, apoptosis of which was lower than that of the control group.

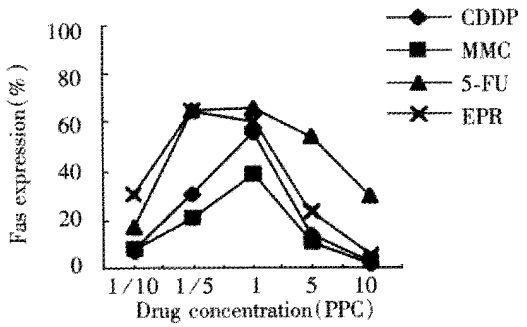

Figure 1 Fas expression of LS174T cells treated with chemotherapy drugs for 48 h.

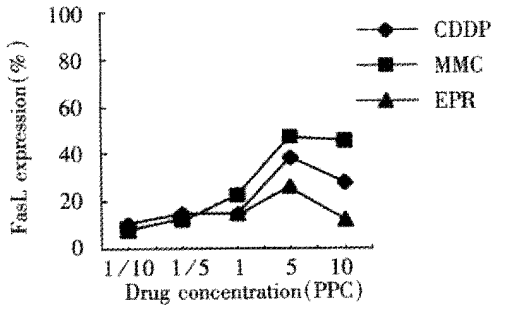

Figure 2 FasL expression of LS174T cells treated with chemotherapy drugs for 48 h.

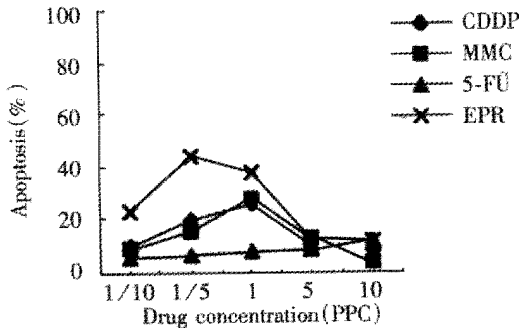

Figure 3 Apoptosis of LS174T cells treated with chemotherapy drugs for 48 h.

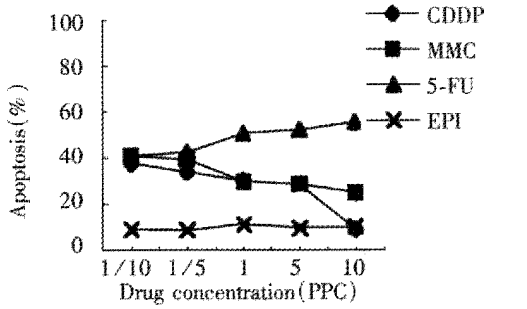

Figure 4 Apoptosis of LoVo cells treated with chemotherapy drugs for 24 h.

We abstracted DNA from the control group of cell lines and the group treated with chemotherapeutic drugs of various concentrations for 24 h and 48 h, and examined DNA ladder by agarose gel electrophoresis. The result showed that DNA ladder was remarkable in the treated group of LS174T cells when drug concentration of CDDP, MMC and EPH was 1/5 PPC or PPC, and 5-Fu concentration was 10 PPC. DNA ladder was remarkable in the treated LoVo cells when CDDP, and MMC concentration was 1/10 PPC, and 5-Fu concentration was 10PPC.There was no obvious difference among the DNA ladders at any concentration of EPH (Figures 5, 6).

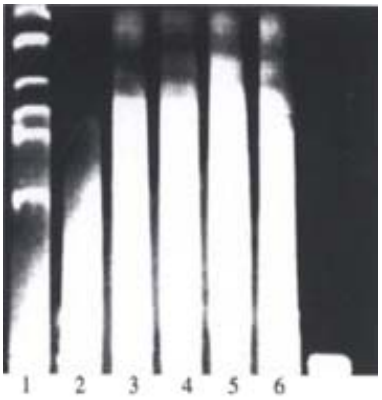

Figure 5 DNA ladder LS174T cells treated with chemotherapy drugs for 48h (1. Markers; 2. The control group; 3. 5-Fu; 4. DDP; 5. EPI; 6. MMC).

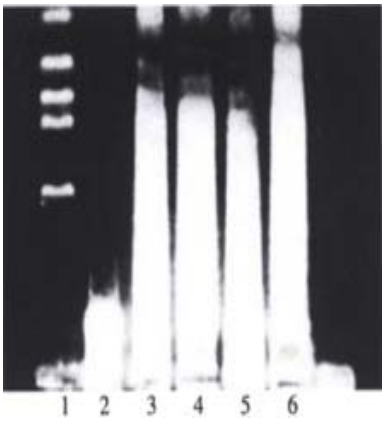

Figure 6 DNA ladder of LoVo cells treated with chemotherapy drugs for 24 h (1. Markers; 2. The control group; 3. 5-Fu; 4. DDP; 5. EPI; 6. MMC).

DISCUSSION

Fas is a 45 kDa type I transmembrane receptor expressed by a variety of normal and neoplastic cells. It belongs to the tumor necrosis factor (TNF) receptor family. When there is no antagonistic factor in the induction of apoptosis, apoptosis of chemosensitive tumor cells is induced following cross-linking of agonistic anti-Fas antibody or FasL with functional Fas expressed by tumor cells. Chemotherapeutic drug could induce tumor cells, which did not express or weakly expressed Fas, to strongly express functional Fas. Our data by FACScan showed that the Fas expression of LS174T cells untreated with chemotherapeutic drugs was only 0.5%, but compared with the Fas expression of the control cells, the Fas expression of LS174T cells treated with CDDP, MMC, 5-Fu and EPH for 48 h was notably upregulated. Fas expression of each treated group reached its peak at 1/5 PPC or PPC, which proved that the appropriate selection of chemotherapeutic drug concentration could effectively induce functional Fas to be strongly expressed on the surface of tumor cells.

In LS174T cells, apoptosis induced by CDDP, MMC and EPH was closely related to Fas-expression. Fas expression of the four LS174T cell groups treated with chemotherapeutic drugs for 48 h and apoptosis reached their peak at 1/5PPC or PPC. Fas expression was downregulated with chemotherapeutic ascending, drug concentration, so was apoptosis. The results of DNA fragmentation studies showed that the DNA ladder was most visible when the concentration of CDDP, MMC and EPH was 1/5 PPC or PPC. Fas expression and apoptosis of CDDP, MMC and EPH groups were positively correlated by relativity analysis ($P<0.05$). In LS174T cells, Fas expression induced by EPH was most notable and apoptosis of this group was the highest of all. There was statistical significance in Fas expression and apoptosis between EPH and CDDP or MMC groups ($P<0.05$). The above data and analysis suggest that kinetics of cell apoptosis correspond to kinetics of Fas induction. We could find the hypersensitive drugs and their appropriate dosage according to apoptosis and functional Fas expression. The different apoptosis paths between LS174T cells and LoVo cells demonstrated the importance of individualized selection of chemotherapeutic drugs.

After treatment with 5-Fu, Fas expression of LS174T cells was remarkablely upregulated while apoptosis was the lowest of all. On the contrary, the anti-tumor effect of 5-Fu on digestive tract tumor is the best among the clinical chemotherapeutic drugs. This contradiction, we believed, may be caused by the different effects between *in vitro* experiment and *in vivo* treatment. *in vitro*, FasL expression of LS174T cells induced by 5-Fu was too low to effectively activate the Fas system and trigger the apoptosis cascade; *in vivo*, FasL expressed strongly on the surface of CTL or NK could mediate autocrine or paracrine chemosensitive cell death by crossing its cognate receptor. This may be the reason why the 5-Fu had best anti-tumor effect in digestive tract tumor. Our study also showed that apoptosis induced by 5-Fu increased with the concentration, which was different from other drugs used in this research.

In LS174T cells, the FasL expression of CDDP,

MMC and EPH groups reached its peak at 5PPC, and there was no significant correlation between FasL expression and apoptosis of each group (P>0.05). FasL was upregulated on the tumor surface upon drug incubation in chemosensitive tumor cells and tumor cells could mediate autocrine or paracrine to release soluble FasL (sFasL). Apoptosis could occur in tumor cells expressing FasL through suicide or fratricide, inducing Fas-mediated apoptosis of peripheral normal cells, CTL and NK which express Fas, to promote local tumor invasion or metastases [18]. Therefore, drug-induced expression of FasL in Fas-negative tumors is not effective and, could result in selective elimination of antitumor lymphocytes. The incorrect chemotherapy could cause drug resistance or immune privilege of tumor cells[19]. Therefore, the induction of FasL by chemotherapeutic drug has dual effects on tumor therapy.

FACScan determination showed that LoVo cells treated with chemotherapeutic drug did not express Fas, weakly expressed FasL, and there was no significant correlation between Fas expression and apoptosis in LoVo cells (P>0.05). However, DNA ladder of LoVo cells treated with chemotherapeutic drug was similar to that of LS174T cells, suggesting that drug-induced apoptosis of LoVo cells did not depend on FasL/Fas interaction. Drug might kill tumor cells through activating other death receptors or directly acting on the downstream factor of Fas system (such as caspases family, etc.), also might trigger apoptosis in another way[20-28]. Nita *et al*[29] used equitoxic (IC50%) doses of 5-Fu to induce apoptosis in LoVo cells and analysed Bcl-2, Bcl-XL, Bax, Bad, Bak and p53 protein expression of LoVo cells by Western blotting, and found that Bcl-XL was expressed in all the cell lines and accompanied by increased expression of Bax and Bak. We are doing further studies to find out whether the ratio of Bcl-XL to Bax is correlated with chemosensitivity of LoVo cells treated with 5-Fu.

The determination of Fas expression, FasL expression and apoptosis of tumor cells treated with chemotherapeutic drug by FACScan indicated that the induction of Fas expression and apoptosis by major chemotherapeutic drugs was the best at the concentration of PPC or below PPC. DNA ladder also proved that the selection of appropriate dosage was of great importance in chemotherapy [30-41]. We could find hypersensitive drugs and their appropriate dosage according to apoptosis determined by FACScan, partly according to Fas expression. The different apoptosis paths between LS174T cells and LoVo cells demonstrated the importance of individualized selection of chemotherapeutic drugs.

REFERENCES

1 Liu HF, Liu WW, Fang DC, Men RP. Relationship between Fas antigen expression and apoptosis in human gastric carcinoma and adjacent noncancerous tissues. *Huaren Xiaohua Zazhi*, 1998;6: 321-322

2 Wei HS, Li DG, Lu HM. Hepatic cell apoptosis and fas gene. *Shijie Huaren Xiaohua Zazhi*, 1999;7:531-532

3 Liu HF, Liu WW, Fang DC, Men RF, Wang ZH. Apoptosis and its relationship with Fas ligand expression in gastric carcinoma and its precancerous lesion. *Shijie Huaren Xiaohua Zazhi*, 1999;7: 561-563

4 Liu HF, Liu WW, Fang DC. Induction of apoptosis in human gastric carcinoma cell line SGC-7901 by anti-Fas monoclonal antibody. *Shijie Huaren Xiaohua Zazhi*, 1999;7:476-478

5 Liu HF, Liu WW, Fang DC. Study of the relationship between apoptosis and proliferation in gastric carcinoma and its precancerous lesion. *Shijie Huaren Xiaohua Zazhi*, 1999;7:649-651

6 Pan CJ, Zhong P, Huang XR, Liu KY, Wang SX. Study on the correlation between proliferation and apoptosis in atrophy and intestinal metaplasia of gastric mucosa. *Shijie Huaren Xiaohua Zazhi*, 2000;8:143-146

7 Wang LS, Pan LJ, Chen CL, Li MS, Shun Y, Zhang YL, Zhou DY. Effect of Bifidobacterium on proliferation and apoptosis of experimental large bowel carcinoma in situ. *Shijie Huaren Xiaohua Zazhi*, 2000;8:429-431

8 Liang WJ, Huang ZY, Ding YQ. Time effect of TNFα on apoptosis of Lovo cells of human colorectal carcinoma. *Huaren Xiaohua Zazhi*, 1998;6:27-29

9 Tu SP, Jiang SH, Qiao MM, Cheng SD, Wang LF, Wu YL, Yuan YZ, Wu YX. Effect of trichosanthin on cytotoxicity and induction of apoptosis of multiple drugs resistence cells in gastric cancer. *Shijie Huaren Xiaohua Zazhi*, 2000;8:150-152

10 Liang WJ, Zhang WD. Signal conducting mechanism of tumor necrosis factor inducing apoptosis. *Shijie Huaren Xiaohua Zazhi*, 2000;8:329-331

11 Li MS, Yuan AL, Zhang WD, Chen XQ, Tian XH, Piao YJ. Immune response induced by dendritic cells induce apoptosis and inhibit proliferation of tumor cells. *Shijie Huaren Xiaohua Zazhi*, 2000;8:56-58

12 Chen HY, Liu WH, Qin SK. Induction of arsenic trioxide on apoptosis of hepatocarcinoma cell lines. *Shijie Huaren Xiaohua Zazhi*, 2000;8:532-535

13 Xin ZP, Xu CF, Huang YX, Wen QS, Xu CZ, Zhao YF. Experimental study on induction of apoptosis by cisplatin in human gastric carcinoma cell line SGC-7901. *Huaren Xiaohua Zazhi*, 1998;6:844-846

14 Tu SP, Jiang SH, Tan JH, Jiang XH, Qiao MM, Zhang YP, Wu YL, Wu YX. Proliferation inhibition and apoptosis induction by arsenic trioxide on gastric cancer cell SGC-7901. *Shijie Huaren Xiaohua Zazhi*, 1999;7:18-21

15 Werner S, Garym C, Sydeny ES, Galle PR. Model for estimation of clinically achievable plasma concentrations for investigational anticancer drugs in man. *Cancer Treat Rep*, 1986;70:1379-1382

16 Simone F, Marek L, Claudia F, Klaus MD. Chemosensitivity of solid tumor cells in vitro is related to activation of the Fas system. *Int J Cancer*, 1998;76:105-114

17 Peters GJ, Lanklma J, Kok RM, Noordhuis P, van Groeningen CJ, van der Wilt CL, Meyer S, Pindeo HM. Prolonged retention of high concentration of 5-fluorouracil in human and murine tumors as compared with plasma. *Cancer Chemother Pharmacol*, 1993; 31:269-276

18 Ding EX, Hizuta A, Morimoto Y, Tanida T, Hongo T, Ishii T, Yamano T, Fujiwara T, Iwagaki H, Tanaka W. Human colon cancer cells express the functional Fas-ligand. *Res Commun Mol Pathol Pharmacol*, 1998;101:13-24

19 Khong FY, Simon CA, Satinder R, Stefan GH, David HA. Fas/FasL ligand interaction in human colorectal hepatic metastases. *Am J Pathol*, 1999;154:693-703

20 Liu HF, Liu WW, Fang DC, Yang SM, Wang RQ. Bax gene expression and its relationship with apoptosis in human gastric carcinoma and precancerous lesions. *Shijie Huaren Xiaohua Zazhi*, 2000;8:665-668

21 Yang XJ, Chen SB, Bao JZ, Wang Y, Zhang ZB, Zhang XK, Zhang XR. Effect of HGF on etoposide-induced apoptosis and bcl-2 gene expression for hepatocellular carcinoma. *Xin Xiaohuabingxue Zazhi*, 1997;5:518-519

22 Li XL, Hao YR, Zou JX, Yang JH, Geng JH. Relationship between C-myc and Bcl-2 alterations and biological behavior and apoptosis in gastric cancer. *Xin Xiaohuabingxue Zazhi*, 1997;5:773-774

23 Sun YX, Zhou HG, Xie DY, Shi YQ. Intestinal tumors and

apoptosis. *Xin Xiaohuabingxue Zazhi*, 1997;5:791-792
24 Yang XJ, Chen SB. ras gene and apoptosis. *Huaren Xiaohua Zazhi*, 1998;6:82-83
25 Yuan RW, Ding Q, Jiang HY, Qin XF, Zou SQ, Xia SS. Bcl-2, P53 protein expression and apoptosis in pancreatic cancer. *Shijie Huaren Xiaohua Zazhi*, 1999;7:851-854
26 Peng XM, Peng WW, Chen Q, Yao JL. Apoptosis, Bcl-2 and P53 protein expressions in tissues from hepatocellular carcinoma. *Huaren Xiaohua Zazhi*, 1998;6:834-836
27 Zhang CS, Wang WL, Peng WD, Hu PZ, Chai YB, Ma FC. Promotion of apoptosis of SMMC7721 cells by Bcl-2 ribozyme. *Shijie Huaren Xiaohua Zazhi*, 2000;8:417-419
28 Qiao Q, Wu JS, Zhang J, Ma QJ, Lai DN. Expression and significance of apoptosis related gene bcl-2, bax in human large intestine adenocarcinoma. *Shijie Huaren Xiaohua Zazhi*, 1999;7: 936-938
29 Nita ME, Nagawa H, Tominaga O, Tsuno N, Fujii S, Sasaki S, Fu CG, Takenoue T, Tsuruo T. 5-fluorouracil induces apoptosis in human colon cancer cell lines with modulation of Bcl-2 family proteins. *Br J Cancer*, 1998;78:986-992
30 Peng ZH, Han GX, Tang HM, Yu H, Yi MY. The effect of Bcl-2 and Fas/FasL system on hepatic apoptosis in hepatocellular carcinoma. *Zhonghua Waike Zazhi*, 2000;17:38-39
31 Ge CH, Wang XL, Li DG, Huang WG, Gu HD, Jiang ZM, Xu QF, Lu HM. Cytotoxic effect of chemotherapeutic agents with verapamil on human gastric cancer cells. *Xin Xiaohuabingxue Zazhi*, 1996;4:66-68
32 Wang ZG, Zhang AL, Ding FQ, Liu GZ. Local transfusion of LAK cell with chemotherapy in the treatment of patients and advanced liver cancer with IDDS. *Xin Xiaohuabingxue Zazhi*, 1996;4:448-449
33 Zhang XQ, Yang XM, Sun HL, Li ZR. Effects and effective factors of hepatic artery chemoembolization for hepatic carcinoma. *Xin Xiaohuabingxue Zazhi*, 1997;5:112-113
34 Liu WQ, Huang DX, Zhang WG. Preoperative parenteral nutrition and chemotherapy in patients with gastroenteral carcinoma. *Xin Xiaohuabingxue Zazhi*, 1997;5:621-623
35 Wang GT, Zhu JS, Xu WY, Wang Y, Zhou AG. Clinical and experimental studies on Fuzheng anti-cancer granula combined with chemotherapy in advanced gastric cancer. *Huaren Xiaohua Zazhi*, 1998;6:214-218
36 Xu J, Chen JK, Liu FK, Wu B, Huang W, Cao JM, Li CL. Histologic study on colorectal cancer with preoperative chemotherapy. *Huaren Xiaohua Zazhi*, 1998;6:891-893
37 Meng ZQ, Yu EX, Song MZ. Inhibition of telomerase activity of human liver cancer cell SMMC-7721 by chemotherapeutic drugs. *Shijie Huaren Xiaohua Zazhi*, 1999;7:252-254
38 Lu XP, Li BJ, Chen SL, Lu B, Jiang NY. Anti-CEA monoclonal antibody targeting therapy for colorectal carcinoma. *Shijie Huaren Xiaohua Zazhi*, 1999;7:329-331
39 Lu XP, Li BJ, Chen SL, Lu B, Jiang NY. Effect of chemotherapy or targeting chemotherapy on apoptosis of colorectal carcinoma. *Shijie Huaren Xiaohua Zazhi*, 1999;7:332-334
40 Li XF, Wang GX, Chen J, Hong BZ. Effect of regional antineoplastics infusion on local recurrence and hepatic metastasis after colon carcinoma resection. *Shijie Huaren Xiaohua Zazhi*, 1999;7:958-959
41 Hou BH, Qing SH, Dong FY, Qi DL,Zhang GQ, Zhao F, Yao XQ, Peng M. Effects of continuous hyperthermia peritoneal perfusion chemotherapy on peritoneal implantation of human colonic cancer cells in nude mice. *Shijie Huaren Xiaohua Zazhi*, 2000;8:650-653

Edited by Ma JY

P.O.Box 2345 Beijing 100023, China
Fax. 0086·10·65891893 Tel. 0086·10·65897901
E-mail.wcjd@public.bta.net.cn www.wd.org.cn

World J Gastroentero, 2001; 7(1):93 - 97
World Journal of Gastroenterology
Copyright © 2001 by the WJG Press ISSN 1007 - 9327

Activity of boanmycin against colorectal cancer

Yong Chuan Deng[1], Yong Su Zhen[2], Shu Zheng[1] and Yu Chuan Xue[2]

Subject headings colorectal neoplasms; boanmycin; antineoplastic agents; neoplasm transplantation; mitomycin C; fluorouracil; mice, nude

Deng YC, Zhen YS, Zheng S, Xue YC. Activity of boanmycin against colorectal cancer. ***World J Gastroenterol***, 2001;7(1):93-97

INTRODUCTION

Boanmycin (Bleomycin A6, BAM), a new antitumor antibiotic, was isolated from many components of bleomycin (BLM) produced by streptomyces pingyangensis which were obtained from a soil sample collected in Pingyang County, Zhejiang Province, China. Boanmycin has a similar chemical structure to that of BLM, but the terminal amine moiety is different [1]. Pingyangmycin (bleomycin A5), one of multicomponent bleomycin complex produced by the strain, was found to have a high activity against a wide spectrum of murine transplantable tumors, but have a relatively low pulmonary toxicity in mice[2-4]. Pingyangmycin, as a single agent, shows marked inhibition on the growth of human colon cancer, stomach cancer and nasopharyngeal cancer xenografts in nude mice[5-7]. It has been widely used clinically in the treatment of tumors since 1979 in China[8]. Because of a good antitumor efficacy of pingyangmycin as a single agent and low marrow toxicity, attempts have been made to develop new superior bleomycin derivatives[9]. BAM, a minor component of bleomycin complex, was also found to be highly active against murine tumors, human liver cancer and colorectal xenografts in nude mice, and markedly inhibit the spontaneous pulmonary metastasis of Lewis carcinoma in mice[10-14]. BAM-monoclonal antibody immunoconjugates were highly effective against related human tumor *in vivo* and *in vitro*[15-19]. BAM also reached a higher concentration and remained for a longer time in murine transplantable carcinomas as compared with other bleomycin components[3]. As observed under electron microscopy, the pulmonary toxic damage caused by BAM was less than that induced by bleomycin[20]. Phase I clinical study of BAM showed no myelosuppression and cardiac toxicity, and its major adverse reactions were fever, gastrointestinal reactions and hardening at the site of i.m. injection. All adverse effects disappeared after discontinuation of the therapy[21].

An ideal animal model for cancer is one that mimics human disease in every respect. Most tumor xenograft studies, including colorectal tumor, for the evaluation of antitumor activity of drugs used subcutaneous implantation system due to its convenience and access to direct detection and therapeutic effect. However, those models have limitations for the study of interaction of tumor cells with their relevant organ environment or organ distribution of drugs. Alteration of microenvironment surrounding tumor tissue will not only influence growth and spread of tumor but also is important for drug delivery[22-24]. Recently, use of orthotopic models for the growth of tumors in mice or rat has aroused more interest, including lung cancer, colorectal cancer, breast cancer, pancreatic cancer, etc[25-30]. However, whether such orthotopic colorectal tumor models apply to the evaluation of new anticancer agents remains unknown.

In the present study, human colorectal tumor xenograft model in nude mice and the orthotopic model of murine colon cancer were used to clarify the antitumor effect of BAM in comparison with that of mitomycin C and 5-fluorouracil, drugs commonly used in clinics against colorectal cancer. We attempted to determine the effect of BAM against colorectal cancer and whether the organ microenvironment could influence the response of a murine colon cancer to systemic therapy with BAM.

MATERIALS AND METHODS

Mice

Nude mice with a BALB/c genetic background were bred under specific pathogen-free conditions at the Institute of Laboratory Animal Sciences, Chinese Academy of Medical Sciences (CAMS). All experiments were carried out in the Institute of Laboratory Animal Sciences under specific pathogen-free conditions using laminar airflow racks. Six to seven week old male or female nude

[1]Cancer Institute, Medical School, Zhejiang University, Hangzhou 310009, Zhejiang Province, China
[2]Institute of Medicinal Biotechnology, CAMS & PUMC, Beijing 100050, China
Dr. Yong Chuan Deng, graduated from Zhejiang Medical University as a Ph.D. of Oncology in 1991, now associated professor of surgery, specialized in oncological surgery, having 20 papers published.
Supported by the National Natural Science Foundation of China, No. 93090012-03
Correspondence to: Yong Chuan Deng, 68 Jiefang Road, Cancer Institute, Medical School, Zhejiang University, Hangzhou 310009, Zhejiang Province, China
Tel. 0086-571-7783572, Fax 0086-571-7214404
Email. dengyc@mail.hz.zj.cn
Received 2000-04-24 **Accepted** 2000-12-10

mice weighing 18 g-22 g were used for the experiment. All food, water and bedding were sterilized.

Tumors

Two human cell lines of colorectal cancer, HT-29 and Hce-8693, transplanted into nude mice, were used. HT-29 was an adenocarcinoma of the colon established in the Memorial Sloan-Kettering Cancer Center, New York. Hce-8693 was a poorly differentiated adenocarcinoma of the cecum established in the Zhejiang Tumor Hospital, Hangzhou.

Colon tumor NO. 26 (CT-26), a murine colon adenocarcinoma, was induced in a BALB/c mouse by chemical carcinogens. Initially, CT-26 cells were serially transplanted and then established as a cell line and used in a large number of chemotherapy studies.

Drugs

Commercially available mitomycin C (MMC) and 5-fluorouracil (5-FU) were used for the experiment. BAM, a single component of bleomycin A6, was purified from bleomycin complex at Institute of Medicinal Biotechnology, CAMS & PUMC, Beijing. A 1/9 LD50 equitoxic dose for each drug, MMC 1.0 mg/kg per injection, 5-FU 27 mg/kg per injection and BAM 10 mg/kg per injection, was used for *in vivo* comparative studies[12].

Chemotherapy of human colorectal cancer xenografted in nude mice

Two human tumor fragments of about 2 mm^3 were inoculated subcutaneously into the right axillary region of nude mice. When diameter of tumor reached 3 mm-4 mm, tumor-bearing mice were randomized into test groups of 5-6 each and drug treatment was initiated. Test mouse was weighed and size of tumor was measured with sliding calipers two times weekly, and tumor weight (W) was calculated by the formula W (mg) = a(mm) × b^2(mm)/2 where a was the width and b is the length. The drugs were administered i.p., *b.i.w.*, a total of 10 injections. Next day after last treatment, mice were killed and the tumors were removed and weighed. The antitumor effect of drug was evaluated in terms of inhibitory ratio [1-(mean tumor weight of treated group - mean tumor weight of control group)] × 100%[12].

Chemotherapy of murine CT-26

Orthotopic tumor implantation Six-week-old (18 g-20 g) female BALB/c mice were anesthetized with diethylether, and the abdomen was prepared for sterile surgery. A small incision was made, the cecum was exteriorized and CT-26 cells (1 × 10^6/0.02 mL) were injected with a 30-G needle between the submucosa and the subserosa. The lack of extra-cecal leakage was the criterion for a successful injection. The cecum was returned to the abdominal cavity, and the wound was closed in one layer[7].

Subcutaneous tumor implantation CT-26 cells (1×10^6/0.02 mL) were injected into *s.c* in right axilla region. Mice were randomized into treatment and control groups based on the body weight next day after tumor cell injection. The drugs were administered *i.m.* (hindlimb), *q.o.d.*, for a total of 10 injections. Mice with *s.c* tumors and cecal tumors were killed on day 21 after tumor cell injection, and tumors were removed and weighed. The antitumor effect of drug was also evaluated in terms of inhibitory ratio [1-(mean tumor weight of treated group - mean tumor weight of control group)] × 100%[7].

Pathologic examination

Samples from untreated and drug-treated tumors were collected from subcutis or cecum and fixed in Bouin's solution, and embedded in paraffin. Sections were made, stained with H & E and observed under microscopy with a rectangular net-like micrometer. Whole area and necrosis area in tumor section was measured, and the necrosis ratio of tumors was calculated. Ten optical fields were examined along the peripheral area of the tumor and the mitotic figures were recorded[12].

Examination of nucleated cells in bone marrow

Femurs were removed and the bone marrow cavity was washed out with 3 mL white-blood-cell diluting solution. The nucleated cells per femur were counted under microscopy[12].

RESULTS

Response of colon cancer to BAM in nude mice

The results shown in Table 1 reveals the same response of the two types of human colon cancer to intraperitoneal BAM in both 10 and 15 mg/kg dose groups. Both doses exerted marked inhibition on the growth of HT-29 and Hce-8693 xenografts in nude mice.

Table 1 Inhibitory effect of BAM on the growth of human colorectal xenografts in nude mice*

Drug	Tumor	No. of mice	Dose (mg/kg)	Tumor weight (g) $\bar{x} \pm s$	Tumor growth inhibition (%)
BAM	HT-29	6		1.300 ± 0.620	
		6	10	0.138 ± 0.064	89[b]
		6	15	0.098 ± 0.074	92[b]
	Hce-8693	5		1.501 ± 1.445	
		5	10	0.154 ± 0.125	90[b]
		5	15	0.122 ± 0.154	92[b]

*Treatment was started on day 3 and day 14 after HT-29 and Hce-8693 tumor transplantation, *ip.*, twice a week, with a total of 10 injections. [b]$P<0.01$, *vs* control group.

Comparative response of colon cancer to BAM, 5-FU and MMC in nude mice

On the basis of equitoxic doses (1/9 LD50), BAM and two clinically active drugs (5-FU and MMC) were evaluated against human colon cancer HT-29 xenografts in nude mice. Table 2 shows the response of the tumor to two weekly treatments with three drugs. BAM is the most active single agent with an inhibition rate of 82% and exerted much stronger growth inhibition against HT-29 xenografts than 5-FU(P<0.01) and MMC(P<0.05). MMC had moderate activity against HT-29 xenografts with an inhibition rate of 53%. 5-FU did not arrest tumor growth throughout the experiment, and tumor increased in size at the same rate as the untreated control with an inhibition rate of 12%.

Comparative response of CT-26 growing at subcutis and cecum to BAM 5-FU and MMC

In the experiment, BALB/c mice were given injections of CT-26 cells into subcutis and cecum, which produced s.c tumor and cecum tumor. In view of the drug distribution, BAM, 5-FU and MMC were administered *i.m.* rather than *i.p.* at an equitoxic dose. In the treatment, the equitoxic dose was administered, and the antitumor activity of the three agents was compared. Table 3 shows the antitumor activity of BAM on the intracecal and *s.c* CT-26 tumor in comparison with that of 5-FU and MMC. BAM displayed a striking activity against intracecal CT-26 tumor; the inhibition of tumor growth was higher at the cecum than at the s.c site (P<0.05). The mean tumor weight after BAM treatment was less than that in the control, 5-FU and MMC groups, and the difference was statistically significant (P<0.01). On the other hand, 5-FU did not effectively suppress the tumor growth, and MMC showed mild activity.

Changes in tumor necrosis and mitosis

In contrast to the control HT-29 tumors that maintained their feature of poorly differentiated adenocarcinoma, the BAM-treated HT-29 xenografts in athymic mice presented extensive tumor necrosis and fibrosis. In areas of residual tumor, tumor cells were frequently found to have giant, bizarre-shaped pyknotic nucleoli, or prominent inclusion-type nucleoli. Xenografts treated with 5-FU and MMC showed scattered giant, bizarre-shaped nuclei and nucleolar prominence but these changes were focal and less apparent than in BAM-treated tumors. More extensive necrosis was found in tumors treated with BAM than in those treated with 5-FU or MMC. The necrotic ratio of tumors (whole necrotic area/whole tumor area) in BAM-treated group (67%) was much higher than that in 5-FU-treated (35%), MMC-treated (43%) and control groups (35%). In contrast to the tumor of the control group, the pathologic mitosis figures in BAM-treated group were reduced by 69%, which were fewer than those in 5-FU-treated, MMC-treated and control group (Table 3).

Table 2 Inhibitory effect of BAM, MMC and 5-Fu on the growth and tumor cell mitosis of human colon cancer HT-29 xenografts in nude mice*

Drug	Dose** (mg/kg)	No. of mice	Tumor weight (g) $\bar{x} \pm s$	Inhibitory rate (%)	Necrotic ratio of tumors△ (%)	Mitotic figures△△ $\bar{x} \pm s$	Mitotic figures△△ (%)
Control		5	0.804±0.173		35[b]	104±12	100
BAM	10	5	0.148±0.059	82	67	41±4	39[b]
MMC	1	5	0.376±0.174	53[a]	43[b]	107±12	103
5-FU	27	5	0.707±0.168	12[b]	35[b]	130±17	130

*Treatment was started on day 9 after tumor transplantation, *ip*., twice a week, with a total of 10 injections;
**Drugs were administered at equitoxic doses (1/9 LD50); △Ratio of necrotic areas in whole section of the tumor.
△△Number of mitotic figures in 10 optical fields of the section of tumor.
[a]P<0.05, *vs* BAM group; [b]P<0.01, *vs* BAM group.

Table 3 Inhibitory effect of BAM, MMC and 5-FU on the growth of CT-26 tumor at the cecum and *s.c* site in mice*

Exp.	Drug	Dose** (mg/kg)	No. of mice	*s.c.* tumor Tumor weight (g) $\bar{x} \pm s$	*s.c.* tumor Inhibitory rate (%)	Cecal tumor Tumor weight (g) $\bar{x} \pm s$	Cecal tumor Inhibitory rate (%)
I	Control		9	0.854±0.151		0.557±0.112	
	BAM	10	9	0.101±0.054	88[b]	0.005±0.010	99[b]
	MMC	1	8	0.311±0.105	64	0.159±0.043	71
	5-FU	27	8	0.459±0.118	46	0.310±0.148	44
II	Control		6	0.900±0.396		0.740±0.446	
	BAM	10	6	0.105±0.088	88[b]	0.011±0.019	99[b]
	MMC	1	5	0.674±0.270	25	0.159±0.510	78
	5-FU	27	6	0.657±0.322	27	0.434±0.255	41

*Treatment was started on next day after tumor cell injection, *im*., *qod*., with a total of 10 injections.
**Drugs were administered at equitoxic doses (1/9 LD50).
[b]P<0.01, *vs* any other group.

Toxicity

No death or body weight loss of more than 20% was seen in the control or treated mice during the experiment. No inhibition on bone marrow cellularity was found in HT-29-bearing nude mice and CT-26-bearing mice at therapeutic doses of BAM. There was no significant difference in nucleated cell counts of marrow between the control and BAM group. In the CT-26-bearing mice, 5-FU and MMC caused significant decrease in bone marrow cellularity (Table 4). At therapeutic doses, no pathologic changes were found in the heart, lung, liver, spleen, kidney and brain of BAM-treated mice.

Table 4 Bone marrow nucleated cells in mice bearing CT-26 treated by BAM, 5-FU and MMC

Exp.	Drug	Dose** (mg/kg)	No. of mice	Nucleated cells (10^6/femur) $\bar{x} \pm s$	%
I	Control		6	13±3	100
	BAM	10	6	13±3	100
	MMC	1	5	7±2	54[b]
	5-FU	27	6	7±2	54[b]
II	Control	9		12±3	100
	BAM	10	9	12±2	100
	MMC	1	8	3±1	25[b]
	5-FU	27	8	4±1	33[b]

*Drugs were administered at equitoxic doses (1/9 LD50).
[b]$P<0.01$, *vs* control group.

DISCUSSION

Colorectal carcinomas are generally not very sensitive to the established chemotherapeutic agents; only 5-FU and MMC have shown some activity against colon carcinomas; the effects achieved, however, are of only a little value with respect to patient survival[31-41]. In the present study, we investigated the antitumor effectiveness of BAM, a new antitumor antibiotic, against human colorectal adenocarcinoma heterotransplanted to nude mice and murine colon adenocarcinoma. On the other hand, BAM, an analog of BLM that is clinically characterized by marked antineoplastic activity against carcinoma of the head and neck[42,43], showed a pronounced antitumor effect against the colorectal carcinoma used in the present study. At a 1/9 LD50 equitoxic dose, BAM exerted much stronger growth inhibition against human colon cancer HT-29 xenograft in nude mice than MMC and 5-FU. However, the tumor that remained after treatment consisted of viable cells with no degenerative changes, which were the source of early recurrence[44]. These results indicated that the effect of cancer chemotherapy should be judged not only by tumor reduction rate but also by histological changes, such as the necrotic ratio of tumors. In the present study, more extensive necrosis and fewer mitosis figures were found in tumors treated with BAM than those with MMC and 5-FU, indicating that BAM was more active against colon cancer HT-29 xenografts among three agents.

Most patients with colorectal carcinoma will die from distant metastases that are not detectable at the initiation of treatment[45,46]. Two major factors that influence the outcome of systemic therapy of cancer are heterogeneity of malignant neoplasms and *in vivo* conditions. Organ environment effects on the response of tumor to systemic chemotherapy are multifactorial, including the nutritional status of cells, the presence of organ-specific growth factors and other single-transducing agents, the degree of oxygenation, pH, extent of the vascular network and its functionality, local immunity, extracellular matrix components and drug metabolism[22-24]. The current model of orthotopic implantation of a colon carcinoma provides a unique opportunity to study a human malignancy in a context that is as close as possible to the clinical condition. Since intracecal tumors were much closer to clinical tumors than *s.c* tumors from the view of the histology of tumor growth or metastasis, this system was applicable to the evaluation of the tumor growth inhibitory effect by BAM. The present study demonstrated that murine adenocarcinoma CT-26 can successfully, using the orthotopic implantation technique, produce an aggressive tumor which retained the morphological biological characteristics of the donor tumor and metastasized to the mesenteric glands. BAM inhibited tumor growth on CT-26 implanted into the cecum and *s.c* more than 5-FU and MMC at the equitoxic dose. Moreover, the inhibitory effect of BAM on the growth of CT-26 tumor was higher at the cecum than at the *s.c* site in mice, which implicates that BAM may have the organ-specific effect. Organ-specific differences in the chemosensitivity of tumor cells have been reported by a few authors. Staroselsky et al have reported that a murine fibrosarcoma growing s.c in syngeneic mice is more sensitive to DXR than the same tumor growing as lung metastases[24]. Pratesi *et al* investigated the antitumor efficacy of flavone acetic acid against human ovarian carcinoma cells xenografted into different organ sites in nude mice, while tumors in the liver and subcutis were sensitive to the flavone, and ascites and lung tumors were resistant[22].

Since current clinical chemotherapy of colorectal cancer generally gives poor results, the finding of the present study is of interest with respect to the growth inhibiting activity of BAM against human colon carcinoma xenograft and murine colon carcinoma. However, further and extensive studies are necessary to confirm this finding and to evaluate the actual antineoplastic effectiveness of BAM against colon carcinomas.

REFERENCES

1 Xu HZ, Dai LH, Zhang HY, Zhao GY, Zhang XR, Zhang GS. Zhengguangmycin A6 and its status in the complex of Zhengguangmycins. *Yaoxue Xuebao*, 1988;23:667-671
2 Xu HZ, Zhang HY. The isolation and identification of pingyangmycin. *Yaoxue Xuebao*, 1980;15:609-614
3 Li DD, Lin FT, Liu HT, Xue SB. Antimicrobial activity of various bleomycin components and their effects on transplantable esophageal cancer in mice. *Kangshengsu*, 1981;6:41-45
4 Zhen YS, Li DD, Lin FT, Li X, Tian PY, Xue YC, Yang XP. Study on antitumor effect and toxicity of bleomycin A5 and bleomycin A2. *Yaoxue Xuebao*,1979;14:83-89
5 Zhen YS, Zhang ZH, Wu SY, Huang J. Inhibitory effect of pingyangmycin on human nasopharyngeal cancer transplanted in nude mice. *Zhongguo Yixue Kexueyuan Xuebao*, 1986;8:51-53
6 Jiang M,Zhen YS.Inhibitory effect of pingyangmycin on human liver cancer and stomach cancer xenografts in nude mice. *Zhonghua Zhongliu Zazhi*, 1988;10:357-360
7 Deng YC, Zhen YS, Zheng S, Xue YC. Antitumor Activity of Pingyangmycin against Colorectal Cancer. *Zhongguo Zhongliu Linchuang*, 1999;26:759-771
8 Zhengguangmycin Coordinating Group. Therapeutic effect of pingyangmycin on Malignant tumors. *Zhonghua Zhongliu Zazhi*, 1979;1:172-175
9 Zhang H, Zhen YS. Pingyangmycin shows no inhibition on the restoration of depressed hemopoiesis and immune function in mice treated with cyclophosphamide. *Proc CAMS & PUMC*, 1987;2:202-206
10 Lin FT, Song KG, Xue YC, Zhen YS. Preclinical pharmacologic evaluation of bleomycin A6. *Zhonghua Zhongliu Zazhi*, 1989; 11:257-259
11 Liu JG, Jiang M, Xu LN, Zhen YS. Minocycline potentiates the antimetastatic effect of boanmycin. *Yaoxue Xuebao*, 1995;30: 668-673
12 Deng YC, Zhen YS, Zheng S, Xue YC. Inhibitory effect of bleomycin A6 on human colon cancer xenografts in nude mice. *Zhongguo Yixue Kexueyuan Xuebao*, 1990;12:335-340
13 Jiang M, Zhen YS. Antitumor activity of bleomycin A6 against human liver cancer in cell culture and in nude mice. *Yaoxue Xuebao*, 1987;22:881-885
14 Li DD, Hu JS, Yu B. Studies on antitumor effect of bleomycin A6. *Kangshengsu*, 1985;10:312-315
15 Peng Z, Zhen YS. Experimental studies on the antitumor activity of monoclonal antibody-bleomycin A6 conjugate against human liver cancer. *Yaoxue Xuebao*, 1991;26:331-335
16 Deng YC, Zhen YS, Zheng S, Jiang M. Experimental studies on the rapeutic effect of rat monoclonal antibody-bleomycin A6 conjugate against human colorectal cancer. *Yaoxue Xuebao*, 1993; 28:410-415
17 Zhen YS, Peng Z, Deng YC, Xu HZ, Chen YX, Tian PY, Li DD, Jiang M.Antitumor activity of immunoconjugates composed of boanmycin and monoclonal antibody. *Chin Med Sci J*, 1994;9: 75-80
18 Zhen YS, Chen YX, Yu B, Zhang H, Wu SY, Du P. Cytotoxicity of the monoclonal antibody anti-CCT2 and bleomycin A6 conjugate to leukemia cells. *Zhongguo Yixue Kexueyuan Xuebao*, 1986;8: 272-275
19 Tian PY, Zhang ML, Huang J, Yu B, Zhen YS. Specific binding and internalization of anti-CCT2 monoclonal antibody and bleomycin A6 conjugate in human leukemia cells. *Yaoxue Xuebao*, 1989;24:16-21
20 Tian PY, Huang J, Zhen YS. An electron-microscopic study on pulmonary toxicity of bleomycin A6 in mice. *Zhongguo Yaolixue Yu Dulixue Zazhi*, 1990;4:221-223
21 Feng FY, Zhou LQ, Man JL, Liu H, Sun Y, Tang ZQ. Phase I clinical study of a new anticancer drug boanmycin. *Zhongguo Yixue Kexueyuan Xuebao*, 1996;18:143-146
22 Pratesi G, Manzotti C, Tortoreto M, Audisio RA, Zunino F. Differential efficacy of flavone acetic against liver versus lung metastases in a human tumour xenograft. *Br J Cancer*, 1991;63:71-74
23 Fidler IJ, Wilmanns C, Staroselsky A, Radinsky R, Dong Z, Fan D. Modulation of tumor cell response to chemotherapy by the organ environment. *Cancer Met Rev*, 1994;13:209-222
24 Staroselsky AN, Fan D, O Brian CA, Bucana CD, Gupta KP, Fidler IJ. Site-dependent differences in response of the UV-2237 murine fibrosarcoma to systemic therapy with adriamycin. *Cancer Res*, 1990;15:7775-7780
25 Rho YS, Lee KT, Jung JC, Yoon C, An Z, Hoffman RM, Chang SG. Efficacy of new platinum analog DPPE in an orthotopic nude mouse model of human colon cancer. *Anticancer Res*, 1999;19: 157-161
26 Sun FX, Sasson AR, Jiang P, An Z, Gamagami R, Li L, Moossa AR, Hoffman RM. An ultra-metastatic model of human colon cancer in nude mice. *Clin Exp Metastasis*, 1999;17:41-48
27 Garcia-Olmo D, Garcia-Rivas M, Garcia-Olmo DC, Atienzar M. Orthotopic implantation of colon carcinoma cells provides an experimental model in the rat that replicates the regional spreading pattern of human colorectal cancer. *Cancer Lett*, 1998;132: 127-133
28 An Z, Jiang P, Wang X, Moossa AR, Hoffman RM. Development of a high metastatic orthotopic model of human renal cell carcinoma in nude mice: benefits of fragment implantation compared to cell-suspension injection. *Clin Exp Metastasis*, 1999; 17: 265-270
29 Pocard M, Muleris M, Hamelin R, Salmon RJ, Dutrillaux B, Poupon MF. Growth dependency of human colon cancer xenograft on organ environment is related with their original clinical stage. *Anticancer Res*, 1998;18:2743-2747
30 Liu QZ, Tuo CW, Wang B, Wu BQ, Zhang YH. Liver metastasis models of human colorectal carcinoma established in nude mice by orthotopic transplantation and their biologic characteristic. *World J Gastroenterol*, 1998;4:409-411
31 Thirion P, Wolmark N, Haddad E, Buyse M, Piedbois P. Survival impact of chemotherapy in patients with colorectal metastases confined to the liver: a re-analysis of 1458 non-operable patients randomised in 22 trials and 4 meta-analyses. Meta-Analysis Group in Cancer. *Ann Oncol*, 1999;10:1317-1320
32 Van Halteren HK, Roumen RM, Coebergh JW, Croiset van Uchelen FA, Keuning JJ, Vreugdenhil G. The impact of 5-FU-based bolus chemotherapy on survival in patients with advanced colorectal cancer. *Anticancer Res*, 1999;19:3447-3449
33 Kokudo N, Seki M, Ohta H, Azekura K, Ueno M, Sato T, Moroguchi A,Matsubara T, Takahashi T, Nakajima T, Aiba K. Effects of systemic and regional chemotherapy after hepatic resection for colorectal metastases. *Ann Surg Oncol*, 1998;5:706-712
34 Seitz JF, Perrier H, Giovannini M, Capodano G, Bernardini D, Bardou VJ. 5-Fluorouracil, high-dose folinic acid and mitomycin C combination chemotherapy in previously treated patients with advanced colorectal carcinoma. *J Chemother*, 1998;10:258-265
35 Li XF,Wang GX, Chen J, Hong BZ. Effect of regional antineoplastics in fusion on local recurrence and hepatic metastasis after colon carcinoma resection. *Shijie Huaren Xiaohua Zazhi*, 1999;7:958-959
36 Lu XP, Li BJ, Chen SL, Lu B, Jiang NY. Effect of chemotherapy or targeting chemotherapy on apoptosis of colorectal carcinoma. *Shijie Huaren Xiaohua Zazhi*, 1999;7:332-334
37 de Gramont A, Figer A, Seymour M, Homerin M, Hmissi A, Cassidy J, Boni C, Cortes-Funes H, Cervantes A, Freyer G, Papamichael D, Le Bail N, Louvet C,Hendler D, de Braud F, Wilson C, Morvan F, Bonetti A. Leucovorin and fluorouracil with or without oxaliplatin as first-line treatment in advanced colorectal cancer. *J Clin Oncol*, 2000;18:2938-2947
38 de Gramont A, Louvet C, Andre T, Tournigand C, Krulik M. A review of GERCOD trials of bimonthly leucovorin plus 5-fluorouracil 48-h continuous infusion in advanced colorectal cancer: evolution of a regimen. Groupe d Etude et de Recherche sur les Cancers de l Ovaire et Digestifs (GERCOD). *Eur J Cancer*, 1998;34: 619-626
39 Seitz JF, Perrier H, Giovannini M, Capodano G, Bernardini D, Bardou VJ. 5-Fluorouracil, high-dose folinic acid and mitomycin C combination chemotherapy in previously treated patients with advanced colorectal carcinoma. *J Chemother*, 1998;10:258-265
40 Kokudo N, Seki M, Ohta H, Azekura K, Ueno M, Sato T, Moroguchi A, Matsubara T,Takahashi T, Nakajima T, Aiba K. Effects of systemic and regional chemotherapy after hepatic resection for colorectal metastases. *Ann Surg Oncol*, 1998;5:706-712
41 Hartmann JT, Harstrick A, Daikeler T, Kollmannsberger C, Muller C,Seeber S, Kanz L, Bokemeyer C. Phase II study of continuous 120 h infusion of mitomycin C as salvage chemotherapy in patients with progressive or rapidly recurrent colorectal cancer. *Anticancer Drugs*, 1998;9:427-431
42 Amrein PC, Colecchi CH, Finkelstein DM, Fabian RL. Adjuvant chemotherapy in advanced head and neck cancer. *Oncologist*, 1997;2:135-141
43 de Vries N, van Zandwijk N, Pastorino U. Chemoprevention of head and neck and lung (pre) cancer. *Recent Results Cancer Res*, 1999;151:13-25
44 Yuan HY, Li Y, Yang GL, Bei DJ, Wang K. Study on the causes of local recurrence of rectal cancer after curative resection: analysis of 213 cases. *World J Gastroenterol*, 1998;4:527-529
45 Yang JH, Rao BQ, Wang Y, Tu XH, Zhang LY, Chen SH, Ou-Yang XN, Dai XH. Clinical significance of detecting the circulating cancer cells in peripheral blood from colorectal cancer. *Shijie Huaren Xiaohua Zazhi*, 2000;8:187-189
46 August DA, Ottow RT, Sugarbaker PH. Clinical perspective of human colorectal cancer metastasis. *Cancer Metastasis Rev*, 1984;3:303-324

Edited by Ma JY

P.O.Box 2345 Beijing 100023, China
Fax. 0086·10·65891893 Tel. 0086·10·65897901
E-mail.wcjd@public.bta.net.cn www.wd.org.cn

World J Gastroentero, 2001; 7(1):98 - 101
World Journal of Gastroenterology
Copyright © 2001 by the WJG Press ISSN 1007 - 9327

Immunogenicity of HGV NS5 protein expressed from Sf9 insect cells

Hao Ren, Fen Lu Zhu, Shi Ying Zhu, Yan Bin Song and Zhong Tian Qi

Subject headings hepatitis agents, GB/immunology; recombinant proteins; electrophoresis, polyacrylamide gel; flaviviridae infections; Blotting, western; insect vectors; polymerase chain reaction

Ren H, Zhu FL, Zhu SY, Song YB, Qi ZT. Immunogenicity of HGV NS5 protein expressed from Sf9 insect cells. *World J Gastroenterol*, 2001;7 (1):98-101

INTRODUCTION

Although reliable assays for the detection of hepatitis C virus and E virus became available, still 10%-20% hepatitis are not caused by hepatitisA-E virus[1-3]. In 1996, two research groups isolated this agent independently and almost simultaneously and named hepatitis G virus and GB virus C, respectively[4-7]. The nucleotide and amino acid homologies between GBV-C and hepatitis G virus (HGV) were 85% and 95%[5-7]. Therefore, GBV-C and HGV were considered as two different isolates of the same virus, referred to as HGV in this paper. HGV is a single-strand, positive sense RNA virus with approximately 9.4kb in length, and classified as a member of *Flaviviridae*. HGV is mainly transmitted through transfusion and could be responsible for chronic liver infection. HGV RNA has been detected in the serum of intravenous drug users (IVDUs), volunteer and commercial blood donors, and patients with cryptogenic hepatitis[8-10]. Until now, RT-PCR is the most commonly used method for the diagnosis of HGV infection. It is necessary to develop a more convenient antibody detection assay. The baculovirus expression system is of a strong polyhedrin promoter[11], and can carry out many types of postranslation modification for a variety of proteins. Most of the expressed proteins were usually shown to be antigenic, immunological, and functionally similar to their authentic counterparts[12-16]. In this study, we used the baculovirus expression system to express HGV NS5 protein in Sf9 cells, and studied its immunogenecity.

Department of Microbiology, Second Military Medical University, Shanghai 200433, China
Dr. Hao Ren, graduated from Shandong Medical University in 1996, got master degree in 1998 from Second Military Medical University, and now is a Ph.D. student, majoring molecular virology.
Supported by the National Natural Science Foundation of China, No.39825116, 39970394.
Correspondence to: Prof. Zhong Tian Qi, Department of Microbiology, Second Military Medical University, Shanghai 200433, China
Tel. 0086-21-25070267, Fax. 0086-21-25070265
Email: qizt@smmu.edu.cn
Received 2000-07-26 **Accepted** 2000-09-29

MATERIALS AND METHODS

Materials

HGV positive sera were collected from HGV RNA positive hemodialyzed patients. The plasmid pFastBac HTa, *E.coli* DH10 Bac cell, *Spodoptera frugiperda* (Sf9) cell and recombinant plasmid HGV Iwh6 were prepared previously in this laboratory[17]. The pPROEX HTa, Lipofectin and Grace's medium were purchased from GIBCO/BRL; and expand™ Long Template PCR System was purchased from Boehringer Mannherm Company. PCR primers were designed according to HGV-Iwh6 and synthesized by Sangon Biotechnology Company. Two restriction enzyme sites *Bam* H I and *Kpn* Iwere added to the 5' end of sense and antisense primers separately. The primer sequences are sense: 5'-GCG GAT CCC TAT CGG CTG CTG TAG CTA AG-3'; antisense: 5'-GCG GTA CCT TAT TGA GCG GCC CTC TTA GC-3'.

Amplification and sequence analysis of HGV NS5 fragment

HGV NS5 fragment was amplified using HGV-Iwh6 clone as the template (PCR condition: predenature 94℃ 2 min, followed by 94℃ 30 s, 60℃ 1 min, 68℃ 2 min, 35 cycles, and extension 10 min before the ending of the reaction). The amplified fragments and pPROEX HTa were digested with *Bam* H I and *Kpn* I. Fragment and vector were recovered respectively and ligated by T4 DNA ligase to obtain recombinant plasmid pHTNS5. Sequence analysis was carried out using ABI PRISM 377 DNA sequencer (PE Company) with M13/pUC primer.

Cloning into transposing vector pFastBac HTa

pHTNS5 and transposing vector pFastBac HTa were digested with *Bam* H I and *Kpn* I, and were ligated by T4 DNA ligase. The ligation mixture was transformed into DH5α competent cell, the positive colonies were chosen on selecting agar plate (ampicillin 100 μg/mL) and identified with endonuclease digestion to obtain the recombinant plasmid pFHTNS5.

Transposon between pFHTNS5 and bacmid

Plasmid pFHTNS5 was transformed into DH10Bac competent cells containing bacmid with a mini-att Tn7 site and helper plasmid. Following hot-shock at 42℃ for 45 s, the transformation mixture was placed in a shaking incubator at 37℃ for 4 h. Recombinant

bacmid was selected on selecting plate agar containing kanamycin 50 μg/mL, gentamicin 7 μg/mL, tetracyline 10 μg/mL, X-gal 200 μg/mL, and IPTG 40 μg/mL after 24 h-48 h incubation at 37℃.

Transfection of Sf9 cells

Recombinant bacmid was extracted according to the procedure of Bac-to-Bac system. For transfection, Sf9 insect cells were grown to 60%-70% confluence. The recombinant bacmid DNA 2 μg was transfected into insect cells Sf9 with Lipofectin. After 5 d-6 d incubation at 27℃ until the morphology of the cells had obvious changes, Sf9 cells and viral supernatant were harvested respectively.

Expression of recombinant protein in insect cells and SDS-PAGE, Western-blot analysis

Twenty μL viral supernatant harvested from the transfected cells was used to infect fresh insect cells. After 5 d-6 d incubation at 27℃, the cells were harvested for protein expression analysis. The cells were washed twice with PBS and analyzed by SDS-PAGE according to the standard procedure. Western-blot was performed using HGV RNA positive sera (1:40 dilution).

RESULTS

Amplification of HGV NS5 fragment and sequence analysis

PCR product was analyzed by agrose gel electrophoresis and the length was the same as expected (Figure 1). Sequence analysis showed that the HGV NS5 fragment was cloned into the vector with correct orientation (data not shown).

Construction of recombinant transposing plasmid pFHTNS5

Figure 2 shows the construction of recombinant transposing plasmid pFHTNS5. Figure 1 shows the analysis of recombinant plasmid on agarose gel by restriction endonuclease digestion which verified that target fragment was correctly cloned into the transposing vector. The results demonstrated a successful construction of recombinant transposing plasmid pFHTNS5.

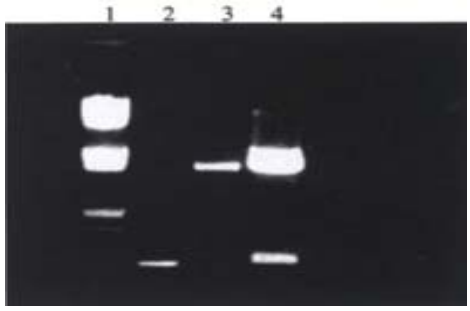

Figure 1 Analysis of recombinant plasmid by restriction endonuclease digestion.
1. λDNA / *Eco* R I + *Hind* III; 2. PCR product; 3. pHTNS5 / *Bam* H I + Kpn I; 4. pFHTNS5 / *Bam* HI + *Kpn* I.

Screening of recombinant bacmid

After transforming competent cell DH10Bac with transposing plasmid pFHTNS, the recombinant bacmid was screened by colour selection. White clones ($lacZ^-$) were selected as positive recombinant bacmid in a background of blue colonies ($lacZ^+$). The recombinant bacmid was extracted according to the procedures described in the manual of Bac-to-Bac system.

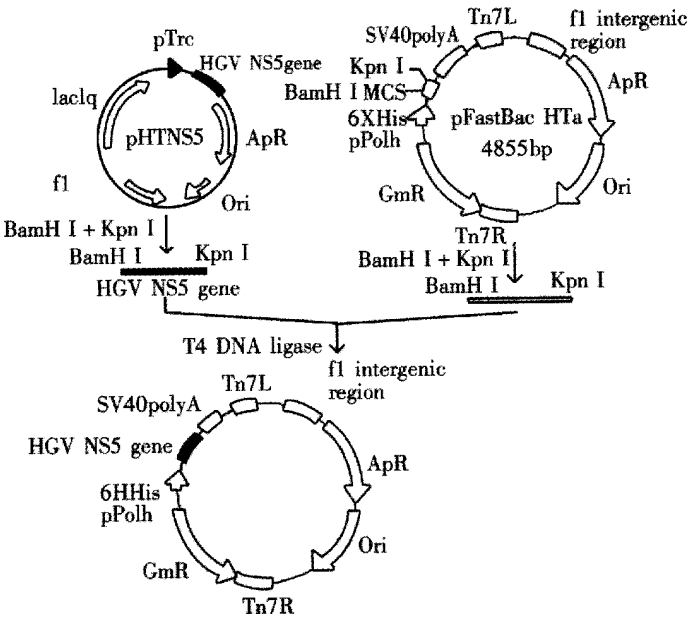

Figure 2 Construction of recombinant plasmid pFHTNS5.

Morphology of transfected or infected Sf9 cells

The morphology of Sf9 cells changed gradually after transfection or infection. The cells became big and round obviously at 4 d-5 d after transfection or infection. Cytopathic effects (CPE) were seen whereas no pathological effects were observed in normal cells (Figure 3).

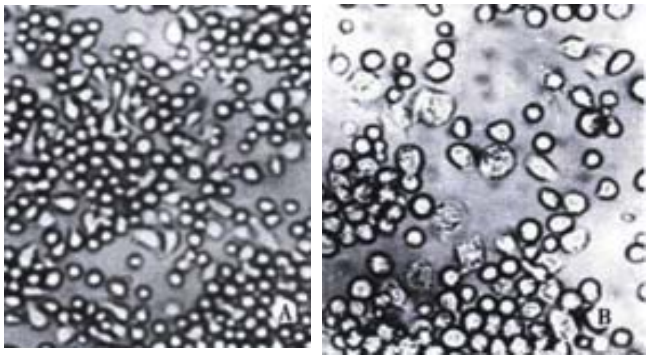

Figure 3 Morphology of uninfected, transfected and infected Sf9 cells (100×). A: Uninfected cells; B: Transfected and infected cells

SDS-PAGE and Western blot analysis of the recombinant protein

Transfected or infected Sf9 cells were harvested and analyzed on 12.5% polyacrylamide gels. Figure 4 shows the result of expressed target HGV NS5 protein with a molecular weight of M_r 41 500. Scanning results indicated that the recombinant protein amounted to 11.7% of the total proteins. Western blot results implied that the recombinant protein could react with HGV RNA positive sera (Figure 5).

Figure 4 SDS-PAGE analysis of expressed HGV NS5 protein. 1. Uninfected sf9 cells; 2. sf9 cells infected with recombinant viruses; 3. Protein relative molecular mass standards. Arrow indicates the position of recombinant protein.

Figure 5 Western-blot analysis of recombinant protein HGV NS5. 1. Uninfected sf9 cells; 2. sf9 cells infected with recombinant viruses; 3. Protein relative molecular mass standards.

DISCUSSION

Although easy and reliable assays for the clinical diagnosis of HBV and HCV infection have been established[18-26], there still existed 10%-20% parenterally and community acquired hepatitis cases of unknown cause[4,5,7]. Transmission and molecular biology of these viruses have been studied thoroughly [27-34]. Clinical studies suggest that some of these may be of viral origin. HGV is a potential aetiological agent for viral hepatitis. As a member of Flaviviridae, HGV is a single-stranded RNA virus with a genome of 9 400 bp in length which includes 5' non-coding region, structural gene region C, E1, E2, non-structural gene region NS2, NS3, NS4, NS5a, NS5b and 3' non-coding region. The genome contains a single open reading frame (ORF) which encodes a 2 900 amino acid polyprotein precursor. Many researches have been carried out since the discovery of HGV,the studies of its antigencity is one of them [17,35-39]. HGV NS5B protein functions as RNA-dependent RNA polymerase]. In addition, Pilot-Matias *et al*[40] also found that C26,C27,C28 (2047-2376 aa) of HGV NS5 gene had potential antigen epitopes. Wang *et al*[41] reported that two linear epitopes (P22, P6) might exist in HGV NS5 gene. The obtained HGV NS5 recombinant protein will provide important materials for studying its structure and function.

The Bac-to-Bac system was established by Luckow[11] in 1993, and a variety of proteins have been expressed with the control of a strong polyhedin promoter since then. It is based on site-specific transposition (transposon Tn7) of an

expression cassette into baculovirus shuttle vector (bacmid) propagated in *Escherichia coli*. After selection of blue-white clonies, recombinant bacmid DNA was extracted for the transfection of Sf9 cells. Insect cells can identify and run many modifications of post-translation and make the expressed protein close to natural protein.

In this study, HGV NS5 gene fragment amplified by PCR was confirmed by restriction enzyme and sequence analysis, and cloned into baculovirus transposing vector pFastBacHTa. Recombinant bacmid was obtained with site-specific transposition, Sf9 cell was transfected with recombinant bacmid or infected with viral supernatant. On the polyacrylamine gel, an expected protein band was seen at M_r 41 500. Western blot found that HGV NS5 recombinant protein could react strongly with HGV RNA positive sera, which implied that recombinant HGV NS5 protein could be used as antigen to detect HGV infection.

REFERENCES

1 Kuo G,Choo QL,Alter HJ,Gitnick GL,Redeker AG, Purcell RH, Miyamura T, Dienstag JL, Alter MJ, Stevens CE. An assay for circulating antibodies to a major etiologic virus of human non-A, non-B hepatitis. *Science*, 1989; 244:362-364

2 Dawson GJ, Chau KH, Cabal CM, Yarbough PO, Reyes GR, Mushahwar IK. Solid-phase enzyme-linked immunosorbent assay for hepatitis E virus IgG and IgM antibodies utilizing recombinant antigens and synthetic peptides. *J Virol Methods*, 1992;38:175-186

3 Schlauder GG, Mushahwar IK. Detection of hepatitis C and E virus by the polymerase chain reaction. *J Virol Methods*, 1994;47:243-253

4 Simons JN, Pilot-Matias TJ, Leary TP, Dawson GJ, Desai SM, Schlauder GG, Muerhoff AS, Erker JC, Buijk SL, Chalmers ML. Identification of two flavivir us-like genomes in the GB hepatitis agent. *Proc Natl Acad Sci USA*, 1995;92:3401-3405

5 Leary TP, Muerhoff AS, Simons JN, Pilot-Matias TJ, Erker JC, Chalmers ML, Schlauder GG, Dawson GJ, Desai SM, Mushahwar IK. Sequence and genomic organization of GBV-C: a novel member of the flaviviridae associated with human non-A-E hepatitis. *J Med Virol*, 1996;48:60-67

6 Linnen J, Wages J Jr, Zhang-Keck ZY, Fry KE, Krawczynski KZ, Alter H, Koonin E, Gallagher M, Alter M, Hadziyannis S, Karayiannis P, Fung K, Nakatsuji Y, Shih JW, Young L, Piatak M Jr, Hoover C, Fernandez J, Chen S, Zou JC, Morris T, Hyams KC, Ismay S, Lifson JD, Hess G, Foung SKH, Thomas H, Bradley D, Margolis H, Kim JP. Molecular cloning and disease association of hepatitis G virus: a transfusion-transmissible agent. *Science*, 1996;271:505-508

7 Simons JN, Leary TP, Dawson GJ, Pilot-Matias TJ, Muerhoff AS, Schlauder GG, Desai SM, Mushahwar IK. Isolation of novel virus-like sequences associated with human hepatitis. *Nat Med*, 1995;1:564-569

8 Zhuang H. Study of hepatitis G virus infection in our country. *Zhonghua Ganzangbing Zazhi*, 1998;6:3-4

9 Chang JH, Wei L, Du SC, Wang H, Sun Y, Tao QM. Hepatitis G virus infection in patients with chronic non-A-E hepatitis. *China Natl J New Gastroenterol*, 1997;3:143-146

10 Wang XT, Zhuang H, Song HB, Li HM, Zhang HY, Yu Y. Partial sequencing of 5 non-coding region of 7 HGV strains isolated from different areas of China. *World J Gastroentero*, 1999;5:432-434

11 Luckow VA, Lee SC, Barry GF, Olins PO. Efficient generation of infec tious recombinant baculoviruses by site-specific transposon-mediated insertion of foreign genes into a baculovirus genome propagated in Escherichia coli. *J Virol*, 1993;67:4566-4579

12 Deng XZ, Diao ZY, He L, Qiao RL, Zhang LY. HBeAg gene expression with baculovirus vector in silk worm cells. *World J Gastroenterol*, 1999;5: 167-171

13 Bae JE, Toth TE. Cloning and kinetics of expression of Brucella abortus heat shock proteins by baculovirus recombinants. *Vet Microbiol*, 2000;75: 199-204

14 Nermut MV, Hockley DJ, Bron P, Thomas D, Zhang WH, Jones IM. Further evidence for hexagonal organization of HIV gag protein in prebudding assemblies and immature virus-like particles. *J Struct Biol*, 1998;123:143-149

15 Li TC, Yamakawa Y, Suzuki K, Tatsumi M, Razak MA, Uchida T, Takeda N, Miyamura T. Expression and self-assembly of empty virus-like particles of hepatitis E virus. *J Virol*, 1997;71:7207-7213

16 Conner ME, Zarley CD, Hu B, Parsons S, Drabinski D, Greiner S, Smith R, Jiang B, Corsaro B, Barniak V, Madore HP, Crawford S, Estes MK. Virus-like particles as a rotavirus subunit vaccine. *J Infect Dis*, 1996;174 (Suppl 1):S88-92

17 Zhu FL, Qi ZT, Ren H, Song YB, Shao L. Splicing and cloning of the full-length genomic cDNA of GBV virus C/hepatitis G virus. *Dier Junyi DaxueXuebao*, 1998;19:301-306

18 Song CH, Wu MY, Wang XL, Dong Q, Tang RH, Fan XL. Correlation between HDV infection and HBV serum markers. *China Natl J New Gastroenterol*, 1996;2:230-231

19 Zhou P, Cai Q, Chen YC, Zhang MS, Guan J, Li XJ. Hepatitis C virus RNA detection in serum and peripheral blood mononuclear cells of patients with hepatitis C. *China Natl J New Gastroenterol*,1997;3:108-110

20 Assy N, Minuk GY. A comparison between previous and present histologic assessments of chronic hepatitis C viral infections in humans. *World J Gastroentero*, 1999;5:107-110

21 Yu SJ.A comparative study on the proliferating activity between HBV-related and HCV-related small HCC. *China Natl J New Gastroenterol*, 1997;3:236-237

22 Zhang LF, Peng WW, Yao JL, Tang YH. Immunohistochemical detection of HCV infection in patients with hepatocellular carcinoma and other liver diseases. *World J Gastroenterol*, 1998;4:64-65

23 Zheng Z, Yang SW, Xiao W, Sun P, Li XJ, Hu YQ. Evaluation of the HBV in HBsAg by HBV DNA measured with PCR. *World J Gastroenterol*, 1998;4(Suppl 2):77

24 Tang RX, Gao FG, Zeng LY, Wang YW, Wang YL. Detection of HBV DNA and its existence status in liver tissues and peripheral blood lymphocytes from chronic hepatitis B patients. *World J Gastroenterol*, 1999;5: 359-361

25 Chen K, Han BG, Ma XK, Zhang HQ, Meng L, Wang GH, Xia F, Song XG, Ling SG. Establishment and preliminery use of hepatitis B virus preS1/2 antigen assay. *World J Gastroenterol*, 1999;5:550-552

26 Gao JE, Tao QM, Guo JP, Ji HP, Lang ZW, Ji Y, Feng BF. Preparation and application of monoclonal antibodies against hepatitis C virus nonstructural proteins. *China Natl J New Gastroenterol*, 1997;3:114-116

27 Zhu FL, Lu HY, Li Z, Qi ZT. Cloning and expression of NS3 cDNA fragment of HCV genome of Hebei isolate in *E. coli*. *World J Gastroenterol*, 1998;4:165-168

28 Sun DG, Liu CY, Meng ZD, Sun YD, Wang SC, Yang YQ, Liang ZL, Zhuang H. A prospective study of vertical transmission of hepatitis C virus. *China Natl J New Gastroenterol*, 1997;3:111-113

29 Zhang SZ, Liang JJ, Qi ZT, Hu YP. Cloning of the non-structural gene 3 of hepatitis C virus and its inducible expression in cultured cells. *World J Gastroentero*, 1999;5:125-127

30 Wei L, Wang Y, Chen HS, Tao QM. Sequencing of hepatitis C virus cDNA with polymerase chain reaction directed sequencing. *China Natl J New Gastroenterol*, 1997;3:12-15

31 Zhang SL, Han XB, Yue YF. Relationship between HBV viremia level of pregnant women and intrauterine infection: neated PCR for detection of HBV DNA. *World J Gastroenterol*, 1998;4:61-63

32 Jiang RL, Lu QS, Luo KX. Cloning and expression of core gene cDNA of Chinese hepatitis C virus in cosmid pTM3. *World J Gastroenterol*, 2000; 6:220-222

33 Dai YM, Shou ZP, Ni CR, Wang NJ, Zhang SP. Localization of HCV RNA and capsid protein in human hepatocellular carcinoma. *World J Gastroenterol*, 2000;6:136-137

34 Zhao LS, Qin S, Zhou TY, Tang H, Liu L, Lei BJ. DNA-based vaccination induces humoral and cellular immune responses against hepatitis B virus surface antigen in mice without activation of C-myc. *World J Gastroenterol*, 2000;6:239-243

35 Wang XT, Zhuang H, Song HB, Li HM, Zhang HY, Yu Y. Partial sequencing of 5 non-coding region of 7 HGV strains isolated from different areas of China. *World J Gastroenterol*, 1999;5:432-434

36 Zhu FL,Qi ZT, Zhu SY, Ren H, Shao L. A Preliminary Study on Macaca Mulatta Infected by Intrahepatic Injection of GHV-C/HGV RNA Transcripts produced *in vitro*. *Bingdu Xuebao*, 2000;16:176-178

37 Zhu FL, Ren H, Zhu SY, Song YB, Qi ZT. High-level Expression of GBV-C/HGV NS3 protein in Sf9 Insect cells Using Baca-to-2Bac Vectors. *Bingdu Xuebao*, 2000;16:273-275

38 Zhu FL, Ren H, Song YB, Qi ZT. Expression of GBV-C/HGV NS3 protein in Escherichia coli. *Zhonghua Weishengwuxue He Mianyixue Zazhi*, 1999; 19:475-478

39 Zhu SY, Pan W, Qi ZT. Expression of E2 glycoprotein gene of hepatitis G virus in insect cells. *Zhongguo Bingduxue*, 1999;14:135-139

40 Pilot-Matias TJ, Muerhoff AS, Simons JN, Leary TP, Buijk SL, Chalmers ML, Erker JC, Dawson GJ, Desai SM, Mushahwar IK. Identification of antigenic regions in the GB hepatitis viruses GBV-A,GBV-B,and GBV-C. *J Med Virol*, 1996;48:329-338

41 Wang XT, Zhuang H, Li HM, Zhang HY, Qi ZB, Wang YC, Pan HP, Chen ZY. Evaluation of peptide antigens for detection of antibodies to GBV-C. *Zhong hua Weishengwuxue He Mianyixue Zazhi*, 1997;17:157-159

Edited by Ma JY

P.O.Box 2345 Beijing 100023, China
Fax. 0086·10·65891893 Tel. 0086·10·65897901
E-mail.wcjd@public.bta.net.cn www.wd.org.cn

World J Gastroentero, 2001; 7(1):102 - 106
World Journal of Gastroenterology
Copyright © 2001 by the WJG Press ISSN 1007 - 9327

Humoral and cellular immunogenecity of DNA vaccine based on hepatitis B core gene in rhesus monkeys

Zu Hu Huang[1], Hui Zhuang[2], Shan Lu[3], Ren Hua Guo[1], Guo Min Xu[2], Jie Cai[1] and Wan Fu Zhu[2]

Subject headings hepatitis B virus; DNA vaccine; hepatitis B core antigens; nucleic acid vaccine; enzyme-linked immunosorbent assay; macaca mulatta

Huang ZH, Zhuang H, Lu S, Guo RH, Xu GM, Cai J, Zhu WF. Humoral and cellular immunogenecity of DNA vaccine based on hepatitis B core gene in rhesus monkeys. ***World J Gastroenterol***, 2001;7(1):102-106

INTRODUCTION

Hepatitis B virus (HBV) is the most common etiologic agent for infectious liver diseases. It is estimated that there are more than 250 million chronic HBV carriers in the world today and there is a significant association among persistent infection, liver cirrhosis and hepatocellular carcinoma[1-3]. The control of HBV infections is thought to be mediated by both humoral and cellular immune responses involving neutralizing antibodies as well as class I and class II major histocompatibility complex (MHC)-restricted T- cells[4,5]. Among the HBV antigens, a number of studies have highlighted the importance of the human immune response against the HBcAg and HBeAg during HBV infections. During acute HBV infection, cytotoxicity T lymphocyte (CTL) specific for HBcAg and HBeAg can be detected in the circulation of the infected host. In contrast, in chronic HBV infection, HBcAg and HBeAg-specific CTL and T-helper cell activity are not readily detected. The cumulated data suggest that CTL activity may play an important role in resolving HBV infection[6-11].

DNA mediated immunization has been shown to be an novel method to induce both humoral and cell-mediated immune responses against many different antigens including HBV antigens[12,13]. We have demonstrated that the DNA vaccine based on HBV core gene has strong humoral and cellular immunogenecity in different species of mice[14,15]. In our experiments, we have further investigated the immunogenecity of this DNA vaccine in rhesus monkeys. The results show that the DNA vaccine of HBV core gene can prime obvious antigen-specific antibody and cell mediated immune responses.

[1]Department of Infectious Diseases, The First Affiliated Hospital of Nanjing Medical University, Nanjing 210029, Jiangsu Province, China
[2]Faculty of Microbiology, Beijing University, Beijing 100000, China
[3]University of Massachusetts Medical Center
Dr. Zu Hu Huang, graduated from Nanjing Medical University in 1982 and earned his Master Degree of Medicine from NMU in 1988, trained in molecular biology and virology in Australia and United States, now Professor and Director of Department of Infectious Diseases, specialized in clinical molecular biology for diagnosis and treatment of viral hepatitis, having 35 papers published.
Project supported by the grant from Science Foundation of Ministry of Health of China, No.96-1-347.
Correspondence to: Zu Hu Huang, The First Affiliated Hospital of Nanjing Medical University, 300 Guangzhou Road, Nanjing 210029, Jiangsu Province, China
Tel. 0086-25-3737024, Fax. 0086-25-3724440
Received 2000-08-08 **Accepted** 2000-10-29

MATERIALS AND METHODS

Preparation of DNA vaccine of HBV core gene

The control plasmid (pJW4303) and DNA vaccine of HBV core gene (pJW4303/HBc) were propagated by a large amount of culture of the transformed *E.coli* strain of HB101. Plasmid DNA was purified with QIAGEN Plasmid Mega Kit (QIAGEN, Germany).

Rhesus monkeys

Four rhesus monkeys (2 male, 2 female, 3 years of age) were purchased from Special Animal Breeding and Raising Center, Xingye, Henan Province, China and maintained at the animal house in Beijing Medical University. The monkeys were divided into experimental group and control group (2 monkeys in each group).

Protocols of DNA immunization

The monkeys in the experimental group were immunized with plasmid pJW4303/HBc and that in the control group were immunized with plasmid pJW4303. The plasmids were dissolved in normal saline to a final concentration of 1 g/L. Each time one monkey received 4-site intramuscular injections with a total volume of 2 mL plasmid solution containing 2 mg plasmid DNA. Three boosts with same dose were given at an interval of 2 months. The monkeys' sera before and after immunizations were collected and stored at -30℃.

Detection of anti-HBc antibody

Anti-HBc antibodies in monkeys' sera were first detected by Abbott Imx System (Abbott, USA) according to the manufacturer's instructions and end-point titers of anti-HBc antibody were then detected by an enzyme linked immunosorbent assay (ELISA). The procedures were as follows: ① The 96-well microplates were coated with recombinant HBcAg (1 mg/L) and blocked with PBS containing

10% FCS. ② Three-fold dilutions of monkeys' sera (1: 50, 1:150, 1:450 …… 1:984150) were added to triplicate wells. ③ HRP labeled rabbit anti-human IgG (Sino-American Biotechnology Co.) at the dilution of 1:3000 was used as second antibody. ④ The substrate solution (TMB) was then added to each well and reaction was stopped by 2M H_2SO_4. ⑤ The absorbence value was measured at wavelength of 450 nm by an ELISA reader. Microplate washings were performed between each step with PBST solution. The end-point of anti-HBc titer was defined as the highest serum dilution that resulted in an absorbence value two times that of non-immune or control serum.

Detection of IgG subclasses of anti-HBc

Subclasses of anti-HBc antibodies were detected in the sera of the monkeys positive for anti-HBc. The procedures were similar to the ELISA method mentioned above for detecting anti-HBc, except that serum was diluted to 1:30. 1:500 diluted sheep anti-human IgG1, IgG2, IgG3 and IgG4 (Nordic Immunological Laboratories, Tilburg, the Netherlands) were used as the second antibody, and 1:5000 diluted HRP labeled rabbit anti-sheep IgG (Jackson Immuno-Research Laboratories Inc, PA, USA) was used as the third antibody.

Detection of IFN-γ and IL-4 in PBMC culture supernatant

The procedures were as follows: ① PBMCs were separated from heparinized monkey blood by Ficoll gradient sedimentation method. ② PBMCs were resuspended with RPMI-1640 containing 10% FCS to a final concentration of 2×10^6 cells/ mL. ③ PBMC suspension 250 μL (5×10^5 cells) was added to triplicate wells in a 24-well cell culture plate, and recombinant human IL-2 (500U/well) was added as well. ④ Except for control wells, PBMCs in each triplicate wells were restimulated with recombinant HBcAg at different doses of 5 μg/well, 10 μg/well and 12.5 μg/well. ⑤ After 48 h incubation under the condition of 37℃, 5% CO_2, the supernatant was collected from each well and stored at once at -70℃. ⑥ IFN-γ and IL-4 concentrations were detected by the ELISA kits (Jinmei Biotechnology Co., Shenzheng, China).

PBMC proliferation assay

The procedures were similar to that for detecting IFN-γ and IL-4 in PBMC culture supernatant, except that ① PBMCs were incubated for 72 h; ② 0.5 μCi ^{3}H-TdR was added to each well and followed by another 4h incubation; PBMCs were then collected onto filter membrane which were then backed 2 h at 80℃; and the radioactivity (CPM) was determined by a beta-scintillation counter (Beckman). The PBMC proliferation activity was expressed by Stimulation Index (SI), which was calculated according to the following formula: (SI = CPM of HBcAg stimulated well/CPM of non HBcAg stimulated well). SI value greater than 2 was generally considered as having antigen specific PBMC proliferation.

RESULTS

Anti-HBc IgG and its end-point titer in monkey's sera

The results of anti-HBc IgG and its end-point titer in monkey's sera are shown in Table 1.

Table 1 Anti-HBc in sera of experimental and control monkeys

Monkey No.	Group	Anti-HBc antibody					End-point
		0 month	2 month	4 month	6 month	8 month	
1	Experimental	N[a]	P[b]	N/D[c]	N/D	N/D	1:36450
2	Experimental	N	N	P	P	P	1:109350
3	Control	N	N	N	N	N	1:150
4	Control	N	N	N	N	N	1:150

[a]N: negative
[b] P: positive (in Abbott Imx System, the detected value less than 1.00 was considered positive for anti-HBc).
[c] not detected because of death.

Subclasses of anti-HBc IgG in sera of experimental group of rhesus monkeys

Subclasses of anti-HBc IgG (IgG1, IgG2, IgG3 and IgG4) were detected in the experimental monkeys (No.1 and No.2), which were found to be positive for anti-HBc in the previous tests. The results are shown in Table 2.

Table 2 Subclasses of anti-HBc IgG and IgG1/IgG2 ratio in rhesus monkeys' sera

Monkey No.	IgG1	IgG2	IgG3	IgG4	IgG1/IgG2
1	0.61 + 0.01[a]	1.02 + 0.08	0.32 + 0.02	0.12 + 0.01	0.60
2	0.61 + 0.04	1.05 + 0.04	0.40 + 0.01	0.18 + 0.03	0.58

[a] The values indicated $\bar{x} \pm s$ of triplicate wells.

IFN-γ and IL-4 levels in culture supernatant of PBMCs stimulated with recombinant HBcAg

IFN-γ and IL-4 levels were detected in monkey No.2 (experimental group) and monkey No.3 (control group). Monkey No.1 and No.4 died before this test was performed. The results are shown in Table 3.

Table 3 IFN-γ and IL-4 values in culture supernatant of PBMCs

Monkey No.	Group	IFN-γ (ng/L)	IL-4 (ng/L)
2	Experimental	15.63	6.25
3	Control	<3.13	6.25

HBcAg specific PBMCs proliferation activity in experimental and control groups of rhesus monkeys

HBcAg specific PBMCs proliferation activities were measured in monkey No.2 and No.3 by the time of 12 months after first immunization. The results are listed in Table 4.

Table 4 HBcAg specific PBMC proliferation activity*

Monkey No.	Group	HBcAg dose for stimulation (μg/well)			
		0	5	10	12.5
2	Experimental	354.4 ± 64.5	984.9 ± 105.4[a] (2.74)	1364.9 ± 47.9[a] (3.83)	890 ± 155.6[a] (2.12)
3	Control	198.4 ± 3.9	274.5 ± 33.2 (1.37)	261.5 ± 28.2 (1.32)	250 ± 70.0 (1.24)

*The values in the table refer to CPM ($\bar{x} \pm s$ from each triplicate well), the values in the brackets indicate stimulation index (SI). [a]$P<0.05$ *vs* control monkey.

DISCUSSION

DNA-mediated immunization refers to the induction of an immune response to antigen expressed *in vivo* subsequent to the introduction of DNA carrying the protein coding sequences and the regulatory elements needed to express them[16,17]. An important feature of DNA-based immunization is the *in situ* production of the expressed protein (s), mimicking a viral infection. The endogenous synthesis should allow presentation of antigens by class I molecules of MHC, resulting in the induction of CD8 + cytotoxic T lymphocytes (CTL)[18]. There have been several experimented reports in which recombinant plasmid DNA was used to induce immune responses to particular pathogens, including malaria[19], herpes simplex virus (HSV)[20], influenza A[21], rabies virus[22], simian immunodeficiency virus (SIV)[23], human immunodeficiency virus type I (HIV)[24] and hepatitis B virus (HBV)[25-32].

In our earlier work, the HBV core gene fragment, which was modified to assure the high level expression of HBcAg[33], was successfully cloned into the plasmid pJW4303, the vector containing CMV immediate early promotor. This recombinant plasmid was named pJW4303/HBc. The DNA immunization using pJW4303/HBc among Balb/c (H_2d) and C57BL/6 (H_2b) mice showed that this recombinant could induce strong humoral (antibody) and cellular (CTL) immune responses[34].

When evaluating the immunogenecity and safety of potential DNA vaccine for eventual use in humans, the nonhuman primate models should be considered. The best nonhuman primate candidate would be those closest to humans on a phylogenetic basis. However, cost and other considerations may preclude studies in hominoid species, such as chimpanzee, orang utans, gorillas, and gibbons. Based on the cost and availability, nonhominoid primate species including rhesus monkeys, represent the alternative candidate nonhuman primate species for pre-clinical immunogenecity studies[35,36].

Townsend *et al*[37] observed the specific immune responses in mouse and rhesus monkeys after genetic immunization with retrovirus vectors expressing different forms of the hepatitis B virus core and e antigens. Their results showed that intramuscular injections with 10^8 CFU of the the LHBc-Neo retrovirus vector into rhesus monkeys induced HBc/eAg-specific antibody production and CD8 + CTLs. The CTL response is long-lasting, and being detectable as late as 16 weeks after immunization.

We used the plasmid as the vector to carry HBV core gene for DNA immunization in rhesus monkeys, which was different from the observation above the reason for that is that the safety of the vector for retrovirus vector was integratable to the host genome.

In our experiments, all 4 monkeys were negative for anti-HBc before DNA immunization. After intramuscular immunization of pJW4303/HBc and pJW4303, the monkeys in the experimental group all developed anti-HBc antibody while the monkeys in the control group all negative for this antibody, indicating that this DNA vaccine could induce antigen specific humoral response in rhesus monkeys. We also found that the monkeys in the experimental group could show different antibody response profiles. Monkey No.1 became positive for anti-HBc (1:36450) after the first immunization while monkey No.2 was not negative for anti-HBc until the second immunization and the antibody titer became higher (1: 103 950) as late as the total four immunizations were accomplished. This different antibody production profiles might indicate the individual difference in response to DNA immunization.

In human and other hominoid primates, the serum IgG exhibited four subclasses, i.e., IgG1, IgG2, IgG3 and IgG4. The relative concentrations of these IgG subclasses were 60%-70% for IgG1, 15%-20% for IgG2, 5%-10% for IgG3, and 1%-7% for IgG4. When looked into the antigen specific IgG antibodies the concentration of IgG1 and IgG2 and its ratio IgG1/IgG2 could reflect the response profiles of helper T cells (T-H1 type or T-H2 type) to some extent. Generally speaking, IgG1/IgG2<1 or IgG1/IgG2>1 reflected T-H1 type or T-H2 type immune responses. The previous data showed that T-H1 type response was beneficial for the clearance or eradication of chronic infected viruses while the T-H2 type- response was usually correlated to the exacerbation of immunopathogenic damage of host tissues[38]. Feltquate *et al* had found that intramuscular immunization of DNA vaccines was prone to induce T-H1 type of immune response, thereby facilitating the recovery of the host from chronic viral infection[39]. Our results also

demonstrated that two monkeys intramuscularly immunized with HBV core DNA vaccine all exhibited T-H1 type of immune response based on the fact that their IgG1/IgG2 ratios were all less than 1 (0.60 and 0.58, respectively).

The profiles of cytokine production were another indicators of helper T cell responses[40-44]. IFN-γ, IL-2, TNF-α and GM-CSF were usually considered as T-H1 type cytokines, while IL-4, IL-5 and IL-10 were T-H2 type cytokines. IFN-γ and IL-4 were chosen in this experiment to observe helper T cell responses after DNA immunization of HBV core gene in rhesus monkeys. IFN-γ level was significantly higher in the culture supernatant of PBMC from the monkeys immunized with HBV core DNA vaccine than that from monkeys injected only with control plasmid (15.63 ng/L *vs* <3.13 ng/L). At the same time, IL-4 levels in both monkeys with injections of pJW4303/HBc or PJW4303 were similar (6.25 ng/L *vs* 6.25 ng/L). The results indicated IFN-γ prominent cytokine profile in the monkey immunized with HBV core DNA vaccine. This result combined with the result of IgG1/IgG2 ratios mentioned above further confirmed the T-H1 type immune responses in the monkeys of the experimental group.

Cell-mediated immune response is critical for the termination of chronic HBV infections[45-47]. Antigen specific lymphocyte proliferation assay is an alternative for the CTL assay to evaluate the cell-mediated immune response[48]. In this experiment, the HBcAg specific PBMC proliferation activity was seen in the monkey immunized with pJW4303/HBc but not in the monkey injected with pJW4303 ($P<0.05$). After stimulation with three different doses of HBcAg, the stimulation index (SI) was all >2 in the experimental monkeys but all <2 in the control monkeys, which strongly indicated that DNA vaccine of pJW4303/HBc could induce antigen-specific cell-mediated immune response in rhesus monkeys.

Sallberg *et al* reported that DNA immunization of HBV core gene using retrovirus as vector could markedly decrease the HBV DNA level in the sera of experimental chimpanzees, and even induce the seroconversion of HBeAg to anti-HBe[49]. Our results showed that using plasmid as vector the DNA vaccine could also stimulate the immune responses in nonhuman primate rhesus monkeys, which was obviously helpful and beneficial for the host to inhibit and eventually eradicate chronically infected virus, including hepatitis B virus. As the designer vaccines for the 21st century, DNA vaccines demonstrated its feasibility of inducing specific cellular immunity in humans[50]. We believed that DNA vaccine of HBV core gene may become a potential therapeutics for the treatment of chronic HBV infection in humans in the near future.

REFERENCES

1 Chan HL, Ghany MG, Lok ASF. Hepatitis B. Schiff's diseases of the liver. 8th Ed. Philadelphia: Lippincott-Raven Publishers, 1999: 757-784

2 Gerlich WH, Thomssen R.The viruses of hepatitis. In: 2nd ed. Bircher J, Benhamou JP, McIntyre N, eds. Oxford textbook of clinical hepatology. Oxford: *Oxford University Press*, 1999: 828-954

3 Wang XL, Guo H, Li ZZ, Jia SY, Zhang ZR, Liu H. Hemodynamic study of HBV carriers. *World J Gastroenterol*, 1998;4(Suppl 2):85

4 Milich DR. Immune response to the hepatitis B virus: infection, animal models, vaccination. *Viral Hepat Rev*, 1997;3:63-103

5 Bertoletti A, Southwood S, Chesnut R, Sette A, Falco M, Ferrara GB, Penna A, Boni C, Fiaccadori F, Ferrari C. Molecular features of the hepatitis B virus nucleocapsid T-cell epitope 18-27: interaction with HLA and T-cell receptor. *Hepatology*, 1997;26:1027-1034

6 Lee WM. Hepatitis B virus infection. *N Engl J Med*, 1997;337: 1733-1745

7 Ferrari C, Penna A, Bertoletti A, Valli A, Antoni AD, Giuberti T, Cavalli A, Petit MA, Fiaccadori F. Cellular immune response to hepatitis B virus-encoded antigens in acute and chronic hepatitis B virus infection. *J Immunol*, 1990;145:3442-3449

8 Bertoletti A, Ferrari C, Fiaccadori F, Penna A, Margolskee R, Schlicht HJ, Fowler P, Guilhot S, Chisari FV. HLA class I-restricted human cytotoxic T cells recognize endogenously synthesized hepatitis B virus nucleocapsid antigen. *Proc Natl Acad Sci USA*, 1991;88:10445-10449

9 Penna A,Chisari FV,Bertoletti A, Missale G, Fowler P, Giuberti T, Fiaccadori F, Ferrari C. Cytotoxic T lymphocytes recognize an HLA-restricted epitope within the hepatitis B virus nucleocapsid antigen. *J Exp Med*, 1991;174:1565-1570

10 Tsai SL, Chen PJ, Lai MY, Yang PM, Sung JL, Huang JH, Hwang LH, Chang TH, Chen DS. Acute exacerbations of chronic type B hepatitis are accompanied by increased T cell responses to hepatitis B core and e antigens. *J Clin Invest*, 1992;89:87-96

11 Lau GKK. Immunological approaches to the breakdown of hepatitis B viral persistence. *World J Gastroenterol*, 1998;4(Suppl 2): 32

12 Robinson HL. Nucleic acid vaccines: an overview. *Vaccine*, 1997; 15:785-787

13 Zhao LS, Qin S, Zhou TY, Tang H, Liu L, Lei BJ. DNA-based vaccination induces humoral and cellular immune responses against hepatitis B virus surface antigen in mice without activation of C-myc. *World J Gastroenterol*, 2000;6:239-243

14 Huang ZH, Lu S, Liu N, Wang SX. Specific immune responses in H-2d mice after DNA immunization of HBV core gene. *ZhonghuaGanzangbing Zazhi*, 1999;7:107-109

15 Huang ZH, Lu S, Liu N, Wang SX. Specific cellular and humoral immune responses in H-2b mice induced by DNA immunization of HBV core gene. *Zhonghua Chuanranbing Zazhi*, 1999;17:104-107

16 Wolff JA, Malone RW, Williams P, Chong W, Acsadi G, Jani A, Felgner PL. Direct gene transfer into mouse muscle *in vivo*. *Science*, 1990;247:1465-1468

17 Tang DC, Devit M, Johnston SA. Genetic immunization is a simple method for eliciting an immune response. *Nature*, 1992;356:152-154

18 McDonnell WM, Askari FK. Molecular medicine DNA vaccines. *N Engl J Med*, 1996;334:42-45

19 Hoffman SL, Doolan DL, Sedegah M, Wang R, Scheller LF, Kumar A, Weiss WR, Le TP, Klinman DM, Hobart P, Norman JA, Hedstrom RC. Toward clinical trials of DNA vaccines against malaria. *Immunol Cell Biol*, 1997;75:376-381

20 Manickan E, Rouse RJD, Yu Z, Wire WS,Rouse BT. Genetic immunization against herpes simplex virus: protection is mediated by CD4+ T lymphocytes. *J Immunol*, 1995;155:259-265

21 Justewicz DM, Morin MJ, Robinson HL, Webster RG. Antibody-forming cell response to virus challenge in mice immunized with DNA encoding the influenza virus hemagglutinin. *J Virol*, 1995; 69:7712-7717

22 Xiang ZQ, Spitalnik S, Tran M, Wunner WH,Cheng J, Ertl HCJ. Vaccination with a plasmid vector carrying the rabies virus glycoprotein gene induces protective immunity against rabies virus. *Virology*, 1994;199:132-140

23 Yasutomi Y, Robinson HL, Lu S, Mustafa F, Lekutis C, Arthos J, Mullins JI, Voss G, Manson K, Wyand M, Letvin NL. Simian immunodeficiency virus-specific cytotoxic T-lymphocyte induction through DNA vaccination of rhesus monkeys. *J Virol*, 1996; 70:678-681

24 Lu S, Santoro JC, Fuller DH, Haynes JR, Robinson HL. Use of DNAs expressing HIV-1 env and noninfectious HIV-1 particles to raise antibody responses in mice. *Virology*, 1995;209:147-154

25 Davis HL, McCluskie MJ, Gerin JL, Purcell RH.DNA vaccine for

hepatitis B: evidence for immunogenicity in chimpanzees and comparison with other vaccines. *Proc Natl Acad Sci USA*, 1996; 93:7213-7218

26 Davis HL, Millan CLB, Mancini M, McCluskie MJ, Hadchouel M, Comanita L, Tiollais P, Whalen RG, Michel ML. DNA-based immunization against hepatitis B surface antigen (HBsAg) in normal and HBsAg-transgenic mice. *Vaccine*, 1997;15:849-852

27 Schirmbeck R, Böhm W, Ando K, Chisari FV, Reimann J. Nucleic acid va ccination primes hepatitis B virus surface antigena-specific cytotoxic T lymphocytes in nonresponder mice. *J Virol*, 1995;69:5929-5934

28 Michel ML, Davis HL, Schleef M, Mancini M, Tiollais P, Whalen RG. DNAa-mediated immunization to the hepatitis B surface antigen in mice: Aspects of the humoral response mimic hepatitis B viral infection in humans. *Proc Natl Acad Sci USA*, 1995;92: 5307-5311

29 Mancini M, Hadchouel M, Davis HL, Whalen RG, Tiollais P, Michel ML.DNA- mediated immunization in a transgenic mouse model of the hepatitis B surface antigen chronic carrier state. *Proc Natl Acad Sci USA*, 1996;93:12496-12501

30 Sllberg M, Townsend K, Chen M, O dea J, Banks T, Jolly DJ, Chang SM, Lee WT, Milich DR. Characterization of humoral and $CD4^+$ cellular responses after genetic immunization with retroviral vectors expressing different forms of the hepatitis B virus core and e antigens. *J Virol*, 1997;71:5295-5303

31 Kuhröber A, Wild J, Pudollek HP, Chisari FV, Reimann J. DNA vaccination with plasmids encoding the intracellular (HBcAg) or secreted (HBeAg) form of the core protein of hepatitis B virus primes T cell responses to two overlapping Kaba- and Kada-restricted epitopes. *Inter Immunol*, 1997;9:1203-1212

32 Geissler M, Tokushige K, Chante CC, Zurawski VR Jr, Wands JR. Cellular and humoral immune response to hepatitis B virus structural proteins in mice after DNA-based immunization. *Gastroenterology*, 1997;112:1307-1320

33 Ye YA, Zhan MY. High efficient expression in E.coli of hepatitis B virus core gene after 5 end modification. *Bingdu Xuebao*, 1988; 4:312-318

34 Huang ZH, Lu S, Liu N, Wang SX, Li J, Tang BY.Humoral and cellular immunogenecity of genetic vaccine on core gene of hepatitis B virus in mice. *Zhonghua Yixue Zazhi*, 1999;79:456-459

35 Kennedy RC, Shearer MH, Hildebrand W.Nonhuman primate models to evaluate vaccine safety and immunogenicity. *Vaccine*, 1997; 15:903-908

36 Liu MA, McClements W, Ulmer JB, Shiver J, Donnelly J. Immunization of non-human primates with DNA vaccines. *Vaccine*, 1997;15:909-912

37 Townsend K, Sällberg M, O dea, J, Banks T, Driver D, Sauter S, Chang SM, Jolly DJ, Mento SJ, Milich DR, Lee WTL. Characterization of $CD8^+$ cytotoxic Ta-Lymphocyte responses after genetic immunization with retrovirus vectors expressing different forms of the hepatitis B virus core and e antigens. *J Virol*, 1997;71:3365-3374

38 Scott P, Kaufmann SHE. The role of T-cell subsets and cytokines in the regulation of infection. *Immunol Today*, 1991;12:346-348

39 Feltquate DM, Heaney S, Webster RG, Robinson HL. Different T. Helpercell types and antibody isotypes generated by saline and gene gun DNA immunization. *J Immunol*, 1997;158:2278-2284

40 Actor JK, Shirai M, Kullberg MC, Buller R ML, Sher A, Berzofsky JA. Helminth infection results in decreased virus-specific $CD8^+$ cytotoxic T-cell and Th1 cytokine responses as well as delayed virus clearance. *Proc Natl Acad Sci USA*, 1993;90:948-952

41 Clerici M, Hakim FT, Venzon DJ, Blatt S, Hendrix CW, Wynn TA, Shearer GM. Changes in interleukin-2 and interleukin-4 production in asymptomatic, human immunodeficiency virus-seropositive individuals. *J Clin Invest*, 1993;91:759-765

42 Milich DR, Wolf SF, Hughes JL, Jones JE. Interleukin 12 suppresses autoantibody production by reversing helper T-cell phenotype in hepatitis B e antigen transgenic mice. *Proc Natl Acad Sci USA*, 1995;92:6847-6851

43 Milich DR, Peterson DL, Sch¡éidel F, Jones JE, Hughes JL. Preferential recognition of hepatitis B nucleocapsid antigens by Th1 or Th2 cells is epitopeand major histocompatibility complex dependent. *J Virol*, 1995;69:2776-2785

44 Geissler M, Gesien A, Tokushige K, Wands JR. Enhancement of cellular and humoral immune responses to hepatitis C virus core protein using DNA-based vaccines augmented with cytokine-expressing plasmids. *J Immunol*, 1997;158:1231-1237

45 Lee HG, Lim JS, Lee KY, Choi YK, Choe IS, Chung TW, Kim K. Peptide-Specific CTL induction in HBV-seropositive PBMC by stimulation with peptides *in vitro*: novel epitopes identified from chronic carriers. *Virus Res*, 1997;50:185-194

46 Jung MC, Diepolder HM, Spengler U, Wierenga EA, Zachoval R, Hoffmann RM, Eichenlaub D, Frosner G, Will H, Pape GR. Activation of a heterogeneous hepatitis B core and e antigen-specific $CD4^+$ T-cell population during seroconversion to antia-HBe and anti-HBs in hepatitis B virus infection. *J Virol*, 1995;69:3358-3368

47 Mondelli M, Vergani GM, Alberti A, Vergani D, Portmann B, Eddleston ALWF, Williams R. Specificity of T lymphocyte cytotoxicity to autologous hepatocytes in chronic hepatitis B virus infection: evidence that T cells are directed against HBV core antigen expressed on hepatocytes. *J Immunol*, 1982;129:2773-2778

48 Löhr HF, Weber W, Schlaak J, Goergen B, Büschenfelde KHMZ, Gerken G. Proliferative response of $CD4^+$ T cells and hepatitis B virus clearance in chronic hepatitis with or without hepatitis B e-minus hepatitis B virus mutants. *Hepatology*, 1995;22:61-68

49 Sällberg M, Hughes J, Javadian A, Ronlov G, Hultgren C, Townsend K, Anderson CG, O Dea J, Alfonso J, Eason R, Murthy KK, Jolly DJ, Chang SM, Mento SJ, Milich D, Lee WT. Genetic immunization of chimpanzees chronically infected with the hepatitis B virus, using a recombinant retroviral vector encoding the hepatitis B virus core antigen. *Hum Gene Ther*, 1998;9:1719-1729

50 Seder RA, Gurunathan S. DNA vaccines - designer vaccines for the 21st century. *N Engl J Med*, 1999;341:277-278

Edited by Ma JY

P.O.Box 2345 Beijing 100023, China
Fax. 0086·10·65891893 Tel. 0086·10·65897901
E-mail.wcjd@public.bta.net.cn www.wd.org.cn

World J Gastroentero, 2001; 7(1):107 - 110
World Journal of Gastroenterology
Copyright © 2001 by the WJG Press ISSN 1007 - 9327

A comparative study on serologic profiles of virus hepatitis B

Jin Nü Fang[1], Chang Ji Jin[1], Lian Hua Cui[1], Zhen Yu Quan[1], BoYoul Choi[2], Moran Ki[3] and Hung Bae Park[2]

Subject headings hepatitis B virus; immunoenzyme techniques; serologic tests; hepatitis B surface antigens; hepatitis B/epidemiology; enzyme-linked immunosorbent assay

Fang JN, Jin CJ, Cui LH, Quan ZY, Choi BY, Ki MR, Park HB. A comparative study on serologic profiles of virus hepatitis B. ***World J Gastroenterol***, 2001;7(1):107-110

INTRODUCTION

Hepatitis B viral infection, one of the most-prevalent liver disorders in China and Korea, is a serious infectious disease as it has the potential of progressing into liver cirrhosis and primary hepatic carcinoma. China and Korea both belong to high-risk endemic regions of viral hepatitis[1]. The HBsAg positive rates in China ranged from 6.9%-17.9% by age, race and test methods[2-5]. In Korea, they were 6.5%-13.3% in all age groups[6-9], and 3.9%-5.9% in childhood groups[10-11]. There have been few comparative studies on Korean-Chinese and other Chinese. Considering the high mortality rates of liver cirrhosis or hepatoma among Korean-Chinese, HBsAg positive rate of Korean-Chinese must be higher than that of other Chinese. The positive rates of Korean-Chinese in Yanji and Longjing cities of Yanbian area by RPHA method were 7.5% and 7.1% respectively, which were higher than 6.2% and 4.7% in Han-Chinese respectively[12].

In regard to the possible reasons of such differences, some studies have laid special emphasis on social, economic and demographic variables such as age, sex, life style, and environment.

This study was conducted in order to assess the pattern of hepatitis B infection prevailing among Han-Chinese, Korean-Chinese, and Koreans. For collection of data, two serological surveys were carried out in 1996 in Korea and China respectively.

[1]Department of Epidemiology, Yanbian University College of Medicine, Yanji 133000, Jilin Province, China
[2]Department of Preventive Medicine, Hanyang University College of Medicine, Seoul 133791, Korea
[3]Department of Preventive Medicine, Eulji University School of Medicine, Taejon 301110, Korea
Dr. Jin Nü Fang, graduated from Norman Bethune University of Medical Sciences in 1985, Hanyang University College of Medicine with a doctoral degree in 1999, now associate professor of epidemiology, specialized in infectious disease epidemiology and cardiovascular epidemiology, having 10 papers published.
Project supported by the National Natural Science Foundation of China, No. 39560074 and Korea Science and Engineering Foundation, 965-0700-001-2.
Correspondence to: Dr. Jin Nü Fang, Department of Epidemiology, Yanbian University College of Medicine, Yanji 133000, Jilin Province, China
Tel. 0086-433-2660621
Email. epidem@public.yj.jl.cn
Received 2000-09-19 **Accepted** 2000-09-29

MATERIALS AND METHODS

Study areas

Study areas were Yangpyung County of Kyonggi Province in Korea and Helong County of Yanbian, a Korean Autonomous Prefecture in China. In Helong County, the proportion of residents by ethnicity were 55% for Korean-Chinese and 44% for Han-Chinese[13]. To compare the prevalence of hepatitis B between Korea and China, we carefully considered the characteristics of selected areas. In both areas, 70% of the residents were farmers. But the pattern of age distribution was different; the majority residing in Yangpyung County in Korea were more than 50 years old, while those in Helong County in China were over 40 years old.

Study subjects

Study subjects among ethnic groups were 556 Korean (male 41.7%, female 58.3%, $P<0.05$), 541 Korean-Chinese (male 51.6%, female 48.4%) and 261 Han-Chinese (male 39.5%, female 60.5%, $P<0.05$). These distributions by gender were statistically significant in Korean and Han-Chinese. Age distributions by ethnic groups were also significantly different; and the Koreans had older age and the Chinese had younger age. Age distributions by gender were not different between Korean and Korean-Chinese, but they were significantly different in Han-Chinese (Table 1). Therefore, this study showed the results with age-adjusted rates by gender.

Table 1 Characteristics of subject by ethnic groups[d]

Ethnic groups	Age (years)	Gender		Total
		Male	Female	
Korean-Chinese[b,c]	20-39	103	117	220
	40-49	89	77	166
	50-	87	68	155
Total	279	262	541	
Han-Chinese[a,b,c]	20-39	42	103	145
	40-49	30	44	74
	50-	26	16	42
Total	98	163	261	
Koreans[a,b]	20-39	43	70	113
	40-49	37	60	97
	50-	152	194	346
Total	232	324	556	

[a]$P<0.05$ between sex, by χ^2 test; [b]$P<0.05$ among age groups, by χ^2 test; [c]$P<0.05$ among age groups by sex, by χ^2 test;
[d]Koreans-Chinese: Koreans in Yanbian in China, Han-Chinese: Chinese in Yanbian in China, Koreans: Koreans in Yangpyung in Korea.

Questionnaires

The questionnaire survey gave direct interviews, including the relative factors on hepatitis B infection such as demographic characteristics, life style, vaccination and disease history.

Serologic tests

Serological markers on hepatitis B virus (HBsAg, anti-HBs and anti-HBc) were tested by EIA (enzyme immunoassays). Sera were stored in a deep freezer, at -30℃ until this test. The serologic tests were all done in Korea.

Statistical analysis

For comparison by ethnic groups, age-adjusted rates by direct method were used. The statistical significance was determined using χ^2 test or Mantel-Haenszel's χ^2-test on SPSS or EPISTAT.

RESULTS

There were no vaccinees on hepatitis B among Chinese, but the vaccination rate among Koreans was 32.4% (36.5% for males and 29.0% for females). The vaccination rate was 44.2% for the age group of 20-39 years, 45.4% for the age group of 40-49 years, and 24.4% among those aged 50 and over (Table 2). In order to compare hepatitis B virus markers among ethnic groups, the vaccinees were excluded.

HBsAg positive rate of males was higher than that of females in the three ethnic groups. Age-adjusted HBsAg positive rates were 7.2%, 12.0% and 4.1% in Han-Chinese, Korean-Chinese, and Korean respectively (P<0.05). This order was same in both genders. But, the difference was statistically significant only in males (P<0.05). Anti-HBs positive rates of males were higher than those of females in Korean-Chinese and Korean, but the differences were not statistically significant. There was also no difference by gender in the Han-Chinese. The age-adjusted anti-HBs positive rate of Korean (62.5%) was the highest, of Korean-Chinese was 57.6%, and of Han-Chinese 49.2%. This order was true in males and females, but the differences among the three ethnic groups were not significant. Anti-HBc positive rates of males were higher than those of females in all three groups, but these differences were not significant. Age-adjusted anti-HBc positive rate was 69.7%, the highest in Korean-Chinese, 60.9% in Korean and 54.0% in Han-Chinese. This order was also found by gender, and these differences were all statistically significant (P<0.05).

The definition of hepatitis B infection was determined as cases that have any hepatitis B virus markers among HBsAg, anti-HBs and anti-HBc. The infection rate was higher in males than in females among the three ethnic groups. But the difference was significant only in Koreans (P<0.05). Age-adjusted infection rates were 78.6% in Korean, 77.0% in Korean-Chinese and 60.7% in Han-Chinese. These differences among the three ethnic groups were significant (P<0.05) in males, females and the total.

In Koreans, the HBsAg positive rate was lower than that of Korean-Chinese, but the HBV infection rate was not different from Korean-Chinese, and was higher than that of the Han-Chinese. In Korean-Chinese, the HBsAg positive rate and HBV infection rate were higher than those of the Han-Chinese. In the Han-Chinese, the HBV infection rate was the lowest and the percentage of those who are susceptible was the highest (Table 3).

We classified the serologic profiles into 8 types by 3 HBV markers, which are HBsAg, anti-HBc and anti-HBs. Mushahwar *et al* (1981)[21] used 15 classifications by 5 HBV markers including HBeAg and anti-HBe, to determine the HBV infectivity. We used 8 types for the description of HBV serologic profiles in the cross-sectional study. Type I of our classification means those susceptible who have all three negative markers. These percentages of those susceptibles were higher in females than in males in all three ethnic groups. The percentage was 18.6% for Koreans or Korean-Chinese, and 36.7% for Han-Chinese. In females, the percentage was 40.5% for Han-Chinese, 29.6% for Korean, and 23.7% for Korean-Chinese. Among HBsAg positive serologic profiles, type VII was dominant. But, varied types such as V, VI and VIII were found only in Korean-Chinese and Han-Chinese excluding Koreans. Koreans had only one type VII, among HBsAg positive profiles. The percentage of HBsAg negative combination (HBsAg- and anti-HBs+ and/or anti-HBc+), were 78.5% and 65.5% for Korean, 67.5% and 67.6% for Korean-Chinese and 53.1% and 52.1% for Han-Chinese. Among these profiles, type IV was dominant in all three ethnic groups (Table 4).

Table 2 Rate of vaccination by sex and age in Koreans[b]

Age (yrs)	Male[a]			Female[a]			Total		
	No. of respondents	No. of vaccinces	%	No. of respondents	No. of vaccinces	%	No. of respondents	No. of vaccinces	%
20-39	43	19	44.2	70	31	44.3	113	50	44.2
40-49	37	23	62.2	60	21	35.0	97	44	45.4
50-	152	44	28.9	194	42	21.6	346	86	24.9
Total	232	86	37.1	324	94	29.0	556	180	32.4

[a]P<0.05 among age groups, by χ^2 test; bKoreans: Koreans in Yangpung in Korea.

Table 3 Positive rates and infection rate of Hepatitis B virus by sex and ethnic groups[e]

	Male			Female			Total		
	No. of tested	Crude rate(%)	Age-adjusted rate[d](%)	No. of tested	Crude rate(%)	Age-adjusted rate[d](%)	No. of tested	Crude rate(%)	A ge-adjusted rate[d](%)
HBsAg positive rate[a,c]									
Korean-Chinese	279	14.0	14.8	262	8.8	8.8	541	11.5	12.0
Han-Chinese	98	10.2	9.4	163	7.4	6.0	261	8.4	7.2
Korean	146	2.7	6.1	230	4.8	3.0	376	4.0	4.1
Anti-HBc positive rate[a,b,c]									
Korean-Chinese	279	74.6	73.2	262	68.3	66.0	541	71.5	69.7
Han-Chinese	98	58.2	59.1	163	50.9	50.4	261	53.6	54.0
Korean	140	69.3	61.3	226	58.0	60.0	366	62.3	60.9
Anti-HBc positive rate									
Korean-Chinese	279	62.4	61.1	262	56.5	54.0	541	59.5	57.6
Han-Chinese	98	46.9	48.4	163	49.1	51.7	261	48.3	49.2
Korean	146	62.3	69.1	230	55.7	58.6	376	58.2	62.5
HBV infection rate[a,b,c]									
Korean	140	81.4	85.3	226	70.4	74.0	366	74.6	78.6
Korean-Chinese	279	81.4	79.7	262	76.3	74.1	541	78.9	77.0
Han-Chinese	98	63.3	63.4	163	59.5	59.8	261	60.9	60.7

[a]$P<0.05$ among 3 ethnic groups in male, by χ^2 test; [b]$P<0.05$ among 3 ethnic groups in female, by χ^2 test; [c]$P<0.05$ among 3 ethnic groups in total, by χ^2 test; [d]Age-standardized rates (standard population; Helong in 1997 and Yangpyung in 1995); [e]Korean-Chinese: Koreans in Yanbian in China, Han-Chinese: Chinese in Yanbian in China, Koreans: Koreans in Yangpyung in Korea.

Table 4 Serological profiles of hepatitis B virus markers by sex and ethnic groups[a]

Gender ethnic groups	Serological profiles* (%)								Total
	I	II	III	IV	V	VI	VII	VIII	
HBsAg	-	-	-	-	+	+	+	+	
Anti-HBc	-	-	+	+	-	-	+	+	
Anti-HBs	-	+	-	+	-	+	-	+	
Male Korean-Chinese	52(18.6)	16(5.8)	27(9.7)	145(52.0)	1(0.4)	2(0.7)	25(9.0)	11(3.9)	279(100.0)
Han-Chinese	36(36.7)	3(3.1)	8(8.2)	41(41.8)	2(2.0)	0(0.0)	6(6.1)	2(2.0)	98(100.0)
Koreans	26(18.6)	17(12.1)	22(15.7)	71(50.7)			4(2.9)		140(100.0)
Female Korean-Chinese	62(23.7)	17(6.5)	35(13.4)	125(47.7)	3(1.1)	1(0.4)	14(5.3)	5(1.9)	262(100.0)
Han-Chinese	66(40.5)	9(5.5)	8(4.9)	68(41.7)	4(2.5)	1(0.6)	5(3.1)	2(1.2)	163(100.0)
Koreans	67(29.6)	28(12.4)	21(9.3)	99(43.8)			11(4.9)		226(100.0)

[a]Korean-Chinese: Koreans in Yanbian in China, Han-Chinese: Chinese in Yanbian in China, Koreans: Koreans in Yangpung in Korea.

DISCUSSION

Since 1980, China has produced hepatitis B vaccines and by regulations, children must be vaccinated. However, vaccination against HBV was not mandatory in adults. Therefore, none of study subjects in China were vaccinated, while in Korea, 32.4% were vaccinated. It implies that the circumstances of HBV infection and transmission were different between China and Korea. Age-adjusted HBsAg positive rate of Korean-Chinese was 12.0%, higher than the 10% previously reported in China as a whole[14]. Moreover, the rate was higher than the 8.0% for the Korean-Chinese in Yanbian area during the 1980s[12]. The rate for Han-Chinese (7.2%) was less than the national level (10%) in China, and the same or less than that of other reports[2-5]. However, no other reports were found from Yanbian area, the differences did not reflect the chronological change. In Koreans, the rate for non-vaccinees was 4.1%, which was less than other reports (6.5%-13.3%)[6-10,15,16].

Korean and Korean-Chinese are the same race, but HBsAg positive rates were different and increased with time for Korean-Chinese and decreased with time for Koreans. The difference between Korean and Korean-Chinese seems to be caused mostly by vaccination. Other factors such as socioeconomic status, sanitary status and medical support appear to influence HBV infection and transmission[6,7,11,17]. The difference between Korean-Chinese and Han-Chinese resulted from cultural difference such as life style, food habits and susceptibility[6,7,11,17]. The rate for Korean-Chinese was more similar to the Han-Chinese than to Koreans, which suggests that environmental factors are more important than genetic factors on HBV.

Positive anti-HBc is difficult to determine definitely. Type IV (anti-HBs+, anti-HBc+, and HBsAg-) and VIII (anti-HBs+ anti-HBc+, and HBsAg+) are in recovery phases caused by the positive anti-HBs. But type III (anti-HBs-, anti-HBc+, and HBsAg-) and VII (anti-HBs- anti-HBc+, and HBsAg+) mean acute or chronic infection. The order of high anti-HBc positive rates among the three ethnic groups was Korean-Chinese, Korean and Han-Chinese. This order was too

difficult to interpret like the anti-HBc.

Positive anti-HBs means having immunity against HBV. Age-adjusted anti-HBs positive rate for Chinese (57.6% for Korean-Chinese and 49.2% for Han-Chinese) was higher than that of other reports[2-5], however, in Korean (the 62.5%) it was higher[8,18] or lower than that of other reports[7,19]. Even though the difference among the three ethnic groups was not statistically significant, the reason why the anti-HBs positive rate for Korean (62.5%) was the highest, can be explained by the different serological profiles. Among the anti-HBs positive Koreans, 20.9% was type II (anti-HBs+, anti-HBc-, and HBsAg-), which indicates remote past infection, but, 10.3% and 9.5% among Korean-Chinese and Han-Chinese. Other types like IV (anti-HBs+, anti-HBc+, and HBsAg-), VI (anti-HBs+, anti-HBc-, and HBsAg+) and VIII (anti-HBs+, anti-HBc+, and HBsAg+) indicate the recovery phase of acute infection as a whole (IV, recovery phase of HBV infection; VI, unknown; and VIII, circulating immune complex of HBsAg or reinfection with different HBsAg subtype or process of seroconversion from HBsAg to anti-HBs). Therefore, positive anti-HBs Koreans had more remote infections than Korean-Chinese and Han-Chinese, which could be also applied to the exploration of HBV infection rates. HBV infection was determined by having had any one of the positive HBV markers among HBsAg, anti-HBs and anti-HBc. The order of high HBV infection rates among the three ethnic groups was the same as anti-HBs, Korean, Korean-Chinese and Han-Chinese. The difference was statistically significant ($P<0.05$).

HBV infection rates in Korean-Chinese were 81.4% in males and 76.3% in females, which were 80.8% in males of Hunan area and 75.5% in female of Guangxi of China[5]. The rates for Koreans were 81.4% in males and 70.4% in females. Therefore, even if the HBsAg rates have been decreasing as compared with that of the 1980s, HBV infection rate did not drop. According to Maynard *et al*[20]. 70%-90% of the population were infected with HBV in the highly endemic areas. Hence, Korea and Yanbian were included in the endemic area.

The fact that HBV infection rates for Korean-Chinese and Koreans were higher than those of the Han-Chinese seems to be caused by susceptibility and cultural factors such as life style and dining habits. Ahn *et al*[19] reported the association between HBV infection and behavioral characteristics such as life style, dining habit and sanitary status. Therefore, to determine the reason for the higher rate of HBV in Koreans and Korean-Chinese, more studies dealing with genetic factors and behavioral factors are needed.

In regard to positive HBsAg rate, the results showed difference by ethnic groups in the same area. Consequently, for each of the areas and the ethnic groups, the HBV infection and transmission must be differentiated[21]. For the clarification of the natural course on HBV, more detailed immigration studies and follow-up efforts should also be made.

REFERENCES

1 Kim DJ, Choi BY, Park HB. A study of hepatitis B infection rates of the school children in a rural area of korea. *Hanyang Daxue Yixuexuebao*, 1986;6:99-107

2 Wang HT, Jiang YT, Ma J, Zhu MB, Zhang XD. An epidemiological study of hepatitis B virus infection in a rural production brigadein the suburb of Beijing. *Zhonghua Liuxingbingxue Zazhi*, 1985;6: 141-144

3 Mi EY, Zhang FK, Liu YP, Lu TL. A seroepidemiologic study on HBV infection among villagers in Shanxi Province. *Zhonghua Liuxingbingxue Zazhi*, 1984;5:325-327

4 Viral hepatitis investigation group of Zhengding County, Hebei Province. The prevalence of HBV infection in rural area of Hebei Province. *Zhonghua Liuxingbingxue Zazhi*, 1987;8:70-74

5 Xiao YJ, Tang XM, Tang SL, Yang TB, Wen SW, Peng KJ. Seroepidemiologic study of HBV infection in Hunan Area. *Zhonghua Liuxingbingxue Zazhi*, 1990;11:133-137

6 Kim JS, Lee WY, Lee SW, Yoon HS, Yang SJ, Lee DH, Kim HC. An epidemiological study on HBsAg and anti-HBs prevalence in relation to liver function tests among farmers in korea. *Korean J Epidemiol*, 1985;7:16-27

7 Choo IH, Han DH, Hwang SJ, Min CH, Cho MK, Yoon CS. An epidemiological study on the occurrence of hepatitis B virus markers in a part of the population of Kwangwon Province. *Korean J Epidemio*, 1986;8:314-322

8 Kim IS, Oh HC, Lee Y, Kim JD, Lee WY. Prevalence and changes of HBsAg and anti-HBs for one year period in natural status and after hepatitis B vaccination. *Korean J Epidemio*, 1987;9:40-48

9 Shin HC, Kim JS. A study on HBsAg positive rate among Korean adults and the immunogenicity of hepatitis B vaccine. *Korean J Epidemio*, 1989;11:98-106

10 Choi BY, Song JC, Park HB, Ko UR. A seroepidemiological study on the aspects of hepatitis B virus infection in a rural community. *J Hanyang Med Coll*, 1990;10:245-265

11 Kim JS, Chung MH, Suh SC. HBsAg positive rate among korean urban and rural middle school children. *Korean J Epidemio*, 1986; 8:115-126

12 Li WY, Li CJ, Jin H. Epidemiology of hepatitis B virus infection in the population of Yanji city. *Zhonghua Yufangyixuehui Yanbian Fenhui Lunwenji*, 1987;1:56

13 Yanbian Renmin Chubanshe. *Yanbian Tongji Nianjian*, 2000. 2000:75

14 Wo GK, Yuan W, Chen HP, Duan XX, Mao MJ. Baseline survey of hepatitis B virus infection in ningbo city. *Zhonghua Liuxingbingxue Zazhi*, 1994;15:191

15 Chun BY, Lee MK, Rho YK. The prevalence of hepatitis B surface antigen among Korean by literature review. *Korean J Epidemio*, 1992;14:54-62

16 Shin HR, Kim JB. Markers after vaccination among healthy worker. *Korean J Epidemio*, 1994;16:163-171

17 Yoo KY. A review study on epidemiology of viral hepatitis. *Korean J Epidemio*, 1982;4:11-34

18 Hahm YS, Shin HR, Park HJ, Kim SR. A study on the relationship between HBsAg and hepatitis B virus DNA among healthy HBsAg carriers. *Korean J Epidemio*, 1992;14:13-23

19 Ahn YO, Yoo KY, Park BJ. An epidemiology study on risk factors of hepatitis B infection in Korea. *Korean J Epidemio*, 1987;9:57-65

20 Maynard JE, Kane MA, Hadler SC. Global control of hepatitis B through vaccination: Role of hepatitis B vaccine in the expanded program on immunization. *Rev Infect Dis*, 1989;11 (Suppl 3):574-78

21 Mushahwar IK, Dienstag JL, Polesky HF. Interpretation of various serological profiles of hepatitis B virus infection. *Am J Clin Path*, 1981;76:773-777

Edited by Ma JY

P.O.Box 2345 Beijing 100023, China
Fax. 0086·10·65891893 Tel. 0086·10·65897901
E-mail.wcjd@public.bta.net.cn www.wd.org.cn

World J Gastroentero, 2001; 7(1):111 - 114
World Journal of Gastroenterology
Copyright © 2001 by the WJG Press ISSN 1007 - 9327

Establishment of transgenic mouse harboring hepatitis B virus (adr subtype) genomes

Yi Ping Hu[1], Wei Jiang Hu[1], Wen Chao Zheng[2], Jian Xiu Li[1], De Shun Dai[1], Xin Min Wang[1], Shu Zhong Zhang[1], Hong Yu Yu[3], Wei Sun[4] and Guang Rong Hao[4]

Subject headings hepatitis B virus; mice transgenic; genome; polymerase chain reaction; immunohistochemistry; microscopy, electron; danes particles

Hu YP, Hu WJ, Zheng WC, Li JX, Dai DS, Wang XM, Zhang SZ, Yu HY, Sun W, Hao GR. Establishment of transgenic mouse harboring hepatitis B virus (adr subtype) genomes. *World J Gastroenterol*, 2001;7 (1):111-114

INTRODUCTION

Hepatitis B virus (HBV) belongs to the group of hepatovirus, a major pathogen of human acute and chronic hepatitis B[1-4], which has a very close association with human hepatocellular carcinoma (HCC)[5-8]. For example, a statistical data from a hospital in Shanghai showed that 80% of HCC patients were positive for HBsAg (personal communication). The published data reported that people infected with HBV have a 200-fold greater risk of developing HCC than age-matched population not infected with HBV[9-11]. So HBV infection, including its consequences, is one of the key problems for the human health in the world. Since HBV only infects human beings and a few kinds of higher primates[12-14], the lack of culture cell and animal model impede the study of biological characteristics of HBV and human hepatitis B in the laboratory[15,16]. In 1985, the first transgenic mouse carrying HBV genes was generated[17], and thereafter the transgenic mouse system was applied in HBV studies[18-26].

HBV prevailing in the world has at least 4 subtypes[27-30], ayw, adr, ayr and adw, among which subtype adr is the most prevailing in China[31,32]. The complete genome of subtype adr has been cloned and analyzed from HBV infected population in China. It was identified that subtype adr was different from other 3 subtypes in DNA and protein sequence[33]. In order to produce the animal model for exploring adr subtype of HBV associated biomedical issues, we generated transgenic mice harboring complete genome from subtype adr of HBV by microinjection method, in which the HBsAg gene and HBeAg gene could be expressed, and the genomic DNA of HBV could be replicated and packed into complete virus particles. This model will be very useful for examination of many aspects of HBV and its associated biomedical issues *in vivo*.

MATERIALS AND METHODS

HBV genome of *adr* subtype was obtained from plasmid -padr-1-dimer. C57 mouse strain was bought from Animal Center of Shanghai Birth Control Research Institute. PCR primers for identification were designed by ourselves according to S region of HBV genome, primer 1: 5'CCCAACCTCCAATCACTCACC3', primer 2: 5'ACGAACCACTGAACAAATGGC3', synthesized by GIBCO BRL company (USA). The themostable DNA polymerase was bought from Sangon Co. (Canada), antigen-antibody ELISA kit of HBV was the product of Sino-American Bio-Engineering Co. (China). Primera gene Labeling System kit was bought from Promega Co. (USA). Antibodies for immunohistochemistry assay were products of Dako Co. (USA). Reagents for transmission electron microscopy were standard ones (China).

Preparation of HBV DNA and microinjection

padr-1-dimer has two copies of intact HBV (adr subtype) genome head to tail, cloned in BamHI site of plasmid pBR322 (Figure 1). Restriction enzymes *Sal* I and *Cla* I were used to digest *Padr*-1-dimer, followed by 7 $g \cdot L^{-1}$ agarose gel electrophoresis of the digested products, the 7.0 kb band was retrieved, purified and dissolved in TE buffer for microinjection. Microinjection and embryo manipulation were performed according to the methods described in References[34-36].

PCR and Southern-blotting of integrated transgenes

Genomic DNA from tail tissue of transgenic mice and normal mouse were prepared, and amplified with primers in S region according to the cycling program: 94℃, 30s; 60℃, 40s; 72℃, 45s; run 35

[1]Department of Cell Biology, Second Military Medical University, Shanghai 200433, China
[2]University of Wisconsin, Madison, WI 53705, USA
[3]Department of Pathology, Second Military Medical University, Shanghai 200433, China
[4]Center of Laboratory Animals, Second Military Medical University, Shanghai 200433, China
Yi Ping Hu, Professor, and now is working at Second Military Medical University , having more then 40 papers published.
This work was supported by Projects of Tackling Key Problems in Science and Technology from the State Science and Technology Ministry (TJ99-LA01) and Shanghai Science and Technology Commission (994919033)
Correspondence to: Professor Yi Ping Hu, Department of Cell Biology, Second Military Medical University Shanghai 200433, China
Tel. 0086-21-25070240, Fax. 0086-21-25070240
Email. yphu@ smmu.edu.cn
Received 2000-05-30 **Accepted** 2000-06-23

cycles in 50 μL reaction system. Fifteen μL of PCR products were loaded on 15 $g \cdot L^{-1}$ agarose gel in the presence of 0.5 μg ethidium bromide per mL. 380 bp band was visualized by UV fluorescence. Southern blot was performed on genomic DNA by agarose electrophoresis of 30 μg restricted DNA with *Bam* HI. Nylon filtrates were hybridized with the probe including HBV genome labeled with α-P^{32}-dATP for further characterization of the transgenic mice.

HBV gene expression in transgenic mice

HBV gene expression in serum Venous blood in eye sockets of mice was collected, serum was isolated by centrifugation, and then used for HBsAg and HBeAg ELISA or RIA.

HBV gene expression in tissues The distribution of HBsAg and HBcAg was assessed by the labeled-avidin-biotin detection procedure. Briefly paraffin-embedded sections were treated for 10 min at 37℃ with 30 $mL \cdot L^{-1}$ hydrogen peroxide and washed with PBS. Rabbit anti-HBsAg primary antiserum at 1:100 dilution, and goat anti-HBcAg primary antiserum at 1:200 dilution were applied over night at room temperature. After washing with PBS, a secondary antiserum consisting of biotin-conjugated goat anti-rabbit IgG and rabbit anti-goat IgG was applied at 1:200 dilution for 40 min at 37℃, and then washed with PBS. Then the preparation was treated with 1:100 dilution ABC complex stained with DAB, and finally counterstained with hematoxylin.

Assay of serum antibody of transgenic mice

Fifty μL of the serum from transgenic mouse was assayed for anti-HBsAg, anti-HBeAg and anti-HBcAg by ELISA according to the Kit protocol.

Pathological findings analysis

Serum ALT and AST Serum ALT and AST were tested with auto-biochemical analyzer.

Histopathological study The specimens of liver, kidney, heart, spleen from transgenic mice were fixed in formalin, paraffin embedded, sectioned and stained with HE.

Examination of HBV Dane's particles in liver tissue from transgenic mice under TEM Several immunohistochemically HBV-positive mouse liver specimens were fixed over night at 4 ℃ in 40 $mL \cdot L^{-1}$ paraformaldehyde and 1 $g \cdot L^{-1}$ glutaradehyde in PBS. They were then postfixed in 10 $g \cdot L^{-1}$ OsO_4 in cacodylate buffer for 1hr at room temperature, dehydrated in gradient ethanol, and embedded in epoxy resin. This sections were cut on an LKB Ultratome III, mounted on copper grids, stained in uranyl acetate and lead citrate, and examined with electron microscope.

RESULTS

Microinjection and embryo manipulation

Hundreds of molecules of target fragment were microinjected into male pronuclei of fertilized eggs. Of 355 fertilized eggs microinjected, 262 of manipulated eggs survived; the survival rate was 73.8%. Thirteen of female recipient mice were transplanted with microinjected eggs through one of the ovarioles, and 2 of the transplanted mice were pregnant; the pregnant rate was 15.4%. Six small mice were born and all of them survived; the survival rate was 100%.

Founder mice and the identification of HBV DNA integration in transgenic mice

PCR and Southern-blotting results indicated that 4 mice were positive. So four founders were obtained. The founder mice were named HB *adr* dimer-*x*. The positive rate was 66%. Then the founders were mated with the normal mice of the same line. 27 F_1 offspring of the founder mice were born. In 14 of them PCR showed positive genomic DNA PCR. The offspring of F_1 were 56 mice, 28 of them were positive, and the positive rate was 50%. The exogenous genes can be transmitted through the germ line (Figure 2).

HBV genes expression in transgenic mice

HBV gene expression in serum The HBsAg and HBeAg were detected in the serum with ELISA and RIA. And the expression level of HBsAg was higher than that of HBeAg, and the gene expression was different in different founders (Table 1). The concentration of HBsAg in the serum was about 3000 $IU \cdot L^{-1}$.

Table 1 The ELISA result of founder mice and normal mice (A450)

Antigen	Control		Transgenic mice			
	Negative	Positive	HB-2	HB-3	HB-4	HB-5
HBsAg	0.01	1.42	0.17	0.06	0.26	0.23
HBeAg	0.01	1.56	0.06	0.06	0.08	0.09

Distribution of HBsAg and HBcAg in transgenic mice Immunohistochemical study of liver and kidney tissues from transgenic mice indicated that the distribution of positive hepatocytes was uneven, HBsAg-positive particles were located mainly in cytoplasm of hepatocytes. HBsAg expression level was weaker in kidney than in liver; the products of immune reactions of HBcAg-positive were not very certain, and mainly emerged in a few nuclei of hepatocytes from the individuals that were invariably HBsAg-positive (Figure 3). No obvious product of immune reaction from HBsAg and HBcAg positive mice was found in spleen, skin, testis and other detected tissues.

Serum antibody in transgenic mice The ELISA test indicated that there was no significant positive result of HBV antibodies in HBV transgenic mouse serum.

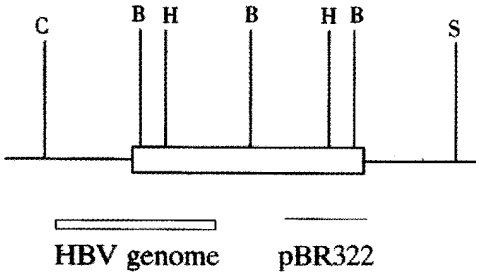

Figure 1 Restriction map and microinfection fragment of padr-1-dimer.
C: *Cla* I; B: *Bam* HI; H: *Hind* III; S: *Sal*I

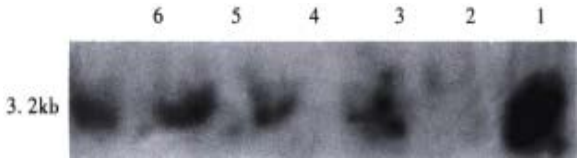

Figure 2 Southern-blot analysis of the HBV transgenic mice.
Lane 1: positive control; Lane 2: negative control;
Lane3-6: transgenic mouse

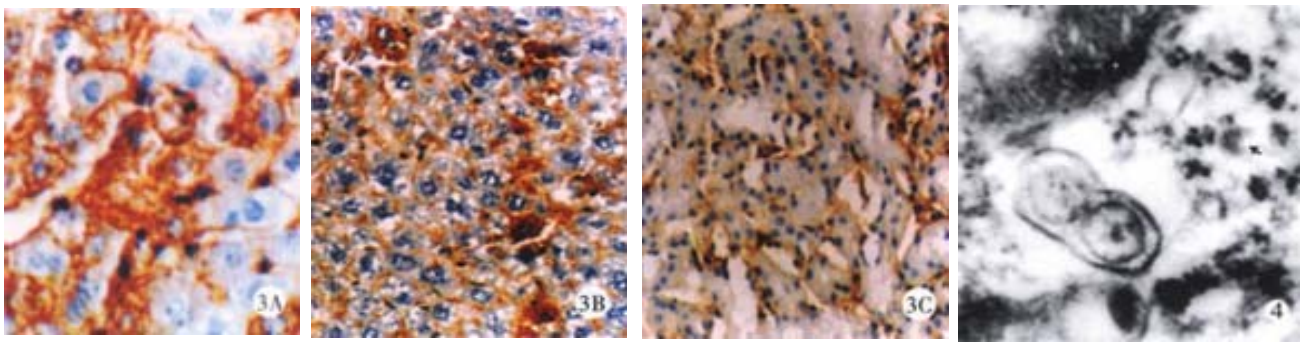

Figure 3 Immunohistochemical analysis of HBV antigens in transgenic mouse tissues.
A. HBsAg in the liver; B. HBcAg in the liver; C. HBsAg in the kidney
Figure 4 Dane's particles under electron microscope.

HBV Dane's particles in liver in transgenic mice under TEM HBsAg particles (spherial and filamental) were found in the endoplasmic reticulum of some hepatocytes, a few of in renal tubule-epithalia, and the cytoplasm of a few Kupffer cells (Figure 4).

Histopathological findings in transgenic mice

Histopathologic observation in transgenic mice tissues Mice have been monitored histologically for over 1 year without evidence of pathological changes in any organ, especially the liver and kidney. The serum ALT and AST assays indicated that there was no significant difference between the transgenic mice and the normal ones.(P>0.05) (Table 2).

Table 2 Aminotransferase in the transgenic mice (n = 12, $x \pm s$)

Mice	ALT(nkat·L^{-1})	AST(nkat·L^{-1})
Normal	698.5 ± 471.8	3597.4 ± 7669.9
Transgenic	708.5 ± 491.8	4349.2 ± 7248.1

DISCUSSION

The HBV transgenic mice show replication of the HB virus in the hepatocytes, but have no evidence of cytopathology of the liver and other organs or tissues.

In theory, HBV genes microinjected are complete in structure, and can be expressed and replicated in their bodies[37,38], because we have purposefully prepared the fragment which contains two copies of intact HBV (*adr* subtype) genomes head-to-tail to make it sure that all of four open reading frames of HBV genome are complete in structure. Four of the founders all showed serum HBsAg-positive, but the expression level is different. We think this is due to the different integrated site of HBV DNA. In general, the exogenous gene will be integrated into multi-sites in transgenic mice. This is similar with the other reports[39,40].

Immunohistochemical assays of several tissues from transgenic mice revealed that HBV gene tissue-dependent expressions were tissue-dependent, and the genes were mainly expressed in the liver and kidney, but the expression level was different; this is similar to HBV-infection in nature. Examination of liver and kidney tissue from transgenic mice under transmission electron microscope revealed the existence of Dane's particles and HBsAg particles in hepatocytes, which confirmed the ability of HBV genome replication in the transgenic mice.

Serum anti-HBs, anti-HBc and anti-HBe detected by ELISA were negative in all of the transgenic mice, and suggested that these mice were tolerant to HBsAg, HBcAg and HBeAg; this result was consistent with that of other author's reports[41]. Now, we obtain the F_3 generation positive mice. The HBV DNAs were able to be transmitted through the germ line of the mice from one generation to another.

The results of our experiments shows that HBVgenome introduced by microinjection is integrated into the mouse genome, and the HBV genes can be expressed, replicated and packaged. So these lines of HBV transgenic mice may be used as the animal model for the study on HBV and its associated biomedical issue. And it can also be applied in the selection of anti-HBV drugs and vaccine[42,43]. It is also useful for exploring the mechanism of HBV infection.

REFERENCES

1 Lok AS. Hepatitis B infection: pathogenesis and management. *J Hepatol*, 2000;32(Suppl 1):89-97
2 Wu XN. Update therapy of chronic hepatitis B in China: Recent progress. *China Natl J New Gastroenterol*, 1996;2:65-68
3 Tang ZY. Clinical research of hepatocellular carcinoma in the 21st century. *China Natl J New Gastroenterol*, 1995;1:2-3
4 Pan BR, Yang SF, Ma LS. Acute liver failure: a progress report. *China Natl J New Gastroenterol*, 1995;1:4-8
5 Chisari FV, Ferrari C. Hepatitis B virus immunopathogenesis. *Annu Rev Immunol*, 1995;13:29-60
6 Tiollais P, Pineau P, Wei Y, Dejean A, Buendia MA. Hepatitis B virus and hepatocellular carcinoma. *Bull Acad Natl Med*, 1998; 182:73-78
7 Cromlish JA. Hepatitis B virus-induced hepatocellular carcinoma: possible roles for HBx. *Trends Microbiol*, 1996;4:270-274
8 Tiollais P, Pineau P, Wei Y. Hepatitis B virus and hepatocellular carcinoma. *Bull Acad Natl Med*, 1998;182:73-77
9 Wu MC. Clinical research advances in primary liver cancer. *World J Gastroentero*, 1998;4:471-474
10 Wu GY, Wu CH. Gene therapy and liver diseases. *World J Gastroentero*, 1998;4(Suppl 2):18-19
11 Tangkijvanich P, Hirsch P, Theamboonlers A, Nuchprayoo I, Poovorawan Y. Association of hepatitis viruses with hepatocellular carcinoma in Thailand. *J Gastroenterol*, 1999;34:227-233
12 Hu X, Margolis HS, Purcell RH, Ebert J, Robertson BH. Identification of hepatitis B virus indigenous to chimpanzees. *Proc Natl Acad Sci USA*, 2000;97:1661-1664
13 Lanford RE, Chavez D, Brasky KM, Burns RB, Rico-Hesse R. Isolation of a hepadnavirus from the woolly monkey, a new world primate. *Proc Natl Acad Sci USA*, 1998;95:5757-5761
14 Pugh JC, Bassendine MF. Molecular biology of hepadnavirus replication. *Br Med Bull*, 1990;46:329-353
15 Xu XP, Yang JZ, Gao Y. Recent advances in the application of cultured hepatocytes into bioartificial liver. *China Natl J New Gastroenterol*, 1996;2:182-184
16 Peeples ME, Komai K, Radek R, Bankowski MJ. A cultured cell receptor for the small S protein of hepatitis B virus. *Virology*, 1987;160:135-142
17 Chisari FV, Pinkert CA, Milich DR, Filippi P, McLachlan A, Palmiter RD, Brinster RL. A transgenic mouse model of the chronic hepatitis B surface antigen carrier state. *Science*, 1985;230:1157-1160
18 Zhu HZ, Cheng GX, Chen JQ, Kuang SY, Cheng Y, Zhang XL, Li HD, Xu SF, Shi JQ, Qian GS, Gu JR. Preliminary study on the production of transgenic mice harboring hepatitis B virus X gene. *World J Gastroenterol*, 1998;4:536-539
19 Larkin J, Clayton M, Sun B, Perchonock CE, Morgan JL, Siracusa LD, Michaels FH, Feitelson MA. Hepatitis B virus transgenic mouse model of chronic liver disease. *Nat Med*, 1999;5:907-912
20 Yamamura K, Araki K. Developmental regulation of hepatitis B surface antigen expression in two lines of hepatitis B virus transgenic mice. *J Virol*, 1989;63:4069-4073
21 Chisari FV, Filippi P, Buras J, McLachlan A, Popper H, Pinkert CA, PaLmiter RD, Brinster RL. Structural and pathological effects of synthesis of hepatitis B virus large envelope polypeptide in transgenic mice. *Proc Natl Acad Sci USA*, 1987;84:6909-6913
22 Reifenberg K, Lohler J, Pudollek HP. Long-term expression of the hepatitis B virus core-e- and X proteins does not cause pathologic changes in tran sgenic mice. *J Hepatol*, 1997;26:119-130
23 Koike K, Moriya K, Yotsuyanagi H, Shintani Y, Fujie H, Tsutsumi T, Kimura S. Compensatory apoptosis in preneoplastic liver of a transgenic mouse model for viral hepatocarcinogenesis. *Cancer Lett*, 1998;134:181-186
24 Guidotti LG, Matzke B, Pasquinelli C. The hepatitis B virus (HBV) precore protein inhibits HBV replication in transgenic mice. *J Virol*, 1996;70:7056-7061
25 Koike K, Moriya K, Iino S, Yotsuyanagi H, Endo Y, Miyamura T, Kurokawa K. High-level expression of hepatitis B virus HBx gene and hepatocarcinogenesis in transgenic mice. *Hepatology*, 1994; 19:810-819
26 Chisari FV. Hepatitis B virus transgenic mice: models of viral immunobiology and pathogenesis. *Hepatology*, 1995;22:1316-1325
27 Echevarria JE, Leon P, Lopez JA, Tenorio A, Domingo CJ, Echevarria JM. HBsAg subtype distribution among different populations of HBsAg carriers in Spain. *Eur J Epidemiol*, 1995;11:39-45
28 Kidd-Ljunggren K, Courouce AM, Oberg M, Kidd AH. Genetic conservation within subtypes in the hepatitis B virus pre-S2 region. *J Gen Virol*, 1994;75(Pt 6):1485-1490
29 Echevarria JE, Tenorio A, Courouce AM, Leon P, Echevarria JM. Polymerase chain reaction can resolve some undefined cases of hepatitis B virus antigenic subtyping. *J Med Virol*, 1994;42:217-223
30 Okamoto H, Imai M, Tsuda F, Tanaka T, Miyakawa Y, Mayumi M. Point mutation in the S gene of hepatitis B virus for a d/y or w/r subtypic change in two blood donors carrying a surface antigen of compound subtype adyr or adwr. *J Virol*, 1987;61:3030-3034
31 Fan J, Zhuang H, Li Y. Comparison of sequences of hepatitis B virus S gene fragment in eight cities of China. *Zhonghua Yufang Yixue Zazhi*, 1997;31:140-143
32 Yuan TT, Tai PC, Shih C. Subtype-independent immature secretion and subtype-dependent replication deficiency of a highly frequent, naturally occurring mutation of human hepatitis B virus core antigen. *J Virol*, 1999;73:10122-10128
33 Gan RB, Chu MJ, Shen LP, Qian SW, Li ZP. The complete nucleotide sequence of the cloned DNA of hepatitis B virus subtype adrin pADR-1. *Sci Sin BY*, 1987;30:507-521
34 Hu YP, Qin SZ, Xu YF, Liu ZD. The chimeric 8kpF gene express with tissue specificly in transgenic mice. *Yichuan Xuebao*, 1992; 19:27-33
35 Kupriyanov S, Zeh K, Baribault H. Double pronuclei injection of DNA into zygotes increases yields of transgenic mouse lines. *Transgenic Res*, 1998;7:223-226
36 Gordon K, Ruddle FH. Gene transfer into mouse embryos. *Dev Biol* (*NY* 1985), 1986;4:1-36
37 Guidotti LG, Matzke B, Schaller H, Chisari FV. High-level hepatitis B virus replication in transgenic mice. *J Virol*, 1995;69:6158-6169
38 Farza H, Hadchouel M, Scotto J, Tiollais P, Babinet C, Pourcel C. Replication and gene expression of hepatitis B virus in a transgenic mouse that contains the complete viral genome. *J Virol*, 1988;62: 649-654
39 Araki K, Miyazaki J, Hino O, Tomita N, Chisaka O, Matsubara K, Yamamura K. Expression and replication of hepatitis B virus genome in transgenic mice. *Proc Natl Acad Sci USA*, 1989;86:207-211
40 Guidotti LG, Matzke B, Schaller H. High-level hepatitis B virus replication in transgenic mice. *J Virol*, 1995;69:6158-6169
41 Wirth S, Guidotti LG, Ando K, Schlicht HJ, Chisari FV. Breaking tolerance leads to autoantibody production but not autoimmune liver disease in hepatitis B virus envelope transgenic mice. *J Immunol*, 1995;154:2504-2515
42 Zhong S, Wen SM, Zhang DF, Wang QL, Wang SQ, Ren H. Sequencing of PCR amplified HBV DNA pre-c and c regions in the 2. 2.15 cells and antiviral action by targeted antisense oligonucleotide directed against sequence. *World J Gastroentero*, 1998;4: 434-436
43 Li H, Li RC, Liao SS, Yang JY, Zeng XJ, Wang SS. Persistence of hepatitis B vaccine immune protection and response to hepatitisB booster immunization. *World J Gastroenterol*, 1998;4:493-496

Edited by Lu HM
proofread by Ma JY

P.O.Box 2345 Beijing 100023, China
Fax. 0086·10·65891893 Tel. 0086·10·65897901
E-mail.wcjd@public.bta.net.cn www.wd.org.cn

World J Gastroentero, 2001; 7(1):115 - 119
World Journal of Gastroenterology
Copyright © 2001 by the WJG Press ISSN 1007 - 9327

Effects of glycyrrhetinic acid on collagen metabolism of hepatic stellate cells at different stages of liver fibrosis in rats

Ji Yao Wang, Qi Sheng Zhang, Ji Sheng Guo and Mei Yu Hu

Subject headings liver cirrhosis; glycyrrhetinic acid; procollagen; clostridium histolyticum collagenase; extracellular matrix; gene expression; immunohistochemistry

Wang JY, Zhang QS, Guo JS, Hu MY. Effects of glycyrrhetinic acid on collagen metabolism of hepatic stellate cells at different stages of liver fibrosis in rats. ***World J Gastroenterol***, 2001;7(1):115-119

INTRODUCTION

Liver fibrosis is a dynamic course leading to cirrhosis from a various chronic liver diseases. The pathological basis of fibrosis is the disturbance of production and degradation of the extracellular matrix (ECM), which causes accumulation of ECM in the liver[1,2]. The deposition of collagen is derived primarily from collagen types I and III in liver fibrosis[3]. The main sources of ECM are the hepatic stellate cells (HSCs)[4,5], especially when HSCs are activated by hepatic injury[6,7]. One of the important methods for preventing liver fibrosis is the inhibition of proliferation and activation of HSCs so as to reduce production of collagen. Glycyrrhetinic acid (GA) has been clinically used in the treatment of liver diseases. It has anti-injury[8-10] and anti-viral[11-13] effects on hepatic diseases. The clinical trials have shown that GA could lower the serum aminotransferase level both in Asian[14,15] and European patients[16] with chronic hepatitis. Our previous studies also indicated that GA could down-regulate mRNA expression of types I and III procollagen in NIH3T3 cells[17] and in fibrotic livers of rats induced by alcohol and CCl_4[18]. However, the effect of GA on HSCs mRNA expression of types I and III procollagen is unclear. In this study, the effects of GA on HSCs mRNA expression of procollagen types I and III and collagenase were investigated and deposition of types I and III collagen in different stages of fibrotic livers in rats was also observed.

Department of Gastroenterology, Zhongshan Hospital, Medical Center, Fu Dan University (Shanghai Medical University), Shanghai 200032, China
Dr. Ji Yao Wang, graduated from Shanghai Medical University in 1967 and got the Master Degree of Medicine in 1981, Shanghai; Master Degree of Science in 1986, Canada. She is the Chairperson of Dept. Internal Medicine; Chief of the Division of Gastroenterology; Director of the Lab of Internal Medicine, professor of internal medicine and supervisor of postgraduate students in the Zhongshan Hospital. She has published more than 100 articles and is the chief editor of *Modern Treatment on Liver Disease* and *Textbook of Internal Medicine* (for 7-year curriculum medical students). She is also the associate editor-in-chief of *Clinical Economics.*
Project supported by the National Natural Science Foundation of China, No.39500138
Correspondence to: Prof. Ji Yao Wang, Department of Internal Medicine, Zhongshan Hospital, Medical Center, Fu Dan University (Former Shanghai?Medical University), Shanghai 200032, China
Received 2000-06-08 **Accepted** 2000-08-19

MATERIALS AND METHODS

Animal model of liver fibrosis and drug treatment

Adult SD rats weighing 250 g-300 g were selected. They were distributed as the normal group, the model group, and the GA group. Each group contained the early (2 weeks), middle (6 weeks), and late stage (9 weeks) subgroups. There were 30 rats in each group and 10 rats in each subgroup. The liver fibrosis model was induced by the administration of CCl_4 and alcohol. Potenlini, an injectable compound whose active component is GA, was administered introperitoneally in the GA group with 3 mL per rat three times a week, begining at 2 weeks prior to sacrifice. Rats were killed by the end of 2, 6 and 9 weeks respectively.

Isolation and culture of HSCs

HSCs were isolated from rat liver as described by Hu[19] with slight modifications. The HSCs showed a typical stellate-like shape containing fat droplet in cytoplasm. During the culture period, HSCs became larger and contained less amounts of fat droplet. By the end of 2 weeks, HSCs looked like myofibroblast. Cells were seeded in culture flask and maintained in DMEM media supplemented with 20% FCS and antibiotics. The media was changed every 48 h. After 2 weeks, when cell confluence was attained, they were harvested by the trypsinized method and applied to further studies or stored in liquid nitrogen.

Identification of HSCs

Freshly isolated HSCs could be distinguished by its autofluoresence characteristic of vitamin A in the lipid droplets at 328 NM. Immunohistochemistry showed that desmin and α-SMA were positive in 99% of cells after 2 weeks of culture. Besides, transmission electron microscopy confirmed the existence of lipid droplet in cytoplasm and revealed a purification of about 90% in freshly isolated cells.

^{3}H-TdR and ^{3}H-proline incorporating test

After two weeks of culture, the HSCs were collected and seeded on 96-well culture plates at a density of 1 × 10^5 cells/mL cultured media. Forty-eight hours later, GA (i.e.potenlini) was added into wells at a final concentration of 1.0, 0.5, 0.25, 0.125 and 0.0625 mg/L, respectively, and incubated for 4 h, 24 h or 48 h, then ^{3}H-TdR or ^{3}H-Proline at a density of 18.5 KBq/per well were added and incubated for 24 h. The cells were then harvested with trypsin and the adhered cells were placed into glass fiber filter by multiple cell collector. The cells were baked at 80℃ for 2 h, scintillation fluid was added and the radioactivity in the cells was determined using scintillation counter.

Plasmid amplification and probe labeling

Plasmid pUCAU1U (containing procollagen type I cDNA fragment)[20], pHFS3 (containing procollagen type III Cdna fragment)[21], and pUC19A (containing collagenase cDNA fragment)[22], were amplificated in LB culture media. The plasmid DNA was extracted with a plasmid extracting kit (QIAGEN Incorporation, Germany). Plasmid was cleaved with restriction endonuclease and the target cDNA fragment was retrieved and phenolized. The cDNA fragment was labeled with DIG high primer technique (Boehringer Maannheim Incorparation,Germany). The probe was further purified by ethanol precipitation. Finally, the efficiency of probe labeling was determined using pseudo-hybridization, the optimal probe concentration of procollagen types I and III and collagenase was found to be 25, 35 and 25ìg/L respectively.

RNA extraction and Northern blot

HSCs RNA was extracted with a Rneasy mini-kit (Boehringer Maannheim Incorparation, Germany). Total RNA 5 μg was electrophorized on a 1% agarose/ 3% formadehyde gel. The RNA samples were stained with ethidium bromide and transferred overnight by capillary blotting in 20 × SSC to nylon membrane. The RNA was immobilized by baking for 30 min, at 120℃. Membranes were prehybridized (2 h) and hybridized (overnight) at 60℃ in high SDS solution. The membranes were washed at a stringency of 2 × SSC with 0.1% SDS at room temperature for 30 min and 0. 1 × SSC with 0.1% SDS at 68℃ for 30 min. The hybridization band was obtained by the chemoiluminescent method after film exposure for 5-10 min and then quantified by the scanning laser densitomitry.

Dot blots of types I and III collagen

The types I and III collagens were isolated by limited pepsin digestion. The livers were minced and homogenized thoroughly in cold distilled water and then centrifuged at 12 000rpm for 20 min. The precipitate (5 g) was suspended in 0.5M acetic acid and digested with pepsin for 24 h at 4℃ with stirring, and then centrifuged. The supernatant was incubated with NaCl (1.0M) overnight. The precipitate contained types I and III collagen which were purified by salt fractionation and their concentration was estimated by ultraviolet spectroscopy. Twenty μL of each sample was loaded on PVDF membrane and was blocked with 10% BSA for 60 min. The polyclonal antibodies (1:250 dilution) of types I and III collagen were added and incubated overnight. The membrane was then washed with PBST 3 times and blocked again with 10% BSA for 30 min. It was then incubated with the secondary antibody for 2 h at room temperature. After washing with 50mM Tris-HCl, the dot was obtained 5-10 min after incubation with DAB. The dot intensity was quantified by scanning laser densitomitry.

Statistical analysis

Data were expressed as mean ± SD. One way ANOVA and *t* test were applied for data analysis.

RESULTS

Histological examination and identification of HSCs

Histological examination (H&E and collagen specific staining) revealed the successful establishment of the rat liver fibrosis models at different stages. Two weeks after CCl_4 and ethanol treatment, denaturation and necrosis were the main microscopic changes in liver. By 6 weeks, except for denaturation, connective tissues began to enlarge and extend. By 9 weeks, pseudo-nodules formed and bands of connective tissues were found in the portal areas. The yield of HSCs was 1.6-1.8 × 10^7 cells per liver. The result of transmission electron microscopy, fluorescence microscopy (Figure 2) and immnohistochemical staining all showed that the purity of HSCs was high, which met the demand of further studies.

^{3}H-TdR and ^{3}H-proline incorporating test

Compared with the control group, GA had an inhibitory effect on cultured HSCs on incorporation of ^{3}H-TdR and ^{3}H-proline at 4 h, 24 h, and 48 h (Table 1), with a time dependent relationship. This inhibitory effect was significant in a dose-dependent manner when the concentration of GA was above 0.25 mg/L (^{3}H-TdR), and 0.125 mg/L (^{3}H-proline), respectively (Table 2).

Table 1 Effect of GA treatment with different duration on ^{3}H-TdR and ^{3}H-proline incorporation of HSCs

Drug	Duration (hrs)	^{3}H-TdR incorporation		^{3}H-proline incorporation	
		cpm	Inhibition rate(%)	cpm	Inhibition rate(%)
None		1540 ± 120		542 ± 102	
GA	4	1327 ± 198	15[a]	421 ± 16	22[a]
	24	1217 ± 254	21[a]	316 ± 18	42[b]
	48	1057 ± 121	31[b]	265 ± 84	51[b]

[a] Compared with control values, $P<0.05$; [b] Compared with control values, $P<0.01$.

Table 2 Effect of GA of different doses on ^{3}H-TdR and ^{3}H-proline incorporation of HSCs

Drug	Duration (hrs)	^{3}H-TdR incorporation		^{3}H-proline incorporation	
		cpm	Inhibition rate(%)	cpm	Inhibition rate(%)
None		1540 ± 120		542 ± 102	
GA	0.0625	1427 ± 175	7	441 ± 76	19[a]
	0.125	1321 ± 126	14	327 ± 71	40[b]
	0.25	1211 ± 137	21[a]	316 ± 57	42[b]
	0.5	1176 ± 134	24[a]	295 ± 81	46[b]
	1.0	1027 ± 121	33[b]	220 ± 63	59[b]

[a]Compared with control values, $P<0.05$; [b]Compared with control values, $P<0.01$.

Plasmid amplification and probe labeling

The purity of extracted plasmid DNA was high, and the ratio OD260/OD280 was over 1.6. The DNA yield of three kinds of plasmid all exceeded 130 μg. Electrophoresis showed that the yield of DNA fragment, which was cleaved with restriction enzyme, was satisfactory. On the other hand, the probe concentration of type I and III procollagen and collagenase was determined to be 15 mg/L, 35 mg/L and 100 mg/L, respectively.

The effect of GA on HSCs mRNA expression of types I and III procollagen and collagenase

At the end of 2, 6 and 9 weeks after the induction of rat liver fibrosis, HSCs mRNA expression of types I and III procollagen in the model group was higher than in normal group ($P<0.05$). However, HSCs mRNA expression of types I and III procollagen in GA group was lower than that in the model group, but was higher than the normal group (GA group vs model group and GA group vs normal group, $P<0.05$). HSCs mRNA expression of collagenase in the model group was higher than in normal group at each stage of liver fibrosis ($P<0.05$). And at the end of 9 weeks, the mRNA expression of HSCs showed a dropping tendency. HSCs mRNA expression of collagenase in GA group was also higher than in normal group, but there was no difference between the GA and the model group (Figure 1).

The effect of GA on liver deposition of types I and III collagen

At the end of the 2nd, 6th and 9th week, the liver deposition of types I and III collagen in the model group was higher than in normal group ($P<0.05$). The liver deposition of types I and III collagn in GA group was lower than in model group ($P<0.05$), but was still higher than in the normal group. In addition, the density of type I and III collagen in treatment groups were closer to the model group at the end of the 9th week than at the 2nd and 6th weeks (Figure 2).

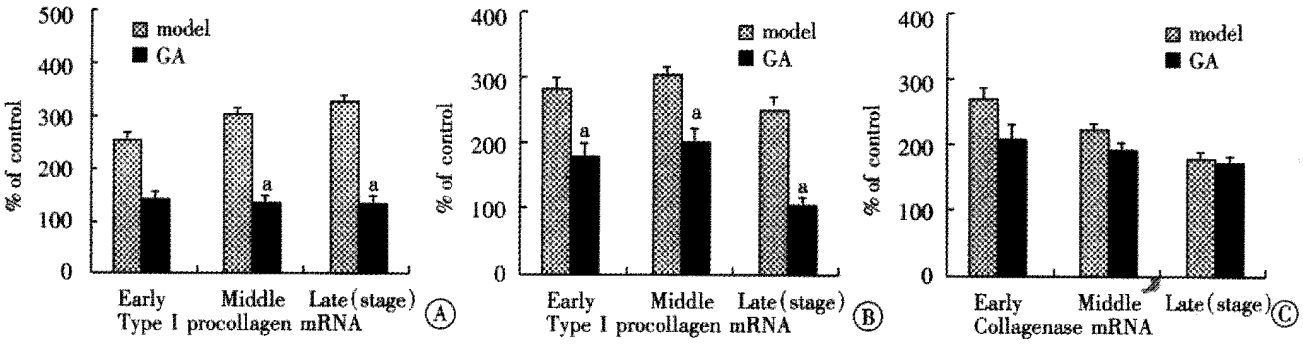

Figure 1 Densitometric analysis of collagenase, type III and I procollagen mRNA Northern blot. The result of Densitometric analysis after normalization against hybridization signals for normal groups was expressed as mean percentage ± SD of the control values (n = 5). The level of types I and III procollagen mRNA expression of HSCs in GA groups was lower than in model groups ([a]$P<0.05$). For the collagenase mRNA expression of HSCs, there was no significant difference between GA groups and model groups.

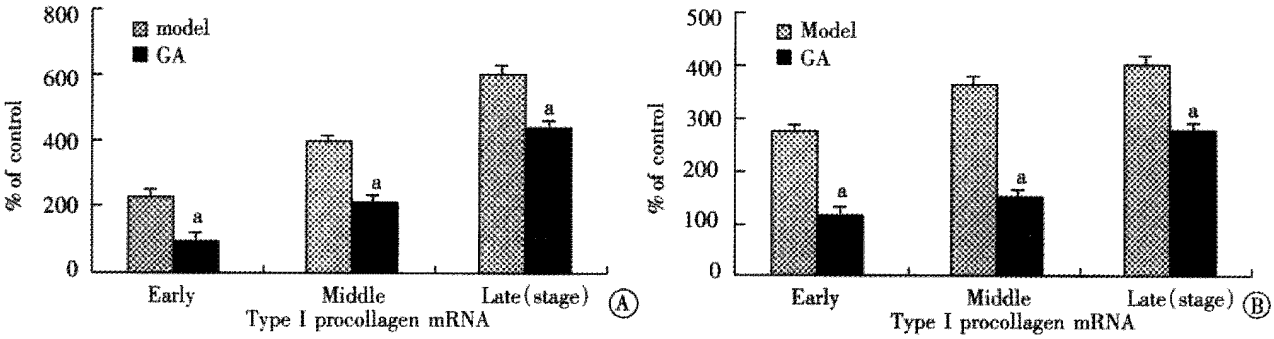

Figure 2 Dot blot densitometric analysis of types I and III collagen. The result of densitometric analysis after normalization against hybridization signals for normal groups was expressed as mean percentage ± SD of the control values (n = 5). The level of types I and III collagen densitometric values in GA groups was lower than in model groups ([a]$P<0.05$).

DISCUSSION

In normal livers, HSCs are situated in the Disse£§s spaces, separating hepatocytes from sinusoidal endothelium and being rich in fat drips. It has been well known that HSCs are responsible for the excessive production of ECM[23-25]. The central event in liver fibrosis is the activation of HSCs and subsequent transformation from quiescent vitamin A-rich cells to proliferative, fibrogenic and contractile myofibroblasts[26]. *In situ* hybridization demonstrated the specific transcript of procollagen[27,28]. It is rationale to choose HSCs as a target for pharmacological therapies for anti-fibrosis of liver. In this study, we observed that GA had an inhibitory effect on proliferation and collagen production of HSCs *in vitro*, which could be associated with the inhibition of activation of HSCs. The activation of HSCs is a pleiotrofic process. It involves a series of gene transcriptions. Finally, HSCs display a shape that is similar to myofibroblast-like cells while addition of GA delayed the transformation of HSCs into myofibroblast-like cells. It suggests that GA could serve as a proximal segment modulator to decrease the activation and collagen production of HSCs in culture.

It has been proved that the expression of type I and III procollagen is up-regulated in hepatic fibrosis [29,30]. In this study, we demonstrated that the expression of types I and III procollagen of HSCs increased in hepatic fibrosis of rats. At the end of the 2nd, 6th and 9th week, the expression of types I and III procollagen was down-regulated in GA treated group, but still higher than in normal group, which indicates that GA only decreases the expression of types I and III procollagen partially. We have previously reported that GA inhibits nuclear factor-κB (NF-κB) binding activity[31]. NF-κB is a pleiotropic transcription activator[33] that exists in many kinds of cells[32]. It binds NF-κB inhibitors (IκB) in the cytoplasm as an inactive form. A wide spectrum of cellular stimulating signals, including mitogen, cytokines, bacterial lipopolysaccharides, viruses and viral proteins, and oxidative injury, could induce the activity of NF-κB[34]. Inducers of NF-κB activity resulted in phosphorylation, ubiquitination and degradation of IκB proteins, thus releasing free NF-κB for its translocation into the nucleus to activate transcription. We presume that by this way, GA can down-regulate the expression of types I and III procollagen of HSCs. In normal liver, the production of collagen is relatively static, and only with moderate expression of mRNA of type III and IV procollagen and laminin. The mRNA expression of type I procollagen increased significantly in the formation of hepatic fibrosis. The ratio of type I:III was about 4:1[35] as observed in our study.

Recently, it has been found that the activity of interstitial collagenase is elevated in the early stage of hepatic fibrosis[23]. However, in the development of fibrosis, the activity of collagenase decreased[36-40]. In our study, the activity of collagenase increased at the early and middle stage of fibrosis, i.e. 2 or 6 weeks after CCl_4 treatment. At the end of the 9th week (late stage), it dropped to the level similar to that of normal groups. It could be due to the overexpression of tissue inhibitor of metalloproteinase in late stage of hepatic fibrosis[41,42]. GA reduced the mRNA expression of types I and III procollagen of HSCs, but not elevated the mRNA expression of collagenase of HSCs, which indicates that GA decreases the deposition of types I and III collagen by reducing the production of collagen, instead of dissolving the collagen. Therefore, at the end of the 9th week, GA was unable to obviously decrease the deposition of collagen. It suggested that the treatment for hepatic fibrosis with GA should begin at the early stage of fibrosis.

Based on the well-known mechanism of fibrosis, the treatment of fibrosis should include the following elements: removing the injurious stimuli; suppressing the hepatic inflammation; down-regulating the stellate cell activation and promoting the matrix degradation[26]. As we know, the major etiological factor of cirrhosis in patients in China is chronic hepatitis B. Histological improvement was found in the patients responding to antiviral therapy with lamivudine for HBV[43]. The result of a long-term follow-up study suggested that the proliferation of fibrous tissues was reversible[44]. Sun *et al*[45] indicated that antifibrotic therapy is important even in cirrhotic stage in which the fibrogenesis is still active. The results of our studies indicated that the effects on antifibrosis of GA might be exerted by down-regulating the binding activity of NF-κB and HSC activation, and by suppressing the hepatic inflammation. Our previous study also showed that the effect of GA on serum conversion of HBeAg[14]. Sato *et al*[46] reported that GA could inhibit the release of HBsAg from the infected hepatocytes. Therefore, GA appears to function at multiple phases of hepatic fibrogenesis. Furthermore, the more exciting report is that GA treatment could inhibit the occurrence of hepatocellular carcinoma[47]. It has been also reported that long term (2-16 years.) treatment by GA in chronic hepatitis C patients had no side-effect and was effective in preventing liver carcinogenesis[48].

Other Chinese herbal recipes have shown their features in antifibrosis. Varieties of recipes or herbal extracts, such as Xiao Chaihu Tang[49], Recipe 861[50], Yiganxian[51], Ganyanping[52], and Matrine[53] have been shown to be effective in prevention and treatment of liver injury and fibrosis with different mechanism and pathway. It implies that the clinical application using the combination of glycyrrhetinic acid with these medicines is an

interesting area for further investigations.

In conclusion, GA inhibits the proliferation and collagen production of HSCs in culture, down-regulates the mRNA expression of type III and I procollagen, and reduces the deposition of type III and I collagen in fibrotic liver. It can be a very useful drug for anti-fibrotic treatment in patients with chronic liver disease.

ACKNOWLEDGEMENTS The authors would like to thank Dr. EdgarLiu (Dept. of Pharmacology, Hong Kong University) and Dr. Xia Hua Xiang (Dept. of Medicine, Queen Mary Hospital, Hong Kong University) for their review of the mamuscript.

REFERENCES

1 Scott JE, Bosworth TR, Cribb AM, Gressner AM. The chemical morphology of extracellular matrix in experimental rat liver fibrosis resembles that of normal developing connective tissue. *Virchows Arch*, 1994;424:89-98
2 Kovalszky I. Fibrogenesis in the liver-afibrosis, cirrhosis. *Orv Hetil*, 1993; 134:59-64
3 Schuppan D. Structure of the extracellular matrix in normal and fibrotic liver: collagens and glycoproteins. *Semin Liver Dis*, 1990;10:1-10
4 Friedman SL, Roll FJ, Boyles J, Bissell DM. Hepatic lipocytes:the principal collagen-producing cells of normal rat liver. *Proc Natl Acad Sci USA*, 1985;82:8681-8685
5 Arenson DM, Friedman SL, Bissell DM. Formation of extracellular matrix in normal rat liver: lipocytes as a major source of proteoglycan. *Gastroenterology*, 1988;95:441-447
6 Pierce RA, Glaug MR, Greco RS, Mackenzie JW, Boyd CD, Deak SB. Increased procollagen mRNA levels in carbon tetrachloridea-induced liver fibrosis in rats. *J Biol Chem*, 1987;262:1652-1658
7 Maher JJ, McGuire RF. Extracellular matrix gene expression increases preferentially in rat lipocytes and sinusoidal endothelial cells during hepatic fibrosis *in vivo*. *J Clin Invest*, 1990;86:1641-1648
8 Shibayama Y. Prevention of hepatotoxic responses to chemicals by glycyrrhizin in rats. *Experiment Molecul Pathol*, 1989;51:48-55
9 Wang Z, Okamoto M, Kurosaki Y, Nakayama T, Kimura T. Pharmacokinetics of Glycyrrhizin in rats with Da-Galactosaminea-induced hepatic disease. *Biol Pharm Bull*, 1996;19:901-904
10 Nose M, Ito M, Kamimura K, Shimizu M, Ogihara Y. A comparison of the antihepatotoxic activity between glycyrrhizin and glycyrrhetinic acid. *Planta Med*, 1994;60:136-139
11 Pompei R, Flore O, Marccialis MA, Pani A, Loddo B. Glycyrrhizic acid inhibits virus growth and inactivates virus particles. Nature(London), 1979; 281:689
12 Takahara T, Watanabe A, Shiraki K. Effects of glycyrrhizin on hepatitis B surface antigen: a biochemical and morphological study. *J Hepatol*, 1994; 21:601-609
13 Crance JM, Leveque F, Biziagos E, van Cuyck-Gandre H, Jouan A,Deloince R. Studies on mechanism of action of glycyrrhizin against hepatitis A virus replication in vitro. *Antiviral Res*, 1994;23:63-76
14 Wang JY, Liu HY, Wu DC, Xia DQ. RCT of potenlin for treatment of chronic active hepatitis B. *Zhonghua Chuanranbing Zazhi*, 1991;4:207-210
15 Suzuki H, Ohza Y, Takino Y, Fujusawa K, Hirayama C. Effects of glycyrrhizin on biochemical tests in patients with chronic hepatitis: double blind trial. *Asian Med J*, 1983;23:423
16 Rossum TGV, Vulto AG, Hop MC, Brouwer JT, Niesters HG, Schalm SW. Intravenous glycyrrhizin for the treatment of chronic hepatitis C: A doublea-blind, randomized, placeboa-controlled phase I/IItrial. *J Gastroenterol Hepatol*, 1999;14:1093-1099
17 Wang JY, Liu WT, Hu MY, Zhu WN, Tong JQ. The inhibitory effect of procollagen type (r) mRNA expressions of fibroblasts by glycyrrhizin acid (Potenlini). *Zhonghua Xiaohua Zazhi*, 1997;17:60-61
18 Guo JS, Wang JY, Liu WT, Yu ZY. Effects of Potenlini on mRNA expression of procollagen type (r) in CCla-4 plus ethanol induced liver injury and hepatic fibrosis in rats. *Weichangbingxue He Ganbingxue Zazhi*, 1998;7:173-177
19 Hu MY, Liu WT, Wang JY, Zhu WN. Isolation and identification of fata-storing cells from fibrous dog liver with a modified centrifugation. *Shanghai Yike Daxue Xuebao*, 1996;23:375-377
20 Mäkelä JK, Raassina M, Virta A, Vuorio E. Human Pro α1(I) collagen: cDNA sequence for the C propeptide domain. *Nucleic Acids Res*, 1988;16:349
21 Sandberg M, Makela JK, Multinaki P. Construction of a human alpha 1(III) collagen cDNA clone and localization of type III collagen expression in fetal tissues. *Matrix*, 1989;9:82
22 Quinn CO, Scott DK, Brinckerhoff CE, Matrisian LM, Jeffrey JJ, Partridge NC. Rat collagenase: cloning, amino acid sequence comparison, and parathyroid hormone regulation in osteoblastic cells. *J Biol Chem*, 1990;265: 22342-22348
23 Maher JJ, McGuire RF. Extracellular matrix gene expression increases preferentially in rat lipocytes and sinusoidal endothelial cells during hepatic fibrosis *in vivo*. *J Clin Invest*, 1990;86:1641-1648
24 Nakatsukasa H, Nagy P, Evarts RP, Hsia CC, Marsden E, Thorgeirsson SS. Cellular distribution of transforming growth factor-β 1 and procollagen types III, and I transcripts in carbon tetrachloride-induced rat liver fibrosis. *J Clin Invest*, 1990;85:1833-1843
25 Wu J, Zern MA. Hepatic stellate cells: a target for the treatment of liver fibrosis. *J Gastroenterol*, 2000;35:665-672
26 Li D, Friedman SL. Liver fibrogenesis and the role of hepatic stellate cells: New insights and prospects for therapy. *J Gastroenterol Hepatol*, 1999;14:618-633
27 Goddard CJR, Smith A, Hoyland JA, Baird P, McMahon RFT, Freemont AJ, Shomaf M, Haboubi NY, Warnes TW. Localisation and semiquantitative assessment of hepatic procollagen mRNA in primary biliary cirrhosis. *Gut*, 1998;43:433-440
28 Ramm GA, Nair VG, Bridle KR, Shepherd RW, Crawford DHG. Contribution of hepatic parenchymal and nonparenchymal cells to hepatic fibrogenesis in biliary atresia. *Am J Pathol*, 1998;153:527-535
29 Ma J, Zhai WR, Zhang YE, Zhou YM, Du WD. Significance of collagen III in human and rat liver fibrosis. *Shanghai Yike Daxue Xuebao*, 1995;22:245-249
30 Friedman SL. The cellular basis of hepatic fibrosis: mechanisms and treatment strategies. *New Eng J Med*, 1993;328:1828-1835
31 Wang JY, Guo JS, Li H, Liu SL, Zern MA. Inhibitory effect of glycyrrhizin on NF-κB binding activity in CCl_4-plus ethanola-induced liver cirrhosis in rats. *Liver*, 1998;18:180-185
32 Sun SC, Ganchi PA, Ballard DW, Greene WC. NF-κB controls expression of inhibitor IκBα: Evidence for an inducible autoregulatory pathway. *Science*, 1993;259:1912-1915
33 Baldwin AS. The NF-κB and IκB proteins: new discoveries and insights. *Ann Rev Immunol*, 1996;14:649-681
34 Meyer M, Caselmann WH, Schlüter V, Schreck R, Hofschneider PH, Baeuerle PA. Hepatitis B virus transactivator MHBs^t: activation of NF-κB, selective inhibition by antioxidants and integral membrane localization. *EMBO J*, 1992;11:2991-3001
35 Pierce RA, Glang MR, Greco RS, Mackenzie JW, Boyd CD, Deak S. Increased procallogen mRNA levels in carbona-tetracloridea-induced liver fibrosis in rats. *J Biol Chem*, 1987;262:1652-1658
36 Maruyama K, Feinman L, Fainsilber Z, Nakano M, Okazaki I, Lieber CS. Mammalian collagenase increases in early alcoholic liver disease and decreases with cirrhosis. *Life Sci*, 1982;30:1379-1384
37 Perez-Tamayo R, Montfort I, Gonzalez E. Collagenolytic activity in experimental cirrhosis of the liver. *Exp Mol Pathol*, 1987;47:300-308
38 Gimenez A, Pares A, Alie S, Camps J, Deulofeu R, CaballerÍa J, Rodes J. Fibrogenic and collagenolytic activity in carbon-tetrachloridea-injured rats: beneficial effects of zinc administration. *J Hepatol*, 1994;21:292-298
39 Wang AM, Wang BN, Dong ZH, Li XM. Dynamic change of the activity of interstitial collagenase in experimental liver fibrosis. *Chin J Dig*, 1998;18:213-216
40 Murawaki Y, Koda M, Yamada S, Kawasaki H, Shima H, Burkhardt H. Serum collagenase activity in patients with chronic liver disease. *J Hepatol*, 1993;18:328-334
41 Benyon RC, Iredale JP, Goddard S, Winwood PJ, Arthur MJP. Expression of tissue inhibitor of metalloproteinases 1 and 2 is increased in fibrotic human liver. *Gastroenterology*, 1996;110:821-831
42 Murawaki Y, Ikuta Y, Idobe Y, Kitamura Y, Kawasaki H. Tissue inhibitor of metalloproteinase-1 in the liver of patients with chronic liver disease. *J Hepatol*, 1997;26:1213-1219
43 Lai CL, Chien RN, Leung NWY, Chang TT, Guan R, Tai DI, Ng KY, Wu PC, Dent JC, Barber J, Stephenson SL, Gray DF. A onea-year trial of lamivudine for chronic hepatitis B. Asia Hepatitis Lamivudine Study Group. *N Engl J Med*, 1998;339:61-68
44 Yan JC, Ma Y, Chen WB, Shun XH. Dynamic observation on liver fibrosis and cirrhosis of hepatitis B. *Huaren Xiaohua Zazhi*, 1998;6:699-702
45 Sun DL, Sun SQ, Li TZ, Lu XL. Serologic study on extracellular matrix metabolism in patients with viral liver cirrhosis. *Shijie Huaren Xiaohua Zazhi*, 1999;7:55-56
46 Sato H, Goto W, Yamamura J, Kurokawa M, Kageyama S, Takahara T, Watanabe A, Shiraki K. Therapeutic basis of glycyrrhhizin on chronic hepatitis B. *Antiviral Res*, 1996;(30):171-177
47 Shiota G, Harada K, Ishida M, Tomie Y, Okubo M, Katayama S, Ito H, Kawasaki H. Inhibition of hepatocellular carcinoma by glycyrrhizin in diethylnitrosamine-treated mice. *Carcinogenesis*, 1999;20:59-63
48 Arase Y, Ikeda K, Murashima N, Chayama K, Tsubota A, Koida I, Suzuki Y, Saitoh S, Kobayashi M, Kumada H. The long term efficacy of glycyrrhizin in chronic hepatitis C patients. *Cancer*, 1997;79:1494-1500
49 Shimizu I, Ma YR, Mizobuchi Y, Liu F, Miura T, Nakai Y, Yasuda M, Shiba M, Horie T, Amagaya S, Kawada N, Hori H, Ito S. Effects of Shosaiko-to, a Japanese herbal medicine, on hepatic fibrosis in rats. *Hepatology*, 1999;29:149-160
50 Wang BE, Wang TL, Jia JD, Ma H, Duan ZP, Li ZM. Experimental and clinical study on inhibition and reversion of liver fibrosis with integrated Chinese and Western medicine. *Chin J Integrated Tradit Western Med*, 1999;5:6-11
51 Li BS, Wang J, Zhen YJ, Wang XG, Sun YH, Wang SQ, Wu ZQ. Blocking effect of Chinese herbs Yiganxian and PHGF on immuno-damaged hepatic fibrosis in rats. *Huaren Xiaohua Zazhi*, 1998;6:786-788
52 Du LJ, Tang WX, Dan ZL, Zhang WY, Li SB. Protective effect of Ganyanyping on CCla-4 induced liver fibrosis in rats. *Huaren Xiaohua Zazhi*, 1998;6:21-22
53 Liang P,Bo AH,Xue GP, Han R, Li HF, Xu YL. Study on the mechanism of matrine on immune liver injury in rats. *Shijie Huaren Xiaohua Zazhi*, 1999;7: 104-108

Edited by Ma JY

P.O.Box 2345 Beijing 100023, China
Fax. 0086·10·65891893 Tel. 0086·10·65897901
E-mail.wcjd@public.bta.net.cn www.wd.org.cn

World J Gastroentero, 2001; 7(1):120 - 125
World Journal of Gastroenterology
Copyright © 2001 by the WJG Press ISSN 1007 - 9327

Expressions of ICAM-1 and its mRNA in sera and tissues of patients with hepatocellular carcinoma

Jing Xu[1], Ming Hui Mei[1], Si En Zeng[2], Qing Fen Shi[3], Yong Ming Liu[4] and Li Ling Qin[3]

Subject headings liver neoplasms/diagnosis; intercellular adhesion molecule-1; RNA, messenger; alpha-fetoprotein; immunohistochemistry; polymerase chain reaction; radioimmunoassay

Xu J, Mei MH, Zeng SE, Shi QF, Liu YM, Qin LL. Expressions of ICAM-1 and its mRNA in sera and tissues of patients with hepatocellular carcinoma. ***World J Gastroentero***, 2001;7(1):120-125

INTRODUCTION

The increased expression of ICAM-1 on a wide range of cells and in the sera of patients with malignancies, chronic liver diseases and inflammation diseases has been described since the late 1980s[1-22]. Recently rapid progress in studies on expression of ICAM-1 in patients with hepatocellular carcinoma (HCC) have been achieved, including clinical and experimental researches [23-31]. It is well known now that ICAM-1 expressed in two ways in HCC: ① membrane-bounded ICAM-1 on the surface of HCC cells (mbICAM-1), which did not express in normal liver cells, and ② soluble ICAM-1 (sICAM-1) in sera of the patients, the concentration of which is well correlated with the progress and prognosis of the disease[32]. However, little is known about whether sICAM-1 is a diagnostic marker for early detecting HCC and monitoring its postoperative recurrence. It has been demonstrated that measurement of sICAM-1 might be of clinical values for early diagnosis and monitoring recurrence of HCC, particularly in patients with normal or low serum level of α-fetoprotein (AFP)[33-37]. Another controversy in this field is what is the main source of high levels of circulating sICAM-1 in HCC patients. It was reported that there were two forms of sICAM-1: HCC-specific circulating form of ICAM-1 shedding from HCC cells, and inflammation-associated ICAM-1 upregulated by several cytokines, of which interferon-gamma (INF-gamma) was the main cytokine trigger for ICAM-1 expression[38]. To solve the two problems mentioned above has become the key to the study. For this purpose, we have further confirmed the clinical values of sICAM-1 detection in HCC compared with benign liver diseases and normal control, analyzed the serum levels of AFP and sICAM-1 in HCC; observed mbICAM-1 expression in different regions of HCC tissues with the immunohistochemistry, and measured the expression of ICAM-1 mRNA in tissue samples by reverse transcriptase polymerase chain reaction (RT-PCR).

MATERIALS AND METHODS

Patients

Between January 1997 and July 2000, 151 patients with pathologically proven HCC either by surgical resection of liver tumors or by liver biopsies (131 men and 20 women; aged from 14 to 80 years, median 49) were treated in our department. Tumor was less than 5 cm in diameter in 21 patients,less than 10 cm in 43 and more than 10 cm or with extrahepatic metastasis in 87 cases. Liver cirrhosis was found in 137 patients. Hepatitis B surface antigen (HBsAg) was positive in 129 patients. Hepatitis C antibody was positive in 14 patients. The serum concentration of AFP was measured in all cases by radioimmunoassay (RIA) and its reference ranges were classified as follows: >200 μg/L as positive in 93; 20 μg/L-200 μg/L as questionable positive in 33 and <20 μg/L as negative in 25[35]. Treatment included surgical procedures (in 90 cases), interventioanl radiology (IR in 46) and percuteneous ethanol injection (PEI in 15). Among the surgically-treated patients, tumor resection was performed in 75, including radical resection in 42, nonradical in 33 due to intrahepatic vascular invasion on the resected margin pathologically or intrahepatic metastasis of tumor found intraoperatively. Laparotomy cathterization of the hepatic artery was undertaken in 15. The 46 patients underwent IR therapies including transcatheter arterial embolization (TAE) in 30 and transcatheter arterial infusion (TAI) in 16.

Follow-up of the patients undergoing hepatectomies

The patients undergoing hepatectomies were followed up monthly in the first year and once every two months in the second year postoperatively. During the follow-up, serum concentration of AFP and sICAM-1, liver function and image

[1]Department of Hepatobiliary Surgery, [2]Department of Pathology, [3]Institute of Hepatobiliary Surgery, [4]Department of Biochemistry, Guilin 541001, Guangxi Province, China
Jing Xu, graduated from Tongji Medical University as a postgraduate, now associate professor, specialized in hepatology, having 15 papers.
Supported by the grant from the Guangxi Science and Technology Committee, No.9811003
Correspondence to: Dr. Jing Xu, 95 Leque Road, Department of Hepatobiliary Surgery, Guilin Medical College, Guilin 541001, Guangxi, China
Tel. 0086-773-2810411, Fax. 0086-773-2822194
Email. Jxu@gliet.edu.cn
Received 2000-09-01 **Accepted** 2000-09-29

examinations including BUS, CT or selective hepatic angiography were undertaken. Tumor recurrence was confirmed when intrahepatic lesion or portal vein tumor thrombi were found by liver image, and pathological diagnosis was established by reoperation or biopsy of the tumor.

ELISA for sICAM-1

Concentrations of sICAM-1 were measured with an enzyme-linked immunosorbent assay kit (Biosource Europe, Fleurus, Belgium) as described previously[31-37]. In all HCC patients, sICAM-1 levels were compared with their levels of serum AFP. As controls, serum levels of sICAM-1 were measured in 62 patients with chronic hepatitis B (CH), 60 with liver cirrhosis (LC) and 50 healthy blood donors.Immunohistochemistry of liver tissues -Tissues from tumor and adjacent region were obtained from 52 patients with surgical resection. Histologically normal liver tissues were obtained from 3 patients with liver hemangioma. To demonstrate the presence of ICAM-1 in the resected liver tissues, each fresh specimen was cut at -20℃ with the cryostat (4 μm- thick), mounted on sialinized adhesion microscope slides, dried overnight at room temperature, fixed with cold acetone (-20℃) for 10 min and chloroform for 20 min. Anti-human ICAM-1 mouse monoclonal antibody (Clone HA58, Pharmigen) was used. The slides were washed twice in TRIS/0.2% BSA and then incubated with sheep-anti-mouse-Ig (DAKO, Copenhagen, Denmark). And then the staining reaction was developed with a streptavidin-biotinylated-alkaline-phosphatase-complex (DAKO),slides were counterstained with hematoxylin, and nonreacting monoclonal antibody of IgG-1-isotype (DAKO) was used as negative control.

RNA extraction and DNA amplification

The total RNA was isolated from the fresh resected liver tissues by the acid guanidium thiocynate-phennol-chloroform method[39](Gstract, Maxim Biotech, Inc., San Francisco, USA). The concentration of RNA was determined from absorption at 260nm, and A 260: -80 ratios were > 1.7. RNA (10 μg)was subjected to electrophoresis in 1.5% agarose gels. The PCR primer for ICAM-1 and GAPDH were designed according to Vigano *et al*[40]. The following four primers presented by Dr. Shraven were used: ① (105) 5'-TGATGACATCAAGAAGGTGGTGAAG-3'; ② (1047)5'-TCCTTGAGGCCATGTGGGC-CAT-3'; ③ (825) 5'-GTCCCCTCAAAAGTCATCC-3'; ④ (1064) 5'-AACCCCATTCAGCGTCACCT-3'. The primer set was used to amplify an intron-spanning region of the human glyceraldeyde-3-phosphate dehydrogenase (GAPDH) gene. The latter gene provided a constitutively expressed internal control for complementary DNA contamination. The presence of ICAM-1 and GAPDH mRNAs was demonstrated by amplifying respective target sequences using PCR according to the instruction provided with the Technical Bulletin Kit (Promega). In brief, 3 μL (2.5 mM) RNA, and 50 pmol/L primers for ICAM-1 or GAPDH were added to each reaction mixture respectively, which included 0.4mM dNTPs 2 μL, 3 μL (1.5 mM) $MgSO_4$, AM V reverse transcriptase 1 μL (5U), TfI DNA polymerase 1 μL (5U), and AMV/TfI 5 × buffer 10 μL. The final reaction volume was 50 μL and was covered with 20 μL mineral oil. Then with PCR thermal cycle(Hema 480, China), RT-PCR reaction was run in the following procedures: ① 48℃ for 45 min, 1 circle; ② 94℃ for 2 min, 1 circle; ③ 94℃ for 30s, 60℃ for 1 min, 38℃ for 2 min, 30 circles; and ④ 68℃ for 7min, 1 circle. Five μL PCR product was placed on 1.5% agarose gel and observed by EB staining under UV light, the electrophoresis photo was transformed into computer, and ICAM-1 intensity was analyzed with MPIAS500 image system, while the GAPDH band intensity was subtracted as an internal standard.

Statistical analysis

Groups were compared by the Kruskal-Wallsi test and the *t* test.

RESULTS

sICAM-1 measurement

The concentrations of sICAM-1 measured in different groups are illustrated in Figure 1. The levels of sICAM-1 in the patients with CH (median -462 μg/L), LC (median-587 μg/L) and HCC (median -1120 μg/L) were significantly higher than that in the normal control (median -285 μg/L) (P<0.01). The levels of sICAM-1 in HCC group was also significantly higher than those in CH and LC groups (P<0.01).

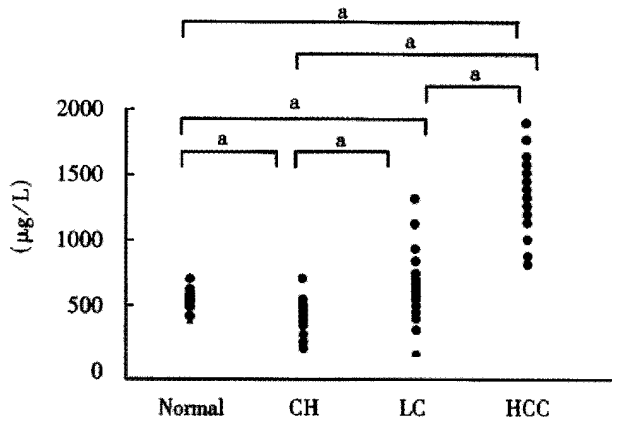

Figure 1 Serum concentration of sICAM-1 in normal controls (n = 50), in patients with chronic hepatitis (CH, n = 62), cirrhosis (LC, n=60), and hepatocellular carcinoma (HCC, n =151). ^aP<0.05, ^bP<0.01.

Comparative analysis of the serum values of sICAM-1 and AFP in HCC patients is listed in Table 1. There were 93 (62%) patients with positive serum AFP, and 58 (38%) with questionable and negative (33 and 25). However, the median values of sICAM-1 in these patients were 1597, 1456 and 1271 μg/L respectively. Statistical analysis showed no significant differences. In addition, analysis of ranges of sICAM-1 of HCC patients showed that 129 (85.4%) patients had a serum concentration exceeding 1000 μg/L, which was higher than the positive rate of serum AFP in the group of same patients.

Table 1 Comparative analysis of serum levels of sICAM-1 and AFP in HCC patients

Group	Number of patients	sICAM-1(μg/L)	AFP(μg/L)
AFP<20 μg/L	25	1271	18
AFP 20-200 μg/L	33	1456	121
AFP>200 μg/L	93	1597	26280

During the postoperative follow-up period of 6-61 months, tumor recurrence was confirmed in 41 patients. The median level of sICAM-1 of the patients was 1051 μg/L and 30 (73.2%) cases had a value higher than 1000 μg/L. On the other hand, there were 25 (60%) patients with serum AFP positive (>200 μg/L). In 6 patients with negative AFP, tumor recurrence was not detected by liver image until their serum levels of sICAM-1 had exceeded 2-4 times higher than before for 1-4 months.

Immunohistochemical staining

In all HCC samples, cancerous regions showed positive membrane staining for ICAM-1 with a honeycomb pattern (Figure 2). Parts of plasma of HCC cells showed strong positive reactions. In contrast to the cancerous areas, in noncancerous adjacent areas (Figure 3), the expression of ICAM-1 was negative, except those hepatocytes in severe cirrhotic areas. Normal liver tissue showed negative or very weak staining of the vascular endothelial cells and hepatocyts for ICAM-1 (Figure 4).

RT-PCR detection of ICAM-1

ICAM-1 mRNA in HCC tissues was detected by RT-PCR analysis (Figure 5). The result showed that freshly aspirated liver tissues expressed the gene coding for ICAM-1 because RT-PCR generated a DNA fragment corresponding to the predicted length, 943bp, of the ICAM-1 amplification product. In each tissue sample, all GAPDH amplification products were of 240bp length. The results revealed that the expression of ICAM-1 was stronger in the carcinomatous tissues of 28/43 cases (65.1%) than that in the paracacinomatous tissues of 13/43(30.2%) cases. Thirty-two of 43 cases had the levels of sICAM-1 >1000 μg/L.

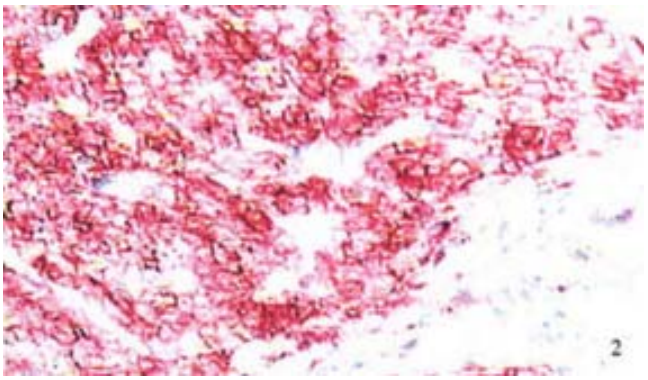

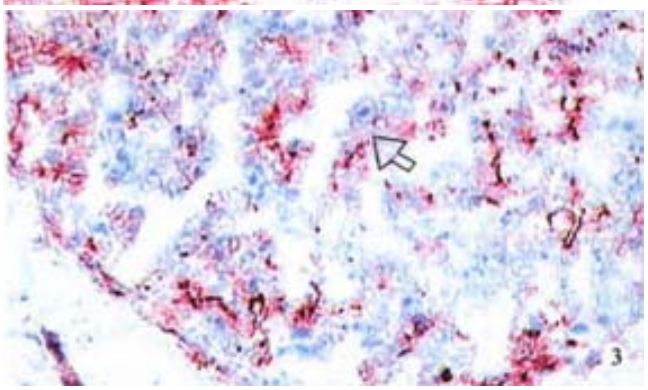

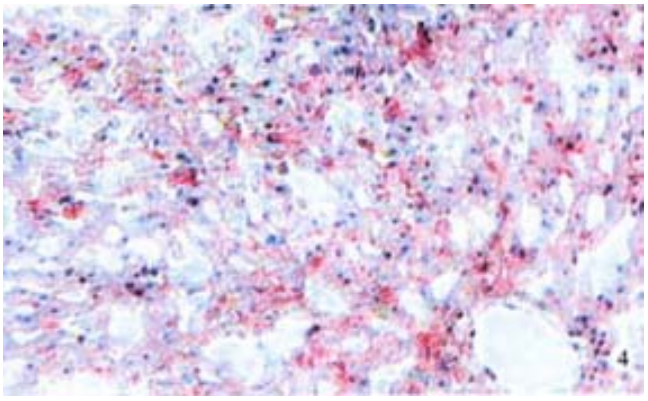

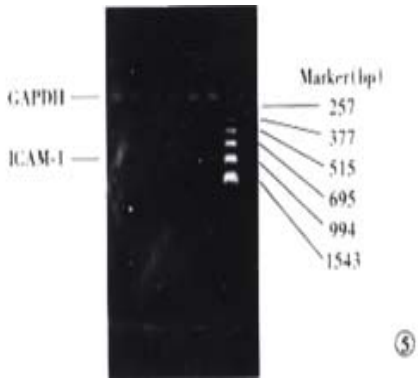

Figure 2 Immunohistochemical staining of ICAM-1 in hepatocellular carcinoma tissue is positive on the surface of tumor cells and in a honeycomb pattern.

Figure 3 Increased expression of ICAM-1 in paracancerous tissue was shown with severe cirrhosis by immunohistochemical staining.

Figure 4 ICAM-1 expression was negative in normal liver tissue by immunohistochemical staining (AEC method).

Figure 5 RT-PCR product gel electrophoresis. Three ìL RT-PCR products of ICAM-1 and GAPDH run on 1.5% agarose gel stained with EB. Lane 1 and Lane 4: the control for ICAM-1 and GAPDH. Lane 2 and 5: paracarcinomatous tissue for ICAM-1 and GAPDH. Lane and 6: HCC tissues for ICAM-1 and GAPDH.

The clinicopathological analysis of ICAM-1 mRNA and HCC is shown in Table 2. In the patients with serum levels of sICAM-1 above 1000 μg/L, the expression rates of ICAM-1 mRNA in HCC and adjacent tissues were 75.0% and 34.4%, respectively (P<0.01), however, in group with sICAM-1 lower than 1000 μg/L, the expression rate in those tissues were 36.4% and 18.2%, respectively (P>0.05). It is noticed that the expression rate of ICAM-1 mRNA was related to the severity of liver cirrhosis and intrahepatic metastasis of tumor. However, the expression rates of ICAM-1 mRNA were not correlated with the serum levels of AFP, differentiation of tumor and tumor sizes.

Table 2 Clinicopathological analysis of ICAM-1 mRNA and HCC %(n)

Clinical data	Cases	Positive tumor ICAM-1 mRNA	Positive paratumor ICAM-1 mRNA
Serum AFP>400 μg/L	25	68.0 (17/25)	32.0(8/25)
Serum AFP<400 μg/L	18	61.1(11/18)	27.8(5/18)
sICAM-1>1000 μg/L[a]	32	75.0(25/32)	34.4(11/32)
<1000 μg/L	11	36.4(3/11)	18.2(2/11)
Severe cirrhosis[a] Yes	30	80.0(24/30)	36.7(11/30)
No	13	30.8(4/13)	15.4(2/13)
Differentiation High	15	66.7(10/15)	33.3(4/15)
Low	28	64.3(18/28)	32.1(9/28)
Tumor size >5 cm	31	66.7(8/12)	25.0(3/12)
<5 cm	12	64.5(20/31)	32.3(10/31)
Intrahepatic metastasis[b] Yes	15	86.7(13/15)	40.0(6/15)
No	28	46.4 (13/28)	25.0(7/28)

[a]P<0.01; [b]P<0.05.

DISCUSSION

HCC is one of the malignancies, which inflicts Chinese population severely. The prognosis of the disease is still dismal due to a delayed diagnosis, low resected rate and high recurrence rate of the tumor. Thus early diagnosis and effective postoperative monitoring are important to improve the surgical effectiveness for HCC[41]. The present study further confirmed our previous observations and other reports, in which elevated serum sICAM-1 was found in HCC, which was significantly higher than in benign liver diseases and the normal controls (Figure 1). As described by Shimizu *et al*[42], a sICAM-1 level above 1000 μg/L is a determinant for prognosis and progression of HCC. In our 151 patients with HCC, 129 (85.4%) cases had a high serum concentration of ICAM-1 above 1000 μg/L, which suggested that the positivity of sICAM-1 was higher than that of serum AFP. Although the serum levels of AFP in the HCC patients were different (Table 1), the sICAM-1 levels in the same group of patients showed no significant differences, particularly in cases with low levels of or negative AFP, indicating that measurement of sICAM-1 might be of diagnostic value for HCC.

Another interesting finding from our study is that in patients with AFP negative or questionable positive, sICAM-1 is a more sensitive serum diagnostic marker than AFP and other procedures, including BUS, CT, etc. In 41 patients with tumor recurrence detected during the postoperative follow-up, 73.2% patients had a high level of sICAM-1 above 1000 μg/L, however, the proportion of positive serum AFP in the same cases was only 60%. Moreover, in 6 of the 41 patients with negative AFP, tumor recurrence was diagnosed 1-4 months earlier by sICAM-1 than by liver image examination. We believe that sICAM-1 is not only a useful marker for predicting the progression and prognosis of the disease, but also a sensitive marker for diagnosing and monitoring HCC and its recurrence, especially for patients with low serum concentrations of AFP when the serum level of sICAM-1 was above 1000 μg/L[32-36].

As mentioned above, our clinical observations strongly supported that sICAM-1 might be of diagnostic value for HCC. However, it is unknown what is the main source of high level of sICAM-1 in HCC: HCC- specific ICAM-1 shedding from mbICAM-1 or inflammation-associated ICAM-1[38]. To distinguish the two forms of ICAM-1 is the ultimate goal of the study in this field[38]. Clinically, we have got the evidence that sICAM-1 is derived from HCC tumor cells, because we found in non-radical resected patients, the sICAM-1 concentrations maintained at a high level after the operation compared with those who underwent a radical resection of tumors, whose sICAM-1 levels would be decreased to the normal within 1-2 months postoperatively. This suggested that circulating sICAM-1 in HCC may originate mainly from tumor cell itself[36,37].

To verify our clinical findings that sICAM-1 is mainly derived from the HCC cells, we investigated the expression of ICAM-1 in HCC and its adjacent tissues with immunohistochemistry. The results showed that ICAM-1 expressed strongly in all specimens of HCC, but did not express in noncancerous regions, which reflected such a fact that high serum sICAM-1 levels of HCC patients might be attributable to tumor cells and a malignant transformation of hepatocytes. Our inference was supported by other authors[24,30,43,44]. Torri and Momosaky reported a high expression rate of ICAM-1 in HCC (80%-96%). Although three possible mechanisms for the expression of ICAM-1 were considered, Torri *et al* hold that malignant transformation of liver cells appeared to be the most important mechanism for the ICAM-1 expression in HCC. Thus they concluded that examination of ICAM-1 might yield significant information on the process of malignant transformation of hepatocytes[41,43]. In the nude mouse liver cancer metastasis model, Sun JJ *et al* demostrated that tissue ICAM-1 and sICAM-1 could indicate the stage

of HCC, potential of hepatoma cells for invasion and metastasis[45]. In addition, *in vitro* study by Momosaky *et al* showed that HCC cell itself markedly secreted soluble ICAM-1 into the culture supernantant in tumor cell lines[43]. On the other hand, no soluble ICAM-1 was shed from normal mouse hepatocytes regardless of the presence or absence of cytokine stimuli[43]. According to the observations from the present and other studies mentioned above, we think that high levels of sICAM-1 in HCC patients might be released mostly from the tumor cells.

After the clinical and immunohistochemical studies, we have recently investigated the correlation between serum levels of sICAM-1 and expression of its mRNA in HCC tissues. The results (Table 2) suggested that hepatocytes transformation may be the essential cause for strong expression of ICAM-1 mRNA, as in carcinomatous tissues of the 43 patients, the positive rate of expression was 65.1% (28/43). However, that in non-carcinomatous tissues was only 30% (13/43), which was quite different from the HCC tissues ($P<0.01$), and in normal liver tissues expression of ICAM-1 mRNA did not exist. Furthermore, the same correlation between the expression of ICAM-1 mRNA and the serum concentrations of sICAM-1 was observed. In patients with serum levels of sICAM-1 above 1000 μg/L, the expression rates of ICAM-1 mRNA in HCC and adjacent tissues were 75% and 34.4%, respectively, however, in group with sICAM-1 lower than 1000 μg/L, the expression rates were 36.4% and 18.2% respectively, which indicated that the expression of ICAM-1 protein was controlled by its correlative gene at the level of transcription regulation.

The expression rate of ICAM-1 mRNA was also related to the severity of liver cirrhosis and intrahepatic metastasis of tumor. Particularly in the later circumstances, the expression rate was much higher in metastatic patients (86.7%) than those without metastasis (53.6%), which suggested that the expression of ICAM-1 mRNA may play an important role in tumor intra and extrahepatic spread. These results were identical to our clinical observations, in which the proportion of sICAM-1 level >1000 μg/L was higher than that of AFP (73. 2% vs 60%) and sICAM-1 level was more sensitive than liver image examinations in indicating tumor recurrence.

Based on our studies on expressions of ICAM-1 and its mRNA in serum and tissues of HCC, we concluded that: ① Serum levels of sICAM-1 in HCC were significantly higher than that in benign liver diseases and normal controls, which indicated that it is useful to measure sICAM-1 to differentiate HCC from other benign lesions when the level of sICAM-1 is higher than 1000 μg/L. ② The high expression level of sICAM-1 might result from the strong expression of ICAM-1 in HCC tissue, which was controlled by its related gene. The source of sICAM-1 in HCC was originated mainly from HCC cells. ③ In HCC with intrahepatic metastasis, the expression of ICAM-1 mRNA was significantly high, which suggested that detecting sICAM-1 is of important value in predicting tumor recurrence after surgery. ④ With understanding of the mechanism of ICAM-1 expression and its origination, we believe that measurement of sICAM-1 may be of diagnostic value for HCC, particularly in patients with low levels of serum AFP.

ACKNOWLEDGEMENT We gratefully acknowledge Prof. Meuer for his cooperation, Dr. Shraven for the primers of PCR; and Yong Ming Liu, and Si En Zen for their excellent works in this study.

REFERENCES

1 Marlin SD, Springer TA. Purified intercellular adhesion molecule-1 (ICAM-1) is a ligand for lymphocyte functiona-associated antigen 1 (LFA-1). *Cell*, 1987;51:813-819
2 Wang YJ, Sun ZQ, Yu JJ, Xu XZ, Zhang X, Quan QZ. Biological effects of type I and III collagens in human hepatocellular carcinoma tissue. *China Natl J New Gastroenterol*, 1995;1:18-20
3 Osborn L, Hession C, Tizard R, Vassallo C, Luhowskyl S, Chi-Rosso G, Lobb R. Direct expression cloning of vascular cell adhesion molecule 1, a cytokinea-induced endothelial protein that binds to lymphocytes. *Cell*, 1989;59:1203-1211
4 Staunton DE, Merluzzi VJ, Rothlein R, Barton R, Marlin S, Springer TA. A cell adhesion molecule, ICAM-1, is the major surface receptor for rhinoviruses. *Cell*, 1989;56:849-853
5 Adams DH, Hubscher SG, Shaw J, Rothlein R, Neuberger JM. Intercellular adhesion molecule 1 on liver allografts during rejection. *Lancet*, 1989;11:1122-1124
6 Vogetseder W, Feichinger H, Schulz TF, Schwaeble W, Tabaczewski P, Mitterer M, Böck G, Marth C, Dapunt O, Mikuz G, Dierich MP. Expression of 7F7-antigen, ahuman adhesion molecule identical to intercellular adhesion molecule-1 (ICAM-1) in human carcinomas and their stromal fibroblasts. *Int J Cancer*, 1989;43:768-773
7 Adams DH, Hubscher SG, Shaw J, Johnson GD, Babbs C, Rothlein R, Neuberger JM.Increased expression of intercellular adhesion molecule 1 on bile ducts in primary biliary cirrhosis and primary sclerosing cholangitis. *Hepatology*, 1991;14:426-431
8 Zöhrens G, Armbrust T, Pirzer U, zum Büschenfelde KHM, Ramadori G. Intercellular adhesion molecule-1 concentration in sera of patients with acute and chronic liver disease: relationship to disease activity and cirrhosis. *Hepatology*, 1993;18:798-802
9 Morita M, Watanabe Y, Akaike T. Inflammatory cytokines up-regulate intercellular adhesion molecule-1 expression on primary cultured mouse hepatocytes and T-lymphocyte adhesion. *Hepatology*, 1994;19:426-431
10 Hutchins D, Steel CM. Regulation of ICAM-1 (CD54) expression in human breast cancer cell lines by interleukin 6 and fibroblast-derived factors. *Int J Cancer*, 1993;58:80-84
11 Zhang BH, Wu MC. Evaluation of serum AFP-reactive-lentil lectin determined by its mAb in the diagnosis of hepatocellular carcinoma. *China Natl J New Gastroenterol*, 1995;1:33-36
12 Seth R, Raymond FD, Makgoba MW. Circulating ICAM-1 isoforms: diagnostic prospects for inflammatory and immune disorders. *Lancet*, 1991;338:83-84
13 Schwaeble W, Kerlin M, zum B¨1schenfelde KHM, Dippold W. De novo expression of intercellular adhesion molecule 1 (ICAM-1, CD54) in pancreas cancer. *Int J Cancer*, 1993;53:328-333
14 Voraberger G, Schäfer R, Stratowa C. Cloning of the human gene for intercellular adhesion molecule-1 and analysis of its 5-regulatory region: induction by cytokines and phorbol ester. *J Immunol*, 1991;147:2777-2786
15 Adams DH, Mainolfi E, Burra P, Neuberrger JM, Ayres R, Elias E, Rothlein R. Detection of circulating intercellular adhesion molecule-1 in chronic liver diseases. *Hepatology*, 1992;16:810-814
16 Chen J, Gong XY, Zhang YF. Clinical significance and immunogical measurement of cell adhesion molecules. *Guowai Yixue Mianyixue Fence*, 1993;6:310-313
17 Tanaka Y, Hayashi M, Takagi S, Yoshie O. Differential

transactivation of the intercellular adhesion molecule-1 gene promoter by Tax1 and Tax2 of human T-cell leukemia viruses. *J Virol*, 1996;70:8508-8517
18 Zhang JF, Zhang B, Liu SF. Clinical significance of soluble intercellular adhesion molecule-1. *Shanghai Mianyixue Zazhi*, 1994; 14:374-375
19 Chen GY, Cao XT, Yu YZ, Zhang WP, Tao Q. Interleukin (IL)-2. Or IL-4 gene transfer in human melanoma cell, expression and function of intercellular adhesion molecule-1. *Zhongguo Mianyixue Zazhi*, 1996;12:20-22
20 Muòoz C, Castellanos MC, Alfranca A, Vara A, Esteban MA, Redondo JM,de Landázuri MO. Transcriptional up-regulation of intracellular adhesion molecule-1 in human endothelial cells by the antioxidant pyrrolidine dithiocarbamate involves the actication of activating protein-1. *J Immunol*, 1996;157:3587-3597
21 Dustin ML, Springer TA. Lymphocyte function-associated antigen-1 (LFA-1) interaction with intercellular adhesion molecule-1 (ICAM-1) is one of at least three mechanisms for lymphocyte adhesion to cultured endothelial cells. *J Cell Biol*, 1988;107:321-331
22 Budnik A, Grewe M, Gyufko K, Krutmann J. Analysis of the production of soluble ICAM-1 molecules by human cells. *Experiment Hematol*, 1996;24:352-359
23 Tsujisaki M, Imai K, Hirata H, Hanzawa Y, Masuya J, Nakano T, Sugiyama T, Matsui M, Hinoda Y, Yachi A. Detection of circulating intercellular adhesion molecule-1 antigen in malignant diseases. *Clin Exp Immunol*, 1991;85:3-8
24 Torii A, Harada A, Nakao A, Nonami T, Ito M, Takagi H. Expression of intercellular adhesion molecule-1 in hepatocellular carcinoma. *J Surg Oncol*, 1993;53:239-242
25 Feng GS, Kramann B, Zheng CS, Zhou RM, Liang B, Zhang YF. Comparative study on the effects of hepatic arterial embolization with Bletilla Striata or gelfoam in the treatment of primary hepatic carcinoma. *China Natl J New Gastroenterol*, 1996;2:158-160
26 Wang D, Shi JQ. Overexpression and mutations of tumor suppressor gene p53 in hepatocellular carcinoma. *China Natl J New Gastroenterol*, 1996;2:161-164
27 Hu SX, Fang GY. Clinical use of hepatic carcinoma associated membrane protein antigen (HAg18-1) for detection of primary hepatocellular carcinoma. *China Natl J New Gastroenterol*, 1996; 2:165-166
28 Sun JJ, Zhou XD, Liu YK, Zhou G, Chen J, Tang ZY. Phasic expression of tissue intercellular adhesion molecule-1 in human liver cancer metastasis model in nude mice. *Zhonghua Shiyan Waike Zazhi*, 1999;16:155-156
29 Sun JJ, Zhou XD, Zhou G, Liu YK. Expression of intercellular adhesive molecule-1 in liver cancer tissues andliver cancer metastasis. *World J Gastroentero*, 1998;4:202-205
30 Sun JJ, Zhou XD, Liu YK, Zhou G. Phase tissue intercellular adhesion molecule-1 expression in nude mice human liver cancer metastasis model. *World J Gastroentero*, 1998;4:314-316
31 Xu J, Mei MH, Dai ZB. Significance of detecting intercellular adhesion molecule-1 in hepatocellular carcinoma. *Guowai Yixue Mianyixue Fence*, 1998;21:86-89
32 Mei MH, Xu J, Chen Q, Yang JH, Deng W, Shi QF, Tan LL. Measurement of serum and bile intercellular adhesion molecule-1 in patients with obstructive jaundice. *Huazhong Yixue Zazhi*, 2000; 24:2-3
33 Xu J, Mei MH, Shi QF. Clinical value of serum circulating intercellular adhesion molecule-1 in hepatocellular carcinoma. *Zhonghua Shiyan Waike Zazhi*, 1998;15:514-515
34 Mei MH, Xu J, Shi QF, Chen Q, Qin LL. Measurement of serum circulating intercellular adhesion molecule-1 and its clinical significance in hepatocellular carcinoma. *J Hepatobiliary Pancreat Surg*, 1999;6:181-185
35 Mei MH, Xu J, Shi QF, Yang JH, Chen Q, Qin LL. Clinical significance of serum intercellular adhesion molecule-1 detection in patients with hepatocellular carcinoma. *World J Gastroenterol*, 2000; 6:408-410
36 Xu J, Mei MH, Shi QF. Combining with sevral marks for diagnosis of primary in hepatocellular carcinoma. *Huazhong Yixue Zazhi*, 2000;24:81-82
37 Hyodo I, Jinno K, Tanimizu M, Doi T, Nishikawa Y, Hosokawa Y, Moriwaki S. Intercellular adhesion molecule-1 release from human hepatocellular carcinoma. *Cancer Detection Prevention*, 1996;20:308-315
38 Chomczynski P, Sacchi N. Single-step method of RNA isolation by acid guanidinium thiocyanate-phenol-chloroform extraction. *Analyt Biochem*, 1987;162:156-159
40 Viganñ P, Gaffuri B, Ragni G, Di Blasio AM, Vignali M. Intercellular adhesion molecule-1 is expressed on human granulosa cells and mediates their binding to lymphoid cells. *J Clinic Endocrinol Metabolism*, 1997;82:101-105
41 Tang ZY. Clinical research of hepatocellular carcinoma in the 21st century. *China Natl J New Gastroenterol*, 1995;1:2-3
42 Shimizu Y, Minemura M, Tsukishiro T, Kashii Y, Miyamoto M, Nishimori H, Higlichi K, Watanabe A. Serum concentration of intercellular adhesion molecule-1 in patients with hepatocellular carcinoma is a marker of the disease progre ssion and prognosis. *Hepatology*, 1995;22:525-531
43 Sun JJ, Zhou XD, Liu YK, Tang ZY, Feng JX, Zhou G, Xue Q, Chen J. Invasion and metastasis of liver cancer: expression of intercellular adhesion molecule 1. *J Cancer Clin Oncol*, 1999; 125:28-34
44 Momosaki S, Yano H, Ogasawara S, Higaki K, Hisaka T, Kojiro M. Expression of intercellular adhesion molecule 1 in human hepatocellular carcinoma. *Hepatology*, 1995;22:1708-1713
45 Hyodo I, Jinno K, Tanimizu M, Hosokawa Y, Nishikawa Y, Akiyama M, Mandai K, Moriwaki S. Detection of circulating intercellular adhesion molecule-1 in hepatocellular carcinoma. *Int J Cancer*, 1993;55:775-779

Edited by Ma JY

P.O.Box 2345 Beijing 100023, China
Fax. 0086·10·65891893 Tel. 0086·10·65897901
E-mail.wcjd@public.bta.net.cn www.wd.org.cn

World J Gastroentero, 2001; 7(1):126 - 127
World Journal of Gastroenterology
Copyright © 2001 by the WJG Press ISSN 1007 - 9327

Plasma endothelin in patients with endotoxemia and dynamic comparison between vasoconstrictor and vasodilator in cirrhotic patients

Feng Liu[1], Ji Xin Li[2], Chun Mei Li[2] and Xi Sheng Leng[2]

Subject headings hypertension, portal; liver cirrhosis; portosystemic shunt, surgical; endothelins; radioimmunoassay; epoprostenol; liver cirrhosis

Liu F, Li JX, Li CM, Leng XS. Plasma endothelin in patients with endotoxemia and dynamic comparison between vasoconstrictor and vasodilator in cirrhotic patients. ***World J Gastroenterol***, 2001;7(1): 126-127

INTRODUCTION

Portal hypertension is a common clinical syndrome characterized by an abnormal increase in portal blood to the systemic circulation, bypassing the liver. Recent studies have reported that humoral substances play an important role in the pathogenesis of portal hypertension, either by increasing vascular resistance at both the intrahepatic and porto-collateral sites or affecting splanchnic vasodilation with a concomitant increase in parto-collateral blood flow[1-6].

Endothelin (ET) released by endothelial cells is a 21-amino acid peptide with potent vasoconstrictor action. Endothelin comprises a family of four homologous isopeptides in human and animals (ET-1, ET-2, and ET-3, VIC)[7-14]. Most reported data are related to ET-1, which is the most powerful vasoconstrictor. Owing to a variety of reasons, reports concerning endothelin levels in cirrhotics are not consistent with each other. Endothelin concentrations in plasma have been reported to be increased in some studies and normal or reduced in others[15-20]. Present evidence suggests that endothelin may play an important role in modulating intrahepatic vascular resistance[21-24]. However, the relationship between vasoconstrictor (ET, TX-) and vasodilator (PGI_2) during portosystemic shunt has not been documented.

[1]Department of General Surgery, the Fifth Affiliated Hospital, Harbin Medical University, Harbin 150036, Heilongjiang Province, China
[2]Department of General Surgery, People's Hospital, Medical University, Beijing 100044, China
Dr. Feng Liu, graduated from Beijing Medical University as a postgraduate in 1995, now associate professor of general surgery, majoring hepatobilliary surgery, having 12 papers published.
Project supported by the National Natural Science Foundation and Ministry of Public Health of China, No.37600481
Correspondence to: Dr. Feng Liu, Department of General Surgery, the Fifth Affiliated Hospital, Harbin Medical University, Harbin 150036, Heilongjiang Province, China
Tel. 0086-51-5314098, Fax. 0098-51-5314088
Email.lfdlyy.163.net.
Received 2000-07-26 **Accepted** 2000-09-29

METHODS

We measured the concentration of endothelin in plasma using radioimmunoassay in 121 patients with cirrhosis and compared these values with 50 age- and sex-matched control subjects, and evaluated systemic endotoxemia. At the same time, perioperative plasma vasoconstrictor and vasodilator were clinically observed in 30 portohypertensive cirrhotic patients undergoing portosystemic shunt.

RESULTS

Plasma endothelin levels were higher in cirrhotic patients with ascites than in those without ascites. Femoral venous plasma endothelin levels averaged 90 ± 23 ng/L in cirrhotic patients versus 34 ± 8 ng/L in controls (P = 0. 000), and that of cirrhotics with ascites was higher than those without 106 ± 17 ng/L *vs* 90 ± 23 ng/L(P = 0.002). Moreover, plasma endothelin levels increased in proportion to the severity of endotoxemia (r_s = 0.61, P = 0.034). Both the levels of plasma vasoconstrictors (ET, TX-) and of the vasodilator (PGI_2) were higher in portohypertensive cirrhotic patients (ET: 107.8 ± 25.9 ng/L*vs* 48.1 ± 9.4 (P = 0.000); TX-: 349.7 ± 198.4 ng/L *vs* 156.3 ± 54 (P = 0.000); PGI_2: 463.1 ± 108.3 ng/L *vs* 227.2 ± 46 (P = 0.000), and their concentrations decreased significantly in patients after portosystemic shunt (P = 0.002).

DISCUSSION

These results suggest that endothelin has significant influence on the portal vascular resistance of cirrhotic liver *in vivo* and may play an important role in the pathogenesis of portal hypertension[25-28]. Endotoxin may lead to the increased synthesis and release of endothelin. It could be that a dynamic balance between levels of vasoconstrictor and vasodilator in plasma exists in the pathophysiology of portohypertensive cirrhotic patients after portosystemic shunt.

REFERENCES

1 Boyer TD. Portal hypertensive hemorrhage: pathogenesis and risk factors. *Seminars Gastrointest Dis*, 1995;6:125-133
2 Zhang ZY, Ren XL, Yao XX. Alterations and relationship of plasma endotoxin and nitric oxide in patients with cirrhosis. *Xin Xiaohuabingxue Zazhi*, 1997;5:369-370
3 Yu Y, Tian HM, Shi ZG, Yao YM, Wang YP, Lu LR, Yu Y, Chang GY, Ma NS, Sheng ZY. Relationship between endotoxemia and dysfunction of intestinal immunoa-barrier after scald in rats.

Huaren Xiaohua Zazhi, 1998;6:703-704
4 Chen S, Liu B, Cai XM, Gu CH. Clinical significance of changes of endothelin and nitric oxide levels in peripheral blood of patients with severe hepatitis. *Shijie Huaren Xiaohua Zazhi*, 1999;7:122-124
5 Assy N, Paizi M, Gaitini D, Baruch Y, Spira G. Clinical implication of VEGF serum levels in cirrhotic patients with or without portal hypertension. *World J Gastroentero*, 1999;5:296-300
6 Huang YQ, Xiao SD, Zhang DZ, Mo JZ. Nitric oxide synthase distribution in esophageal mucosa and hemodynamic changes in rats with cirrhosis. *World J Gastroentero*, 1999;5:213-216
7 Wang JY, Wang XL, Liu P. Detection of serum TNF-α, IFN-γ, IL-26 and IL-28 in patients with hepatitis B. *World J Gastroentero*, 1999;5:38-40
8 Xu KD, Liu TF, Cing X. Significance of detection of plasma nitric oxide, endothelin, endotoxin in patients with liver cirrhosis. *World J Gastroenterol*, 1998;4(Suppl 2):64
9 Liu ZH. Clinical study of therapeutic effect of dong fang gan kang no.1 on fatty liver. *World J Gastroenterol*, 1998;4(Suppl 2):73
10 Xu YJ, Liu XN, Guan HW, Zhu LH, Bai DS. Diagnosis and treatment of spontaneous rupture of liver carcinoma with bleeding. *World J Gastroentero*, 1998;4(Suppl 2):81
11 Wu MC. Clinical research advances in primary liver cancer. *World J Gastroentero*, 1998;4:471-474
12 Yao XX, Cui DL, Sui YF, Li XT. Clinical and experimental study of effect of Raondix Salviae Militiorrhiza and other blood-activating and stasisa-eliminating Chinese herbs on hemodynamics of portal hypertension. *World J Gastroentero*, 1998;4:439-442
13 Yu YY, Si CW, Tian XL, He Q, Xue HP. Effect of cytokines on liver necrosis. *World J Gastroenterol*, 1998;4:311-313
14 Jia JB, Han DW, Xu RL, Gao F, Zhao LF, Zhao YC, Yan JP, Ma XH. Effect of endotoxin on fibronectin synthesis of rat primary cultured hepatocytes. *World J Gastroenterol*, 1998;4:329-331
15 Yang JM, Han DW, Xie CM, Liang QC, Zhao YC, Ma XH. Endotoxins enhance hepatocarcinogenesis induced by oral intake of thioacetamide in rats. *World J Gastroentero*, 1998;4:128-132
16 Liu GS, Huang YX, Li SW, Pan BR, Wang X, Sun DY, Wang QL. Experimental study on mechanism and protection of stress ulcer produced by explosive noise. *World J Gastroenterol*, 1998;4:519-523
17 Lu MD, Yin YY, Ren W. A study of portal vein embolization with absolute ethanol injection in cirrhotic rats. *World J Gastroenterol*, 1998;4:415-417
18 Assy N, Gong YW, Zhang M, Minuk GY. Appearance of an inhibitory cell nuclear antigen in rat and human serum during variable degrees of hepatic regenerative activity. *World J Gastroenterol*, 1999;5:103-106
19 Assy N, Minuk GY. A comparison between previous and present histologic assessments of chronic hepatitis C viral infections in humans. *World J Gastroentero*, 1999;5:107-110
20 He P, Tang ZY, Ye SL, Liu BB. Relationship between expression of fetoprotein messenger RNA and some clinical parameters of human hepatocellular carcinoma. *World J Gastroenterol*, 1999;5:111-115
21 Peng XM, Yao CL, Chen XJ, Peng WW, Gao ZL. Codon 249 mutations of p53 gene in non-neoplastic liver tissues. *World J Gastroenterol*, 1999;5:324-326
22 Saitoh O, Sugi K, Kojima K, Matsumoto H, Nakagawa K, Kayazawa M, Tanaka S, Teranishi T, Hirata I, Katsu KI. Increased prevalence of intestinal inflammation in patients with liver cirrhosis. *World J Gastroenterol*, 1999;5:391-396
23 Li ZZ, Wei CD, Wang Y, Xing C, Guo H, Cai W, Liu H. The effect of cold upon upper gastrointestinal hemorrhage resulting from liver cirhosis and its mechanism. *World J Gastroenterol*, 1998;4 (Suppl 2):74
24 Pan RM, Shao XD. Clinical characteristics of alcoholic liver disease. *World J Gastroenterol*, 1998;4(Suppl 2):95-96
25 Wei H, Wang YX. A clinical analysis of 36 cases of hepatopulmonary syndrome. *World J Gastroenterol*, 1998;4(Suppl 2):101
26 Gu SQ, Li LY, Li Z, He D. Analysis on clinical features of hepatic encephalopathy of 108 cases. *World J Gastroenterol*, 1998;4(Suppl 2):101
27 Wu CH. Fibrodynamics-aelucidation of the mechanisms and sites of liver fibrogenesis. *World J Gastroenterol*, 1999;5:388-390
28 Cheng ML, Wu YY, Huang KF, Luo TY, Ding YS, Lu YY, Liu RC, Wu J. Clinical study on the treatment of liver fibrosis due to hepatitis B by IFN-α_1 and traditional medicine preparation. *World J Gastroenterol*, 1999;5:267-269

Edited by Jason Carr

P.O.Box 2345 Beijing 100023, China
Fax. 0086·10·65891893 Tel. 0086·10·65897901
E-mail.wcjd@public.bta.net.cn www.wd.org.cn

World J Gastroentero, 2001; 7(1):128 - 130
World Journal of Gastroenterology
Copyright © 2001 by the WJG Press ISSN 1007 - 9327

Adhesion molecule and proinflammatory cytokine gene expression in hepatic sinusoidal endothelial cells following cecal ligation and puncture

Rong Qian Wu, Ying Xin Xu, Xu Hua Song, Li Jun Chen and Xian Jun Meng

Subject headings cell adhesion molecules; sepsis; endothelium; cytokines; gene expression; polymerase chain reaction; RNA, messenger; liver/injuries; cecal diseases

Wu RQ, Xu YX, Song XH, Chen LJ, Meng XJ. Adhesion molecule and proinflammatory cytokine gene expression in hepatic sinusoidal endothelial cells following cecal ligation and puncture. ***World J Gastroenterol***, 2001;7(1):128-130

INTRODUCTION

Multiple organ dysfunction syndrome (MODS) is thought to be a frequent consequence of sepsis[1-3]. Despite substantial advances in our knowledge and understanding of the basic pathophysiologic mechanisms[4-7], in critically ill patients infections and sepsis are still associated with a high mortality[8,9]. There is evidence that the development of tissue damage in sepsis and shock is closely associated with the release of an ever increasing number of mediators and accumulation of neutrophils at the sites of infection or injury[10,11].

The endothelium is an intimal layer of simple squamous cells which provides a continuous, fluent surface for circulating blood. It is not the passive, metabolically inert barrier that it was once thought to be, and it is now known to be a metabolically and physiologically dynamic tissue with multiple functions. On the basis of recent discoveries in the field of endothelial cell biology (such as endothelium-derived mediators and the expression of adhesion molecules), end othelial cells are now thought to be not only target cells of injury, but also actively involved in inflammatory reactions and subsequent organ damage[12,13].

Polymicrobial sepsis induced by cecal ligation and puncture (CLP) is a model of sepsis which reproduces many of the inflammatory and pathological sequelae that are observed clinically. Following CLP, animals develop bacteremia, hypothermia, hypotension, and damage to multiple organ systems[14]. The present study was designed to observe the gene expression of adhesion molecules and proinflammatory cytokines in hepatic sinusoidal endothelial cells with a CLP model, in order to investigate the role of endothelial cells in tissue damage during sepsis.

Institute of Surgical Research , General Hospital of PLA, Beijing 100853, China
Dr. Rong Qian Wu, graduated from General Hospital of PLA as a M.D. in 1999, now attending surgeon of general surgery, major field of research in sepsis and MODS, having 15 papers published.
Supported by the National Natural Science Foundation of China, No.39870796
Correspondence to: Dr. Rong Qian Wu, Institute of surgical Research, General Hospital of PLA, Beijing 100853, China
Received 2000-09-04 **Accepted** 2000-09-29

MATERIALS AND METHODS

Animal model and CLP

NIH mice were obtained from the animal center of the General Hospital of PLA. The mice were randomly divided into 2 groups: CLP group and sham group. Sepsis was induced in the CLP group by CLP. The mice were anesthetized, and the cecum was ligated below the ileocecal junction: intestinal continuity was maintained. The cecum was punctured twice with a 20-gauge needle and a small amount of cecal contents was expressed through the punctures. The incision was closed and 1 mL of normal saline was administered subcutaneously. Sham-operated mice underwent the same surgical procedure, but without CLP. The mice were sacrificed at 3 or 12 h after the procedure.

Isolation and purification of hepatic sinusoidal endothelial cells

Hepatic sinusoidal endothelial cells were isolated by collagenase perfusion of the liver, isopyknic sedimentation in a two-step percoll gradient, and selective adherence [15]. The purified sinusoidal endothelial cells were identified by staining with anti-von willebrand factor (vWF, factor VII I-related antigen). Flow cytometric analysis showed a purity greater than 85% in hepatic sinusoidal endothelial cells.

Analysis of adhesion molecules and proinflammatory cytokines mRNA by reverse transcription-PCR

Total RNA was extracted from endothelial cells. We used a phenol-chloroform extraction method reported by Chomczynski. The RNA was then quantitated spectrophotometrically. Total RNA from experimental samples was used to synthesize cDNA using AMV reverse transcriptase. β-actin and β_2-MG were used as internal control primers. The primers for the adhesion molecules and controls were as follows: β- actin (478bp), 5'AGG GAA ATC GTG CGT GAC ATC AAA 3', 5'ACT CAT CGT ACT CCT GCT TGC TGA 3'; β_2-MG (300 bp), 5'GGC TCG CTC GGT GAC CCT AGT CTT T 3',

5'TCT GCA GGC GTA TGT ATC AGT CTC A 3'; VCAM-1 (442bp), 5'CCT CAC TTG CAG CAC TAC GGG CT 3', 5' TTT TCC AAT ATC CTC AAT GAC GGG 3'; ICAM-1 (326bp), 5'TGC GTT TTG GAG CTA GCG GAC CA 3', 5' CGA GGA CCA TAC AGC ACG TGC AG 3'; E-selectin (435bp), 5'CCT GAA CTG CTC CCA CCC GTT CG 3', 5' GTG AAG TTA CAG GAT GAC TTA AAC GCA 3'; TNF-α (349 bp), 5'TTC TGT CCC TTT CAC TCA CTG G3', 5'TTG GTG GTT TGC TAC GAC GTG G 3' IL-1β (441bp), 5'ATT AGA CAG CTG CAC TAC AGG CTC 3', 5'AGA TTC CAT GGT GAA GTC AAT TAT 3' IL-6 (156bp), 5'TGG AGT CAC AGA AGG AGT GGC TAA G 3', 5'TCT GAC CAC AGT GAG GAA TGT CCA C 3'. Polymerase chain reactions were performed in a 25 μL reaction volume. A hot start was applied for 5min at 95℃. The amplification cycle (denaturation step at 94℃ for 30s, an annealing step at 55℃ for 30s and an extension step at 72℃ for 90s) was repeated 30 times and followed by a final extension for 10 min at 72℃. Amplified products were separated by electrophoresis in ethidium bromide-stained 1.5% agarose gel and visualized with UV illumination. The bands representing reaction product on the film were scanned by densitometry. A normalization quotient (Q) was calculated between the integrated optical density values (IOD) for the adhesion molecules and the β-actin or β_2-MG bands (Q = IOD, adhesion molecules band/internal control band). The level of adhesion molecules mRNA were expressed as the quotient of the integrated optical density values for the adhesion molecules and the β-actin or β_2-MG bands.

Statistical analysis

All data were reported as means ± SD. Data were analyzed by *t* test for comparisons between the two groups. A *P* value of less than 0.05 was deemed significant.

RESULTS

Adhesion molecules mRNA expression in hepatic sinusoidal endothelial cells

E-selectin mRNA levels markedly increased at 3 h after CLP in hepatic sinusoidal endothelial cells, and returned to baseline at 12 h after CLP. Increases in ICAM-1 mRNA level was found at 3 h after CLP, and this level became higher at 12 h after CLP. VCAM-1 mRNA expression in hepatic sinusoidal endothelial cells increased significantly 3h after CLP but declined at 12h after CLP (Table 1).

Table 1 Adhesion molecules mRNA expression in hepatic sinusoidal endothelial cells ($x \pm s$)

	E-selectin		ICAM-1		VCAM-1	
	3h	12h	3h	12h	3h	12h
Sham	0.22 ± 0.04	0.23 ± 0.04	0.26 ± 0.03	0.30 ± 0.05	0.37 ± 0.04	0.30 ± 0.05
CLP	0.85 ± 0.06[b]	0.24 ± 0.03	0.67 ± 0.04[b]	1.02 ± 0.10[b]	1.04 ± 0.14[b]	0.86 ± 0.05[b]

[b]$P<0.01$ *vs* sham group.

Proinflammatory cytokines mRNA expression in hepatic sinusoidal endothelial cells

A significant increase in TNF, IL-1 and IL-6 gene expression was observed at 3 and 12 hours after CLP. The level of TNFα and IL-1β at 3 hours was higher than 12 hours, and the level of IL-6 gene expression at 12 hours was higher than 3 hours (Table 2).

Table 2 Proinflammatory cytokines mRNA expression in hepatic sinusoidal endothelial cells ($x \pm s$)

	TNFα		IL-1β		IL-6	
	3h	12h	3h	12h	3h	12h
Sham	0.23 ± 0.04	0.22 ± 0.04	0.30 ± 0.04	0.39 ± 0.06	0.47 ± 0.05	0.49 ± 0.05
CLP	0.71 ± 0.03[b]	0.54 ± 0.07[b]	1.02 ± 0.12[b]	0.78 ± 0.08[b]	0.90 ± 0.05[b]	1.11 ± 0.14[b]

[b]$P<0.01$ *vs* sham group.

DISCUSSION

The liver, with its rich supply of blood and sinusoid, is directly exposed to bacteria and endotoxins drained from the GI tract[16-19]. Previously, researchers in our institute have reported that the liver is the most susceptible and vulnerable organ during sepsis and multiple organ failure [20].

Vascular endothelial cells form an interface between tissues and inflammatory cells. This unique location allows localization of the inflammatory reaction to the site of injury while protecting adjacent healthy tissue. Endothelial cells mediate the local inflammatory response through modulation of vascular tone, vascular permeability and stimulation of leukocyte extravasation[21,22]. The role of neutrophil extravasation and accumulation has been emphasized in recent years[23,24]. This is mediated by the induced expression of multiple cell adhesion molecules on the surface of neutrophils and endothelial cells[25,26]. These include the selectins which are a group of surface glycoproteins essential to leukocyte margination and rolling along the vascular endothelium. Specifically, endothelial E- and P- selectin and L-selectin are expressed on neutrophils[27]. Another group of cell adhesion molecules involved in endothelial cell-leukocyte interaction is the immunoglobulin supergene family. This group comprises intercellular adhesion molecules-1 and 2 (ICAM-1, ICAM-2), vascular cell adhesion molecules-1 (VCAM-1)[28]. The most well studied of these molecules is ICAM-1, which play a critical role in events subsequent to initial leukocyte margination. In this study, we found that the up-regulation of the expressions of adhesion molecules in liver sinusoidal endothelial cells is a crucial step for the migration of leukocytes to and accumulation at the site of inflammation. Although neutrophils are important for killing microorganisms, activation of recruited neutrophils coupled with excessive release of oxygen metabolites and proinflammatory mediators may induce tissue injury which can lead to organ dysfunction[29,30].

Cytokines are polypeptides or glycoproteins of low molecular weight. Most cytokines are not stored as preformed molecules, hence their production requires new gene transcription and translation. Unlike mediators derived from the classical endocrine system, cytokines are produced. The production of cytokines at various tissue sites depends, in part, on the proximity of the site to the injurious stimulus. In this study we assessed the gene expression of proinflammatory cytokines in hepatic sinusoid endothelial cells. Recent discoveries in the field of endothelial cell biology have shown its capability of production cytokines[31-33], but the role of endothelial cell-derived cytokines in sepsis induced tissue injury was largely ignored. Proinflammatory cytokines TNF and IL-1 are known to play predominant roles in the normal inflammatory response. Exaggerated endogenous production is likely responsible for the complications associated with sepsis such as tissue injury and ultimate organ failure[34-36]. We observed a significant increase in TNF and IL-1 gene expression shortly after the induction of sepsis. This indicates that endothelium is an important source of cytokines during sepsis, and may play a role in sepsis induced organ dysfunction. The consensus of the concept of systemic inflammatory responses has brought about a likely promising approach in the treatment of SIRS/MODS[37]-anti-inflammatory instead of anti-infection[38,39]. Various approaches aimed at interrupting the cascade of host inflammatory responses have been tested. These include interventions targeted at the inflammation effector cells as monoclonal antibodies or receptor antagonist to pro-inflammatory cytokines. However, many of these seemingly effective measures in experimental study failed when moved from the laboratory bench to clinical ward [40-44].

REFERENCES

1 Livingston DH, Mosenthal AC, Deitch EA. Sepsis and multiple organ dysfunction syndrome: a clinical-mechanistic overview. *New Horiz*, 1995;3:257-266
2 Goris RJA. MODS/SIRS: Result of an overwhelming inflammatory response? *World J Surg*, 1996;20:418-421
3 Gullo A, Berlot G. Sepsis. *Intensive Care Med*, 1999;25:869-871
4 Bone RC. Toward a theory regarding the pathogenesis of the systemic inflammatory response syndrome: what we do and do not know about cytokine regulation. *Crit Care Med*, 1996;24: 163-172
5 Deitch EA. Multiple organ failure: pathophysiology and potential future therapy. *Ann Surg*, 1992;216:117-134
6 Nieuwenhuijzen GAP, Deitch EA, Goris RJA. Infection, the gut and the development of the multiple organ dysfunction syndrome. *Eur J Surg*, 1996;162:259-273
7 Gullo A, Berlot G. Ingredients of organ dysfunction or failure. *World J Surg*, 1996;20:430-436
8 Sands KE, Bates DW, Lanken PN, Graman PS, Hibberd PL, Kahn KL, Parsonnet J, Panzer R, Orav EJ, Snydman DR, Black E, Schwartz JS, Moore R, Johnson BL, Platt R. Epidemiology of sepsis syndrome in 8 academic medical centers. *JAMA*, 1997;278: 234-240
9 Teplick R, Rubin R. Therapy of sepsis: why have we made such little progress. *Crit Care Med*, 1999;27:1682-1683
10 Davies MG, Hagen PO. Systemic inflammatory response syndrome. *Br J Surg*, 1997;84:920-935
11 Gutierrez-Ramos JC, Bluethmann H. Molecules and mechanisms operatingin septic shock: lessons from knockout mice. *Immunol Today*, 1997;18:329-334
12 Wang XD, Andersson R. The role of endothelial cells in the systemic inflammatory response syndrome and multiple system organ failure. *Eur J Surg*, 1995;161:703-713
13 McGill SN, Ahmed NA, Christou NV. Endothelial cells: role in infectionand inflammation. *World J Surg*, 1998;22:171-178
14 Salkowski CA, Detore G, Franks A, Falk MC, Vogel SN. Pulmonary and hepatic gene expression following cecal ligation and puncture: monophosphoryl lipid A prophylaxis attenuates sepsis-induced cytokine and chemokine expression and neutrophil infiltration. *Infect Immun*, 1998; 66:3569-3578
15 Braet F, De zanger R, Sasaoki T, Baekeland M, Janssens P, Smedsrød B, Wisse E. Assessment of a method of isolation, purification, and cultivation of rat liver sinusoidal endothelial cells. *Lab Invest*, 1994;70:944-952
16 Han DW. The clinical sine of subsequent liver injury induced by gut derived endotoxemia. *Shijie Huaren Xiaohua Zazhi*, 1999;7:1055-1058
17 Swank GM, Deitch EA. Role of the gut in multiple organ failure: bacterial translocation and permeability changes. *World J Surg*, 1996;20:411-417
18 Qin RY, Zou SQ, Wu ZD, Qiu FZ. Influence of splanchnic vascular infusion on the content of endotoxins in plasma and the translocation of intestinal bacteria in rats with acute hemorrhage necrosis pancreatitis. *World J Gastroentero*, 2000;6:577-580
19 Zhang SC, Dai Q, Wang JY, He BM, Zhou K. Gut-derived endotoxemia: one of the factors leading to production of cytokines in liver diseases. *World J Gastroenterol*, 2000;6(Suppl 3):16
20 Meng XJ, Wang P, Zhang P. The role of liver in the development of multiple organ failure. *Zhonghua Waike Zazhi*, 1988;26:13-15
21 Liu XJ, Liu F, Xiao WJ, Huang MH, Huang SM, Wang YP. Effects of sinusoidal endothelial cell conditioned medium on the expression of connective tissue growth factor in rat hepatic stellate cells. *World J Gastroenterol*, 2000;6(Suppl 3):42
22 Braet F, Zanger RD, Spector I, Wisse E. Structure and dynamics of hepatic endothelial fenestrae. *World J Gastroenterol*, 2000;6(Suppl 3):1
23 Van Oosten M, Van De Bilt E, De Vries HE, Van Berkel TJC, Kuiper J. Vascular adhesion molecule-1 and intercellular adhesion molecule-1 expression on rat liver cells after lipopolysaccharide administration *in vivo*. *Hepatology*, 1995;22:1538-1546
24 Tanaka Y, Adams DH, Shaw S. Proteoglycans on endothelial cells present adhesion-inducing cytokines to leukocytes. *Immunol Today*, 1993;14:111-114
25 Furie B, Furie BC. Leukocyte crosstalk at the vascular wall. *Thromb Haemostas*, 1997;78:306-309
26 Adams DH, Nash GB. Disturbance of leukocyte circulation and adhesion to the endothelium as factors in circulatory pathology. *Br J Anaesth*, 1996;77:17-31
27 Mackay CR, Imhof BA. Cell adhesion in the immune system. *Immunol Today*, 1993;14:99-102
28 Wang JH, Springer TA. Structural specializations of immunoglobulin superfamily members for adhesion to integrins and viruses. *Immunol Reviews*, 1998;163:197-215
29 Wu P, Li X, Zhou T, Zhang MJ, Chen JL, Wang WM, Chen N, Dong DC. Role of P-selectin and anti-P-selectin monoclonal antibody in apoptosis during hepatic/renal ischemia-reperfusion injury. *World J Gastroenterol*, 2000;6:244-247
30 Marzi I, Maier M, Herzog C, Bauer M. Influence of pentoxifylline and albifylline on liver microcirculation and leukocyte adhesion after hemorrhagic shock in the rat. *J Trauma*, 1996;40:90-96
31 Mantovani A, Bussolino F, Dejana E. Cytokine regulation of endothelial cell function. *FASEB J*, 1992;6:2591-2599
32 Mantovani A, Bussolino F, Introna M. Cytokine regulation of endothelial cell function: from molecular level to the bedside. *Immunol Today*, 1997;18:231-240
33 Mantovani A, Garlanda C, Introna M, Vecchi A. Regulation of endothelial cell function by pro- and anti-inflammatory cytokines. *Transplant Proc*, 1998;30:4239-4243
34 Zhang GQ, Yu H, Zhou XQ, Liao D, Xie Q, Wang B. TNF-α induced apoptosis and necrosis of mice hepatocytes. *Shijie Huaren Xiaohua Zazhi*, 2000;8:303-306
35 Schlag G, Redl H. Mediators of injury and inflammation. *World J Surg*, 1996;20:406-410
36 Jansen MJJM, Hendriks T, Vogels MTE, van der Meer JWM, Goris RJA. Inflammatory cytokines in an experimental model for the multiple organ dysfunction syndrome. *Crit Care Med*, 1996;24:1196-1202
37 Bone RC. Immunologic Dissonance: A continuing evolution in our understanding of the systemic inflammatory response syndrome (SIRS) and the multiple organ dysfunction syndrome (MODS). *Ann Intern Med*, 1996;125:680-691
38 Smail N, Messiah A, Edouard A, Descorps-Declere A, Duranteau J, Vigue B, Mimoz O, Samii K. Role of systemicinflammatory response syndrome and infection in the occurrence of early multiple organ dysfunction syndrome following severe trauma. *Intensive Care Med*, 1995;21:813-816
39 Faist E, Kim C. Therapeutic immunomodulatory approaches for the control of systemic inflammatory response syndrome and the prevention of sepsis. *New Horiz*, 1998;6:S97-S102
40 Bernard GR. Research in sepsis and acute respiratory distress syndrome: are we changing course? *Crit Care Med*, 1999;27:434-436
41 Bone RC. Why sepsis trials fail. *JAMA*, 1996;276:565-566
42 Piper RD, Cook DJ, Bone RC, Sibbald WJ. Introducing Critical Appraisal to studies of animal models investigating novel therapies in sepsis. *Crit Care Med*, 1996;24:2059-2070
43 Abraham E. Why immunomodulatory therapies have not worked in sepsis. *Intensive Care Med*, 1999;25:556-566
44 Nasraway SA. Sepsis research: we must change course. *Crit Care Med*, 1999; 27:427-430

Edited by Jason Carr

P.O.Box 2345 Beijing 100023, China
Fax. 0086·10·65891893 Tel. 0086·10·65897901
E-mail.wcjd@public.bta.net.cn www.wd.org.cn

World J Gastroentero, 2001; 7(1):131 - 135
World Journal of Gastroenterology
Copyright © 2001 by the WJG Press ISSN 1007 - 9327

Effect of 5-2Aza-2'-deoxycytidine on the P16 tumor suppressor gene in hepatocellular carcinoma cell line HepG2

Li Hua Liu[1], Wen Hua Xiao[2] and Wei Wen Liu[3]

Subject headings liver neoplasms; genes, p16; methylation; genes, suppressor, tumor; flow cytometry; immunohistochemistry; polymerase chain reaction

Liu LH, Xiao WH, Liu WW. Effect of 5-2Aza-2'-deoxycytidine on the P16 tumor suppressor gene in hepatocellular carcinoma cell line HepG2. ***World J Gastroentero***, 2001;7(1):131-135

INTRODUCTION

Hepatocellular carcinoma (HCC) is one of the most common human malignancies world wide[1,2], and is closely associated with infection of HBV and HCV and contamination of aflatoxin B1[3-6]. Although the molecular mechanisms of hepatocarcinogenesis remain poorly understood, an increasing number of genetic abnormalities have been recognized[7-10], for example, the *p*16 gene[11,12] the p53 gene[13-18], the E-cadherin gene[19], and the c-myc gene[20]. In relevance to HCC, inactivation of a tumor suppressor gene *p*16, which is important in the regulation of cell cycling, has recently been described in a significant proportion of patients with HCC[11]. An important mechanism of gene inactivation is aberrant methylation in the promoter region of the gene[11,21,22]. Evidence of p16 hypermethylation has also been documented in several human cancers[21-26]. However, to our knowledge, there were few studies on the *p*16 gene in HCC. 5-Aza-2'-deoxycytidine (5-Aza-cdR) is thought to act by inhibiting DNA methyltransferase that methylates cytosine residues in eukaryotic DNA[27]. Cedar *et al*[28] even took it as an experimental tool for demethylation. This drug appears to incorporate into the cellular DNA where it acts as a noncompetitive inhibitor of the maintenance methylase[29]. Methel moieties are thus passively removed when the DNA undergoes replication, and indeed, numerous inactive cellular and viral genes can be turned on following exposure to 5-Aza-cdR[30]. In order to determine whether *p*16 hypermethylation is involved in hepatocarcinogenesis, we determined the *p*16 gene protein, mRNA expression and methylation status in HCC cell line HepG2 before and after treatment with 5-Aza-cdR, and observed the growth change.

MATHERIALS AND METHODS

Cell line culture

Human hepatocellular carcinoma cell line HepG2 was obtained from the Laboratory of Gastroenterology, Southwest Hospital. It was cultured in RPMI 1640 supplemented with 100 mL/L fetal bovine serum, 100KU/L penicillin/ streptomycin and 5% sodium pyruvate at 37℃ in humidified atmosphere of 50 mL/L CO_2.

5-Aza-CdR treatment

Cells (approximately 1×10^5/mL) were plated in the vial, and treated with 5×10^{-7}M 5-Aza-cdR (Sigma Co.) for 24 h. The medium was changed after 24 h drug treatment and cultured for 9 days, to ensure complete recovery from the immediate toxic effects of 5-Aza-cdR[31]. Untreated cells were analyzed under similar conditions as a control.

Determination of cell cycle profile

Cells (2×10^6/100 mL vial) were plated and treated with 5×10^{-7} M 5-Aza-cdR. Cells were fixed after 7 days with 700 mL/L ethanol, and stained with propidium iodide (50 mg/L: Crze Co.). DNA content at each cell cycle stage was determined via flow cytometry.

Effects of 5-Aza-CdR on tumorigenicity

HepG2 cells (2×10^6) were injected into the right flank of 4-week-old Balb/c male nude mice 11 days after treatment with 5-Aza-cdR. Untreated cells were injected into the left flank under the same condition as a control. Tumor sizes were measured 4 weeks after injection.

[1]Department of Oncology, Southwest Hospital, Third Military Medical University, Chongqing 400038, China (now working in Department of Gastroenterology, General Hospital of PLA, Lanzhou 730050, Gansu Province, China)
[2]Department of Oncology,[3]Department of Gastroenterology, Southwest Hospital, Third Military Medical University, Chongqing 400038, China
Dr. Li Hua Liu, graduated from Third Military Medical University as a postgraduate in 2000, associate professor of gastroenterology,majoring in pathology of hepatocellular carcinoma, having 5 papers published.
Project supported partly by the National Natural Science Foundation of China, No.39870344
Correspondence to: Wen Hua Xiao, Department of Gastroenterology, 304th Hospital of PLA, Beijing 100037, China
Tel. 0086-10-66867321
Email. wenhua_x@mailcity.com
Received 2000-07-05 **Accepted** 2000-07-21

Immunohistochemistry

Cells (1×10^6/3 cm dish) were cultured onto acid-washed 0.8 × 0.8 (mm) coverslips. The cells were fixed in 4% parafomaldehyde for 30 min at room temperature. The slides were washed in phosphate-buffered saline (PBS) three times for 3 minutes. The endogenous peroxidase activity was quenched by 10 minute incubation in methanol with 3% hydrogen peroxide (Zhongshan Chemical Co.). The fixation slides were then cleared with PBS. Nonspecific binding was blocked by applying normal goat serum in humidity chamber in a dilution of 1:10
for 30 minutes. Slides were blotted, and the anti-entire-human p16 antibody (Zhongshan Chemical Co.) (ready to use) as a primary antibody was applied for 1 hour at 37℃ in a humidity chamber. Secondary antibody (rabbit anti-mouse IgG) (Zhongshan Chemical Co.) diluted with PBS and normal human serum (40 μL rabbit anti-mouse antibody, 50 μL normal human serum, and 910 μL PBS) was applied for 1 hour at 37 ℃ in a humidity chamber. Finally, peroxidase-antiperoxidase conjugate diluted 1:100 in PBS was applied for 1 hour at 37℃ after washing with PBS. Slides were kept in diaminobenzidine tetrahydrochloride for 10 minutes (50 mg in 200 mL PBS with 25 μL of 30% H_2O_2) (DAB; Zhongshan Chemical Co.) . The manufacturer provides the presence (+) and absence (-) controls. The expression of p16 gene was observed under the light microscope and analyzed by the figure analysis method.

RT-PCR

RNA was isolated using Tripure isolation reagent (Boehringer Mannheim Co.). RNA was reverse transcribed according to the manufacturer's instructions of the access RT-PCR system (Promega Co.). cDNA was amplified using primers specific for both the p16 gene and GAPDH gene, the latter being used as a control. The primers used for *p*16 amplifications were located in exon 1 and exon 2 of the gene. Their sequences were 5'-AGCCTTCGGCTGACTGGCTGG-3'(sense) and 5'-CTGCCCATCATCATGACCTGGA-3'- (antisense). (Shanghai Sheng Gong Chemical Co., PAG pure). Standard PCR reaction was performed in total volume of 25 μL reaction mixture, including dNTP 0.2mM, 1 mM each primer 1 (sense) and Primer 2 (antisense), 1 mM $MgSO_4$, 0.1 U/mL of reverse transcriptase AMV, 0.1U/mL of Taq DNA polymerase and 100ng RNA. Conditions for *p*16 amplifications were 94℃ for 2 min, 40 cycles of 94 ℃ for 30s; 60℃ for 45s; and 68℃ for 90s , followed by incubation at 68℃ for 7 min. RT-PCR amplification product is 428 base pair[bp]. Primers for the GAPDH gene were 5'-CCACCCATGGCAAATTCCATGGCA-3' (sense), and 5'-TCTAGACGG CAGGTCAGGTCCAC-3'. (antisense) Conditions for GAPDH amplifications were 94℃ for 2 min, 40 cycles of 94℃ for 30s , 60℃ for 40s and 68℃ for 60s, followed by incubation at 68℃ for 7min. The amplification product is 598 bp. RT-PCR products were resolved on 2% agarose gel by figure analysis method.

PCR-based methylation assay

DNA was isolated with the Tripure isolation reagent. A PCR assay relying on the inability of some restriction enzymes, e.g. Hpa II or *Msp* I, to cut methylated sequences was used to analyze the methylation status of the second exon of the *p*16. DNA digests were performed according to the manufacturer's directions (Boehringer Mannheim Co.). DNA (1 μg) was digested for 2 h with 10 units of enzyme/μg of DNA. 200 ng of the digested DNA were amplified with primers flanking the restriction sites. The primers set used for methylation analysis of *p*16 exon 2 were 5'-CTGCTTGGCGGTGAGGGGG-3'(sense) and 5'-CCTCACCTGAGGGACCTTC-3'(antisense). The amplifiction products was 402 bp. Conditions were: 94 ℃ for 3 min, 35 cycles of 94℃ for 1 min, 57℃ 30s, and 72℃ for 40s, followed by incubation at 72℃ for 1 min. PCR products were resolved on 2% agarose gel. To rule out the possibility of incomplete restriction, all samples were digested twice with each of the enzymes in independent experiments. PCR ampifications from each of the duplicate digests were repeated at least twice to ensure reproducibility of the results.

Statistical analysis

t tests were used for statistical analysis. Significance was defined as $P<0.05$.

RESULTS

Cell cycle arrest after treatment with 5-Aza-cdR

HepG2 cells treated with 5-Aza-cdR were analyzed by flow cytometry to identify any change in its cell cycle profiles. The treated cells showed an increase in the proportion in G1,from 79.4% to 82.2% and a decrease in S, from 11.9% to 6.4%. Apoptotic rate increased from 6. 5% to 14.5%. These results indicated that 5-Aza-cdR may induce cancer cell division and apoptosis.

Effects of 5-Aza-cdR on tumorigenicity

Tumors induced via the injection of untreated HepG2 cells were approximately 1.32 cm^3 in size, whereas the tumors induced by HepG2 cells treated with 5-Aza-cdR averaged 0.98 cm^3 in size. These demonstrated that the growth-inhibitory effects of 5-Aza-cdR treatment *in vivo* were still recognizable.

Effect of 5-Aza-cdR on P16 protein expression

The positive 5-Aza-cdR-treated cells showed intense

homogenous brown staining of their nucler. After treatment with 5×10^{-7} M 5-A2a-cdR, HepG2 showed a higher expression of P16 protein than untreated cells. We observed under light microscope 5 fields in every slide at random, measured the staining degree of every 124 positive cells by the figure analysis method, IOD was 212.81 ± 62.56 and 495.89 ± 52.12 respectively in the untreated group and the treated group. This showed a significant difference ($P<0.05$). Although *P*16 protein expression alternations are very complicated and still undefined, our data showed that *P*16 protein expression could be silenced by hyper methylation of *p*16 gene (Figures 1,2).

Effect of 5-Aza-CdR on p16 mRNA expression

Figure 3 shows that expression level of *p*16 mRNA in HepG2 cells was increased after treated with 5×10^{-7} M 5-aza-cdR. The *p*16 gene, was selected for this study, because it was known to frequently undergo *de novo* methylation during tumorigenesis and because 5-Aza-cdR might be highly effective in inducing the expression of the gene inappropriately silenced by *de novo* methylation[18]. These results demonstrated a strong correlation between hypermethylation of the *p*16 and transcriptional silencing of this gene.

Effect of 5-Aza-CdR on p16 gene methylation status

Before 5-aza-cdR treatment the *p*16 exon2 showed hypermethylation, and therefore could not be deaved by loth HpaII and *Msp* I. It has been known that only the DNA indigested with *Hpa* II or *Msp* I can be amplified. After treated with 5-aza-cdR, the *p*16 gene became demethylated, then could be deaved by loth of the enzymes, and this failed to be emplified. Our experiment demonstrated that after hypermethylation in the *p*16 exon2 and 5-aza-cdR could enhance demethylation (Figure 4).

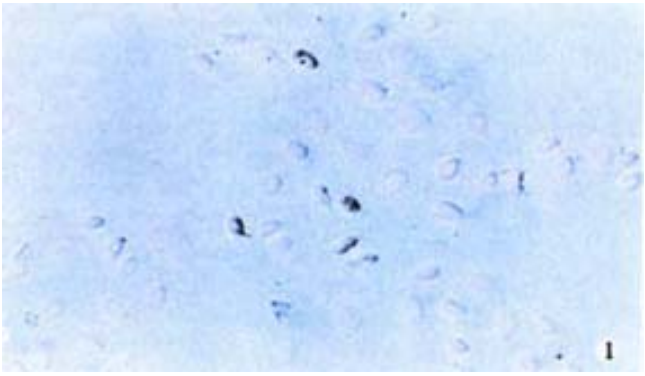

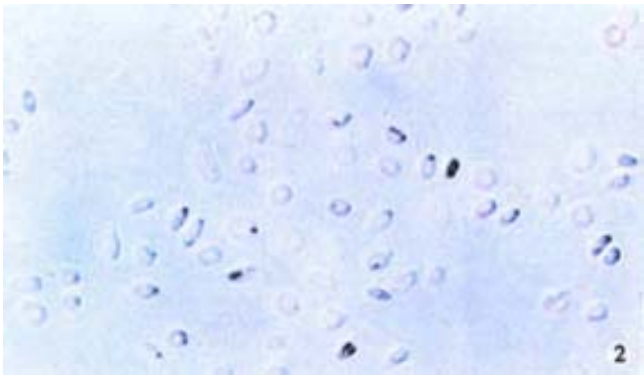

Figure 1 Immunohistochemical demonstration of p16 protein expression in HepG2 cell line before treatment with 5-Aza-cdR. SABC × 200
Figure 2 Immunohistochemical demonstration of p16 protein expression in HepG2 cell line after treatment with 5-Aza-cdR. SABC × 200

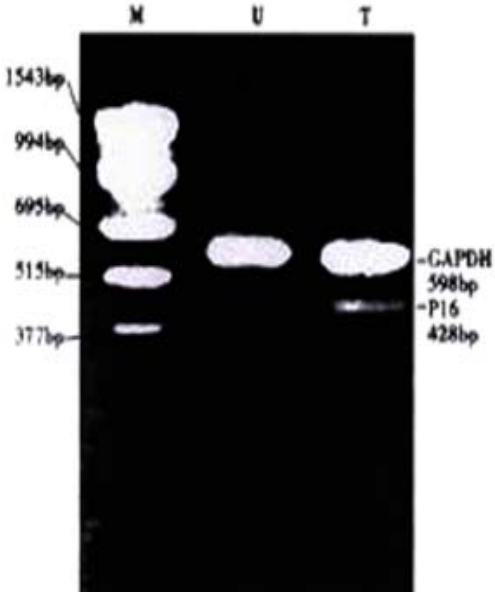

Figure 3 Effects of 5-Aza-cdR on the p16 mRNA expression in HepG2 cell line. Cells were treated with 5×10^{-7} M 5-Aza-cdR for 24 hours; after culturing for 9 days, p16 mRNA were determined by RT-PCR. U: untreated T: treated with 5-Aza-CdR

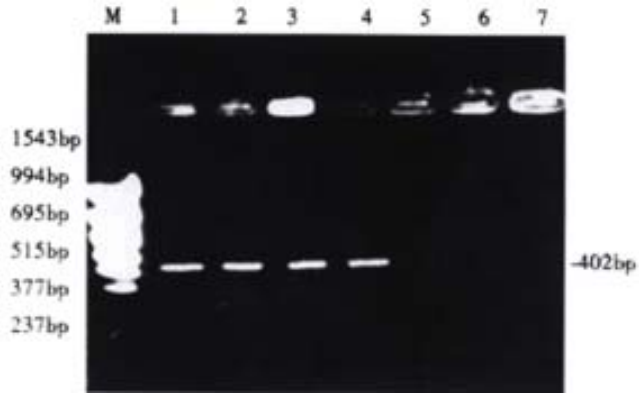

Figure 4 Detection of aberrant methylation of the p16 gene in HCC cell line HepG2. *Lane M*: molecular weight marker; *Lane 1*: Neither treated with 5-aza-cdR nor digested with *Hpa* II or *Msp* I; *Lane 2*: Untreated with 5-aza-cdR, but digested with *Hpa* II; *Lane 3*: Untreated with 5-Aza-cdR, but digested with *Msp* I; *Lane 4*: Treated with 5-aza-cdR, but not digested with *Hpa* II or *Msp* I; *Lane 5*: Treated with 5-aza-cdR, and digested with *Hpa* II; *Lane 6*: Treated with 5-aza-cdR, and digested with *Msp* I.

DISCUSSION

HCC is one of the most frequent human malignances worldwide. A number of tumor suppressor genic abnormalities are being recognized involving in the development of HCC[7-20]. The tumor-suppressor gene, p16,coding for an inhibitor of cyclin-dependant kinase (cdk) 4, was isolated and mapped to chromosome 9p21 [32,33], a locus frequently lost in diverse malignancies [34]. The *p*16 gene product p16 protein was originally isolated as a protein that was associated with cdk complexes[35] and thought to exert a negative type of control on cell proliferation through its binding to cdk4, thereby preventing cdk4 from forming an active complex with cyclin D protein[36]. As one of cancer-associated genes, the p16 gene abnormalities is arousing more and more attention. Germ-line mutations of the p16 gene have been identified in hereditary melanomas[37]. In addition,the gene is homozygously deleted or mutated in uncultured tumors of diverse origin[38], including pancreatic adenocarcinomas[39], melanomas[37], esophageal carcinomas[40,41], gliomas [42]lung cancer[43] and hepatocellular carcinoma[44]. Recently, it has been reported that inactivation of the *p*16 gene is frequently associated with aberrant DNA met hylation in all common human cancers[26]. However, there have been relatively few studies on expression of *p*16 in HCC.

Sun *et al*[45] found that DNA methyltransferase (MTase) mRNA levels were significantly higher in HCC and HCC cell lines (including HepG2 cell line), but they did not study the related genic methylation. Wong *et al*[46] demonstrated that aberrant methylation of the p16 gene occurred in 73% of HCC tissues. Hui *et al*[44] studied six HCC cell lines and found no p16 mRNA and protein in only one of them. After ruling out mutation and homozygous deletion of the p16 gene, they guessed that the silence of p16 gene might be associated with enhanced methylation of p16 gene, although the methylation status was not tested. However, p16 mRNA was detected in the other five HCC cell lines, and they thought that the lack of p16 gene transcription was not a frequent event in HCC cell line. The absence of p16 protein and presence of p16 mRNA expression strongly suggested that inactivation of p16 gene function could occur at the posttranscriptional level, but, the presence of expressions of both *p*16 mRNA and protein in HepG2, could not be explained. Boyes *et al*[47] discovered that the inhibition of gene transcription correlated with density of DNA methylation and the length of the promoter region. Hsieh[48] also found that the expression of gene transcription depended on CpG island methylation density; lower levels of methylation yielded a 67% to 90% inhibition of gene expression, higher levels of methylation extinguished gene expression completely. Numerous investigations described reactivation of genes by 5-Aza-cdR by acting on various loci of the inactive X chromosome[49], the VHL gene[50], the E-cadherin gene [51], the estrogen receptor gene[52] and the p16 gene[31]. In order to detect similar methylation changes in HepG2 cell line, we also used 5-Aza-cdR.

In this study, HepG2 cells treated with 5-Aza-cdR, showed demethylation of the p16 gene. The p16 mRNA and protein were all increased dramatically, cell cycle was arrested in G1, apoptototic rate increased and implanted tumor grew more slowly. According to our results, we thought that: p16 hypermethyla tion is associated with HCC cell line; MTase is increased in HepG2 cell line; 5'CpG island of p16 promoter was not methylated completely in this HCC cell line; p16 gene can be reactivated by inhibiting the activities of MTase; p16 methylation may be a common event during the establishment of the cell line *in vitro*; and p16 gene encodes a cell cycle regulatory protein that belongs to the cyclin-dependent kinase inhibitory protein family and regulates the G1/S phase cell cycle transition, and therefore, reactivated p16 may affect the growth of the HCC cell line. Xiao *et al*[53,54] found that 17p13.3 CpG island, PYN22.1, Rb gene all showed hypermethylation, we guess that 5-Aza-cdR may reactivate those genes.

The induction of p16 activation by 5-Aza-cdR *in vivo* and the decreased tumorigenicity in animal experiment suggest the chemotherapeutic potential of 5-Aza-cdR in the management of cancer.

REFERENCES

1 Chen CJ, Yu MW, Iiaw YF. Epidemiological characteristics and risk factors of hepatocellular carcinoma. *J Gastroenterol Hepatol*, 1997;12:S294-S308

2 Tang ZY. Clinical research of hepatocellular carcinoma in the 21st century. *China Natl J New Gastroenterol*,1995;1:2-3

3 Yang JM, Wang RQ, Bu BG, Zhou ZC, Fang DC, Luo YH. Effect of hepatitis C virus infection on expression of several cancer-associated gene products in hepatocellular carcinoma. *World J Gastroentero*, 1999;5:25-27

4 Feng DY, Chen RX, Peng Y, Zheng H, Yan YH. Effect of HCV NS_3 protein on P53 protein expression in hepatocarcinogenesis. *World J Gastroentero*, 1999;5:45-46

5 Wang Y, Liu H, Zhou Q, Li X. Analysis of point mutation in site 1896 of HBV precore and its detection in the tissues and serum of HCC patients. *World J Gastroentero*, 2000;6:395-397

6 Deng ZL, Ma Y. Aflatoxin sufferer and p53 gene mutation in hepatocellular carcinoma. *World J Gastroenterol*, 1998;4:28-29

7 Sheu JC. Molecular mechanism of hepatocarcinogenesis. *J Gastroenterol Hepatol*, 1997;12:S309-S313

8 Sun BH, Zhang J, Wang BJ, Zhao XP, Wang YK, Yu ZQ, Yang DL, Hao LJ. Analysis of *in vivo* patterns of caspase 3 gene expression in primary hepatocellular carcinoma and its relationship to $p21^{WAF1}$ expression and hepatic apoptosis. *World J Gastroenterol*, 2000;6: 356-360

9 Roberts LR, LaRusso NF. Potential roles of tumor suppressor genes and microsatellite instability in hepatocellular carcinogenesis in southern African blacks. *World J Gastroenterol*, 2000; 6:37-41

10 Martins C, Kedda MA, Kew MC. Characterization of six tumor suppressor genes and microsatellite instability in hepatocellular carcinoma in southern African blacks. *World J Gastroenterol*, 1999;5:470-476

11 Chaubert P, Gayer R, Zimmermann A, Fontolliet C, Stamm B, Bosman F, Shaw P. Germ-line mutations of the $p16^{INK4}$ (MTSI) gene occur in a subset of patients with hepatocellular carcinoma.

Hepatology, 1997;25:1376-1381
12 Qin Y, Li B, Tan YS, Sun ZL, Zuo FQ, Sun ZF. Polymorphism of p16INK4a gene and rare mutation of p15INK4b gene exon2 in primary hepatocarcinoma. *World J Gastroenterol*, 2000;6:411-414
13 Challen C, Lunec J, Warren W, Collier J, Bassendine MF. Analysis of the p53 tumor-suppressor gene in hepatocellular carcinomas from Britain. *Hepatology*, 1992;16:1362-1366
14 Kress S, Jahn UR, Buchmann A, Bannash P, Schwarz M. p53 mutations in human hepatocellular carcinomas. *Cancer Res*, 1992; 52:3220-3223
15 Xiao WH, Liu WW, Lu YY, Li Z. Mutation of p53 tumor suppressor gene in hepatocellular carcinoma. *Xin Xiaohuabingxue Zazhi*, 1997;5:573-574
16 Lin GY, Chen ZL, Lu CM, Li Y, Ping XJ, Huang R. Immunohistochemical study on p53, H-rasp21, c-erbB-2 protein and PCNA expression in HCC tissues of Han and minority ethnic patients. *World J Gastroenterol*, 2000;6:234-238
17 Wang D, Shi JQ. Overexpression and mutations of tumor suppressor gene p53 in hepatocellular carcinoma. *China Natl J New Gastroenterol*, 1996;2:161-164
18 Peng XM, Peng WW, Yao JL. Codon 249 mutations of p53 gene in development of hepatocellular carcinoma. *World J Gastroenterol*, 1998;4:125-127
19 Kanai Y, Ushijima S, Hui AM, Ochiai A, Tsuda H, Sakamoto M, Hirohashi S. The E-cadherin gene is silenced by CpG methylation in human hepatocellular carcinomas. *Int J Cancer*, 1997;71:355-359
20 Simile MM, Pascale R, De Miglio MR, Nufris A, Daino L, Seddaiu MA, Gaspa L, Feo F. Correlation between Sa-denosyla-L-methionine content and production of c-myc,c-Ha-ras and c-Ki-ras mRNA transcripts in the early stages of rat liver carcinogenesis. *Cancer Lett*, 1994;79:9-16
21 Merlo A, Herman JG, Mao L, Lee DJ, Gabrielson E, Burger PC, Baylin SB, Sidransky D. 5 CpG island methytation is associated with transcriptional silencing of the tumor suppressor. p16/CDKN$_2$/MTS$_1$ in human cancers. *Nat Med*, 1995;1:686-692
22 Zhang J, Lai MD, Chen J. Methylation status of p16 gene in colorectal carcinoma and normal colonic mucosa. *World J Gastroenterol*, 1999;5:451-454
23 Gonzalez-Zulueta M, Bender CM, Yang AS, Nguyen T, Beart RW, Van Tornout JM, Jones PA. Methylation of the 5- CpG island of the p16/CDKN2 tumor suppressor gene in normal and transformed human tissues correlates with gene silencing. *Cancer Res*, 1995; 55:4531-4537
24 Costello JF, Berger MS, Huang HT, Cavence WK. Silencing of p16/CDKN2 expression in human gliomas by methylovtion and chromatin condensation. *Cancer Res*, 1996;56:2405-2410
25 Ottersen GA, Khlief SN, Chen W, Coxon AB, Kaye FJ. CDKN2 gene silencing in lung cancer by DNA hypermethylation and kinetics of *p*16^{INK4} protein induction by 5-aza-2'-deoxycytidine. *Oncogene*, 1995;11:1211-1216
26 Herman JG, Merlo A, Mao L, Lapidus RG, Issa JPJ, Davidson NE, Sidransky D, Baylin SB. Inactivation of the CDKN2/p16/MTS1 gene is frequently associated with aberrant DNA methylation in all common human cancers. *CancerRes*, 1995;55:4525-4530
27 Pinto A, Zagonel V. 5-Aza-2 -deoxycytidine and 5-Aza-cytidine in the treatment of acute myeloid leukemias and myelodysplastic syndromes: past, present, and future trends. *Leukemia (Baltimore)*, 1993;1:51-60
28 Cedar H, Razin A. DNA methylation and development. *Biochimica et Biophysica Acta*, 1990;1049:1-8
29 Jones PA, Taylor SM. Cellular differentiation,cytidine analogs and DNA methylation. *Cell*, 1980;20:85-93
30 Jones PA. Altering gene expression with 5-azacytidine. *Cell*, 1985; 40:485-486
31 Bender CM, Pao MM, Jones PA. Inhibition of DNA methylation by 5-Az--deoxycytidine suppresses the growth of human tumor cell lines. *Cancer Res*, 1998;58:95-101
32 Serrano M, Hannon GJ, Beach D. A new regulatory motif in cell-cycle control causing specific inhibition of cyclin D/cdk4. *Nature*, 1993;366:704-707
33 Nobori T, Miura K, Wu DJ, Lois A, Takabayashi K, Carson DA. Deletions of the cyclin-dependent kinase-4 inhibitor gene in multiple human cancers. *Nature*, 1994;368:753-756
34 Cannon-Albright LA, Goldgar DE, Meyer LJ, Lewis CM, Anderson DE, Fountain JW, Hegi ME, Wiseman RW, Petty EM, Bale AE. Assignment of a locus for familial melanoma, MLM, to chromosome 9p13-p22. *Science*, 1992;258:1148-1152
35 Xiong Y, Zhang H, Beach D. Subunit rearrangement of the cyclin-dependend kinases is associated with cellular transformation. *Gene Dev*, 1993;7:1572-1583
36 Serrano M, Gomez-Lahoz E, Depinho RA, Beach D, Bar-Sagi D. Inhibition of Ras-induced proliferation and cellular transformation by p16. *Science*, 1995;267:249-252
37 Hussussian CJ, Struewing JP, Goldstein AM, Higgins PA, Ally DS, Sheahan MD, Clark WH, Tucker MA, Dracopoli NC. Germline p16 mutations in familial melanoma. *Nat Genet*, 1994;8:15-21
38 Spruck CH, Gonzalez-Zulueta M, Shibata A, Simoneau AR, Lin MF, Gonzales F, Tsai YC. P16 gene in uncultured tumors. *Nature*, 1994;370:183-184
39 Caldas C, Hahn SA, Dacosta LT, Redston MS, Schutte M, Seymour AB, Weinstein CL. Frequent somatic mutations and homozygous deletions of the p16 (MTS1) gene in pancreatic adenocarcinoma. *Nat Genet*, 1994;8:27-32
40 Mori T, Miura K, Aoki T, Nishihira T, Mori S, Nakamura Y. Frequent somatic mutation of the MTS1/CDK4 gene in esophageal squamous cell carcinoma. *Cancer Res*, 1994;54:3396-3397
41 Zhou X, Tarmin L, Yin J, Jiang HY, Suzuki H, Rhyu MG, Abraham JM, Meltzer SJ. The MTS1 gene is frequently mutated in primary human esophageal tumors. *Oncogene*, 1994;9:3737-3741
42 Giani C, Finocchiaro G. Mutation rate of the CDKN2 gene in malignant gliomas. *Cancer Res*, 1994;54:6338-6339
43 Otterson GA, Demetrick DJ, Spillare EA, Hagiwara K, Hussain SP, Bennett WP, Forrester K. Mutations and altered expression of p16 in human cancer. *Proc Natl Acad Sci*, 1994;91:11045-11049
44 Hui AM,Sakamoto M,Kanai Y,Ino Y,Gotoh M, Yokota J, Hirohashi S.Inactivation of p16^{INK4} in Hepatocellular carcinoma. *Hepatology*, 1996;24:575-579
45 Sun L, Hui AM, Kanai Y, Sakamoto M, Hirohashi S. Increased DNA methyltransferase expression is associated with an early stage of human hepato-carcinogenesis. *Jpn J Cancer Res*, 1997; 88:1165-1170
46 Wong IHN, Lo YMD, Zhang J, Liew CT, Ng MHL, Wong N, Lai PBS, Lau WY, Hjelm NM, Johnson PJ. Detection of aberrant p16 methylation in the plasma and serum of liver cancer patients. *Cancer Res*, 1999;59:71-73
47 Boyes J, Bird A. Repression of genes by DNA methylation depends on CpG density and promoter strength evidence for involvement of a methyl-CpG binding protein. *EMBO J*, 1992;11:327-333
48 Hsieh CL. Dependence of transcriptional repression on CpG methylation density. *Mol Cell Biol*, 1994;14:5487-5494
49 Jones PA, Taylor SM, Mohandas T, Shapiro LJ. Cell cycle-specific reactivation of an inactive X-chromosome locus by 5-azadeoxycytidine. *Proc Natl Acad Sci USA*, 1982;79:1215-1219
50 Herman JG, Latif F, Weng Y, Lerman MI, Zbar B, Liu S, Samid D, Duan DSR, Gnarra JR, Linehan WM, Baylin SB. Silencing of the VHL tumor-suppressor gene by DNA methylation in renal carcinoma. *Proc Natl Acad Sci USA*, 1994;91:9700-9704
51 Yoshiura K, Kanai Y, Ochiai A, Shimoyama Y, Sugimura T, Hirohashi S. Silencing of the E-cadherin invasion-suppressor gene by CpG methylation in human carcinomas. *Proc Natl Acad Sci USA*, 1995;92:7416-7419
52 Ottaviome YL, Issa JP, Parl FF, Smith HS, Baylin SB, Davidson NE. Methylation of the estrogen receptor gene CpG island marks loss of estrogen receptor expression in human breast cancer cells. *Cancer Res*, 1994;54:2552-2555
53 Xiao WH, Liu WW, Lu YY, Gao CF, Chui JT, Lu R. Analysis of methylation states of CpG island at locus 17p13.3 and its significance in hepatocellular carcinoma. *Zhonghua Yixue Yichuanxue Zazhi*, 1997;14:297-299
54 Xiao WH, Liu WW, Lu YY, Gao CF. Study the mechanisms of many suppresses genes inactivation. *Disan Junyi Daxue Xuebao*, 1997;19: 324-327

Edited by Lu HM
proofread by Ma JY

P.O.Box 2345 Beijing 100023, China
Fax. 0086·10·65891893 Tel. 0086·10·65897901
E-mail.wcjd@public.bta.net.cn www.wd.org.cn

World J Gastroentero, 2001; 7(1):136 - 139
World Journal of Gastroenterology
Copyright © 2001 by the WJG Press ISSN 1007 - 9327

Methylation status of c-fms oncogene in HCC and its relationship with clinical pathology

Jun Cui, Dong Hua Yang, Xiang Jun Bi and Zi Rong Fan

Subject headings carcinoma, hepatocellular/pathology; oncogenes; DNA methylation; receptors, colony-stimulating factor; genes, fms; gene expression

Cui J, Yang DH, Bi XJ, Fan ZR. Methylation status of c-fms oncogenein HCC and its relationship with clinical pathology. ***World J Gastroenterol***, 2001;7(1):136-139

INTRODUCTION

The mechanism that DNA hypomethylation leads to activation of oncogene and occurrence of malignant neoplasm is being increasingly recognized by researchers. Normal DNA methylation plays important role in stabilizing the phenotype of cell. DNA methylation status reduction and/or pattern alteration are related to activation and abnormally high expression of some oncogenes and cellular malignancy [1-6]. c-fms oncogene encodes for colony stimulating factor 1 receptor (CSF-1R)[7], c-fms/CSF-1R was highlyexpressed in hepatocellular carcinoma (HCC) tissue, but the mechanism remained obscure[8,9]. In this study, restrictive endonucleases *Hpa* II/*Msp* I digestion and Southern blot were used to study methylation status alteration of c-fms oncogene in HCC tissue and matching circum-cancer liver tissue, meanwhile the relationship between the alteration and clinical pathology of HCC was investigated. The gist of this study was to clarify the mechanism leading to c-fms oncogene high expression in hepatocellular carcinogenesis.

MATERIALS AND METHODS

Subjects

Thirty HCC patients were verified with pathological examination (25 males and 5 females, age range 32 -76 years, mean 55 years). Fresh hepatic tissue of HCC focus and circum-tissues 2 cm from HCC focus were cut off, normal control was from HBV negative hepatic tissue of renal transplantation donor. All the tissues were washed with physiological saline and put in freezing tube, and then they were put in liquid nitrogen for storage.

Main reagents

Restrictive endonucleases *Hpa* II/*Msp* I were purchased from Japan TaKaRa Bio-Company. DIG random labeling and detection kit were purchased from Boster Bio-Company. Nylon transfer membranes used for Southern blot were purchased from Shanghai Bio-Company. c-fms plasmid was kindly provided by academician Gu Jianren in the National Laboratory for Oncogene and Related Genes, Shanghai Cancer Institute.

METHODS

DNA extraction About 0.5g hepatic tissue was triturated in mortar, and a dissolvent (10 mmol/L Tris-Cl pH 8.0,10 mmol/L EDTA pH 8.0, 0.5% SDS) 500 μL was added. The preparation was digested with proteinase K and RNase, then it was extracted twice with saturated hydroxybenzene and once with chloroform isoamyl alcohol (chloroform:isoamyl alcohol = 24:1), and at last 2.5 volumes of absolute alcohol and 0.1 volume of 3 mol/L sodium acetate (pH 5.2) were added to precipitate the DNA. The extracted DNA was dissolved in TE buffer (pH 8.0), and DNA concentration was detersmined with an ultraviolet spectrophotometer.

Probe labeling

Plasmid extraction, restrictive endonucleases digestion, reclamation and purification were performed as the methods recorded in Molecular Cloning. The probe was labeled with DIG random labeling and detection kit.

Southern blot

Genome DNA 10 μg was digested with restrictive endonucleases Hpa II and *Msp* I 50U each for 12 hours respectively. Digested DNA was examined with 0.8% agarose electrophoresis. The buffer used for electrophoresis was 0.5 × TBE. Electrophoresis was ended when 2 kb marker shifted to the middle of the gel. Photo was taken under ultraviolet ray transmission. The gel was immersed in 0.25 mol/L

Department of Gastroenterology, Zhujiang Hospital, The First Military Medical University, Guangzhou 510282, Guangdong Province, China
Jun Cui, graduated from North China Coal Medical College in 1994 and got bachelor degree, graduated from China Medical University in 1997 with master degree, worked in Yantai Yu Huang-Ding Hospital, came to the First Military Medical University in 1998 to continue the study of doctor degree. Now physician-in-charge, lecturer, specialized in the genetic diagnosis and therapy for hepatocellular carcinoma, having 10 papers published.
Supported by the Natural Science Foundation of Guangdong Province, No 990422
Correspondence to: Jun Cui, Department of Gastroenterology, Zhujiang Hospital, The First Military Medical University, Guangzhou 510282, Guangdong Province, China
Tel. 0086-20-85143369
Email. Fanzr@fimmu.edu.cn
Received 2000-07-22 **Accepted** 2000-09-29

HCl for 10 minutes, washed with distilled water for 20-30 minutes, and then immersed in denaturalizing liquid twice for 15 minutes each time. The gel was again washed twice with distilled water, and then it was immersed into neutralizing liquid twice for 15 minutes each time. A piece of nylon membrane of the same size as the gel was cut, it was immersed into 2 × SSC for 20 minutes. Transfer was performed for 18 hours at room temperature by the capillary transfer method. Then the nylon membrane was taken out and washed several times with 2 × SSC. After this, it was fixed for 20 minutes under long wave ultraviolet radiation. The transferred nylon membrane was sealed in a plastic bag and then pre-hybridizing reagent was perfused into the bag. The bag was put in a 42℃ water bath for 2 hours, and then pre-hybridizing reagent was decanted off. The bag was sealed, after the hybridizing reagent containing the DIG-labeled probe had been put in. The bag was put into a 42℃ water bath and hybridized for 20 hours. After hybridization the nylon membrane was taken out, and showed coloration according to the instruction of the DIG random labeling and detection kit.

Pathological examination and classification

The tumors were variously classified into unifocal or multifocal, and massive or nodular (a main tumor mass with satellites). The size and inner-condition of the tumors were recorded. The histological grading was based on Edmondson standard I-IV scale.

RESULTS

Southern blot of HCC tumor tissue and circum-cancer liver tissue

Hpa II and *Msp* I are isoschizomers. Both can digest CCGG sequence, but when the sequence is methylated into C-mCGG, only *Msp* I can digest while *Hpa* II can not. Methylation status of the gene may thus be determined by relying on such a difference. The data in this study showed that after digestion with *Hpa* II, hybridizing bands of less than 6.5kb in size were observed in 36.7%(11/30) of HCC tissue and 13.3%(4/30) of circum-cancer liver tissue, which resembled those of the hybridizing bands digested with *Msp* I. The results indicated that the methylation status of c-fms oncogene in the tissue was decreased (Figures 1,2).

Methylation status comparison of c-fms oncogene in HCC tissue and circum-cancer liver tissue

Hypomethylation rate of c-fms oncogene in HCC tissue and circum-cancer liver tissue was compared, the difference was determined, the result is shown in Table 1.

Table 1 Methylation status of c-fms oncogene (number of patients)

Methylation status	HCC tissue	Circum-cancer liver tissue
Normal methylation	19	26
Hypomethylation	11	4

Note: χ^2=4.36, P<0.05, hypomethylation rate of c-fms oncogene in HCC tissue was higher than that in circum-cancer liver tissue.

Relationship between hypomethylation of c-fms oncogene and clinical pathology

The relationship between hypomethylation of c-fms oncogene in hepatic tissue and the sex, age and pathological Edmondson scale of patients was analysed; the results are shown in Table 2.

Table 2 Relationship between hypomethylation of c-fms oncogene and clinical pathology

Item		Total number	HCC tissue		Circum-cancer liver tissue	
			Number	%	Number	%
Sex	Male	25	10	41.0	3	12.0
	Female	5	1	20.0	1	20.0
Age(yrs)	<60	22	7	31.8	2	9.1
	⩾60	8	4	50.0	2	25.0
Edmondson	I-II	14	2	14.3	1	7.1
scale	III-IV	16	9	56.3[b]	3	18.8

[b]P<0.05, *vs* Edmondson I-II.

Chi-square test showed that there was no significant relationship between hypomethylation of c-fms oncogene and sex and age of patients (P>0.05). There was significant relationship between Edmondson scale and hypomethylation of c-fms oncogene in HCC tissue (χ^2=5.66, P<0.05), while there was no significant relationship between Edmondson scale and hypomethylation of c-fms oncogene in circum-cancer liver tissue(P>0.05).

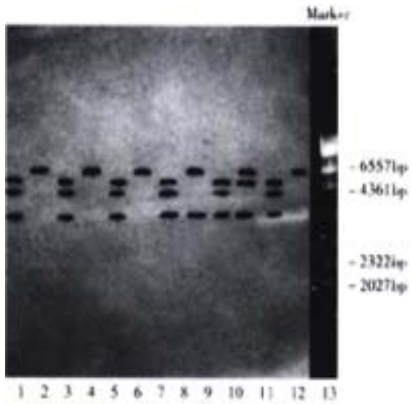

Figure 1 Southern blot of HCC tissue genome DNA digested with *Hpa* II / *Msp* I.
Lane 1, 3, 5, 7, 9, 11 *Msp* I digestion;
Lane 2, 4, 6, 8, 10, 12 *Hpa* II digestion;
Lane 13 λDNA / *Hind* III markers;
Lane 1, 2 normal control hepatic tissue;
Lane 3-12 HCC tissue;
Lane 8, 10 hybridizing bands of less than 6.5kb in size appeared after *Hpa* II digestion

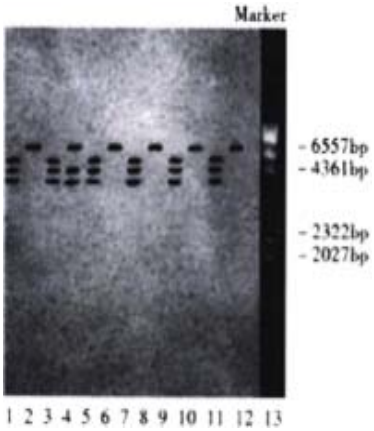

Figure 2 Southern blot of circum[a2]cancer liver tissue genome DNA digested with *Hpa* II / *Msp* I. Lane 1, 3, 5, 7, 9, 11 *Msp* I digestion; Lane 2, 4, 6, 8, 10, 12 *Hpa* II digestion;
Lane 13 λDNA / *Hind* III markers;
Lane 1, 2 normal control hepatic tissue;
Lane 3-12 circum-cancer liver tissue;
Lane 4 hybridizing bands of less than 6.5kb in size appeared after *Hpa* II digestion

DISCUSSION

In the process of cellular carcinogenesis, genetic and epigenetic mechanism contributes to abnormal expression of gene. The genetic mechanism involves the mutation and chromosome rearrangement, with which genetic products of abnormal molecular structures can be produced[10-19]. The epigenetic mechanism mainly refers to an altered methylation status of 5'-cytosine in the DNA sequence, which leads to an abnormal expression of gene in quantity, but no change in DNA sequence and genetic product [20-24]. In the process of cellular carcinogenesis, the methyl groups in CpG islands of DNA are lost gradually. Although the accurate mechanism between DNA hypomethylation and cellular carcinogenesis remains obscure, some data showed that DNA hypomethylation could affect chromatin condensation in the middle stage, which led to a change and/or rupture of chromosome[25-31]. DNA hypomethylation is a kind of molecular structure leading to abnormal expression of gene; it facilitates a high expression of gene[32]. Highly specific DNA methylation types exist in human genomes, and are reflected in genetic characteristics of DNA, such as transcription, duplication, recombination, transposition and mutation. One biological function of human genome DNA methylation is to keep promoter of gene in silent status for long. 5' methyl-cytosine in special DNA sequence can mediate the specific combination and interaction between DNA and some functional proteins. As the interactions locate in the core region which regulates biological function of gene, sequence-specific methylation of DNA can affect cellular function[33-39]. Furthermore, DNA methylation depends on combining special proteins, and it directly or indirectly induced conformational alterations of DNA. DNA methylation is a kind of modificatory mode of cellular DNA at transcription level. In human genome, CpG islands in house keeping genes including a great number of oncogenes are in the form of methylation. Transcription and expression of the methylated genes especially oncogenes are limited. Decline of DNA methylation status at special sites of oncogene induces abnormal expression of the gene[28,40-43].

c-fms oncogene locates at 5q 33.3 of human chromosome and encodes CSF 1R, which has tyrosine kinase activity[44]. c-fms/CSF-1R is highly expressed in hepatocellular carcinogenesis, and its expressing level in HCC tissue is higher than that in circum-cancer liver tissue. Through the mechanism of signal transduction, CSF-1R stimulates the growth and development of HCC [45-50]. The whole length of c-fms oncogene is 43kb, in which there are 49 CCGG sites. The data in this study indicated that the hypomethylation rate of c-fms oncogene in HCC tissue was higher than that in circum-cancer liver tissue, while no hypomethylation of c-fms oncogene in normal hepatic tissue was observed. So hypomethylation is an important activating mechanism of c-fms oncogene in hepatocellular carcinogenesis. The data also showed that the hypomethylation rate of c-fms oncogene in Edmondson III-IV HCC was higher than that in Edmondson I-II HCC. All the evidence indicated that hypomethylation of c-fms oncogene might be an important late genetic incident in hepatocellular carcinogenesis. HCC with hypomethylation of c-fms oncogene may show the characteristics of higher malignancy and rapid development, and provide a clinical guide in the selection of surgery, radiotherapy and chemotherapy, and also in judging the prognosis of patients.

c-fms/CSF-1R is abnormally high-expressed in hepatocellular carcinogenesis at a late stage, meanwhile hypomethylation of c-fms oncogene occurs, and the hypomethylation rate of c-fms oncogene in HCC tissue is higher than that in the circum-cancer liver tissue. These data indicate that hypomethylation of c-fms oncogene is a kind of molecular mechanism leading to abnormally high CSF-1R expression and promoting the occurrence and development of HCC. So blocking the process of hypomethylation of c-fms oncogene, consequently decreasing a high expression of CSF-1R may have great clinical significance in decreasing malignant phenotype of HCC and improving prognosis of patients.

REFERENCES

1 Yao D, Jiang D, Huang Z, Lu J, Tao Q, Yu Z, Meng X. Abnormal expression of hepatoma specific gamma-glutamyl transferase and alteration of gamma-glutamyl transferase gene methylation status in patients with hepatocellular carcinoma. *Cancer*, 2000;88:761-769
2 Nagai H, Kim YS, Yasuda T, Ohmachi Y, Yokouchi H, Monden M, Emi M, Konishi N, Nogami M, Okumura K, Matsubara K. A novel sperm-specific hypomethylation sequence is a demethylation hotspot in human hepatocellular carcinomas. *Gene*, 1999;237:15-20
3 Tsujiuchi T, Tsutsumi M, Sasaki Y, Takahama M. Konishi Y. Hypomethylation of CpG sites and c-myc gene overexpression in hepatocellular carcinomas, but not hyperplastic nodules, induced by a choline-deficient L-amino acid-defined diet in rats. *Jpn J Cancer Res*,

1999;90:909-913
4 Dong Z, Wang X, Zhao Q, Townsend CM Jr, Evers BM. DNA methylation contributes to expression of the human neurotensin/neuromedin N gene. *Am J Physiol*, 1998;274:G535-543
5 Yakoob J, Fan XG, Hu GL, Zhang Z. DNA methylation and carcinogenesis in digestive neoplasms. *World J Gastroenterol*, 1998; 4:174-177
6 Zhang J, Lai MD, Chen J. Methylation status of p16 gene in colorectal carcinoma and normal colonic mucosa. *World J Gastroenterol*, 1999;5:451-454
7 Sherr CJ. The fms oncogene. *Biochimica et Biophys Acta*, 1988; 948:225-243
8 Yang DH, Liu WW, Gu JR, Wan DF, Li HN, Ma AQ, Qu SM, Xu XL. Expression of cancer gene products of IGF-II, IGF-II receptors, CSF-1 receptors in primary hepatic cancer and non-cancerous liver tissue. *Zhonghua Yixue Zazhi*, 1992;72:476-480
9 Motoo Y, Mahmoudi M, Osther K, Bollon AP. Oncogene expression in human hepatoma cells PLC/PRF/5. *Biochem Biophys Res Commun*, 1986;135:262-268
10 Huang H, Fujii H, Sankila A, Mahler Araujo BM, Matsuda M, Cathomas G, Ohgaki H. Beta-catenin mutations are frequent in human hepatocellular carcinomas associated with hepatitis C virus infection. *Am J Pathol*, 1999;155:1795-1801
11 Yang SM, Zhou H, Chen RC, Wang YF, Chen F, Zhang CG, Zhen Y, Yan JH,Su JH. Sequencing of p53 mutation in established human hepatocellular carcinoma cell line of HHC4 and HHC15 in nude mice. *World J Gastroenterol*, 1998;4:506-510
12 Martins C, Kedda MA, Kew MC. Characterization of six tumor suppressor genes and microsatellite instability in hepatocellular carcinoma in southern African blacks. *World J Gastroenterol*, 1999; 5:470-476
13 Liew CT, Li HM, Lo KW, Leow CK, Chan JY, Hin LY, Lau WY, Lai PB, Lim BK, Huang J, Leung WT, Wu S, Lee JC. High frequency of p16INK4A gene alterationsin hepatocellular carcinoma. *Oncogene*, 1999;18:789-795
14 Yano M, Asahara T, Dohi K, Mizuno T, Iwamoto KS, Seyama T. Close correlation between a p53 or hMSH2 gene mutation in the tumor and survival of hepatoc ellular carcinoma patients. *Int J Oncol*, 1999;14:447-451
15 Qin Y, Li B, Tan YS, Sun ZL, Zuo FQ, Sun ZF. Polymorphism of p16INK4a gene and rare mutation of p15INK4b gene exon2 in primary hepatocarcinoma. *World J Gastroentero*, 2000;6:411-414
16 Yakicier MC, Irmak MB, Romano A, Kew M, Ozturk M. Smad2 and Smad4 gene mutations in hepatocellular carcinoma. *Oncogene*, 1999;18:4879-4883
17 Park WS, Dong SM, Kim SY, Na EY, Shin MS, Pi JH, Kim BJ, Bae JH, Hong YK, Lee KS, Lee SH, Yoo NJ, Jang JJ, Pack S, Zhuang Z, Schmidt L, Zbar B, Lee JY. Somatic mutations in the kinase domain of the Met/hepatocyte growth factor receptor gene in childhood hepatocellular carcinomas. *Cancer Res*, 1999;59:307-310
18 Luo D, Liu QF, Gove C, Naomov NV, Su JJ, Williams R. Analysis of Na-ras gene mutation and p53 gene expression in human hepatocellular carcinomas. *World J Gastroenterol*, 1998;4:97-99
19 Peng XM, Peng WW, Yao JL. Codon 249 mutations of p53 gene in development of hepatocellular carcinoma. *World J Gastroenterol*, 1998;4:125-127
20 Lai DN, Xie YF, Bian L, Yao X. Study on p16 gene aberrant methylation of colon cancer cell lines. *Shijie Huaren Xiaohua Zazhi*, 1999;7:676-678
21 Kitamura T, Watanabe S, Sato N. Liver regeneration, liver cancers and cyclins. *J Gastroenterol Hepatol*, 1998;13(Suppl):S96-99
22 Koyama M, Nagai H, Bando K, Ito M, Moriyama Y, Emi M. Localization of a target region of allelic loss to a 1-cM interval on chromosome 16p 13.13 in hepatocellular carcinoma. *Jpn J Cancer Res*, 1999;90:951-956
23 Kim KS, Lee YI. Biallelic expression of the H19 and IGF2 genes in hepatocellular carcinoma. *Cancer Lett*, 1997;119:143-148
24 Hada H, Koide N, Morita T, Shiraha H, Shinji T, Nakamura M, Ujike K,Takayama N, Oka T, Hanafusa T, Yumoto Y, Hamazaki K, Tsuji T. Promoter-independent loss of mRNA and protein of the Rb gene in a human hepatocellular carcinoma. *Hepatogastroenterology*, 1996;43:1185-1189
25 Robertson KD, Jones PA. DNA methylation: past, present and future directions. *Carcinogenesis*, 2000;21:461-467
26 Rizwana R, Hahn PJ. CpG methylation reduces genomic instability. *J Cell Sci*, 1999;112:4513-4519
27 Qu GZ, Grundy PE, Narayan A, Ehrlich M. Frequent hypomethylation in Wilms tumors of pericentromeric DNA in chromosomes 1 and 16. *Cancer Genet Cytogenet*, 1999;109:34-39
28 Qu G, Dubeau L, Narayan A, Yu MC, Ehrlich M. Satellite DNA hypomethylation *vs* overall genomic hypomethylation in ovarian epithelial tumors of different malignant potential. *Mutat Res*, 1999;423:91-101
29 Jeddeloh JA, Stokes TL, Richards EJ. Maintenance of genomic methylation requires a SWI2/SNF2-like protein. *Nat Genet*, 1999;22:94-97
30 Dao D, Walsh CP, Yuan L, Gorelov D, Feng L, Hensle T, Nisen P, Yamashiro DJ, Bestor TH, Tycko B. Multipoint analysis of human chromosome 11p15/mouse distal chromosome 7: inclusion of H19/IGF2 in the minimal WT2 region, gene specificity of H19 silencing in Wilms tumorigenesis and methylation hyper-dependence of H19 imprinting. *Hum Mol Genet*, 1999;8:1337-1352
31 Goto T, Christians E, Monk M. Expression of an Xist promoter-luciferase construct during spermatogenesis and in preimplantation embryos: regulation by DNA methylation. *Mol Reprod Dev*, 1998;49:356-367
32 Wachsman JT. DNA methylation and the association between genetic and epigenetic changes: relation to carcinogenesis. *Mutat Res*, 1997;375:1-8
33 Lu S, Davies PJA. Regulation of the expression of the tissue transglutaminase gene by DNA methylation. *Proc Natl Acad Sci USA*, 1997;94:4692-4697
34 Hansen RS, Wijmenga C, Luo P, Stanek AM, Canfield TK, Weemaes CM, Gartler SM. The DNMT3B DNA methyltransferase gene is mutated in the ICF immunodeficiency syndrome. *Proc Natl Acad Sci USA*, 1999;96:14412-14417
35 Kovarik A, Van-Houdt H, Holy A, Depicker A. Drug-induced hypomethylation of a posttranscriptionally silenced transgene locus of tobacco leads to partial release of silencing. *FEBS Lett*, 2000;467:47-51
36 Schmutte C, Fishel R. Genomic instability: first step to carcinogenesis. *Anticancer Res*, 1999;19:4665-4696
37 Cho M, Grabmaier K, Kitahori Y, Hiasa Y, Nakagawa Y, Uemura H, Hirao Y, Ohnishi T, Yoshikawa K, Ooesterwijk E. Activation of the MN/CA9 gene is associated with hypomethylation in human renal cell carcinoma cell lines. *Mol Carcino*, 2000;27:184-189
38 Felgner J, Heidorn K, Korbacher D, Frahm SO, Parwaresch R. Cell lineage specificity in G-CSF receptor gene methylation. *Leukemia*, 1999;13:530-534
39 Florl AR, Lower R, Schmitz-Drager BJ, Schulz WA. DNA methylation and expression of LINE-1 and HERV-K provirus sequences in urothelial and renal cell carcinomas. *Br J Cancer*, 1999;80:1312-1321
40 Jones PL, Wolffe AP. Relationships between chromatin organization and DNA methylation in determining gene expression. *Semin Cancer Biol*, 1999;9:339-347
41 Chiurazzi P, Pomponi MG, Pietrobono R, Bakker CE, Neri G, Oostra BA. Synergistic effect of histone hyperacetylation and DNA demethylation in the reactivation of the FMR1 gene. *Hum Mol Genet*, 1999;8:2317-2323
42 Devereux TR, Horikawa I, Anna CH, Annab LA, Afshari CA, Barrett JC. DNA methylation analysis of the promoter region of the human telomerase reverse transcriptase (hTERT) gene. *Cancer Res*, 1999;59:6087-6090
43 Torres L, Avila MA, Carretero MV, Latasa MU, Caballeria J, Lopez-Rodas G, Boukaba A, Lu SC, Franco L, Mato JM. Liver-specific methionine adenosyltransferase MAT1A gene expression is associated with a specific pattern of promoter methylation and histone acetylation: implications for MAT1A silencing during transformation. *FASEB J*, 2000;14:95-102
44 Cui J, Yang DH. CSF-1 receptor/c-fms and liver cancer. *Shijie Huaren Xiaohua Zazhi*, 2000;8:696-697
45 Hamilton JA. CSF-1 signal transduction. *J Leukoc Biol*, 1997;62: 145-155
46 Choudhury GG, Sylvia VL, Pfeifer A, Wang LM, Smith EA, Sakaguchi AY. Human colony stimulating factor-1 receptor activates the C-raf-1 proto-oncogene kinase. *Biochem Biophys Res Commun*, 1990;172:154-159
47 Roussel MF. Signal transduction by the macrophage-colony-stimulating factor receptor (CSF-1R). *J Cell Sci*, 1994;18(Suppl):105-108
48 Flick MB, Sapi E, Perrotta PL, Maher MG, Halaban R, Carter D, Kacinski BM. Recognition of activated CSF-1 receptor in breast carcinomas by a tyrosine 723 phosphospecific antibody. *Oncogene*, 1997;14:2553-2561
49 Hatch WC, Ganju RK, Hiregowdara D, Avraham S, Groopman JE. The related adhesion focal tyrosine kinase (RAFTK) is tyrosine phosphorylated and participates in colony-stimulating factor-1/macrophage colony-stimulating factor signaling in monocyte-macrophages. *Blood*, 1998;91:3967-3973
50 Rohrschneider LR, Bourette RP, Lioubin MN, Algate PA, Myles GM, Carlberg K. Growth and differentiation signals regulated by the M-CSF receptor. *Mol Reprod Dev*, 1997;46:96-103

Edited by Lu HM
proofread by Ma JY

P.O.Box 2345 Beijing 100023, China
Fax. 0086·10·65891893 Tel. 0086·10·65897901
E-mail.wcjd@public.bta.net.cn www.wd.org.cn

World J Gastroentero, 2001; 7(1):140 - 142
World Journal of Gastroenterology
Copyright © 2001 by the WJG Press ISSN 1007 - 9327

Influencing factors of rat small intestinal epithelial cell cultivation and effects of radiation on cell proliferation

Xin Ze Ran, Yong Ping Su, Yong Jiang Wei, Guo Ping Ai, Tian Min Cheng and Yuan Lin

Subject headings intestine, small; intestinal epithelial cell; radiation; cells, cultured; radiation dosage; immunohistochemistry; microscopy, electron

Ran XZ, Su YP, Wei YJ, Ai GP, Cheng TM, Lin Y. Influencing factors of rat small intestinal epithelial cell cultivation and effects of radiation on cell proliferation. ***World J Gastroenterol***, 2001;7(1):140-142

INTRODUCTION

Crypt epithelial cells in normal small intestine proliferate at a high speed. But they are very difficult to culture *in vitro* and passage stably. A lot of studies have been done [1-16]. Some domestic labs isolated and cultured crypt cells from embryonal intestines and aseptic animal intestine, but failed. We introduced normal rat epithelial cell line IEC-6 from the USA and its living condition for stable passage was successfully established after trials. The cell line was testified to be the small intestinal epithelial cell by electronmicroscopy,immunihistochemistryandenzymatic-histoch-emistry. It has been applied to some related research work[17-21]. It was found that many factors were involved in the culture system. Our present study focuses on the culture method and the influencing factors on IEC-6.

MATERIALS AND METHODS

Reagents

Dulbecco's modified Eagle Medium (DMEM), HEPES from Sigma Cooperation, ^{3}H-TdR with the radioactive concentration of 37 MBq/mL and activity ratio of 740GBp/mL is the product of the Chinese Nuclear Science Institute.

Apparatus

Carbon dioxide culture case, Model Queue 2721, USA; automatic liquid scintillation counter, Model 1217, Sweden; cell harvester, Model 2T-II, Zhejiang Province; and microplate, Japan.

Institute of Combined Injury, PLA, School of Preventive Medicine, Third Military Medical University, Chongqing 400038, China
Dr. Xin Ze Ran, graduated from Third Military Medical University in 1980, now engaged in the research of combined radiation injuries for 20 years and having 40 papers published.
Supported by the National Natural Science Foundation of China, No. 39100119
Correspondence to: Dr. Xin Ze Ran, Institute of Combined Injury, PLA School of Preventive Medicine, Third Military Medical University, Chongqing 400038, China
Tel. 0086-23-68752278, Fax 0086-23-68752279
Email. Rxz@mail.tmmu.com.cn
Received 2000-08-08 **Accepted** 2000-09-29

Cell line

Intestinal epithelial cell line, No. 6, IEC-6 was provided by the General Hospital of Massachusetts, Boston, USA.

Culture liquid medium

Liquid DMEM/L was made up according to the protocol supplemented with HEPES 10 mmol, penicillin 10^5U, streptomycin 100 mg, sodium carbonate 3.7 g and fetal bovine serum 100 mmol. L-glutamine 200 mmol/L was added before use.

Establishment of cell passage and detection of activity

IEC-6 cell line was immediately put into 40℃ water bath to thaw after being taken from liquid nitrogen, centrifuged for 10 minutes at 1000r/min. Liquid medium was added per bottle after the supernatant was deserted. Then the bottle was put into the carbon dioxide case (10% CO_2, 18.6% O_2 100% relative humidity, 37℃). After the cells adhered to the wall, change the liquid once, then passage on the 5th day. When the cell was passaged or the activity was detected, the liquid medium was deserted and 0.02% EDTA 8 mL was added for digestion of 30 minutes at 37℃. The incompletely digested cells were scraped softly with curved tube, passed into centrifuge tube and centrifuged for 8 minutes at 1000r/min. Supernatant was deserted and the liquid medium was added to a certain concentration. The cells were then seeded onto 96-well plates and cultured for 72 hours. ^{3}H-TdR, 1.5uCi per well, was added at the 12th hour before the culture was stopped. At the end of the culture, the cells were digested with 0.02% EDTA, harvested on the glass fiber filter membrane, and heated at 80℃. When the membrane cooled down to the room temperature, 8 mL scintillation liquid was added, Cpm was measured with automatic liquid scintillation counter.

Scintillation liquid contained POPOP 0.4 g, PPo 4 g, xylene 1000 mL.

RESULTS AND DISCUSSION

Effect of IEC-6 density

IEC-6 cells at various densities in microplate wells were labeled with ^{3}H-TdR 18.5kBq and cultured for 72 hours to investigate its effect on proliferation. Table 1 shows that at a certain range of densities, ^{3}H-TdR incorporation increased with the IEC-6 amount, the peak was at 10×10^4/well. Positive

correlation was found between cell density (X) and ^{3}H-TdR incorporation (y) at the range of 1.25×10^4-10×10^4/well with the correlation coefficient $r = 0.956$ and regression equation $y = 2177X+3575$(min^{-1}). When the cell density was more than 11.25×10^4/well, there was negative correlation ($r = 0.986$, y) = 36782-1253 X), possibly due to the limit amount of nutrition, liquid evaporation and subject to changes of culture condition[22].

Table 1 Effect of density on ^{3}H-TdR incorporation in culture cell ($\bar{x} \pm s$)

Density ($\times10^4$/ well)	n	Min^{-1}	Density ($\times10^4$/ well)	n	Min^{-1}
1.25	18	3547 ± 681	11.25	20	23648 ± 1398
2.50	20	9941 ± 413	12.50	18	20593 ± 2245
5.00	18	17931 ± 2051	13.75	20	19812 ± 2310
7.50	18	19825 ± 2135	15.00	18	17638 ± 959
10.00	24	23789 ± 2536	17.50	22	14874 ± 881

Effect of culture time

Incorporation of ^{3}H-TdR was different after IEC-6 was cultured for 6, 12, 24, 48, 72 and 96 hours (Table 2). Within 72 hours, incorporation increased from 1846 ± 146 to 25727 ± 4006 (min^{-1}) along with the time prolongation and it reached its peak at 72 hour. But when the culture time extended to 96 hours, the incorporation decreased. This may be caused by the activity inhibition of some IEC-6 under non-physical conditions.

Table 2 Effect of culture time on IEC-6 cell proliferation ($\bar{x} \pm s$)

Culture time (h)	n	Min^{-1}	Culture time (h)	n	Min^{-1}
6	24	1846 ± 146	48	24	21258 ± 1240
12	26	4038 ± 363	72	24	25727 ± 2006
24	24	6367 ± 588	96	24	24355 ± 2079

Effect of different ^{3}H-TdR dosage

In this study, different dosage of ^{3}H-TdR was administered in the IEC-6 culture system. A linear correlation was found between the ^{3}H-TdR incorporation and dosage when the dose was below 55.5KBq/well. When larger dosage was used, the incorporations slightly increased or decreased (Table 3). The radioactive damage to cells and consequent inhibition of DNA synthesis by high concentration of ^{3}H-TdR contributed to the incorporation decrease. Generally, the dosage of 18.5 KBq/well ^{3}H-TdR to 10×10^4 cell yielded a satisfactory result of incorporation 2.5×10^4.

Table 3 Effect of ^{3}H-TdR dosage on IEC-6 cell proliferation ($\bar{x} \pm s$)

^{3}H-TdR dosage (kBq / well)	n	Min^{-1}	^{3}H-TdR dosage (kBq / well)	n	Min^{-1}
0.00	20	139 ± 29	27.75	21	27555 ± 1637
2.31	22	1333 ± 118	37.00	21	37235 ± 1485
4.62		10136 ± 1083	46.25	22	41874 ± 1213
9.25	24	16880 ± 1447	55.05	24	48072 ± 1676
18.50	24	24890 ± 1623	74.00	20	42430 ± 1735

Effect of pH in lipid medium

pH of culture medium is one of the most important factors in cell culture. To optimize the culture condition, the pH value was set at 6.0, 6.6, 7.26, 7.6, 8.0 and 8.8, and ^{3}H-TdR incorporation was measured respectively (Table 4). The incorporation was the highest at pH 7.26, lower pH at 6.6 and 7.6, and the lowest at pH 6.0 and 8.0. In the common sense, cells can survive when pH ranged from 6 to 8. Variant cells and animal species do not have the same optimal pH. It is believed that optimal pH has an effect on the survival of cells *in vitro* by adjusting the intracellular enzymes and proliferation factors. We therefore set the optimal pH 7.26 in IEC-6 culture medium.

Table 4 Effect of pH of culture medium on ^{3}H-TdR incorporation ($\bar{x} \pm s$)

pH	n	Min^{-1}	pH	n	Min^{-1}
6.0	20	4528 ± 660	7.6	28	12897 ± 1301
6.6	24	18771 ± 920	8.0	20	1305 ± 146
7.26	24	22510 ± 1448	8.8	20	636 ± 102

Effect of insulin and concentration of fetal bovine serum

Fetal bovine serum is one of the essential factors in cell culture *in vitro*. If the concentration of fetal bovine serum is too low, cells will die or have proliferation prohibited. When the concentration is too high, the osmotic pressure in culture medium will change and it will influence the survival of cells. In this study, we found that 10% of fetal bovine serum was optimal in culture medium. Content of glucose in DMEM was high (4500 mg/L) and insulin can speed up glucose oxygenolysis and transportation through cell membrane, so the use of glucose was accelerated in the cells. The results showed that incorporation of ^{3}H-TdR was higher in cells treated with insulin than in the cells (Table 5) without insulin treatment.

Table 5 Effect of insulin and concentration of fetal bovine serum on IEC-6 cell proliferation ($\bar{x} \pm s$)

Fetal bovine serum(%)	n	Min^{-1}	
		Insulin group	Control group
0.0	18	476 ± 22	510 ± 101
2.5	20	13111 ± 978	1901 ± 580
5.0	22	14756 ± 1094	9097 ± 1069
7.5	22	20262 ± 2012	14569 ± 1136
10.0	24	23666 ± 1114	18775 ± 1361
15.0	20	22743 ± 1728	17645 ± 1289
20.0	18	22590 ± 1603	16965 ± 1147

Repeatability measurement

To investigate the experimental method, stability and the researcher's error, repeatability was measured by dividing the same culture system of IEC-6 into 30 parts. The incorporation of ^{3}H-TdR was 24327 ± 808 (min^{-1}). The value ranged from 23921 to 24733 when $P<0.01$ and coefficient of variation was 3.32%.

Effect of ionizing radiation on IEC-6

Intestinal epithelial cells are sensitive to ionizing radiation. The changes of incorporation of ^{3}H-TdR showed the damage of ionizing radiation on cells which reflected the cell biological characteristics. When IEC-6 was not exposed to radiation, the incorporation was 24327 ± 808. Incorporation after 4Gy, 8Gy, 16Gy, 2Gy and 26y irradiation were 31.8%, 24.1%, 15.2%, 11.2% and 8. 3% of control. Significantly negative dose-effect relation was found with the relative coefficient r = -0.970 (Table 6).

Table 6 Effect of ionizing radiation dosage on ^{3}H-TdR incorporation in IEC-6 cell ($\bar{x} \pm s$)

Dosage(Gy)	Min^{-1}	(%)	Dosage(Gy)	Min^{-1}	(%)
0	13427 ± 803	100.0	16	3698 ± 371	15.2
4	7736 ± 765	31.8	18	3381 ± 235	13.9
6	7249 ± 472	29.8	20	3041 ± 327	12.5
8	5863 ± 594	24.1	22	2725 ± 348	11.2
10	4865 ± 586	20.0	24	2481 ± 263	10.2
14	4136 ± 424	17.0	26	2019 ± 154	8.3
			r = -0.970		

In summary, methods of IEC-6 culture, passage and activity detection established in this study have the advantage of easy handling, being reliable in results, using less amounts of cells and a good repeatability. Subjective error can be avoided in measurement of epithelial proliferation with radioactivity. These will provide an ideal method for the research[23-35] on intestinal epithelimm[36-42].

REFERENCES

1 Rogler G, Aschenbrenner E, Gross V, Stange EF, Scholmerich J. Intracellular transport of high-density lipoprotein 3 in intestinal epithelial cells ($Caco_2$) is tubulin associated. *Digestion*, 2000;61:47-58

2 Hofman P, Piche M, Far DF, Le-Negrate G, Selva E, Landraud L, Alliana-Schmid A, Boquet P, Rossi B. Increased Escherichia coli phagocytosis in neutrophils that have transmigrated across a cultured intestinal epithelium. *Infect Immun*, 2000;68:449-455

3 Said HM. Cellular uptake of biotin: mechanisms and regulation. *J Nutr*, 1999;129(2S Suppl):490S-493S

4 Eckmann L, Stenson WF, Savidge TC, Lowe DC, Barrett KE, Fierer J, Smith JR, Kagnoff MF. Role of intestinal epithelial cells in the host secretory response to infection by invasive bacteria. Bacterial entry induces epithelial prostaglandin h synthase-2 expression and prostaglandin E2 and F2alpha production. *J Clin Invest*, 1997;100:296-309

5 Tripuraneni J, Koutsouris A, Pestic L, De-Lanerolle P, Hecht G. The toxin of diarrheic shellfish poisoning, okadaic acid, increases intestinal epithelial paracellular permeability. *Gastroenterology*, 1997;112:100-108

6 Hidalgo IJ. Cultured intestinal epithelial cell models. *Pharm Biotechnol*, 1996;8:35-50

7 Augustijns PF, Borchardt RT. Transport and metabolism of delta sleep-inducing peptide in cultured human intestinal epithelial cell monolayers. *Drug Metab Dispos*, 1995;23:1372-1378

8 Zheng L,Chen J, Zhu Y, Yang H, Elmquist W, Hu M. Comparison of the transport characteristics of D- and L-methionine in a human intestinal epithelial model (Caco-2) and in a perfused rat intestinal model. *Pharm Res*, 1994;11:1771-1776

9 Chikhale PJ, Borchardt RT. Metabolism of L-alpha-methyldopa in cultured human intestinal epithelial (Caco-2) cell monolayers. Comparison with metabolism *in vivo*. *Drug Metab Dispos*, 1994;22:592-600

10 Das S, Traynor-Kaplan A, Kachintorn U, Aley SB, Gillin FD.GP49, an invariant GPI-anchored antigen of Giardia lamblia. *Braz J Med Biol Res*, 1994;27:463-469

11 Rokutan K, Sakai A, Teramoto F, Kido Y, Shizuka F, Kishi K. Epidermal growth factor-induced mitogen signals in cultured intestinal epithelial cells. *J Gastroenterol*, 1994;29(Suppl 7):59-62

12 Lambert RW, Kelleher RS, Wickham LA, Vaerman JP, Sullivan DA. Neuroendocrinimmune modulation of secretory component production by ratlacrimal,salivary, and intestinal epithelial cells. *Invest Ophthalmol Vis Sci*, 1994;35:1192-1201

13 Sunitha I, Meighen DL, Hartman DP, Thompson EW, Byers SW, Avigan MI.Hepatocyte growth factor stimulates invasion across reconstituted basement membranes by a new human small intestinal cell line. *Clin Exp Metastasis*, 1994;12:143-154

14 Sanderson IR, He Y. Nucleotide uptake and metabolism by intestinal epithelial cells. *J Nutr*, 1994;124(1 Suppl):131S-137S

15 Quaroni A, Wands J, Trelstad RL, Isselbacher KJ. Epithelioid cell cultures from rat small intestine. Characterization by morphologic and immunologic criteria. *J Cell Biol*, 1979;80:248-265

16 Gike M, Kanai M, Lynch-Devaney K, Podolsky DK. Rapid mitogen-activated protein kinase activation by transforming growth factor in wounded rat intestinal epithelial cells.*World J Gastroenterol*, 1998;4:263

17 Wang XH, Zhou Z, Zhu GX, Lou SF, Ran XZ, Cheng TM, Yu ZP. Protective effect of keratinocyte growth factor on intestinal epithelial cell line No.6 after irradiation. *Disan Junyi Daxue Xuebao*, 2000;22:713-715

18 Bai XD, Liu XH, Su YP. Inhibitory effects intestinal mucus on bacterial adherence to cultured intestinal epithelial cell after burns. *Disan Junyi Daxue Xuebao*, 1998;20:214-216

19 Zhang WJ, Ke JX, Shi TZ, L¨1 YH, Su YP, Bai XD, Ran XZ. An improving method of ultramicrotomy for cultured cell. *Disan Junyi Daxue Xuebao*, 1996;18:A48-A49

20 Wang JP, Hu CM, Su YP, Cheng TM. Preliminary identification of the genes expressed in intestinal epithelial cell after radiation injury in mice. *Disan Junyi Daxue Xuebao*, 1999;21:387-389

21 Xu H, Cheng TM, Su YP, Lin Y. Effects of total body irradiation on functions of small intestinal intraepithelial lymphocytes. *Zhonghua Fangshe Yixue Yu Fanghu Zazhi*, 1999;19:18-21

2 Zhou DH, Shen YS, Zhao MR. The application of MTT colorimetric aeasured the proliferation of lymphocytes and activity of rat/mouse IL-2. *Zhongguo Mianyixue Zazhi*, 1986;2:39-44

23 Zhang XL, Wang GH, Han L, Su L,Sheng Z, Zou JH, Liu JY. Transformation and influencing factors of the peripheral blood T lymphocytes of dometic rabbits. *Beijing Yike Daxue Xuebao*, 1988;20:10

24 Peng ZS, Liang ZC, Liu MC, Ouyang NT. Studies on gastric epithelial cell proliferation and apoptosis in Hp associated gastric ulcer. *Shijie Huaren Xiaohua Zazhi*, 1999;7:218-219

25 Wu YZ, Wu JS, Lai DN, Ma QJ, He ZS, Gao DM. Relationship between ectasias in gastric microvascular system and cytokinetics in gastric mucous epithelial cell group in PHG-MH rats. *Huaren Xiaohua Zazhi*, 1998;6:752-754

26 Fang DC, Liu W, Lang HJ, Liu WW. Effects of Naa-2SeOa-3 on UnscheduledDNA synthesis, lipid peroxidation and ras P21 expression in gastric epithelial cells. *Huaren Xiaohua Zazhi*, 1998;6:421-422

27 Wang LD, Zhou Q, Gao SS, Li YX, Yang WC. Measurements of cell proliferation in esophageal and gastric cardia epithelia of subjects in a high incidence area for esophageal cancer. *China Natl J New Gastroenterol*, 1996;2:82-85

28 Chen XM, Han DW, Noguchi K, Tanikawa K. Uptake of bacterial lipopolysaccharide and expression of tumor necrosis factor-mRNA in isolated rat intrahepatic bile duct epithelial cells. *China Natl J New Gastroenterol*, 1997;3:3-5

29 Wang ZX, Shen HF, Chen HJ. Adherent properties of Helicobacter pylori to human epithelial cells. *China Natl J New Gastroenterol*,1997;3:35-37

30 I ndaram AVK, Nandi S, Weissman S, Lam S, Bailey B, Blumstein M, Greenberg R, Bank S. Elevated basal intestinal mucosal cytokine levels in asymptomatic first-degree relatives of patients with Crohn s disease. *World J Gastroenterol*, 2000;6:49-52

31 Lai YC, Yang SS, Wu CH, Chen TK. Endoscopic hemoclip treatment for bleeding peptic ulcer. *World J Gastroenterol*, 2000;6:53-56

32 Pan QS, Fang ZP, Zhao YX. Immunocytochemical identification and localization of APUD cells in the gut of seven stomachless teleost fishes. *World J Gastroentero*, 2000;6:96-101

33 Li YX, Li JS, Li N. Improved technique of vascular anastomosis for small intestinal transplantation in rats. *World J Gastroenterol*, 2000;6:259-262

34 Liu BH, Chen HS, Zhou JH, Xiao N. Effects of endotoxin on endothelin receptor in hepatic and intestinal tissues after endotoxemia| in rats. *World J Gastroentero*, 2000;6:298-300

35 Fu XB, Yang YH, Sun TZ, Gu XM, Jiang LX, Sun XQ, Sheng ZY. Effect of intestinal ischemia-reperfusion on expressions of endogenous basic fibroblast growth factor and transforming growth factor B in lung and its relation with lung repair. *World J Gastroenterol*, 2000;6:353-355

36 Wang QG, He LY, Chen YW, Hu SL. Enzymohistochemical study on burn effect on rat intestinal NOS. *World J Gastroenterol*, 2000;6:421-423

37 Chen XM, LaRusso NF. Human intestinal and biliary cryptosporidiosis. *World J Gastroentero*, 1999;5:424-429

38 Komatsu S, Nimura Y, Granger DN. Intestinal stasis-associated bowel inflammation. *World J Gastroenterol*, 1999;5:518-521

39 Zhou Q, Xu TR, Fan QH, Zhen ZX. Clinicopathologic study of primary intestinal B cell malignant lymphoma. *World J Gastroenterol*, 1999;5:538-540

40 Huang B, Wu ZB, Ruan YB. Expression of nm23 gene in hepatocellular carcinoma tissue and its relation with metastasis. *World J Gastroenterol*, 1998;4:266-267

41 Xu CT, Pan BR, Wang YM, Zhang RY, Substance P. Vasoactive intestinal peptide and leu-enkephalin in plasma and gastric juice of patients with precancerous lesions and gastric cancer. *China Natl J New Gastroenterol*, 1995;1:27-29

42 Xu CT, Wang RL, Pan BR. Endoscopic evaluation of gastrointestinal tract lesions in patients with iron-deficiency anemia. *China Natl J New Gastroenterol*, 1996;2:95-98

Edited by Ma JY

P.O.Box 2345 Beijing 100023, China
Fax. 0086·10·65891893 Tel. 0086·10·65897901
E-mail.wcjd@public.bta.net.cn www.wd.org.cn

World J Gastroentero, 2001; 7(1):143 - 148
World Journal of Gastroenterology
Copyright © 2001 by the WJG Press ISSN 1007 - 9327

Effects of Taxotere on invasive potential and multidrug resistance phenotype in pancreatic carcinoma cell line SUIT-2

Bin Liu[1], Edgar Staren[2], Takeshi Iwamura[3], Hubert Appert[2] and John Howard[2]

Subject headings pancreatic neoplasms; drug therapy, combination; drug resistance; glycoproteins; neoplasm invasiveness; polymerase chain reaction; taxotere; multidrug resistance

Liu B, Staren E, Iwamura T, Appert H, Howard J. Effects of Taxotere on invasive potential and multidrug resistance phenotype in pancreatic carcinoma cell line SUIT-2. ***World J Gastroenterol***, 2001;7(1):143-148

INTRODUCTION

Development of drug-resistance to chemotherapy and subsequent metastasis of tumor are primarily responsible for treatment failure and the death from cancer. There have been many previous studies on the relationship between expression of multidrug resistance (MDR) phenotype P-glycoprotein (P-gp) and the malignant properties of tumors, but the results are often conflicting[1-8]. The difference in tumor types or MDR phenotype induced by specific agents might account for this discrepancy. Taxotere (TXT), a member of the family of taxanes, has antitumor activity through its effect of promoting the polymerization of tubulin[9,10]. Since microtubules are involved in many respects of cell functions, such as cell movement, intracellular protein translocation, an altered invasive ability has been confirmed in *in vitro* invasion assay[11-14] and *in vivo* metastasis assay[15] in tumor cells treated with taxane. Taxane has also been found to down-or up- regulate the expressions of metastasis-associated proteins or genes, such as metallo-poteinase[13,16-18], urokinase-type plasminogen activator[18], and E-cadherin[19]. Our previous work demonstrated that the intrinsic and acquired resistance to TXT in pancreatic adenocarcinoma (PAC) cell line SUIT-2 was mediated mainly by P-gp[20]. This study demonstrated that the invasive ability of TXT-resistant cells S2/TXT was not significantly greater than that of SUIT-2. However, S2/TXT cells have increased resistance to the anti-invasion effects of TXT as compared with their parental cells, SUIT-2.

[1]Department of General Surgery, the Affiliated Hospital of Xuzhou Medical College, Xuzhou 221002, Jiangsu Province, China
[2]Department of Surgery, Medical College of Ohio, Toledo, Ohio, USA
[3]Department of Surgery, Miyazaki Medical College, Miyazaki, Japan
Bin Liu, graduated from Xuzhou Medical College in 1983, having 14 papers published. He is an associate professor and Deputy Director of the Department of General Surgery.
Supported in part by Phône-Poulenc Rorer Pharmaceuticals INC.
Correspondence to: Dr. Bin Liu, Department of General Surgery, the Affiliated Hospital of Xuzhou Medical College, Xuzhou 221002, Jiangsu, China
Tel. 0086-516-5802003
Email. Liubinxy@pub.xz.jsinfo.net
Received 2000-08-08 **Accepted** 2000-09-30

MATERIALS AND METHODS

Reagents

Taxotere, obtained from Rhone-Poulenc Rorer Pharmaceuticals Inc., was stored as 10mM stock solution in absolute ethanol at -20℃. This solution was further diluted in the medium and used in the cell culture immediately before each experiment. MTT (3-[4, 5dimethylthiazol-2-yl]-2,5-diphenyltetrazoliumbromide) was dissolved in phosphate buffered saline (PBS) at a concentration of 5 g/L and filtered. The MTT solution was stored in the dark at 4℃ before use.

Cell cultures

Human pancreatic cancer cell line SUIT-2 was established by Iwamura *et al*[21]. This cell line was derived from a metastatic liver tumor of human moderately differentiated pancreatic carcinoma. Its sublines including S2-007, S2-013, S2-020 and S2-028 were cloned by soft agar culture and showed different metastatic potential[22]. Cells were cultured in plastic flasks with McCoy's modified medium supplemented with 10% fetal bovine serum (FBS) (Sigma) and 1. 25% penicillin-streptomycin solution (Sigma) (designated as "culture medium" below) and maintained at 37℃ in humidified atmosphere containing 5% CO_2.

Development of TXT resistant SUIT-2 cell line (S2/TXT)

A SUIT-2 TXT resistance derivative was developed by growing the parental cell line SUIT-2 in increasing concentration of TXT. Initially, the cells were grown as monolayers in culture medium at 37 ℃ in 5% CO_2 humidity atmosphere and exposed to 0.1nM TXT with addition of fresh culture medium and drugs every 3 days. After 2 weeks, the cells were exposed sequentially to stepwise increasing concentration of the drug until a TXT concentration of 2 nM was achieved. These cells were maintained in a drug-free culture medium for at least 3 weeks before used in experiments.

MTT colorimetric assay

The MTT colorimetric assay was performed as described by Page *et al*[23]. Briefly, SUIT-2 and S2/TXT cells were grown within 96well microtitre plates (Costar) at 2×10^4 cells/100 μL of culture medium per well and acclimated for 6 hours. Various concentrations of drugs (100 μL) diluted in culture medium were added. Five duplicate wells were used for each determination. The plates were incubated at 37℃ in 5% CO_2 for 72 hours when the control cells reached 90% confluence, and 30 μL of MTT solution was then added to each well and the plates were incubated at 37℃ for another 4 h. The medium and MTT solutions were then aspirated and 150 μL of dimethyl sulfoxide (DMSO) (Sigma) was added. The plates were agitated on the shaker for 15 minutes and read on Bio-Tek Microplate reader EL 800 (Bio-Tek Instruments, Inc.) with DeltaSoft 3 software. Fraction of cell proliferation was defined as the ratio of optical density volume to that of controls. The IC_{50} was defined as the concentration of the drugs required to reduce the optical density by 50% in treated cells to that of the controls.

Reverse transcription-polymerase chain reaction (RT-PCR)

The isolation of total RNA was based on the method of Chomczynski and Sacchi[24]. After the SUIT-2 and S2/TXT cell lines grew to 90% confluence, the total RNAs were extracted from the cell lines using Trireagent (Biotechnique, Molecular Research Center, Inc.). The total RNA was also isolated from the SUIT-2 cells incubated with 0.4 nM of TXT for 24 h. The messenger RNA was quantitated by measuring its absorbance at 260 nm. Equal amounts of RNA were reversed transcribed using SuperScriptTM One-stepTM RT-PCR System (Life Technologies). The 25 μL PCR mixed in each tube containing 0.5 μL RT/Tag Mix, 3 μL of 5 mM $MgSO_4$, 5 μL diethy pyrocarbonate (DEPC, Sigma) treated distilled water, 3 μL mixed primer pairs, 12. 5 μL 2X reaction mix and 1 μg template RNA in DEPC water. After an initial denaturation in a programmable thermocycler at 94℃ for 2 minutes, PCR was carried out for 30 cycles with the thermal profile: denaturing at 94℃ for 30 seconds, annealing at 55℃ for 30 seconds and extension at 72℃ for 1 minute with an extra 10 minutes extension for the last cycle. After completion of the amplification cycles, 5 μL of each PCR product was electrophoresed at 60V for 1.5 h on a 1.2% agarose gel (GIBCOBRL) in Trizma base and glacial acetic acid EDTA buffer, together with a 100-bp DNA (GIBCOBRL). The specific primers for mdr1 used in this study were sense 5'-CCC ATC ATT GCA ATA GCA GG-3', antisense: 5'- GTT CAA ACT TCT GCT CCT GA-3'. The metastasis of the carcinoma involved many kinds of genes. The primers used to detect the metastasis-related genes in this study were MMP-2: sense 5'-GAG CTG AAG GAC ACA CTA AAG AAG A-3'; antisense 5'-TTG CCA TCC TTC TCA AAG TTG TAG G-3', MMP-9: Sense 5'-CAC TGT CCA CCC CTC AGA GC-3'; antisense 5'-GCC ACT TGT CGG CGA TAA GG-3', Intigrin α5: sense 5'-CAT TTC CAA GTC TGG GCC AA-3'; antisense 5'-TGG AGG CTT GAG CTG AGC TT-3', intigrin β1: sense 5'-TGT TCA GTG CAG AGC CTT CA-3'; antisense 5'-CCT CAT ACT TCG GAT TGA CC-3' and E-Cadherin: sense 5'-GTG ACT GAT GCT GAT GCC CCC AAT ACC-3'; antisense 5'-GAC GCA GAA TCA GAA TAA GAA AAG CAA G-3'. β-actin was used as controls. Its sense primer was: 5'-TGA CGG GGT CAC CCA CAC TGT GCC CAT CTA-3'; antisense primer was: 5'- CTA GAA GCA TTT GCG GTG GAC GAT GGA GGG-3'.

Flow cytometry for Rhodamine-123 (Rho-123) accumulation assay

SUIT-2 and its subline S2/TXT cells were harvested in logarithmic growth phase with 0.25% trypsin and resuspended in phenol red-free DMEM medium at 1×10^6 cells/mL. For Rho-123 accumulation assay, aliquots of 1 mL cell suspension were preincubated with or without 5 μM Verapamil for 45 minutes at 37℃. Rho-123, 200 μg/L dissolved in DMEM, was added and incubated for 40 minutes at 37℃ in the dark. After incubation, cells were washed twice with and resuspended in ice-cold Rho-123 free DMEM with 5 μM Ver. The accumulation of Rho-123 in cells was analyzed with flow cytometry. Ten thousand cells per sample were analyzed. The fluorescence was measured on a logarithmic scale of 4 decades of log. These cell lines, which had not been exposed to Rho-123, were used to determine the background of autofluorescence under this condition.

Fibroblast conditioned medium (FCM)

The FCM was obtained by incubating NIH 3T3 cells (ATCC) in a serum free medium. Briefly, after NIH 3T3 cells grew to 70%-80% confluence in 10% FBS McCoy's medium, the medium was changed to DMEM containing ascorbic acid (50 mg/L), the cells were then incubated at 37℃ for 24 h. The medium was collected after spinning down the cells and stored at -80℃[25].

Cell invasion assay

Matrigel invasion ability of cells was assayed using a Transwell cell culture chamber[25] with an 8 μm pore size polyvinylpyrrolidone-free polycarbonate filter (Costar, Cambridge, MA). At first, the filter was coated with 200 μL Matrigel (Invitrogen, 0.25 μg/μL) and allowed to air-dry overnight. The Matrigel was reconstituted the following day with

200 μL DMEM at room temperature for 30 minutes. SUIT-2 and S2/TXT cells were harvested by trypsinization and resuspended in the culture medium at concentration of 2×10^5 cells/mL. Single cell suspension (400 μL) were placed in the upper chamber of the Transwell in the presence or absence of 0.4 nM of taxotere. The lower chamber contained 1 mL conditioned medium. After the cells were incubated at 37℃ for 24 h, the cells on the upper surface of the filter were removed by wiping with a cotton swab. The filter was fixed with 3% glutaraldehyde, stained with Hematoxylin. Cells which had invaded to the lower surface of the filter in five microscopic fields of 150 × magnification, were counted in each filter. Triplicate samples were conducted. The data were expressed as the average cell number of 15 fields.

Statistics

The significance of different invasion ability between SUIT-2 and S2/TXT, before and after treatment with TXT, was analyzed with Student's *t* test. Values were expressed as mean ± SD.

RESULTS

The sensitivity of SUIT-2 and S2/TXT cells to TXT

The acquired TXT resistant cell line S2/TXT was established from SUIT-2 by culturing with stepwise increasing concentrations of TXT as described in the Materials and Methods. Its IC_{50} (8.1 nM) was 9.5 folds that of its parental cell line SUIT-2 (IC_{50}: 0.85 nM). No change of sensitivity to TXT was found in this cell line during 4 months of study. The doubling time and morphology were similar to that of its parental cell line SUIT-2.

Expressions of mdr1 and other metastasis related genes

The expressions of the major drug transporter pump gene *mdr1* were studied by RT-PCR. There were strong expressions of *mdr1* in TXT-resistant cell line S2/TXT and SUIT-2 cells treated with 0.4 nM TXT for 24 h, and no expressions in the parental cell line SUIT-2, which were sensitive to TXT. Expression of metastasis-related genes in S2/TXT, including MMP-2, MMP-9, Integrin α5, Integrin β and E-Cadherin, was different from the parental cell line SUIT-2. Incubated with 0.4 nM of TXT for 24 h, TXT did not up- or down-regulate these metastasis-related gene expressions (Figure 1).

Rho-123 accumulation assay

Transporter activity of P-gp in S2/TXT cells was assayed by accumulation and efflux of Rho-123 tested with flow cytometry. The accumulation of Rho-123 in SUIT-2 cells is much higher than that of S2/TXT cells. The addition of 5 μM Ver significantly elevated the intracellular Rho-123 level in the TXT-resistant SUIT-2/TXT cells but not in the TXT-sensitive SUIT-2 cells.

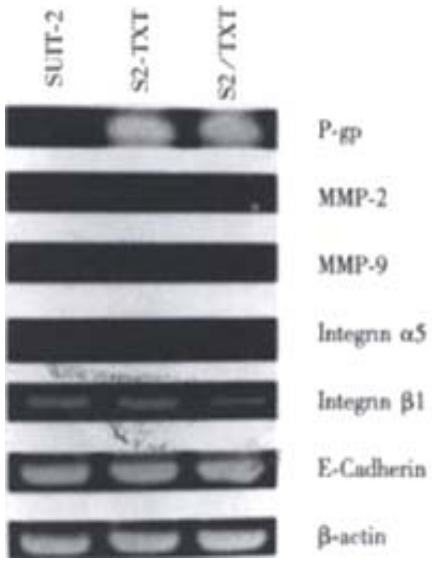

Figure 1 Reverse transcription-polymerase chain reaction (RT-PCR) analysis of drug resistance gene messenger RNA *mdr1* in SUIT-2 and S2/TXT cell lines. RT-PCR was performed with 30 cycles of PCR amplification. The β-actin gene RT-PCR products confirms that intact mRNA is equally present in each of the cell lines. This figure shows that there were strong expressions of *mdr1* in TXT-resistant cell line S2/TXT and SUIT-2 cells treated with 0.4 nM TXT for 24 h, no expressions in the parental cell line SUIT-2. Metastasis-related gene expressions had no difference in these cells.

Invasion assay

The effects of TXT on the *in vitro* invasion ability of SUIT-2 and S2/TXT were examined using an invasion assay system with reconstituted Matrigel membrane. The invasion ability of S2/TXT, which expressed P-gp, was not significantly different from that of SUIT-2 (83 ± 28 *vs* 71 ± 22 cells per field, $P>0.05$). Treatment of the cells with 0.4 nM of TXT for 24 h significantly inhibited the cell invasion of SUIT-2 through the Matrigel basement membrane (71 ± 22 *vs* 17 ± 5 cells per field, $P<0.01$). However, the TXT, in the concentration tested, had no effect on invasion of drug resistant cell line S2/TXT (83 ± 28 vs 68 ± 24 cells per field before and after TXT treatment, $P>0.05$).

DISCUSSION

Pancreatic adenocarcinoma (PAC) currently remains one of the leading causes of cancer death throughout the world. Most patients are surgically unresectable at the time of diagnosis. For those who were resected, the risk of recurrence was extremely high[26]. Consequently, chemotherapy is an important approach for most patients with PAC. Taxane as a promising antitumor agent has been widely used in treatment of cancers. Unfortunately, the initial response to this agent may be hampered by the development of multidrug-resistant cells[27] and possible enhancement of malignant potential[28]. Taxane resistance of tumor cells may involve many mechanisms, but were most often

related to the expression of P-gp[20]. In this study, examination of the TXT effect on the *in vitro* proliferation capacity of SUIT-2 and S2/TXT cells revealed a higher sensitivity of SUIT-2 when compared to the S2/TXT variant. TXT challenge of the initially drug sensitive parental SUIT-2 cell lines resulted in the development of multidrug resistance together with simultaneous expression of P-gp. Active drug transporter pump P-gp in these TXT[a2]resistant cells was confirmed by Rhodamine accumulation assay. However, in a study by Dumontet *et al*, only 44% of resistant clones were found to express the *mdr1* gene, and studies with labeled paclitaxel (Taxol, PTX) did not show altered accumulation in *mdr1* negative clones[29]. Other studies on the mechanisms of Taxane-resistance included the composition and the mutations in β-tubulin isotypes[29,30]. The different expression of P-gp or tubulin mutation might be related to the means by which the resistant cells were selected [31]. Multi-step selected cells often present a high level of Taxane-resistance mediated by P-gp, while single-step selection yields a low level Taxane-resistance cells with tubulin mutations[31]. Since severe tubulin mutations are very likely to affect cell survival, these cells will generally be lost during the selection.

As shown in this study, TXT had marked inhibitory effects on tumor cell invasion. These effects were also found in other tumor cells treated with taxol[11-13,32]. The basic effects of Taxane on tumor cell promoted the polymerization of tubulin and stabilizing microtubule assembly, thereby blocking cell replication in the late G2 mitotic phase of the cell cycle[10,33,34]. Since microtubules are also important components of cell motility and intracellular transport [19,35,36], it is possible that TXT inhibits the invasive and migratory ability through interference with the function of the fundamental part of the cytoskeleton, such as inducing rearrangements or changes of the microtubules, which might interfere with their functional ability to mediate cell movement and protease vesicle transports and secretions of the gelatinase[13]. Direct observation by microinterferometry demonstrated that taxol can suppress the mean area of protrusion and retraction of cells and reduced the spread of cell translocation [35]. The prevention of microtubule depolyme rization by taxol can freeze the cell in a spread conformation, thereby blocking motility[37]. In some cell types, microtubules are known to serve as tracks to transport vesicles and organelles[38]. Mark *et al* reported that relatively low levels of taxol can inhibit secretion of the M_r 72 000 and M_r 92 000 type IV collagenases plus an M_r 57 000 glatinase by blocking the cytoplasmic processing and packaging of the protease and completely inhibit cell attachment to matrigel, type IV collagen and plastic substrates *in vitro*. This has been shown to contribute to the reduced *in vitro* invasive ability and the establishment, growth and long-term survival of prostate tumor cells in SCID mice[13]. TXT did not, however, increase Integrin-mediated cell adhesion and cell spreading, which are attributable to microtubule depolymerization induced by microtubule disrupting agents[39].

Like other neoplasms, this pancreatic carcinoma cell line SUIT-2 is heterogeneous and consists of multiple subpopulations of cells with different invasive and metastatic properties[22]. These cells may be heterogeneous with regard to their sensitivity to chemotherapeutic agent and may contain different expressions of drug resistant phenotypes. Our previous studies have shown that the most TXT-resistant cell line in SUIT-2 and its subline (S2-007, S2-013, S2-020, S2-028) was S2-020 with strong expression of P-gp[21]. Although an *in vitro* study showed that S2-020 was also the most invasive toward Matrigel among these cell lines[22], there was no direct evidence that the expression of P-gp in this cell lines is responsible for its high invasive potential. On the contrary, it has been demonstrated that type I and IV collagenolytic activities are related to the malignancy of these cell lines[22,40].

The existence of different subpopulations in tumor increases the chance that cells with a high probability of survival will be selected when environmental conditions change. When SUIT-2 cell lines were treated with TXT, the highly invasive S2-020 with positive P-gp expression would be selected. However, the morphology of S2/TXT is totally different from that of S2-020 and *in vitro* invasive ability and morphology are similar to that of SUIT-2. Therefore, the expression of P-gp in S2/TXT was not due to the selection effect of TXT but to creation of TXT-resistant clone caused by potential of genetic mutation of TXT. In addition to the development of MDR, exposure tumor cells to some chemotherapeutic agents can cause activation or inactivation of genes with altered behavioral phenotype[41]. There was, however, no evidence that this occurred in this specific cell line treated with TXT, as shown by analysis of a number of metastasis-related genes. Thus, TXT appears capable of inducing the expression of P-gp without changing the intrinsic malignant characteristics of SUIT-2 cells.

In contrast to the study by Belotti *et al*, which show the PTX inhibits the motility of parental and PTX resistant cells equally[11], TXT did not inhibit the invasiveness of the TXT-resistant cell SUIT-2. This difference might be related to the mechanisms of taxane-resistance. Although the effect of PTX on cell motility and invasiveness is independent of

its effect on cell proliferation[11], these effects might still be based on the intracellular concentration of the drug. Studies have shown that the tumor cells can present TXT-resistance with normal intracellular concentration of TXT. This kind of resistance usually is mediated by changes of beta tubulin isotypes[31]. In such cases, the normal intracellular drug concentration in the TXT-resistance cell can be reached as in the TXT sensitive cells. In the S2/TXT cell line, which expresses active drug transporter pump P-gp, the intracellular concentration of TXT might not be high enough to act on microtubule and to inhibit cell invasion. It indicates that the resistance to the cytotoxic activity of TXT also confers resistance to the anti-invasion of the drug in the cell line SUIT-2. Therefore, the collateral anti-tumor effects of chemotherapeutic agents, as proposed by other studies[13], will disappear in this TXT-resistant cell line when treated with taxotere.

The relationship between P-gp expression and tumor malignancy is controversial. Although some studies have found that the expression of P-gp is casually related to a less aggressive pheno-type[4,42,43], in numerous cases, metastases exhibit a multidrug resistant pattern. Clinical and *in vitro* studies have also provided correlative results concerning the changes of metastatic potential following acquisition of the MDR phenotype[2,3,8,44]. To date, there has been no direct evidence showing that P-gp is involved intumor malignant potential. The invasive ability in the P-gp-positive S2/TXT cell line was not different from its P-gp-negative parental cell line SUIT-2, suggesting that TXT has no direct effect on increasing tumor malignant potential related to the induction of P-gp expression in this PAC cell line. The higher malignant potential associated with positive P-gp expression found in the other studies might be due to other invasive or metastatic related gene expressed simultaneously with P-gp.

From this study, we conclude that P-gp is primarily responsible for TXT resistance in PAC cell lines SUIT-2. However, expression of P-gp does not confer a more malignant invasive potential in this cell line with TXT resistance. Furthermore, TXT can inhibit the invasive ability of drug-sensitive cells but not drug-resistant cells.

REFERENCES

1 Zhang LJ, Chen KN, Xu GW, Xing HP, Shi XT. Congenital expression of *mdr*-1 gene in tissues of carcinoma and its relation with patho morphology and prognosis. *World J Gastroentero*, 1999;5:53-56

2 Staroselsky AN, Mahlin T, Savion N, Klein O, Nordenberg J, Donin N, Michowitz M, Leibovici J. Metastatic potential and multidrug resistance correlation in the B16 melanoma system. *J Exp Ther Oncol*, 1996;1:251-259

3 Kakehi Y, Wu WJ, Kim WJ, Arao S, Fukumoto M, Yoshida O. Comparison of multidrug resistance gene expression levels with malignant potentials and influence of chemotherapy in urothelial cancers. *Int J Urol*, 1995;2:309-315

4 Mitsumoto M, Kamura T, Kobayashi H, Sonoda T, Kaku T, Nakano H. Emergence of higher levels of invasive and metastatic properties in the drug resistant cancer cell lines after the repeated administration of cisplatin in tumor-bearing mice. *J Cancer Res Clin Oncol*, 1998;124:607-614

5 Scotlandi K, Manara MC, Serra M, Benini S, Maurici D, Caputo A, De Giovanni C, Lollini PL, Nanni P, Picci P, Campanacci M, Baldini N. The expression of P-glycoprotein is causally related to a less aggressive phenotype in human osteosarcoma cells. *Oncogene*, 1999;18:739-746

6 Anzai H, Kitadai Y, Bucana CD, Sanchez R, Omoto R, Fidler IJ. Expression of metastasis-related genes in surgical specimens of human gastric cancer can predict disease recurrence. *Eur J Cancer*, 1998;34:558-565

7 Scotlandi K, Serra M, Nicoletti G, Vaccari M, Manara MC, Nini G, Landuzzi L, Colacci A, Bacci G, Bertoni F, Picci P, Campanacci M, Baldini N. Multidrug resistance and malignancy in human osteosarcoma. *Cancer Res*, 1996;56:2434-2439

8 Greene GF, Kitadai Y, Pettaway CA, von Eschenbach AC, Bucana CD, Fidler IJ. Correlation of metastasis-related gene expression with metastatic potential in human prostate carcinoma cells implanted in nude mice using an in situ messenger RNA hybridization technique. *Am J Pathol*, 1997;150:1571-1582

9 Bissery MC, Guenard D, Gueritte-Voegelein F, Lavelle F. Experimental antitumor activity of taxotere (RP 56976, NSC 628503), a taxol analogue. *Cancer Res*, 1991;51:4845-4852

10 Yuan JH, Zhang RP, Zhang RG, Guo LX, Wang XW, Luo D, Xie Y, Xie H. Growth-inhibiting effects of taxol on human liver cancer *in vitro* and in nude mice. *World J Gastroenterol*, 2000;6:210-215

11 Belotti D, Rieppi M, Nicoletti MI, Casazza AM, Fojo T, Taraboletti G, Giavazzi R. Paclitaxel (Taxol(R)) inhibits motility of paclitaxel-resistant human ovarian carcinoma cells. *Clin Cancer Res*, 1996; 2:1725-1730

12 Terzis AJ, Thorsen F, Heese O, Visted T, Bjerkvig R, Dahl O, Arnold H, Gundersen G. Proliferation, migration and invasion of human glioma cells exposed to paclitaxel (Taxol) *in vitro*. *Br J Cancer*, 1997;75:1744-1752

13 Stearns ME, Wang M. Taxol blocks processes essential for prostate tumor cell (PC-3 ML) invasion and metastases. *Cancer Res*, 1992;52:3776-3781

14 Westerlund A, Hujanen E, Hoyhtya M, Puistola U, Turpeenniemi-Hujanen T. Ovarian cancer cell invasion is inhibited by paclitaxel. *Clin Exp Metastasis*, 1997;15:318-328

15 Belotti D, Vergani V, Drudis T, Borsotti P, Pitelli MR, Viale G, Giavazzi R, Taraboletti G. The microtubule-affecting drug paclitaxel has antiangiogenic activity. *Clin Cancer Res*, 1996;2:1843-1849

16 Stearns ME, Wang M. Immunoassays of the metalloproteinase (MMP-2) and tissue inhibitor of metalloproteinase (TIMP 1 and 2) levels in noninvasive and metastatic PC-3 clones: effects of taxol. *Oncol Res*, 1994;6:195-201

17 Jardillier JC, Affoue M, Bobichon H, Delvincourt C, Madoulet C. Detection of metastatic activity of the MCF-7 multidrug resistant cell line cultured in spheroids. *Bull Acad Natl Med*, 1998;182: 651-661

18 Alonso DF, Farina HG, Arregui C, Aon MA, Gomez DE. Modulation of urokinase-type plasminogen activator and metalloproteinase activities in cultured mouse mammary-carcinoma cells: enhancement by paclitaxel and inhibition by nocodazole. *Int J Cancer*, 1999;83:242-246

19 Eckert K, Fuhrmann-Selter T, Maurer HR. Docetaxel enhances the expression of E-cadherin and carcinoembryonic antigen (CEA) on human colon cancer cell lines *in vitro*. *Anticancer Res*, 1997; 17:7-12

20 Liu B, Staren E, Iwamura T, Appert H, Howard J. Mechanisms of intrinsic and acquired Taxotere-related drug resistance in pancreatic carcinoma cell SUIT-2 and its sublines. *Proc Am Asso Can Res*, 2000;41:616

21 Iwamura T, Katsuki T, Ide K. Establishment and characterization of a human pancreatic cancer cell line (SUIT-2) producing carcinoembryonic antigen and carbohydrate antigen 19-9. *Jpn J Cancer Res*, 1987;78:54-62

22 Taniguchi S, Iwamura T, Kitamura N, Yamanari H, Setoguchi T. Heterogeneities of attachment, chemotaxis, and protease production among clones with different metastatic potentials from a human pancreatic cancer cell line. *Clin Exp Metastasis*, 1994;12: 238-244

23 Page M, Bejaoui N, Cinq-Mars B, Lemieux P.Optimization of the tetraz olium-based colorimetric assay for the measurement of cell number and cytotoxicity. *Int J Immunopharmacol*, 1988;10:785-793

24 Chomczynski P, Sacchi N. Single-step method of RNA isolation by acidguanidinium thiocyanate-phenol-chloroform extraction. *Anal Biochem*, 1987;162:156-159

25 Albini A, Iwamoto Y, Kleinman HK, Martin GR, Aaronson SA, Kozlowski JM, McEwan RN. A rapid *in vitro* assay for quantitating the invasive potential of tumor cells. *Cancer Res*, 1987;47: 3239-3245
26 Zhou ZH, Song MZ. Current therapies of pancreatic cancer. *Shijie Huaren Xiaohua Zazhi*, 2000;8:214-215
27 Parekh H, Wiesen K, Simpkins H. Acquisition of taxol resistance via P-glycoprotein and non-P-glycoprotein-mediated mechanisms in human ovarian carcinoma cells. *Biochem Pharmacol*, 1997; 53:461-470
28 Emanuel SL, Chamberlin HA, Cohen D. Antimitotic drugs cause increased tumorigenicity of multidrug resistant cells. *Int J Oncol*, 1999;14:487-494
29 Dumontet C, Duran GE, Steger KA, Beketic-Oreskovic L, Sikic BI. Resistance mechanisms in human sarcoma mutants derived by single-step exposure to paclitaxel (Taxol). *Cancer Res*, 1996;56:1091-1097
30 Kapoor P, Ghosh A, Madhubala R. Isolation of a taxol-resistant Leishmania donovani promastigote mutant that exhibits a multidrug-resistant phenotype. *FEMS Microbiol Lett*, 1999;176:437-441
31 Gonzalez-Garay ML, Chang L, Blade K, Menick DR, Cabral F. A beta-tubulin leucine cluster involved in microtubule assembly and paclitaxel resistance. *J Biol Chem*, 1999;274:23875-23882
32 Verschueren H, Dewit J, De Braekeleer J, Schirrmacher V, De Baetselier P. Motility and invasive potency of murine T-lymphoma cells: effect of microtubule inhibitors. *Cell Biol Int*, 1994;18:11-19
33 Bissery MC, Guenard D, Gueritte-Voegelein F, Lavelle F. Experimental antitumor activity of taxotere (RP 56976, NSC 628503), a taxol analogue. *Cancer Res*, 1991;51:4845-4852
34 Hill BT, Whelan RD, Shellard SA, McClean S, Hosking LK. Differential cytotoxic effects of docetaxel in a range of mammalian tumor cell lines and certain drug resistant sublines *in vitro*. *Invest New Drugs*, 1994;12:169-182
35 Dunn GA, Zicha D, Fraylich PE. Rapid, microtubule-dependent fluctuations of the cell margin. *J Cell Sci*, 1997;110:3091-3098
36 Mooney DJ, Langer R, Ingber DE. Cytoskeletal filament assembly and the control of cell spreading and function by extracellular matrix. *J Cell Sci*, 1995;108:2311-2320
37 Stracke ML, Soroush M, Liotta LA, Schiffmann E. Cytoskeletal agents in hibit motility and adherence of human tumor cells. *Kidney Int*, 1993;43:151-157
38 Robin P, Rossignol B, Raymond MN. Effect of microtubule network disturbance by nocodazole and docetaxel (Taxotere) on protein secretion in rat extraor bital lacrimal and parotid glands. *Eur J Cell Biol*, 1995;67:227-237
39 Kadi A, Pichard V, Lehmann M, Briand C, Braguer D, Marvaldi J, Rognoni JB, Luis J. Effect of microtubule disruption on cell adhesion and spreading. *Biochem Biophys Res Commun*, 1998;246: 690-695
40 Taniguchi S, Iwamura T, Katsuki T. Correlation between spontaneous metastatic potential and type I collagenolytic activity in a human pancreatic cancer cell line (SUIT-2) and sublines. *Clin Exp Metastasis*, 1992;10:259-266
41 Bashir I, Sikora K, Foster CS. Multidrug resistance and behavioural phenotype of cancer cells. *Cell Biol Int*, 1993;17:907-917
42 Serra M, Scotlandi K, Manara MC, Maurici D, Lollini PL, De Giovanni C, Toffoli G, Baldini N. Establishment and characterization of multidrug-resistant human osteosarcoma cell lines. *Anticancer Res*, 1993;13:323-329
43 Suwa H, Ohshio G, Arao S, Imamura T, Yamaki K, Manabe T, Imamura M, Hiai H, Fukumoto M. Immunohistochemical localization of P-glycoprotein and expression of the multidrug resistance-1 gene in human pancreatic cancer: relevance to indicator of better prognosis. *Jpn J Cancer Res*, 1996;87:641-649
44 Yao XQ, Qing SH. Detection of multidrug resistance gene in progvessive colon cancer and its significance. *Shijie Huaren Xiaohua Zazhi*, 1999;7:535-536

Edited by Ma JY